

# MEDICAL PHYSICS *International*

- EDITORIALS
- GLOBAL NUMBER OF MEDICAL PHYSICISTS AND ITS GROWTH 1965-2015
- PROFESSIONAL SURVEY IN SWITZERLAND: MEDICAL PHYSICISTS IN RADIODIAGNOSTICS
- MEDICAL PHYSICS PROFESSIONAL DEVELOPMENT AND EDUCATION IN INDIA
- STATUS OF MEDICAL PHYSICS PROFESSIONAL DEVELOPMENT AND EDUCATION IN NEPAL
- MEDICAL PHYSICS PROFESSIONAL DEVELOPMENT AND EDUCATION IN NIGERIA
- AN INTRODUCTION TO HOSPITAL NETWORKS
- PERFORMANCE AND PITFALLS OF DIAGNOSTIC X-RAY ...
- OPTIMISATION OF PLANAR CHEST PA EXPOSURES ...
- EMERGING MODELS FOR GLOBAL HEALTH ...
- ICMP2016 BOOK OF ABSTRACTS



## BOOK OF ABSTRACTS



The Journal of the International Organization for Medical Physics

Volume 4, Number 2, December 2016

MPI



# **MEDICAL PHYSICS INTERNATIONAL**

---

**THE JOURNAL OF  
THE INTERNATIONAL ORGANIZATION FOR MEDICAL PHYSICS**



Volume 4, Number 2, December 2016

## **MEDICAL PHYSICS INTERNATIONAL**

The Journal of the International Organization for Medical Physics

---

### **Aims and Coverage:**

Medical Physics International (MPI) is the official IOMP journal. The journal provides a new platform for medical physicists to share their experience, ideas and new information generated from their work of scientific, educational and professional nature. The e- journal is available free of charge to IOMP members.

### **Co-Editors**

Slavik Tabakov, IOMP President, UK and Perry Sprawls, Atlanta, USA

### **Editorial Board**

KY Cheung , IOMP Past President, Hong Kong, China

Madan Rehani, IOMP Vice President, IAEA

William Hendee , IOMP Scientific Com Past-Chair, Wisconsin, USA

Tae Suk Suh , President AFOMP, IOMP Publication Com Chair, South Korea

John Damilakis, EFOMP President, IOMP ETC Chair, Greece

Virginia Tsapaki, IOMP Secretary General, Greece

Raymond Wu, IOMP PRC Past Chair, USA

Simone Kodlulovich Dias, President ALFIM, IOMP Awards Committee Chair, Brazil

Anchali Krisanachinda, Past President SEAFOMP, IOMP Treasurer, Thailand

Toafeeq Ige, FAMPO Secretary General, Nigeria

Technical Editors: Magdalena Stoeva and Asen Cvetkov, Bulgaria

Editorial Assistant: Vassilka Tabakova, UK

MPI web address: [www.mpjournal.org](http://www.mpjournal.org)

Published by: The International Organization for Medical Physics (IOMP), web address: [www.iomp.org](http://www.iomp.org) ; post address: IOMP c/o IPEM, 230 Tadcaster Road, York YO24 1ES, UK.

Copyright ©2013 International Organisation Medical Physics. All rights reserved. No part of this publication may be reproduced, stored, transmitted or disseminated in any form, or by any means, without prior permission from the Editors-in-Chief of the Journal, to whom all request to reproduce copyright material should be directed in writing.

All opinions expressed in the Medical Physics International Journal are those of the respective authors and not the Publisher. The Editorial Board makes every effort to ensure the information and data contained in this Journal are as accurate as possible at the time of going to press. However IOMP makes no warranties as to the accuracy, completeness or suitability for any purpose of the content and disclaim all such representations and warranties whether expressed or implied.

**ISSN 2306 - 4609**

## CONTENTS

|   |            |
|---|------------|
| <b>Contents</b>   | <b>75</b>  |
| <b>EDITORIALS</b>   | <b>77</b>  |
| EDITORIAL   | 77         |
| <i>Perry Sprawls</i>  |            |
| EDITORIAL   | 77         |
| <i>Slavik Tabakov</i>   |            |
| <b>EDUCATIONAL RESOURCES</b>  | <b>78</b>  |
| GLOBAL NUMBER OF MEDICAL PHYSICISTS AND ITS GROWTH 1965-2015  | 78         |
| <i>S. Tabakov</i>   |            |
| <b>PROFESSIONAL ISSUES</b>  | <b>82</b>  |
| PROFESSIONAL SURVEY IN SWITZERLAND: MEDICAL PHYSICISTS IN RADIODIAGNOSTICS                                    | 82         |
| <i>Eleni-Theano Samara, Robert Schöpflin, Stefano Presilla</i>  |            |
| MEDICAL PHYSICS PROFESSIONAL DEVELOPMENT AND EDUCATION IN INDIA   | 88         |
| <i>Neeraj Dixit, G. Sahani, S. Mahalakshmi, Pankaj Tandon, Sunil D. Sharma, A. U. Sonawane, Arun Chougule</i> |            |
| STATUS OF MEDICAL PHYSICS PROFESSIONAL DEVELOPMENT AND EDUCATION IN NEPAL                                     | 94         |
| <i>Matrika P. Adhikari 1, Pradumna P. Chaurasia</i>   |            |
| MEDICAL PHYSICS PROFESSIONAL DEVELOPMENT AND EDUCATION IN NIGERIA   | 96         |
| <i>Obed R.I, Ekpo M.E, Omojola A.D, Abdulkadir M.K</i>  |            |
| <b>TECHNOLOGY INNOVATIONS</b>   | <b>99</b>  |
| AN INTRODUCTION TO HOSPITAL NETWORKS  | 99         |
| <i>P.S. Ganney</i>  |            |
| PERFORMANCE AND PITFALLS OF DIAGNOSTIC X-RAY SOURCES: AN OVERVIEW   | 107        |
| <i>R. Behling</i>   |            |
| <b>HOW-TO</b>   | <b>115</b> |
| OPTIMISATION OF PLANAR CHEST PA EXPOSURES USING THE CDRAD CONTRAST DETAIL PHANTOM                             | 115        |
| <i>K. Thomson, J. Lynch</i>   |            |
| <b>INVITED PAPERS</b>   | <b>121</b> |
| EMERGING MODELS FOR GLOBAL HEALTH IN RADIATION ONCOLOGY   | 121        |
| <i>W. Ngwa, T. Ngoma</i>  |            |
| <b>INFORMATION FOR AUTHORS</b>  | <b>131</b> |
| PUBLICATION OF DOCTORAL THESIS AND DISSERTATION ABSTRACTS   | 131        |
| INSTRUCTIONS FOR AUTHORS  | 132        |
| <b>ICMP2016 BOOK OF ABSTRACTS</b>   | <b>135</b> |
| ICMP 2016 ORGANISATIONAL STRUCTURE  | 137        |
| ICMP 2016 PRESIDENT MESSAGE   | 138        |
| IOMP PRESIDENT MESSAGE  | 139        |
| AFOMP PRESIDENT MESSAGE   | 140        |
| SEAFOMP PRESIDENT MESSAGE   | 141        |
| ORAL PRESENTATIONS  | 143        |
| POSTER PRESENTATIONS  | 367        |
| MINI SIMPOSIA   | 534        |



## EDITORIALS

### **Connecting Our Global Medical Physics Community**

*Perry Sprawls, Co-Editor*

All of us medical physicists generally work in our local hospitals, clinics, and educational institutions. We are members of regional or national medical physics organizations but often separated and isolated from all of the other medical physicists around the world because of great distances and limitations to travel. As a profession, we benefit from being connected so that we can share experiences, especially as we move into the future with the many developments and innovations in both radiation oncology and diagnostic imaging. As these technologies and clinical methods become available and spread around the world there is a critical need for medical physicists with knowledge and experience to support the evolving, and often complex, clinical methods.

The internet and world-wide web (WWW) now provides the foundation for connecting our global community and sharing experiences that can benefit others. The value is in the specific programs that post materials, three examples are considered here.

This journal, Medical Physics International, provides an opportunity for medical physicists in the various countries to share their experience in professional and education program development. It also provides educational resources on many of the advances in clinical methods requiring physics involvement.

The Virtual Library of the American Association of Physicists in Medicine (AAPM) is an extensive source of educational presentations at: <http://aapm.org/education/VL>. It is available to AAPM members and to medical physicists in any of the Developing Countries who register as a Developing Country Education Associate at: <http://aapm.org/international>.

The Windows to the World of Medical Physics at: <http://www.sprawls.org/PhysicsWindows/> is a resource to support medical physics educators in all countries with high-quality visuals to enhance their classroom activities.

As the global medical physics community becomes even more connected through the internet we all benefit by sharing experiences and resources.

---

### **2016 – Year dedicated to Medical Physics Education and Training**

*Slavik Tabakov, Co-Editor*

One of the most important aspects for development of any profession is education and training. Many medical physicists take part in various education and training activities, but it is the dissemination of these, what supports the global growth of the profession. With this on mind we initiated in 2013 the new IOMP Journal Medical Physics International, which now surpasses 6000 readers per month. In 2016 IOMP decided to dedicate the International Day of Medical Physics to Education and Training. This coincided with the double growth of the global number of medical physicists in the past 20 years, which is strongly related with the increased number of international education projects and activities and the introduction of e-learning (please see the related paper in this issues of MPI).

To further support the dissemination of education and training activities I proposed to the IOMP ExCom to discuss a new initiative, aiming to increase the educational elements of the International Conference in Medical Physics (ICMP). This new initiative, IOMP School includes educational Symposia and Workshops.

The first IOMP School was launched at the ICMP 2016, in Bangkok. The IOMP School 2016, aims to introduce young medical physicists to the newest developments in the profession. It also includes a Workshop aiming to help colleagues from low-and-middle income countries to build medical physics capacities in their societies and countries. More than 40 educational mini-Symposia were proposed to the ICMP2016 Organisers by colleagues from USA, UK, EFOMP, Japan, Korea, Australis and other AFOMP countries. These formed an educational block covering almost all mornings of the ICMP2016 in Bangkok. The interest to these mini-Symposia from colleagues of Asia is substantial, what is a clear indication of the need of such activity. IOMP plans to carry such IOMP Schools at all future ICMP.

# EDUCATIONAL RESOURCES

## GLOBAL NUMBER OF MEDICAL PHYSICISTS AND ITS GROWTH 1965-2015

S. Tabakov<sup>1,2</sup>

<sup>1</sup> Dept. Medical Engineering and Physics, King's College London, King's College Hospital, London SE5 9RS, UK

<sup>2</sup> President IOMP (International Organization for Medical Physics), IPEM, York YO24 1ES, UK

**Abstract—** The paper presents the global growth of medical physicists during the period 1965-2015, supported by the archive data of IOMP ([www.iomp.org](http://www.iomp.org)). Medical physicists work in various institutions and thus it is not possible to have their exact global number, but the available IOMP data gives a good estimate and presents the distribution of medical physicists in different continents. The growth of the profession is discussed as strongly linked with the Education and Training activities in medical physics. Based on the recent (2015) report of the Global Task Force on Radiotherapy for Cancer, further activities are discussed to reflect the expected significant need of more medical physicists by 2035.

**Keywords—** Medical Physics Professional development, Education and Training, e-Learning

### I. INTRODUCTION

Medical physicists have a very important role in contemporary medicine, associated with the clinical application of all medical imaging and radiotherapy equipment. This way it is only natural to see increasing of medical physicists with the increased use of this equipment.

Medical physicists work mainly in hospitals, but also in Universities, Research Institutions, Regulatory bodies, Industry, etc. Due to this reason it is not possible to establish the exact global number of medical physicists. However, the data from various medical physics societies, collected by the International Organization for Medical Physics (IOMP), presents a good estimate of this number. The IOMP archive data on Fig.1 shows the growth of the profession in the past 50+ years.

### II. GLOBAL NUMBER OF MEDICAL PHYSICISTS 1965-2015

The history of IOMP has been subject of previous publications [1, 2]. For the purposes of this paper we shall make a brief summary here below. IOMP has been formed in 1963 by 4 National Organisations – from the

UK, USA, Canada and Sweden. In the next two years new Medical Physics Societies joined the Organization – namely from East Germany (DDR), Hungary, Israel, Poland and South Africa. As per the IOMP data, around the time of IOMP formation there had been about 6,000 medical physicists globally. Outside this statistics would be professionals in countries where medical physics societies had not yet been formed, as well as non-members of national societies, hence it would not be possible to have an accurate number of the medical physicists globally at this period.

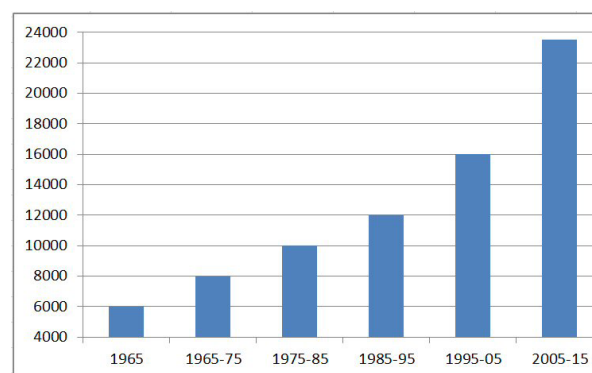


Fig.1 Growth of medical physicists globally in the period 1965-2015 – per decade (IOMP data)

Further, IOMP data shows that during the first decade of the Organization (1965-1975) the global number of medical physicists (members of national societies) increased to about 8,000. During this period new national societies joined IOMP – namely: West Germany, Brazil, Finland, France, Greece and Mexico.

In the next decade 1975-1985 the global number of medical physicists (members of national societies) increased to about 10,000. During this period the new national societies joining IOMP are from: Netherlands, New Zealand, Ireland, Norway, Italy, Japan, Spain,

Austria, Belgium, Denmark, India, Switzerland and Thailand.

The growth of approximately 2,000 professionals per decade continued also in the next period 1985-1995, when the global number of medical physicists (members of national societies) increased to about 12,000. This was one of the most active decades of IOMP, with 30 new member societies joining the Organization (although some are from small countries, and one is uniting two existing societies – Germany). The new national societies joining IOMP in this decade were from: Nigeria, People's Republic of China, Columbia, Turkey, Australia, Hong Kong, Philippine, Sri Lanka, Malaysia, Cyprus, Argentina, Bulgaria, Ghana, Republic of Korea, Romania, Yugoslavia, Tanzania, Germany (united); Moldova, Pakistan, Russia, Slovenia, Sudan, Trinidad & Tobago, Algeria, Indonesia, Iran, Jordan, Panama, Venezuela, Zimbabwe. This way about 30 years after the formation of IOMP the global number of medical physicists doubled.

The period 1995-2005 included 18 relatively small new member societies to the IOMP family – namely from Cuba, Estonia, Georgia, Lithuania, Morocco, Ukraine, Zambia, Ecuador, Portugal, Bangladesh, Chile, Egypt, Nepal, Republic of Taiwan, Singapore, Uganda, Mexico and Mongolia. However in this period the growth per decade doubled (to 4000) and by 2005 the global number of medical physicists reached about 16,000. This period also marks extensive development of medical physics education and training. Many countries established new MSc (or related) University courses. For example, after the International Conference in Medical Radiation Physics Post-graduate Education (Budapest, 1994, [3]) almost all countries from Eastern Europe developed their own medical physics education courses. Also during this period was the introduction of e-learning in medical physics and the opening of a number of educational web sites [4]. Obviously this has influenced the professional growth. This argument is supported by the developments in the next decade.

The strong emphasis on education and training continued also in the decade 2005-2015 [5]. The number of new member societies joining IOMP in this period was relatively small, from: Croatia, Cameroon, Czech Republic, Arab Emirates, Macedonia, Lebanon, Peru, Qatar, Saudi Arabia, Vietnam and Iraq. However the global growth of medical physicists was the largest so far – close to 6000 per decade. During 2016 the global number of medical physicist reached 24,000. This is doubling of this number in the past 20 years. This way about 50 years after its establishment IOMP data shows quadrupling of medical physicists globally. During this period the strongest growth of the profession was in Asia (over 120% increase) and this was supported by many Educational Workshops (including two large ones,

satellite to the World Congresses in Sydney and Seoul, focused on establishment of MSc courses). As a further argument for the importance of education, we have to underline that half of all medical physicists are from USA and UK - members of the AAPM and IPEM – the largest medical physics societies with best developed education, training and professional development.

During this decade e-learning in medical physics developed very strongly and availability of teaching materials through Internet supported many colleagues from low-and-middle income countries [5]. These colleagues also received strong support from the ICTP International College on Medical Physics, where in the period after 1999 about 1000 medical physicists from 82 such countries passed intensive courses [6]. All these colleagues received free e-learning and other teaching materials, which had allowed them to start courses in their own countries. Currently about 20 new MSc courses have been established by graduates of the ICTP College. This was also supported by the IOMP Model Curriculum and the special Guides of the IAEA.

### III. CURRENT GLOBAL DISTRIBUTION OF MEDICAL PHYSICISTS AND PREDICTIONS OF THE GLOBAL TASK FORCE ON RADIOTHERAPY FOR CANCER

The approximate distribution of medical physicists around the world is quite uneven, as shown in Fig. 2, where the number is shown per IOMP Regional Organisations (Federations, formed by IOMP to support the profession in their continents/regions). Obviously additional work is necessary to support the increase of medical physicists in Latin America and Africa. A number of projects are supporting the professional development in these continents, especially through the IAEA, which developed packages of materials and Guides for education and training courses [7]. To help with the dissemination of education, training and professional related information, IOMP launched in 2013 a special free online e-Journal Medical Physics International ([www.mpijournal.org](http://www.mpijournal.org)), which quickly established itself as one of the most accessed Journals in the profession. Further, IOMP formed in 2015 a new body – Regional Coordination Board, aiming to assist the international coordination of the efforts for harmonised development of the profession. The Board includes the leads of all Regional Organisations (Federations) of IOMP and the largest medical physics societies.

These concerted activities will be very important for the coming two decades, where we shall have to expect further very strong increase of the global number of medical physicists. The recently published report [8] of the Global Task Force on Radiotherapy for Cancer estimates that, only for the needs of Radiotherapy by

2035, the global number of newly trained medical physicists will be of the order of: 17,200 (for High-income countries); 12,500 (for Upper-middle-income countries); 7,200 (for Lower-middle-income countries); 2,400 (for Low-income countries). Adding the needs of Medical Imaging will result in approximately tripling the number of medical physicists in the coming two decades (2015-2035).

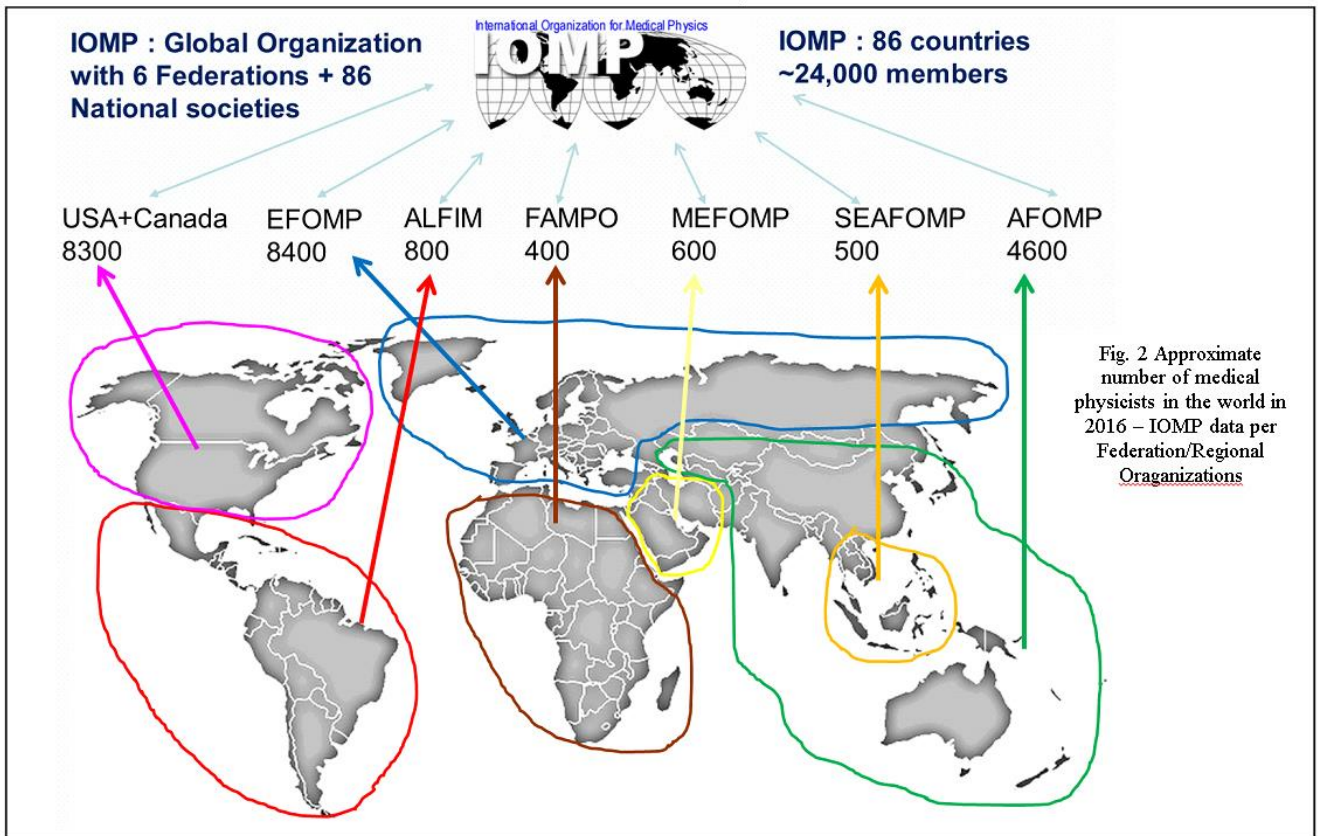
#### IV. CONCLUSION

The huge challenge, shown in the previous paragraph, will need special attention and actions. In the first place this will be the further development of education and training – something of special importance for a dynamic profession such as medical physics. We as profession will need to specially emphasize activities as sharing teaching expertise and materials, developing of new e-learning activities and more effective education methodologies [9]. Another very important action is continuing discussions in all IOMP Regional Organizations on the subject – such as Topical Conferences, Workshops and other activities. The new IOMP activity, satellite to the ICMP2016 – IOMP School, is an existing step in this direction. Further this can be supplemented by the establishment of Regional Training Centres, what would be of great help especially for smaller countries. The activities of ICTP can be used as a model in such development.

Today it is impossible to even imagine contemporary medicine without the sophisticated Medical Imaging and Radiotherapy equipment. Due to this reason, when the high-level UNESCO World Conference “Physics and Sustainable Development” (Durban, South Africa, 2005) discussed the main topics of applied physics in the 21st century, one of the highlighted topics was ‘Physics and Health’ (presented by IOMP). This way increasing the medical physics workforce is not simply a professional need, it is also of main importance for the development of global healthcare.

#### V. REFERENCES

1. Azam Niroomand-Rad, C Orton, P Smith, S Tabakov (2013), A History of the International Organization for Medical Physics – 50 Year Anniversary – Part I, Journal Medical Physics International, vol. 1, No.2, 2013, p.113 (available free from: <http://www.mpijournal.org/pdf/2013-02/MPI-2013-02-p113.pdf>)
  2. Azam Niroomand-Rad, C Orton, P Smith, S Tabakov (2014), A History of the International Organization for Medical Physics – 50 Year Anniversary – Part II, Journal Medical Physics International, vol. 2, No.1, 2014, p.7 (available free from: <http://www.mpijournal.org/pdf/2014-01/MPI-2014-01-p007.pdf>)
  3. C. Roberts, Tabakov S., Lewis C. - editors, (1995) "Medical Radiation Physics - A European Perspective", London, King's College London, ISBN 1 870722 02 7 (available free from: [http://www.emerald2.eu/mep/e-book95/MedRadPhys\\_95b.pdf](http://www.emerald2.eu/mep/e-book95/MedRadPhys_95b.pdf))
  4. S. Tabakov, V Tabakova, (2015), The Pioneering of e-Learning in Medical Physics, London, ISBN 978-0-9552108-3-9 (available free from: <http://www.emerald2.eu/mep/e-learning>)
  5. S. Tabakov, P Sprawls, A Krisanachinda, C Lewis, Editors and Co-Authors (2011), Medical Physics and Engineering Education and Training – part I, ISBN 92-95003-44-6, ICTP, Trieste, Italy (available free from: [http://www.emerald2.eu/mep/e-book11/ETC\\_BOOK\\_2011\\_ebook\\_s.pdf](http://www.emerald2.eu/mep/e-book11/ETC_BOOK_2011_ebook_s.pdf))
  6. L Bertocchi, A Benini, F Milano, R Padovani, P Sprawls, S Tabakov (2014), 50 Years ICTP and its Activities in the Field of Medical Physics, Journal Medical Physics International, vol. 2, No.2, 2014, p.410, (available free from: <http://www.mpijournal.org/pdf/2014-02/MPI-2014-02-p410.pdf>)
  7. G. Loreti, H. Delis, B. Healy, J. Izewska, G.L. Poli, A. Meghziene (2015), IAEA Education and Training Activities in Medical Physics, Journal Medical Physics International, vol. 3, No.2, 2015, p.81, (available free from: <http://www.mpijournal.org/pdf/2015-02/MPI-2015-02-p081.pdf>)
  8. Rifat Atun, D A Jaffray, M B Barton, F Bray, M Baumann, B Vikram, T P Hanna, F M Knaul, Y Lievens, T Y M Lui, M Milosevic, B O'Sullivan, D L Rodin, E Rosenblatt, J Van Dyk, M L Yap, E Zubizarreta, M Gospodarowicz (2015), Expanding global access to radiotherapy, Lancet Oncol 2015; 16: 1153–86
  9. P Sprawls (2016), Windows to the World of Medical Imaging Physics Visuals for Effective and Efficient Learning and Teaching, Journal Medical Physics International, vol. 4, No.1, 2016, p.20, (available free from: <http://www.mpijournal.org/pdf/2016-01/MPI-2016-01-p020.pdf>)
- Author:** Slavik Tabakov, PhD, FIPEM, FHEA, FIOMP, President IOMP, Institute: King's College London, UK, [slavik.tabakov@emerald2.co.uk](mailto:slavik.tabakov@emerald2.co.uk)



# PROFESSIONAL ISSUES

## PROFESSIONAL SURVEY IN SWITZERLAND: MEDICAL PHYSICISTS IN RADIODIAGNOSTICS

Eleni-Theano Samara<sup>1</sup>, Robert Schöpflin<sup>2</sup>, Stefano Presilla<sup>3</sup>

<sup>1</sup> Radiation oncology service, Valais Hospital, Sion, Switzerland

<sup>2</sup> Radiation protection, Radiation oncology service, St. Gallen Cantonal Hospital, St. Gallen, Switzerland

<sup>3</sup> Medical physics service, Ente Ospedaliero Cantonale, Bellinzona, Switzerland

**Abstract—** In Switzerland, medical physicists (MP) started officially working in the field of radiology and nuclear medicine in 2012. In the end of 2015, a survey was conducted to examine the situation of the MP working in the field and the future of the profession. MP were shown to be highly motivated to work in this field. The work of MP in radiodiagnosics should evolve towards radiation management. In Switzerland, we need to define our mission and responsibilities as MP in radiology and nuclear medicine in order to develop our profession.

**Keywords—** Survey, Radiology, Nuclear medicine, Switzerland

### VI. INTRODUCTION

Medical physicists (MP) in radiodiagnosics (radiology and nuclear medicine) started officially working in Swiss hospitals in 2012, final date imposed by the Swiss law (Radiological protection ordinance, art.74, p.7) [1]

The general framework about the duties and responsibilities of MP was published in 2011 as recommendations without, however, reaching a full agreement of different societies [2]. In the same document, the minimum hiring times were also defined (Table 1). MP in Switzerland are hired as consultants and their principal tasks are the following:

- Measurements of patient, staff and public safety related dosimetric quantities during quality controls (QC)
- Improving patient protection by optimization of practices, procedures and acquisition protocols
- Improving protection of the medical staff by giving advice on machine operation and personal protective equipment, including protective garments, fixed and mobile shielding

- Establishing an effective education system in radioprotection for healthcare professionals.

QC to the machines are carried out by the manufacturers. MP perform measurements that are exclusively related to radiation dose in order to optimize it, without, though, repeating the controls that are already made by the manufacturers. Radiation protection remains under the responsibility of the radiation protection experts.

Table 1 Minimum hiring times for MP in Switzerland

| Equipment   | Minimum hiring time per year (day) |
|---|------------------------------------|
| <b>Radiology</b>  |                                    |
| CT  | 3                                  |
| Fluoroscopy units (dedicated for interventional procedures) | 3.4                                |
| Other fluoroscopy units                                     | 1                                  |
| <b>Nuclear medicine</b>                                     |                                    |
| Gamma-camera  | 2.5                                |
| SPECT/CT  | 5.5                                |
| PET   | 2.75                               |
| PET/CT  | 5.75                               |

Several schemas for the occupation of the MP were adopted by the different hospitals and clinics: i) MP work exclusively for radiodiagnosics, ii) MP that work principally in radiation therapy cover the requirements in radiodiagnosics for their hospital, and iii) enterprises provide external services of MP. These enterprises can be independent MP, big hospitals that provide services to other smaller ones or any other institute.

## VII. SURVEY

A survey was conducted in the end of 2015 to examine the current situation of the MP working in radiodiagnostics and gather the opinions about the future of the profession. All MP working in radiodiagnostics in the country were asked to participate to the survey. The survey was conducted using the Google forms and the statistical analysis was made by means of the MedCalc software, v. 14.12.0.

Twenty-two physicists took part in the survey. The majority of the MP that took part in the survey work in public hospitals (73%), 23% work in private hospitals and only one participant reported to be self-employed. Half of the institutes reported that they provide external services of MP to thirds.

The activity rate between the different modalities is presented in Figure 1 (Some MP seem to work more than 100%, either did their respond concern more than one MP or simply a mistake was introduced. The original data are presented here with no corrections.). Radiology tasks concern almost all MP with a rate between 10% and 80%. MP with no responsibilities in diagnostic radiology, work either exclusively in radiation therapy or nuclear medicine. Nuclear medicine, on the other hand, has very low rates of occupation, between 10% and 30%. As expected, radiation therapy MP work primarily in this domain, for instance participants 4, 5, 9, 10, 11, 21 and cover the needs of their institution for radiodiagnostics and typically do not provide external services. Only one person (participant 20) reported an occupational rate balanced between all modalities.

Very interestingly, almost all MP have tasks related to radiation protection. This may be officially written in their job description or simply required by their everyday work. Moreover, to the question “Are you involved in the radiation protection policy of your hospital?”, 81% of the MP answered positively with one participant specifying that this task is “not official”.

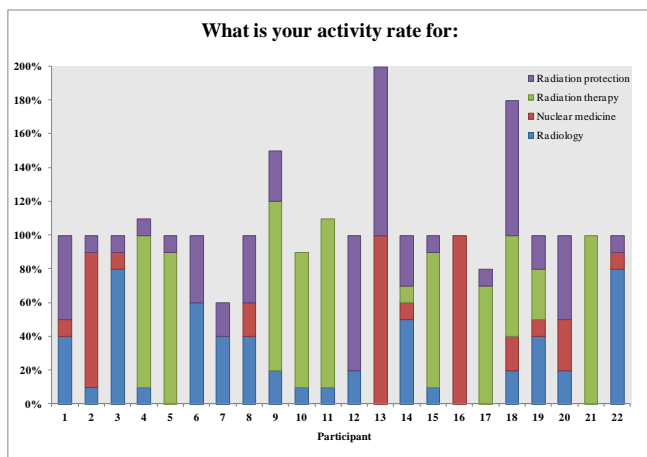
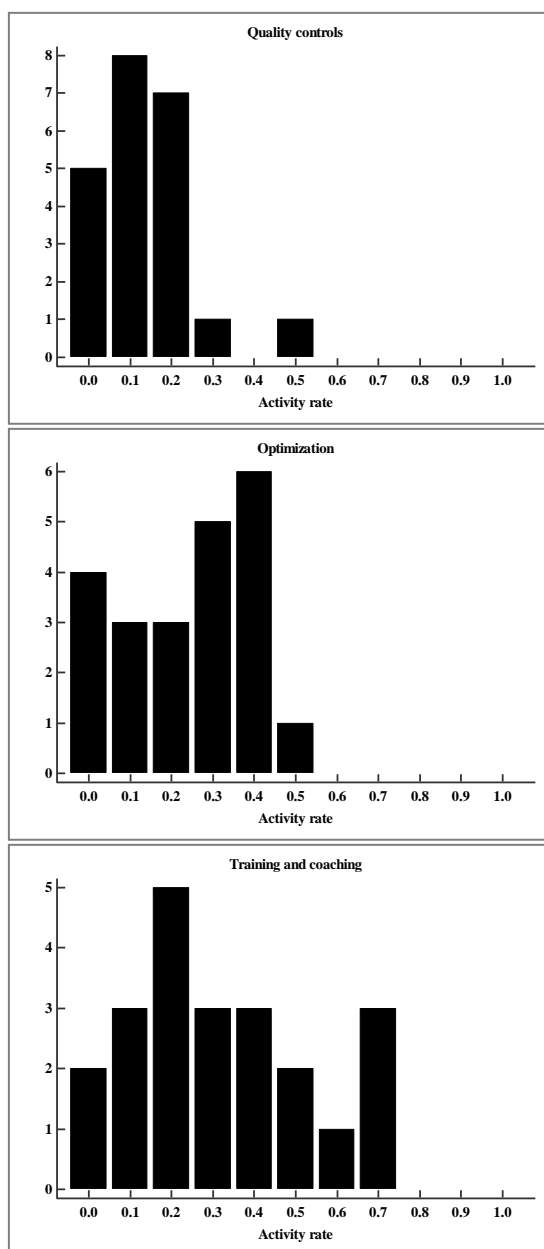


Fig. 1 The activity rate of MP in radiation protection, radiation therapy, nuclear medicine and radiology

According to the “Guidelines and recommendations for application of the radioprotection ordinance Article 74”, published in 2011, the tasks of the MP include i) quality controls of radiological equipment, ii) optimization of protocols and techniques used for patient and personnel safety and iii) training of the personnel in medical physics matters. The results of this survey showed that MP are concentrated to the training and coaching of the personnel (Figure 2). Optimization comes second, while quality controls are rarely performed by MP. Other tasks related to radiology and nuclear medicine may include IT activities or research in the field, but they only occupy a small amount of time.



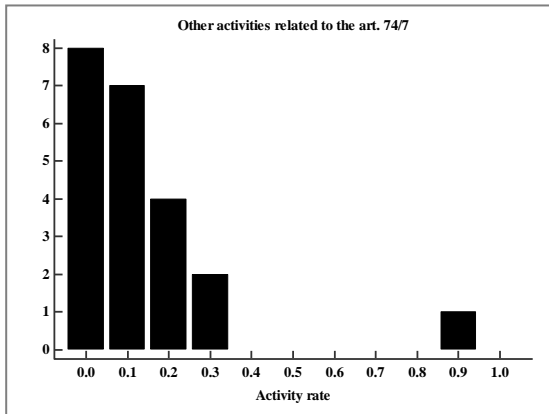


Fig. 2 The activity rate of the tasks of MP working in radiology and nuclear medicine

The majority of the MP working in radiodiagnosics believes that the work of the MP should be oriented towards the management of the radiation instead of quality controls of the radiological machines, as depicted in the Figure 3. This comes to no surprise as already the current activities in radiodiagnosics include only few quality controls. Moreover, the colleagues mentioned that a MP should:

- consider radiation dose optimization taking into account other clinical factors, such as contrast agent
- analyze the clinical practice for avoidable risks
- be consulted from the purchase of the radiological equipment to its end-of-life
- be active in the field of medical informatics as it becomes an every-day tool for our work.

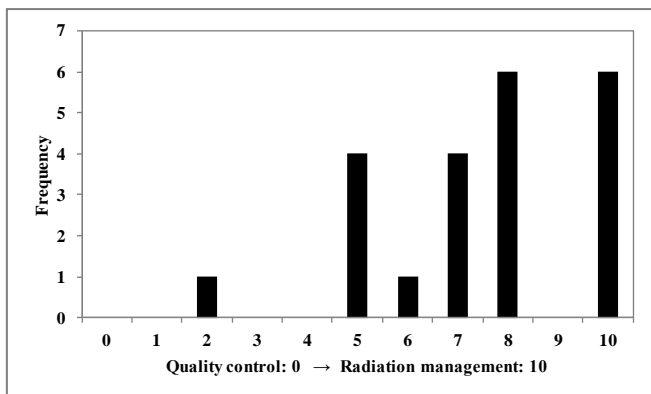


Figure 3: Answers to the question “Should the work of the MP-74/7 be more quality-control oriented or radiation management-oriented?”

A positive and motivating point for the profession of MP in radiodiagnosics, which remains an open field at least in Switzerland, is that the MP feel that their responsibilities and tasks have evolved and continue to evolve according to Figure 4.

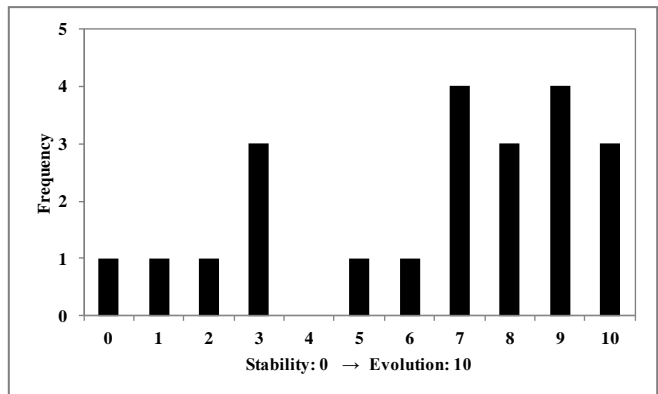


Figure 4: Answers to the question “Do you feel that your responsibilities and tasks have been evolving with time or do you feel that they have been stable since the day you started in radiology and/or nuclear medicine?”

The same positive perspective is also depicted in Figure 5 that gives the answers about the motivation of the MP to continue working in the field (A) and motivate younger MP to consider careers in radiology and nuclear medicine (B). It is interesting to remark here that all four MP that noted very low scores in both questions work principally in radiation therapy (participants 5, 11, 15, and 21).

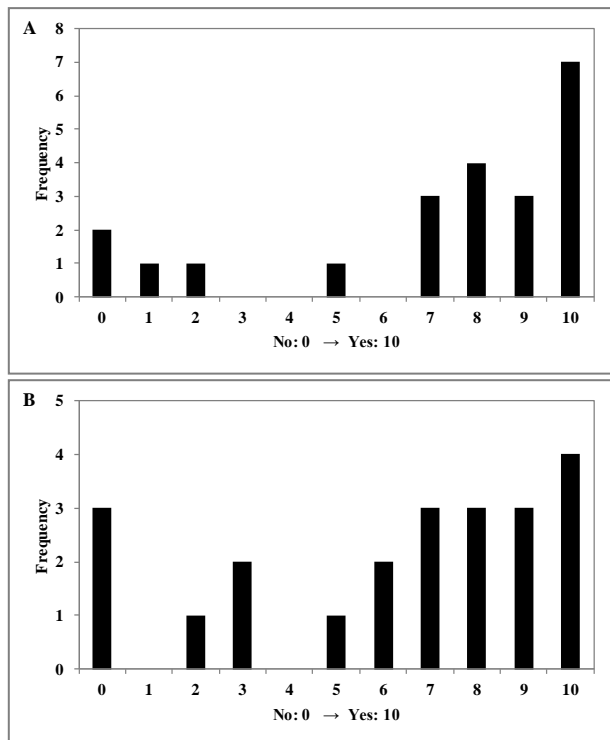


Figure 5: Motivation of the MP to continue working in the field (A) and motivate younger MP to consider careers in radiology and nuclear medicine (B)

This frustration may be related to the equivocal responsibilities of the MP in radiology and nuclear medicine

according to the Swiss legislation or in the institute where they work (Figure 6). The approval towards the definition of the responsibilities of the MP in the institutes, where they work, is higher than the one in the Swiss legislation (mean values for institute definition was 5.7, while the mean value for the Swiss legislation definition was 4.3, p-value=0.006 for paired T-test).

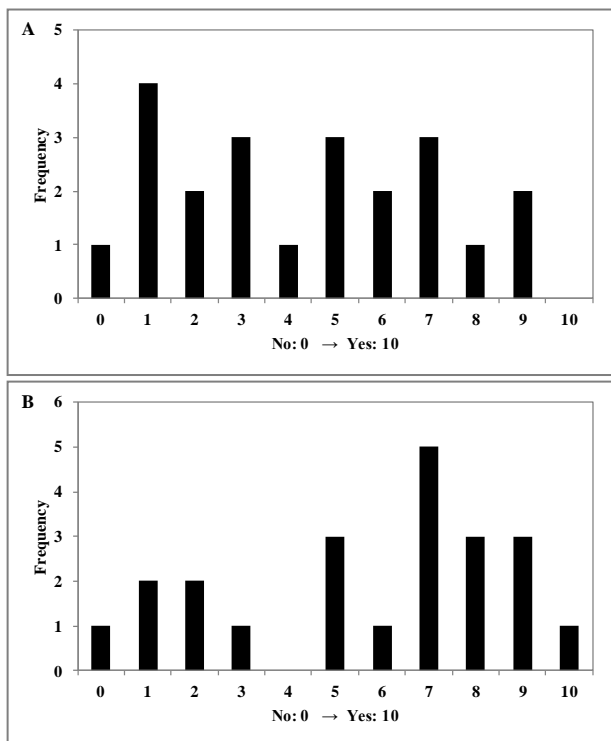


Figure 6: Answers to the question “Are you satisfied with the definition of your responsibilities in radiology and/or nuclear medicine according to the Swiss legislation (A) and within your hospital (B)?”

Figure 7 shows a correlation between the motivation of the MP to continue working in the field and the definition of their responsibilities in their hospital. A clearer definition of responsibilities is related to higher motivation of the personnel as one may observe. The fact that MP in radiation therapy have limited time to determine the needs and develop a concept for radiodiagnostics tasks may also explain this finding. Medical physics in radiology and nuclear medicine is a quite young profession in Switzerland and time was and may still be necessary to clarify our responsibilities.

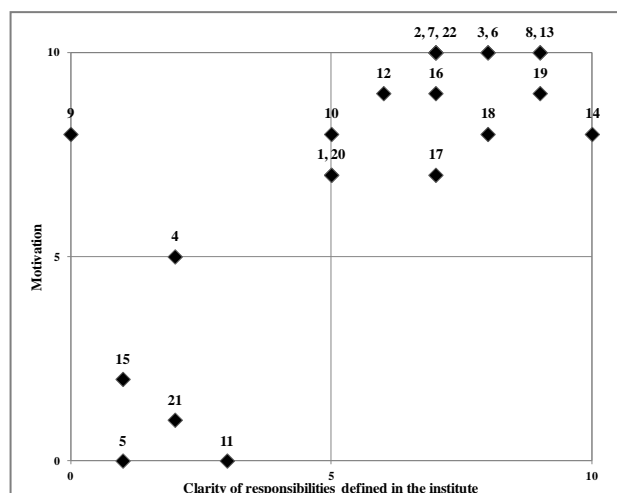
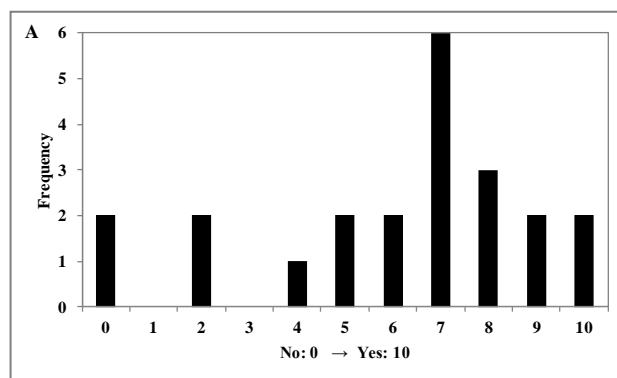


Figure 7: Correlation between the motivation of the MP to continue working in the field and the definition of their responsibilities in their hospital. The data labels correspond to the participant number.

Two questions concerned the feeling of the MP about the recognition of their work, one towards their direct colleagues, i.e. medical physicists and one their colleagues with different occupation (radiologists, technologists, etc.). What was particularly interesting was that for both questions the mean score was equal to 6 (Figure 8) with no significant difference. However, lack of recognition of a MP’s work in his/her institute does not necessarily mean lack of recognition among other colleagues (no correlation was found between the two answers of the participants). The fact that one may feel that his/her work is not recognized by colleagues with different background is understandable and we should work hard to better communicate the importance of our work. However, it is urgent, in our opinion, to improve the esteem of the work of the MP in radiology and nuclear medicine at least among medical physicists that work in radiation therapy.



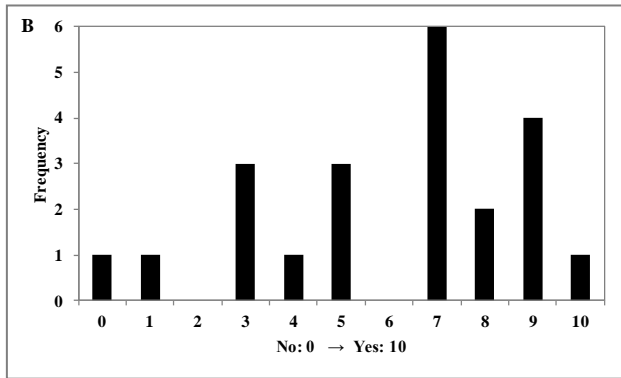


Figure 8: Answers to the question “Do you feel that your work is recognized a) among your colleagues (medical physicists) and b) in the hospital (physicians, radiographers, etc.)?”

An open question about any recommendation to improve our profession was asked and a summary of the proposals of the colleagues is presented here:

- Definition of the role of the MP in radiology and nuclear medicine
- Definition of the responsibilities of the MP in the Swiss legislation
- Strong communication about the role of the MP to other professionals and the related importance and impact in the clinical workflow.
- Reasonable hiring times of MP according to institute activities and needs
- Realistic funding of medical physics activities.

The next question concerned the collaboration of the MP with the physicians, radiographers and manufacturers in order to optimize radiation protocols. The general feeling is encouraging as showed in Figure 9. Furthermore, the participants described the collaboration as satisfying (32%) and mentioned that “it is changing with time towards the best” (55%), while no one believes the contrary. One more positive aspect is the mutual collaboration in radiation protection matters, where people feel free to express to MP their own ideas (46%) and apply the propositions of the MP (32%). Naturally, there are cases where the collaboration is described as difficult or that it should be closer, as mentioned by 27% of the participants or that there are still people that do not know what an MP does in radiodiagnosics.

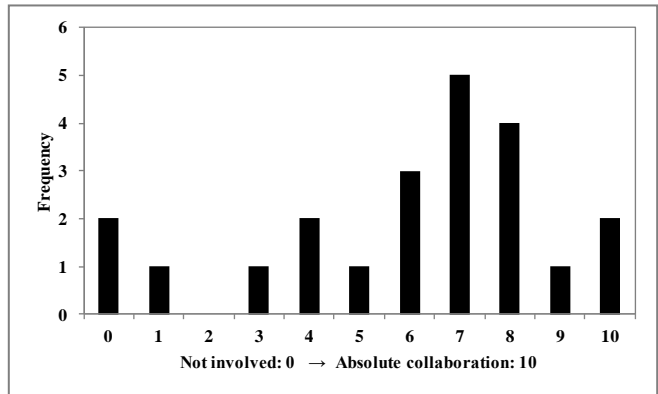


Figure 9: Answers to the question “How closely do you work with physicians, radiographers and manufacturers in order to optimize radiation protocols?”

Lastly, soft skills are necessary to our profession (Figure 10). We need to teach and train in medical physics people with different background, we need to convince people to change their habits in order to protect effectively their patient and themselves, we need to prove to the institute management that we provide good service and we improve the quality of the institute where we work and as shown from the previous questions we need to improve the collaborations with our partners.

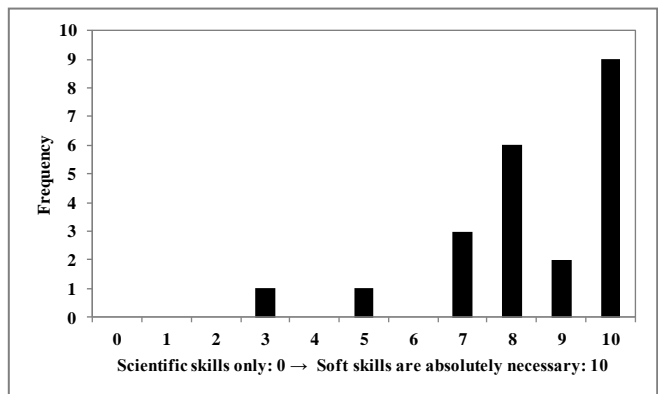


Figure 10: Answers to the question “Do you feel that the medical physicist has to develop skills other than scientific in order to work in radiology and/or nuclear medicine (for example effective communication, dialogue, management, decision making, teaching, etc.)?”

### VIII. CONCLUSIONS

In conclusion, the survey showed encouraging results about the future of medical physics in radiodiagnosics. MP actually working in the different institutes are highly motivated to work in this field. Most of MP agree that the work in radiodiagnosics should evolve towards radiation management. In Switzerland, we need to define our mission and responsibilities as MP in radiology and nuclear medicine in order to develop our profession. This will improve our every-day work in terms of collaboration with other professions and raise our personal satisfaction.

## REFERENCES

1. Radiological protection ordinance (RPO) at <https://www.admin.ch/opc/en/classified-compilation/19940157/index.html>
2. Requirements for medical physicists in nuclear medicine and radiology at <http://www.bag.admin.ch/themen/strahlung/02883/02885/index.html?lang=fr>

### Contacts of the corresponding author:

Author: Eleni-Theano Samara  
Institute: Valais Hospital  
Street: Avenue du Grand Champsec 80, CH-1951  
City: Sion  
Country: Switzerland  
Email: Elina.Samara@hopitalvs.ch

### Conflict of Interest Statement

The authors have no conflict of interest to declare

## MEDICAL PHYSICS PROFESSIONAL DEVELOPMENT AND EDUCATION IN INDIA

Neeraj Dixit<sup>1</sup>, G. Sahani<sup>1</sup>, S. Mahalakshmi<sup>1</sup>, Pankaj Tandon<sup>1</sup>, Sunil D. Sharma<sup>2</sup>, A. U. Sonawane<sup>1</sup>,  
Arun Chougule<sup>3</sup>

<sup>1</sup> Radiological Safety Division, Atomic Energy Regulatory Board, Mumbai, India

<sup>2</sup> Radiological Physics & Advisory Division, Bhabha Atomic Research Centre, Mumbai, India

<sup>3</sup> Department of Radiological Physics, S.M.S. Medical College & Hospital, Jaipur, India  
& President of Association of Medical Physicists of India

**Abstract**—In the treatment of cancer, Medical Physicist works in a hospital environment as a part of a wide clinical team and plays important roles such as treatment planning, radiation dosimetry, quality assurance (QA) of the equipment in order to deliver accurate radiation dose for better tumour control. Medical Physicist also contributes in performance evaluation of radiation generating equipment used in nuclear medicine and diagnostic radiology practice and optimization of radiation doses in imaging modalities. Bhabha Atomic Research Centre had started one year Post Graduate Diploma in Radiological Physics programme in 1962 with support from world health organization (WHO), which was the first course in India in the field of Medical Radiation Physics. Presently, there are 20 universities/institutions conducting Post M.Sc./Post Graduate degree/diploma in Medical Physics across India. Considering the tremendous scope for research in Medical Radiation Physics, some of the universities/institutions are offering Doctor of Philosophy (Ph.D.) in Medical Physics. National Regulatory Authority i.e., Atomic Energy Regulatory Board (AERB) made the provision for internship/ residency programme for Medical Physicists considering the need of clinical training. Each qualified Medical Physicist is registered with the AERB through online e-LORA (Electronic Licensing of Radiation Applications) system and a unique registration number is allotted to them. As on date, there are 1270 qualified Medical Physicists registered with AERB. There are 410 radiotherapy institutions having various types of radiotherapy equipments (conventional to advanced) in the country and there is no dearth of Medical Physicists to cater the present need. In addition to playing crucial role in Radiotherapy, Medical Physicists also contribute in diagnostic radiology and nuclear medicine practices for optimizing image quality and thereby optimizing the radiation doses from these imaging modalities. Association of Medical Physicists of India (AMPI) was founded in 1976 with the objective to work for strengthening medical physics knowledge through conducting annual conferences/workshop/CME, publishing Journal on Medical Physics. For maintaining standard in the practice of medical physics, AMPI has also started College of Medical Physics of India (CMPI), to initiate the evaluation and certification programme for the qualified medical physicists.

**Keywords**—Medical Physics, Internship, Course, Qualification, e-LORA, AERB

### IX. INTRODUCTION

It is well established that ionizing radiation is being used worldwide for the treatment of cancer and diagnosis of the various diseases for past several decades. In treatment, the goal is to deliver the maximum radiation dose to the tumour and minimum radiation dose to the surrounding healthy tissues for obtaining better treatment outcome whereas in diagnosis the aim is to obtain better image quality with minimum radiation dose. Medical Physics is the branch of science that mainly deals with the applications of ionizing radiation in health care through radiotherapy, diagnostic radiology, nuclear medicine and the associated radiological protection. In the treatment of cancer Medical Physicist works in a hospital environment as a part of a wide clinical team and plays an important role for treatment planning, radiation dosimetry, quality assurance (QA) of the equipment in order to deliver accurate radiation dose for maximizing tumor control probability and minimizing normal tissue complication probability[1-2]. Medical Physicist also contributes in QA of the equipment used in nuclear medicine and diagnostic radiology practice and optimization of radiation doses in imaging modalities. Medical Physicists work alongside clinicians in providing scientific and technical expertise and conducting research. Role of a Medical Physicist is multifold and consists of treatment planning, estimation of dose for patients and personnel, the quality assurance tests of radiological equipment, the calculation for radiation shielding requirements and the training of several health professionals (doctors, medical physicists, radiologists, technicians, and nurses). Additionally, Medical Physicist is assigned the responsibilities of Radiological Safety Officer (RSO) in medical radiation facility, subject to qualifying the competency test and approval from AERB, for ensuring radiation safety of workers and members of public. According to GLOBOCAN data of International Agency for Research on Cancer (IARC), a World Health Organization(WHO) entity, about a million new cases were recorded while about 683,000 deaths due to cancer were registered in 2012[3]. Out of these 1 million cancer patients around 60% patients need radiation therapy. At present there are only 600 Teletherapy equipments (Medical Linear Accelerators, Cyberknife, Tomotherapy, Telecobalt units) in

India which is far below the required number of Teletherapy equipments to cater the new cancer patients, even though rapid growth of hospitals with radiation therapy facilities with advanced technologies is seen in India in the last decade. Moreover, considering complexity of the equipments, stringent QA (patient specific QA in addition to equipment) in advanced technologies is needed. In view of the above, there would be requirement of more number of medical physicists which is mandatory requirements as per the national regulatory authority- Atomic Energy Regulatory Board (AERB). This paper presents the current status of Medical Physics professional development in India.

## X. MATERIALS AND METHODS:

### *Ila) Historical Development of Medical Physics Programme in India*

In treatment of cancer, Medical Physicist is a part of clinical team and plays vital role to deliver accurate radiation dose for desired treatment outcome by carrying out radiation dosimetry, quality assurance (QA), treatment planning and other important task. Expertise of the Medical Physicist is also required in nuclear medicine and diagnostic radiology practices for optimization of radiation doses to obtain good image quality. Considering the importance of the Medical Physicist in health care sector, Bhabha Atomic Research Centre (BARC) started one year post graduate Diploma in Radiological Physics programme in 1962 with support from world health organization (WHO), which was the first course in India[4-7]. To cater the need of rising demand of more number of Medical Physicist in the country many more universities started offering Medical Physics courses in addition to BARC[8]. There are two types of courses offered by the various universities in India to become a qualified Medical Physicist namely i) One year post M.Sc. Course in Medical Physics/Radiological physics; and ii) Two years postgraduate degree course in Medical Physics/Medical Radiation Physics after graduation in science with physics as major subject. As per the stipulation by the AERB, minimum qualifications required to work as Medical Physicist in India are [9]:

- i) A post graduate degree in Physics from a recognized university;
- ii) A Post M.Sc. diploma in radiological/medical physics from a recognized university; &
- iii) An internship of minimum 12 months duration in a recognized well-equipped radiation therapy department.

OR

- i) A basic degree in science from a recognized university with Physics as one of the main subjects;
- ii) A post graduate degree in radiological/medical physics from a recognized university; and

- iii) An internship of minimum 12 months in a recognized well-equipped radiation therapy department.

Further, the qualification required, as per the AERB, to work as Radiological Safety Officer (RSO) in Radiotherapy facility in India is as follows:

- i) Minimum qualifications required for a Medical Physicist and ;
- ii) Certification for competency to work as RSO
- iii) An approval from the competent authority to function as RSO.

### *Iib) Medical Physics Programme in India:*

Only those candidates who successfully complete the Medical Physics course and one year internship from a well equipped radiotherapy centre meeting the internship criteria are eligible to work as Medical Physicist in the country [7-9]. These candidates become eligible to work as RSO in medical institutions after evaluation through competency test and allowed to function as RSO with approval from AERB.

List of the institutions whose Medical Physics course is in accordance with AERB requirements are given in Table-1. As per constitution of AERB, one of its mandates is to prescribe the syllabi for training of personnel in radiation safety aspects at all levels. To meet with the pace of the technological advancement in the field, syllabus of Medical Physics course is reviewed and revised periodically to incorporate the advanced technologies.

### *Iic) Medical Physics Internship/Residency Programme:*

A medical physicist is professional who is competent to independently practice one or more subfields of medical physics. In a hospital, Medical Physicist is primarily involved with different activities, such as dosimetry, performance evaluation, QA, treatment planning, research and development, and teaching related to use of ionizing radiation and radiation safety. Medical physicist plays an important role in ensuring accurate radiation dose delivery for intended treatment outcome. Significant technological advancements in radiation dose delivery and imaging modalities have led to availability of high precision radiotherapy with highly conformal radiation doses. A number of complex equipments and procedures are used to fulfil the objectives of effective and safe radiotherapy. The use of fully computer controlled radiotherapy equipment e.g. advanced medical accelerator equipped with advanced treatment techniques [e.g. 3D conformal radiotherapy (3D-CRT), intensity modulated radiotherapy (IMRT), image-guided radiotherapy (IGRT), Stereotactic radio-surgery (SRS)/Stereotactic Radiotherapy (SRT), and Volumetric Modulation Arc Therapy (VMAT)] require highly skilled and competent medical physicist. A mere holder of a university degree in radiological/medical physics, without

the acquiring adequate hospital training, cannot be considered as competent Medical Physicist [10]. Therefore, it is necessary for the Medical Physicist to undergo internship/ residency programme from a well equipped radiotherapy centre to gain competence in the field. Internship/ residency is now an integral part of the Medical Physics education and training programmes in most of the developed countries [11-16]. To maintain the quality of the medical physics courses at par with international standards, it is necessary to incorporate and implement internship/ residency in Medical Physics education and training programmes in India. Therefore, considering need of clinical training, AERB made the provision for internship/residency programme for Medical Physicists by stipulating the same as a mandatory requirement in the revised Safety Code [9].

In India, the candidates after successfully completing course from any of the institutions as listed in Table-1, need to undergo mandatory internship/residency of minimum 12 months duration in a radiation therapy department, meeting the AERB laid down criteria, to become qualified Medical Physicist. To fulfil this requirement, all the Medical Physicists passing out from different academic courses in the country undergo internship/residency in Medical Physics programme under the supervision of a qualified and experienced Medical Physicist at a recognised well-equipped radiotherapy centre in the country for a duration not less than 12 months[8-9]. Minimum syllabus prescribed by AERB for the internship/residency programme for Medical Physics includes 1) Radiotherapy Equipment (treatment and imaging) and QA; 2) Beam Calibration and Dosimetry; 3) External Beam Treatment Planning; 4) Brachytherapy Dosimetry and Treatment Planning; 5) In-Vivo Dosimetry and Patient Dose Verification; 6) Radiation Protection and Safety; 6) Clinical Orientation; and 7) Professional Skill Development and Career Planning. Well equipped radiotherapy centre for the purpose of internship/residency programme must have at least 1) One Linear Accelerator (with photon and electron beams) ; 2) One HDR Brachytherapy Unit; 3) One Simulator/ CT-Simulator; 4) One Treatment Planning System; 5) Adequate dosimetry and monitoring instruments; 6) at least one Medical Physicist with minimum 5 years of experience to become internship supervisor. The ratio of Medical Physicist intern and Internship Supervisor is 1:1. However, a medical physicist with more than 3 years of working experience in a Radiotherapy Department can also be considered as an internship supervisor subject to availability of at least one Medical Physicist having minimum 5 years of experience in the department.

*IId) Growth of the Medical Radiation Facilities and availability of Medical Physicists*

The usages of ionising radiation sources (radioisotopes and radiation generating equipment) for medical applications have been enormously increasing all over the world. Applications of radiation sources in medical applications (radiotherapy, nuclear medicine and diagnostic radiology) in India have seen huge growth during the last decade. For analysis of growth of radiotherapy facilities in India, eight years data (2009-2016) is depicted in Fig.1. India witnessed rapid growth of medical institutions using ionising radiation for diagnosis and treatment purposes for the last decade.

*Ile) Higher Studies and R& D activities in Medical Physics*

Considering the tremendous scope for research in Medical Radiation Physics, some of the universities/institutions are now offering Ph.D. in Medical Physics e.g. Anna University, Homi Bhabha national Institute (a deemed to be university) Punjab University, Baba Farid University of Health Sciences, D.Y. Patil University etc. There are various Government organisations e.g. Department of Atomic Energy (DAE), AERB, Department of Science and Technology (DST), Council for Scientific and Industrial Research (CSIR) etc. which are also providing financial assistance for research projects pertaining to the Medical Physics and Radiation Safety.

XI. RESULTS

From the Fig.1, it is observed that institutions using radiotherapy facilities were 266 in 2009 whereas 410 in 2016. We can also observe from Fig.1 that number of accelerators and remote afterloading HDR brachytherapy equipments were 167 and 160 in 2009 whereas this number increased to 374 and 258 in 2016. However, there is decline trend seen in case of Telecobalt equipments which decreased from 300 in 2009 to 224 in 2016.

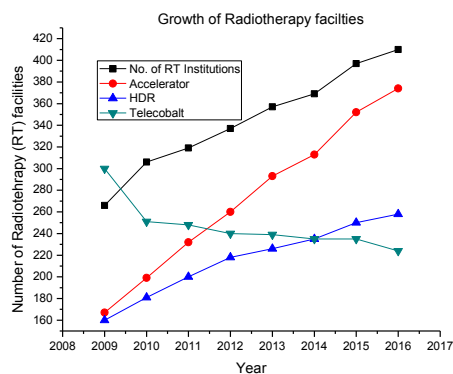


**Fig 1:** Growth of Radiotherapy facilities in India

Presently twenty institutions/universities are conducting Medical Physics courses and producing on an average 150

Medical Physicists annually across the country. Fig.2 represents the growth of number of Medical Physics courses over a decade (2007-2016). Currently there are total 236 Nuclear Medicine institutions equipped with 125 PET-CT, 163 Gamma Camera and 61 High Dose therapy facilities which are licensed by AERB. The status of these Nuclear Medicine facilities is shown in Fig.3. (Computed Tomography, Fixed, Mobile, Portable, Radiography & Fluoroscopy, Mammography, C-Arm, Dental, OPG, Dental Cone Beam CT and BMD) registered with AERB.

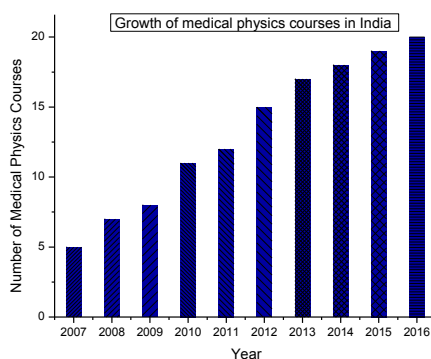


Fig.2: Growth of Medical Physics courses in India

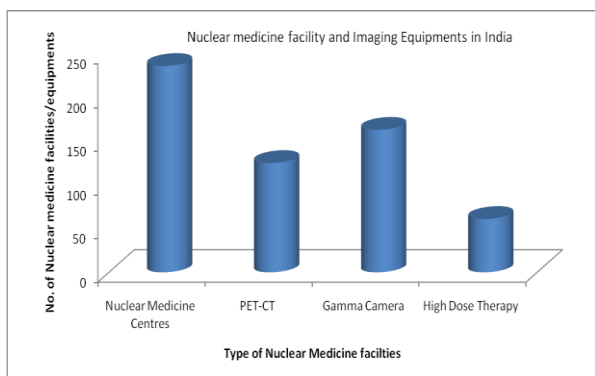


Fig.3: Present status of Nuclear Medicine facilities

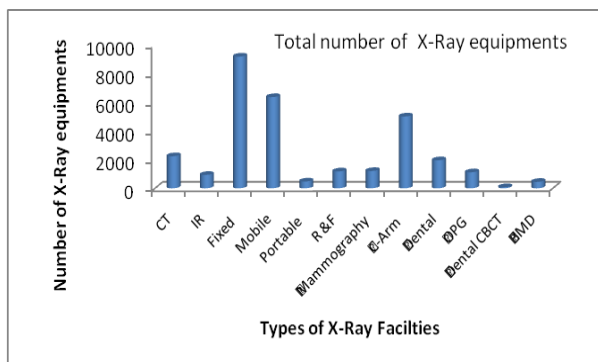


Fig.4: Present status of diagnostic X-Ray facilities

XII. DISCUSSION

The maximum number of cancer patients that can be treated annually is around 500 per Teletherapy equipments. Therefore, using present 600 teletherapy equipments available in India, the maximum number of patients that can be treated annually is about 300000, which is far below the required equipments to cater the total cancer patients in India (~600000 as per the WHO report). Thus there is a need for double the number of existing teletherapy equipments which in-turn requires large number of Medical Physicists to cater the need. The required number of Medical Physicists will further increase considering complexity as it will require more man-hours for performing QA of the equipment & patient specific QA, treatment planning etc. in advanced technologies. Initially BARC has started One year post graduate diploma in radiological physics course (Dip.R.P.) in 1962 whereas presently 19 more institutions conducting various Post M.Sc./ Post Graduate courses in Medical/Radiological physics due to growing demand of Medical Physicists producing 150 on an average number of Medical Physicists annually across the India.

Each qualified Medical Physicist is registered with AERB through online e-LORA (Electronic Licensing of Radiation Applications) system and a unique registration number is allotted to them [17]. As per the records, there are 1270 qualified Medical Physicists registered with AERB. There are 410 radiotherapy institutions in the country and therefore the ratio of available Medical Physicists to number of radiotherapy institution is around 3:1. Similarly, available number of Medical Physicists per Teletherapy equipment is more than 2. Therefore, there is no dearth of Medical Physicists to cater the present need. The average growth rate of radiotherapy equipments (addition of new equipments) in the radiotherapy institutions spread across the country is around 60 over the past 5 years whereas the average number of Medical Physicists being produced around 150 annually i.e. by a factor of >3 per equipment. Therefore, no shortfall of required number of Medical Physicists is anticipated with the current growth trend of radiotherapy equipments in India.

Further, in India, Medical Physics activities started in the mid 40s with the appointment of Dr. Ramaiah Naidu as the first Medical Physicist at the Tata Memorial Hospital [18]. The Association of Medical Physicists of India (AMPI), an affiliate of the Indian National Science Academy and the International Organization for Medical Physics, was founded in 1976 with the objective to work for strengthening Medical Physics knowledge through conducting annual conferences/workshop/CME, publishing Journal on Medical Physics, encourage Research and Development and Education in the field of medical physics, and disseminate world-wide information in this field to all

members of the association and to participate actively in programmes on Medical Physics conducted by international organisations such as International Organization for Medical Physics (IOMP), The Asia-Oceania Federation of Organizations for Medical Physics (AFOMP) etc. For maintaining standard in the practice of Medical Physics in human healthcare programme towards the fulfilment of objectives of medical imaging and radiation therapy, AMPI has also started College of Medical Physics of India (CMPI), to initiate the evaluation and certification programme for the qualified Medical Physicists. Currently AMPI has an active membership more than 2000.

### XIII. CONCLUSIONS

India has vast experience in the field of Medical Physics. Medical Physics courses are being conducted in the country since more than five decades. All types of radiotherapy equipments with conventional to advanced treatment technologies (Telecobalt, standard and advanced medical accelerator, IORT) and specialized equipments (Cyber Knife, Gamma Knife and Tomotherapy) are in operation in the country. India has well structured Medical Physics courses and presently several Medical Physics courses are being conducted by various universities in different parts of the country producing adequate number of Medical Physicists annually to cater the need in the healthcare sector of the country. India has initiated various steps for strengthening its Medical Physics programme by reviewing and revising syllabus periodically to incorporate the topics related to advanced techniques introduced in the field of Medical Physics and introducing one year compulsory internship/residency programme by AERB. AMPI is also taking keen initiative in conducting workshop/seminar/CME/conferences on various topics in order to update and share the knowledge among the professionals. India is also promoting research and development activities by providing financial aid to the institutions/universities carrying out research activities in the Medical Physics. In addition to playing crucial role in Radiotherapy, Medical Physicists also contribute in diagnostic radiology and nuclear medicine practices for optimizing image quality and thereby optimizing the radiation doses from these imaging modalities.

### ACKNOWLEDGEMENT

Authors sincerely express their gratitude to the Chairman, AERB and Executive Director, AERB, for their encouragement and support to undertake this activity.

### REFERENCES

1. Khan F. M. Physics of Radiation Therapy, 4th Edition; Lippincott Williams & Wilkins, USA (2010).
2. International Atomic Energy Agency (IAEA) Setting-up a radiotherapy programme: Clinical, medical physics, radiation protection and safety aspects, STI/PUB/1296 Vienna: IAEA. 2008.
3. Sankaranarayanan R. Cancer prevention and care in India: an unfinished agenda; *www.thelancet.com/oncology* Vol 15 May 2014; DOI: [http://dx.doi.org/10.1016/S1470-2045\(14\)70140-8](http://dx.doi.org/10.1016/S1470-2045(14)70140-8)
4. AAPM at [www.aapm.org/meetings/amos2/pdf/41-11901-28262-192.pdf](http://www.aapm.org/meetings/amos2/pdf/41-11901-28262-192.pdf)
5. Grover, R.B. & Puri, R.R. Sadhana (2013. Development of human resources for Indian nuclear power programme) 38: 1051. doi:10.1007/s12046-013-0171-z
6. S. D. Sharma, S. Kannan. Medical radiation physics and medical physicists in India. In: Medical Physics and Engineering Education and Training-Part I (Eds: S. Tabakov, P. Sprawls, A. Krishnachinda, C. Lewis), 2011, pp 48-58. Available at: [www.emerald2.eu](http://www.emerald2.eu).
7. S. D. Sharma. Medical radiation physics courses in India. AFOMP Newsletter, 6(1), 8-9, 2014.
8. AERB at <http://www.aerb.gov.in/AERBPortal/pages/English/t/forms/regforms/radiotherapy/medphycourse.pdf>
9. Atomic Energy Regulatory Board (AERB) Safety Code: Radiation Therapy Sources, Equipment And Installations, AERB/RF-MED/SC-1 (Rev.1), 2011
10. S. D. Sharma. Issues related to implementation of internship/residency program for qualified medical radiation physicists. J. Med. Phys. 34(1), 1-3, 2009.
11. American Association of Physicists in Medicine (AAPM) Essentials and guidelines for hospital-based Medical Physics residency training programs. AAPM Report No. 90. 2006.
12. American Association of Physicists in Medicine (AAPM) Alternative clinical training pathways for medical physicists: Report of AAPM Task Group 133. AAPM Report No. 133. 2008.
13. EFOMP Policy Statement No.12. The present status of Medical Physics education and training in Europe. New perspectives and EFOMP recommendations. Available from: <http://www.efomp.org>.
14. Syllabus for the radiation oncology Medical Physics (ROMP) training program. Available from: <http://www.acpsem.org.au>.
15. ROMP clinical training guide. Available from: <http://www.acpsem.org.au>.
16. Eudaldo T, Olsen K. The present status of Medical Physics education and training in Europe: An EFOMP survey. Phys Med. 2008;24:3-20. [PubMed: 18061501]
17. AERB at <https://elora.aerb.gov.in/ELORA/registerRP>Action.htm>
18. AMPI at [http://www.ampi.org.in/?page\\_id=4](http://www.ampi.org.in/?page_id=4)

Contacts of the corresponding author:

Author: Neeraj Dixit  
 Institute: Atomic Energy Regulatory Board  
 Street: Anushaktinagar  
 City: Mumbai  
 Country: India  
 Email: [neerajdixit@aerb.gov.in](mailto:neerajdixit@aerb.gov.in)

Table 1: List of Medical Physics courses in india

| Sr. No. | Name of the Institute   | Affiliated by  | Entry level qualification                    | Course Name  | Duration |
|---------|---|--|--|--|----------|
| 1.      | Radiological Physics & Advisory Division, Bhabha Atomic Reseraach Centre Mumbai , | Homi Bhabha National Institute (Deemed University), Mumbai   | Master's degree in science (Physics)         | Post M.Sc. Diploma Course in Radiological Physics (Dip. R. P.)   | 1 Year   |
| 2.      | Osmania University, Hyderabad   | Osmania University, Hyderabad                                | -do-   | -do-   | -do-     |
| 3.      | * Pt. J. N. M. Medical College & Dr. B.R. Ambedkar Memorial Hospital,Raipur       | AYUSH and Health Sciences University of Chhattisgarh, Raipur | -do-   | -do-   | -do-     |
| 4.      | Guru Gobind Singh Indraprastha University,New Delhi                               | Guru Gobind Singh Indraprastha University, New Delhi         | -do-   | -do-   | -do-     |
| 5.      | Regional Cancer Center,Thiruvananthapuram   | Kerala University of Health Sciences, Thrissur               | -do-   | -do-   | -do-     |
| 6.      | Amrita Institute of Medical Science & Research Center,Kochi                       | Amrita Vishwa Vidyapeetham, Coimbatore                       | -do-   | Post Graduate Diploma in Medical Radiological Sciences( PG DMRP) | -do-     |
| 7.      | Jadavpur University,Kolkata   | Jadavpur University, Kolkata                                 | -do-   | Post M.Sc. Diploma in Medical Physics                            | -do-     |
| 8.      | *Mahavir Cancer Sansthan, Patna   | Aryabhatta Knowledge University, Patna                       | -do-   | -do-   | -do-     |
| 9.      | Anna University, Chennai  | Anna University, Chennai                                     | Bachelor's degree in science (Physics major) | M.Sc.(Medical Physics)   | 2 Years  |
| 10.     | Dr. B. Borooah Cancer Institute, Guwahati   | Gauhati University, Guwahati                                 | -do-   | M.Sc. (Radiological Physics)                                     | -do-     |
| 11.     | Vydehi Institute of Medical Sciences,Bangalore                                    | Rajiv Gandhi University of Health Sciences, Bangalore        | -do-   | M.Sc.(Radiation Physics)   | -do-     |
| 12.     | Kidwai Memorial Institute of Oncology,Bangalore                                   | Rajiv Gandhi University of Health Sciences, Bangalore        | -do-   | -do-   | -do-     |
| 13.     | Calicut University,Calicut  | Calicut University, Calicut                                  | -do-   | -do-   | -do-     |
| 14.     | Manipal University,Manipal  | Manipal University, Manipal, Karnataka                       | -do-   | M.Sc.( Medical Radiation Physics)                                | -do-     |
| 15.     | Panjab University Chandigarh  | Panjab University, Chandigarh                                | -do-   | M.Sc.(Medical Physics)   | -do-     |
| 16.     | *PSG College of Technology,Coimbatore   | Anna University, Chennai                                     | -do-   | M.Sc.(Medical Physics)   | -do-     |
| 17.     | Christan Medical College, Vellore   | The Tamil Nadu Dr M. G. R. Medical University, Chennai       | -do-   | -do-   | -do-     |
| 18.     | Bharthiar University, Coimbatore  | Bharthiar University, Coimbatore                             | -do-   | -do-   | -do-     |
| 19.     | Dr. N.G.P. Arts & Science College, Coimbatore                                     | Bharthiar University, Coimbatore                             | -do-   | -do-   | -do-     |
| 20.     | D.Y. Patil University, Kolhapur   | D.Y.Patil University, Kolhapur                               | -do-   | -do-   | -do-     |

\*Although the courses are in line with AERB requirement but temporally not offered by the institutions/Universities

# STATUS OF MEDICAL PHYSICS PROFESSIONAL DEVELOPMENT AND EDUCATION IN NEPAL

Matrika P. Adhikari <sup>1</sup>, Pradumna P. Chaurasia <sup>1</sup>

<sup>1</sup>Department of Radiation Oncology, B.P. Koirala Memorial Cancer Hospital, Bharatpur, Chitwan, Nepal

## I. INTRODUCTION

Nepal is a mountainous landlocked country surrounded by India from east, west and south and by Tibet of china from north. Its longitude is 80.10 East to 88.0 East and latitude is 26.20 North to 30.40 North.[1] It is 94th largest and 45st most populous country in the world with area 147181 Sq. Kilometer and 27.8 million populations[2]. GDP Per capita income is \$2313[3]



## II. HISTORICAL BACKGROUND

The First use of radiation in Nepal dates back to 1923 when the first X-Ray machine was installed at Military hospital. In 1987 Bir Hospital, Kathmandu started the first nuclear medicine service with gamma camera. The same hospital started the first CT scan in 1988 and Radiotherapy unit with tele Cobalt machine in 1991. First linear accelerator, brachytherapy and simulator established and treatment started in 2002, at B.P. Koirala Memorial Cancer Hospital (BPKMCH) Bharatpur, Chitwan. 3DCRT started in 2007 and IMRT in 2012. Nowadays there are many new Universities and Medical College coming up which led to the installation of new radiation modalities. The number of x-ray Machines, MRI, CT scanners, Linear accelerators and brachytherapy is increasing.

## III. MAJOR CANCER CENTERS IN NEPAL

There are few centers in Nepal. Though it is not adequate, there is potential to grow new centers in future. Few of them are as following.

1. B.P. Koirala Memorial Cancer Hospital, (BPKMCH), Bharatpur, Chitwan
2. National Academy of Medical Sciences, (NAMS), Bir Hospital, Kathmandu
3. Bhaktapur Cancer Hospital (BCH), Bhaktapur
4. Manipal Medical College, Pokhara
5. Kathmandu Cancer Care and Research Center (KCC&RC), Bhaktapur
6. Nepal Cancer Hospital and Research Center (NCC&RC) Lalitpur
7. National Cancer Hospital, lalitpur
8. Nepal Cancer Hospital, Banke

## IV. PRESENT STATISTICS OF MACHINE AND MANPOWER

The First use of radiation in Nepal dates back to 1923 when the first X-Ray machine was installed

Table 1 Radiology and Nuclear medicine

| S.no. | Machine      | Number |
|-------|--------------|--------|
| 1     | MRI Unit     | 18     |
| 2     | CT scanner   | 45     |
| 3     | FLuro/X-ray  | 1000+  |
| 4     | DR           | 05     |
| 5     | CR           | 45     |
| 6     | Mammography  | 12     |
| 7     | Gamma Camera | 03     |
| 8     | PET Scan     | 01     |

Table 2 Radiotherapy

| S.No. | Machine                      | Number |
|-------|------------------------------|--------|
| 1     | Tele-Cobalt machines         | 4      |
| 2     | Linear Accelerators          | 5      |
| 3     | Simulators                   | 4      |
| 4     | High Dose Rate Brachytherapy | 3      |
| 5     | Ortho voltage                | 1      |

Table 3 Manpower

| S.No. | Machine                     | Number |
|-------|-----------------------------|--------|
| 1     | Radiologists                | 110    |
| 2     | Medical Physicists          | 11     |
| 3     | Radiation Oncologists       | 27     |
| 4     | Radiographer/Technologists  | 250    |
| 5     | Radiotherapy Technologist   | 18     |
| 6     | Nuclear medicine Physicians | 03     |

## V. PROFESSIONAL ORGANIZATIONS

Some of the major organizations are as following

1. Nepalese Association of Medical Physicists (NAMP)
2. Nepalese society for Radiation Oncologist (NESTRO)
3. Nepal Radiological Society
4. Nepal Radiologist's Association
5. Nuclear Society of Nepal
6. Nepal Radiological Technology Student's Society

## VI. ABOUT MEDICAL PHYSICIST I NEPAL

The entry criteria for Medical Physicist are M.Sc in Physics plus one year Post Graduate Diploma in Medical Physics or M.Sc in Medical Physics or M.Sc. Physics plus one year clinical training.

According to "Reviewing country and Regional Programs RAS/0/057" from the IAEA fact-finding and programming mission to Nepal, Nepal should have at least 25 qualified Medical Physicist [4].

Nepalese association of medical Physicist (NAMP) has been established in 2009 and is actively working for the development and welfare of Medical Physics profession and professionals.

## VII. CONTRIBUTION OF ICTP AND IAEA TO NEPAL.

Most of the physicists have participated the college on Medical Physics that encouraged them to continue in the field and supported a lot by providing high standard teaching learning materials and training on modern trends and technology. We have got opportunity to participate medical Physics related training from ICTP and IAEA. Two fellows are doing Master in Medical Physics in ICTP.

Nepal became IAEA member in 2008, since then IAEA has provided short and long term fellowship training for the development and promotion of Medical Physicist. It is conducting project to support Nepal and also helping to formulate the Radiation Act.

## VIII. ACADEMIC ACTIVITIES AND PHYSICIST INVOLVEMENT

Biomedical physics is an Optional paper in M.Sc. Program in the Central Department of Physics and Prithvi Narayan Campus Pokhara. Thesis on Biomedical physics is going on in B.P. Koirala Memorial Cancer Hospital, Bir Hospital and Bhaktapur cancer Hospital. Medical physicists are actively involved in as thesis guide in this program. B.Sc. Medical imaging program is going on in 5 different places with intake of about 40 students per year. National Academy of Medical Science (NAMS), is conducting MD Radiotherapy course in collaboration with B.P. Koirala Memorial cancer Hospital. Medical Physicists are involved in as teaching faculty. Eight centers are conducting M D Radio-diagnosis program.

## IX. VARIOUS ACTIVITIES OF NEPALESE ASSOCIATION OF MEDICAL PHYSICIST (NAMP)

Since its establishment in 2009, NAMP has been recognized nationally and internationally as an authorized and representative organization for medical Physicist in Nepal. It has been involved in national and international activities for the promotion and development of Medical Physics profession. It is conducting talk program, Seminar, conferences etc. for the promotion of Medical Physics activities.

NAMP conducted an interaction program on the occasion of 116th year of discovery of x-ray in 2011. In the same year it conducted scientific talk program with UN-ICTP visiting Scholar Professor Anna Benini. One day symposium was organized on the occasion of first International day of Medical Physics (IDMP) on 7th Nov 2013. International conference on Medical Physics in Radiation Oncology and Imaging (ICMPROI-2014)[5] was jointly organized by Bangladesh Medical Physics Society (BMPS), Association of Medical Physicist of India, (AMPI) and Nepalese Association of Medical Physicist (NAMP) in Dhaka, Bangladesh. In 2015 a seminar on CT Imaging was conducted with guest speakers from Japan. NAMP is constantly lobbying for the formulation of radiation act and to conduct academic program in Medical Physics. NAMP is in constant communication with international organizations such as IOMP, IAEA,

AFOMP, SEAFOMP, AMPI, BMP and participating and representing Nepal in international forum.

## X. ISSUES TO BE ADDRESSED

There are some major issues to be solved in proper time for the strengthening of medical Physics.

Draft of Radiation act is ready and expect to get approved by Parliament in 2017. Formation of Regulatory body is in high demand. Medical Physics certification board is must. Strengthening academic programs for Medical Physicist is felt to fulfill the demand of qualified medical Physicist. Training and increasing opportunities for the Medical Physics professionals is must. The Medical Physicist have specialized skill and rare, so better facilities and moral support from policy maker is necessary to stop brain drain. Establishing guidelines is necessary for the safe and effective use of ionizing radiation and to meet international standards.

There are many universities and medical colleges conducting M.D. in Radio-diagnosis but they have not appointed diagnostic Medical Physicist till date.

## XI. DISPOSAL ISSUE OF OLD USED SOURCE

Old cobalt source made in Russia, donated by china could not be sent back to the point of origin and disposed safely in BPKMCH premises. Some Radium needles used to treat cervix cancer are said to be dumped in Kathmandu, near prasuti griha (Maternity Hospital), Kathmandu. Old sources from B.P. Koirala Memorial Cancer Hospital (BPKMCH) and Bhaktapur Cancer Hospital (BCH) are sent back to origin and replaced with new source.

## XII. REFERENCES

1. [www.worldatlas.com/webimage/countrys/asia/nepa](http://www.worldatlas.com/webimage/countrys/asia/nepa)
2. World fact book- 2014
3. <http://www.tradingeconomics.com/nepal/gdp-per-capita-ppp>
4. Kanchan P. Adhikari (2011), e-book, Medical Physics and engineering education and training Part- I, ICTP, Italy, 61-64
5. [www.bmps-bd.org/Conference](http://www.bmps-bd.org/Conference)



## ADDRESS FOR CORRESPONDENCE

Matrika Prasad Adhikari  
 Medical Physicist  
 B.P. Koirala Memorial Cancer Hospital  
 Bharatpur, Chitwan, Nepal  
 E mail: [adhikarimp10@yahoo.com](mailto:adhikarimp10@yahoo.com)  
 Phone no: +977 9842060365

## MEDICAL PHYSICS PROFESSIONAL DEVELOPMENT AND EDUCATION IN NIGERIA

Obed R.I<sup>1</sup>, Ekpo M.E<sup>1</sup>, Omojola A.D<sup>2</sup>, Abdulkadir M.K<sup>3</sup>

<sup>1</sup> Department of Physics, Faculty of Science, University of Ibadan, Ibadan, Oyo State, Nigeria.

<sup>2</sup>Department of Radiology, Federal Medical Centre Asaba, Delta State, Nigeria

<sup>3</sup>Department of Radiology, Kwara State General Hospital, Ilorin, Kwara State, Nigeria

**Abstract** — The evolution of medical physics profession and its awareness in Nigeria is developing at a rate faster than it was fifteen years ago. Notwithstanding, the profession as well as its development is facing challenges both in the academia and health sector. The aim of this project is to highlight challenges in the academia and in the health sector, and to give an overview of the number of institutions running the medical physics programme and its related fields. Sources for this project were from universities and pioneers in Medical Physics in Nigeria. Currently, there are only seven universities running the post-graduate academic curriculum (Masters of Science – M.Sc and Doctor of Philosophy – Ph.D programmes) in Medical Physics. The International Atomic Energy Agency had partnered with the country’s Ministry of Health in the year 2012 to start up a residency training program but it has experienced several challenges due to slow government policies in passing the Medical physics bill which would have necessitated the establishment of a Postgraduate College for Medical Physics in Nigeria.

**Keywords**— Nigeria Nuclear Regulatory Authority, Medical Physics, National University Commission

### I. INTRODUCTION

Nigeria, popularly called the “giant of Africa” is situated on the Gulf of Guinea in West Africa, with a population of well over 188 million people and has Abuja as its Capital city based on the latest United Nations estimate<sup>1</sup>. The first Department of Radiology started as far back as 1953 at the University College Hospital in Ibadan Oyo state under Professor Alexander Brown who was the first head of department<sup>2</sup>. Also, first radiation therapy and nuclear medicine services in West Africa was established in Nigeria at the College of Medicine of the University of Lagos in 1968 and commenced radiation therapy work in 1969 with a superficial X-ray machine. A Theratron 780 Cobalt-60 machine was later donated by the Canadian government in 1975 for the treatment of cancer and other malignancies. It was also the first department to offer courses in Radiation Biology, Radiation therapy and Medical Physics in Nigeria and West Africa at large. Since the emergence of these specialties (Radiology and Radiotherapy) in Nigeria, it has raised the quest to have adequate man power like

Radiologist, Oncologist and Radiographer with Medical Physicist being at the tail end due to its non popularity. In a bid to improve health services, the then President Olusegun Obasanjo in 2003 launched the VAMED Hospital Equipment Project, in which fourteen (14) teaching hospitals acquired up to date equipments through the project<sup>3</sup>. However, the increase in the number of imaging equipment has not resulted in commensurate increase in additional training as many government hospitals especially the specialist and teaching hospitals do not have these facilities. The activation of the Nigerian Nuclear Regulatory Authority (NNRA) in 2001 and the National Institute of Radiation Protection and Research (NIRPR) in 2006 (which is a body under the former), has brought to limelight the importance of medical physics in the country especially in the health establishment as well as the implementation of radiation protection in industrial sector with particular emphasis on the petroleum industry where a substantial amount of radioactive materials are in use<sup>4</sup>. The ongoing medical physics residency programme with training only in radiotherapy due to national exigencies commenced in 2012 and has been plagued with challenges primarily due to funding and delayed legislative instruments. The registered professional body of Medical Physicists in Nigeria is the Nigerian Association of Medical Physicist (NAMP). This association includes Clinical Physicists and other Medical Physicists working in the academia and the industries. Figure 1 shows the distribution of Medical Physicists in Nigerian Hospitals.

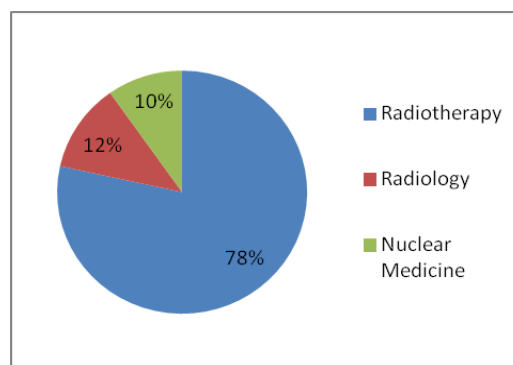


Figure1. Distribution of Medical Physicists in Hospitals in Nigeria

## II. MATERIALS AND METHODS

Materials for this write up was gathered from various universities in Nigeria with respect to institutions that run the medical physics program: through their academic prospectus, and first-hand information from colleagues who are currently lecturers in those institutions. All the Medical Physics courses in Nigeria are post-graduate programmes and their organisation is vested in the senate of the various universities running them with the National University Commission (NUC) providing some bench-marking criteria and some oversight functions. Other closely related fields like Radiation and Health Physics, Biophysics, Nuclear and Radiation Physics among others are not reported in this project.

## III. RESULT

Table 1: Institutions in Nigeria that offer Medical Physics program

|   | Institution                  | REGION        | STATE    | DEGREE        |
|---|------------------------------|---------------|----------|---------------|
| 1 | University of Lagos          | South-West    | Lagos    | MSc/MPhil/PhD |
| 2 | Benue State University       | North-Central | Benue    | MSc/ PhD      |
| 3 | Obafemi Awolowo University   | South-West    | Osun     | MSc/MPhil/PhD |
| 4 | University of Nigeria NsuKka | South-East    | Enugu    | MSc/MPhil/PhD |
| 5 | Nasarawa State University    | North-Central | Nasarawa | MSc           |
| 6 | Nnamdi Azikiwe University    | South-East    | Anambra  | MSc/MPhil/PhD |
| 7 | University of Benin          | South-South   | Edo      | MSc/MPhil/PhD |

MSc = Master of Science, MPhil = Master of Philosophy, Ph.D = Doctor of Philosophy

No university in Nigeria offer Medical Physics at undergraduate level, it can only be done from the Masters level. The results in Table 1 show Universities currently offering the Medical Physics course. All the Universities, except Nasarawa State University, offer the course at Masters and PhD levels, simultaneously. A student can opt to do an MPhil program directly, if the student did not qualify for PhD directly based on his or her grade point.



Figure 2: Map of Nigeria showing areas where Medical Physics is done at M.Sc/MPhil/Ph.D.

Also, figure 2 show regions where the Medical Physics course is done. Two in the South-west, two in the North-central, two in the South-east and one in the South-south.

## IV. DISCUSSION

Figure 1 shows a distribution of clinical Medical Physicists in Nigeria with 78% in Radiotherapy Department, 12% in Radiology and 10% Nuclear Medicine. The above distribution is an estimated figure obtained from hospitals with radiation facilities. The institutions running the Medical Physics program are presented in table 1. General courses for this program Include: Radiotherapy Physics, Diagnostic Physics, Radiation Protection, Nuclear Medicine among others. Most of the Universities have now added Anatomy and Physiology to their curriculum. Medical Physics program in universities in Nigeria are administered in the faculty of science, only College of Medicine, University of Lagos offers the course in the faculty of Medicine. Nasarawa State University offers it as Radiation and Medical Physics only at Masters level. Most of the courses taught appear to lack real practical sessions due to lack of appropriate facility, equipment and manpower. Generally, Medical Physicists with Masters in Nigeria have increased with an average turnover of seven (7) graduates every year. Currently, there are over seventy (70) Medical Physicists in Nigeria with only few employed in the twenty-one Federal Teaching Hospitals and less than six (6) in the twenty-three Federal Medical Centres across the nation. A preponderance of these physicists is in the academia.

## CONCLUSIONS

Medical Physics academic program is currently available in 7 (seven) Universities in Nigeria. To a large extent, most

Medical Physicists in Nigeria are not clinically qualified and this necessitated the IAEA supported medical physics residency programme which currently has 4 (four) residents preparing for their Part II undertaking in Radiotherapy stream. Only few were employed with Bachelor of Science in Physics. A large number have Master of Science in Medical Physics. The current challenge is in the delayed action at the national parliament (assembly) on the Medical Physics bill which will fully compliment the academic program when it is finally passed into law and diligently implemented.

#### V. ACKNOWLEDGMENT

Thanks goes to all the contributors to this mini project and the participants from Nigeria at the College on Medical Physics held at the Abdus Salam International Centre for Theoretical Physics (ICTP), Trieste, Italy from 3-25 September, 2016. The authors also want to appreciate the contribution of Dr Taofeeq Ige in editing the manuscript.

#### VI. REFERENCES

1. The current population in Nigeria, United Nation Estimate 2016: <http://www.worldometers.info/world-population/nigeria-population/> Accessed on 13 September, 2016.
2. Brief history: <http://uch-ibadan.org.ng/Radiology> Accessed on 14 September, 2016.
3. Nigerian Nuclear Regulatory Authority (NNRA) (2003). Nigerian basic ionizing radiation regulations. Lagos, Nigeria: The Federal Government Press.
4. Transforming healthcare delivery in Nigeria 2011: <http://www.vanguardngr.com/2011/12/transforming-healthcare-delivery-in-nigeria/> Accessed on 23 September, 2016.
5. Ige TA and Okonkwo EC (2010) . Medical Physics in Nigeria - A road map . Deutsche Gesellschaft fur Medizinische Physik – ISBN 3-925218-88-2, 2010.

---

# TECHNOLOGY INNOVATION

---

## AN INTRODUCTION TO HOSPITAL NETWORKS

P.S. Ganney<sup>1</sup>

<sup>1</sup> University College London Hospitals NHS Trust, London, England

**Abstract—** Computer networks in healthcare settings increasingly contain systems that fall under the classification of Medical Devices. Such items are under the jurisdiction of Clinical Engineering and Medical Physics staff who have not been formally trained in networking. This article provides an introduction to many of the concepts.

**Keywords—** Computer, Network, Connectivity, LAN, Medical Device

### X. INTRODUCTION

The emergence of the computer-based medical device has led naturally to a desire to interconnect such devices. This paper gives an overview of networking concepts, together with the applicability of them to a healthcare environment.

### XI. NETWORKING CONCEPTS

Whilst a computer on its own is a powerful device, the possibilities and the power increase greatly when such devices are linked together in a network.

The minimum number of devices in a network is 2 (otherwise you're talking to yourself). The maximum number depends on the addressing method: standard IP addresses allow for 4,294,967,296 ( $256^4$ ) but there are lots of ways to extend this, as we shall see.

In a hospital environment, devices are usually connected physically – i.e. with a cable. This improves reliability as well as giving larger bandwidth and higher speed. There are multiple ways of connecting devices, but the simplest is via a hub, which is essentially a connection box where all incoming signals are sent to all connected devices.

#### A. The Network Packet

All networking is described in terms of packets so it is useful to describe this first. A network packet is a formatted unit of data carried by a packet-switched network.

Computer communications links that do not support packets, such as traditional point-to-point telecommunications links, simply transmit data as a bit stream.

A packet consists of control information and user data, which is also known as the payload. Control information provides data for delivering the payload, for example: source and destination network addresses, error detection codes, and sequencing information. Typically, control information is found in packet headers and trailers.

Different communications protocols use different conventions for distinguishing between the elements and for formatting the data. For example, in Point-to-Point Protocol, the packet is formatted in 8-bit bytes, and special characters are used to delimit the different elements. Other protocols like Ethernet, establish the start of the header and data elements by their location relative to the start of the packet. Some protocols format the information at a bit level instead of a byte level.

A good analogy is to consider a packet to be like a letter: the header is like the envelope, and the data area is whatever the person puts inside the envelope.

In the seven-layer OSI model of computer networking (see later), packet strictly refers to a data unit at layer 3, the Network Layer. The correct term for a data unit at Layer 2, the Data Link Layer, is a frame, and at Layer 4, the Transport Layer, the correct term is a segment or datagram. For the case of TCP/IP communication over Ethernet, a TCP segment is carried in one or more IP packets, which are each carried in one or more Ethernet frames.

#### B. Hardware

We shall first examine the three main hardware components – hub, switch and router.



Fig. 1. A network hub (source: Wikimedia Commons)

A hub is a simple connection box, operating at the Physical Layer (layer 1) of the OSI model (see later). Like a transport hub, it's where everything comes together. Unlike a transport hub, though, whatever comes in on one connection goes out on all other connections. It's up to the receiver to decide whether or not the message is for them. Hubs therefore work well for small networks, but get messy and slow down for larger ones. It is therefore often common to find them in small networks (e.g. at home) or in sub-networks (e.g. in an office).

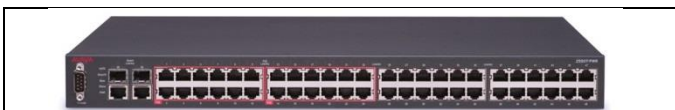


Fig. 2. A network switch (source: Wikimedia Commons)

A switch is a device that filters and forwards packets between LAN segments. Switches operate at the data link layer (layer 2) and sometimes the network layer (layer 3) of the OSI Reference Model (see later) and therefore support any packet protocol. LANs that use switches to join segments are called switched LANs or, in the case of Ethernet networks, switched Ethernet LANs.



Fig. 3. A network router (source: Wikimedia Commons)

A router forwards data packets along networks. A router is connected to at least two networks and is located at a gateway, the place where two or more networks connect.

Routers use headers and forwarding tables to determine the best path for forwarding the packets, and they use protocols such as ICMP (Internet Control Message Protocol) to communicate with each other and configure the best route between any two hosts.

A large network will therefore contain all 3 of these types of devices.

Today most routers have become something of a Swiss Army knife, combining the features and functionality of a router and switch/hub into a single unit (and may contain a basic Domain Name Service (DNS)).

The functions of a router, hub and a switch are all quite different from one another, even if at times they are all integrated into a single device. We will start with the hub and the switch since these two devices have similar roles on the network.

Each serves as a central connection for all of the network equipment and handles a data type known as frames. Frames carry data. When a frame is received, it is amplified and then transmitted on to the port of the destination device. The big difference between these two devices is in the method in which frames are being delivered.

In a hub, a frame is passed along or "broadcast" to every one of its ports. It doesn't matter that the frame is only destined for one port. The hub has no way of distinguishing which port a frame should be sent to. Passing it along to every port ensures that it will reach its intended destination. This places a lot of traffic on the network and can lead to poor network response times.

Additionally, a 10/100Mbps hub must share its bandwidth with each and every one of its ports. So when only one device is broadcasting, it will have access to the maximum available bandwidth. If, however, multiple devices are broadcasting, then that bandwidth will need to be divided among all of those systems, which will degrade performance.

A switch, however, keeps a record of the MAC addresses of all the devices connected to it. With this information, a switch can identify which system is sitting on which port. So when a frame is received, it knows exactly which port to send it to, without significantly increasing network response times. And, unlike a hub, a 10/100Mbps switch will allocate a full 10/100Mbps to each of its ports. So regardless of the number of devices transmitting, users will always have access to the maximum amount of bandwidth. For these reasons a switch is considered to be a much better choice than a hub.

Routers are completely different devices. Where a hub or switch is concerned with transmitting frames, a router's job, as its name implies, is to route packets to other networks until that packet ultimately reaches its destination. One of the key features of a packet is that it not only contains data, but the destination address of where it's going.

A router is typically connected to at least two networks, commonly two Local Area Networks (LANs) or Wide Area Networks (WANs) or a LAN and its ISP's network. For example, a PC or workgroup and Broadband.

Routers might have a single WAN port and a single LAN port and are designed to connect an existing LAN hub or switch to a WAN. Ethernet switches and hubs can be connected to a router with multiple PC ports to expand a LAN. Depending on the capabilities (kinds of available ports) of the router and the switches or hubs, the connection between the router and switches/hubs may require either straight-through or crossover (null-modem) cables. Some routers even have USB ports, and more commonly, wireless access points built into them.

Besides the inherent protection features provided by the NAT, many routers will also have a built-in, configurable, hardware-based firewall. Firewall capabilities can range from the very basic to quite sophisticated devices. Among the capabilities found on leading routers are those that permit configuring TCP/UDP ports for games, chat services, and the like, on the LAN behind the firewall.

So, in summary, a hub glues together an Ethernet network segment, a switch can connect multiple Ethernet segments more efficiently and a router can do those functions plus route TCP/IP packets between multiple LANs and/or WANs; and much more.

### C. Network Topologies

The topology of the network can be thought of as its shape. Not its physical shape, but its logical one: much like the tube map shows how stations connect, not where they are. The five basic topologies are bus, ring, star, tree and mesh, which we now examine.

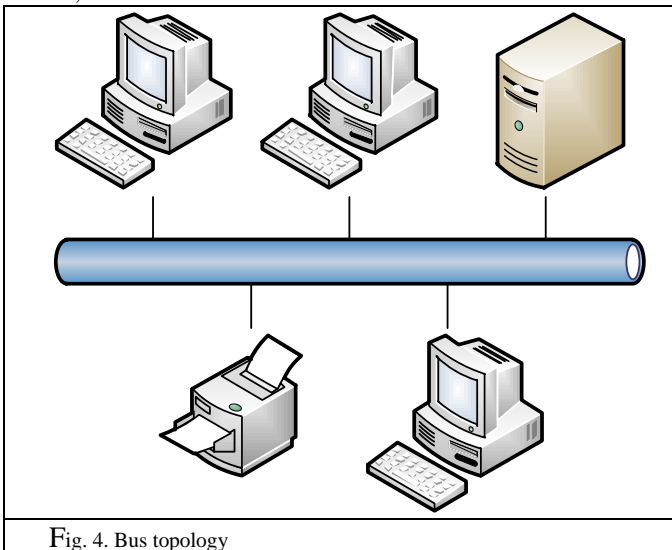


Fig. 4. Bus topology

Bus networks use a common backbone to connect all devices. A single cable, the backbone functions as a shared communication medium that devices attach or tap into with an interface connector. A device wanting to communicate with another device on the network sends a broadcast message onto the wire that all other devices see, but only the intended recipient actually accepts and processes the message.

Ethernet bus topologies are relatively easy to install and don't require much cabling compared to the alternatives. However, bus networks work best with a limited number of devices. If more than a few dozen computers are added to a network bus, performance problems will likely result. In addition, if the backbone cable fails, the entire network effectively becomes unusable.

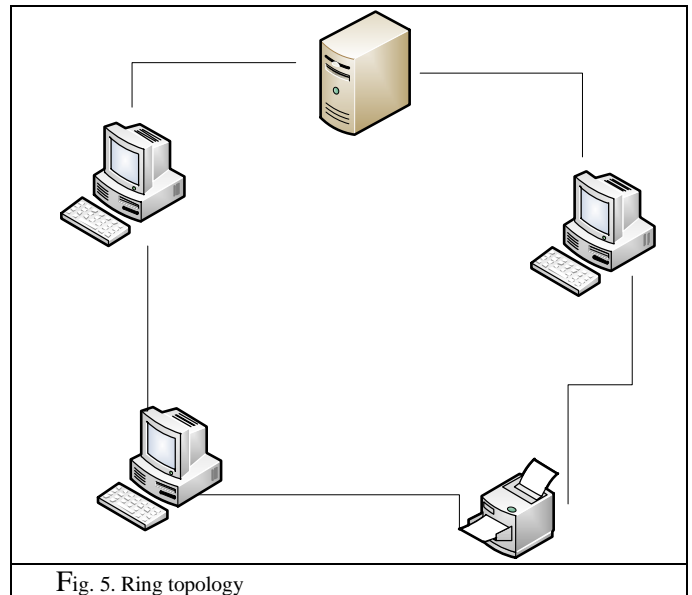


Fig. 5. Ring topology

In a ring network, every device has exactly two neighbours for communication purposes. All messages travel through a ring in the same direction (either "clockwise" or "counterclockwise"). A failure in any cable or device breaks the loop and can take down the entire network.

To implement a ring network, one typically uses FDDI<sup>1</sup>, SONET<sup>2</sup>, or Token Ring technology<sup>3</sup>.

1. <sup>1</sup> Fiber Distributed Data Interface – a set of ANSI and ISO standards for data transmission on fibre optic lines in a LAN that can extend in range up to 200 km (124 miles).
2. <sup>2</sup> Synchronous Optical Network – the American National Standards Institute standard for synchronous data transmission on optical media.
3. <sup>3</sup> In a token ring, a "token" is passed around the network. The device holding the "token" is permitted to transmit – nothing else is. If a device has nothing to transmit, it passes the token on.

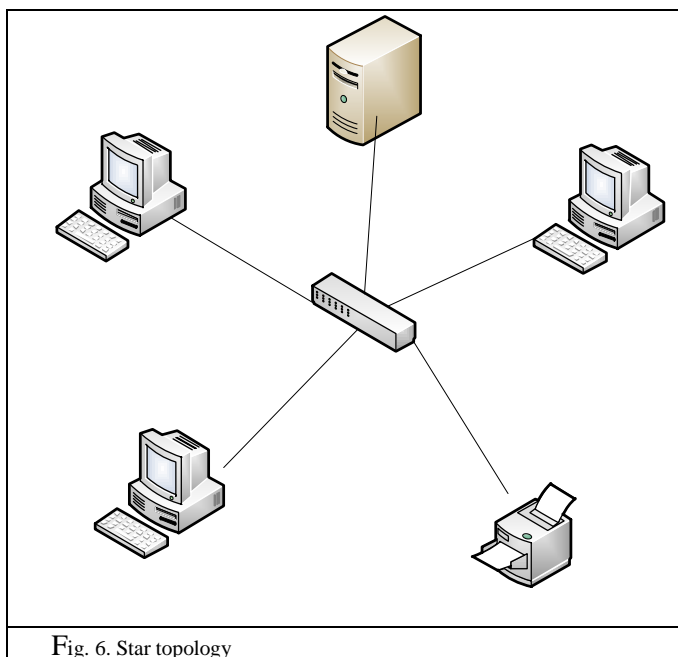


Fig. 6. Star topology

Most small (e.g. home) networks use the star topology. A star network features a central connection point called a "hub node" that may be a network hub, switch or (more likely) a router. Devices typically connect to the hub with Unshielded Twisted Pair (UTP) Ethernet.

Compared to the bus topology, a star network generally requires more cable, but a failure in any star network cable will only take down one computer's network access and not the entire LAN. (If the hub fails, however, the entire network also fails.)

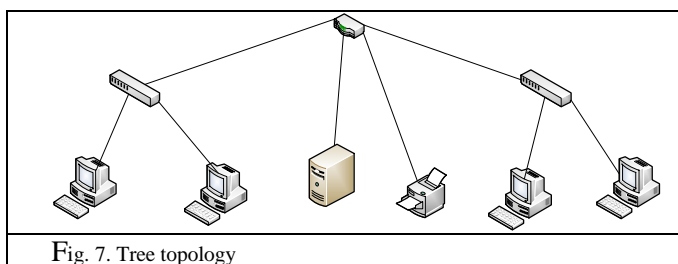


Fig. 7. Tree topology

Tree topologies integrate multiple star topologies together onto a bus. In its simplest form, only hub devices connect directly to the tree bus, and each hub functions as the root of a tree of devices. This bus/star hybrid approach supports future expandability of the network much better than a bus (limited in the number of devices due to the broadcast traffic it generates) or a star (limited by the number of hub connection points) alone.

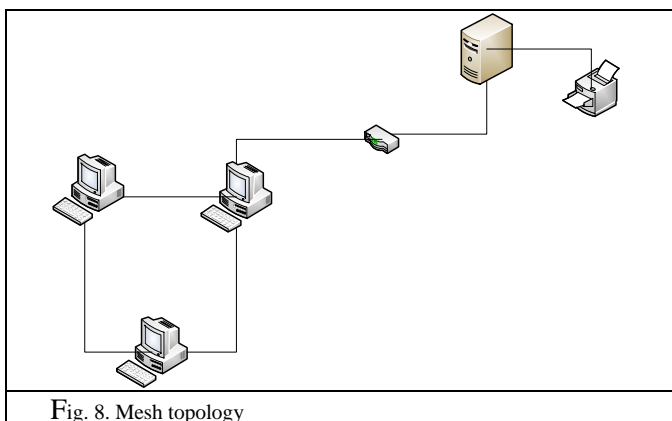


Fig. 8. Mesh topology

Mesh topologies involve the concept of routes. Unlike each of the previous topologies, messages sent on a mesh network can take any of several possible paths from source to destination. (Recall that even in a ring, although two cable paths exist, messages can only travel in one direction.) Some WANs, most notably the Internet, employ mesh routing, specifically for the resilience that it brings.

A mesh network in which every device connects to every other is called a full mesh. As shown in the illustration above, partial mesh networks also exist in which some devices connect only indirectly to others.

#### D. IP addressing and DNS

People like to communicate using names. Therefore we call our devices "Linac B PC", "Endoscopy control" and so on rather than "1", "2" or "3.1412".

Computers prefer numbers. When they're communicating, they require unique numbers. Therefore they use IP addresses. An IP (Internet Protocol) version 4 address is formed of 4 groups of digits, separated by dots<sup>4</sup>. Each group of digits can range in value from 0 to 255 – 256<sup>5</sup> unique numbers. The combination of these 4 groups should uniquely identify the device on the network. If it's not unique then chaos ensues.

Of course, we still like to call our devices by names, so a network service called a DNS (Domain Name Server) is usually available to translate "LinacA" into 123.45.67.89 so that the command "ping LinacA"<sup>6</sup> can be issued and a reply can come from 123.45.67.89 without having to know the IP address of LinacA.

The four-byte IP address allows us to perform grouping. A set of devices may be given addresses in the same range – i.e. they have the same first 2 or 3 bytes, differing only in the final one or two. Given that we have a DNS to do the translation and can therefore give our devices sensible

<sup>4</sup> IPv6 also exists, but is not widespread (yet), but does allow 296 addresses.

<sup>5</sup> Due to binary: 256 is 2<sup>8</sup> so each group of digits is composed of 8 bits.

<sup>6</sup> A command that sends an "are you there" message.

names, this may seem unnecessary, but it does allow us to segregate our network using masking.

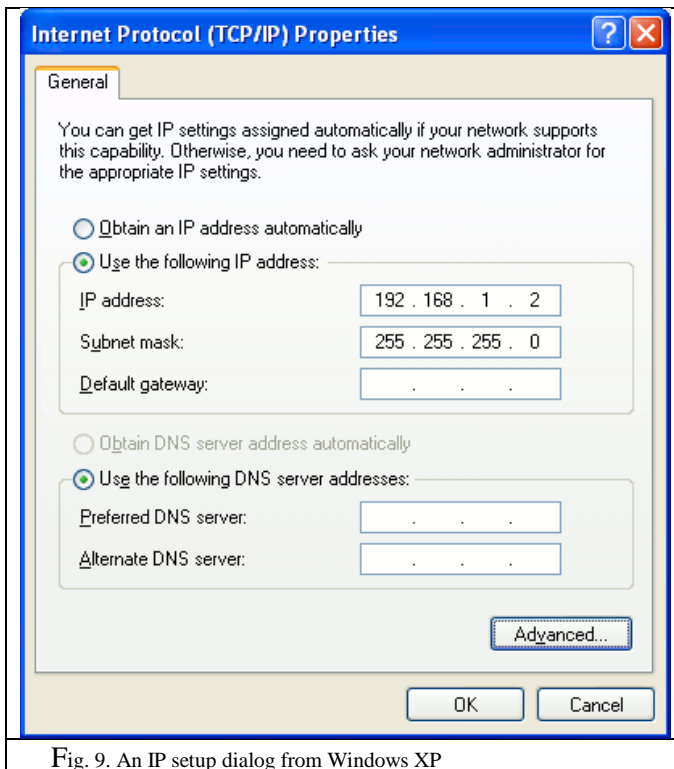


Fig. 9. An IP setup dialog from Windows XP

An IP mask of 255.255.255.0 allows us to separate out the network prefix and the host number using bitwise AND<sup>7</sup>.

Thus, in the example in Fig. 9, the network address is 192.168.1 and the host number is 2. Networks can be further divided to produce smaller subnets by putting more bits into the mask. For example a mask of 255.255.255.192 leaves this example with the same host number, but a host number previously of 130 would now be rendered as 2.

The modern way of specifying a network mask is to specify the number of bits in it, as masks are always 1s to the left and 0s to the right and no intermingling. Thus 192.168.1.2, netmask 255.255.255.0 is written as 192.168.1.2/24. This is known as CIDR (Classless Inter-Domain Routing) notation.

It is this subnetting that allows us to write simple router rules as they can be produced for groups of IPs instead of for each one individually.

There are 3 main ways of giving a device an IP address. Firstly, and most simply, is static. This is where the 4-byte number is given to that device and that device only (see Fig. 9 where this is the case).

The second is dynamic. This is where a device requests an IP address from the DHCP<sup>8</sup> controller and is provided

with the next spare one. This system works well with hot-spots and networks where there are more devices than IP addresses, but never has all the devices switched on at once. It's also very useful in networks where the number of devices changes frequently (e.g. a hospital network): it is not necessary to keep note of the addresses issued so far and no-one has to check whether a device has been decommissioned. Administratively it's the simplest method, but it too has drawbacks.

The main one is that some protocols have to communicate via fixed IP addresses. DICOM is one such (although later devices can often take the device name, many can't). One solution to this is to run a mixed addressing network, with some static IPs (usually in the same range so they can be easily administered) and the rest dynamic. One other solution is to use reserved IPs – in this case it is again all controlled by the DHCP controller (often part of the DNS), but when a device requests an IP it is always served the same one, which has been reserved for it. That way the network runs only in dynamic mode but the needs of static addressing are met.

Which brings us to the question of 2 Devices with the same IP address. Locally this is impossible, but globally not so. If a device's IP address is only visible up to the router, then it is not visible beyond it (e.g. on the Internet) and therefore another device on the other side of the router can have exactly the same IP address and they will never conflict.

### E. Security

The first question to address is: where is your data? It may be on a local machine, on a local server or in "the cloud".

Cloud Computing is where the software and data do not reside on local servers, in the local organisation or possibly even in the same country. Whilst this frees up a lot of infrastructure and makes mobile computing more possible, it does have 2 main drawbacks:

The first is that a reliable network connection is essential to use the cloud.

The second is that the laws of data protection that apply to data are those that exist in the country in which the data resides: in the USA, for example, companies are allowed to sell the data they have on their network. Not to anyone, of course, but they can sell health records to insurance agencies, email addresses to marketers etc. So it is important, for health records, to know where the data is being held (for further information see the Data Protection Act, which is beyond the scope of this article). In the UK there is a G-Cloud, a cloud solution hosted there for public service use, thus making it subject to the UK's data protection laws. There are also more and more assured clouds being marketed.

There are great advantages in connecting together ICT equipment to enable data sharing, together with the enhanced safety from a reduction in transcription errors and

7.<sup>7</sup> Where two binary numbers are compared, bit by bit and an AND operation is performed on them to produce the result.

8.<sup>8</sup> Dynamic Host Configuration Protocol

the increased availability and speed of access to information. However, this connectedness brings with it additional system security issues: a failure in one part may be swiftly replicated across the IT estate. There are many ways to tackle these issues and this section details some of these. It should be noted that best practice will utilise a range of security methods.

The first method is one of segregation, using a firewall. A firewall is, in the simplest sense, a pair of network cards (or a router) and a set of rules. A network packet arrives at one card, is tested against the rules and (if it passes) is passed to the other card for transmission. In this way, a part (or the whole of) a network can be protected from activity on the rest of the network by restricting the messages that can pass through it to a predefined and pre-approved set. The rules controlling this may be as simple as only allowing a predefined set of IP addresses through. Refinements include port numbers, the direction the message is travelling in, whether the incoming message is a response to an outgoing one (e.g. a web page) and specific exceptions to general rules. This is all achieved via packet filtering, where the header of the packet is examined in order to extract the information required for the rules.

The above description is of a hardware firewall. Software firewalls run on the device after the network traffic has been received. They can therefore be more sophisticated in their rules in that they can have additional information such as the program that made the request. Software firewalls can also include privacy controls and content filtering. As the software firewall runs on the device, if the device becomes compromised, then the firewall may also be compromised. The Windows 7 firewall only blocks incoming traffic, so will not prevent a compromised device from sending malicious network packets.

#### F. Bandwidth

Bandwidth in a computer network sense is its transmission capacity, which (as it is a function of the speed of transmission) is usually expressed in bps (bits per second). The most common wired bandwidths are 1 Gbps (often called “Gigabit Ethernet”), 10 Mbps (standard Ethernet) and 100 Mbps (fast Ethernet). Wireless is generally slower – 802.11g supports up to 54 Mbps, for example. Note that these are maximums and a wired network stands a better chance of providing the full bandwidth due to less interference. As bandwidth is actually the capacity, binding together several cables can increase the total bandwidth whilst not increasing the speed – although this would not normally be done in a departmental network, the point at which a hospital meets the national N3 network may be implemented this way (provided both sides of the connection can handle it – which is usually by routing pre-defined packets to specified lines, e.g. by IP address range).

It is never a good idea to reach 100% bandwidth utilisation and the average in order to avoid this may be as

low as 30%, although 50% would be more common. The amount of “spare” capacity is often termed “headroom”. At 75% the throughput versus offered traffic curve starts to depart from a linear proportional increase of throughput for increase of offered traffic. At 80% the channel could be approaching overload. Much is dependent upon the traffic type - data traffic can cope with higher utilisation levels than voice as delay and jitter have more effect on the user experience for voice traffic than data traffic. Optimisation techniques such as QoS<sup>9</sup> can be used to prioritise voice traffic (or any other traffic that is time-critical).

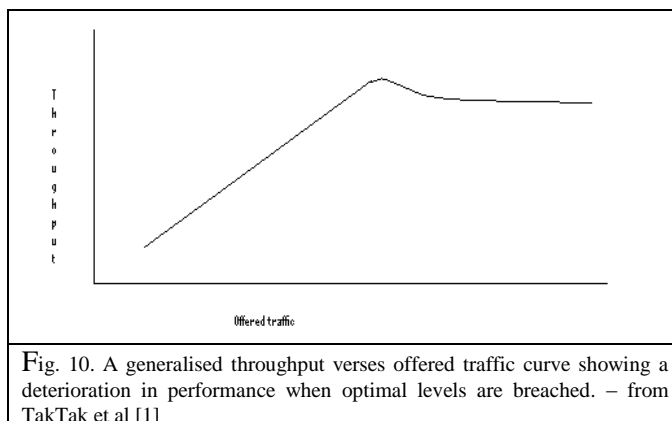


Fig. 10. A generalised throughput versus offered traffic curve showing a deterioration in performance when optimal levels are breached. – from TakTak et al [1]

The above utilisation levels are generally for non collision based channels. In the case of Ethernet which uses CSMA<sup>10</sup> with collision detection as the access mechanism, utilisation should be much lower. An overdriven CSMA channel can result in throughput reduction rather than an increase with increasing offered traffic. Retrys as a result of a collision lead to more retrys and more collisions and so on. Collision detection with a limitation on the number of retrys and back off between the retrys is aimed at keeping the channel stable but throughput will tail off. Kleinrock [2] provides good further reading.

All the resilience methods outlined here require a level of redundancy: be it a copy, checksums or headroom. Thus a resilient system will always be over-engineered – in the case of bandwidth, over-engineering can remove the need for optimisation systems such as QOS, thus making the design (and therefore the support) simpler.

## XII. STANDARDS

There are several international standards covering IT networks, but the one of particular interest here is IEC 80001-1 (2010). This standard, titled “Application of risk management for IT-networks incorporating medical devices -- Part 1: Roles, responsibilities and activities” contains

9. <sup>9</sup> Quality-of-service, a Cisco product.

10. <sup>10</sup> Carrier Sense Multiple Access, a protocol in which a node verifies the absence of other traffic before transmitting on a shared transmission medium.

many definitions. The main one for consideration here is that of the “*Medical IT Network*”, which is defined as “*an IT-NETWORK that incorporates at least one MEDICAL DEVICE*”. An IT-NETWORK is defined as “*a system or systems composed of communicating nodes and transmission links to provide physically linked or wireless transmission between two or more specified communication nodes*” and is adapted from IEC 61907:2009, definition 3.1.1. The MEDICAL DEVICE definition is from the Medical Device Directive. Thus a hospital that connects even one medical device into its standard network (or, indeed, loads medical device software onto a non-medical device so connected) has thereby created a medical IT-Network. The bounds of this network are that of the responsible organisation<sup>11</sup> but do bring different responsibilities into play, as detailed in the standard. In particular, the role of the medical IT-network risk manager, the person accountable for risk management of the medical IT-network is specified.

This family of standards could stimulate cross disciplinary teams in hospitals, involving IT departments, Informatics Departments and Clinical Departments in establishing quality systems for Clinical Computing. This would include assurance of finance, planning of procurement and upgrades, and the monitoring of adequate support arrangements. Medical Physicists and Clinical Engineers would have an important role to play in these groups, particularly with regard to day to day running and relationships with device suppliers.

XIII. THE OSI 7-LAYER MODEL [3]

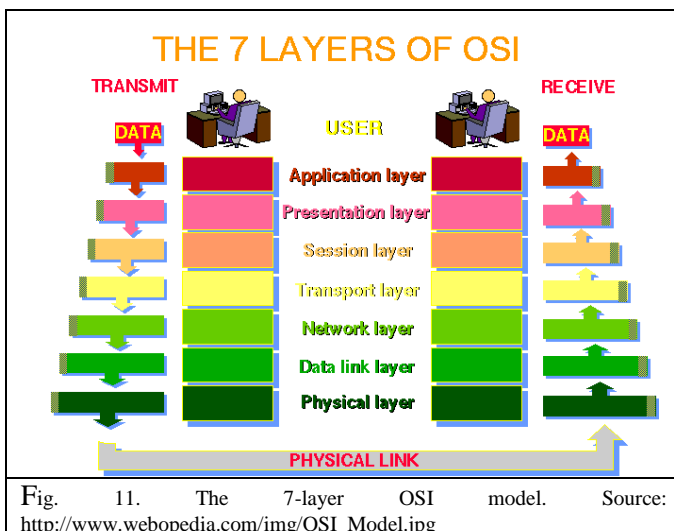


Fig. 11. The 7-layer OSI model. Source: [http://www.webopedia.com/img/OSI\\_Model.jpg](http://www.webopedia.com/img/OSI_Model.jpg)

The OSI 7-layer model describes the transmission of messages. In sending a message, each layer (from the highest – the Application – to the lowest – the Physical)

adds a wrapper to the message, which is removed after physical transmission as the message makes its way back up the layers into the receiving application.

The physical layer, the lowest layer of the OSI model, is concerned with the transmission and reception of the unstructured raw bit stream over a physical medium. It describes the electrical/optical, mechanical, and functional interfaces to the physical medium, and carries the signals for all of the higher layers. It deal with such matters as what signal state represents a binary 1, how many pins are on a connector (and what they do) and how many volts/db should be used to represent a given signal state.

The data link layer provides error-free transfer of data frames from one node to another over the physical layer, allowing layers above it to assume virtually error-free transmission over the link. The data link layer handles matters such as establishing and terminating the logical link between two nodes, transmitting/receiving frames sequentially and determining when the node "has the right" to use the physical medium (see the description of “token ring” earlier).

The network layer controls the operation of the subnet, deciding which physical path the data should take based on network conditions, priority of service, and other factors. It is concerned with routing, subnet traffic control and logical-physical address mapping.

The transport layer ensures that messages are delivered error-free, in sequence, and with no losses or duplications. It relieves the higher layer protocols from any concern with the transfer of data between them and their peers. It handles such matters as message segmentation, message acknowledgement and session multiplexing (multiplexing several message streams, or sessions onto one logical link and keeping track of which messages belong to which sessions).

The session layer allows session establishment between processes running on different stations. It handles session establishment, maintenance and termination, allowing two application processes on different machines to establish, use and terminate a connection, called a session.

The presentation layer formats the data to be presented to the application layer. It can be viewed as the translator for the network. This layer may translate data from a format used by the application layer into a common format at the sending station, then translate the common format to a format known to the application layer at the receiving station. It handles code conversions such as ASCII to EBCDIC, bit-order and CR/LF. Data compression and encryption take place at this layer.

The application layer serves as the window for users and application processes to access network services. This layer contains a variety of commonly needed functions such as resource sharing, remote printing and file access and directory services.

11. <sup>11</sup> Thus a connection to the Internet does not render a network a medical IT-network.

#### XIV. CONCLUSIONS

Hospital networks are useful conduits for distributing and sharing information, which thereby enhance patient care. They do, however, require correct implementation in order to do so safely.

#### ACKNOWLEDGMENT

The author wishes to acknowledge colleagues past and present, especially Bill Webster, who assisted the development of this material over several years.

#### REFERENCES

8. Taktak AFG, Ganney PS, Long D & White P (2013) Clinical Engineering. Academic Press, Oxford. especially chapters 8-10 by Claridge, Ganney, McDonagh & Pisharody
9. Kleinrock L (1975-2011) Queuing Systems Volumes 1-3. John Wiley & Sons, London
10. <https://support.microsoft.com/en-us/kb/103884>

Contacts of the corresponding author:

Author: Paul Ganney  
Institute: University College London Hospitals NHS Trust  
Street: Euston Road  
City: London  
Country: England  
Email: [paul.ganney@uclh.nhs.uk](mailto:paul.ganney@uclh.nhs.uk)

## PERFORMANCE AND PITFALLS OF DIAGNOSTIC X-RAY SOURCES: AN OVERVIEW

R. Behling

Philips, Hamburg, Germany

This article is derived from the book, *Modern Diagnostic X-Ray Sources: Technology, Manufacturing, Reliability* by Rolf Behling (© Taylor & Francis / CRC Press, 2016). Portions of the book are reproduced herein with the publisher's permission.

**Abstract**— Performance and reliability of medical X-ray sources for imaging humans are crucial from ethical, clinical and economic perspectives. This overview will treat the aspects to consider for investment of equipment for medical X-ray imaging. Recent X-ray tubes deliver enhanced reliability and unprecedented performance. But, metric for benchmarking has to change. Modern terms for product comparison still need to penetrate the market and to be implemented in practice. It is time to abandon *heat units* and comply with latest standards, which consider current technology.

In view of the increasing number of interventional procedures and the risks associated with ionizing radiation, toxic contrast agents, and the potentially hazardous combination thereof, system reliability is of paramount importance. This paper will discuss tube life time aspects.

The speed of scientific and industrial development of new diagnostic and therapeutic X-ray sources remains high. Still, system developers and clinicians suffer from gaps between aspirations and reality in day-to-day diagnostic routine. X-ray sources are still limiting cutting-edge medical procedures. Undesired side-effects, wear and tear, limitations of the clinical work flow, costs, and undesired characteristics of the X-ray source must be further addressed. New applications and modalities, like spectral CT, and phase-contrast or dark-field imaging will impact the course of new developments of X-ray sources. High performance and flawless operation of the very special kind of vacuum electronics of X-ray tubes can only be safeguarded by quality manufacturing and highly skilled craftsmanship. Joint development of semiconductor and vacuum based electronics, i.e. X-ray generators and tubes, has proven key to success in the medical industry to guarantee a seamless match of the once separate devices. Thus, the terminology is expected to morph from *X-ray tube* and *high-voltage generator* to *X-ray source segment*.

**Keywords**— X-ray tube, X-ray generator, tube failures, X-ray tube metric, reliability.

### XV. INTRODUCTION

Physics, history, technology and manufacturing of X-ray sources for medical diagnostic imaging are treated in many textbooks of medical imaging, usually as sub-chapters. A comprehensive description of the many aspects related to diagnostic X-ray sources, issues of reliability and their possible future can be found in [1]. Instead, the present paper will briefly touch a small

selected sample of deficits and pitfalls, which are relevant for the practical clinical use.

### XVI. HISTORY

The discovery of Conrad Wilhelm Roentgen, who created X-ray photons for the first time on purpose, which are capable of gathering detailed information about the anatomy of patients, was a quantum leap for medical diagnostics and therapy. Besides many laboratory type installations, the world's first X-ray machine in a clinic was installed and used in March 1896 in a patient preparation room of an operation theater in the New General Hospital (now UKE) in Hamburg, Germany. This city has since then been home of an industrial center of X-ray technology. Only a few places worldwide house the required expertise. Initially, the technology evolved with overwhelming enthusiasm and speed. But, at the time the hazards of ionizing radiation were unknown, yet. Highly flexible construction materials like glass provided lots of freedom of experimenting in those days.



Fig. 1 Replica of an early ion X-ray tube as used by C. W. Roentgen. When the electron collector (short wire, right) is charged positively during the cycle of alternating high-voltage from the inductor and acts as an anode ions generated in the residual gas hit the aluminum slab on the left, the cathode. Cathode rays (electrons) are released, accelerated in the electric field, by-pass the anode wire and hit the glass wall at the right. Greenish fluorescence signals electronic current flow and X-ray generation. Backscattered electrons are collected by the anode wire. Roentgen wrote on Feb. 26<sup>th</sup>, 1896: "Namely, I discovered, that X-rays are not only created in glass, but also all other solid bodies (and perhaps even in liquids and gasses)..." (Translated from [2], pg. 56). (Photo courtesy of Philips.)

XVII. X-RAY SOURCES

This extraordinary situation resulted in product cycle times of weeks rather than decades, which we are facing today. But, at the same time the extreme innovation rate was also paired with deep frustration. Summarizing an exhaustive year of ups and downs, Roentgen complained in January 1897 in a letter to his friend and assistant Ludwig Zehnder, see [2], pg. 65 (translated): “Meanwhile, I have provisionally sworn, that I do not want to deal with the behavior of the [X-ray] tubes, as these dingus are even more capricious and erratic than the women.” (Remark: A bowl of chocolate on his desk proves that Roentgen dearly loved his wife Bertha and vice versa, other than the above quote could suggest. To keep him happy, she replenished the chocolate daily. The bowl is still on exhibit at the German Roentgen Museum, Remscheid-Lennep, Germany.) But still, even after decades of technology development, the world of diagnostic X-ray sources surprises users and developers

Roentgen’s interface between tube and high voltage generator consisted of merely two wires: one charging the cathode, the other the anode, see Fig. 1. The tube current was simply defined by gas content and electrode geometry and was a simple monotonic function of the applied tube voltage. X-ray tubes and high voltage generators were developed in separate departments, sometimes even in separate companies. The first X-ray tube for use in a clinic came from C.H.F Mueller, later Philips, Hamburg, the inductor from Berlin, Germany. Today, experts prefer using the term *X-ray segment* instead of *tube* and *high voltage generator*. The complexity of the interface and the degree of interleaved R&D activity have both risen dramatically over time, latest with the advent of magnetic focusing and focal spot

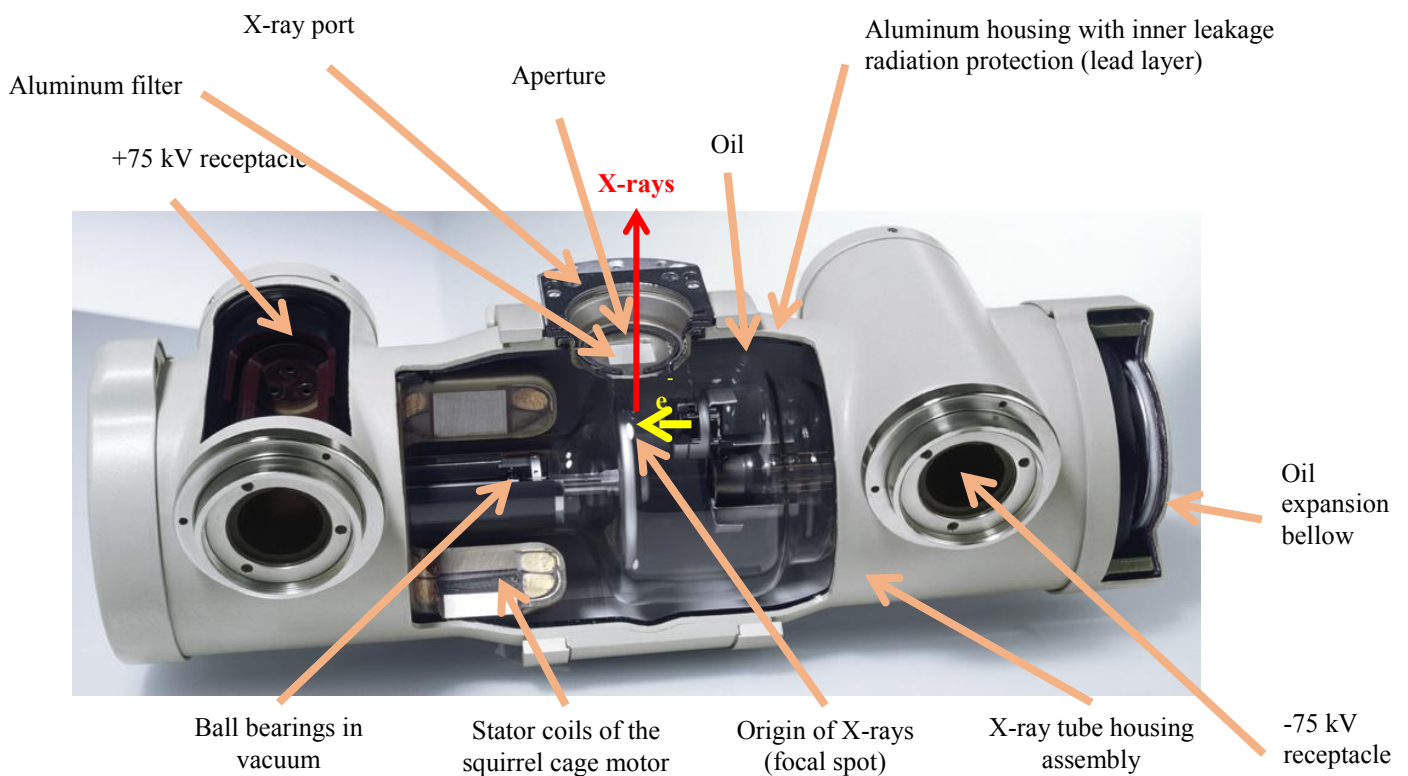


Fig. 2 Rotating anode X-ray tube housing assembly

with pitfalls and in extreme cases, frustration. Besides evolving X-ray system technology, this is one of the many reasons for ongoing annual multi-million dollar industrial R&D investment.

deflection. Other than with electrostatic focusing, magnetic control requires permanent fine tuning of the electrical supply of focusing magnets by the generator. Electron trajectories depend on the selected technique factors tube voltage and tube current which may vary during exposure. In addition, grid switching the tube current and focal spot deflection may require control voltages of several kilovolts to be supplied by the

generator to the cathode. Thermal and vacuum discharge management have become state-of-the-art. Intelligent X-ray dose control, rotor drives, safety management, service functionality, web connectivity add. The majority of large industrial vendors have therefore established integrated R&D departments, which have been given the joint responsibility for tube and generator development under single management. High performance X-ray tubes have morphed to X-ray source sub-segments of imaging systems rather than stand-alone items.

XVIII. BASICS OF FUNCTIONING

Before branching into the various possible pitfalls, it may be helpful to recall the basic functioning of rotating anode X-ray tubes. Figure 2 shows a sample cut model of a rotating anode X-ray tube housing assembly equipped with a rotor system with ball bearings, driven by an asynchronous squirrel-cage type motor. An electron beam is released into vacuum by a directly current heated thermionic tungsten electron emitter. Electrons are then accelerated in the electric field between cathode and anode. Photons emerge from a micrometer thin layer

below the surface of the target during interaction of the electron beam with high-z and high density material, preferably tungsten. A small percentage of primary electrons shot into the extremely high electric field around the nuclei of the target convert their kinetic energy into electromagnetic X-radiation in the focal spot (FS). The tube voltage defines the X-ray photon spectrum with a Duane-Hunt cut-off energy at  $-eU_t$ ,  $e$  being the electron charge,  $U_t$  the tube voltage. Undesired X-ray photons of lowest energy are taken out of the used beam. The soft end of the spectrum is defined by X-ray filters in the beam path, typically made of aluminum slabs with a thickness in the order of 2.5 mm or more, depending on the application. Due to their high absorption rate per length of tissue passed, photons with energies below ca. 15 keV to 30 keV would merely raise the patient's skin dose without delivering information to the detector.

The factor of conversion of electrical power to used X-ray intensity is in the order of  $10^{-4}$ , for details see [1], chapter 2.2. Thus, typically the generation of bremsstrahlung (brake radiation) for imaging, means management of kilowatts of electric power and sophisticated heat management, see Figure 4.

• GE

- Thermionic cathode (Coolidge, 1913)
- Graphite anodes (CGR, 1967)
- Largest anode (2005)

• Philips

- 1<sup>st</sup> clinic (Hamburg, Germany, Müller, 3/20/1896)
- Line focus (Goetze, 1919)
- Metal frame + finned rotating anode (Bowers, 1929)
- All metal ceramics (1980)
- Liquid bearing (1989), dual suspended (2007)
- Double quadrupole (2007)

• Siemens

- Graphite backed anodes (1973)
- Flat electron emitter (1998)
- Rotating frame (2003)
- Magnetic quadrupole, z-deflection (2007)

• Varian

- Largest anode heat capacity (1980s)
- Liquid cooled e<sup>-</sup> - trap (1998)

• Others

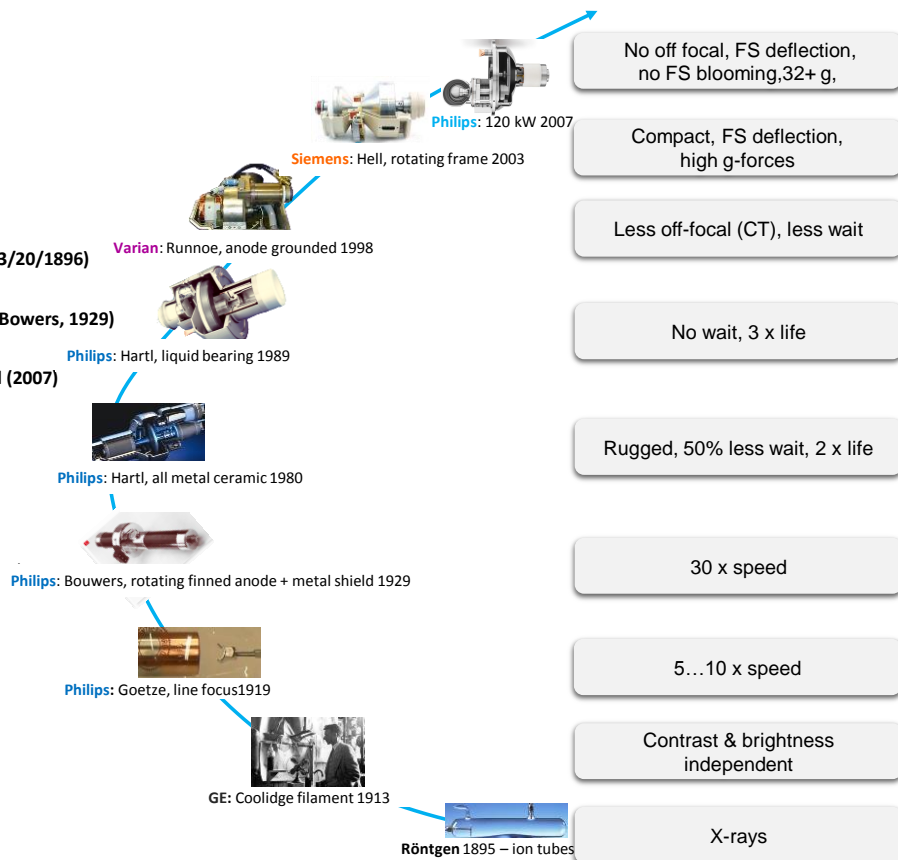


Fig. 3 Key achievements by various vendors (in alphabetic order) and their historic predecessors

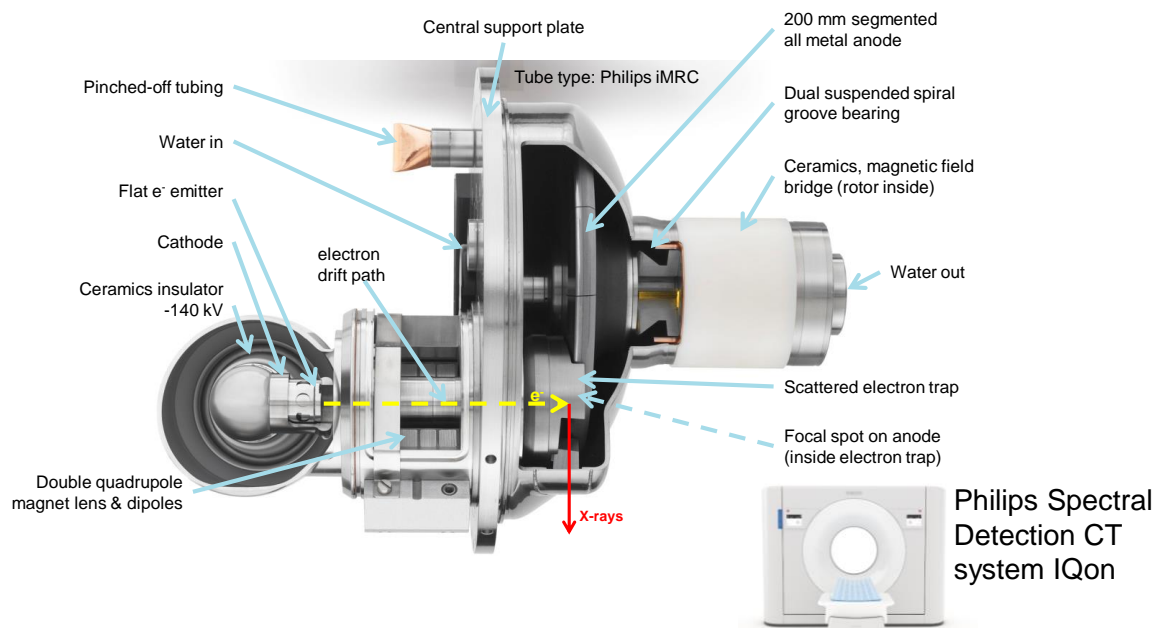


Fig. 4: Latest premium tube technology. Cut view of the Philips iMRC® tube in CT systems iCT® and IQon®, see text. (Picture courtesy of Philips.)

### XIX. IMPROVEMENTS

Roentgen's discovery started fierce race for technical improvement. Figure 3 points to major milestones. As a consequence of the great simplification of the way to operate X-ray systems, a division between medical physicists and radiologists occurred with Lilienfeld's and Coolidge's introduction of thermionic electron sources instead of a pure gas discharge. They both aimed at softening X-ray tubes. Lilienfeld attached an incandescent light bulb to the ion tube to boost electron production at low tube voltage. Coolidge, then working at GE, a little later inferred a ductile tungsten wire as the electron source and abandoned residual gas. From now on, contrast (spectrum, beam hardness) and brightness (tube current) of the X-ray image could be adjusted independently. Simplification of use allowed for a split of radiographers into medical physicists and radiologists. A significant improvement was the introduction of a rectangular Götze line focus by the manufacturer C.H.F. Müller, later Philips, which helped improving the brightness of the FS. This invention made use of the isotropic angular intensity distribution of bremsstrahlung which extends down to low take-off angles. The next quantum leap was accomplished by Bouwers of the Philips research laboratories, who industrialized a rotating anode with finned structure. Götze focus and rotating anodes helped cutting exposure times by more than two

orders of magnitude. Siemens improved these anodes by speeding them up and backing the metal disk with graphite. Again, Philips resumed the lead and implemented all metal ceramics technology in medical tubes, which has become state-of-the-art for the entire industry. Wait times could be reduced and eventually completely eliminated by introducing hydrodynamic bearings and unprecedented large anodes in computed tomography and interventional X-ray systems. Varian bettered the heat balance by improving the capturing of back-scattered electrons, dissipating their waste energy and reducing off-focal radiation. A quest for compactness and operation at high centrifugal forces stimulated Siemens to realize an idea from General Electric and Metropolitan Vickers of the late 1940ies: The rotating anode was made an integral part of the now rotating tube frame with immediate contact to the surrounding oil. The rotating frame tube Straton® was born in 2003 which allows for focal spot deflection in azimuthal and axial direction, see [3] and [1], chapter 1.3.9. Some limitations of FS power density and FS stability at high tube current became apparent, however.

With their iMRC platform Philips introduced the latest major technological leap. The company launched in 2007 the iMRC® tube, which is shown as a cut model in Figure 4. The iMRC® tube family is a premium tier CT tube platform which allows for high speed rotation of a segmented anode at high centrifugal acceleration in a fast revolving CT gantry. Unprecedented FS power density

for very high spatial image resolution is accompanied by high and exactly shaped photon flux for low image noise. This is of particular importance for detection based spectral CT imaging. The electron beam of the iMRC® tube originates from a directly heated meandered surface of a comparatively large planar thermionic tungsten emitter. This technology combines mechanical and chemo-physical robustness and totally eliminates for the first time space charge limitations of the tube current in rotating anode tubes. Double quadrupole magnetic focusing and deflection and a highly efficient electron trap eliminate FS blooming, and artifacts from aliasing and off-focal radiation, see below. Siemens adapted their latest tube development to this set of technologies with their Vectron® tube and launched it in 2013. More details are in [1], chapter 1.3.12.

## XX. LATENT PITFALLS

Despite of great progress, X-ray tube technology still suffers from a number of technical pitfalls, which should be known to assess and avoid image artifacts, optimize system design and enable efficient fault finding in practice. Attention should be paid to tube life time which may depend on gantry speed in CT, gyroscopic forces in interventional systems, and power requested. Other aspects comprise degradation of the dose output over time, preparation time, electrical stability and means in the generator to cope with vacuum discharges. Image quality and spatial definition depend on focal spot size and stability under rotation, thermal capacity, off-focal and leakage radiation, and scattered radiation from the tube port. The work flow depends on cooling time, short and long term.

## XXI. THERMAL ISSUES AND NEW METRIC

The inefficiency of X-ray generation has produced the most severe bottleneck for the clinical routine: target cooling, see figure 5. Stationary anodes were the only available technology for more than three decades, which resulted in long exposure times and motion blur. The focal spot of Bouwers' rotating anode is cooled by convection cooling, instead. Heated material is removed by rotation. Cooling of the bulk material is challenging, however. Ball bearings, which were initially employed and which have become industry standard until now for conventional tubes, substantially block heat conduction. The alternative thermal radiation is efficient at high temperatures, but ceases with fading visible glow of the body. Thus, heat had to be stored in the target before heat radiation could slowly dissipate it in preparation of the next patient. In view of this technology, anode heat storage capacity has become the primary figure of merit for tube selection from the 1930ies. More *heat units* (HU)

suggested better performance. The terms *heat unit* or *mega heat unit* (MHU) have never been exactly standardized, and originally refer to rotating anode X-ray tubes supplied by dual-phase high voltage generators, an electronics technology of the 1920ies.

The IEC began specifying the storable heat content in SI units instead, defined single level heat integration algorithms in the form of heating and cooling charts and the method of validation of the heat storage capacity of an anode. Eventually, by the launch of novel tube and generator technology *maximum anode heat content* turned from a historic key performance indicator into a confusing term. As a consequence of the advent of electron traps in metal ceramics tubes (Philips SRC, molybdenum aperture, 1980), heat conducting liquid metal hydro-dynamic bearings (Philips MRC, 1989), and definitely by the launch of rotating frame technology (Siemens Straton®, 2003, see [3]), the IEC amended the standard IEC 60613 in 2010. Without even mentioning anode heat content anymore, tube performance, e.g. for CT, is now simply rated by the *Nominal CT power*, defined as the power which a tube can sustain during a demanding realistic sequence of scans: 4 seconds exposure within an endlessly repeated cycle of 600 s duration each. Other than before, compliance with this metric can most simply be validated by the user. It is time to finally abandon HU's and MHU's for tube comparison.

## XXII. CURRENT ISSUES

There are other pitfalls related to the production of electrons and their fate after impact on the target. Figure 6 shows an exemplary electron emission curve for an interventional angiography tube with tungsten coil electron emitter. The characteristics is best described by both, space charge limited emission according the Child-Langmuir  $V_t^{3/2}/d^2$  - law for high currents,  $V_t$  being the tube voltage and  $d$  the cathode-to-anode distance, and the Richardson equation with its exponential temperature dependency, which is appropriate for low currents.

The left part of the chart, where the tube current is small and the emitter temperature low, is dominated by thermionic emission without major space charge effects. The emission current density  $j_c$  and the tube current  $I_{\text{tube}}$  both rise steeply with temperature according to Richardson's law  $j_c \propto T^2 e^{-W_w/(k_B/T)}$ , where  $T$  is the temperature of the tungsten emitter with its work function  $W_w$  and  $k_B$  is Boltzmann's constant. For the sample tube shown the temperature  $T$  is rising about linearly with the indicated heating current  $I_{\text{fil}}$ . The majority of emitted electrons successfully escape from the cathode and are collected by the anode. Tube voltage does not matter in this saturation emission approximation (left). Ideally, the tube current should be unlimited in the entire specified range of tube voltages and tube power. Generally, this is indeed so for stationary anode tubes. But, the permitted



Fig. 5 Thermal picture of a rotating anode in operation. The rectangular focal spot, 10 mm in length and about 1 mm wide, points radially and is located at the right on the anode, trailed by a comet tail of the hot surface of the focal spot track. The X-ray focal spot is located about half a focal spot width further to the right. Some reflected light is visible from the heated electron emitter coil in the cathode at the left. The anode rotated counter clock wise with about 50 Hz. (Adapted from [1].)

current and power density in the focal spot of a rotating anode is by one to two orders of magnitude higher. Negative electronic space charge between cathode and anode limits tube performance at low tube voltages and high tube currents. Indicated by the blue squares in Figure 6 at the maximum permitted temperature, coiled electron emitters present an approximately linear decrease of the

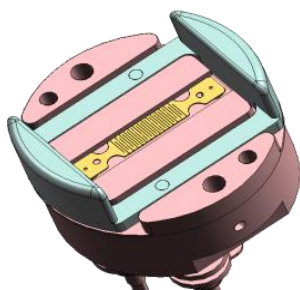


Fig. 7 CAD model of the cathode of the Philips iMRC® tube for CT (systems iCT® and IQon®). The use of a meandered flat electron emitter (yellow) enables generation of unprecedented high tube currents even at low tube voltages. The emitter is robust enough to withstand adverse conditions of residual gas pressure, ion bombardment and vacuum discharges. Space charge limitations are practically absent.

maximal tube current  $I_{\text{tube}}$  with the tube voltage in practice. Only for voltages above the so-called isowatt point, where cathode and anode performance meet, the anode is the limiting component, indicated by red circles.

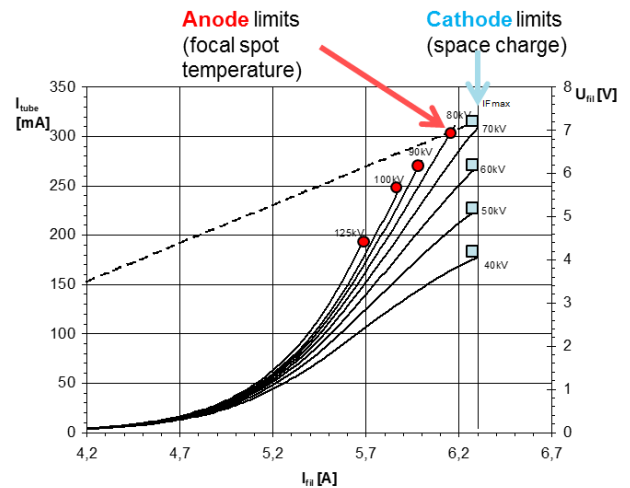


Fig. 6 Sample emission curves for the small focal spot of the rotating anode tube Philips MRC 0407 with tungsten coil emitters.  $I_{\text{tube}}$  (left axis) represents the tube current, which depends on tube voltage (parameter indicated) and heating current  $I_{\text{fil}}$  (abscissa). Red circles indicate anode limits, blue squares cathode limits. Dotted curve:  $U_{\text{fil}}$  (right axis) is the voltage to drive the filament heating current  $I_{\text{fil}}$ . (Graphics adapted from [1].)

The approximately linear relationship between maximal permitted tube current tube voltage at low electric field strengths results from a mixed type of emission, the contribution of thermionic and space charge limited electron emission from the different surfaces of the emitter. As said, the Child-Langmuir law would suggest proportionality between  $I_t$  and  $V_t^{3/2}$  for pure space

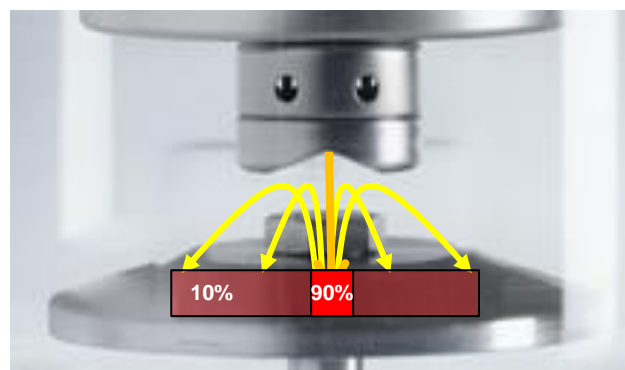


Fig. 8 Backscattered electrons (yellow) causing off-focal radiation in a bipolar glass tube. These electrons are reflected by the cathode (in this design facing the anode), hit the anode outside the border of the primary focal spot (red). Cathode: top, rotating anode: bottom. Percentage figures roughly quantify the intensity of X-rays. (Adapted from [1].)

charge limited emission at low tube voltages and high filament temperatures. But, for the exemplary cathode referenced in Figure 6 this behavior is somewhat obscured. Regions on the emitter which are subject to large enough electric fields, which suppress the space

charge effects, add current and partly counter-balance the current deficit. The advent of flat emitters greatly improved the situation, see Figure 7. With reference to figure 6, the absence of space charge limitations would mean that all emission curves would coincide with the 125 kV-curve and extend beyond it to the right, no matter how small the tube voltage would be within the interesting range.

XXIII. IMPAIRED IMAGE QUALITY AND REMEDY

Another pitfall is caused by the intense interaction of electrons with the target material tungsten. The origin of X-rays in conventional glass tubes, as shown in Figure 2, is typically an extended area, about a few micrometers below the surface surrounding the center of the intersection of the beam of primary electrons with the anode surface. Scattering of electrons at the nuclei of the target creates photons, but also severely alters the direction of the electrons. Given the high electric potential inside the tungsten nuclei, which peaks at more than 20 megavolts, a few scattering events will suffice to cause rapid angular diffusion of the primary electrons in the vicinity of the surface. Thus, about half of the impinging particles are backscattered and lost into vacuum. On average, they carry nearly 40% of the primary power. In typical standard tube designs, where the cathode is located directly facing the anode, like the one shown in Figure 2, backscattered electrons will be mirrored back and experience a second impact. Soft off-focal radiation is generated outside the desired focal spot and may impair the definition of the image. It may cause shadows around highly contrasting objects, like iodinated vessels in angiography application.



Fig. 9 Suppression of so-called windmill artifacts at sharply contrasting edges using axial deflection of the focal spot (FS) position between projections in CT. (Adapted from [1].)

Off-focal radiation may even mimic a bleeding and confound the differentiation between hemorrhagic and ischemic stroke. Therefore, electron traps in high performance tubes, as shown in figure 4, are built in to gather the majority of these backscattered electrons. For those tubes, like the one shown in Figure 4, X-ray scattering in the tube window remains as the only cause of off-focal radiation.

XXIV. SUPPRESSION OF ARTIFACTS

Modern features of X-ray sources augment artifact suppression in computed tomography. Figure 9 demonstrates the efficient remediation of aliasing artifacts by axial and azimuthal deflection of the FS between projections in CT. The electron beam of the suitable X-ray tube, as shown in figure 4, is magnetically deflected in radial direction by about half a focal spot length, which translates to an apparent axial displacement of the projected focal spot. The additional information can be used by the reconstruction algorithm to suppress so-called windmill artifacts at sharp edges in axial direction, as shown in figure 9.

XXV. CONSUMABLE X-RAY TUBE

The most costly issue with medical X-ray tubes remains short tube life. There is little public data available. Erdi, see [4] and Table 1, reports an average of 19.2 and 22.4 months in 50 replacements of high-performance CT tubes at 13 GE scanners in the Sloan Kettering Center NY, USA. But, tube life differs significantly between vendors. Differences of settings in imaging systems, local adaptations and preferences, frequency and ways of usage further broaden the life time distribution. Outliers are often caused by defects in the rotor drive, long periods of operation in preparation mode, extraordinary high tube voltages or unusual low tube voltages and high emission currents used. Other than e.g. for incandescent light bulbs, the temporal failure distribution for X-ray tubes is typically very broad, as can be seen from the columns Spread and Min.-max. in Table 1. This underscores the need of commercial insurance policies, ideally by signing tube-included service contracts with the supplier. There are many ways for the user to save costs and extend reliability. Typical causes of failure and Pareto distributions are treated in [1], chapter 9.5.

Table 1 Average Tube life of GE CT tubes (adapted from [4], see text).

| Tube type            | Av. Life (months) | Spread (months) | Min.-max. (months) |
|----------------------|-------------------|-----------------|--------------------|
| GE Performix Ultra ® | 19.2              | ±12.5           | 7-48               |
| GE Performix Pro ®   | 22.4              | ±9.6            | 12-32              |

The multitude of typical failure modes, e.g. for typical CT tubes, includes arcing, vacuum leakage and subsequent vacuum discharges, see figure 10, run-away arcing by thermal overheat of the target, electron field emission from irregularities on electrodes and loose particles, low X-output, hardening of the X-ray beam, pollution of the X-ray window, notably by carbonization of cooling oil, rotor vibration, bearing noise, frozen rotors, evaporated electron emitters and short circuits, implosion of glass tubes, damaged or polluted heat exchangers and pumps, broken anodes, burnt-out stator coils, damaged mechanics, and more.



Fig. 10 Foot point craters on a used cathode head after severe vacuum discharge activity (arcing), adapted from [1].

## XXVI. CONCLUSION

A number of pitfalls and limitations of current technology of generation of medical diagnostic X-rays

still exist and demand attention by system developers, medical physicists and clinicians.

Instead of adhering to outdated terminology, selection and investment of medical diagnostic X-ray sources should be supported by applying the latest metric and standards which reflect most recent technology.

Tube life remains an issue. Commercial risks should be managed by selecting experienced suppliers which offer well matching premium quality tubes and generators. The commercial burden of tube failure may be imposed on the vendor by signing tube-included service contracts.

## REFERENCES

1. Behling, R., 2016. *Modern Diagnostic X-Ray Sources: Technology, Manufacturing, Reliability*. CRC Press, Taylor & Francis, Boca Raton, USA. ISBN 978-1-4822-4132-7.
2. Zehnder, L. 1935. *W. C. Röntgen – Briefe an L. Zehnder*. (W. C. Roentgen – letters to L. Zehnder). Switzerland: Rascher & Cie, AG Verlag.
3. Schardt, P. et al. 2004. New X-ray tube performance in computed tomography by introducing the rotating envelope tube technology. *Med. Phys.* 31(9): 2699–706.
4. Erdi, Y., E. 2013. Computed tomography X-ray tube life analysis: A multiyear study. *Radiologic Technology* 84: 567.

Contacts of the corresponding author:

Author: Rolf Behling  
 Company: Philips Medical Systems DMC GmbH  
 Street: Roentgenstrasse 24  
 City: 22335 Hamburg  
 Country: Germany  
 Email: Rolf.Behling@Philips.com

# HOW-TO

## OPTIMISATION OF PLANAR CHEST PA EXPOSURES USING THE CDRAD CONTRAST DETAIL PHANTOM

K. Thomson<sup>1</sup>, J. Lynch<sup>2</sup>

<sup>1</sup> Medical Physics, Musgrove Park Hospital, Taunton and Somerset NHS Foundation Trust, Taunton, UK

<sup>2</sup> Radiation Physics and Protection, Oxford University Hospitals NHS Foundation Trust, Oxford, UK

*Abstract*— Optimization is a vital process for minimizing the risk of detriment from diagnostic radiation use, while ensuring adequate image quality for diagnosis. It is a legal requirement in most countries worldwide, and there are a number of strategies available. One such technique is the use of quantitative and anthropomorphic phantoms to adjust exposure factors, in combination with dosimetric techniques, to achieve acceptable image quality at a minimum dose. A case study is described, which uses the CDRAD contrast detail phantom and a thorax phantom to optimize exposure factors for chest posterior-anterior (PA) exposures.

*Keywords*— Optimization, image quality, CDRAD, contrast detail phantom

### I. INTRODUCTION

Section I discusses the legislative requirements for optimization and strategies for undertaking it. A case study is then presented describing the use of several of these strategies to optimize chest PA exposures, based on image quality and patient dose.

Section II describes the materials and methods used in this case study, with section III, IV and V containing results, discussion and conclusions, respectively.

#### A. Legislation and Motivation

The principle of optimization is enshrined in legislation worldwide, and is defined as the process of ensuring that all radiodiagnostic doses are as low as reasonably achievable, consistent with obtaining adequate information to allow a diagnosis [1].

Optimization is one of the three general principles of radiation protection, along with justification and dose limitation, and is given as Principle 5 in the International Atomic Energy Agency's latest edition of "Radiation Protection and Safety of Radiation Sources: International

Basic Safety Standards (BSS), published in July 2014 [2].

Under Requirement 38 of the BSS, the exposure to the patient from a diagnostic procedure must be "the minimum necessary to fulfil the clinical purpose of the radiological procedure, with account taken of relevant norms of acceptable image quality ... and of relevant diagnostic reference levels."

According to the BSS, special attention should be paid to optimizing certain types of exposure, including doses to pregnant women or pediatric patients, volunteers, screening programs and exposures giving relatively high doses. Exposures that fall into this last category might include computed tomography (CT), extended image-guided interventional procedures or high activity nuclear medicine administrations.

The dose to a patient from a planar radiographic exposure is comparatively low when set against these "high dose procedures". A 2010 review of the UK population's radiation doses from medical exposures found that conventional radiography accounted for only 19% of the total population dose in man Sv, compared with 68% due to CT scans [3]. The conventional proportion had reduced from 44% in 2007/8, due the increase in CT examinations, a trend mirrored worldwide. However, the number of conventional radiographs performed, 90% of the total in 2008 [4], means that rigorous optimization is still required.

#### B. Strategies for Optimization

A number of different strategies can be used as part of the optimization process. This paper focuses on planar diagnostic radiographs. The same principles apply to modalities such as CT, fluoroscopy, mammography and diagnostic nuclear medicine, but the technical and clinical methods will vary.

It is important to remember that the object of optimization is not just to reduce the dose; the image quality must be of sufficient diagnostic quality to answer the clinical question, or the exposure may have to be repeated.

### 1. Technological tools

In general, the condition of the equipment used for x-ray imaging has a large impact on the doses to patients and the resultant image quality, and all x-ray equipment should be part of a rigorous quality control system, from acceptance testing and commissioning to routine testing.

One key technological aid to optimization is the automatic exposure control (AEC) device. A table or chest bucky may contain such a device, usually located behind a grid, which terminates the beam when a fixed exposure parameter is met (such as air kerma or detector dose indicator) [5]. This achieves consistency across exposures, ensures the detector receives sufficient dose to form an adequate image, and stops additional exposure above that level. Ensuring that the dose at which the AECs cut off the beam is at the correct level is a vital optimization strategy, and may be done by the manufacturer's engineer, in cooperation with medical physicists or x-ray technicians. The receptor dose may be recommended by the manufacturer, and is lower for more efficient detectors.

Also important is regular testing of AECs, for reproducibility, consistency between different AEC chambers, and repeatability for multiple exposures.

Advancements in x-ray imaging technology should aid optimization by reducing doses for a fixed level of image quality, or, conversely, improving diagnostic information for a particular dose. Improvements may be in the form of superior image processing or imaging plate design, such as increased detective quantum efficiency (DQE) or spatial resolution. It is important to have good communication between the equipment manufacturer, installer and local users, so that the best use of the equipment can be made, for example in using and setting up optimized protocols at commissioning.

### 2. Positioning and Orientation

Patient dose can be altered by choosing a particular projection and positioning the patient accordingly. For example, a recent study compared the effective doses to patients from lumbar spine exposures in eight different projections and found variations of up to 60% [6]. This is due to the varying radiation dose to organs of different radiosensitivities; there may be no difference in the dose-area product (DAP) recorded. The position of overlying organs will also need to be considered.

### 3. Diagnostic Reference Levels

Diagnostic reference levels (DRLs) are a means of monitoring typical imaging doses and indicating the need for a review or investigation. Established DRLs are published, for example by governments or national bodies, based on large data surveys and can be used as a comparison with local doses for a particular procedure.

DRLs may be set locally, but should not normally exceed national levels. Typical calculation methods involve finding the median of a distribution of DAPs for a room and procedure and for patients of mean mass within a certain range, while national DRLs may be the third quartile of mean doses from local centers [5]. Periodically, local doses should be assessed and compared against published DRLs, both for exceeding it and falling significantly below, the latter of which may indicate poor image quality. The distribution of doses, often in the form of DAPs, provides a useful indication of variation. For an individual patient, there may be a valid reason for exceeding a DRL; for example, a patient may have a substantially larger than average body mass. However, the process of assessing local doses against local and national DRLs should indicate the need for an investigation and initiate a cycle of the optimization process.

### 4. Exposure Factors

The choice of radiation quality, determined by kVp and filtration, for a particular exposure will depend on the anatomy, detector type, acceptable noise and receptor dose needed. Different detectors will have particular energy dependences and peak sensitivities. In general, detector sensitivity increases at lower kVp and image contrast improves, but patient dose increases as more x-ray photons are absorbed in the body [5]. Filtration, in the form of sheets of metal such as aluminium or copper, are used to remove photons of such low energy that they will contribute to patient dose without adding to the image. Recommended exposure factors are published, for example by the European Commission [7]; these provide good references but may not be maximally optimized for particular exposures on local equipment.

Increases in tube current and time (mAs) will increase the patient dose. When AECs are in use, the mAs is not selected, and the AECs provide assurance that the detector receives an adequate but not unnecessarily large dose. However, the choice of beam quality still affects the patient dose when AECs are in use.

The choice of anti-scatter grid, and whether to use one, also influences patient dose and image quality. Grids may be parallel or focused (the latter requiring a fixed distance from the beam focal spot), and eliminate scattered photons, which degrade the image. The grid ratio, which is the height of radiopaque strips divided by the thickness of the inter-strip spaces, controls how much scattered radiation is transmitted. However, the primary beam is also attenuated, so patient dose increases for a given

receptor dose. This may be justified if the level of scatter without a grid is unlikely to give adequate image quality for diagnosis.

### 5. Phantom Measurements

Phantoms can be exposed using the settings for a particular clinical examination, allowing the operator to adjust exposure factors, successively altering the dose and assessing the resulting image quality.

This can be done quantitatively, using a phantom with contrast and resolution details of known dimensions, and qualitatively, using a phantom as close as possible to the clinical reality so that the image quality achieved by the optimization process is mirrored in real patient images subsequently produced using the final choice of parameters.

#### C. Case Study: Chest PA exposures, radiographic room

The case study described here uses a combination of several of the techniques described above to optimize chest posterior-anterior (PA) exposures at a large radiology department, the Churchill Hospital, part of the Oxford University Hospitals NHS Foundation Trust (OUH). It focuses on methods that can be employed by a local medical physics team, rather than improvements to imaging equipment design or changes to clinical positioning.

Chest radiographs may be requested for a range of clinical questions, and must have adequate image quality for small lung field details, possibly obscured by mediastinum and ribs. The current UK national DRL for chest PA examinations is 10 cGycm<sup>2</sup> [8]. However, the OUH local DRLs were 8 cGycm<sup>2</sup> for computed radiography (CR) systems and 7 cGycm<sup>2</sup> for direct radiography (DR) systems, reflecting local equipment and DR's superior DQE.

## II. MATERIALS AND METHODS

The first step in this optimization process was analysis of the patient doses for a range of clinical examinations and x-ray rooms across the hospital Trust. Data was taken in the form of DAPs from the RIS system, and inevitably contained some spurious data due to incorrect recording or unit errors, some of which were revealed on investigation of outliers. The distribution for chest PA for the room featured in this case study is given in Figure 1 below:

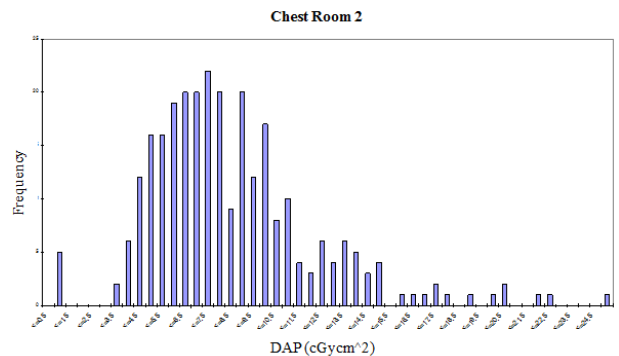


Fig.1 Distribution of doses for chest radiography room

Distributions for different rooms were then compared, highlighting areas where there was particularly high variation or a large number of outliers. The room means were then compared with each other and with national and local DRLs, as shown in Figure 2.

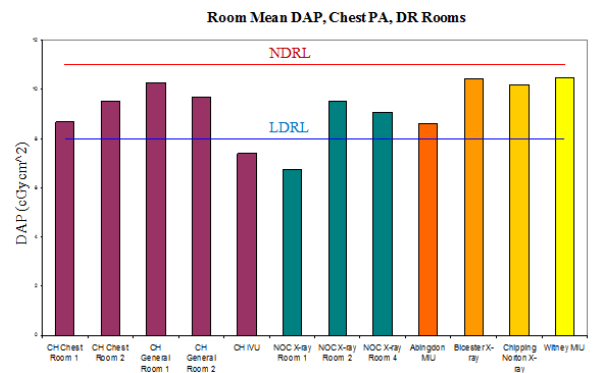


Fig.2 Doses for different radiography rooms

Although none of the room means here exceed the national DRL, many were exceeding the local DRL based on previous data across several hospitals. The variation also prompted an investigation and an effort to optimize doses. In some cases the variation could be explained, for example where certain rooms are used for imaging inpatients. The exposure factors for different rooms were compared, including whether there were protocols built in for each examination type or selected with reference to a chart, and whether AECs were used and at what exposure termination level.

Thought was also given as to whether images from these systems were always of acceptable diagnostic quality. This can be addressed by discussion with radiologists and radiographers, and analysis of rejected images.

In this optimization process, one room was chosen for initial further optimization work, on the basis that its doses were on the higher end of the distribution, and because the equipment was typical of that used across the Trust for chest PA exposures. The room in question had a GE Definium 8000 DR x-ray system, and was used with

clinical exposure parameters of 120 kV and no additional filtration, with left and right AECs, an anti-scatter grid and a focus to detector distance of 180 cm. The AEC performance had been previously optimized according to local protocol. However, its inherently poorer energy response at high kV settings (greater than 100 kV) could not be mitigated against, resulting in higher terminating exposures at these beam energies.

Having ascertained the normal clinical parameters and that these were used for all chest PA exposures except in extraordinary circumstances, the next step was to decide what factors to vary to test the effect on dose and image quality. In general, it is better to not vary too many parameters at once, or to move too far away from the current clinical practice. At this stage, it is also important to be aware of recommendations given by the manufacturer, professional bodies and national guidelines, as well as to find out if the results of similar optimization work is available.

The parameter chosen for testing was beam quality in the form of kVp and filtration. In addition to the current clinical exposure parameters (120 kVp, no filtration), we considered 90, 100 and 110 kVp, and 0.1 and 0.2 mm copper (Cu). This gave twelve combinations in total.

A. CDRAD Contrast Detail Phantom

Image quality was assessed quantitatively using a CDRAD contrast detail phantom, which has dimensions of 26.4 by 26.4 cm, with thickness 0.76 cm, and incorporates a 15 by 15 grid of squares, each containing two cylindrical holes. These vary in depth and diameter from 0.3 to 8 mm, in 15 exponential steps, and test a system’s detection of objects as they become smaller and of lower contrast [9].

The phantom was positioned between 5 cm thicknesses of Perspex as a scattering medium. The field size was set to cover the whole phantom, and five exposures were taken for each set of parameters.

“Unprocessed” images were used for this analysis and the images were automatically scored using the Artinis CD Analyser program [10], which gives an inverse image quality figure, IQFinv, for each set of images:

$$IQFinv = 100 / \Sigma(C.D) \tag{1}$$

Where C and D are the threshold detection contrasts and diameters, respectively, for each set of images of the CDRAD phantom. Increased detectability, i.e. the ability to detect smaller and less contrasted objects, gives a higher IQFinv.

B. Chest Phantom Images

Having chosen sets of parameters which gave an improvement in image quality as measured using a

CDRAD phantom, it was important to assess the effect on image quality for more realistic clinical images. An anatomical chest phantom was positioned by a radiographer as if for a chest PA exposure, and images acquired at the settings tested above, to be reviewed by a radiologist to confirm that a change in parameters would still give adequate image quality.

C. Effective Doses

Effective doses for each combination of kVp and filtration were calculated using Monte Carlo simulation and the PCXMC v. 2.0 software package. Organ and effective doses were calculated using ICRP 103 weighting factors, the same field size set as for clinical chest PA examinations, and knowledge of the inherent half-value layer and filtration of the x-ray unit, with each combination of varying kVp and additional filtration.

III. RESULTS

A. IQFinv and Effective Doses

A sample contrast detail score diagram (for 110 kV and 0.1 mm Cu) is given in Figure 3, with the contrast detail curve for all twelve combinations in Figure 4.

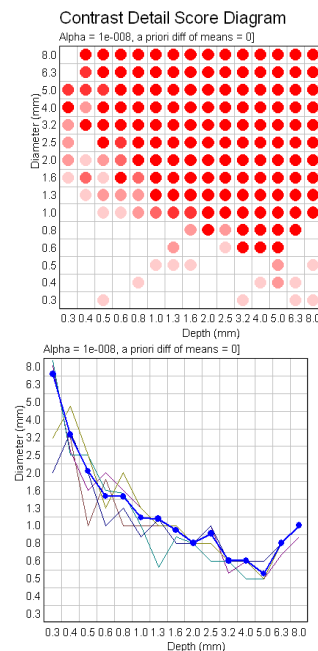


Fig.3 Contrast Detail Score Diagram and Curve for 110 kV and 0.1 mm Cu (five exposures)

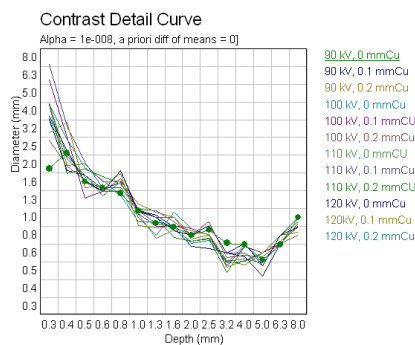


Fig.4 Contrast Detail Score Curve for all twelve combinations

Inverse image quality figures and effective doses for each of the combinations of kVp and filtration are given in Table 1 below, and in graphical format in Figure 5.

Table 1 Effective doses and IQFinv

| Exposure Parameters | Effective Dose ( $\mu\text{Sv}$ ) | IQFinv |
|---------------------|-----------------------------------|--------|
| 90 kV, 0 mm Cu      | 9.3                               | 3.13   |
| 90 kV, 0.1 mm Cu    | 8.1                               | 3.09   |
| 90 kV, 0.2 mm Cu    | 7.6                               | 3.20   |
| 100 kV, 0 mm Cu     | 9.4                               | 3.22   |
| 100 kV, 0.1 mm Cu   | 8.0                               | 3.07   |
| 100 kV, 0.2 mm Cu   | 7.5                               | 3.28   |
| 110 kV, 0 mm Cu     | 9.7                               | 3.29   |
| 110 kV, 0.1 mm Cu   | 8.5                               | 2.89   |
| 110 kV, 0.2 mm Cu   | 7.8                               | 3.11   |
| 120 kV, 0 mm Cu     | 10.1                              | 3.34   |
| 120 kV, 0.1 mm Cu   | 8.8                               | 3.16   |
| 120 kV, 0.2 mm Cu   | 8.2                               | 3.20   |

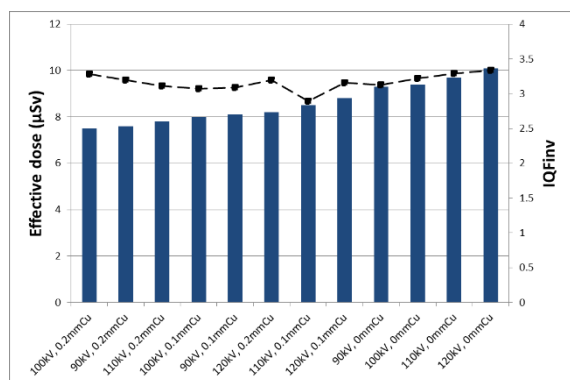


Fig.5 Effective doses and IQFinv

There is not a great change in detectability, as indicated by the IQFinv values and the contrast detail curve, between the twelve combinations (13% between the least and most detectable). However, the increase in effective dose from the lowest (100 kV, 0.2 mm Cu, 7.5  $\mu\text{Sv}$ ) to the highest (120 kV, 0 mm Cu, 10.1  $\mu\text{Sv}$ ) is 26%. There can be some confidence, therefore, that choosing one of these other combinations will reduce effective dose without significant loss in image quality.

B. Phantom images

The highest effective dose comes from the current clinical parameters, 120 kV and 0 mm Cu. Changing to the lowest dose parameters, 100 kV and 0.2 mm Cu, reduces the effective dose by 26% for a change in IQFinv of 1.8%.

The phantom images for these two combinations of kV and filtration are shown in Figure 6.

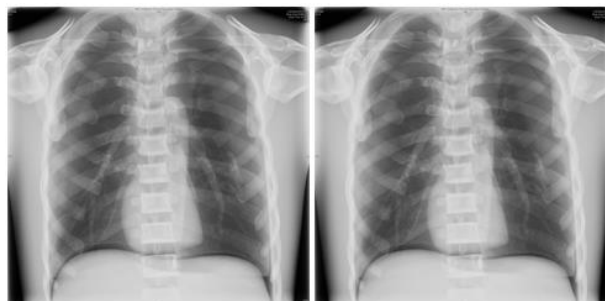


Fig.6 Left: 120 kV, 0 mm Cu (10.1  $\mu\text{Sv}$ , IQFinv 3.34; Right: 100 kV, 0.2 mm Cu (7.5  $\mu\text{Sv}$ , IQFinv 3.28)

The two images were judged to be of equivalent diagnostic image quality. We therefore chose to implement these new settings for future chest PA exposures using this equipment.

IV. DISCUSSION

A. Implementation and extension

The reduction in effective dose expected from changing the beam quality is a reduction in average risk to a population. However, it is reasonable to assume a reduced risk to an individual patient, consistent with the principle of keeping doses as low as reasonably practicable while achieving images of diagnostic quality.

It is important to work in cooperation with all users of the equipment when making changes, especially radiographers and radiologists. Radiographers and other operators must be clear about any changes to equipment settings or clinical procedures, and radiologists must approve the expected image quality post-changes, and

feed back any problems as soon as possible after a change.

For these reasons it is sensible not to make too many changes at once, and to only make small adjustments, so that there are no undiagnostic or repeated images.

The effect on the room dose mean and distribution should be monitored and compared with local and national DRLs.

Ideally, each type of exposure should be optimized for every piece of x-ray equipment. However, it may be better to have the same parameters for a set of similar equipment or in the same department. This will depend on the variation in optimum parameters between equipment, and whether each unit has built in exposure factors or if they are selected from an exposure chart.

Having a clear system for inputting doses and exposure factors into RIS after exposures allows greater confidence when examining room dose distributions and comparing with DRLs. The implementation of dose management systems which record these automatically may improve this process.

The variation in dose and image quality for different clinical examinations and equipment may influence the decision on subsequent choices of equipment.

#### B. Limitations of this method

This method is time-consuming to complete for all examinations and x-ray units. The greatest benefit may be achieved by investigating units with the highest and most variable doses or which record many repeated exposures.

CDRAD images and IQFinv values are not direct measures of image quality. It may be difficult to find phantoms which adequately reflect the range of clinical questions requiring diagnosis. Similarly, it is difficult to optimize for a range of patient sizes. In particular, larger patients may have poor image quality due to increased scattered radiation, and are usually excluded from data used to produce DRLs. If they form the majority of patients in a particular center, a local DRL may be formulated specially. If they form a minority or are outliers for a number of units, it may be appropriate to form adjusted reference levels and exposure parameters for these patients.

## V. CONCLUSIONS

A number of strategies are available to optimize diagnostic radiographs for individual x-ray units and across hospitals. The case study presented here used qualitative and quantitative assessment of image quality using exposures of phantoms, and calculations of effective dose, to choose exposure parameters for future chest PA examinations. This is part of an iterative process

of optimization across many x-ray units and clinical examinations, with the aim of reducing the risk of detriment from radiation and achieving adequate diagnostic image quality.

## ACKNOWLEDGMENT

I would like to thank the radiography and medical physics staff at Oxford University Hospitals NHS Foundation Trust.

## BIBLIOGRAPHY

- [1] *Ionising Radiation (Medical Exposure) Regulations 2000, SI 2000/1059 reg 7*, London: HMSO, 2000.
- [2] International Atomic Energy Agency, *Radiation Protection and Safety of Radiation Sources: International Basic Safety Standards*, Vienna, 2014.
- [3] W. Oatway, A. Jones, et al., "Ionising Radiation Exposure of the UK Population: 2010 Review," Public Health England, Chilton, 2016.
- [4] D. Hart and B. Wall, et al., "Frequency and Collective Dose for Medical and Dental X-ray Examinations in the UK, 2008," Health Protection Agency, Chilton, 2010.
- [5] C. J. Martin, "Optimisation in general radiography," *Biomedical Imaging and Intervention Journal*, vol. 3(2), 2007.
- [6] A. Chaparian, A. Kanani and M. Baghbanian, "Reduction of radiation risks in patients undergoing some X-ray examinations by using optimal projections: A Monte Carlo program-based mathematical calculation," *Journal of Medical Physics*, vol. 39, no. 1, pp. 32-39, 2014.
- [7] European Commission, *European guidelines on quality criteria for diagnostic radiographic images*, Luxembourg: European Commission, 1996.
- [8] D. Hart, M. C. Hillier and P. C. Shrimpton, *Doses to Patients from Radiographic and Fluoroscopic X-ray Imaging Procedures in the UK - 2010 Review*, Chilton: Health Protection Agency, 2012.
- [9] Artinis Medical Systems, *CDRAD Type 2.0 Manual V. 5*.
- [10] Artinis Medical Systems, *Artinis CDRAD Analyser Manual V. 1.1*.

Contacts of the corresponding author:

Author: Katharine Thomson  
 Institute: Medical Physics, Musgrove Park Hospital  
 Street: Parkfield Drive  
 City: Taunton  
 Country: United Kingdom  
 Email: Katharine.thomson@tst.nhs.uk

## INVITED PAPERS

### EMERGING MODELS FOR GLOBAL HEALTH IN RADIATION ONCOLOGY

W. Ngwa<sup>1,2</sup>, T. Ngoma<sup>3</sup>

<sup>1</sup> Department of Radiation Oncology, Brigham and Women's Hospital, Dana Farber Cancer Institute and Harvard Medical School, Boston, USA

<sup>2</sup> Department of Physics and Applied Physics, University of Massachusetts, Lowell, USA

<sup>3</sup> Department of Clinical Oncology, Muhimbili University of Health and Allied Sciences, Dar es Salaam, Tanzania

**Abstract**— Global health is an emerging cross-disciplinary field, bringing together the best of science, medicine and humanity. It is a field which recognizes that in today's world "Global Health is Local Health and Local Health is Global Health", a field where everyone can participate, and where collaborations are crucial. Highlighting urgency for collaborations, the recent World Health Organization Cancer Report describes the growing global burden of cancer as alarming, a major obstacle to human development and well-being, with a growing annual economic cost of ca. US\$ 2 trillion. The report also highlights major global cancer disparities, with over 60% of 14 million new cases and 70% of 8.2 million deaths per year occurring in low and middle income countries (LMIC), some of which, sadly, are the least capable of dealing with cancer without some form of collaboration. With the growing scourge of cancer costing millions of lives and trillions of dollars across the world each year, people are increasingly coming together across institutions, cultures, countries and continents to work together with a greater sense of purpose, and urgency to stop this scourge and reduce the disparities. Medical Physicists are no exception; they are increasing reaching out beyond the bunker to impact the world and collaborate to close the cancer divide. Many yet are interested but do not know how or where to participate or collaborate. A recent Institute of Physics (IOP) book by Ngwa and Ngoma, recognizes this gap and the need for an educational resource that can serve as a useful reference for the emerging field of global health in radiation oncology. This article reviews the content of this book, with a particular focus on Medical Physics, and emerging models in global health, or greater effective international collaborations that will save lives, eliminate global cancer disparities.

**Keywords**— Physics, Global Health, Radiology, Oncology

#### VI. INTRODUCTION

In 2013, the International Organization for Medical Physics (IOMP) and the American Association of Physicists in Medicine (AAPM) joined other medical physicists around the world to recognize the inaugural International Day of

Medical Physics. This celebration recognizes the critical role medical physicists play in providing quality health care for millions of people around the world every day and ensuring the safety and efficacy of radiation. However, in many Low and Middle Income Countries (LMIC) round the world, no one joins the celebration, because there are still few or no Medical Physicists in these countries. This sad reality epitomizes the major global health disparities that currently exist in radiology (diagnostic and therapeutic). For example, radiotherapy, which is needed in the treatment of over 50% of cancer patients, is not available in 31 of Africa's 54 countries. 55 out of 139 LMIC, reportedly have no radiation therapy services at present. In LMIC, the range of radiotherapy needs which are currently covered vary from 0% and 3% - 4% in low income countries up to 59–79% in upper-middle income countries in Europe and Central Asia [1]. According to Zubizaretta et al., [1] the estimated number of additional medical physicist, radiation oncologists, dosimetrists and radiation therapists needed is over 43000 professionals.

In parallel to the growing cancer burden, there has been a major upsurge of global health interests in radiology, including Medical Physics, with a growing number of initiatives and activities highlighted at different Medical Physics conferences and Symposia. Appurtenant to this upsurge in global radiology interest, a common issue expressed at global health summits, seminars, or symposia is that people really want to participate in global health but do not know how. This tacitly expressed need for a book that can serve as a one stop reference for the emerging area of global health and facilitate participation as well as education and training efforts, in global radiation oncology. Cognizant of this, Ngwa and Ngoma published the e-book titled "Emerging Models for Radiation Oncology Global Health" (figure 1). This article reviews this book, which has been of great interest to Medical Physicists and others looking to reach beyond the bunker to impact the world, in ways still few and far between.

## VII. GLOBAL HEALTH IN RADIATION ONCOLOGY RISES

Chapter 1 of the book “Emerging Models for Global Health in Radiation Oncology” introduces global health and the rationale for greater active involvement by Medical Physicists in global health action. A major rationale is the level of disparities that currently exist in global radiation oncology care, education and research. The book recalls the different meetings, symposia and conferences where there have been a consistent call for greater international collaborations to close the cancer divide. These calls [2], recognize that such collaborations will benefit both LMIC and high-income countries. For example, until now, hundreds of millions of people in LMIC with tremendous potential are essentially left out of research efforts to find a cure for cancer. Empowering these potential laden people through collaborations provides opportunity to unleash greater human resources, and brainpower in the global war on cancer, and facilitate the development of new globally beneficial technologies for cancer care or cure, which will benefit people from all countries. This proffers global health as local health, or vice versa.

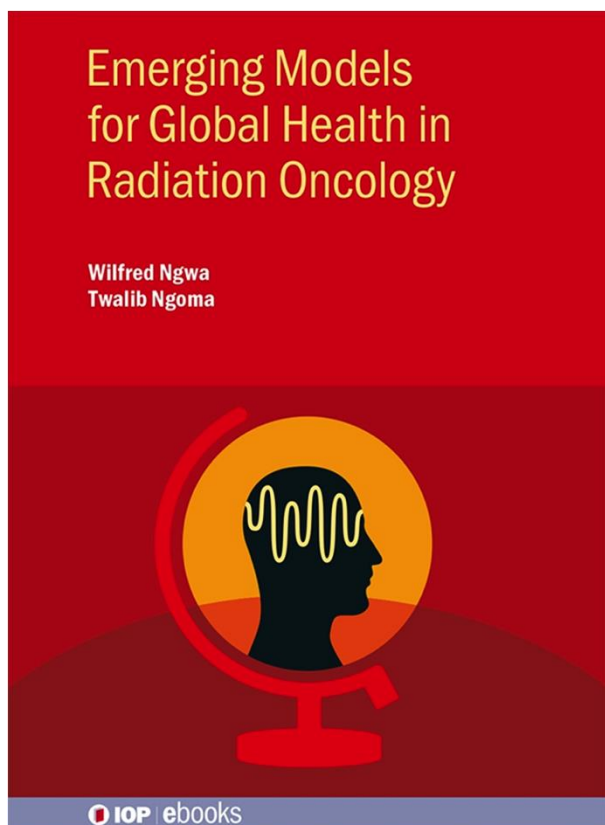


Figure 1: First book in IOP e-book series on global health

One area, where collaborations are greatly needed is in the development or deployment of lower cost technologies for cancer care, research and education. Capacity building programs to address the drastic shortage of Medical Physicists and other oncology professionals is also examined as an area of great need. Capacity building is

also in demand in high-income countries like the USA, where about 90% of residents surveyed [3] would like to have a global radiation oncology experience, which could prepare them to be the next cadre of global health leaders. As Anthony Zietman, Editor of the Red Journal puts it, [4] “Bringing radiation therapy to LMIC is an increasingly global need or responsibility...”. A recent Lancet study [5] demonstrates the substantial health and economic benefits that can be derived by investing in radiotherapy, especially in LMIC. Medical Physicists are greatly needed in this effort.

AAPM symposia, yearly summits at Harvard, and other conferences continue to show that there is great interest and enthusiasm amongst Medical Physicists for global health. It is increasingly evident that this field will see major growth in the coming years. A key focus going forward is on how to facilitate participation.

Chapter 1 closes by highlighting different models for participation and action at all levels, from the individual volunteer, through institutional to supra-national level organizations like the International Atomic Energy Agency.

## VIII. CHALLENGES AND NEW OPPORTUNITIES IN GLOBAL RADIATION ONCOLOGY

At the 2015 Global Health Catalyst cancer summit at Harvard University, global health leaders were asked about the major challenges in the emerging field of global radiation oncology.<sup>6</sup> In response, some of the main issues highlighted included: lack of political will, infrastructure, funding for research/collaborations, dearth in human capacity/resources, space-time, culture, bandwidth for use of information and communication technologies, commitment, no pellucid career advancement path in global radiation oncology, lack of access to care, adverse perceptions about radiotherapy among other things.

In chapter 2 of the book, these major challenges are examined, along with possible solutions and associated opportunities for advancing global radiation oncology. Examples of opportunities include the IAEA internship program, Radiating Hope, Seed Global Health amongst many others. More opportunities continue to emerge and are becoming a major feature of the yearly global health events.

## IX. CURRENT MODELS OF GLOBAL RADIATION ONCOLOGY

Collaborations are a central component of global health, and this is no different in global radiation oncology. At the fundamental level, global health collaborations constitute a mutually beneficial relationship between two or more entities working toward common goals, by sharing responsibility, authority, and accountability for achieving results. Chapter 3 examines the different models of collaborations, with illustrative examples. This is designed to help those entering the field to learn about what is

working, what can be adopted or scaled or further adapted/optimized for maximal impact and sustainability. Models under which most current collaborative activities in global radiation oncology fall include: twinning partnerships, consortium partnership model, and non-profit models.

The book covers the anatomy of successful collaborative partnerships from the planning phase, bonding phase, implementation and evaluation phase, dissemination and finally the scaling phase.

X. ICT-POWERED MODELS OF GLOBAL RADIATION ONCOLOGY

In today’s hyper-connected world, Information and Communication Technologies (ICTs) will increasingly play an integral role in healthcare. Here, ICTs refer to devices or systems that allow the storage, retrieval, manipulation, transmission and receipt of digital/electronic information. Examples include, smart phones, personal computers, digital television, email, social media platforms, radio, Skype, etc. Following a 2014 AAPM symposium on ICTs and Medical Physics, Ngwa and co-authors published a Red Journal article highlighting the tremendous potential of ICTs in global radiation oncology. This chapter builds on this article, showing how ICTs can make it easier for Medical Physicists and other Radiation Oncology health professionals to participate in global health more effectively or without physically travelling. From telemedicine (remote consultations, remote treatment planning support, remote quality assurance, etc) to online learning and e-research, ICTs are shown to be becoming an indispensable part of global health with potential to elide some of the spatio-temporal or financial barriers to global radiation oncology. This chapter delves into examples of ICT-powered approaches or models currently being deployed in global radiation oncology. This includes remote treatment planning platforms, platforms based on CERR for clinical oncology trials, online learning platforms, and cloud computing platforms for ICT-powered research collaborations. Successful programs in global radiation oncology powered by ICTs are also described. A sample of these is shown in table 1.

Table 1: Sample of ICT-powered global radiation oncology programs

| Model programs            | ICT-powered activities  |
|---------------------------|---|
| BOTSOGO                   | Tumor boards using ICT platforms like Adobe Connect                     |
| Chartrounds.com           | Bringing disease specialists to discuss patient cases by teleconference |
| Radiating Hope            | Remote treatment planning using screen-sharing software                 |
| IAEA PACT VUCCnet<br>AAPM | Online learning Platform<br>International Education                     |

Committee, AAPM online learning Center

The Global Cancer Project Map (GCPM): Provide resources to view and better understand international efforts in cancer research

QARC Remote review in support of cancer clinical trials

The Sprawls Education Foundation ([www.sprawls.org](http://www.sprawls.org)) has also emerged as an exemplary online learning platform with focus on utilizing technology to enhance human performance in medical physics education and training. A recent e-book on the pioneering of e-Learning in Medical Physics by Tabakov and Tabakova chronicles 7 international projects, which are among the first to develop and introduce original e-learning in the teaching process, among a growing number of online learning and ICT-powered programs.

XI. LOW COST TECHNOLOGIES FOR GLOBAL RADIATION ONCOLOGY

Given the vast disparities in disease burden between developed countries and LMICs, researchers are also working to accelerate the development of new health technologies that may help to bridge this gap. The National Cancer Institute Center for Global Health in the USA and others are increasing funding mechanisms to promote the development of lower cost technologies that can make treatments including radiotherapy more affordable in LMICs. In chapter 5, some of the lower cost technologies by radiotherapy equipment suppliers are highlighted as well as a number of promising emerging technologies that could help increase affordability and access to radiotherapy services. Example technologies include: 1) NanoX, A compact radiotherapy system intended to lower the costs of building and operating a radiotherapy center being developed by Keall et al.; 2) low-cost enabling technology for image-guided photodynamic therapy of oral cancer; 3) RO-ILS, an online portal that allows radiation oncology centers to provide non-patient-specific data about the radiation therapy near-misses and safety incidents that have occurred at their facility in a secure, non-punitive environment. Many other examples are highlighted in the book that inspire greater efforts for research by Medical physicists in this direction

XII. PRACTICAL GUIDE AND RECOMMENDATIONS FOR HIGH IMPACT RADIATION ONCOLOGY GLOBAL HEALTH

Chapter 6 includes recommendations culled from feedback by global health leaders for facilitating high impact global radiation oncology. This includes recommendations on working to secure funding, cross-cultural interaction, diaspora involvement, professional development pathways,

crowdsourcing and crowdfunding, advocacy and other important aspects.

The authors asked a number of global health leaders about what they would recommend based on their experience in collaborating or working with partners in LMIC. Some of the recommendations included:

- Equal partnership with high functioning organizations in the LMIC
- Cultural differences be respected and taken into account
- Keeping ICT implementation simple
- Significant investment in local capacity
- Encouraging at least short duration site (exchange) visits by collaboration partners
- Being flexible and ensure regular communication
- Engage with LMIC community, build local contacts, build a network, work together
- Establish trusting human relationships
- Need to focus on how to create a sustainable model with Education and training at the core.

It is evident as new initiatives emerge on global health that we continue to update recommendations and learn from the experience of those who have gone before, not to re-invent the wheel or repeat the same mistakes.

### XIII. GLOBAL RADIATION ONCOLOGY: QUO VADIS

At the start of the 21st century, when the global health community rose up to confront the challenge of HIV/AIDs, it looked like an impossible task. The remarkable global progress that has been made in confronting HIV/AIDs provides hope and confidence that similar success can be achieved in cancer control and global radiation oncology efforts. The Lancet Oncology Commission report on expanding global access to radiotherapy has set key goals or targets that could be met to help curb the growing global burden of cancer and end needless suffering and deaths in this frontier. The commission has made an explicit call for greater action to work towards meeting these targets. These targets provide measurable goals for the future of global radiation oncology. Chapter 7 looks at the role of collaborations in meeting these goals, and examines how to better leverage the upsurge in activity and interest in global radiation oncology for high impact action.

Many years ago, President John F. Kennedy stood before a joint session of the United States Congress and said, "I believe we should go to the moon." It was a call to mankind that inspired a generation in pursuit of science and innovation, where they literally pushed the boundaries of what was possible. In 2016, another USA President, Obama,

also stood before congress to announce the 'moonshot to cure cancer' initiative. The USA government followed this announcement with a two point execution plan: first for increased resources, both private and public—to support cancer work, and secondly to break down silos and catalyze collaborations and sharing of information to "end cancer as we know it". This execution plan is also relevant in advancing global radiation oncology, and physicists will be central to its success, just as they were in successfully putting man on the moon. In conclusion, the book "Emerging Models for Global Health in Radiation Oncology" provides a one-stop reference educational resource in this field. It has seeded a new IOP e-book series on global health that will indubitably be a major driver of knowledge sharing and education in this emerging field towards improved healthcare outcomes, saved lives, and the elimination of global cancer disparities.

### ACKNOWLEDGMENT

Funding support is acknowledged from the Joint Center for Radiation Therapy foundation.

### REFERENCES

- [1] Zubizarreta EH, Fidarova E, Healy B, Rosenblatt E: Need for radiotherapy in low and middle income countries - the silent crisis continues. *Clin Oncol (R Coll Radiol)* 2015, 27:107-14.
- [2] Varmus H, Kumar HS: Addressing the growing international challenge of cancer: a multinational perspective. *Science translational medicine* 2013, 5:175cm2.
- [3] Dad L, Shah MM, Mutter R, Olsen J, Dominello M, Miller SM, Fisher B, Lee N, Komaki R: Why target the globe?: 4-year report (2009-2013) of the Association of Residents in Radiation Oncology Global Health Initiative. *International journal of radiation oncology, biology, physics* 2014, 89:485-91.
- [4] Zietman A: Bringing radiation therapy to underserved nations: an increasingly global responsibility in an ever-shrinking world. *International journal of radiation oncology, biology, physics* 2014, 89:440-2.
- [5] Atun R, Jaffray DA, Barton MB, Bray F, Baumann M, Vikram B, Hanna TP, Knaul FM, Lievens Y, Lui TY, Milosevic M, O'Sullivan B, Rodin DL, Rosenblatt E, Van Dyk J, Yap ML, Zubizarreta E, Gospodarowicz M: Expanding global access to radiotherapy. *Lancet Oncol* 2015, 16:1153-86.



The Abdus Salam  
**International Centre  
 for Theoretical Physics**  
 www.ictp.it



**EFOMP**



# SCHOOL ON MEDICAL PHYSICS FOR RADIATION THERAPY: DOSIMETRY AND TREATMENT PLANNING FOR BASIC AND ADVANCED APPLICATIONS

27 March - 7 April, 2017  
 Miramare, Trieste, Italy

The Abdus Salam International Centre for Theoretical Physics (ICTP) will organize, with the support of the International Organization for Medical Physics (IOMP), the European Federation of Organisations for Medical Physics (EFOMP), the American Association of Physicists in Medicine (AAPM) and the Associazione Italiana di Fisica Medica (AIFM), a School on Medical Physics for Radiation Therapy to take place from 27 March to 7 April, 2017. The topic will be: Applied Physics of Medical Radiation Therapy - Dosimetry and Treatment Planning for Basic and Advanced Applications. The School will specially address the needs of Healthcare in low and middle income countries.

#### OBJECTIVE OF THE SCHOOL

The objective of the School is to contribute to the understanding of Physics applied to Radiation Therapy and the development of competent medical physicists who can make a direct contribution to the improvement of health care in their countries through better radiation therapy.

This will be achieved by providing participants with education and practical training to enhance their effectiveness as future disseminators of this knowledge, who can provide in turn educational and training opportunities to other medical professionals and students.

#### PROGRAM

The program of the School will consist of lectures, interactive discussions and problem solving sessions and applied learning experiences in local hospitals.

The two-week School will be devoted to the Physics applied to Radiation Therapy with the aim to introduce to conventional and advanced therapy principles, methods and technology:

- disseminating information about issues on radiotherapy physics and defining innovations that could improve the quality of radiotherapy services;
- outlining a systematic approach to the assessment of the appropriateness of conventional and advanced radiotherapy techniques; and
- facilitating the creation of a network for the exchange of information on radiotherapy physics among scientists in developing and developed Member States.

Traditionally, medical physicists have played a significant role in driving development in radiation medicine. This school will take a comprehensive approach for the implementation of conventional and advanced therapy methods, including the integration in treatment planning and patient setup of imaging modalities relevant in radiation therapy.

#### PARTICIPATION

Medical Physics scientists and students from all countries which are members of the United Nations, UNESCO or IAEA may attend the School. Participants should hold a university degree in medical physics or related subjects and have some professional experience in medical physics related to radiation therapy. As it will be conducted in English, participants should have an adequate working knowledge of this language.

Although the main purpose of the Centre is to help research workers from developing countries, through a program of training activities within a framework of international cooperation, post-doctoral scientists from developed countries are also welcome to attend.

As a rule, travel and subsistence expenses of the participants should be borne by the home institution. Every effort should be made by candidates to secure support for their fare (or at least half-fare). However, limited funds are available for some participants from developing countries, to be selected by the organizers. There is no registration fee.

#### HOW TO APPLY FOR PARTICIPATION

The application form can be accessed at the activity website

<https://e-applications.ictp.it/applicant/login/3110>

Once in the website, comprehensive instructions will guide you step-by-step, on how to fill out and submit the application form.

ACTIVITY SECRETARIAT: Telephone: +39-040-2240-226

Fax: +39-040-2240-7226

E-mail: [smr3110@ictp.it](mailto:smr3110@ictp.it)

ICTP Home Page: <http://www.ictp.it>

## DIRECTORS

- C. Cavedon (AIFM)
- M. De Denaro (Trieste, Italy)
- G. Hartmann (EFOMP)
- M.R. Malisan (Udine, Italy)
- C.G. Orton (IOMP)
- R. Padovani (ICTP)
- Y Pipman (AAPM)
- A. Torresin (EFOMP)

## LOCAL ORGANISER

- L. Bertocchi (ICTP)

## TOPICS

- Radiobiology
- Dosimetry
- Dosimetry algorithms
- 3D conformal, advanced (IMRT, VMAT) treatment delivery and brachytherapy
- Imaging and image integration
- Treatment planning and its practical implementation
- Treatment verification
- Quality assurance
- Case studies

## APPLICATION DEADLINE

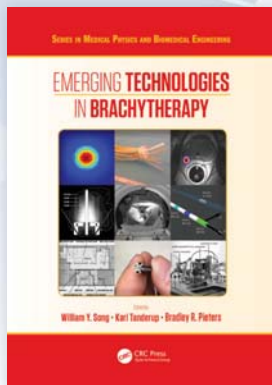
31 December 2016



SAVE  
25%

## EXCLUSIVE DISCOUNTS FOR MEMBERS OF THE IOMP

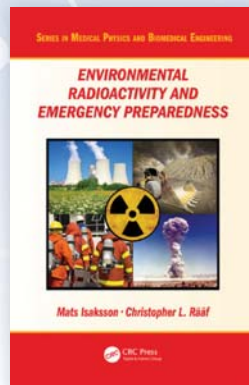
on new books in the *Series in Medical Physics and Biomedical Engineering*, the official book series of the IOMP



### Emerging Technologies in Brachytherapy

Brachytherapy is continuously advancing. Years of accumulated experience have led to clinical evidence of its benefit in numerous clinical sites such as gynecological, prostate, breast, rectum, ocular, and many other cancers. Brachytherapy continues to expand in its scope of practice and complexity, driven by strong academic and commercial research, by advances in competing modalities, and due to the diversity in the political and economic landscape. It is a true challenge for practicing professionals and students to readily grasp the overarching trends of the field, especially of those technologies and innovative practices that are not yet established but are certainly on the rise.

March 2017 • 978-1-4987-3652-7

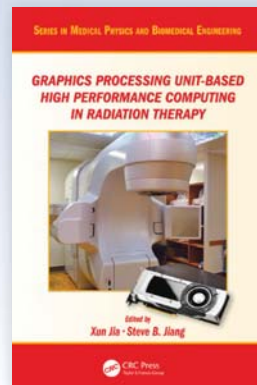


### Environmental Radioactivity and Emergency Preparedness

Radioactive sources such as nuclear power installations can pose a great threat to both humans and our environment. How do we measure, model and regulate such threats? *Environmental Radioactivity and Emergency Preparedness* addresses these topical questions and aims to plug the gap in the lack of comprehensive literature in this field.

The book explores how to deal with the threats posed by different radiological sources, including those that are lost or hidden, and the issues posed by the use of such sources. It presents measurement methods and approaches to model and quantify the extent of threat, and also presents strategies for emergency preparedness, such as strategies for first-responders and radiological triage in case an accident should happen.

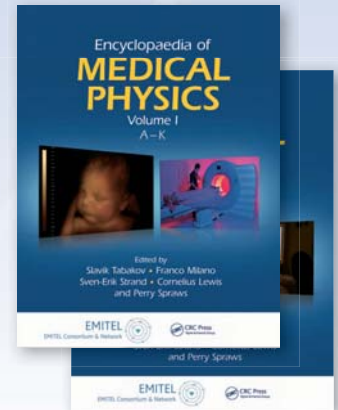
December 2016 • 978-1-4822-4464-9



### Graphics Processing Unit-Based High Performance Computing in Radiation Therapy

**"Graphics Processing Unit-Based High Performance Computing in Radiation Therapy provides comprehensive and timely information on state-of-the-art GPU techniques and is certainly a must-have book for medical physicists, engineers, and students engaged in research and development involving high performance computing."** – Lei Xing, Jacob Haimson Professor of Medical Physics, Stanford University

October 2015 • 978-1-4822-4478-6



### Encyclopaedia of Medical Physics

**"The breadth of topics is considerable and the consortium has made significant progress towards satisfying their goal of a global resource. The editors and translators have certainly put much effort into collecting and disseminating information and the global community can be grateful."** – Joseph Driewer, PhD, University of Nebraska Medical Center, Omaha, USA

December 2012 • 978-1-4398-4652-0

SAVE  
25%

When you order online and enter Promo Code **LMQ84**.

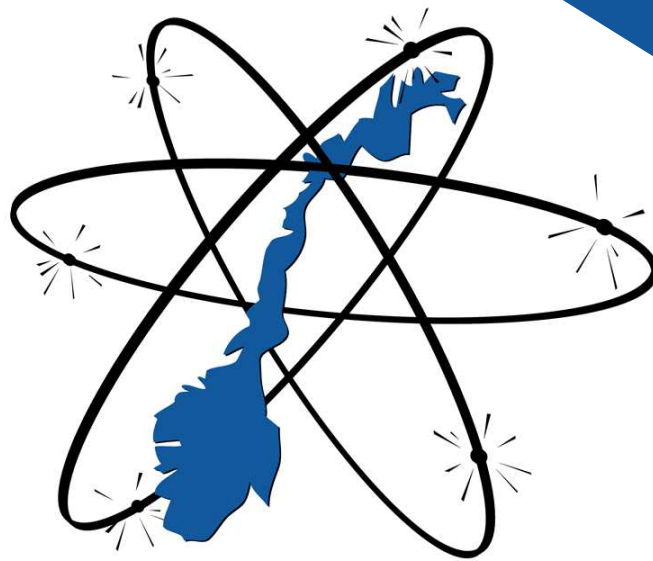
FREE standard shipping when you order online.



# Norwegian Association for Medical Physics

– A professional interest organisation–

- Supports and shows the way for development in medical physics
  - Stimulates development and exchange of experience
  - Contributes to a professional practice of the discipline
  - Certify medical physicist in Norway



**NFMF**

Norsk Forening for Medisinsk Fysikk

1976 — 40 år — 2016

[www.nfmf.org](http://www.nfmf.org)

40 years

of knowledge and experience

# Norwegian Association for Medical Physics

## 40 years



Norwegian Association for Medical Physics (NFMF) celebrates 40 years in 2016! The disciplines of medical physics has been continuously in development since the start but we still have the professional basic that we have applied for several years, both in radiotherapy physics and diagnostic physics. The association consists of about 190 members, and they contribute mainly in diagnostics and radiotherapy in Norwegian hospitals. We are especially happy for the increase in physicists in diagnostic imaging the recent years – and this contributes to a more even distribution of radiotherapy physicists and diagnostic physicists than ever! In addition we have members working within radiation protection.

NFMF has arranged a yearly conference since 1993 – at that time the MedFys-days were started at “Teknisk museum” in Oslo. With a few exceptions when the society had the yearly conference at the NACP-symposia in Århus and Uppsala, the MedFys-days have been arranged every year since. From 2012 the MedFys-days have been arranged at Kvitfjell during week 6 – and the conference has been growing for each year. It is obvious that the members, exhibitors and lecturers do appreciate a medical physics conference in the Norwegian winter nature! The association will of course celebrate the 40 years jubilee on MedFys-2016.

During the centennial we will also reveal ourselves by being present on meetings arranged in collaboration with other associations and by spreading information about medical physics and medical physicists at other occasions. We will use the anniversary both to give a historical review and at the same time to look ahead! Thank you to the anniversary committee, lead by Rune Hafslund, for the work put into a great 40 year anniversary for NFMF!

Kind regards  
Einar Waldeland  
Leader



Norwegian Association for Medical Physics

NFMF was  
founded



1976

The longest linear  
Accelerator in the Nordic  
with an energy of 32 MeV



1979

Hyperthermia



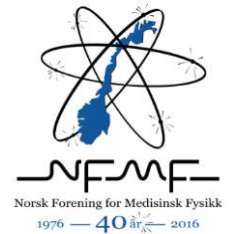
1983

Norway's first  
MR image



1986

# Norwegian Association for Medical Physics



Norwegian Association for Medical Physics (NFMF) was founded in 1976. The association is a professional association of interest for individuals working in the field of medical physics. The association works towards high professional standards and for a professional practice. A medical physicist has an important role in medical diagnostics and therapy, and is part of an interdisciplinary team for the best of the patient. A medical physicist participate in clinical practice, research, teaching, and in the development of the profession.

The association participate in a formalized Nordic cooperation through the umbrella organization Nordic Association for Clinical Physics (NACP) and is affiliated with the international organizations for medical physics: European Federation of Organizations for Medical Physics (EFOMP) and International Organization for Medical Physics (IOMP).

## What does a medical physicist do?

Medical physics includes development and usage of advanced physical methods for diagnostics and therapy of patients. In addition to excellent understanding of physical principles, medical physicists should have good insight into medical issues and physiology.

Most medical physicists have their work in health services and may have tasks within the disciplines; radiotherapy, radiology, nuclear medicine, MR and radiation protection. The medical physicist have a central role to assure proper, recognized and effective use of radiation. The medical physicists main tasks can be summarized to:

- Participation in daily operations in patient diagnostics and therapy
- Method development and introduction of new techniques and new technology
- Quality assurance and quality control
- Optimization of medical use of radiation
- Expertise in estimation, calculation and measurement of radiation dose
- Participation in procurement processes of medical equipment
- Run own research projects or contribute to others projects
- Teaching and training of students and personnel working in healthcare

The first and only  
gamma knife in Norway



1988

Rapid development  
in radiotherapy



1990 -

Opening of the first  
PET-centre in Norway



2006

First PET/MR  
in Norway



2013

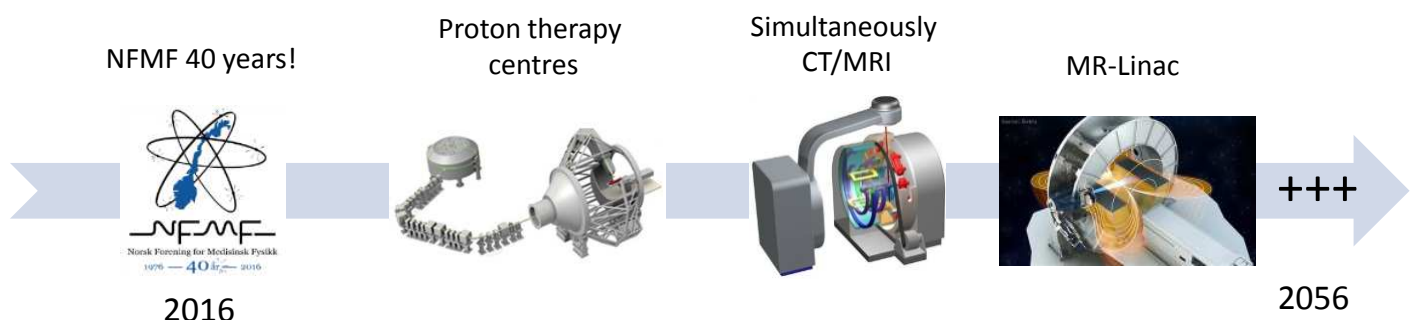
# Medical physics in the future



Medical physics do develop at high speed both within diagnostics and therapy, and medical physicists participate increasingly in this development. Medical physicists participate in multidisciplinary cooperation, which asks for good and effective communication with other professions/disciplines and show the importance of speaking the same language.

Exciting things are happening within the fields of medical physics in Norway. Several centres with PET cyclotron and production of radiopharmaceuticals are planned and build . During 2018 you will find these PET centres in all four health regions. Centres for proton therapy are also in progress in all four health regions. In this process medical physicists have key roles. Within hybrid modalities a rapid development is happening - SPECT/CT, PET/CT, SPECT/MR and PET/MR. Simultaneous CT/MR is also under development and is predicted to be the next chapter within multimodal imaging. Important areas of priority in radiotherapy are: particle therapy, adaptive radiotherapy, radiobiological customization by dose-painting, and use of PET/MR/SPECT for dose planning. The first MR-linac's are already installed in international clinical environments.

**The latest 40 years have made an excellent foundation for the next 40 years!**



## INFORMATION FOR AUTHORS

---



### PUBLICATION OF DOCTORAL THESIS AND DISSERTATION ABSTRACTS

A special feature of Medical Physics International (online at [www.mpijournal.org](http://www.mpijournal.org)) is the publication of thesis and dissertation abstracts for recent graduates, specifically those receiving doctoral degrees in medical physics or closely related fields in 2010 or later. This is an opportunity for recent graduates to inform the global medical physics community about their research and special interests.

Abstracts should be submitted by the author along with a letter/message requesting and giving permission for publication, stating the field of study, the degree that was received, and the date of graduation. The abstracts must

be in English and no longer than 2 pages (using the MPI manuscript template) and can include color images and illustrations. The abstract document should contain the thesis title, author's name, and the institution granting the degree.

Complete information on manuscript preparation is available in the INSTRUCTIONS FOR AUTHORS section of the online journal: [www.mpijournal.org](http://www.mpijournal.org).

For publication in the next edition abstracts must be submitted not later than /august 1, 2014.

## INSTRUCTIONS FOR AUTHORS

The goal of the new IOMP Journal Medical Physics International (<http://mpijournal.org>) is to publish manuscripts that will enhance medical physics education and professional development on a global basis. There is a special emphasis on general review articles, reports on specific educational methods, programs, and resources. In general, this will be limited to resources that are available at no cost to medical physicists and related professionals in all countries of the world. Information on commercial educational products and services can be published as paid advertisements. Research reports are not published unless the subject is educational methodology or activities relating to professional development. High-quality review articles that are comprehensive and describe significant developments in medical physics and related technology are encouraged. These will become part of a series providing a record of the history and heritage of the medical physics profession.

A special feature of the IOMP MPI Journal will be the publication of thesis and dissertation abstracts for will be the publication of thesis and dissertation abstracts for recent doctoral graduates, specifically those receiving their doctoral degrees in medical physics (or closely related fields) in 2010 or later.

### MANUSCRIPT STYLE

Manuscripts shall be in English and submitted in WORD. Either American or British spelling can be used but it must be the same throughout the manuscript. Authors for whom English is not their first language are encouraged to have their manuscripts edited and checked for appropriate grammar and spelling. Manuscripts can be up to 10 journal pages (approximately 8000 words reduced by the space occupied by tables and illustrations) and should include an unstructured abstract of no more than 100 words.

The style should follow the template that can be downloaded from the website at:

[http://mpijournal.org/authors\\_submitpaper.aspx](http://mpijournal.org/authors_submitpaper.aspx)

### ILLUSTRATIONS SPECIAL REQUIREMENTS

Illustrations can be inserted into the manuscript for the review process but must be submitted as individual files when a manuscript is accepted for publication.

The use of high-quality color visuals is encouraged. Any published visuals will be available to readers to use in their educational activities without additional approvals.

### REFERENCE WEBSITES

Websites that relate to the manuscript topic and are sources for additional supporting information should be included and linked from within the article or as references.

### EDITORIAL POLICIES, PERMISSIONS AND

#### APPROVALS

#### AUTHORSHIP

Only persons who have made substantial contributions to the manuscript or the work described in the manuscript shall be listed as authors. All persons who have contributed to the preparation of the manuscript or the work through technical assistance, writing assistance, financial support shall be listed in an acknowledgements section.

### CONFLICT OF INTEREST

When they submit a manuscript, whether an article or a letter, authors are responsible for recognizing and disclosing financial and other conflicts of interest that might bias their work. They should acknowledge in the manuscript all financial support for the work and other financial or personal connections to the work.

All submitted manuscripts must be supported by a document (form provided by MPI) that:

- Is signed by all co-authors verifying that they have participated in the project and approve the manuscript as submitted.
- Stating where the manuscript, or a substantially similar manuscript has been presented, published, or is being submitted for publication. Note: presentation of a paper at a conference or meeting does not prevent it from being published in MPI and where it was presented can be indicated in the published manuscript.

- Permission to publish any copyrighted material, or material created by other than the co-authors, has been obtained.
- Permission is granted to MPI to copyright, or use with permission copyrighted materials, the manuscripts to be published.
- Permission is granted for the free use of any published materials for non-commercial educational purposes.

SUBMISSION OF MANUSCRIPTS

Manuscripts to be considered for publication should be submitted as a WORD document to: Slavik Tabakov, Co-editor: slavik.tabakov@emerald2.co.uk

MANUSCRIPT PROPOSALS

Authors considering the development of a manuscript for a Review Article can first submit a brief proposal to the editors. This should include the title, list of authors, an abstract, and other supporting information that is appropriate. After review of the proposal the editors will consider issuing an invitation for a manuscript. When the manuscript is received it will go through the usual peer-review process.

MEDICAL PHYSICS INTERNATIONAL Journal

MEDICAL PHYSICS INTERNATIONAL INSTRUCTION FOR AUTHORS

A. FamilyName<sup>1</sup>, B.C. CoauthorFamilyName<sup>2</sup>, D. CoauthorFamilyName<sup>1</sup>

<sup>1</sup> Institution/Department, Affiliation, City, Country  
<sup>2</sup> Institution/Department, Affiliation, City, Country

**Abstract**— Paper abstract should not exceed 300 words. Detailed instructions for preparing the papers are available to guide the authors during the submission process. The official language is English.

**Keywords**— List maximum 5 keywords, separated by commas.

I. INTRODUCTION

These are the instructions for preparing papers for the Medical Physics International Journal. English is the official language of the Journal. Read the instructions in this template paper carefully before proceeding with your paper.

II. DETAILED INSTRUCTIONS

**Paper Size:** A4

**Length:** The maximum document size is usually 8 pages. For longer papers please contact the Editor(s).

**Margins:** The page margins to be set to: "mirror margins", top margin 4 cm, bottom margin 2,5 cm, inside margin 1,9 cm and outside margin 1,4 cm.

**Page Layout:** 2 columns layout.

**Alignment:** Justified.

**Fonts:** Times New Roman with single line spacing throughout the paper.

**Title:** Maximum length - 2 lines. Avoid unusual abbreviations. Font size - 14 point bold, uppercase. Authors' names and affiliations (Institution/Department, City, Country) shall span the entire page.

**Indentation:** 8 point after the title, 10 point after the authors' names and affiliations, 20 point between author's info and the beginning of the paper.

**Abstract:** Font - 9 point bold. Maximum length - 300 words.

**Style:** Use separate sections for introduction, materials and methods, results, discussion, conclusions, acknowledgments and references.

**Headings:** Enumerate Chapter Headings by Roman numbers (I, II, etc.). For Chapter Headings use ALL CAPS. First letter of Chapter Heading is font size 12, regular and other letters are font 8 regular style. Indents - 20 point before and 10 point after each Chapter Heading. Subchapter Headings are font 10, italic. Enumerate Subchapter Headings by capital letters (A., B., etc.). Indents

- 15 point before and 7,5 point after each Subchapter Heading.

**Body Text:** Use Roman typeface (10 point regular) throughout. Only if you want to emphasize special parts of the text use *Italics*. Start a new paragraph by indenting it from the left margin by 4 mm (and not by inserting a blank line). Font sizes and styles to be used in the paper are summarized in Table 1.

**Tables:** Insert tables as close as possible to where they are mentioned in the text. If necessary, span them over both columns. Enumerate them consecutively using Arabic numbers and provide a caption for each table (e.g. Table 1, Table 2, ...). Use font 10 regular for Table caption, 1<sup>st</sup> letter, and font 8 regular for the rest of table caption and table legend. Place table captions and table legend above the table. Indents - 15 point before and 5 point after the captions.

Table 1 Font sizes and styles

| Item                             | Font Size, pt | Font Style | Indent, points       |
|----------------------------------|---------------|------------|----------------------|
| Title                            | 14            | Bold       | Aft: 5               |
| Author                           | 12            | Regular    | Aft: 10              |
| Authors' info                    | 9             | Regular    | Aft: 20              |
| Abstract                         | 9             | Bold       |                      |
| Keywords                         | 9             | Bold       |                      |
| <b>Chapters</b>                  |               |            |                      |
| Heading - 1 <sup>st</sup> letter | 12            | Regular    | Before: 20           |
| Heading - other letters          | 8             | Regular    | Aft: 10              |
| Subchapter heading               | 10            | Italic     | Before: 15, Aft: 7,5 |
| Body text                        | 10            | Regular    | First line left: 4mm |
| Acknowledgment                   | 8             | Regular    | First line left: 4mm |
| References                       | 8             | Regular    | First line left: 4mm |
| Author's address                 | 8             | Regular    |                      |
| <b>Tables</b>                    |               |            |                      |
| Caption, 1 <sup>st</sup> letter  | 10            | Regular    | Before: 15           |
| Caption - other letters          | 8             | Regular    | Aft: 5               |
| Legend                           | 8             | Regular    |                      |
| Column titles                    | 8             | Regular    |                      |
| Data                             | 8             | Regular    |                      |
| <b>Figures</b>                   |               |            |                      |
| Caption - 1 <sup>st</sup> letter | 10            | Regular    | Before: 15           |
| Caption - other letters          | 8             | Regular    | Aft: 5               |
| Legend                           | 8             | Regular    |                      |

MEDICAL PHYSICS INTERNATIONAL Journal

**Figures:** Insert figures where appropriate as close as possible to where they are mentioned in the text. If necessary, span them over both columns. Enumerate them consecutively using Arabic numbers and provide a caption for each figure (e.g. Fig. 1, Fig. 2, ...). Use font 10 regular for Figure caption, 1<sup>st</sup> letter, and font 8 regular for the rest of figure caption and figure legend. Place figure legend beneath figures. Indents - 15 point before and 5 point after the captions. Figures are going to be reproduced in color in the electronic versions of the Journal, but may be printed in grayscale or black & white.

**'REFERENCES':** Examples of citations for Journal articles [1], books [2], the Digital Object Identifier (DOI) of the cited literature [3], Proceedings papers [4] and electronic publications [5].

III. CONCLUSIONS

Send your papers only in electronic form. Papers to be submitted prior the deadline. Check the on-line Editorial Process section for more information on Paper Submission and Review process.

ACKNOWLEDGMENT

Format the Acknowledgment headlines without numbering.

REFERENCES

The list of References should only include papers that are cited in the text and that have been published or accepted for publication. Citations in the text should be identified by numbers in square brackets and the list of references at the end of the paper should be numbered according to the order of appearance in the text.

Cited papers that have been accepted for publication should be included in the list of references with the name of the journal and marked as "in press". The author is responsible for the accuracy of the references. Journal titles should be abbreviated according to Engineering Index Inc. References with correct punctuation.



Fig. 1 Medical Physics International Journal

**Equations:** Write the equation in equation editor. Enumerate equations consecutively using Arabic numbers

$$A + B = C \quad (1)$$

$$X = A \times e^{2t} + 2kt \quad (2)$$

**Items/Bullets:** In case you need to itemize parts of your text, use either bullets or numbers, as shown below:

- First item
- Second item

1. Numbered first item
2. Numbered second item

**References:** Use Arabic numbers in square brackets to number references in such order as they appear in the text. List them in numerical order as presented under the heading

1. LeadingAuthor A, CoAuthor B, CoAuthor C et al. (2012) Paper Title Journal 111:220-230
2. LeadingAuthor D, CoAuthor E (2009) Title. Publisher: London
3. LeadingAuthor A, CoAuthor B, CoAuthor C (2012) Paper Title Journal 111:330-340 DOI:123456789
4. LeadingAuthor F, CoAuthor G (2012) Title. IOMP Proceedings, vol. 4, World Congress on Med. Phys. & Biomed. Eng., City, Country, 2012, pp 300-304
5. MPI at <http://www.mpijournal.org>

Contacts of the corresponding author:

Author:  
Institute:  
Street:  
City:  
Country:  
Email:



## ICMP 2016



## BOOK OF ABSTRACTS

---

**Editing: S Tabakov, M Stoeva, A Krisanachinda, V Tabakova**



## **ICMP 2016 ORGANISATIONAL STRUCTURE**

**President:** Anchali Krisanachinda  
**Co-Presidents:** Slavik Tabakov, Tae-Suk Suh

**Congress Organising Committee (COC):**  
**President TMPS** Anchali Krisanachinda  
**President IOMP** Slavik Tabakov  
**President AFOMP** Tae Suk Suh  
**President SEAFOMP** James Lee  
**Secretary General IOMP** Virginia Tsapaki

**International Advisory Committee**  
**Chair:** Slavik Tabakov  
**Co-Chair:** Hu Yi Min  
**Members:** Akio Ogura  
Franco Milano  
Agnette Peralta

**Scientific/Programme Committee**  
**Co-Chairs:** Geoffrey Ibbott  
Arun Chogule  
Howell Round  
**Local Committee:** PuangpenTangboonduangjit

**Educational Committee (IOMP School):**  
**Co-Chairs:** John Damilakis,  
Kwan HoongNg,  
Shigekazu Fukuda

**Special Activities Committee:**  
**Co-Chairs:** KY Cheung  
Madan Rehani  
Yakov Pipman

**Commercial Exhibition and Marketing**  
**Chair:** Sivalee Suriyapee  
**Co-Chair:** Napapong Pongnapang

**Social Committee**  
**Co-Chairs:** Kitiwat Khamwan

## ICMP 2016 PRESIDENT MESSAGE



On behalf of the ICMP2016, it is our great honor to welcome all of you to the 22<sup>nd</sup> International Conference on Medical Physics host by International Organization on Medical Physics (IOMP), Asia-Oceania Federation of Organizations on Medical Physics (AFOMP) and South East Asian Federation of Organizations on Medical Physics (SEAFOMP), International Union of Pure and Applied Physics (IUPAP), Thai Medical Physicist Society (TMPS) and Thailand Convention and Exhibition Bureau (TCEB). ICMP 2016 receives the support from other Regional Federations and Societies such as EFOMP, MEFOMP, ALFIM, FAMPO, IAEA, JSMP and JSRT. Many thanks for the kind support from Commercial Exhibitors to make this Conference completion and successful.

My sincere thanks are forwarded to distinguished speakers and all participants who made the total number of participants at over 500 from 40 countries all over the world. The number Mini Symposium is 42 and Oral presentations with electronic poster are 392. The numbers of booth are 34.

We wish you enjoy the Conference during these four days at Shangri La Hotel on scientific program and other functional program arrange under IOMP activities. Please give me the sincere apology for any conveniences during and before the Conference.

Thank you,

A handwritten signature in blue ink, which appears to read "Anchali".

Anchali Krisanachinda, Ph.D.  
President, ICMP2016

## IOMP PRESIDENT MESSAGE



Dear Colleagues,

On behalf of the International Organization for Medical Physics (IOMP), I welcome you to the International Conference on Medical Physics in Bangkok, Thailand (9-12 December 2016).

This will be the 22<sup>nd</sup> International Conference on Medical Physics of IOMP. A long path has been walked from the 1<sup>st</sup> such Conference in Harrogate, UK in 1965 (when the number of medical physicists globally was around 6000). For these 50+ years medical physicists contributed enormously to the progress of contemporary medicine. They developed and introduced in clinical practice many new methods and equipment, which are now a firm basis of healthcare. These resulted in three Nobel Awards, a participation in the Nobel Peace Award and many National and International Awards. Medical physicists are now an intrinsic part of the healthcare team, what led to the official recognition of the occupation “medical physicist” by the International Labour Organisation, where our profession is now included, linked with two fields – Physics and Health Professionals. This achievement of IOMP, IFMBE and IUPESM is of great importance for thousands of colleagues around the world.

IOMP supports strongly the development of education and training in medical physics. Our profession is recognised as one of the first in the world to fully embrace e-learning – a subject to which I dedicated my professional life. Now medical physicists have original e-learning materials, used by thousands of colleagues each month. To further support this IOMP launched in 2013 a specific Journal related to professional and educational issues (Medical Physics International – [www.mpijournal.org](http://www.mpijournal.org)), which rapidly established itself as one of the important publications of the profession. All these activities were very effective and IOMP continues them in Bangkok 2016 with the introduction of its new initiative “IOMP School”, which includes more than 40 educational symposia. Today IOMP is proud to announce that in the past 20 years these educational activities were pivotal for the doubling of medical physicists globally – from 12,000 in 1995 to 24,000 at present.

The 22<sup>nd</sup> International Conference on Medical Physics (ICMP2016) in Bangkok is dedicated to the topic of “Medical Physics Propelling Global Health”. It will include a number of presentations and symposia related to the newest developments in our profession and their importance for healthcare. I want to thank the Scientific Committee and all Organisers of ICMP2016 for their hard work for the success of the Conference, which is important both for the region and for all colleagues worldwide. I want also to extend my thanks to the IOMP Regional Organisations – AFOMP, led by Prof. Tae Suk Suh, and SEAFOMP, led by Prof. James Lee Cheow Lei for their strong support for the Conference. I would also want to express gratitude to the Thai Medical Physicist Society, hosting the Conference, and especially to the ICMP2016 President Prof. Anchali Krisanachinda.

I am looking forward to see you at the ICMP2016 in Bangkok and am sending you my best wishes

Prof. Dr Slavik Tabakov, FIPEM, FIOMP

President IOMP

## AFOMP PRESIDENT MESSAGE



I am pleased to welcome all delegates to the 22nd International Conference on Medical Physics (ICMP 2016), held in conjunction with the 16th Asia-Oceania Congress of Medical Physics (AOCMP 2016). It is also my great honor and privilege to deliver a congratulatory remark on behalf of the Asia-Oceania Federation of Organization for Medical Physics (AFOMP) in this beautiful and historical city, Bangkok, Thailand. As the president of the AFOMP, I would like to take this opportunity to thank Prof. Anchali Krisanachinda, the Organizing Chair of ICMP 2016, the Thai Medical Physicist Society (TMPS) and South-East Asia Federation of organization for Medical Physics (SEAFOMP), led by Prof. James Lee. Further, I express my sincere gratitude to Prof. Slavik Tabakov, the President of IOMP, and other members of the society for making this joint meeting possible.

The Organizing Committee of ICMP 2016 has planned a very interesting congress that covers a wide range of issues, including various Mini Symposia on different topic in medical physics. The ICMP 2016 program comprises three parts: scientific interactions, education and training in medical physics, and special oriental cultural experiences. Several specific workshops and symposia have been designed to address the specific issues in medical physics relevant to the Asia-Pacific region. I am sure that they will provide a strong foundation for the ongoing development of medical physics in the Asia-Pacific region, based on appropriate affordable technology and professional development.

The role and status of medical physicists in the AFOMP region has gradually improved as can be seen by its increasing recognition in societies. However, neither the governments nor the public has yet recognized the importance of medical physics and the necessity for accreditation. I believe that a well-prepared strategy and a strong action plan are crucial for the AFOMP to move forward. The AFOMP will help build a strong relationship between other sub-regional organizations in the Asia-Oceania region and international bodies such as the IOMP, IAEA, WHO, etc., and encourage the exchange of information among them.

This is the first time that the AOCMP is being held in conjunction with ICMP in Asia. It is hoped that the meeting will provide an informative and stimulating discussion essential for further advancement of medical physics for improvement in health care. It is my pleasure to announce the opening of ICMP 2016 and AOCMP 2016. I wish the members of these associations every success and continuous prosperity.

Thanks to you all.

Tae Suk Suh,

President of AFOMP

## SEAFOMP PRESIDENT MESSAGE



Dear Medical Physics colleagues,

Welcome to ICMP 2016! It is indeed exciting that this important conference is hosted for the first time in Thailand and South-East Asia. I am particularly grateful to the Thai Medical Physicist Society for putting in their best and tireless effort to organise this event and also for IOMP's huge support behind them. It is my wish that you would greatly benefit from the comprehensive array of topics and good speakers at ICMP. For those of you with posters and oral presentations, it will also be an important platform to present your research ideas and findings with like-minded professionals. As the global Medical Physics community meets, it is my hope that there will be stimulating exchange of ideas and new friendships forged while enjoying the conference and making time to visit Thailand, the land of smiles.

Once again, on behalf of the South East Asian Federation of Organizations for Medical Physics, we would like to express our heartfelt thanks to Thailand for hosting the ICMP 2016 and indeed my warmest welcome to all participants around the world.

Enjoy!

James C L Lee, PhD

SEAFOMP President



## ICMP 2016



## ORAL PRESENTATIONS

## **1.1 Particle Beam**

## THE EVALUATION OF THE PROTON PENCIL BEAM USING MULTILAYER IONIZATION CHAMBER SYSTEM (GIRAFFE)

Kunihiko Tateoka<sup>1</sup>

<sup>1</sup> Proton Therapy Center, Sapporo Teishinkai Hospital, Japan

**Key words:** Proton Therapy, Bragg-Peak, Depth-Dose

### Purpose

For pencil (spot or line) scanned clinical proton beam delivery modes, depth-dose distributions are measured using the plane-parallel ionization chambers of the large electrode radius. This method is used for a long time. The Giraffe consists of a stack of 180 independent air-vented, plane-parallel ionization chambers and can measure the depth-dose distributions in a short time. In this study, the Giraffe-measured depth-dose distributions were compared with those measured by the Stingray chamber, the plane-parallel ionization chamber and the three dimensional water tank dosimetry system.

### Methods

For pencil-beam by SUMITOMO cyclotron delivery system, the Giraffe-measured depth-dose distributions were compared with those measured with the water tank system and the Stingray chamber regarding range, the depth of the distal 90% dose, the region between the proximal 95% and distal 90% dose and distal-dose fall off (DDF): the region between the distal 80% and 20% dose.

### Results

The reproducibility of measured data from the Giraffe has showed better than 1%. For pencil-beam PDD distributions showed about 2% agreement. Range values agreed within about 1.0mm. DDF values agreed within 0.5mm. Moreover, the setup and measurement time for all Giraffe measurements was 3 to 20 times less, respectively, compared to the water tank measurements.

### Conclusions

The Giraffe can measure the depth-dose distributions for pencil proton beams for a short time. Fathomer, Range values and DDF values obtained with the Giraffe are within the acceptable variations compared with the water tank measurements system.

## **DEVELOPMENT OF A PROTON THERAPY TREATMENT PLANNING SOFTWARE FOR RESEARCH AND EDUCATIONAL PURPOSES**

Thiansin Liamsuwan<sup>1</sup>, Puangpen Tangboonduangjit<sup>2</sup>, Thanaphat Chongsan<sup>3</sup>

<sup>1</sup>Thailand Institute of Nuclear Technology

<sup>2</sup>School of Medical Physics, Faculty of Medicine Ramathibodi Hospital, Mahidol University

<sup>3</sup>Thammasat Radiation Oncology Center, Thammasat University

**Key words:** Proton therapy, treatment planning, pencil beam scanning (PBS), single field uniform dose (SFUD)

### **Purpose**

The aim of this work was to develop a treatment planning system (TPS) for the proton pencil beam scanning (PBS) technique to be used for research and educational purposes.

### **Methods**

The software was developed using MATLAB and structured into different modules. Each module represents specific functionality of the TPS, including reading and interpretation of CT-DICOM files, dose calculation of proton pencil beams, dose optimization and calculation of dose-volume histogram (DVH). Users are allowed to provide CT data of a patient and an arbitrary set of pencil beam parameters such as spot size, proton energy distribution, depth increment of PBS and source-to-isocenter distance, along with the default values that were compiled from published literature. At present, the software is able to calculate single field uniform dose (SFUD) plans of the PBS technique, for which each optimized field delivers homogeneous dose to the target volume.

### **Results**

The functionality of the TPS was successfully tested with CT data of a pediatric patient diagnosed with a primary brain tumor and the default pencil beam parameters obtained from published literature. The overview and outputs of the program as well as the comparison of dose distributions and computational time at different planning scenarios will be presented.

### **Conclusions**

The modular structure and the accessibility to modify beam parameters of the developed TPS will facilitate medical physicists and researchers to perform dosimetric investigation of proton therapy at different scenarios despite limited or unavailable access to proton therapy machines.

## **EVALUATION OF DOSIMETRIC CHARACTERISTIC OF AN ALUMINA BASED CERAMICS TLD FOR HIGH ENERGY PHOTON AND PROTON BEAMS**

Weishan Chang<sup>1</sup>, Yusuke Koba<sup>2</sup>, Kiyomitsu Shinsho<sup>3</sup>, Hidetoshi Saitoh<sup>3</sup>, Kazuki Matsumoto<sup>4</sup>, Hiroaki Ushiba<sup>4</sup>, Takayuki Ando<sup>4</sup>

<sup>1</sup>Tokyo Metropolitan University

<sup>2</sup>National Institute Of Quantum And Radiological Sciences Technology

<sup>3</sup>Tokyo Metropolitan University

<sup>4</sup>Chiyoda Technol. Corporation

**Key words:** TLD, proton beam, photon beam

### **Purpose**

It has been reported that the main glow peak of alumina based ceramics TLD (A8, Chibacera Co.) is less LET dependent compared to other commercial TLD. The purpose of this report is to investigate the basic dosimetric characteristics of A8 for proton dosimetry.

### **Methods**

The dosimetric characteristics that are independent of radiation such as reproducibility and fading effect were investigated using a 6 MV photon beam. Dose response linearity and the depth dose distribution were investigated using a 70 MeV proton beam. The depth dose distribution measured with the A8 was compared with that measured with a plane parallel ionization chamber (type34045, PTW-Freiburg, Germany). The LET at each depth was also calculated to evaluate the LET dependence and the potential of A8 for proton dosimetry.

### **Results**

The reproducibility of A8 was within 3 % and the fading effect was within 10% for 1 week.

The TL signal of A8 was linear as a function of dose in the range of 0.5–5 Gy. Depth dose distribution measured with A8 showed good agreement with ionization chamber in plateau region, and the position of Bragg peak determined with A8 shifts towards to shallower depth compared with that determined with ionization chamber. The variation of the response of A8 was within 5 % at LET range from 1 keV/m to 5 keV/m.

### **Conclusions**

The dosimetric characteristics of A8 were demonstrated and the suitability for proton dosimetry was evaluated.

## **DEVELOPMENT OF TREATMENT PLANNING SYSTEM ENGINE BASED ON MONTE CARLO SIMULATION FOR PROTON BORON FUSION THERAPY**

Sunmi Kim<sup>1</sup>, Do-Kun Yoon<sup>1</sup>, Han-Back Shin<sup>1</sup>, Joo-Young Jung<sup>1</sup>, Moo-Sub Kim<sup>1</sup>, Tae Suk Suh<sup>1</sup>

<sup>1</sup>The Catholic University of Korea

**Key words:** Proton, Boron, Monte Carlo Simulation, Treatment Planning System Engine

### **Purpose**

In this study, we present the introduction of a therapy method using the proton boron fusion reaction. The purpose of this research is to develop the treatment planning system engine for proton boron fusion therapy using Monte Carlo Simulation.

### **Methods**

A series of simulations has been carried out using MCNPX code for designing the treatment planning system(TPS) engine for proton boron fusion therapy(PBFT). First step is an import of the CT images for the planning. Those images were converted to the code including the geometry information for MCNPX. Second step is the simulation with this code according to the treatment plan. The simulation results show the dose distribution of the proton beam. Surely, an influence of the boron is also involved in the results. Last step is the evaluation of the Monte Carlo engine based treatment planning of PBFT.

### **Results**

MCNPX simulation results and analysis of these results show the theoretical validity of the developed TPS Engine for proton boron fusion therapy. It demonstrates the advantage as depth dose rate, treatment time, maximum normal tissue dose. Their corresponding values are compared with other results of conventional proton beam therapy.

### **Conclusions**

In present work, in order to prove the merit of use of boron when proton therapy, we have performed the simulation works for treatment planning of PBFT. In the future, we will try to establish the protocol for a clinical application.

## DEVELOPMENT OF THE STEREOTACTIC RADIOSURGERY FOR CARBON PARTICLE BEAM

Mintra Keawsamur<sup>1</sup>, Tatsuaki Kanai<sup>2</sup>

<sup>1</sup>Gunma University

<sup>2</sup>Graduate School Of Medicine, Gunma University, Gunma, Japan

**Key words:** carbon beam, stereotactic radiosurgery, small field dosimetry

### Purpose

The main objective of this research is to develop the stereotactic radiosurgery for Carbon beam to treat the small brain tumor that we call Carbon knife. Gunma university heavy ion medical center has developed a raster-scanning irradiation method to perform carbon knife radiotherapy with higher accuracy. Layout of the raster scanning carbon knife system consists of the scanning magnets, dose monitors, position monitor, mini ridge filter, and collimator.

### Methods

The mini-ridge filter with 5mm, 7.5mm, and 10mm width of SOBP, which is included the fluence attenuation factor, was set at 1200 mm upstream from isocenter. The 3 sizes of the collimator, which is set at 50 mm upstream from the patient surface, were 2x2 mm<sup>2</sup>, 3x3 mm<sup>2</sup>, and 10x10 mm<sup>2</sup>

For the precise measurement, a specially designed small parallel plate ionization chamber with 0.003 cm<sup>3</sup> effective volume has been developed.

### Results

The correction factor for saturation of the 0.003 cm<sup>3</sup> IC at 1000 operating voltage was 1.0214. The obtained a calibration coefficient in terms of absorbed dose to water when calibrated against the parallel plate Markus ionization chamber, which has been calibrated by SDL, was 1.016x10<sup>10</sup> Gy/C. Depth dose and beam profile data were compared with the diode dosimetry PR type 60020 and our in-house ionization chamber. The measurement points for lateral profile are at the start, the middle, and the end point of SOBP.

### Conclusions

The suitable mini-ridge filter and collimator will be selected for therapeutic usage depending on the target volume and tumor site.

## **DESIGN OF A NOVEL RADIATION THERAPY REGIMEN BASED ON THE ANALYSIS OF FACTORS AFFECTING ITS EFFICACY FOR BIOLOGICALLY HETEROGENEOUS TUMOR TARGETS**

Narayan Sahoo<sup>1</sup>, Yasumasa Nishimura<sup>2</sup>, Avilash Rath<sup>3</sup>, Falk Poenisch<sup>1</sup>, Xiaodong Zhang<sup>1</sup>, Wei Liu<sup>4</sup>, Xiaorong Zhu<sup>1</sup>, Michael Gillin<sup>1</sup>

<sup>1</sup>UT MD Anderson Cancer Center, USA

<sup>2</sup>Kindai University

<sup>3</sup>University of Texas at Austin

<sup>4</sup>Mayo Clinic, Arizona

**Key words:** Dose painting, IMPT

### **Purpose**

To analyze the sensitivity of radiation induced cell killing to repopulation rates (R) and radiation sensitivity (S) for malignant cells, and to explore the usefulness of intensity modulated proton therapy (IMPT) to improve the efficacy of radiation therapy for biologically heterogeneous tumor targets.

### **Methods**

An exponential radiation cell killing model was used to quantify the survival fraction (SF) as a function of R and S for fractionated radiation therapy. IMPT plans were designed for test cases to study the feasibility of giving higher doses to the radio-resistant target volumes in breast and prostate for increasing the cell killing in these volumes without exceeding the acceptable tolerance doses to the organs at risk (OAR).

### **Results**

It is found that SF is minimally affected by the increase in R, but increases significantly with the decrease in S requiring higher doses to achieve the same level of cell killing that can be achieved for standard values of these parameters. For the test cases in this study, it is shown that two times higher doses of currently used prescription dose for hypo-fractionated treatments, which is given to other regions of the target, can be delivered with IMPT to radio-resistant target volumes while keeping the OAR doses to their acceptable limits.

### **Conclusions**

Our proposed dose painting with higher doses to the radio-resistance cancer cells and more normal tissue sparing with IMPT has the potential to achieve higher complication-free tumor control for biologically heterogeneous tumor targets.

## THE IMPACT OF RESPIRATORY MOVEMENT IN SPOT SCANNING PROTON THERAPY

Y. Ueshima<sup>1</sup>, N. Hayashi<sup>2</sup>, C. Nakagami<sup>1</sup>, K. Yasui<sup>3</sup>

<sup>1</sup>Graduate School of Health Sciences, Fujita Health University, Aichi, Japan; <sup>2</sup>School of Health Sciences, Fujita Health University, Aichi, Japan; <sup>3</sup>Nagoya Proton Therapy Center, Nagoya City West Medical Center, Aichi, Japan;

**Keywords:** spot scanning proton therapy, respiratory movement, dose distribution, dose calculation program, MATLAB

**Introduction:** Respiratory movement is important factor in spot scanning proton therapy(SSPT) [1][2]. However, dose measurement including respiratory movement is difficult. The purpose of this study is to evaluate four-dimensional dose distributions in various respiratory movements.

**Methods:** We created specific program with MATLAB for this research. The program can simulate dose distributions including various respiratory movements. We simulated dose distributions in various amplitudes and respiratory cycles using sine and cos<sup>2n</sup> waves [3]. Then we compared the dose distributions with- and without-respiratory gating technique. The gating rate of 25% was used for simulations.

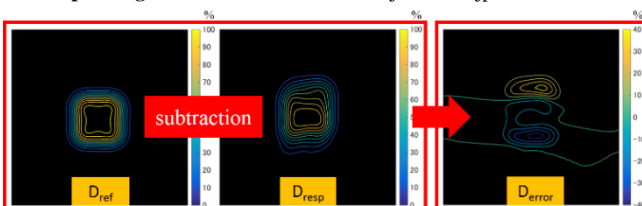
**Results:** The dose distributions with various respiratory patterns were verified with simple field size. The larger amplitude or shorter respiratory cycle were input, the larger error in a dose distribution was obtained (Maximum error: -52.37% at local dose). When the gating rate of 25% was used, a maximum error of -10.41% was obtained. The usefulness of respiratory gating technique for cos<sup>2n</sup> wave was more significant than those for sine wave.

**Conclusion:** The impact of respiratory movement in SSPT was evaluated with specific program. With this program, the simple dose verification with consideration of respiratory movement is available even if the measurement-based dose verification is impossible. Furthermore, the complicated dose verification with irregular field should be verified for clinical implementation for SSPT in future.

**References:**

1. S. Fukumoto, Trends of Particle Beam Cancer Therapy, Journal of the Atomic Energy Society of Japan, Vol.35, No.10, 885-890, 1993.
2. M. Phillips, et al “Effects of respiratory movement on dose uniformity with a charged particle scanning method.” Phys. Med. Biol. 37, 223-234, 1992.
3. Seppenwoolde et al, “Precise and real-time measurement of 3D tumor motion in lung due to breathing and heartbeat, measured during radiotherapy.” Int. J. Radiation Oncology Biol. Phys., 53, 822-834, 2002.

Corresponding authoremail:82016302@fujita-hu.ac.jp



**INFORMATION ABOUT THE ABSTRACT**

Recently, SSPT is expected to create dose distributions with high conformity. Although this method has some fundamental advantages, it's a dynamic irradiation method, respiratory movement causes a serious impact on dose irradiation accuracy. It's useful to simulate independent verification by using our in-house dose calculation program.

We constructed a dose calculation program by using MATLAB (MathWorks). This program was modeled on PROBEAT-III (Hitachi). Parameters of the treatment plan was output using the treatment planning system VQA (Hitachi).

Dose calculation algorithm used in SSPT is pencil beam algorithm. In this algorithm, the energy loss and scattering caused by passing through pencil beams in materials, treated as the interaction in a kernel. The kernel was calculated by depth and lateral dose distribution function. The depth dose distribution function, using Percent Depth Dose; PDD which output by Monte Carlo code; GEANT4 (Geometry and Tracking version4).The lateral dose distribution function, using a two-dimensional standard normal distribution (Eq. 1).

$$f(x, y) = \frac{1}{2\pi\sigma_x\sigma_y\sqrt{1-\rho}} \times \exp\left[-\frac{1}{2(1-\rho^2)} \times \left\{ \frac{(x-\mu_x)^2}{\sigma_x^2} - 2\rho \frac{(x-\mu_x)(y-\mu_y)}{\sigma_x\sigma_y} + \frac{(y-\mu_y)^2}{\sigma_y^2} \right\}\right] \quad (1)$$

By quoting a spot position and proton energy created by VQA, some dose distribution was created in MATLAB. Treatment volume is 5×5×2 cm<sup>3</sup>, proton energies are 112.7 ~ 125 MeV, Number of spots are 869, etc.

Fig.1 indicates dose distributions with no respiratory movement (D<sub>ref</sub>), with respiratory movement (D<sub>resp</sub>) and a dose error distribution of difference dose (D<sub>error</sub>). D<sub>resp</sub> is subtracted from D<sub>ref</sub>, and D<sub>error</sub>-Maximum difference dose in D<sub>error</sub> is defined as Error<sub>max</sub>. Error<sub>max</sub> are shown in Table 1 and 2. You can see the improvement of administration dose by respiratory gating irradiation in Table 3.

By using our in-house dose calculation program in SSPT, we verified the impact of respiratory movement on dose distributions and indicated that respiratory gating irradiation improved dose distributions.

Table 1 Maximum difference dose at several amplitudes

| Amplitude (15 bpm)       |            |            |             |
|--------------------------|------------|------------|-------------|
| (LR, CC) (mm)            | (0.5, 0.2) | (2.5, 7.7) | (1.8, 24.6) |
| Error <sub>max</sub> (%) | +0.83      | +15.34     | -46.08      |

Table 2 Maximum difference dose at several respiratory cycles

| Respiratory cycle (LR, CC) =<br>(1.8 mm, 24.6 mm) |    |        |        |        |
|---|----|--------|--------|--------|
| Cycle (bpm)                                       | 10 | 15     | 20     |        |
| Error <sub>max</sub> (%)                          |    | -52.37 | -46.08 | -39.56 |

Table 3 Maximum difference dose with-respiratory gating irradiation

| Respiratory gating       | OFF    | ON     |
|--------------------------|--------|--------|
| Error <sub>max</sub> (%) | -46.08 | -10.41 |

Fig.1 Dose distributions with some variation

## BEAM COMMISSIONING OF A NEW PROTON THERAPY FACILITY

Yuya Azuma<sup>1</sup>, Kunihiko Tateoka<sup>1</sup>, Yasuhiro Hasegawa<sup>1</sup>, Noriyuki Araki<sup>2</sup>, Seiichi Adachi<sup>2</sup>, Masaru Takagi<sup>1</sup>, Masato Hareyama<sup>1</sup>

<sup>1</sup>Proton Therapy Center, Sapporo Teishinkai Hospital, Japan

<sup>2</sup>Toyo Medic Co., Ltd.

**Key words:** Proton Therapy, Beam Commissioning, Wobbling Method

### Purpose

Beam commissioning for proton therapy started from this spring in our facility. In the commissioning, performance of proton beams is investigated and dose distributions of proton beam are compared with results of a treatment planning system (TPS) in order to achieve accurate proton therapy.

### Methods

Proton therapy system in Sapporo Teishinkai Hospital (Hokkaido, Japan) consists of a cyclotron (P235, Sumitomo Heavy Industries, Ltd.) and a TPS (Eclipse Protons ver.13.7, Varian Medical Systems, Inc.). Our system has both wobbling system and scanning system. The commissioning for proton therapy with wobbling method started from this spring. In the commissioning, measurements of several parameters of proton broad beams are performed. Beam data are also compared with results from TPS calculation.

### Results

Flatness of spread-out Bragg peak (SOBP) and lateral dose distribution are investigated.

For the most of ridge filters, flatness of SOBP and lateral dose distribution result in less than 2.5%. For some ridge filters, flatness is large due to the ripple in the SOBP, but even in this case, TPS calculation is consistent to the beam data with acceptable error.

### Conclusions

Beam commissioning of proton therapy with wobbling method is held in our facility. TPS calculation is consistent to the beam data with acceptable error for proton therapy.

## DESIGN OF AN EXTERNAL BEAM PORT ON A 16.5 MEV MEDICAL CYCLOTRON

Johan Asp<sup>1</sup>, Shahraam Afshar<sup>2</sup>, Alexandre Santos<sup>3</sup>, Eva Besak Sansom<sup>4</sup>

<sup>1</sup>South Australian Health and Medical Research Institute, Australia

<sup>2</sup>Laser Physics and Photonic Devices, University of South Australia, Australia

<sup>3</sup>Department of Medical Physics, Royal Adelaide Hospital, Australia

<sup>4</sup>Institute for Health Research, University of South Australia, Australia

**Key words:** Monte Carlo simulation

### Purpose

Irradiating biological samples using protons from medical cyclotrons is a promising tool in preclinical radiobiology. This project aims to develop an external beam port on a GE-PETtrace cyclotron. During routine production, the cyclotron uses beam currents around 135 nA. However, 1-10 nA is required for suitable dose rates in radiobiological applications. Therefore, this project aims to reduce beam intensity, measure low beam currents with significantly higher resolution than standard, and add beam scattering foils to reduce beam fluence.

### Methods

A Havar foil was mounted on the end of the cyclotron beamline to produce an external proton beam of 1 cm diameter. The cyclotron was run in manual mode to produce stable low current beams between 10-1000 nA. The low target currents were measured by a picoampere metre controlled using an in-house LabView interface. Additionally, Monte Carlo simulations were performed (SRIM) to model scatter foils to broaden and flatten the beam before hitting the target.

### Results

Stable beam currents below 100 nA have been achieved and accurately monitored by the picoampere meter. However, dose rates delivered by these beam currents are around 500 Gy/s due to the intensity of the beam and the small target volume irradiated by protons. SRIM Monte Carlo simulations have shown that using two 0.127 mm gold foils spreads the beam to  $\sim 4 \times 4 \text{ cm}^2$  and reduces the proton energy to  $7.5 \pm 0.5 \text{ MeV}$ .

### Conclusions

Stable beam currents below 100 nA have been achieved on a medical cyclotron with successful monitoring using a picoampere meter. Dual gold scattering foils achieved biologically relevant doses between 1-10 Gy.

## QUANTITATIVE EVALUATION OF THE RANGE DEGRADATION EFFECT ACCORDING TO THE SLOPE OF THE RANGE COMPENSATOR IN THE PASSIVE SCATTERING PROTON THERAPY

Wook-Geun Shin<sup>1</sup>, Hak Soo Kim<sup>2</sup>, Jong Hwi Jeong<sup>2</sup>, Se Byeong Lee<sup>2</sup>, Chul Hee Min<sup>3</sup>

<sup>1</sup>Yonsei University, Republic of Korea

<sup>2</sup>Proton Therapy Center, National Cancer Center, Ilsan, Republic of Korea

<sup>3</sup>Department of Radiation Convergence Engineering, Yonsei University, Wonju, Republic of Korea

**Key words:** Monte Carlo simulation, proton therapy, range compensator, range degradation, TOPAS

### Purpose

It is known that the pencil beam algorithm (PBA) has a limitation in predicting the scattering effect. The aim of this study is to quantitatively evaluate the range degradation due to the slope of the range compensator using the tool for particle simulation (TOPAS) Monte Carlo (MC) tool.

### Methods

The therapeutic beam with 15-cm-range, 15-cm-modulation, and 10-cm-field-size was employed. To analyze the effect of the slope, the thicknesses of the compensator in the isocentric line were set as 5 cm and the six slopes between 0-5 (dy/dx) were used with MC simulation. To assess the percent depth dose (PDD), the water phantom of 200x200x200 mm<sup>3</sup> was positioned at the downstream of the compensator and the central line was divided into the dose matrices of 1x1x0.1 mm<sup>3</sup>.

### Results

In order to quantitatively evaluate the simulation results, the distal-fall-off-width was defined as the distance between the D20 and D80. The proton beam range was decreased from 91.1 to 87.7 mm and distal-fall-off-widths were from 2.1 to 26.1 mm with the compensator of 0-5 slope. This range degradation was caused by two reasons; those are the changed tracks of the proton beams due to the scattering in the compensator, and the scattering effect in the phantom.

### Conclusions

The current study shows the contribution of the range compensator to the dose distribution with the range degradation. When the compensator slope is steeper than 2, patient dose planned by PBA should be independently validated using MC method.

## INVESTIGATION OF FORMULATION DEPENDENCE ON DOSE-QUENCHING OF *PRESAGE* IN A PROTON BEAM

Mitchell Carroll<sup>1</sup>, Geoffrey Ibbott<sup>1</sup>

<sup>1</sup>MD Anderson Medical Physics, USA

**Key words:** 3D Dosimetry, proton

### **Purpose**

Dose-quenching has been observed in *PRESAGE*® dosimeters when irradiated by protons and has been linked to the relative concentration of radical initiator (RI) to leuco dye responder. This work investigated the magnitude of that relationship.

### **Methods**

Ten *PRESAGE*® dosimeters were manufactured with RI concentrations ranging from 3-30% (w/o) and 2% (w/o) leuco dye. These were stored under the same conditions for 72 hours prior to irradiation. A passively scattered 225-MeV proton beam with 10cm SOBP was selected, and the *PRESAGE*® dosimeters were irradiated to 200cGy in a solid water phantom. Track-averaged LET of the beam was calculated analytically. Point measurements were taken along the dose profiles of the dosimeters and compared with ionization chamber measurements. The magnitude of the under-responding for each formulation was calculated by the residual of these measurements.

### **Results**

*PRESAGE*® formulations below 21% RI under-responded by less than 3% in the most proximal, low-LET, SOBP region. In the most distal, high-LET, SOBP region, the minimum under-response was 12.2% which occurred in the 12% RI formulation. The quenching magnitude was asymmetrical and had greater under-responding at higher concentrations. At 30% RI, the under-response increased to 73.7%.

When the magnitude of under-response was correlated to LET, 9-18% RI formulations under-responded linearly with LET (RMSE $\leq$ 0.7%). Formulations outside this range corresponded superlinearly to LET with the gradient increasing alongside RI concentration.

### **Conclusions**

*PRESAGE*® demonstrated dose-quenching dependence on formulation as well as linearity to LET at specific RI concentrations. This has potential to allow for quenching minimization as well as analytical correction.

## **1.2 Monte Carlo Simulation**

# 1D GAMMA ANALYSIS ON THE EFFECT OF MEAN ELECTRON ENERGY, FWHM AND XY JAW THICKNESS FOR SMALL FIELDS

R. C. X. Soh<sup>1</sup>, L. K. R. Tan<sup>1</sup>, M. S. L. Goh<sup>1</sup>, S. Yani<sup>3</sup>, F. Haryanto<sup>3</sup>, W. S. Lew<sup>1</sup>, J. C. L. Lee<sup>1,2</sup>

<sup>1</sup>School of Physical and Mathematical Sciences, Nanyang Technological University, Singapore

<sup>2</sup>Division of Radiation Oncology, National Cancer Centre Singapore, Singapore

<sup>3</sup>Department of Physics, Faculty of Mathematics and Natural Sciences, Institut Teknologi Bandung, Indonesia

**Key words:** Monte Carlo, 1D gamma analysis, optimal parameters, small fields

**Introduction:** Monte Carlo method is the current gold standard for accurately predicting the dose distribution in any medium for radiotherapy. With the increase in the number of cancer patients that is treated with stereotactic radiosurgery and stereotactic body radiation therapy, there is an accompanying emphasis for small field dosimetric simulations. Most Monte Carlo studies estimate the initial electron beam parameters such as the mean electron energy and the radial intensity (Full Width at Half Maximum, FWHM) by trial and error methods, and concluded that the determination of these parameters must be done independently for small fields [1]. However, this approach can be tedious and time-consuming. The current study propose an alternate approach in the determination of these parameters using 1D gamma analysis on the depth dose and lateral profile, for small field sizes such as  $2 \times 2 \text{cm}^2$ ,  $1 \times 1 \text{cm}^2$  and  $0.5 \times 0.5 \text{cm}^2$ .

**Methods:** EGSnrc-based BEAMnrc code was used to generate the phase space files for a 6 MV photon beam from a Varian Clinac X linear accelerator. EGSnrc-based DOSXYZnrc code was used to calculate the dose in water. Measured data was obtained using Sun Nuclear EDGE Detector and crosschecked against PTW Diode SRS (PTW-60018) measurements in a Sun Nuclear 3D water scanner. In order to obtain the optimal initial mean electron energy and FWHM, 1D gamma analysis was conducted by imposing the passing criteria from  $\gamma_{2.0\%/2.0\text{mm}}$  to  $\gamma_{0.3\%/0.3\text{mm}}$ . The parameter with the highest percentage of gamma passes with the most stringent passing criteria will be deemed optimal. The gamma index for the out-of-field (OOF) dose region was also investigated by varying the thickness of the XY jaws of the linear accelerator. Measurement and

comparison of the lateral beam profile were performed at depth = 1.5 cm.

**Results:** Gamma analysis with a stringent passing criteria of  $\gamma_{0.3\%/0.3\text{mm}}$  shows that unique sets of parameters are required for optimal and accurate simulation for small fields (Fig. 1) [2]. Furthermore, as field sizes decreases, higher initial electron beam energy and smaller FWHM are required to match measured data (Table 1). Doses in the OOF region increases with thinner XY jaws.

Table 1: Optimal parameters for small fields based on 1D gamma analysis

| Field Size                   | Mean Electron Energy (MeV) | FWHM (cm) | Decrease in XY Jaws Thickness / $\Delta t$ (cm) |
|------------------------------|----------------------------|-----------|---|
| $0.5 \times 0.5 \text{cm}^2$ | 6.2                        | 0.1       | 0   |
| $1 \times 1 \text{cm}^2$     | 6.1                        | 0.1       | 0   |
| $2 \times 2 \text{cm}^2$     | 6.1                        | 0.2       | 1.0   |

**Discussion:** Results show that independent determination of small field optimal parameters using 1D gamma analysis is potentially more effective and accurate than using direct dose difference test in trial and error methods [3]. Optimal parameters can be clearly distinguished using increasingly stringent passing criteria. By simulating thinner XY jaws, doses in the OOF region can be increased to match measured data due to higher beam transmission [4].

**Conclusion:** In general, unique sets of parameters are required for an accurate Monte Carlo simulation for small field sizes. The trial and error method to determine the optimal initial electron parameters can be avoided by using the 1D gamma analysis procedure presented in this study.

## References:

- O. Chibani, B. Mofteh, C.M.C. Ma (2011) On Monte Carlo modeling of megavoltage photon beams: A revisited study on the sensitivity of beam parameters. Med. Phys. 38:188-201.
- J. Pena, D.M. Gonzalez-Castano, F. Gomez et al. (2007) Automatic determination of primary electron beam parameters in Monte Carlo simulation. Med Phys 34(3):1076-1084.
- D.A. Low, W.B. Harms, S. Mutic et al. (1998) A technique for the quantitative evaluation of dose distributions. Medical Physics 25(5):656-661.
- F.M. Khan (2003) The Physics of Radiation Therapy. Lippincott Williams & Wilkins. p234-235.

Corresponding author email: rogersohcx@gmail.com

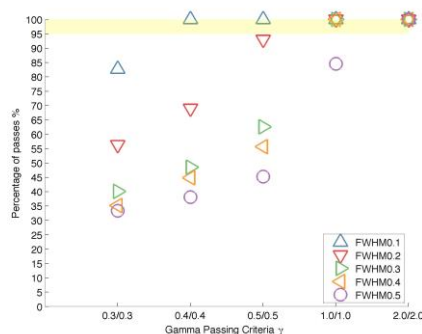


Fig.1 1D Gamma analysis of FWHM for field size  $0.5 \times 0.5 \text{cm}^2$

## **AN ASSESSMENT ON THE USE OF RADCALC TO VERIFY RAYSTATION ELECTRON MONTE CARLO PLANS**

Yunfei Hu<sup>1</sup>, Ben Archibald-Heeren<sup>2</sup>, Mikel Byrne<sup>2</sup>

<sup>1</sup>Radiation Oncology Centres Gosford, Australia

<sup>2</sup>Radiation Oncology Centres Wahroonga

**Key words:** Monte Carlo simulations

### **Purpose**

Raystation is the planning system implemented for electron Monte Carlo (EMC) planning and RadCalc, a pencil-beam- algorithm software, is implemented as the patient-specific quality assurance software. In this study, the authors investigated different types of clinical plans and designed a series of test plans to compare the behaviour of Raystation and Radcalc for electron MU calculation under different circumstances.

### **Methods**

Twenty EMC patients' plans were selected. For each clinical patient in Raystation, three sets of plans were created; 1) Patient's original plans; 2) Plans recalculated with homogenous water density within patient geometry; and 3) Plan recalculated in a standard water phantom free of inhomogeneity or surface curvature. Two series of test plans were also generated, with one focusing on the test of inhomogeneity and the other on the test of surface curvature. Monitor units were compared.

### **Results**

RadCalc agrees well with Raystation with clinical plans of flat surface and homogeneous material. When there is inhomogeneity around the dose point the agreement becomes worse. Difference becomes more significant if surface curvature is involved in the clinical plan. Test plans further proved these conclusions.

### **Conclusions**

Only in very basic plans can RadCalc be used to check EMC plans from Raystation. Complex factors such as surface curvature and inhomogeneity, which are often dominant factors in dose calculation in a patient geometry, fail to be handled by RadCalc's algorithm. Simplifying these plans by copying the plans onto a water phantom greatly improves the accuracy of RadCalc, but also significantly reduces the comprehensiveness and the confidence of the verification.

## **MONTE CARLO-BASED ASSESSMENT OF IMPACTS OF HETEROGENEOUS MATERIALS ON DOSE DISTRIBUTIONS USING THREE-DIMENSIONAL GAMMA ANALYSIS IN INTRACAVITARY BRACHYTHERAPY FOR CERVICAL CANCER**

Tran Thi Thao Nguyen<sup>1</sup>, Hidetaka Arimura<sup>2</sup>, Yoshifumi Oku<sup>3</sup>, Takashi Yoshiura<sup>4</sup>

<sup>1</sup>Kyushu University, Japan

<sup>2</sup>Faculty of Medical Sciences, Kyushu University

<sup>3</sup>Kagoshima University Hospital

<sup>4</sup>Graduate School of Diagnostic Radiotherapy, Kagoshima University

**Key words:** heterogeneous materials, intracavitary brachytherapy, Monte Carlo simulation, 3D gamma analysis

### **Purpose**

The aim of this study was to quantitatively evaluate impacts of heterogeneous materials on dose distributions using three-dimensional (3D) gamma analysis in intracavitary brachytherapy for cervical cancer.

### **Methods**

Monte Carlo (MC) simulations were performed for the comparison of two dose distributions between a water phantom and a 3D patient physical map (PPM) by employing a Particle and Heavy Ion Transport code System (PHITS) (Ver.2.73). The PPM was obtained by converting computed tomography (CT) values of planning CT images of a cervical cancer patient to physical densities and material compositions using the Schneider's conversion table. An encapsulated Ir-192 source (HDR Ir-192 model mHDR-v2r) was set at fifteen dwell positions in a titanium applicator consisting of a uterine tandem and two ovoids. The gamma pass rates (%) representing the degree of agreement between the two dose distributions were evaluated with acceptance criteria of 3 mm/3%. A billion photons were generated from the source in the water phantom and the PPM in the MC simulations. Cut-off energies of photon, electron, and positron were set to 1 keV, 0.512 MeV, and 0.512 MeV, respectively.

### **Results**

The mean  $\pm$  standard deviation of for gamma pass rates was  $84.61\% \pm 2.12\%$  for four fractions. The major discrepancy between the two dose distributions was found around the applicator region.

### **Conclusions**

This work revealed the discrepancy on the dose distributions between the water phantom and the 3D PPM due to the presence of the applicator.

## **OPTIMIZATION OF A NOVEL FLAT PANEL DETECTOR STRUCTURE FOR REMOVING SCATTER RADIATION: EFFECTS OF VERTICAL AND HORIZONTAL ALIGNMENTS OF LEAD TO INCIDENT X-RAYS**

Yongsu Yoon<sup>1</sup>, Junji Morishita<sup>2</sup>, Kihyun Kim<sup>3</sup>, Jungmin Kim<sup>3</sup>

<sup>1</sup>Department of Health Sciences, Graduate School of Medical Sciences, Kyushu University, Republic of Korea

<sup>2</sup>Department of Health Sciences, Faculty of Medical Sciences, Kyushu University

<sup>3</sup>School of Health And Environmental Sciences, Korea Univeristy

**Key words:** Flat panel detector, Scatter radiation

### **Purpose**

To examine the effects of vertical and horizontal lead components of a novel flat panel detector system on its performance with angulated incident X-rays.

### **Methods**

The authors have investigated the feasibility of a novel system with net-like lead in the substrate layer, matching the ineffective area on the thin-film transistor layer to block the scattered radiation such that only primary X-rays could reach the effective area. As the novel system comprises net-like lead in the substrate layer, there were possibilities of vertical lead alignment perpendicular to the direction of the incident X-rays and horizontal lead alignment parallel to the direction of incident X-rays may affect the image quality if the incident X-ray is angulated in clinical usage. To evaluate the effects of vertical and horizontal lead components on the incident X-rays, we measured the image contrast of four systems: the no-grid system, novel system, and novel system with vertical or horizontal lead components by Monte Carlo simulation.

### **Results**

The image contrasts of the four systems were 0.47, 0.57, 0.51, and 0.51 at 0°; 0.18, 0.19, 0.15, and 0.19 at 15°; and 0.24, 0.24, 0.23, and 0.26 at 30°. As the results indicate, the vertical lead components degrade the image quality as the angle of incident X-rays increases.

### **Conclusions**

Although the novel system showed significantly good performance at 0° as well as applicability to angulated incident X-rays, the effects of vertical lead components should be considered to obtain better performance.

## **VERY SMALL CIRCULAR FIELDS OUTPUTS AND CORRECTION FACTORS KQ OF THE MICRODIAMOND AND THE EFD-3G DETECTORS**

Eyad Alhakeem<sup>1</sup>, Sergei Zavgorodni<sup>2</sup>

<sup>1</sup>University of Victoria, Canada

<sup>2</sup>British Columbia Cancer Agency–Vancouver Island Center

**Key words:** small fields, microdiamond, correction factors, Monte Carlo, TrueBeam

### **Purpose**

The purpose of this work was to determine relative output factors (OFs) and kq factors for small circular fields using microDiamond, EFD-3G, and EBT3 detectors as well as MC calculations.

### **Methods**

OFs for Varian TrueBeam with circular cones of 1.3, 2.5, 3.5, 10, 12.5, 15 and 40 mm diameter at isocenter were measured using GafChromic EBT3 films, microDiamond and electron EFD-3G diode detectors. BEAMnrc/DOSXYZnrc codes were used to calculate OFs in water phantom with 1x1x1 mm<sup>3</sup> voxels for the 10-40 mm cones and 0.1x0.1x0.1 mm<sup>3</sup> voxels for the 1.3, 2.5 and 3.5 mm cones, respectively. kq as defined in Alfonso et al formalism were calculated for the microDiamond and EFD-3G detectors using egs\_chamber code. kq factors were also derived experimentally using EBT3 measurements.

### **Results**

OFs determined by different methods agreed within 3.5% for the collimators of 10mm diameter and larger. For cones of 1.3 and 3.5mm OF determined by different methods differed by up to 70.0 and 12.3%, respectively. For the cones of 3.5-15mm MC and experimentally derived kq agree within 4.1% to 1.95% and ranged from 0.9 to 1.0 respectively. Calculated k factors were 1.047, 0.897, 0.891 and 0.961, for 1.3, 2.5, 3.5 and 12.5mm cones, respectively.

### **Conclusions**

MC calculated and experimental output and kq factors agree within 3% for the cones larger than 3.5mm. Dosimetry of the very small 1.3 - 3.5 mm beams presents considerable challenges and requires multiple independent methods of verification.

## **A FIRST STEP TOWARD THE PROMPT GAMMA RAY IMAGING TECHNIQUE DURING ANTI-PROTON THERAPY USING BORON PARTICLE FOR TUMOR MONITORING**

Han-Back Shin<sup>1</sup>, Do-Kun Yoon<sup>1</sup>, Joo-Young Jung<sup>1</sup>, Moo-Sub Kim<sup>1</sup>, Sunmi Kim<sup>1</sup>, Tae Suk Suh<sup>1</sup>

<sup>1</sup>The Catholic University of Korea, Republic of Korea

**Key words:** Antiproton, boron, monitoring, prompt gamma ray

### **Purpose**

In this study, we propose a tumor monitoring technique using prompt gamma rays emitted from the reaction between an antiproton and a boron particle, and verify the improvement of the therapeutic effectiveness of the antiproton boron fusion therapy compared with proton and antiproton beam without boron.

### **Methods**

The tumor monitoring system during the antiproton therapy was simulated using the Monte Carlo simulation. We acquired the percentage depth dose of the antiproton beam from a water phantom with and without three boron uptake regions (BURs; region A, B, and C). The obtained results were compared with the performance of a proton beam. The tomographic image of the BURs was reconstructed using prompt gamma ray events which sorted from the single photon emission tomography (SPECT) during the treatment. In addition, receiver operation characteristic curve (ROC), signal-to-noise ratio and contrast-to-noise ratio were analyzed to evaluate the reconstructed image.

### **Results**

The prompt gamma ray peak was observed at 719 keV in the energy spectrum. Moreover, the maximum peak of antiproton beam with boron is three times greater than that of proton beam. The reconstructed image was successfully identified from the simulation results. In terms of the ROC analysis, the area under the curve values were 0.647 (A), 0.679 (B), and 0.632 (C).

### **Conclusions**

We confirmed the feasibility of tumor monitoring during the antiproton therapy as well as the superior therapeutic effect of the antiproton boron fusion therapy. These findings may be beneficial for the development of a more accurate particle therapy.

## EVALUATION OF MONTE CARLO SIMULATION OF 6 MV FLATTENING FILTER FREE LINAC WITH EXPERIMENTS AND AAA CODE TREATMENT PLANNING SYSTEM

M. Arif Efendi<sup>1</sup>, Amporn Funsian<sup>2</sup>, Thawat Chittrakarn<sup>1</sup>, Tripob Bhongsuwan<sup>1</sup>

<sup>1</sup>Department of Physics, Faculty of Science, Prince of Songkla University, Hatyai, Songkhla 90110, Thailand;

<sup>2</sup>Department of Radiology, Faculty of Medicine, Prince of Songkla University, Hatyai, Songkhla 90110, Thailand

**Key words:** Anisotropic Analytical Algorithm, Gamma Analysis, Linear Accelerator, PRIMO

**Introduction** Monte Carlo (MC) simulations have been used for a long time in calculations of particle traces in Linear Accelerator (LINAC) [1]. MC simulation gives more accurate dose calculation than deterministic system [2]. Currently, treatment planning system just uses deterministic system such as Analytical Anisotropic Algorithm (AAA) [3]. AAA code was developed by Drs. Waldemar Ulmer and Wolfgang Kaissl [4].

TrueBeamSTx is the most modern LINAC machine marketed by Varian Medical Systems (Palo Alto, California, USA) [5]. TrueBeamSTx has several unique features such as Flattening Filter Free (FFF) photon beams, reengineered electron beams with new scattering foil geometries, updated imaging hardware/ software, and automatic control system[6].

The aim of this work is to evaluate the accuracy of MC simulations of TrueBeamSTx Varian LINAC for FFF beams, against experiments and calculations using AAA code.

**Methods** MC simulation using PRIMO code [7], experimental measurement and AAA code calculation were performed for the calculation of depth dose, cross-plane and in-plane beam profiles inside water phantom. Depth dose profiles were determined at 4×4, 10×10, 40×40 cm<sup>2</sup> field sizes. Cross-plane and in-plane beam profiles were made inside water phantom at depth 1.5, 5, 10, and 20 cm for each field size. Experimental result and AAA code calculation were imported to PRIMO code and compared using gamma analysis.

**Results:** Depth dose comparison of PRIMO simulations with experiments and AAA code calculations, together with difference in both of them are shown in figure 1. Blue line is from PRIMO simulation result, red cross for experimental result, and green circle for AAA code calculation.

Comparison between MC simulations of beam profiles for 10×10 cm<sup>2</sup> jaws open field and experiments shows more than 46% passing criteria for cross-plane and more than 47% for in-plane. Comparison with AAA code shows more than 89% and more than 86% passing criteria for cross-plane and in-plane, respectively.

**Discussion:** PRIMO simulation had a good agreement with experiments and AAA calculations in depth dose profiles. PRIMO simulation gave more than 95% passing criteria.

Beam profiles of PRIMO simulations had a better agreement with AAA calculations than experimental results.

The achieved agreement of MC simulations with AAA code calculations was more than 69%.

**Conclusion:** MC simulation using PRIMO code could probably be used as an alternative for dosimetric calculation instead of company AAA code. It gave the same result as AAA code used for treatment planning. However, MC simulation took a very long time to obtain good result. It can be concluded that the period of simulation is still big issue in MC simulation.

### References:

1. Padilla-Cabal, F., Pérez-Liva, M., Lara, E., Alfonso, R., & Lopez-Pino, N. (2015). Monte Carlo calculations of an Elekta Precise SL-25 photon beam model. *Journal of Radiotherapy in Practice*, 14(3), 311–322.
2. Juste, B., Miró, R., Abella, V., Santos, A., & Verdú, G. (2015). Use of MOSFET dosimeters to validate Monte Carlo radiation treatment calculation in an anthropomorphic phantom. *Radiation Physics and Chemistry*, 116, 208–213. doi:10.1016/j.radphyschem.2015.04.025
3. Sievinen, J., Ulmer, W., Kaissl, W., & others. (2005). AAA photon dose calculation model in Eclipse. Palo Alto (CA): Varian Medical Systems, 118, 2894.
4. Ulmer, W., & Harder, D. (1995). A Triple Gaussian Pencil beam Model for Photon beam Treatment Planning. *Zeitschrift für Medizinische Physik*, 5(1), 25–30. doi:10.1016/S0939-3889(15)70758-0
5. Rodriguez, M., Sempau, J., Fogliata, A., Cozzi, L., Sauerwein, W., & Brualla, L. (2015). A geometrical model for the Monte Carlo simulation of the TrueBeam linac. *Physics in medicine and biology*, 60(11), N219.
6. Glide-Hurst, C., Bellon, M., Foster, R., Altunbas, C., Speiser, M., Altman, M., ... others. (2013). Commissioning of the Varian TrueBeam linear accelerator: a multi-institutional study. *Medical physics*, 40(3), 31719.
7. Rodriguez, M., Sempau, J., & Brualla, L. (2013). PRIMO: A graphical environment for the Monte Carlo simulation of Varian and Elekta linacs. *Strahlentherapie und Onkologie*, 189(10), 881–886.

Corresponding author email: tripob.b@psu.ac.th

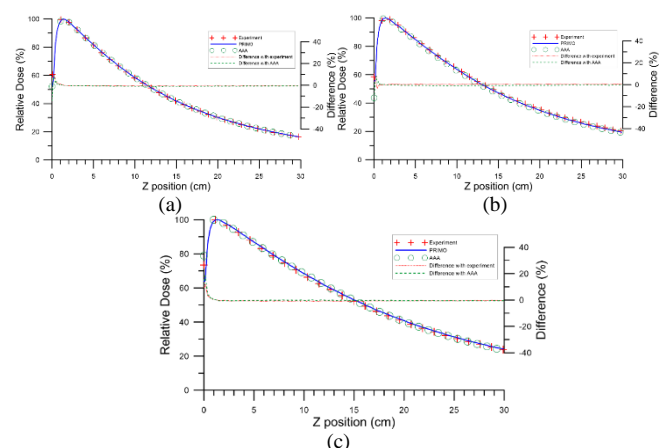


Fig.1 Depth dose profiles comparison for field sizes (a) 4×4, (b) 10×10, and (c) 40×40 cm<sup>2</sup>

## **DOSE VERIFICATION OF LUNG STEREOTACTIC BODY RADIOTHERAPY (SBRT) PLANS USING THE EGSNRC/BEAMNRC MONTE CARLO CODE**

Sri Herwiningsih<sup>1</sup>, Andrew Fielding<sup>1</sup>

<sup>1</sup>Queensland University of Technology, Australia

**Key words:** Early stage NSCLC, dose calculation accuracy, collapsed cone convolution, Monte Carlo simulation

### **Purpose**

This work aims to verify the accuracy of the dose calculation with a collapsed cone convolution (CCC) algorithm in the treatment planning of non-small cell lung cancer (NSCLC) stereotactic body radiation therapy (SBRT) using the Monte Carlo (MC) technique.

### **Methods**

Twenty early stage NSCLC SBRT treatment plans previously calculated using the CCC algorithm (Pinnacle3 RTPS) were re-calculated using the EGSnrc/BEAMnrc MC code. The CCC and MC dose distributions were analysed using the CERR software. The dosimetric parameters to the PTV and organ at risks (OARs) were evaluated based on the dosimetric criteria outlined in the RTOG 1021 trial protocol. A paired student t-test was performed to evaluate the difference between the CCC and MC calculations with a statistical significance defined as  $p \leq 0.05$ .

### **Results**

Although the CCC overestimated the PTV coverage in 11 plans, there was no significant difference in the mean PTV coverage of the prescribed dose between the CCC ( $95.13 \pm 1.62\%$ ) and MC ( $95.14 \pm 2.67\%$ ) calculations ( $p=0.97$ ). In general, the CCC overestimated the dose to the OARs, except for normal lung tissues and the brachial plexus. Underestimation was observed for V10.5Gy and V11.4Gy of the normal lung tissues, however, the mean difference is not statistically significant ( $p=0.45$  and  $p=0.55$ , respectively).

### **Conclusions**

Although the CCC algorithms might still be adequate for dose calculation of the lung SBRT plans, the availability of the commercial fast Monte Carlo-based algorithms TPS would be highly recommended in order to achieve a maximum radiotherapeutic gain.

## **IMPLEMENTATION OF MONTE CARLO DOSE CALCULATIONS TO CLINICAL QUALITY ASSURANCE PROCESS**

Sergei Zavgorodni<sup>1</sup>, Reid Townson<sup>1</sup>

<sup>1</sup>BC Cancer Agency, Vancouver Island Center; University of Victoria, Canada

**Key words:** Monte Carlo, VMAT, IMRT, Quality Assurance, Treatment Planning

### **Purpose**

To implement Monte Carlo (MC) based dose calculations to clinical quality assurance process.

### **Methods**

MC system developed in our institution combines fast modeling of particle transport through the linac head with VMC++ dose calculations. Secondary collimators are presented as perfectly absorbing planes, and collimator positions are synchronized with MLC motions to allow modeling of VMAT and IMRT in jaw-tracking mode. Particle fluence above the secondary collimators is presented as a phase space provided by the linac manufacturer. Conversion of MC calculated dose to absolute units in Gy is performed using experimentally measured backscatter radiation into the linac monitor chamber. Calculations are performed on patients' CT data and the MC dose distributions are imported to the TPS (Varian Eclipse) in "dose-to-water" format. Dose comparison is performed using the tools provided by the TPS.

### **Results**

MC calculations have been accepted into clinical use for independent verification of the dose provided by commercial TPS as of August 2015. Since then all IMRT, VMAT and complex conformal plans produced in our clinic have been calculated using the MC system. Over 500 plans have been calculated so far; the mean PTV dose difference between MC and TPS calculations was -0.3% (1.0% SD), ranging from -2.7% to +2.7% except for two lung cases where the differences were +2.8% and -6%. Typical calculation times for clinical IMRT and VMAT cases are ~5-10 minutes on a 24-core server.

### **Conclusions**

MC calculations are a valuable clinical tool, providing efficient QA for complex treatment plans.

## **MONTE CARLO SIMULATION BEACHEDMARKED AGAINST MEASUREMENT FOR AN ELEKTA SYNERGY LINAC EQUIPPED WITH AN AGILITY 160-LEAF MLC**

Oluwaseyi Michael Oderinde<sup>1</sup>, Freek Du Plessis<sup>1</sup>

<sup>1</sup>University of The Free State, South Africa

**Key words:** Agility 160-leaf MLC, Monte Carlo, Dosimetry parameter, advanced radiotherapy

### **Purpose**

The Agility<sup>TM</sup> multileaf collimator (Elekta AB, Stockholm, Sweden) is designed to meet present day demand for fast, accurate, and efficient radiation treatment. The aim of this study was to characterize photon beams using a detailed linac model in BEAMnrc of the Linac equipped with an Agility MLC and to validate the beam data with measurement.

### **Methods**

The head of the Linac was simulated for 1 x 1 up to 30 x 30 cm<sup>2</sup> square field sizes for 6, 10 and 15 MV photon beams using the BEAMnrc MC Code. Photon beam data were calculated in a homogenous water phantom using the DOSXYZnrc MC Code. The MC calculations were validated by water bath measurements that included beam profiles, depth dose and relative output factors.

### **Results**

For the square field sizes considered, the MC calculations and physical measurements agreed to within 2.6% for percentage depth doses (PDDs), lateral dose profiles and output factors.

### **Conclusions**

BEAMnrc input linac model is highly accurate up to 2%/2 mm. It has the potential to be used for dose calculation in advanced radiotherapy treatment planning.

## EVALUATION OF LATENT UNCERTAINTIES FROM VARIAN TRUEBEAM PHOTON PHASE-SPACES IN MONTE CARLO DOSE CALCULATIONS FOR STANDARD AND SMALL FIELDS

Eyad Alhakeem<sup>1</sup>, Sergei Zavgorodni<sup>2</sup>

<sup>1</sup>University of Victoria, Canada

<sup>2</sup>British Columbia Cancer Agency–Vancouver Island Center

**Key words:** Monte Carlo, Latent uncertainty, TrueBeam, Phase-space file

### **Purpose**

To evaluate the latent variance (LV) of Varian TrueBeam photon phase-space files (PSF) for standard and very small stereotactic fields.

### **Methods**

BEAMnrc/DOSXYZnrc Monte Carlo (MC) software was used to score phase-spaces (PSB) with small number of particles under the jaws or cone collimators. PSB for 6MV, 6MV-FFF, 10MV, 10MV-FFF and 15MV photon beams with 10x10 cm<sup>2</sup> field size as well as those from 6MV scored under circular cones of 0.13, 0.25, 0.35, 1.0, 1.2, 1.5 and 4cm diameter were transported into a water phantom with particle recycling ranging from 10 to 1000. Dose variances were scored and LV evaluated as per Sempau et al.

### **Results**

Calculated LVs were greatest at the phantom surface and decreased with depth until reached a plateau at 10 cm depth. For 10x10cm<sup>2</sup> fields and 0.5x0.5x0.5cm<sup>3</sup> voxel size LVs were found to be 0.96%, 0.54%, 0.69%, 0.35% and 0.57% for the 6MV, 6MV-FFF, 10MV, 10MV-FFF and 15MV PSFs, respectively at the depth of 10cm. For the cones of 0.13cm 0.25cm 0.35cm and 1cm calculated LVs were 75.6%, 24.8%, 17.6% and 8.0% respectively. For voxel sizes of 0.02x0.02x0.5cm<sup>3</sup>, 0.05x0.05x0.5cm<sup>3</sup> and 0.1x0.1x0.5cm<sup>3</sup> and the cone of 2.5cm calculated LV, were 61.2%, 40.7% and 22.6% respectively.

### **Conclusions**

A single PSF could be used in a standard field and voxel size MC simulation to produce results with and acceptable statistical uncertainty of 1%. However, for small beams, a few PSFs would have to be summed up and used to achieve sub-percent uncertainty.

## **SIMULATION BASED DETECTOR MATERIAL COMPARISON FOR PROMPT GAMMA RAY IMAGING DURING BNCT**

Do-Kun Yoon<sup>1</sup>, Joo-Young Jung<sup>1</sup>, Han-Back Shin<sup>1</sup>, Moo-Sub Kim<sup>1</sup>, Sunmi Kim<sup>1</sup>, Tae Suk Suh<sup>1</sup>

<sup>1</sup>The Catholic University of Korea, Republic of Korea

**Key words:** Detector materials, Monte Carlo simulation, prompt gamma ray, BNCT.

### **Purpose**

Purpose of this study was to conclude the best detector materials among commercialized detector materials for prompt gamma ray imaging during BNCT using Monte Carlo simulation results.

### **Methods**

In order to simulate the sixteen detector materials, physical specifications of detectors were collected from the other study results. When each detector material was irradiated by an epi-thermal neutron beam with same conditions, the detection efficiency and energy resolution value were acquired using the Monte Carlo simulation code. In addition, the prompt gamma ray image was reconstructed by using the best six performance detector materials during the BNCT treatment simulation. After the acquisition of images, the image quality evaluation process was performed to compare the detector materials.

### **Results**

The prompt gamma ray images were successfully reconstructed by using the best six detector materials (BGO, GSO, LYSO, CZT, HPGe, CdTe). We could confirm the difference of image quality according to the use of different detectors. Moreover, the quantitative evaluation results support the difference of the quality clearly.

### **Conclusions**

Surely each detector has both the strong point and the weak point. From these results, we can more clearly decide the detector materials for prompt gamma ray imaging during the BNCT according to the preference.

## **VALIDATION OF GEANT4-BASED IMRT AND VMAT DOSE CALCULATION SYSTEM WITH IN-HOUSE DEVELOPED DICOM-RT INTERFACE**

Hyun Joon Choi<sup>1</sup>, Hyo Jun Park<sup>1</sup>, Wook-Geun Shin<sup>1</sup>, Jung-In Kim<sup>2</sup>, Chul Hee Min<sup>1</sup>

<sup>1</sup>Department Of Radiation Convergence Engineering, Yonsei University, Republic of Korea

<sup>2</sup>Seoul National University Hospital, Republic of Korea

**Key words:** Geant4, IMRT, VMAT, DICOM-RT interface

### **Purpose**

For the intensity-modulated radiation therapy (IMRT) and volumetric-modulated arc therapy (VMAT) dose calculation using Monte Carlo (MC) method, it is required to implement and validate the fully automatic system for accurate evaluation of the patient dose distribution. The aim of this study is to develop a precise and automated procedure for IMRT and VMAT simulations using DICOM files and to evaluate the patient dose with Geant4-based 4D simulation.

### **Methods**

The MC commissioning of 6 MV Varian Clinac 2300 IX was performed based on the measurement data. For the MLC validation, the simulated dose distributions calculated using the Geant4 were compared with the measured one using the film with the in-house designed bar pattern opening. Automated DICOM-RT interface was developed for the beam condition setting and the phantom modeling. Finally, IMRT and VMAT plans in heterogeneous and homogeneous phantom were compared between our system and the clinical treatment planning system (TPS).

### **Results**

The maximum local dose difference in each PDD and lateral profile was less than 2%. In MLC validation study, dose distributions were well-matched between MC and measurement within 1% for leakage dose and lateral profile differences. Overall IMRT and VMAT dose distributions showed fairly good agreement between in-house developed system and commercial TPS in the water and lung phantom, especially, gamma pass rates in the PTV region of the lung plan were higher than 94%.

### **Conclusions**

The current study using in-house developed system shows possibility to accurately verify IMRT and VMAT plan based on MC 4D simulations.

## DOSE DISTRIBUTION STUDY OF A HUMAN HEAD PHANTOM USING GEANT4 SIMULATION TOOLS

H C Gooch Jr<sup>1</sup>, S A Nawang<sup>1</sup>, A M Bacala<sup>1</sup>, A Kimura<sup>2</sup>

<sup>1</sup>MSU-Iligan Institute of Technology, Iligan City, Philippines; <sup>2</sup>Ashikaga Institute of Technology, Ashikaga-chi Tochigi, Japan

**Key words:** Medical imaging, DICOM, GEANT4, gMocren, Monte Carlo

**Introduction** In this study, DICOM images were used to create a human head phantom to simulate accurate dose delivery to the patient for treatment planning. Unnecessary dose delivered to the patient is very hazardous, thus Monte Carlo simulation is vital. For this purpose, we demonstrate the Monte Carlo simulation using GEANT4 and gMocren as the visualization tool for treatment planning.

**Methods** The human head phantom was constructed from the actual DICOM image of a human head. The density profile of the DICOM images is used to construct the phantom material. The phantom was irradiated with 10 million electrons and X-rays of energies 6 MeV to 22 MeV. The Monte Carlo simulation is done using GEANT4 and gMocren as the visualization tool.

**Results:** Results show the phantom received a total dose of 0.434 Gy and 0.161 Gy from the 6 MeV electron and X-ray beams, respectively. The dose distribution is peaked at 0.98 cm for the 6 MeV electron beam and increases slightly as the beam energy is increased. For X-rays, the peak is positioned at 2.81 cm and increases to 7.71 cm as the beam energy is increased from 6 MeV to 22 MeV.

**Conclusion:** Monte Carlo simulation using GEANT4 and gMocren can provide analysis and graphical outputs that can be used in a clinical setting. As observed, specific beam of certain energy can be used for treatment at different depths. The dose distribution of electron and X-ray beams for energies 6 MeV to 22 MeV show as expected.

### References:

1. Agostinelli, S., et.al. (2003) Geant4, a simulation toolkit, Nucl.Instrum. Methods Phys. Res. NIM A 506: 250-303.
2. Akinori Kimura, Kyoko Hasegawa, et.al. (2015) gMocren: Visualization software for Monte Carlo simulators for radiotherapy, Journal of Advance Simulations in Science and Engineering. Japan Society for Simulation Technology. Vol.2 No.1 45-62.
3. Podgorzak, E.B. (2006) Radiation Physics for Medical Physicists, Springer-Verlag Berlin Heidelberg.

Corresponding author email: jungoooc@gmail.com

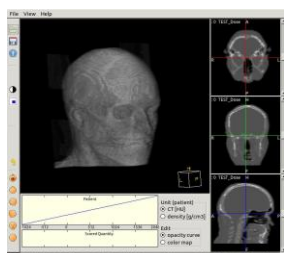


Fig.1 The human head phantom.

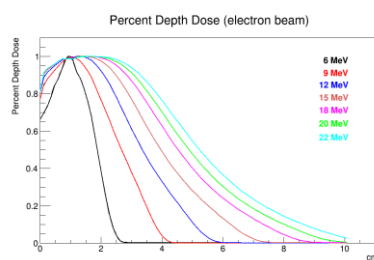


Fig.2 PDD distribution for electron beam.

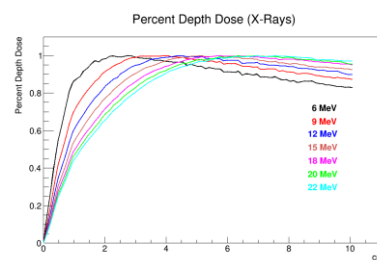


Fig.3 PDD distribution for x-rays.

Currently, about half of all cancer patients receive radiation therapy as part of their treatment plan. The longstanding aim of

radiation therapy is to deliver sufficient radiation dose to eradicate or control the tumor volume with minimal damage to the surrounding normal tissues in the patient. Medical imaging has proved critical in the treatment of patients and improving health care. The most widely used in medical applications is the DICOM. Producing these images require the use of radiation delivered to the different parts of the body of the patient. These procedure is also done when using radiation in treatments of cancer but using higher energies just enough to damage cancerous tissues in a specific area. To accomplish accurate delivery of dose to the patient, simulation tools and treatment planning software and other treatment devices have been developed.

To simulate the passage of radiation to the human body, the Monte Carlo simulation is done using Geant4 (Geometry and Tracking) [1] and gMocren [2] as a visualization tool. Actual DICOM images is used to create the human phantom. The density of the material of each voxel is calculated by taking the average density index of each pixel of the image contained in the voxel. Then the density index of the images is used to construct the phantom material based on the values given by the International Commission on Radiation Units and Measurements (ICRU).

Fig.1 shows the main window of gMocren showing the resulting human head phantom constructed from the actual DICOM images. The simulation setup mirrors the actual clinical setup for radiotherapy. The phantom is subjected to electron and x-ray beam energies of 6, 9, 12, 15, 18, 20 and 22 MeV. The phantom is irradiated with ten (10) million electrons and another independent run with ten (10) million x-rays. Both beams are positioned 100 cm from upper end of the phantom head directed in the x-direction of the patient (z-direction of the accelerator axis). Dose and energy deposits from the beams are calculated to determine the depth dose distribution. The output of the simulation is stored on a gMocren format for visualization and analysis.

The visual outputs from gMocren also show that the dose, in the case of electron beam, is concentrated near the entrance of the beam while the dose is distributed along the direction of the beam and exits the phantom in the case of the x-ray beam. The percent depth dose distribution (PDD) for electron beams is shown in Fig.2 and for x-rays in Fig.3. These plots are comparable when using water as the phantom material as shown in reference [3].

# THE SIMULATION OF LINEAR ACCELERATOR BY USING MONTE CARLO CODE EGSNRC

D T Tai<sup>1,3</sup>, N D Son<sup>2</sup>, T T H Loan<sup>3</sup>, H D Tuan<sup>3</sup>, and H P W Anson<sup>4</sup>

<sup>1</sup>Depart Dong Nai General Hospital, Vietnam; <sup>2</sup>Chi Anh Medical Technology Co.,Ltd, Vietnam; <sup>3</sup>University of Science, Vietnam; <sup>4</sup>PTW-Asia Pacific Ltd, Hong Kong.

**Key words:** Monte Carlo simulation, EGSnrc.

**Introduction:** An accuracy of the simulation linear accelerator (Linac) used in radiotherapy is an essential requirement for calculation algorithm using Monte Carlo (MC) method. In this study, a MC modeling of the High Performance Defining Head (HPD) Siemens Primus linear accelerator in 6 MV photon beams at Dong Nai general hospital was performed. The BEAMnrc and the DOSXYZnrc codes were used to perform all calculation of the dose distribution in the water phantom. Percent depth dose (PDD) and Beam profiles (OCR) obtained from simulation will be compared with corresponding experimental data to evaluate the accuracy of the simulation by using not only the point to point errors but also the gamma evaluation method.

## Methods

### Monte Carlo simulation of the HPD Linac with BEAMnrc

The BEAMnrc user code was used to simulate a 6MV photon beams from a Siemens Primus linear which consist of 9 component modules: Vacuum envelope (SLABS), the target (SLABS), the flattening filter (FLATFILT), chambers for monitoring the Linac output (CHAMBER), mirror made of SiO<sub>2</sub> (MIRROR), the jaws X and jaws Y made of tungsten (JAWS), reticle tray of mica (SLABS), and slab air (SLABS).

### Dose calculation with DOSXYZnrc

The EGSnrc user code DOSXYZnrc was used to calculate dose distribution in a water phantom (50×50×30 cm<sup>3</sup> water tank). The water phantom was located at source to surface distance (SSD) of 100 cm. The electron and photon cut-off energy (ECUT, PCUT) was set to 0.7 MeV and 0.01 MeV, respectively. 10<sup>9</sup> histories were simulated.

### Experimental measurements

All the measurements were made using the IBA Dosimetry "blue phantom" scanning system, controlled by Omnipro-Accept 7.4c software. All measurements were done in water using the Scanditronix Wellhofer CC13 cylindrical ionization chamber having an active volume of 0.13 cm<sup>3</sup>.

### Method to compare measured and simulated data

Conventionally, the agreement between calculations and measurements was usually evaluated by calculating the mean point to point dose error. However, the evaluation of the result using the point to point errors could give rise to high overall errors in low dose areas and high dose gradient regions. Therefore, calculating the gamma index is an alternative method for this analysis recently [2]. This method has become the gold standard for the comparison between measured and calculated dose distributions.

## Results:

### Percent Depth Dose (PDD)

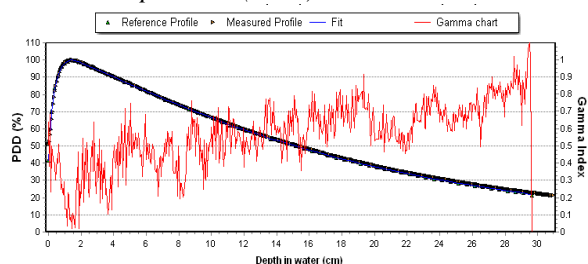


Figure 1. Comparisons of simulated with measured PDD Beam profiles (the off-centre ratio-OCR)

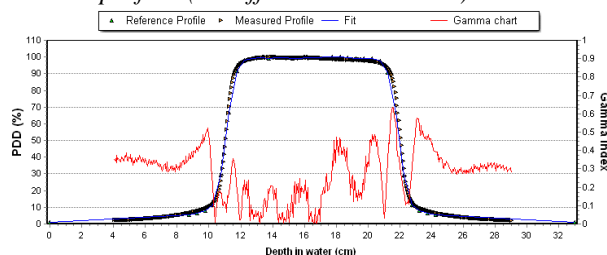


Figure 2. The 6MV photon beam profile in water

## Discussion:

In this work, the Siemens Primus linear accelerator was successful simulated with excellent agreements between simulations and measurements with average dose difference of 0.7% for PDD and beam profile flatness less than 2%. The percentage gamma passing rate is 100% with 1% dose difference and 1 mm distance to agreement as acceptance criteria.

## Conclusion:

The BEAMnrc and DOSXYZnrc codes package have very good accuracy in calculating dose distribution and it can be considered as a bright method for dose calculations in patient. A Monte Carlo simulation of a Siemens Primus M5497 was done the results of which will be used for future studies.

## References:

1. B. Walters, I. Kawrakow and D. W. O. Rogers 2004, DOSXYZnrc User's Manual, National Research Council of Canada Report, PIRS -794, revB, Ottawa: NRC., ISBN 92-95003-44-6
2. Daniel A. Low, William B. Harms and James A. Purdy (1998), A technique for the quantitative evaluation of dose distributions, Med. Phys. 25(5).
3. M. Aljamal and A. Zakaria (2013), Monte Carlo Modeling of a Siemens Primus 6 MV Photon Beam Linear Accelerator, Australian Journal of Basic and Applied Sciences 7(10), 340-346

Corresponding author email: thanhtai\_phys@yahoo.com

## **1.3 Clinical Dosimetry**

## **ADDRESSING CURRENT CHALLENGES IN PRIMARY DOSIMETRY METROLOGY BY GRAPHITE AND WATER CALORIMETRY**

Benjamin Rapp

CEA, France

### **Key words**

Absorbed dose, Graphite and water calorimetry, Small radiation fields

### **Purpose**

Until ten years ago, calorimetry was used to establish and consolidate the absorbed dose to water standards for high energy photon and electron beams, in large and static radiation fields. But, with the fast evolution of radiotherapy a concern was raised regarding the need of new dosimetry reference adapted to the new treatment technics, to fill the gap between the standard reference and clinical conditions. A particularly challenging area is the establishment of standards for small radiation fields.

### **Methods**

Calorimetry is the best technique available to perform absolute measurement of absorbed dose. As a primary laboratory for metrology of ionizing radiations we have a long experience in building and operating both graphite and water calorimeters.

### **Results**

Two new graphite calorimeters were built, and a new approach, based on dose-area product measurement, has been investigated in order to bring the calibration conditions closer to the clinical use with radiation fields of size lower than 2 cm. New dosimetry standards are established simultaneously, by water and graphite calorimetry, on the new medical accelerator TrueBeam from Varian, recently installed in our laboratory. These new detectors, the results obtained and the outcome for customers' detector calibration will be discussed.

### **Conclusions**

It is very valuable to operate both graphite and water calorimetry. It allows to check the consistency of the new dosimetric standards by two independent methods when it is possible, or to select the most efficient type of detector in term of uncertainty.

## **ANALYSIS OF DOSES TO TRIGEMINAL NERVE, BRAINSTEM IN GAMMA KNIFE RADIOSURGERY - A DOSIMETRIC STUDY**

Vindhyavasini Pandey

Govt MVM College, India

### **Key words**

Gamma Knife, Stereotactic Radiosurgery, Trigeminal Neuralgia, Brainstem Dose

### **Purpose**

The present study is to analyse the dose distribution inside the tiny trigeminal nerve target and also to analyse the dose received in brainstem.

### **Methods**

Ten cases are considered in the present study to analyse the dose distribution in TN (Trigeminal Neuralgia) target and organ at risk. The treatment plan was analysed for target dose conformity, homogeneity and dose coverage. Gamma Plan version 8.3.1 is used for planning of cases.

### **Results**

In the brainstem the volume doses  $D_{min}$ ,  $D_{max}$ ,  $D_{mean}$  were taken for analysing the doses in the brain stem. The mean value of maximum dose within the trigeminal nerve target was  $91.04 \pm 1.6$  and minimum dose was  $12 \pm 5.05$ . The mean conformity index was  $1.4 \pm 0.235$  and the homogeneity index was  $2.018 \pm 0.035$ . The mean dose to brainstem was  $1.17 \pm 0.23$  and the mean value of maximum dose to brainstem was  $15.83 \pm 2.2$ .

### **Conclusions**

The present study shows the superior sparing of brainstem and reasonable of target coverage. Use of 4mm Collimator and plugging provides the best result to spare brainstem and deliver the desired dose to the Root Entry Zone in Trigeminal Neuralgia.

## **CLINICAL EXPERIENCE WITH DELTA4 PHANTOM FOR PATIENT SPECIFIC QUALITY ASSURANCE OF MODERN RADIOTHERAPY TREATMENT TECHNIQUES**

Raju Srivastava<sup>1</sup>, Carlos De Wagter<sup>2</sup>

<sup>1</sup>University Hospital Ghent, Belgium

<sup>2</sup>Department of Radiation Oncology, University Hospital Ghent, Belgium

### **Key words**

IMRT VMAT Rapid Arc, Delta4 phantom

### **Purpose**

The new treatment modalities in radiotherapy have made it possible to deliver highly conformal and individually- shaped dose distributions. These techniques require a dedicated QA (Quality Assurance) procedure for dosimetric verification of a planned dose distribution to check for the agreement between a dose distribution calculated by the Treatment Planning System (TPS) and the corresponding measured dose distribution. The result of the QA is also dependent on the evaluation procedure, for example the choice of acceptance criteria and tolerance levels. In this work, The Delta4 phantom was used for verification of intensity-modulated radiation therapy (IMRT) and volumetric modulated arc therapy (VMAT) and Rapid Arc.

### **Methods**

150 patients were analyzed with Delta4 phantom. During verification process, TPS (Pinnacle and Eclipse) plans were transferred to the phantom and the treatment plan is recalculated. All plans were analyzed using the three parameter %DA (limit 3%), DTA (limit 3%), (limit 3 mm), and -index with the 3% dose tolerance and 3 mm distance to agreement in relation to the treatment planning system.

### **Results**

Results confirmed a good agreement between the two distributions with high and conformed dose to the target and low dose to the organ at risk. All measurements passed with at least 95% of the measurements within - criteria.

### **Conclusions**

Our results indicate that Delta4 phantom is an effective and efficient method for the patient specific QA. Although Delta4 appears a straightforward device for measuring dose and allows measure in real time, it is recommended to use with caution for QA.

## **RISK OF DEVICE MALFUNCTION IN CANCER PATIENTS WITH CARDIOVASCULAR IMPLANTABLE ELECTRONIC DEVICES UNDERGOING RADIOTHERAPY: A REVISION TO THE LAST UPDATED GUIDELINES**

Guadalupe Martín-Martín, Elena Moreno Merino, M<sup>a</sup> Nieves Estival Ortega  
H.U.Fuenlabrada, Spain

### **Key words**

Radiotherapy, Pacemakers, ICD, guidelines

### **Purpose**

Practical recommendations for patients undergoing radiation therapy with Cardiac Implantable Electronic Devices (CIEDs) were published in 2012 by the Dutch Society of Radiotherapy. We aimed to investigate the main dosimetric factors that affected our patients in order to update these recommendations.

### **Methods**

Between 2009 and 2016, 60 patients with CIEDs were treated in our institution. Dose to the CIED was assessed for every patient who was classified according to his/her risk.

### **Results**

Our patient focus group consisted of 44, 15 and 1 patients categorized into low, medium and high risk groups, respectively. The median age was 76 (range 54-98) years. Most treatments were prostate (20%), brain metastasis (16%), head and neck (9%), lung (7%), and esophagus (5%). The prescribed dose ranged from 8 to 78 Gy with a daily dose ranging from 1.8 to 8 Gy. The maximum doses to the CIEDs were 179.1 cGy, 751 cGy and 1270 cGy, for the low, medium and high risk groups, respectively. Radiation therapy was safely delivered in all patients, but in two of them we experienced a CIED malfunction, while Cone-Beam acquisition previous to the treatment was taking place.

### **Conclusions**

Radiation dose seems to play a lesser role while beam energy appears to be the essential factor in inducing damaging effects in CIEDs. Inactivation of anti-tachycardia therapies during RT and heart rhythm monitoring seems to be redundant. Photon beam energy should be limited to  $\leq 10$  MV and the CIED should never be included within the cone-beam radiation field.

## **CHARACTERIZATION OF GAFCHROMIC EBT3 FILM FOR IN-VIVO DOSE MEASUREMENT IN INTRAOPERATIVE RADIOTHERAPY (IORT)**

Zainor Zaili, Ung Ngie Min, Jeannie Wong Hsiu Ding, Jong Wei Loong, See Mee Hoong, Nur Aishah Mohd Taib, Lee Kien Yiap  
University of Malaya, Malaysia

### **Key words**

GafChromic EBT3, radiochromic film dosimetry, radiation dosimetry, IORT

### **Purpose**

This project aims to characterize the GafCharomic EBT3 film for radiation dosimetry of 50 kV x-ray beam in IORT methods. The calibration of GafChromic EBT3 film was performed using the Intrabeam IORT system (Carl Zeiss Meditec AG, Oberkochen, Germany) operating using a 50 kV x-ray source. The percentage depth dose (PDD) measurement, net optical density yield at different depths, energy dependence and the surface dose on spherical applicators were measured.

### **Results**

In the PDD measurement, results from the EBT3 film were found to have a maximum deviation of  $4.4 \% \pm 2.2 \%$  (1SD) compared to the ionization chamber measurement. Measurement of a fixed prescribed dose delivered at various depths to obtain the net optical density yield showed a maximum enhanced response by a factor of 1.5 at depth of 3.5 mm due to the beam hardening effect. The energy dependence between 50 kV and 6 MV for dose range 8 Gy and below showed a variation of  $20.6 \% \pm 0.3 \%$ . For dose range above 8 Gy there was energy dependence of  $19.1 \% \pm 0.01 \%$  for the two identical beams qualities. There were maximum deviations of 11.0 % and 19.25 % from the prescribed dose for applicator sizes of 3.5 and 4.0 cm respectively during dose verification on applicator surface.

### **Conclusions**

GafChromic EBT3 film is shown to be useful dosimeter for assessing dose characteristic in IORT.

# **RADIOBIOLOGICAL EVALUATION OF DOSE CALCULATION ALGORITHMS ON PROSTATE STEREOTACTIC BODY RADIOTHERAPY USING FLATTENING FILTER-FREE BEAM**

Sang-Won Kang<sup>1</sup>, Jin-Beom Chung<sup>2</sup>, Jeong-Woo Lee<sup>3</sup>, Tae- Suk Suh<sup>1</sup>

<sup>1</sup>Department of Biomedical Engineering And Research Institute of Biomedical Engineering, College of Medicine, The Catholic University of Korea, South Korea

<sup>2</sup>Department of Radiation Oncology, Seoul National University Bundang Hospital, Seongnam

<sup>3</sup>Department of Radiation Oncology, Kunkuk University Medical Center

## **Key words**

SBRT, Radiobiological evaluation, Acuros XB

## **Purpose**

The purpose of this study is to evaluate the dosimetric and radiobiological impact of Acuros XB (AXB) and Anisotropic Analytic Algorithm (AAA) dose calculation algorithms on prostate stereotactic body radiation therapy plans with flattening-filter free (FFF) modes.

## **Methods**

For thirteen patients with prostate cancer, SBRT planning was performed using 10-MV photon beam with FF and FFF modes. The total dose prescribed to the PTV was 42.7 Gy in 7 fractions. All plans were initially calculated using AAA algorithm in Eclipse treatment planning system (11.0.34), and then were re-calculated using AXB with the same MUs and MLC files. The four types of plans for different algorithms and beam energies were compared in terms of homogeneity and conformity. To evaluate the radiobiological impact, the tumor control probability (TCP) and normal tissue complication probability (NTCP) calculations were performed.

## **Results**

For PTV, both calculation algorithms and beam modes lead to comparable homogeneity and conformity. However, the averaged TCP values in AXB plans were always lower than in AAA plans with an average difference of 5.3% and 6.1% for 10-MV FFF and FF beam, respectively. In addition, the averaged NTCP values for organs at risk (OARs) were comparable.

## **Conclusions**

This study showed that prostate SBRT plan were comparable dosimetric results with different dose calculation algorithms as well as delivery beam modes. For biological results, even though NTCP values for both calculation algorithms and beam modes were similar, AXB plans produced slightly lower TCP compared to the AAA plans.

# **RECOMBINATION CORRECTION FACTOR $K_s$ FOR ARTISTE SIEMENS FLATTENING FILTER FREE X-RAY THERAPY BEAMS. RECOMMENDATIONS FOR A REFERENCE IONIZATION CHAMBER**

Guadalupe Martín  
H.U.Fuenlabrada, Spain

## **Key words**

Absolute dosimetry, Relative dosimetry, Ionization chamber, FFF

## **Purpose**

High dose rate flattening filter free (FFF) beams pose new considerations for accurate reference and relative dosimetry. The purpose of this work was to investigate the recombination effect of three types of commonly used ionization chambers (Farmer, PinPoint and Semiflex) in FFF beams of Siemens Artiste Linacs.

## **Methods**

The recombination correction factors  $K_s$  were measured on two Siemens Artiste Linacs for FFF beams of 7 MV. They were obtained from  $1/V$  versus  $1/Q$  curves (Jaffé plots) for different dose per pulse (DPP) values, and as a function of depth. Volume-averaging effects were determined by two methods: (1) direct measurement of volume-averaging via cross-calibration and (2) through a calculation of the radial profile volume-averaging correction factor,  $Prp$ , previously described in the literature.

## **Results**

Accurate  $K_s$  factors were determined and compared to the obtained with the simplified method of two-voltage analysis. Volume-averaging effects were 0.3% when measured with a Farmer-type chamber. Errors in measured  $K_s$  at different depths were minimal so a factor to correct for the effect of ion recombination in PDD profiles is unnecessary.

## **Conclusions**

The correction factor  $K_s$  depends only on the DPP specific for every Linac and the chamber type. For all chambers investigated more accurate coefficients than  $K_s$  were determined for a greater accuracy on ion recombination effects. Recommendations for a preferred ion chamber for absolute or relative dosimetry are given for Artiste Siemens Linacs. However, accurate commissioning of reference ionization chambers following our methods to apply the established correction factors  $K_s$  and  $Prp$ , is strongly recommended.

## DEVELOPMENT OF PATIENT-SPECIFIC THREE-DIMENSIONAL-PRINTED PHANTOMS FOR ARTIFICIAL *IN VIVO* DOSIMETRY

T Kamomae<sup>1</sup>, H Shimizu<sup>2</sup>, T Nakaya<sup>3</sup>, K Okudaira<sup>3</sup>, Y Miyake<sup>3</sup>,  
M Komori<sup>4</sup>, H Oguchi<sup>4</sup>, T Komada<sup>5</sup>, Y Itoh<sup>1</sup>, S Naganawa<sup>5</sup>

<sup>1</sup>Department of Therapeutic Radiology, Nagoya University Graduate School of Medicine, Nagoya, Japan;

<sup>2</sup>Department of Radiation Oncology, Aichi Cancer Center Central Hospital, Nagoya, Japan;

<sup>3</sup>Department of Radiological Technology, Nagoya University Hospital, Nagoya, Japan;

<sup>4</sup>Department of Radiological Sciences, Nagoya University Graduate School of Medicine, Nagoya, Japan;

<sup>5</sup>Department of Radiology, Nagoya University Graduate School of Medicine, Nagoya, Japan

**Key words:** 3D printing, *in vivo* dosimetry, IMRT

**Purpose:** Pre-treatment intensity-modulated radiation therapy quality assurance is performed using simple rectangular or cylindrical phantoms [1, 2]. Dosimetric errors caused by complex patient-specific anatomy are thus absent in the evaluation. In this study, we developed a system for producing patient-specific three-dimensional (3D)-printed phantoms for artificial *in vivo* dosimetry.

**Methods:** An anthropomorphic head phantom containing bone and paranasal sinus was scanned by computed tomography (CT). The threshold CT value corresponding to the equivalent of the size between the surface rendering and actual phantom was determined. Based on the surface rendering data, the patient-specific phantom was made using a fused-deposition-modeling-based 3D printer. A polylactic acid material was selected as the printing material. The printed phantom has the specification that glass dosimeters and radiochromic films can be inserted. The size, CT value, and physical characteristics of photon beams were evaluated.

**Results:** To obtain the same size for the actual phantom, the optimal threshold CT value for surface rendering was  $-600$  HU. The size difference between the actual and printed phantoms was less than 1 mm. The CT value of the printed phantom was  $-6 \pm 18$  HU. In the treatment planning system, the differences in water-equivalent path lengths were increased for beams passing the bone. When the same MU was irradiated, the dose difference was mostly less than 3%.

**Conclusion:** We developed a system for producing patient-specific 3D-printed phantoms. The modeling accuracy of the printed phantom was acceptable; however, the printing material for the bone still needs improvement.

### References:

1. Ezzell GA, Burmeister JW, Dogan N, et al.: IMRT commissioning: Multiple institution planning and dosimetry comparisons, a report from AAPM Task Group 119, *Med Phys*, 36(11):5359-73, 2009.
2. Kamomae T, Itoh Y, Okudaira K, et al.: Dosimetric impact of dental metallic crown on intensity-modulated radiotherapy and volumetric-modulated arc therapy for head and neck cancer, *J Appl Clin Med Phys*, 17(1):5870, 2016.

Corresponding author email: kamomae@med.nagoya-u.ac.jp

Figure 1 shows the pictures of the anthropomorphic head phantom containing bone and paranasal sinus and the 3D-printed phantom. The total printing time for this part was about 20 hours.

The size difference between the anthropomorphic and 3D-printed phantom was less than 1 mm (Fig. 2a). The 3D-printed objects have a tendency to shrink ( $< 1$  mm) during cooling. This tendency depends on the size, position, and printing material. The printing parameters and scaling factor may correct the volume reduction. The CT value profiles of each phantom showed good agreement except for bone areas (Fig. 2b). The CT value of the soft tissue area in the 3D-printed phantom was  $-6 \pm 18$  HU.

For the single static field irradiation, the measured dose difference between the 3D-printed and the anthropomorphic phantom was  $2.0 \pm 2.1\%$ . Furthermore, for the two-arc volumetric modulated arc therapy (VMAT) plan, the measured dose difference was  $2.9 \pm 2.8\%$ . Measured doses on the 3D-printed phantom were slightly increased compared to the anthropomorphic one. We consider that the main reason for this difference is the low CT value (i.e., electron density) of the printing material in the bone areas.

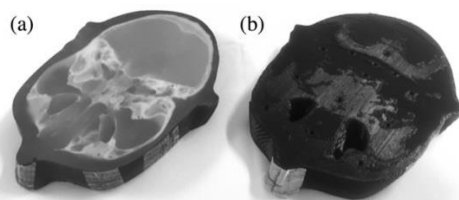


Fig. 1 Picture of the anthropomorphic head phantom containing bone and paranasal sinus (a) and the 3D-printed phantom (b).

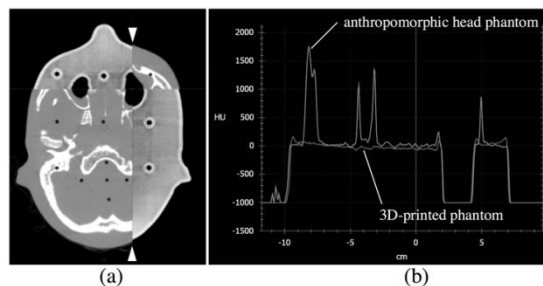


Fig. 2 (a) Overlaid transversal images of the anthropomorphic head phantom and 3D-printed phantom. (b) Hounsfield unit number profiles along the line connecting the white arrows in image (a).

## **FEASIBILITY STUDY OF FABRICATED GERMANIUM DOPED OPTICAL FIBRE AS A POTENTIAL DOSIMETER SUBJECTED TO PROTON BEAM**

Noramaliza Mohd Noor<sup>1</sup>, Mohammad Faizal Hassan<sup>1</sup>, Wan Nordiana Wan Abdul Rahman<sup>2</sup>, Takahiro Tominaga<sup>3</sup>, Moshi Geso<sup>4</sup>, Hiroaki Akasaka<sup>5</sup>, David Andrew Bradley<sup>6</sup>

<sup>1</sup>Department of Imaging, Faculty of Medicine and Health Sciences, Universiti Putra Malaysia, 43400 Serdang, Selangor, Malaysia

<sup>2</sup>School of Health Sciences, Universiti Sains Malaysia, 16150 Kubang Kerian, Kelantan, Malaysia

<sup>3</sup>Department of Clinical Radiology, Faculty of Health Sciences, Hiroshima International University, Higashi-Hiroshima City, Hiroshima 739-2695, Japan

<sup>4</sup>Discipline of Medical Radiations, School of Medical Sciences, Royal Melbourne Institute of Technology University, Bundoora, Victoria 3083, Australia

<sup>5</sup>Division of Radiation Oncology, Kobe University Graduate School of Medicine, Kobe, Hyogo 650-0017, Japan

<sup>6</sup>Centre for Nuclear and Radiation Physics, Department of Physics, University of Surrey, Guildford, Surrey GU2 7XH, United Kingdom

### **Key words**

Dosimetric characteristics, Fabricated Ge-doped optical fibre, Proton beam

### **Purpose**

Thermoluminescence (TL) properties of novel cylindrical germanium (Ge) doped optical fibres have been studied to develop a potential dosimeter for proton beam measurements. The essential dosimetric characteristics that have been investigated are glow curves, linearity, reproducibility and fading.

### **Methods**

The fabricated Ge-doped fibres were sectioned into ~6.0 mm length, weighed and annealed at 400°C for one hour. A Scanning Electron Microscope (SEM) and Energy Dispersive X-ray Spectroscopy (EDXS) analysis were performed to map the Ge distribution across the deposited region. The TLD-100 chips (LiF:Mg, Ti) were used as a reference dosimeter to allow the relative response of the fibres to be evaluated. The commercially available optical fibres (CorActive, Canada) were also used to provide comparable TL response. The irradiations were delivered through use of a proton accelerator at Hyogo Ion Beam Medical Center in Japan with energies of 150 and 210 MeV and doses from 1 to 10 Gy.

### **Results**

As expected, the fabricated fibres have been found to offer excellent linearity of TL yield, with correlation coefficient more than 0.99. The fabricated fibres also demonstrated good reproducibility being within 1.7% to 5.5% following repeated measurements (n=3). The fabricated fibres can also be re-used many times after annealing. After 96 days of storage at room temperature, the fabricated fibres (2.3% Ge-doped) provided the least degree of signal loss (12.1%) compared to the commercial fibres (22.6%).

### **Conclusions**

The novel fabricated Ge-doped optical fibre studied demonstrates an excellent candidate for dose measurement in proton beam therapy.

## **RADIATION DOSE PERTURBATION ON PATIENTS WITH ESOPHAGEAL SELF-EXPANDABLE STENTS: AN EXPERIMENTAL MODEL**

Flor Herrera-Martinez<sup>1</sup>, Javier Altamirano-Garcia<sup>2</sup>, Miguel Rodriguez-Ponce<sup>2</sup>, Francisco Lozano-Garcia<sup>2</sup>, Francisco Rodriguez-Pendas<sup>2</sup>

<sup>1</sup>INCAN, Mexico

<sup>2</sup>Instituto Nacional De Cancerologia

### **Key words**

Esophageal stents, Radiation dosimetry, Treatment planning.

### **Purpose**

To determine the perturbations in the total radiation dose distribution due to self-expandable stents for patients with esophageal carcinoma for each stent model used by the endoscopy department.

### **Methods**

A rectangular phantom was used with a plastic insert where the stents available were disposed; to simulate an air cavity inside each stent, latex balloons were used. Simulations for each stent were performed with and without the air cavity. We used Eclipse treatment planning system to calculate the simplest case of an esophageal carcinoma treatment plan (two opposing fields), on two available energies: 6 and 15 MV photons. All of these plans were irradiated using EBT3 radiochromic films and the results were compared with the TPS results.

### **Results**

Maximum difference between dose distribution with air cavity and without it was about 3% on a poliflex model, and this difference was reduced on higher energies. Water-filled stent cases were compared with a no-stent control case, in order to determine the perturbation due to the stent material, founding differences below 1%.

### **Conclusions**

First esophageal carcinoma patients will be treated on a follow clinical essay to determine if this clinical procedure can be used as a treatment protocol, and their side effects. More measurements will be performed using two more energies, in order to have a complete chart for different photon energies used in clinical practice.

## REFERENCE DOSIMETRY FOR SMALL FIELD MEGAVOLTAGE PHOTON BEAM ON STANDARD SYSTEM

Md. Anwarul Islam<sup>1</sup>, Md. Mahmudul Hasan Manna<sup>2</sup>, Golam Abu Zakaria<sup>3</sup>, Md. Abdul Mannan Chowdhury<sup>1</sup>

<sup>1</sup>Jahangirnagar University, Bangladesh.

<sup>2</sup>Gono University

<sup>3</sup>Gummersbach, Academic Teaching Hospital of the University of Cologne

### Key words

Small Field, Reference dosimetry

### Purpose

To explore the present knowledge of reference dosimetry of small sized photon beams based on different international literature, reports and guidelines.

### Methods

All the dosimetric data of small photon fields have been measured with PTW PinPoint 3D, Semiflex and diode detector and compared with the data calculated by Eclipse V8.6 Treatment Planning System (TPS) which was commissioned by PinPoint chamber data for small field and other internationally published data set. The newly proposed formalism by the IAEA/AAPM small field working group, Cross-Calibration and the Daisy-Chaining method is investigated.

### Results

It is found that the Daisy-Chaining method yields 0.2% more close result than the Cross-Calibration method for a 2x2 cm<sup>2</sup> field size. The detector dependence of small field output factor, Semiflex shows largest absolute percent difference for 1x1 cm<sup>2</sup> field which is about 39.65%. The diode shows the best agreement with the TPS and at 1x1 cm<sup>2</sup> field it shows 4.5% over response. The PinPoint 3D chamber shows a consistent good agreement with TPS for all of the measured fields with a maximum deviation of 1.4%. This study also compares the MLC defined small field output factor data with the RPC provided standard dataset and a maximum percent difference of 4.3% and 2.8% is seen for 6 and 10 MV respectively.

### Conclusions

For 2x2 cm<sup>2</sup> and below field size, the dosimetric accuracy and precision becomes most vulnerable and attention should be paid during measurements with appropriate small field detector in accordance with Monte Carlo and different detector system.

## **JAW POSITION DETECTION METHOD IN JAW TRACKING DELIVERY WITH EPID IN CINE MODE**

Toru Kawabata<sup>1</sup>, Satoru Sugimoto<sup>2</sup>, Chie Kurokawa<sup>2</sup>, Keisuke Usui<sup>2</sup>, Tatsuya Inoue<sup>3</sup>, Hironori Nagata<sup>1</sup>, Hiroyuki Watanabe<sup>1</sup>

<sup>1</sup>Juntendo University, Graduate School of Medicine, Japan

<sup>2</sup>Juntendo University, Department of Radiation Oncology, Japan

<sup>3</sup>Juntendo University Urayasu Hospital, Japan

### **Key words**

Jaw position, Jaw tracking, EPID, Cine mode, Bidirectional picket fence

### **Purpose**

To develop a method for detecting jaw positions during jaw tracking delivery using EPID in cine mode.

### **Methods**

Performance of jaw tracking technique was verified by a newly proposed bidirectional picket fence (BPF) test, in which upper leaf pairs moved in the left to right direction and lower leaf pairs moved in the opposite direction. Leaves and jaws repeated move-and-stop alternately during beam delivery to create a picket fence pattern. In the BPF plan, jaws traced MLC aperture and the irradiated patterns were acquired by EPID in cine mode. As for the EPID images, the jaw positions were defined as the 50% dose level in the transmission region under MLCs.

### **Results**

Jaw positions determined by EPID measurements were compared with those expected from the delivered BPF plan. When the jaws stopped, the mean differences were  $0.40 \pm 0.37$ mm for X1 jaw,  $0.76 \pm 0.42$ mm for X2 jaw. On the other hand, when the jaws were moving, the mean differences were  $1.52 \pm 0.81$ mm for X1 jaw,  $1.28 \pm 0.98$ mm for X2 jaw. The differences obtained via "jaws moved" were larger than those of "jaws stopped" case. It is probably due to blurring in the edge of moving jaws introduced by frame averaging.

### **Conclusions**

The jaw positions during jaw tracking delivery were identified using cine EPID acquisition. It was shown that the jaw positions could be determined with a precision better than 2.0mm.

## EFFICIENCY OF DOSE CONTROL SYSTEM AND QUALITY ASSURANCE IN TOMOTHERAPY TREATMENTS

Diana Binny<sup>1</sup>, Craig M Lancaster<sup>1</sup>, Steven R Sylvander<sup>1</sup>, Tanya Kairn<sup>2</sup>, Jamie V Trapp<sup>3</sup>, Scott Crowe<sup>1</sup>

<sup>1</sup> Royal Brisbane And Women's Hospital, Brisbane, Australia

<sup>2</sup> Genesis Cancer Care Queensland, Brisbane, Australia

<sup>3</sup> Queensland University Of Technology, Brisbane, Australia

**Key words:** Tomotherapy, quality assurance, output variations.

### **Purpose**

The purpose of this study was to assess the pre-set TomoTherapy quality assurance (TQA) tool in measuring beam parameters variations over time and also quantifying the effects of the vendor installed Dose Control System (DCS) servo in treatment delivered dose pre and post upgrade.

### **Methods**

TQA daily measurement results from two treatment machines for a period of up to 4 years were assessed. Analysis of beam quality, helical and static output variations, gantry period and phase angle variations and patient co-ordinate system offsets for pre and post DCS upgrade was made. Treatment delivery output variations from the planned dose were also analysed before and after the DCS upgrade. Effects of gantry period variations on the helical and static output were also studied. Patient co-ordinate systems and the effect of gantry phase angle variations were also retrospectively assessed.

### **Results**

It was observed that post DCS, variations in the helical output using the step helical wedge test pre DCS upgrade was reduced from  $\pm 3\%$  to  $\pm 0.5\%$ . However, there were no significant variations in patient treatment dose outputs after DCS upgrade. Energy variations did seem to be a contributing factor to the higher output dose seen during the later phases of DCS upgrade. Correlations were seen between gantry phase angle variations and patient IECx co-ordinate system.

### **Conclusions**

DCS servo upgrade has drastically improved the dose output variations seen in the helical step wedge testing module with no significant changes seen in treatment delivery variations.

## **DETERMINATION OF OUTPUT FACTOR IN HOMOGENEOUS AND INHOMOGENEOUS MEDIUM FOR SMALL FIELD PHOTON BEAM 6 MV**

Andrian Dede Handika<sup>1</sup>, Wahyu Edy Wibowo<sup>2</sup>, Supriyanto Ardjo Pawiro<sup>1</sup>

<sup>1</sup>Department of Physics, Faculty of Mathematics and Natural Sciences, Universitas Indonesia, Depok, Indonesia

<sup>2</sup>Department of Radiotherapy, Fkui/Rscm, Jakarta

### **Key words**

Homogeneous medium, Inhomogeneous medium, Output factor, Small field.

### **Purpose**

This study was aimed to determine output factors of small field for photon beams in homogeneous and inhomogeneous medium.

### **Methods**

Output factor measurements were performed in two techniques; fixed Source Skin Distance (SSD); and fixed Source- Axis Distace (SAD), being carried out using Exradin A16 ionization chamber and Gafchromic EBT3 Film at 5 g/cm<sup>2</sup> depth and various field sizes of 0.8 cm, 2.4 cm, 4 cm, and 10 cm.

### **Results**

The calculated output factors were compared with Monte-Carlo study by Sanchez-Doblado. Results show deviations of output factor for homogeneous medium being less than 4%, whereas in the field size of 0.8 cm and 2.4 cm for inhomogeneous medium the deviation was found to be more than 10%. Difference of output factors deviation against Monte-Carlo study was found to be less than 3% between SSD and SAD techniques.

### **Conclusions**

Inhomogeneous medium gave more influence to output factor especially for field size smaller than 2.4 cm. Output factor did not significantly differ between fixed SSD and fixed SAD techniques.

## **DETERMINATION OF PION OF ION CHAMBERS USED FOR REFERENCE DOSIMETRY OF PASSIVELY SCATTERED AND SPOT SCANNED PROTON BEAMS PRODUCED BY THE SYNCHROTRON OF HITACHI PROBEAT MACHINE**

Narayan Sahoo<sup>1</sup>, Yuting Li<sup>1</sup>, Falk Poenisch<sup>1</sup>, Aman Anand<sup>2</sup>, Jiajian Shen<sup>2</sup>, Martin Bues<sup>2</sup>, Archana Gautam<sup>1</sup>, Xiaorong Zhu<sup>1</sup>, Michael Gillin<sup>1</sup>

<sup>1</sup>Ut Md Anderson Cancer Center

<sup>2</sup>Mayo Clinic, Arizona

**Key words:** Pion, reference dosimetry, proton

### **Purpose**

To validate the formulas for Pion suggested in IAEA TRS-398 protocol for commonly used chambers for reference dosimetry of passive scattering and spot scanning proton beams of the synchrotron of Hitachi ProBeat machine.

### **Methods**

PTW Farmer, advanced Markus (AM) and Bragg peak (BP), and Exradin A26 chambers were irradiated both in passive scattering (PSB) and spot scanning (SSB) proton beams. The charges (Q) were measured as a function of applied bias (V). The extrapolated charge (Q<sub>ex</sub>) at large bias was determined from curve fitting of Q vs 1/V. The Pion was calculated from the ratio of Q<sub>ex</sub> and Q at the bias used for reference dosimetry and was compared with Pion calculated with the formulas suggested in IAEA TRS-398 protocol.

### **Results**

For PSB, Pion obtained from extrapolation method for PTW Farmer, AM and BP, and Exradin A26 chambers agreed within 0.2%, 0.8%, 0.4% and 0.1% with those from continuous beam formula respectively. For SSB, Pion from extrapolation method was found to be within 0.2% of the continuous beam formula for all chambers. For SSB, the differences of Pion values from the formula for pulse scanned and extrapolation methods were much larger (0.3 to 0.6%), but for PSB the values from the formula for pulsed beam have similar agreements as for the continuous beam formula.

### **Conclusions**

The two voltage formula for the continuous beam was found to be more appropriate for the pulsed and pulse scanned beams from the synchrotron of the Hitachi ProBeat machine for reference dosimetry.

## DOSE MEASUREMENT IN TOTAL BODY IRRADIATION BY GAFCHROMIC EBT3 FILM

V Inphavong<sup>1</sup>, S Suriyapee<sup>1</sup>, T Sanghangthum<sup>1</sup>, S Oonsiri<sup>2</sup>, T Thawonwong<sup>2</sup>

<sup>1</sup>Chulalongkorn University; <sup>2</sup>King Chulalongkorn Memorial Hospital, Thailand

**Key words:** GafchromicEBT3film, Total body irradiation, Dose measurement, 3D conformal.

**Introduction:** Total body irradiation is a type of external beam radiotherapy and considered as a special technique aimed to deliver a uniform dose to the entire body within  $\pm 10\%$  of prescribed dose while keeping lung dose within tolerance level[1]. Treatment of TBI for large fields is usually used at extended source to surface distances (SSD) technique because it is the simplest and most prevalent of the TBI technique used nowadays [2]. The purpose was to measure the dose in the phantom and patients during total body irradiation photon beams by Gafchromic EBT3 film.

**Material and methods:** The films were calibrated with the range of 10-800cGy of 6MV photon beams in virtual water phantom at 1.5cm depth, 10x10cm<sup>2</sup> field size and at 100cm SSD. The techniques of TBI were two lateral parallel opposing fields for 200cGy per fraction, two fractions per day in three days and the thickness in lateral and AP direction were measured during simulation in order to calculate monitor units (MU) by manual calculation aimed 1200cGy at the head and legs at extended source axis distance (SAD) 500cm. The remainder dose of less than 1200cGy in chest and abdomen part was added with anterior-posterior/ posterior-anterior (AP/PA) field by 3D conformal technique with lung and kidney shield in the 7<sup>th</sup> fraction at 100cm source to surface distance (SSD).The measurements in Alderson RANDO phantom and three patients in 3D conformal for chest and abdomen region were performed by film. The films were placed in the middle head of phantom, at the surface of: left side and right side of head, neck, shoulder, chest, umbilicus, abdomen and thighs, for AP/PA fields the films were placed in the phantom section of shoulder, lung blocks, umbilicus, kidney blocks, abdomen and on the surface of phantom of shoulder, chest, umbilicus, abdomen, groin and thighs. In the patients, films were placed only in AP/PA fields of armpits, shoulders, chest, umbilicus, abdomen, groin and thighs for 6MV photon beam by Varian iX (Varian Oncology Systems, Palo Alto, CA, USA) linear accelerator. After irradiation, films were scanned 24 hours irradiation with Epson scanner and determined absolute dose by MapCHECK software.

**Result and discussion:** For the phantom study, dose differences between measured and calculated in lateral fields were within  $\pm 12\%$  (-12.63% to 0.54%), the chest region showed highest dose difference, the films were placed at the inhomogeneous part of the chest region which radiation transmitted more than passing soft tissue resulted in higher measured dose.

The dose differences on surface with bolus were within  $\pm 7\%$  (-6.6% to 3.9%), high difference shows in inhomogeneity part (chest). The dose difference inside phantom were within  $\pm 7\%$  (-6.63% to 2.88%), high differences would be caused by the matching of upper/lower field region in umbilicus. The lung and kidney blocks were shielded by MLC, it showed agreement within  $\pm 3\%$  (-2.88% to 3.44%).For the patients, the percent dose differences between measured and calculated dose were within  $\pm 4\%$  (-4.41 to 3.33) in AP/PA fields, these doses were more agreeable than measured in phantom.

**Conclusion:** TheGafchromic EBT3 film can be used to measure dose in the patient during total body irradiation to assure the accuracy of delivered dose.

### References:

1. Van Dyk, J., Galvin,J.M., Glasgow, G.P., Podgorsak, E.B.: The physical aspects of total and half body photon irradiation. Task Group 29, Radiation Therapy Committee report. AAPM report No. 17, 1986.
2. Ervin B. Podgorsak and Matthew B. Podgorsak et al. (1999) Special Techniques in Radiotherapy. The Modern Technology of Radiation Oncology. Medical Physics Publishing Medison, Wisconsin.
3. Rui, Y., Damian, B., Julius, T., Ross, A et al. (2012). A simplified technique for delivering total body irradiation with improved dose homogeneity. Journal Med. Phys. 39(4).

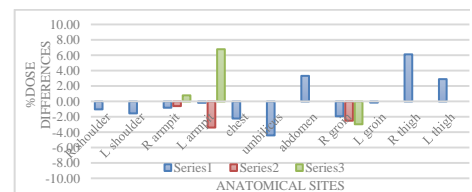


Fig.1 Percent dose differences of three patients in AP/PA fields.

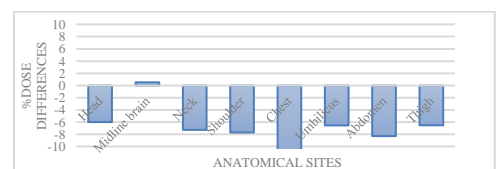
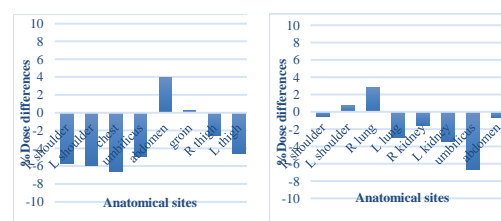


Fig.2 Percent dose differences in each site of phantom in lateral fields.



(a) (b)  
Fig.3 Percent dose differences on surface with bolus (a) and inside phantom (b) in AP/PA fields.

## **DOSIMETRIC VALIDATION OF THE BRAINLAB ELEMENTS TREATMENT PLANNING SYSTEM FOR TREATMENT OF MULTIPLE BRAIN METASTASES USING STEREOTACTIC RADIOSURGERY**

Kumaresh Chandra Paul<sup>1</sup>, Guenther H Hartmann<sup>2</sup>, Golam Abu Zakaria<sup>2</sup>

<sup>1</sup>Gono Bishwabidyalay (University)

<sup>2</sup>Dept. Of Medical Physics In Radiation Oncology, German Cancer Research Center, Im Neuenheimer Feld 280, 69120 Heidelberg

**Key words:** Elements, Brain metastases, stereotactic radiosurgery

### **Purpose**

Brainlab AG have recently released a module in their Elements series which is able to treat multiple metastases using several arc fields. This offers significant clinical and dosimetric benefit compared to other treatments such as whole brain radiotherapy or treating each metastasis individually with SRS beams. The dosimetric beam data used for Elements is the same as used for iPlan Dose RT which had already been released for clinical use. This work describes some of the commissioning and validation of the dose calculation algorithms in Elements.

### **Methods**

For validation of Elements, verification plans were calculated on an in-house solid water “Burger” phantom and compared with measured doses using a PTW PinPoint ionisation chamber. The plans were created to simulate multiple brain metastasis treatments. The brain metastases ranged in diameters between 6 – 30 mm. An end to end test was also performed using Gafchromic EBT-XD film on an ART phantom using ExacTrac technology for alignment and set up.

### **Results**

For the point dose measurements performed in the “Burger” phantom the average agreement was 1.17%, 1.4%, 0.8%, 0.74%, and 0.28% for simulated brain metastases of diameters 6, 10, 15, 20 and 30 mm, respectively. The maximum deviations were between -2.36% and 5.08%. For the End to End test using the Gafchromic EBT-XD film we obtained minimum pass rates of 95.79% for gamma criteria of 3%/3mm.

### **Conclusions**

The accuracy of the commissioning of the Brainlab Elements has been verified using 1D and 2D dose measurements. Agreements with calculated doses were found to be within acceptable tolerances.

## **EXPERIMENTAL STUDY ON THE SHIFT OF EFFECTIVE POINT OF MEASUREMENT AND DISPLACEMENT PERTURBATION FACTOR AT CYLINDRICAL CHAMBERS IN HIGH ENERGY ELECTRON BEAMS**

Kumaresh Chandra Paul<sup>1</sup>, Guenther H Hartmann<sup>2</sup>, Golam Abu Zakaria<sup>2</sup>

<sup>1</sup>Gono Bishwabidyalay (University), Bangladesh

<sup>2</sup>Dept. of Medical Physics in Radiation Oncology, German Cancer Research Center, Im Neuenheimer Feld 280, 69120 Heidelberg, Germany

### **Key words**

Cylindrical ionization chamber, Electron energy, EPOM

### **Purpose**

In clinical practice absorbed dose determination requires the placement of ionization chamber in water which needs the placement of effective point of measurement (EPOM) at the measuring depth. Recent publications have reported that the position of the EPOM is indeed varying with beam energy, field size, and chamber geometry. The aim of this study was to investigate whether the shift of EPOM can be taken to be constant, independent of the beams energy and chamber geometry.

### **Methods**

A Linear accelerator, water phantom, Roos chamber, electrometers, specially prepared cylindrical chambers with the inner radius of 1 to 6 mm, and a Semiflex chamber, were used in the study. Ionization was measured along the beam central axis in the water phantom and normalized to maximum ionization. The vertical electron beams of 6, 8, 10, 12 and 15 MeV and depth-ionization curves were considered. Microsoft Office Excel and Sigma Plots-10 were used for data analysis.

### **Results**

The obtained shift of EPOM for the cylindrical chambers was a range of 0.24 to 0.70 times the chamber radius. The shift was in the upstream direction to the source. The displacement shift was observed increasing with the beam quality. The normalized displacement perturbation factor was found increasing with the chamber radius.

### **Conclusions**

Displacement effect was not in a good agreement with a single value of the protocols moreover, showed to be energy and chamber volume dependent. A modified formula needs to be established for the electron beam dosimetry at cylindrical chambers with reduces uncertainty.

## **DEVELOPMENT OF IN VIVO DOSE VERIFICATION SYSTEM USING TRANSIT DOSE**

Seonghoon Jeong<sup>1</sup>, Myonggeun Yoon<sup>1</sup>, Weon Kuu Chung<sup>2</sup>, Dong Wook Kim<sup>2</sup>, Mijoo Chung<sup>2</sup>

<sup>1</sup>Korea University, South Korea

<sup>2</sup>Kyung Hee University Hospital at Gangdong

### **Key words**

Radiation therapy, Transit dose, Glass dosimeter, Inverse square law, Percentage depth dose

### **Purpose**

To verify the accuracy of planned dose distribution for patient treatment, patient dose quality assurance using the solid water phantom is usually performed. This method, however, is not the method of verifying the absorbed dose in real patient. In this study, as a previous process of developing algorithm in human, we measured the transit dose using the glass dosimeter to develop dose calculation algorithm in phantom.

### **Methods**

We measured the transit dose at 150cm from source of LINAC to calculate the dose in the homogeneous phantom. The homogeneous phantom (10cm, 20cm, 30cm thickness) was located near the isocenter. We can calculate the dose at the bottom of phantom using the measured transit dose, inverse square law value and scatter factor. To develop dose calculation algorithm in homogeneous phantom, we measured the field size dependence of transit dose and bottom dose to calculate the scatter factor, the relative dose response to correct the change of field size and location of isocenter.

### **Results**

The measurement results of the relative dose response for isocenter location change are increased when the SSD decreases. We could calculate the dose in the phantom using the transit dose, inverse square law, scatter factor and percentage depth dose data. The accuracies of algorithm were 0.54%, 1.03% and -1.65% for each phantom.

### **Conclusions**

We developed the phantom-dose calculation algorithm using the transit dose, inverse square law, scatter factor and PDD data to develop dose calculation algorithm

# DOSIMETRIC EVALUATION OF 6MV PHOTON BEAMS FOR ACUROS XB ALGORITHM

Y Phimmakone, SSuriyapee, TSanghangthum, T Tawonwong

Medical Imaging Program, Department of Radiology, Faculty of Medicine, Chulalongkorn University, Bangkok, Thailand.

**Keywords:** AcurosXB, Dose Evaluation, TG53

**Introduction:** This research is conducted to investigate the dosimetric accuracy of Acuros XB software in Eclipse TPS according to AAPM TG53 and IAEA TPS 430 protocol.

**Methods:** The PDD and 10cm depth of profile of 6MV beams from TrueBEAM were measured in water phantom. The PDDs were obtained by scanning with CC13 chamber, while profiles were acquired with PFD diode. The output factors were measured at 10 cm depth using CC13 ionization chamber. The dose of five 3D-CRT and five IMRT plans in solid phantom were measured with FC65P and CC13 chamber, respectively. All of the measurement results were compared with calculated dose in TPS.

**Results and Discussion:** The measured PDD showed a good agreement to TPS of  $\delta_1$  (high dose, small dose gradient) less than 1.5% and  $\delta_2$  (high dose, large dose gradient) within 1.5mm. The profiles displayed the coincidence results with TPS that showed  $\delta_2$  less than 2mm,  $\delta_3$  (high dose, small dose gradient) within 3%,  $\delta_4$  (low dose, small dose gradient) within 3%, and  $\delta_{50-90}$  within 2mm. The maximum output factors differences were only 1.22%. The clinical 3D-CRT plans exhibited larger dose difference compared with open field, however, the dose differences between measurement and calculation were within 1.5%.

**Conclusion:** The dose differences between AcurosXB algorithm calculation and measurement are within the recommendation of AAPM TG53 and IAEA TRS430.

**Table1:** Percentage difference of Measurement and Calculation dose in PDD of various fields size

| Fields size (cm <sup>2</sup> ) | Measurements       |                     | Calculations       |                     | % Difference       |                     |
|--------------------------------|--------------------|---------------------|--------------------|---------------------|--------------------|---------------------|
|                                | d <sub>1</sub> (%) | d <sub>2</sub> (mm) | d <sub>1</sub> (%) | d <sub>2</sub> (mm) | d <sub>1</sub> (%) | d <sub>2</sub> (mm) |
| 5x5                            | 62.4               | 6.4                 | 63                 | 7                   | 0.60               | 0.60                |
| 10x10                          | 66.5               | 6                   | 66.8               | 6.4                 | 0.30               | 0.40                |
| 20x20                          | 69.4               | 5.3                 | 68.3               | 6.4                 | -1.10              | 1.10                |
| 30x30                          | 70.9               | 4.7                 | 71.5               | 5.1                 | 0.60               | 0.40                |
| 10x5                           | 64.7               | 7.7                 | 64.6               | 6.7                 | -0.10              | -1.00               |
| 20x10                          | 67.7               | 5.8                 | 68.3               | 6.4                 | 0.60               | 0.60                |
| 30x10                          | 68                 | 5.7                 | 68.6               | 6.3                 | 0.60               | 0.60                |

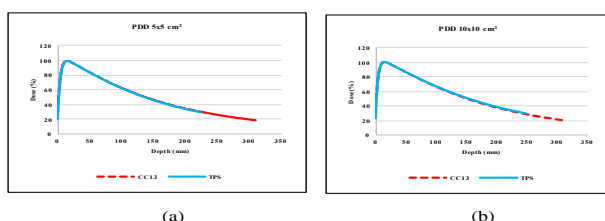


**Figure1:** Percentage depth dose curve comparisons between measurement and calculation dose for the field sizes of (a) 5x5 cm<sup>2</sup> and (b) 10x10 cm<sup>2</sup>.

**Table2:** Percentage difference for output factors between measurement and calculation dose for 6 MV photon beams.

| Fields size (cm <sup>2</sup> ) | Measurements (cGy) | Calculations (cGy) | % Difference |
|--------------------------------|--------------------|--------------------|--------------|
| 5x5                            | 0.8958             | 0.8917             | -0.46        |
| 8x8                            | 0.9659             | 0.9624             | -0.37        |
| 15x15                          | 1.0584             | 1.0586             | 0.02         |
| 20x20                          | 1.0993             | 1.0992             | 0.00         |
| 25x25                          | 1.1276             | 1.1278             | 0.02         |
| 10x5                           | 0.9408             | 0.9293             | -1.22        |
| 10x20                          | 1.0362             | 1.0421             | 0.57         |
| 20x10                          | 1.0421             | 1.0376             | -0.44        |
| 30x10                          | 1.0571             | 1.0481             | -0.85        |

## INFORMATION ABOUT THE ABSTRACT

Acuros XB is a new algorithm from Varian Eclipse treatment planning system (TPS) and dedicated for Radiotherapy TPS. Acuros XB has been developed to administer accuracy and speed in delivering radiation in external beam. Acuros XB is faster for VMAT calculation in single workstation environment [1]. AAPM TG53 has been established in 1998 to guide and assist the medical physicists who work in Radiotherapy field to develop and implement the comprehensiveness in QA radiotherapy treatment planning including software and algorithm in TPS [2,3]. The measured PDD, in-plane and cross-plane profiles, output factors were scanned and measured in Blue phantom, while the clinical application in 3D-CRT and IMRT plans were measured in solid water phantoms. The PDD and profiles were verified in square (5x5, 10x10, 20x20, 30x30cm<sup>2</sup>) and rectangular fields (10x5, 20x10, 30x10 cm<sup>2</sup>), while the output factors were measured in square fields (5x5, 8x8, 10x10, 15x15, 20x20, 25x25 cm<sup>2</sup>) and rectangular (10x5, 10x20, 20x10, 30x10 cm<sup>2</sup>). The PDD was evaluated in  $\delta_1$  (high dose, small dose gradient) of the dose difference at 10 cm depth and  $\delta_2$  (high dose, large dose gradient) of the distance difference at 90% dose, while the profiles were analyzed in  $\delta_2$  (high dose, large dose gradient) of the distance difference at 40% dose,  $\delta_3$  (high dose, small dose gradient) of the dose difference at 60% of field from central axis,  $\delta_4$  (low dose, small dose gradient) of the dose difference at 20% of the field out of the field edge and  $\delta_{50-90}$  for the distance difference between 50% and 90% dose. The PDD comparison between measurement and calculation of 5x5 and 10x10 cm<sup>2</sup> are displayed as the example in figure1, while the  $\delta_1$  and  $\delta_2$  of PDD at various fields are shown in Table1. All of the PDD and profiles comparison were in the acceptable criteria as defined in IAEA TRS 430. The output factors differences are exhibited in Table2 those are within the recommendation as well.

## References:

1. Fregory A. Failla, T.W, Yves A: "Acuros XB advanced dose calculation for the Eclipse treatment planning system". Varian Medical system.
2. IAEA 1998 Report No 430: "Commissioning and QA of Computerized Planning Systems for Radiation Treatment of Cancer".
3. Benedrick. F: "Quality assurance for clinical radiotherapy treatment planning" (AAPM TG53). Medical Physics. 25 (10), October 1998, 1773.

Corresponding email: [ssivalee@yahoo.com](mailto:ssivalee@yahoo.com)

## **ANALYSIS OF BEAM PENUMBRA IN ENERGY MATCHED FLATTENING FILTER FREE BEAMS IN ELEKTA VERSA HD**

Senni Andavar

Shri Mata Vaishno Devi Narayana Superspeciality Hospital, India

### **Key words**

Beam Energy Matching Flattening Filter Free Versa HD

### **Purpose**

The purpose of the study is to report the beam characteristics of energy matched FFF beams in Elekta versa HD. When the flattening filter is removed from a radiation beam, the mean energy in the beam is reduced. Unlike other commercially available FFF beams, the energy of the Elekta FFF beams in High Dose Rate mode is adjusted via the digital control system to produce the same penetrative quality as its flattened beam at a depth of 10cm.

### **Methods**

The measurements include PDDs, Inline and crossline profiles for different field sizes for both 6 and 10 MV flattened as well as FFF beams. All the measurements were obtained in the steps of 1mm increment. Beam penumbra was defined as the distance between the 80% and 20% isodose lines. The field sizes were ranging from 5 x 5cm<sup>2</sup> to 40 x 40cm<sup>2</sup>.

### **Results**

There are no significant changes in the PPDs and penumbra at 10cm depth for both flattened and unflattened beam. Due the higher dose rate in FFF mode the depth of the maximum dose is deeper in 2mm and 1mm for 6FFF and 10FFF beams respectively for reference field sizes. The maximum changes in the penumbra region observed at 5 x 5cm<sup>2</sup> and higher field sizes for 2mm when compared with flattened beam.

### **Conclusions**

The matching of the FFF beams at 10cm depth with flattened beam giving the potential advantage of higher beam quality and penetration ability more closely resembles the flattened beams currently used in clinical practice.

## **ANALYSIS OF INFLECTION POINTS AND BEAM PENUMBRA FOR FFF BEAM USING DIFFERENT TYPES OF DETECTORS**

Senniandavar Andavar, Vikas Roshan

Shri Mata Vaishno Devi Narayana Superspeciality Hospital, India

### **Key words**

Inflection Point Flattening Filter Free Detectors

### **Purpose**

The purpose of the study was to analyse the inflection points and beam penumbra for flattening filter free beam using four different types of radiation detectors.

### **Methods**

The Profile measurements were performed for 6FFF and 10FFF with four different types of detectors namely as semiflex (0.125cc), pinpoint chamber (0.015cc), diode and diamond detector. All the measurements were obtained in the steps of 1mm increments. For to analysis purpose, 20x20 cm<sup>2</sup> field size taken as a reference field size for all four detectors. The inflection points and the beam penumbra was analysed based on the AERB/Quality Assurance/Un flatten beams.

### **Results**

There is no significant difference (200mm  $\pm$ 1) observed in the inflection points measurements with all the detectors. Both the diode E and diamond detectors are showing good agreement with each other in terms of beam penumbra analysis. Negligible difference was observed with pinpoint detector when compared with diode and diamond detector. There was a significant numerical (+4mm) difference was observed in both sides of the penumbra with semiflex chamber measurements when compared with other detectors.

### **Conclusions**

These results were reflecting the relative sensitivity of the each detector. Choosing the type of the detectors in the flattening filter free beams measurement is very important in terms of accurate beam penumbra measurements.

## **A COMPREHENSIVE INTERCOMPARISON STUDY OF THERMOLUMINESCENT AND OPTICALLY STIMULATED DOSIMETERS FOR IN VIVO DOSIMETRY**

Gourav Kumar Jain, Mary Joan, Gurvinder Singh

Department of Radiological Physics, SMS Medical College & Hospitals Jaipur, India

### **Key words**

TLD, OSLD, In vivo dosimetry

### **Purpose**

A comprehensive intercomparison study of thermoluminescent and optically stimulated dosimeters for in vivo dosimetry

### **Methods**

The TLDs used in this study were Nucleonix Ltd., CaSO<sub>4</sub>:Dy discs, CaSO<sub>4</sub>:Dy powder, LiF:Mg,Ti chips and OSLDs were from Landauer Inc., Al<sub>2</sub>O<sub>3</sub>:C nanoDots™. All dose measurements were performed on teletherapy units in solid water phantom. Further, various dosimetric characteristics like accuracy, inter detector response, dose linearity, energy and angular response of dosimeters were investigated and if required the measurements were compared with ionization chamber measurements.

### **Results**

The interdetector variation for CaSO<sub>4</sub>:Dy discs was found to be within  $\pm 9\%$  with a standard deviation of 3.41%. The dose linearity was found linear with R<sup>2</sup> value 0.997. The dose linearity for CaSO<sub>4</sub>:Dy powder was found linear with R<sup>2</sup> value 0.963. The interdetector variation for LiF:Mg,Ti chips was found to be  $\pm 7\%$  with a standard deviation of 3.5%. The dose linearity was found linear with R<sup>2</sup> value 0.993. The interdetector variation of OSL detector was found to be within 3.44% standard deviation. Further, an average response of OSLDs was evaluated 0.982 relative to absolute dose by ionization chamber. The maximum percentage deviation in an OSLD was found to be -4.5%. OSLD provides a good linearity till approximately 250cGy of dose with R<sup>2</sup> value 0.997 but thereafter shows supralinear response at higher doses.

### **Conclusions**

The TL/OSL type and irradiation conditions had varying degrees of uncertainty. The interdetector response variation can be minimized by applying element correction factor. The accuracy of the OSL dosimeters was found better than TLD.

## **SURFACE DOSE MEASUREMENTS IN FFF BEAMS USING A THIN WINDOW CHAMBER**

Peta Lonski<sup>1</sup>, Peta Lonski<sup>1</sup>, Rick Franich<sup>2</sup>, Prabhakar Ramachandran<sup>1</sup>, Tomas Kron<sup>1</sup>

<sup>1</sup>Peter MacCallum Cancer Centre, Australia

<sup>2</sup>RMIT University

### **Key words**

Surface dose, FFF, Polarity

### **Purpose**

Surface dose measurements are important for estimating patient skin dose during external beam radiotherapy. It was the aim of this work to quantify the surface dose from flat and FFF beams from a Varian TrueBeam linear accelerator using a thin window chamber. Chamber recombination and polarity effects were evaluated.

### **Methods**

An Exradin A10 thin window parallel plate chamber was used to measure surface dose for different photon beams for 4x4, 10x10, 20x20 and 40x40 cm<sup>2</sup> fields. A custom-made solid water slab was used to accommodate the chamber. Recombination and polarity effects were measured at surface and depth of maximum dose.

### **Results**

Surface dose was measured for 6MV, 6FFF, 10MV, 10FFF and 18MV and was found to increase with field size. At 10x10cm<sup>2</sup> surface dose was 19.6% for 6 MV, 25.5% for 6FFF, 13.9% for 10MV, 17.0% for 10FFF and 14.5% for 18MV. FFF was associated with higher surface dose in smaller fields but lower surface dose in larger fields indicating that the inhomogeneous fluence distribution of photons also affects surface dose. Polarity correction was as large as 1.10 for both 6MV and 10FFF for a 4x4 cm<sup>2</sup> field at the surface but small (1.001 for 6MV and 1.008 for 10FFF) at d-max.

As expected, softer beam quality was associated with higher surface dose and recombination did not alter with field size.

### **Conclusions**

Surface dose can be quantified using a thin window parallel plate chamber; however, polarity effects at the surface can be large and must be accounted for.

## COMPARISON OF VARIOUS RADIATION THERAPY TECHNIQUES IN BREAST CANCER WITH INCLUSION OF INTERNAL MAMMARY NODES BY USE OF RANDO PHANTOM AND TLD

Mohammad Taghi Bahreyni Toossi<sup>1</sup>, Shokouhozaman Soleymanifard<sup>1</sup>, Ashraf Farkhari<sup>1</sup>, Fatemeh Homaei Shandiz<sup>1</sup>, Elahe Salari<sup>2</sup>

<sup>1</sup>Mashhad University of Medical Sciences, Iran

<sup>2</sup>Reza Radiation Oncology Center

### Key words

Breast cancer, Radiotherapy technique, Lymph nodes, Organs at risk

### Purpose

To compare breast cancer radiotherapy techniques with inclusion of internal mammary nodes in terms of the coverage of regional lymph nodes, chest wall; and the dose received by the heart and lung.

### Methods

After transferring CT images of the RANDO phantom to the treatment planning system, the lungs, heart and regional lymph nodes were contoured. Three treatment plans including wide tangent (WT), oblique parasternal photon (OPP), and oblique parasternal electron (OPE) techniques were performed. For each technique, TLDs were placed in appropriate points of the phantom. 2 types of TLDs were used; TLD-100 for photon dosimetry and TLD-700 for electron dosimetry. Phantom irradiation was repeated 4 times for each technique.

### Results

The mean absorbed dose by the left axillary lymph nodes was statistically similar in all techniques. Left supraclavicular nodes mean dose in the OPE technique was significantly higher than the other two methods, which were statistically similar. The OPE technique produced a significantly lower left internal mammary lymph nodes mean dose than the two other methods. The chest wall mean dose was statistically similar in all techniques. The mean dose received by the left lung was higher than the lung tolerance dose for OPP technique; and no statistically significant differences were observed among the two other methods. The mean absorbed dose by the heart was lowest for WT technique.

### Conclusions

In terms of the target volume coverage and protection of OAR, WT technique is the best technique.

## **EVALUATION OF ELECTRON DOSE CALCULATIONS ACCURACY OF A TREATMENT PLANNING SYSTEM IN RADIOTHERAPY OF BREAST CANCER WITH PHOTON-ELECTRON TECHNIQUE**

Mohammad Taghi Bahreyni Toossi<sup>1</sup>, Shokouhozaman Soleymanifard<sup>1</sup>, Ashraf Farkhari<sup>1</sup>, Bagher Farhood<sup>2</sup>

<sup>1</sup>Mashhad University of Medical Sciences, Iran

<sup>2</sup>Tehran University Of Medical Sciences

### **Key words**

Breast cancer, TPS, Radiotherapy

### **Purpose**

To assess the accuracy of electron dose calculations of Prowess Panther TPS for photon-electron technique. In fact, we assessed the accuracy of the electron dose calculations in an internal mammary field, because only this field is irradiated by electron in photon-electron technique.

### **Methods**

In this study, regions of in-field, under shield and outside field of the internal mammary field were evaluated. TLD-700 chips were placed in the points of interest within the RANDO phantom for dose measurement. Prowess Panther TPS was also applied for dose calculation. Finally, confidence limit values were obtained to quantify the electron dose calculation accuracy of the TPS for the internal mammary field.

### **Results**

The results of this study indicate that Prowess Panther TPS underestimated the dose for outside field and under shield regions compared to the measured doses by TLD700; while the calculated doses by TPS for in-field regions compared to the measured doses, for some points are overestimated and for some other points underestimated. Finally, the confidence limit values were obtained for various regions of internal mammary field. Confidence limits for in-field, under shield and outside field regions were 54.23, 80.51 and 108.20, respectively.

### **Conclusions**

It is conceded that the accuracy of electron dose calculations of Prowess panther TPS is not acceptable in the internal mammary field. Therefore, it is recommended that for fields including electron beam, it should not entirely rely on TPS calculations.

**Keywords:** Photon-electron technique, Radiotherapy, Confidence limit, Dose calculation accuracy, Treatment planning system

## **COMPARISON OF CARDIAC AND LUNG DOSES BETWEEN FREE BREATHING AND DEEP INSPIRATION BREATH HOLD TECHNIQUE FOR LEFT BREAST IRRADIATION - A DOSIMETRIC STUDY**

Mohammad Anisuzzaman Bhuiyan, Karthick Raj Mani

United Hospital Ltd, Dhaka, Bangladesh

### **Key words**

Deep Inspiration Breath Hold, Left Breast

### **Purpose**

To investigate the cardio-pulmonary doses between Deep Inspiration Breath Hold (DIBH) and Free Breathing (FB) technique in left sided breast irradiation

### **Methods**

DIBH CT and FB CT were acquired for 10 left sided breast patients who underwent whole breast irradiation with or without nodal irradiation. Three fields single isocenter technique were used for patients with node positive patients along with two tangential conformal fields whereas only two tangential fields were used in node negative patients. All the critical structures like lungs, heart, esophagus, thyroid, etc were delineated in both DIBH & FB scan. Both DIBH and FB scan were fused with the dicom origin as they were acquired with the same dicom coordinates. The critical structures of the FB scan were transferred to the DIBH dataset with reference to the dicom origin. Plan were created in the DIBH scan for a dose range between 45-50Gy in 25 fractions. Critical structures doses were recorded from the Dose Volume Histogram for both the DIBH and FB data set for evaluation.

### **Results**

V25 (relative volume receiving 25Gy and more) for heart were reduced from 19.14% (FB) to 3.68% (DIBH) using the breath hold technique. Ipsilateral lung V20 volume was also reduced between 25% to 15% with DIBH compared to FB technique.

### **Conclusions**

DIBH shows a substantial reduction of cardiac and pulmonary doses compared with FB technique. Using the simple DIBH technique we can effectively reduce the cardiac morbidity and lung pneumonitis.

## **ORIENTATION-DEPENDENT RESPONSE OF GAFCHROMIC® EBT-2 IRRADIATED IN THE PRESENCE OF A MAGNETIC FIELD**

Hannah Lee<sup>1</sup>, Yvonne Roed<sup>2</sup>, Muhammad Gadhi<sup>3</sup>, Ashley Rubinstein<sup>1</sup>, Zhifei Wen<sup>1</sup>, Gye Won Choi<sup>1</sup>, Mitchell Carroll<sup>1</sup>, Geoffrey Ibbott<sup>1</sup>

<sup>1</sup>UT MD Anderson Cancer Center, USA

<sup>2</sup>UT MD Anderson Cancer Center, University Of Houston

<sup>3</sup>UT MD Anderson Cancer Center, The Islamia University of Bahawalpur & Bino

### **Key words**

Gafchromic film, Magnetic field dosimetry

### **Purpose**

To compare the response of Gafchromic® EBT-2 and EBT-3 film irradiated in the presence of different magnetic field (B-field) strengths for MR-guided radiation therapy QA applications.

### **Methods**

EBT-2 and EBT-3 film were irradiated with a Co-60 source to 2, 4 and 8Gy at 5cm depth in an acrylic phantom placed inside an electromagnet. Films were irradiated perpendicular to the beam and with a reference edge parallel or perpendicular to the B-field. B-field strengths of 0T, 0.35T, and 1.5T were used. Films were scanned 24hr post-irradiation using an EPSON 10000XL flatbed scanner and optical density changes were measured for the red channel.

### **Results**

For EBT-2 at 0.35T, the maximum %change was -5.9% (4Gy) with the reference edge parallel to the B-field; when the edge was perpendicular to the B-field a -3.6% change (4Gy) was observed. At 1.5T, changes of -5.3% (4Gy) for the edge-parallel position and -2.8% (4Gy) for the edge-perpendicular position were measured. EBT-3 exhibited a maximum %change at 0.35T of -2.4% (2Gy) for the edge-parallel position and of -1.0% (2Gy) for the edge-perpendicular position. At 1.5T, the edge-parallel position resulted in a maximum %change of -1.1% (8Gy) and the edge-perpendicular position in a -1.5% change (8Gy).

### **Conclusions**

EBT-2 film under-responded in the presence of B-fields with the greatest % changes observed in the edge-parallel positions. EBT-3 film showed minor % changes for all film positions with respect to the B-field. Consistency in film orientation remains key for dosimetry in B-fields.

## **POLYMER GELS AS POTENTIAL 3D IMRT QA DEVICES FOR MAGNETIC RESONANCE-GUIDED RADIATION THERAPY**

Yvonne Roed<sup>1</sup>, Yao Ding<sup>2</sup>, Jihong Wang<sup>2</sup>, Lawrence Pinsky<sup>3</sup>, Geoffrey Ibbott<sup>2</sup>

<sup>1</sup>UT MD Anderson Cancer Center, University Of Houston, USA

<sup>2</sup>UT MD Anderson Cancer Center

<sup>3</sup>University of Houston

### **Key words**

Polymer gels, 3D dosimetry, MRgRT, IMRT QA

### **Purpose**

To demonstrate the performance of polymer gels as 3D IMRT QA devices in magnetic resonance-guided radiation therapy.

### **Methods**

Custom-designed polymer gel dosimeters were irradiated with an Elekta VERSA 6 MV linac at 10 cm depth and SSD = 100 cm inside a full phantom. 400 cGy was delivered in a single exposure and as 4x100 cGy with 5min beam-off between irradiations. The experiment was repeated inside an electromagnet (B = 1.04T) with the center of the dosimeters at 300 cm from the source. 600 cGy was delivered in a single irradiation and as 6x100 cGy with 5min beam-off between exposures.

2D spin-spin relaxation rate (R2) maps were acquired 24h post-irradiation with a GE 3T MR scanner. R2 values from single and multiple fraction delivery were compared as well as the influence of beam-off time.

### **Results**

Polymer gels exhibited well-behaved responses to dose delivery. However, the R2 values from the fractionated delivery were 25% higher at high dose rates (266 cGy/min) than the single fraction delivery. Beam-on was only 17% of the total elapsed time.

At low dose rates (38 cGy/min) and B = 1.04 T only 1% difference in R2 values were measured between the single and fractionated dose delivery. Beam-on was 35% of the total elapsed time.

### **Conclusions**

Polymer gels showed promise as QA devices for MRgRT. Further investigations are needed because different elapsed times and dose rates introduced differences in response.

## **OFF-AXIS DOSIMETRIC CHANGES IN 6 MV PHOTON BEAM PROFILE IN THE PRESENCE OF CADMIUM FREE COMPENSATOR ALLOY**

Sandeep Kaushik<sup>1</sup>, Rajesh Punia<sup>1</sup>, Rajender Singh Kundu<sup>1</sup>, Atul Tyagi<sup>2</sup>

<sup>1</sup>Guru Jambheshwar University of Science and Technology, India

<sup>2</sup>Dr BLK Super Speciality Hospital

### **Key words**

Compensator, Beam flatness, Beam hardening, Attenuation.

### **Purpose**

Purpose of the study was to investigate off-axis dosimetric changes produced in six megavolt photon beam in the presence of cadmium free compensator alloy.

### **Methods**

Cadmium free alloy of lead, tin and bismuth was prepared with known percentage by weight composition. Total five slabs having thicknesses ranging from 4.3 mm to 41.6 mm were casted. Beam profiles were taken using computer controlled radiation field analyzer at three depths in water phantom for 6 MV photon beam on medical linear accelerator. Off-axis variation was measured with 0.13cc ion chamber at two diagonal points in a plane and at three depths.

### **Results**

Beam flatness was found to decrease with increase in thickness of compensator and field size and also at larger depth in phantom. It may be because of selective beam hardening due to compensator and at larger depths due to phantom attenuation. For compensator thickness up to 20 mm, flatness changes were in tolerance in relevant to clinical use. However, for compensator thickness >20 mm, beam profiles were no more flat. Point dose measurement at a depth of 15mm with slab thickness 30.2mm caused approximately 20 % under dose region at 70 mm off-axis diagonal point for a field size of 200×200 mm<sup>2</sup>. Further deviation at higher depths was negligible.

### **Conclusions**

Flatness of photon beams is sensitive to change in photon beam mean energy. Compensator attenuation changes photon beam mean energy along beam cross-section may result in decreased beam flatness and hence under dose area in target.

## **1.4 Image Guided Radiotherapy**

## **CONCORDANCE BETWEEN SETUP ERRORS AND PTV MARGINS USING CONE-BEAM CT FOR SBRT OF LUNG METASTASIS**

Mayank Tyagi Tyagi, Sharma Sk, Dewan Abhinav, Suresh T

Rajiv Gandhi Cancer Institute and Research Center, India

### **Purpose**

Setup errors problem in the radiation treatment influence the size of safety margins and thereby size of irradiation field. It is introduced by various known and unknown variables which could be related to human or mechanical error; however these can be reduced by daily meticulous procedural checks. They are defined as the difference between the actual and intended treatment position with respect to radiation delivery. Aim of the present study is to assess setup error and its effect on PTV margins for stereotactic body radiotherapy on lung metastasis.

### **Methods**

A total of 20 patients with lung metastasis from different primaries, who underwent stereotactic body radiotherapy treatment, were enrolled in the present study. These patients underwent 3 to 6 fraction on True beam linear accelerator with thermoplastic cast used for immobilization. Daily verification was done using CBCT after initial setup. CBCT images were registered to the planning CT images, and setup errors on x, y, z axis were analyzed. Setup errors were calculated by evaluating the deviations from measured distance between the irradiation field margin and thoracic cage.

### **Results**

A total of 86 CBCT scans were performed. With respect to lateral, cranio-caudal and antero posterior axis, the observed setup error ranged from  $0.39\pm 0.25$ cm,  $0.41\pm 0.15$  cm and  $0.25\pm 0.14$  cm respectively.

### **Conclusions**

Measurement and correction of setup errors before each fraction using CBCT could help to improve the accuracy. Daily CBCT scan verification helps to minimize setup errors and meticulous verification can decrease PTV margins for SBRT in lung metastasis.

### **Key words**

Stereotactic body radiotherapy, CBCT, Setup error

## COMMISSIONING AND VALIDATION OF COMMERCIAL DEFORMABLE IMAGE REGISTRATION SOFTWARE

Reena Devi Phurailatpam<sup>1</sup>, Jamema Swamidas<sup>1</sup>, Siji Paul<sup>1</sup>, Kishore Joshi<sup>1</sup>, Deepak Deshpande<sup>2</sup>

<sup>1</sup> ACTREC, Tata Memorial Centre, India

<sup>2</sup> Tata Memorial Hospital, Tata Memorial Centre, India

### Purpose

To commission and validate the commercially available deformable image registration (DIR) software before clinical implementation.

### Methods

Five phantoms made in-house with various known deformations were used for this analysis. The known deformations introduced were from simple to complex. The first phantom was a cylinder of different diameter, while the second had the same diameter with varying height. Third phantom was a cylinder with known deformations in both diameter and in height. Fourth and fifth phantoms consisted of varying shapes of clay simulating the deformations of pelvic region and with different densities. CT scans were obtained for each phantom with slice thickness of 1.25mm followed by DIR registration in commercially available DIR software (Smart Adapt, Eclipse v 13.6, Varian Medical Systems). Contours were drawn in each phantom and were propagated to registered images which were used for further evaluation using open source software 3D slicer v 4.5.0.1. The following parameters were evaluated: Dice Similarity Co-efficient (DSC), shift in centre of mass (COM) and Hausdorff distances Hf95%.

### Results

For phantoms with simple deformations (Phantoms 1-4), mean  $\pm$ SD of DSC, COM and Hf95% were found to be  $0.915 \pm 0.403$ ,  $0.84 \pm 0.80$  mm, and  $1.86 \pm 1.35$  mm respectively. However for phantom with complex deformations (Phantom 5), the DSC, COM and Hf95% were found to be in the range of 0.516, 14mm and 18mm respectively.

### Conclusions

For simple deformations, the results were found to be quite reasonable; however for complex deformations which involve sliding of organs and large expansion and contraction, the accuracy is limited. Visual validation of the propagated contours may be recommended during clinical implementation.

### Key words

Deformable image registration, validation, commissioning

## **EFFECT OF REGION EXTRACTION AND ASSIGNED ELECTRON DENSITY VALUE ON THE ACCURACY OF DOSE CALCULATION WITH MRI-BASED VMAT PLANNING**

Keisuke Usui<sup>1</sup>, Tatsuya Inoue<sup>2</sup>, Chie Kurokawa<sup>1</sup>, Satoru Sugimoto<sup>1</sup>, Keisuke Sasai<sup>1</sup>, Koichi Ogawa<sup>3</sup>

<sup>1</sup> Juntendo University, Department of Radiation Oncology, Japan

<sup>2</sup> Juntendo University Urayasu Hospital, Japan

<sup>3</sup> Hosei University, Faculty of Science and Engineering, Japan

### **Purpose**

The purpose of our present study is to calculate a patient dose using magnetic resonance imaging (MRI). In this study, we evaluated the accuracy of region extraction and the effect of assigned electron densities (EDs) on the calculated dose using the Boltzmann transport equations in volumetric arc therapy (VMAT) planning.

### **Methods**

Four different regionalized image of the pelvic MRI were applied, (1) MRIw: all water-equivalent; (2) MRIw+b: water and bones; (3) MRIs+b: soft tissues and bones; and (4) MRIs+b+g: soft tissues, bones, and rectal gas. And these regions were assigned to corresponding EDs for calculating doses. Then, we changed the assigned ED values from 0.44 to 1.25. Furthermore, we directly assigned organ material densities corresponding regions. Using an initial planning and optimization parameters, MRI-based VMAT plans were calculated with the Acuros XB algorithm (Eclipse ver. 13.6) and were compared with corresponding, forward-calculated, CT-based plans for the target volumes (TVs) and Organs at Risk.

### **Results**

In the MRIw plan, the mean dose for TVs was overestimated by 2.0%. On the other hand, the MRIw+b plan showed reduced differences to within 0.5%. Further segmentation (MRIs+b) did not produce substantial improvement. Dose deviations affected by the variation of the assigned ED in soft tissues were as small as approximately 1.0%, whereas large deviations were shown in bone and rectal gas regions, especially those with >2% of errors with a direct material allocation. Therefore, assignment values acquired from the patient-specific CTs were suitable and the contouring accuracy of rectal gas regions had large influence on the calculation dose.

### **Conclusions**

Segmented MRI-based VMAT planning with the ED assignment method was feasible.

### **Key words**

## COMPARISON OF 8 DEFORMABLE IMAGE REGISTRATION METHODS ON TOMOTHERAPY MEGAVOLTAGE COMPUTED TOMOGRAPHY IMAGES FOR ADAPTIVE RADIOTHERAPY

Wannapha Nobnop<sup>1</sup>, Hudsaleark Neamin<sup>1</sup>, Imjai Chitapanarux<sup>2</sup>, Somsak Wanwilairat<sup>2</sup>, Vicharn Lorvidhaya<sup>2</sup>, Taweap Sanghangthum<sup>3</sup>

<sup>1</sup> Department Of Radiologic Technology, Faculty Of Associated Medical Sciences, Chiangmai University, Thailand

<sup>2</sup> Division Of Therapeutic Radiology And Oncology, Faculty Of Medicine, Chiangmai University, Thailand

<sup>3</sup> Division Of Therapeutic Radiology And Oncology, Faculty Of Medicine, Chulalongkorn University, Bangkok, Thailand

### Purpose

The Deformable Image Registration (DIR) application on Megavoltage Computed Tomography (MVCT) images is the benefit for adaptive radiotherapy. This study aim to quantify the accuracy of DIR on MVCT images when using the different deformation models which assessed in phantom and nasopharyngeal carcinoma (NPC) patients.

### Methods

In phantom studies, the investigations of DIR accuracy in areas of air-tissue and tissue-tissue interface were observed using twelve shape of acrylic and tissue equivalent materials insert in a cubic phantom. In clinical studies, the MVCT images of seven NPC patients (1st and 20th fraction) were used to evaluate. The eight DIR methods performed by DIRART software vary in (i) DIR registration algorithms (demons or optical flow algorithms), (ii) Transformation framework (asymmetric or symmetric transformation) and (iii) Mapping direction (forward or backward mapping). The accuracy of all methods were compared using an intensity-based criterion (correlation coefficient, CC), and volume-based criterion (Dice Similarity coefficient, DSC).

### Results

The experimental results are consistent between phantom and clinical cases. The asymmetric transformation with optical flow in backward mapping showed the best performance for air-tissue interface areas by the mean value of CC and DSC with  $0.97\pm 0.03$  and  $0.79\pm 0.11$ , respectively. For tissue-tissue interface areas, the symmetric transformation with optical flow algorithm in forward mapping showed the good agreement in mean value of CC ( $0.99\pm 0.01$ ) and DSC ( $0.89 \pm 0.03$ ).

### Conclusions

The different deformation models and also different interface areas were effect the accuracy of DIR. The DIR method in term of intensity correlation and volume overlapping analysis yields clinically acceptable results to use in adaptive radiotherapy.

### Key words

Deformable image registration, DIRART, MVCT, Tomotherapy

## INVESTIGATION OF A TARGET-BASED PATIENT POSITIONING FRAMEWORK FOR IMAGE-GUIDED RADIOTHERAPY IN PROSTATE CANCER TREATMENT

Motoki Sasahara<sup>1</sup>, Hidetaka Arimura<sup>2</sup>, Yusuke Shibayama<sup>3</sup>, Takaaki Hirose<sup>1</sup>, Saiji Ohga<sup>4</sup>, Yoshiyuki Umezu<sup>3</sup>, Hiroshi Honda<sup>4</sup>, Tomonari Sasaki<sup>2</sup>

<sup>1</sup> Department of Health Sciences, Graduate School of Medical Sciences, Kyushu University, Japan

<sup>2</sup> Department of Health Sciences, Faculty of Medical Sciences, Kyushu University, Japan

<sup>3</sup> Department of Medical Technology, Kyushu University Hospital, Japan

<sup>4</sup> Department of Clinical Radiology, Graduate School of Medical Sciences, Kyushu University, Japan

### Purpose

The purpose of this study was to investigate a target-based patient positioning framework for image-guided radiotherapy in prostate cancer treatment.

### Methods

Twenty-four planning CT images with digital imaging and communications in medicine for radiotherapy (DICOM-RT) structures and 33 cone-beam computed tomography (CBCT) images of 5 patients were used for this study. The first step of our proposed framework was the generation of pelvic bone and prostate probabilistic atlases from 24 planning CT images and prostate contours, which were produced in the step of treatment planning. Next, occurrence probabilities of CBCT values within prostate regions were obtained from planning CT images, prostate contours, and CBCT images. Then, the CBCT images were registered to the atlases using a rigid registration with mutual information. Finally, prostate regions were estimated using the Bayesian inference to CBCT images with the probabilistic atlases and the occurrence probabilities of CBCT values within the prostate regions. The proposed framework was evaluated by calculating the Euclidean distance of errors between two centroids of prostate regions determined by the proposed framework and ground truths of manual delineations by a radiation oncologist and a medical physicist on 33 CBCT images of 5 patients.

### Results

The average Euclidean distance (location error) between the centroids of prostate regions determined by our proposed framework and ground truths was  $3.4 \pm 1.5$  mm.

### Conclusions

Our proposed framework based on probabilistic atlases and Bayesian inference might be useful for an automated target-based patient positioning in image-guided radiotherapy of prostate cancer.

### Key words

## **DEVELOPMENT OF SWALLOWING PREDICTION SYSTEM USING PRESSURE SENSOR**

Min-Seok Cho<sup>1</sup>, Siyong Kim<sup>2</sup>, Tae-Ho Kim<sup>1</sup>, Dong-Su Kim<sup>1</sup>, Seong-Hee Kang<sup>1</sup>, Kyeong-Hyun Kim<sup>1</sup>, Dong-Seok Shin<sup>1</sup>, Yu-Yun Noh<sup>1</sup>, Tae-Suk Suh<sup>1</sup>

<sup>1</sup> Catholic University Of Korea, Korea

<sup>2</sup> Department of Radiation Oncology, Virginia Commonwealth University, VA, USA

### **Purpose**

To develop a swallowing prediction system (SPS) using force sensing sensors and evaluate its feasibility.

### **Methods**

The SPS developed consists of force sensing sensor units, a signal transport device and a control PC installed with an in-house software. The SPS is designed to predict the pharyngeal stage of swallowing because it is known that internal organ movement occurs in pharyngeal stage. To detect prediction signal in the SPS, the force sensing sensor unit was attached on the submental muscle region of the thermoplastic mask. A volunteer study was conducted to evaluate the feasibility of the system. In this volunteer study, we intended to verify that the system could predict the pharyngeal stage of the swallowing. sEMG and spirometer were used to verify the pharyngeal stage of the swallowing. We measured time gaps between obtaining the warning signals in the SPS and starting points of the pharyngeal stage of swallowing.

### **Results**

The measured data showed that the time gaps were in reasonable order to be easily utilized.

### **Conclusions**

The proposed method was able to predict the on-set of swallowing of human subjects inside the thermoplastic mask, which has never been possible with other monitoring systems such as camera-based monitoring system. With the prediction ability of swallowing incorporated into the machine control mechanism (in the future), beam delivery can be controlled to skip swallowing periods and significant dosimetric gain is expected in head & neck cancer treatments.

### **Key words**

Swallowing, Prediction, Pressure sensor

## **FEASIBILITY OF A REAL-TIME ALIGNMENT MONITORING SYSTEM USING AN ARRAY OF PHOTODIODES**

Yu-Yun Noh<sup>1</sup>, Siyong Kim<sup>2</sup>, Tae-Ho Kim<sup>1</sup>, Seong-Hee Kang<sup>1</sup>, Dong-Su Kim<sup>1</sup>, Min-Seok Cho<sup>1</sup>, Kyeong-Hyun Kim<sup>1</sup>, Dong-Seok Shin<sup>1</sup>, Tae-Suk Suh<sup>1</sup>

<sup>1</sup> The Catholic University of Korea, Korea

<sup>2</sup> Virginia Commonwealth University, VA, USA

### **Purpose**

To improve the accuracy of patient alignment during treatment, we developed a real-time alignment monitoring system (RAMS) and verified the feasibility by using an in-house designed phantom.

### **Methods**

The RAMS consisted of a room laser sensing array (RLSA) and analog-to-digital converter and control PC. In the RLSA, photodiodes are arranged in a pattern that the RAMS provides alignment in 1 mm resolution. The RAMS can detect misalignments by monitoring signal patterns. To verify the reproducibility of the system, temporal reproducibility and repeatability test was conducted.

The accuracy of the system was tested by measuring signals with varying laser-match positions.

To verify the clinical usability, the system was installed on the phantom, composed of an acrylic box and screw and thermoplastic mask. After set-up, the phantom was moved in positions simulating clinical misalignments and signals of the system were measured in real time.

### **Results**

The results of reproducibility and accuracy tests verified signal stability and resolution of the system.

The results of usability tests which simulated clinical misalignments suggested that the system can accurately detect simulated errors.

### **Conclusions**

The reproducibility and accuracy tests verified that the system is capable of real-time quantitative alignment monitoring. The clinical usability of the system was verified by the phantom study. The system is simple, cost-effective, and easily incorporated into conventional room laser. With these advantages, the system can contribute to improve accuracy of patient alignment during treatment. Through further studies, the clinical applicability of the system will be evaluated by the volunteer study.

### **Key words**

real-time alignment monitoring, room laser

# MARKERLESS TUMOR TRACKING USING PRIOR CONE BEAM COMPUTED TOMOGRAPHY

R B Chhatkuli<sup>1</sup>, KDemachi<sup>1</sup>, MUesaka<sup>1</sup>, AHaga<sup>2</sup>

<sup>1</sup>Department of Nuclear Engineering and Management, The University of Tokyo, Japan; <sup>2</sup>Department of Radiology, The University of Tokyo Hospital

**Key words:** lung tumor, radiation therapy, tracking, markerless

**Introduction**To develop a tumor tracking algorithm for phase recognition during stereotactic body radiation therapy (SBRT) using four dimensional cone beam CT (4D-CBCT) obtained during patient registration [1] and in-treatment cone beam projection images without the use of internal or external markers.

**Methods**In our SBRT protocol [2], both planning 4DCT (for planning) and 4D-CBCT (for patient setup) are acquired during the treatment to create the template projection images for ten phases. In-treatment images can be obtained near real-time during treatment. Template based phase recognition is performed for 4D-CBCT re-projected templates and is compared with the image based recognition called Amsterdam Shroud technique.

**Results:**The offline template matching analysis using the cross correlation indicates that phase recognition performed by using the prior 4D-CBCT has an accuracy up to  $96\pm 2\%$  in comparison with Amsterdam Shroud technique, whereas it has up to  $93\pm 1\%$  for 4DCT. Fig.1 illustrates the template matching for 4D-CBCT and planning 4D-CT at the same angle.

**Discussion:**The mentioned result includes a perfect phase match and  $\pm 1$  phase match. The uncertainties in Amsterdam Shroud technique is believed to be one of the reasons for the mismatch.

**Conclusion:**Markerless tumor tracking based on phase recognition using prior 4D-CBCT has been developed successfully. Though 4DCT is widely used for the tracking of moving tumors [3], 4D-CBCT prove to be more significant as it is taken just prior treatment. We believe this as a first study that reports on the use of prior 4D-CBCT and the comparison of 4DCT with 4D-CBCT for phase recognition

**References:**

1. Nakagawa, Keiichi, et al. "4D registration and 4D verification of lung tumor position for stereotactic volumetric modulated arc therapy using respiratory-correlated cone-beam CT." Journal of radiation research ,2012
2. Haga, Akihiro, et al. "Others: Four-dimensional Cone-Beam CT during SBRT." Stereotactic Body Radiation Therapy, Springer Japan, 2015.

Corresponding author email:ritu@nuclear.jp

**INFORMATION ABOUT THE ABSTRACT**

Image guided radiation therapy (IGRT) has played a major role in the precision of radiation therapy mainly for moving tumors. These IGRT units are used for 2D planar imaging and the acquisition of CBCT. Real-time acquisition of 4D-CBCT however is not possible in principle.

The phase recognition algorithm is divided into four steps, (i) Acquisition of prior 4D-CBCT is a regular part of treatment process using the SBRT protocol in the University of Tokyo Hospital. It is performed just before the treatment for patient setup and registration. (ii) Re-projection of prior 4D-CBCT at one degree interval ( $-180^\circ$  to  $+180^\circ$ ) to create the template images at each angle. (iii) Acquisition of the in-treatment images acquired during the treatment in same position as prior images plus some couch registration. For online acquisition projection streaming client system will be used. (iv) Matching of the template with the in-treatment images at each angles.

For the verification of our algorithm we have used several input data, using linearly driven Quasar Phantom, in built 4D phantom, patients treated in FF (flattening filter) mode, patients treated in FFF (flattening filter free) mode. Finally we also verified the algorithm using planning 4DCT data which is acquired a week before the treatment for the treatment planning and is widely used in tumor tracking. Fig. 1 is one of the example of the template matching for planning 4DCT and 4D-CBCT at the same angle. Though in most of the cases the planning 4DCT and 4D-CBCT shows the similar results, it is believed that in some patient case the amplitude of breathing on treatment day might completely differ from a week before.

4D-CBCT and 4DCT based phase recognition has been successfully completed without the use of any external or internal markers. Real-time tumor tracking using prior images is believed to be significant in the treatment of lung tumor IGRT.

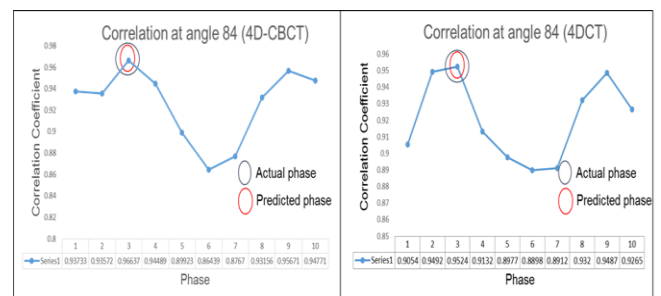


Fig.1 Template matching result for 4D-CBCT (left) and planning CT (right) at the same angle

## IS 3D PATIENT SURFACE OBSERVATION FEASIBLE FOR RESPIRATORY MOTION MONITORING?

Chikae Nakagami<sup>1</sup>, Naoki Hayashi<sup>2</sup>, Takuma Matsunaga<sup>3</sup>, Yusuke Ueshima<sup>1</sup>, Masashi Nozue<sup>4</sup>

<sup>1</sup> Graduate School Of Health Sciences, Fujita Health University

<sup>2</sup> School Of Health Sciences, Fujita Health University

<sup>3</sup> Department Of Radiology, Seirei Hamamatsu General Hospital

<sup>4</sup> Department Of Radiation Oncology, Seirei Hamamatsu General Hospital

### Purpose

Recently the patient surface monitoring technology is widely used to observe intra-setup error in radiotherapy. The scanning technology is evolutionally expanding to three dimensional (3D) scanning. On the other hands, the respiratory motion monitoring is essential in high precision radiotherapy. The purpose of this study is to evaluate the feasibility of 3D scanning procedure for respiratory motion monitoring.

### Methods

We used 3D scanning device (VOXELAN) for observing patient surface. Total of 213 scans (11 patients) was retrospectively analyzed. The scanning field size was up to 15 cm x 60 cm. The raw data of 3D scanning were converted to comma-separated values (CSV) files by a specific in-house program. We selected 9-12 region-of-interests (ROI) from raw data in order to observe kinetic motion and those interrelations. The kinetic motion was compared between medial and peripheral ROIs.

### Results

The processing speed of 3D scanning was 0.15-0.17 seconds even if the maximum scanning field size was set on. According to 3D scanning data, the motion on peripheral ROI was larger than medial ROI. The correlation between those ROIs was better (correlation coefficient ranging from 0.7 to 0.9). Particularly, the peripheral ROI at 7.5 cm from centerline was strong kinetic signal compared to medial ROI when the wider scanning field was set on.

### Conclusions

The motion of 3D patient surface scanning was analyzed. The correlation between medial and peripheral ROIs was confirmed. The 3D scanning technique might be feasible for respiratory motion monitoring in radiotherapy.

### Key words

3D patient surface scanning, respiratory motion, radiotherapy, kinetic analysis

## **SETUP UNCERTAINTY OF HEAD AND NECK CANCER (HNC) PATIENTS TREATED WITH IMAGE GUIDED AND INTENSITY MODULATED RADIOTHERAPY (IG-IMRT)**

Hafiz Zin, Nada Alia M Zamri, Shazril Imran Shaukat, Gokula Kumar Appalanaido  
University Sains, Malaysia

### **Purpose**

IMRT uses sophisticated linac to deliver intensity modulated beams to the tumour target, fraction-by-fraction, over several weeks. The irradiation is guided with imaging modalities incorporated as part of the linac known as image guided radiotherapy (IGRT) to ensure the reproducibility of the patient setup and the accuracy of the delivery. This retrospective study investigates the reproducibility of setup for 27 HNC patients at a new centre using a kV cone- beam CT based-IGRT (Elekta XVI).

### **Methods**

All patients were immobilised with a thermoplastic head mask on a CT scanner during radiotherapy simulation. The clinical target volume (CTV) to planning target volume (PTV) was extended to 3 mm margin in all direction during treatment planning. Cone beam CT images were acquired before radiotherapy treatment and were compared with the intended treatment setup acquired during simulation. The position differences were corrected if exceeded 3 mm. The data were recorded for every patient at every IGRT performed over their course of treatment.

### **Results**

The maximum position differences measured for every patient range between 1.7 mm to 5.0 mm. 14 patients exceeded the 3 mm margin. The results show that a 3 mm margin is sufficient provided that daily imaging and setup correction are performed. Without IGRT modality, a 5 mm margin appears to be safe given that the same immobilisation system is used.

### **Conclusions**

Accurate delivery of IMRT and successful implementation of IGRT in radiotherapy and requires coordinated effort of the medical physicists, the radiation oncologists and the radiation therapists.

### **Key words**

Setup Uncertainty, IGRT, IMRT

## **INTERFRACTIONAL PROSTATE MOTION BEHAVIOR: ASSESSMENT FROM THE EXACTRAC STEREOSCOPIC KV X-RAY SYSTEM WITH FIDUCIAL MARKERS AND CONE BEAM COMPUTED TOMOGRAPHY**

Siwadol Pleanarom, Lalida Tuntipumiamorn, Pittaya Dankulchai  
Siriraj Hospital

### **Purpose**

To evaluate the setup uncertainty for prostate volumetric modulated arc therapy (VMAT) using the ExacTrac system with fiducial marker registration and from cone beam computed tomography (CBCT).

### **Methods**

A total number of 671 stereoscopic x-ray images and 202 OBI CBCT images from 20 prostate VMAT patients treated with TrueBeamSTx were investigated. By daily online matching, the corrections determined from initial laser setup, from the ExacTrac image system, and from CBCT were accumulated. Positioning differences based on fiducial markers registration between Digitally Reconstructed Radiography (DRR) images and the ExacTrac and internal anatomy matching from CBCT were measured in superior-inferior (SI), anterior-posterior (AP) and right-left (RL) directions.

### **Results**

The mean magnitude of shifts ( $\pm$ SD) detected from laser alignment was  $3.01\pm 2.54$  mm in SI,  $5.12\pm 5.24$  mm in AP, and  $2.73\pm 2.76$  mm in RL. With the ExacTrac system, the displacement was reduced to be  $0.78\pm 1.01$  mm in SI,  $0.94\pm 1.45$  mm in AP, and  $0.60\pm 0.76$  mm in RL. Residual setup error assessed from CBCT was  $0.74\pm 1.39$  mm in SI,  $0.93\pm 1.68$  mm in AP and  $0.61\pm 1.38$  mm in RL respectively.

### **Conclusions**

Interfractional prostate motion were found predominantly in AP direction. Using the ExacTrac image guided system with fiducial marker matching was judge to be an efficient method of daily localization. This finding was strongly insisted from the residual setup error results obtained from CBCT.

### **Key words**

Fiducial marker, Prostate cancer, Setup uncertainty, VMAT

## **1.5 Treatment Planning**

## **A COLLISION DETECTION SOFTWARE PROGRAM TO MINIMIZE TREATMENT RE-PLANNING FOR PATIENTS TREATED WITH EXTERNAL BEAM RADIATION THERAPY**

Rasika Rajapakshe

BC Cancer Agency

### **Purpose**

To develop standalone simulation software enabling dosimetrists to pre-determine whether a patient's complex treatment plan would result in any collisions between the linear accelerator components and patient, and/or their immobilization devices.

### **Methods**

Standalone 3D simulation software was developed using Blender, a 3D-graphics suite (<http://www.blender.org>). During the CT imaging session, measurements of the patient's extremities, position, and immobilization devices are recorded. The simulation software uses the measurements to recreate the patient in 3D by scaling a standard human model to the patient's size and position. Immobilization devices are also included in the 3D recreation. Along with the patient, the simulation software reads the treatment plan exported in DICOM format from ARIA and recreates the 3D setup geometry for each beam, allowing the planner to check for collisions and adjust the plan as necessary.

### **Results**

There have been 36 documented collision checks using this software at the Centre during its integration into the treatment work cycle from 30 October 2014 to 1 May 2015. Only plans involving complex treatment setups, with potential for collision, required testing. Of these checked plans, 4 were re-planned prior to delivery due to the detection of a collision during simulation.

### **Conclusions**

We have shown virtual simulations of complex radiation treatments that include patient-specific modeling can be used to accurately detect collisions prior to treatment delivery, saving a considerable amount of time and resources that would otherwise be spent on mock appointments or treatment re-planning.

### **Key words**

External Beam Radiation Therapy, Collision Detection, 3D Patient Model, Patient Safety, Treatment Planning

## **DEEP INSPIRATION BREATH HOLD TECHNIQUES WITH HOMEMADE LPT SYSTEM FOR LEFT BREAST CANCER USING 3DCRT**

Rahman Mohammad Mokhlesur<sup>1</sup>, Zakaria Golam Abu<sup>2</sup>, Azhari Hasin Anupama<sup>1</sup>, Hasan Mahmudul<sup>3</sup>, Rahman Hafizur<sup>1</sup>

<sup>1</sup> Dept of Medical Physics and Biomedical Engineering (MPBME) Gono Bishwabidyalay (University), Savar, Dhaka, Bangladesh

<sup>2</sup> Gummersbach Hospital, Germany

<sup>3</sup> Dept.of Oncology & Radiotherapy Centre, Square Hospitals Ltd, Dhaka, Bangladesh

### **Purpose**

The deep inspiration breath-hold technique (DIBH) can decrease radiation dose delivered to the heart and lung. Deep Inspiration Breath-hold, utilizing a respiration-monitoring device by using LPT system has been used in our clinic to reduce cardiac dose and lung dose for patients receiving left-sided breast irradiation compared to free breathing (FB).

### **Methods**

Between July and October 2015, a total of 10 patients with left-sided breast cancer underwent two computed tomography scans each with the DIBH using LPT system and using FB after mastectomy. The scans were retrospectively re-planned using standardized criteria for the purpose of this study. Treatment plans were generated by 3DCRT technique. The DIBH plans for each patient were compared with FB plans using dosimetric parameters.

### **Results**

All patients were successfully planned with the DIBH technique using LPT system. Significant differences were found between the DIBH and FB plans for mean heart dose (4.49 vs. 5.95Gy,  $p=0.009$ ), heart V30 (4.74 vs. 6.82 %,  $p=0.006$ ), V20 (6.41 vs. 9.12 %,  $p=0.004$ ), and mean left anterior descending coronary artery (LAD) dose (20.39 vs. 24.93Gy,  $p<0.001$ ). The mean left lung dose (8.18 vs. 9.29Gy,  $p=0.001$ ) and lung V20 (20.26 vs. 21.82%,  $p=0.1366$ ).

### **Conclusions**

This study reports that the use of the DIBH technique using LPT system in breathing adapted radiotherapy for left-sided breast cancer is easily feasible in daily practice and significantly reduces the radiation doses to the heart, LAD and lung, therefore potentially reducing cardiac risk.

### **Key words**

LPT system; Breath hold Techniques; Cardiac toxicity; 3DCRT

## **A CLINICAL ESTIMATION OF ESCALATION OF DOSE, USING 3D CRT TO IMRT, IN LUNG CANCER THERAPY: CASE STUDIES IN QUANTIFYING DOSES AT ORGANS AT RISK (OAR) BEYOND THE TUMOR SITE**

Sadiq R. Malik<sup>1</sup>, Motiur Rahman<sup>2</sup>, Shohel Reza<sup>2</sup>

<sup>1</sup> Delta Hospital, Bangladesh

<sup>2</sup> Delta Medical College and Hospital, Bangladesh

### **Purpose**

Lung tissues vary widely in tissue densities with its surrounding organs. This generates immense interest for Radiation Oncologists to estimate doses to OAR (organs at risk) or at proximal and lateral distances from tumor site. Application of advanced imaging and dose calculation algorithm initiated precise treatment planning enabling more sophisticated treatment delivery procedures by 3D Conformal Radiotherapy (3D CRT).

### **Methods**

Lung is a unique organ where special techniques are involved including IGRT (Image Guided Radiation Therapy) and faster imaging. Organs at Risk (OARs) are, therefore, spared. Implementation of comprehensive QA program ensures precise treatment. Intensity-modulated Radiation Therapy (IMRT) which is a more advanced form of 3DCRT. The fact that there is some dose heterogeneity for both the target and normal critical structures in the IMRT planning procedure as compared to the traditional irradiation techniques. IMRT techniques are significantly more complex and advanced than 3DCRT.

### **Results**

IMRT planning and treatment delivery shows significant potential for improving the therapeutic ratio of cancer patient. IAEA-TECDOC-1588 is divided into two parts: 3D CRT and IMRT. It provides guidelines and highlights the milestones that are to be achieved for the transition from 2D RT through 3D CRT to IMRT. The OARs (Organs at Risk) at proximal and distal regions of lung besides Spinal Cord, Other Lung, Ribs, Heart, Esophagus, etc.

### **Conclusions**

Implication of this study in evaluating the plan qualities by Homogeneity and Conformity indexes and DVH (dose volume histogram) analysis prior to approval of treatment plans for delivery.

### **Key words**

3D CRT, IMRT, OAR, QA, DVH

## VERIFICATION OF DOSIMETRIC CALCULATION IN SMALL RADIATION FIELDS FROM ACUROS XB ALGORITHM VERSION 13.6

Buppaungkul S, B.Sc., Asavaphatiboon S, Ph.D, Tangboonduangjit P, Ph.D.

School of Medical Physics, Faculty of Medicine Ramathibodi Hospital, Mahidol University, Bangkok Thailand

**Key words:** MicroDiamond detector, EDGE detector, Diode SRS detector, Acuros XB, Small field, Dose grid resolution

**Introduction:** The aim of this project is to verify the small field dosimetric calculation from Acuros XB (AXB) algorithm version 13.6. Taking a measured data from microDiamond as the reference, the dose calculation from AXB and measurement from EDGE and diode SRS can be compared.

**Methods:** In this study, three detectors were irradiated in 6 MV photon beams with square and rectangular field sizes  $10 \times 10 \text{ cm}^2$  down to  $1 \times 1 \text{ cm}^2$  at a depth of 10 cm in water of SAD technique. In order to achieve the absorbed dose in water, FC-65G and semiflex 31010 were used to calibrate microDiamond, EDGE and diode SRS detector. Then, two methods of collimation field size which are secondary jaws and multileaf collimator (MLC) were used in dosimetric measurement and simulation in AXB for square and rectangular fields. The dosimetric accuracy between measurement and AXB in 1.0 mm and 2.5 mm dose grid resolutions can be evaluated.

**Results:** From Table 1, the difference of absorbed doses from diode SRS is less than 2% for both collimation methods when compared with microdiamond detector. For EDGE detector, the highest different dose can be found as 1.46% and 2.81% in field of  $1 \times 1 \text{ cm}^2$  which is defined by secondary jaws and MLC respectively.

For AXB dose calculation using secondary jaws shaped fields, the dose calculations from AXB 1.0 mm grid resolution ( $AXB_{1.0\text{mm}}$ ) are closer to the dose measured by microDiamond than the AXB dose calculation in 2.5 mm grid resolution ( $AXB_{2.5\text{mm}}$ ). For field sizes of  $1 \times 3$  and  $1 \times 1 \text{ cm}^2$ , the dose difference between  $AXB_{2.5\text{mm}}$  dose calculation and microDiamond are about 2.8 and 3.4% respectively. Using MLC shaped fields, the percentage dose difference in  $AXB_{2.5\text{mm}}$  and  $AXB_{1.0\text{mm}}$  are smaller than 2% for field sizes larger than  $3 \times 3 \text{ cm}^2$ .

**Discussion:** The over response can be observed in  $10 \times 10 \text{ cm}^2$  by using diode SRS detector because of high density of silicon chip. In addition, the doses become decreasingly accurate when EDGE detector is used to measure in smaller field size than  $1.5 \times 1.5 \text{ cm}^2$  [1]. For AXB, the reduction of grid resolution improves in dose accuracy in small fields defined by secondary jaws [2]. However the percentage dose differences for  $AXB_{1.0\text{mm}}$  are higher than  $AXB_{2.5\text{mm}}$  for MLC. This may occur from the reduction of smoothing and averaging of the dose distribution in the high dose gradient regions in small fields and the effect of the scatter or leakage dose calculation for MLC in small fields may influence to  $AXB_{1.0\text{mm}}$  rather than  $AXB_{2.5\text{mm}}$ . In this case, the inaccuracy of dose calculation may cause from the effect of AXB algorithm in modeling of the scatter or leakage dose for MLC in small fields due to only two parameters namely dosimetric leaf gap (DLG) and the leaf transmission (LT) are used to model MLC deliveries in the Eclipse treatment planning [3].

**Conclusion:** This study indicated that smaller AXB grid resolution increases the accuracy of dose calculation for secondary jaws shaped fields. However the results of MLC-shaped fields illustrate the large percent difference of absorbed doses from both  $AXB_{2.5\text{mm}}$  and  $AXB_{1.0\text{mm}}$ . This may be due to the effect of AXB algorithm in modelling of the scatter or leakage dose for MLC in small fields.

**References:**

1. Se An Oh, JiWoon Yea, Rena Lee et al. Dosimetric validation of the output factors in the small field less than  $3 \text{ cm}^2$  using the gafchromic EBT2 films and the various detectors. PROGRESS in MEDICAL PHYSICS, 2014 Dec; 25(4): 218-223.
2. Kan M. W. K, YU P. K. N and Leung L. H. T. Verification of dosimetric impact of Acuros XB algorithm on intensity modulated stereotactic radiotherapy for locally persistent nasopharyngeal carcinoma. Med. Phys. 2012; 39(8): 4705-4714.
3. Fogliata A., Nicolini G., Clivio A. et al. Accuracy of Acuros XB and AAA dose calculation for small fields with reference to RapidArc stereotactic treatments. Med. Phys. 38(11), 6228-6237 (2011).

**Corresponding author email:** sakchai.b@dmsc.mail.go.th

Table 1. The percentage differences of absorbed dose compared with microDiamond for different field sizes. The values in normal and italics are the percentage difference of field sizes defined by secondary jaws and MLC respectively.

| %difference compared with microDiamond detector |              |             |             |              |              |              |             |             |              |             |              |             |             |              |
|---|--------------|-------------|-------------|--------------|--------------|--------------|-------------|-------------|--------------|-------------|--------------|-------------|-------------|--------------|
| Field sizes (cm <sup>2</sup> )                  | 10×10        | 8×8         | 8×2         | 5×5          | 4×4          | 3×3          | 2.5×2.5     | 2.5×1       | 2×2          | 1.5×8       | 1.5×1.5      | 1.2×2       | 1×3         | 1×1          |
| EDGE  | 0.60         | 0.42        | 0.41        | 0.02         | 0.23         | -0.09        | 0.41        | 1.27        | 0.08         | 0.57        | 0.63         | 1.25        | 1.29        | 1.46         |
|   | <i>0.60</i>  | <i>1.49</i> | <i>0.69</i> | <i>1.25</i>  | <i>1.32</i>  | <i>1.23</i>  | <i>0.48</i> | <i>1.61</i> | <i>1.37</i>  | <i>0.62</i> | <i>1.56</i>  | <i>0.87</i> | <i>1.07</i> | <i>2.81</i>  |
| Diode SRS                                       | 1.68         | 0.66        | 0.35        | -0.14        | 0.24         | -0.67        | 0.11        | 0.67        | -0.64        | 0.27        | -0.48        | 0.47        | 0.40        | 0.11         |
|   | <i>1.68</i>  | <i>0.73</i> | <i>0.61</i> | <i>0.03</i>  | <i>-0.16</i> | <i>-0.35</i> | <i>0.13</i> | <i>0.81</i> | <i>-0.49</i> | <i>0.41</i> | <i>-1.09</i> | <i>0.16</i> | <i>0.48</i> | <i>-0.05</i> |
| AXB <sub>2.5 mm</sub>                           | -0.28        | -1.00       | -1.30       | -1.06        | -1.66        | -0.87        | -0.88       | -2.09       | -0.68        | -1.11       | -0.32        | -1.89       | -2.77       | -3.44        |
|   | <i>-0.41</i> | <i>0.09</i> | <i>2.12</i> | <i>-0.14</i> | <i>0.26</i>  | <i>2.19</i>  | <i>2.03</i> | <i>1.79</i> | <i>3.67</i>  | <i>2.47</i> | <i>1.37</i>  | <i>4.16</i> | <i>2.70</i> | <i>2.09</i>  |
| AXB <sub>1.0 mm</sub>                           | -0.28        | -1.00       | -1.30       | -1.06        | -1.66        | -1.03        | -0.88       | -0.54       | -0.85        | -1.11       | -0.66        | -1.21       | -1.40       | -0.70        |
|   | <i>-0.41</i> | <i>0.09</i> | <i>2.12</i> | <i>-0.14</i> | <i>0.26</i>  | <i>1.50</i>  | <i>2.03</i> | <i>3.65</i> | <i>3.52</i>  | <i>2.47</i> | <i>2.85</i>  | <i>4.16</i> | <i>3.68</i> | <i>4.92</i>  |

## **A COMPARATIVE EVALUATION OF 6MV FLATTEN BEAM AND UNFLATTEN BEAM IN CARCINOMA OF CERVIX ? IMRT PLANNING STUDY**

Suresh Tamilarasu<sup>1</sup>, Madeswaran Saminathan<sup>2</sup>, SK Sharma<sup>1</sup>, Anjali Pahuja<sup>1</sup>, Abhinav Dewan<sup>1</sup>, Mayak Tyagi<sup>1</sup>

<sup>1</sup> Rajiv Gandhi Cancer Hospital and Research Center, India

<sup>2</sup> VIT University, India

### **Purpose**

To compare the IMRT plan quality using 6MV Flatten and Unflatten beam in Ca. Cervix cases

### **Methods**

Ten Ca. Cervix patients were selected, Planning Target volume (PTV) and Organ at risk (OAR) were delineated. Dose prescribed to Planning Target volume (PTV) was 50.4Gy in 28 fractions. 6MV FB IMRT and 6MV UFB IMRT plans were generated using True beam Linear accelerator. The planning were performed on Eclipse Treatment Planning system.

### **Results**

All the plans satisfied our dosimetric criterion. FB IMRT plans produces better conformity index (CI) and Homogeneity index (HI) in compared to 6MV UFB IMRT. There is no big difference in isodose distribution. Statically significant difference observed in D50%, D2% of target PTV, V50Gy of bladder, MU, Beam On time (BOT), mean non tumour integral dose (NTID) and low dose volume coverage in normal tissues were statistically significant. MUs delivered per fraction were significantly lower for the FB plans as compared to the FFFB. Dose rate in FFFB plan was 2.3 times higher than FB plan, thereby leading to 48% decrease in beam on time.

### **Conclusions**

6MV Un flatten beam (UFB) produces the dosimetrically and clinically acceptable plan by IMRT technique. Innovative technology plays important role in radiotherapy, by increase patient safety, reduce the patient waiting time. In this study, we recommended that 6MV UF x-ray beam was a good choice for cervical cancer IMRT and further clinical studies are needed.

### **Key words**

Intensity Modulated Radiotherapy, Flatten beam, Unflatten beam

## **DOSIMETRIC COMPARISON OF VMAT AND TOMOTHERAPY FOR SYNCHRONOUS BILATERAL BREAST CASES**

Siji Nojin Paul, Jamema S.V., Kishore Joshi, Prabhat K. Sharma, Reena Phurailatpam, Tabassum W., Rajiv Sarin  
Actrec, Tata Memorial Centre, India

### **Purpose**

Dosimetric comparison of Helical Tomotherapy(HT) and Volumetric Modulated Arc Therapy(VMAT) for synchronous bilateral breast irradiation with tumor bed boost.

### **Methods**

8 patients with pathologically proven bilateral breast carcinoma(5 bilateral breast+3 atleast one breast conserved) were analyzed. CT(GE Discovery) scans(2.5mm slice thickness) were obtained followed by target volume delineation according to ESTRO guidelines. Two plans, HT(v4.2.3) and VMAT Eclipse(v13.5.27) were made for each patient. HT plans were generated with 5cm field-width, 0.287pitch, modulation factor 3 and posterior directional block while VMAT plans were generated with 4 partial arcs avoiding the posterior beam entry. The chestwall/breast and supraclavicular field were prescribed to 50 Gy in 25 fractions while tumor bed was simultaneously boosted to 61 Gy. Planning Target Volumes(PTV) were analysed using Coverage Index(CI) and Homogeneity Index(HI), while lungs and heart were analysed using dose volume parameters(V5,V20,Dmean,V13,D2). The data was compared using Wilcoxon signed rank test ( $p < 0.05$ ; significant).

### **Results**

CI and HI were found to be similar for PTV(CI of breast  $p = 0.26$ , CI,HI of TB  $p = 0.4, 0.2$  respectively) and SC(CI,HI  $p = 0.48, 0.2$  respectively). However the lung dose volume parameters(V5,V20,Dmean) significantly favoured HT( $p = 0.01$ ). Heart dose volumes(V5,V13,D2) were comparable in both plans( $p = 0.33, 0.05, 0.05$  respectively). Mean heart doses favoured HT( $p = 0.04$ ) when TB was not in the inner quadrant( $p = 0.11$ ). The average(SD) monitor units and treatment time for HT and VMAT were 6115(751) and 1539(255)MU & 7.4(0.7) and 2.9(0.3) minutes respectively.

### **Conclusions**

Both HT and VMAT produced similar results for PTV and heart; however HT was favourable for low dose volumes in lungs. VMAT delivery was found to be faster as compared to HT.

### **Key words**

Helical Tomotherapy, VMAT, bilateral breast

# IMAGE TRANSFORMATION APPROACH FOR PAN AND TILT DOSE CALCULATION OF VERO GIMBAL MOTION

H. Prasetio<sup>1</sup>, J. Wölfelschneider<sup>1</sup> and C. Bert<sup>1</sup>

<sup>1</sup>Department of Radiation Oncology, Universitätsklinikum Erlangen, Friedrich-Alexander-Universität Erlangen-Nürnberg, Germany

**Key words:** Tracking, Gimbal motion, 4D dose

**Introduction:** Irradiation of an intra-fractionally moving tumor requires advanced treatment delivery approaches. The development of modern delivery systems makes the treatment of moving tumors possible.<sup>[1-4]</sup> The Vero system has the capability to track moving tumor using its gimbal to inline (tilt) and crossline (pan) direction. Implementing the gimbal motion into a commercial treatment planning system (TPS) is not a straightforward process. This study aims to create the real beam geometry as happens during the treatment to allow a more realistic dose reconstruction.

**Methods:** To simulate an oblique beam geometry, the input images for the TPS have to be rotated using a rotation matrix. The angle of the rotation matrix was based on the target position, whereas the rotation itself was implemented using the Vero center of rotation. Afterwards, the Pinnacle<sup>3</sup> TPS used the rotated images for dose calculation. The final dose distribution was back rotated by reversing the rotation process. Dose verifications were done using static pan-tilt irradiation for field size 10 cm x 10 cm and depth of 1.5 cm, 5 cm and 10 cm using SSD technique. Further studies were done by observing the beam path of a dynamic tracking plan with a synthetic target motion at the tilt direction (Eq. 1) and distributing the MUs according to the target position and time. The amplitude, breathing frequency, initial treatment and total time were defined as A=2.1 cm, c=0,  $\omega=2\pi*0.1$  Hz and t=120 s, while b=8 will define the curve shape. The doses were calculated using SAD technique at depth of 10 cm for field sizes 2 cm x 2 cm and 5 cm x 5 cm. To observe the impact of the image rotation, dose profiles for calculation with and without image rotation were compared.. Irradiation were done at gantry and ring angle of 0°.

$$Y(t) = A * \sqrt{\frac{(1+b^2)}{(1+b^2 \times \cos(\omega t - c))}} \times \cos(\omega t - c) \quad (1)$$

**Results:** The gamma pass rate of the static pan-tilt comparisons were > 99.2% for all depth and positions using 3% / 3 mm  $\gamma$ -criteria. The dose distribution showed an angulated dose distribution, even though the beam was created at gantry and ring 0° (Fig. 1). The dose profile of the calculated dose with the tilt rotation approach was smaller for the region above the target plane, vice versa below the

target plane. The results showed that the image rotation approach is able to simulate the real beam geometry.

**Discussion:** The dose calculation using the image rotation approach at static pan-tilt positions showed good agreement with the measurements. Therefore, the approach is able to simulate the beam geometry during the treatment of dynamic tracking. The dose distribution for a tilt tracking is angulated according to the tilt directions, even though the dose calculations were done at gantry and ring 0°. The dose calculation without implementing the tilt rotation shows under and over dose effects for the dose plane above and below the target. Therefore, the implementation of the image rotation will avoid the under- and over-dose situations, additionally give better insight for the delivered dose. The image rotation will be a promising approach to implement pan-tilt motion in the dose calculation, and can also be implemented at any TPS. Implementing of the image rotation and adding the MUs distributions according the target position and time will make the dose calculation on the TPS closer to the treatment delivery.

**Conclusion:** The gamma passing rate for each individual pan-tilt position > 98.2%, which shows that the image rotation can simulate the real beam geometry of the pan-tilt motion. The implementation of the image rotation can avoid under- and over- dose within the whole dose distribution. Additionally, adding a MUs distribution, which is based on the target position and timing during the motion, would create a more realistic dose calculation during the pan-tilt motion.

**References:**

1. Kamino Y, Takayama K, Kokubo M, et al. Development of a four-dimensional image-guided radiotherapy system with a gimbaled X-ray head. *Int J Radiat Oncol Biol Phys*, (2006),66(1):271–8.
2. Dieterich S, Pawlicki T. Cyberknife Image-Guided Delivery and Quality Assurance. *Int J Radiat Oncol Biol Phys*, (2008),71(1 SUPPL.):126–30.
3. Keall PJ, Cattell H, Pokhrel D, et al. Geometric accuracy of a real-time target tracking system with dynamic multileaf collimator tracking system. *Int J Radiat Oncol Biol Phys* (2006),65(5):1579–84.
4. Menten MJ, Guckenberger M, Herrmann C, et al. Comparison of a multileaf collimator tracking system and a robotic treatment couch tracking system for organ motion compensation during radiotherapy. *Med Phys*, (2012),39(11):7032.

Corresponding author email: heru.prasetio@uk-erlangen.de

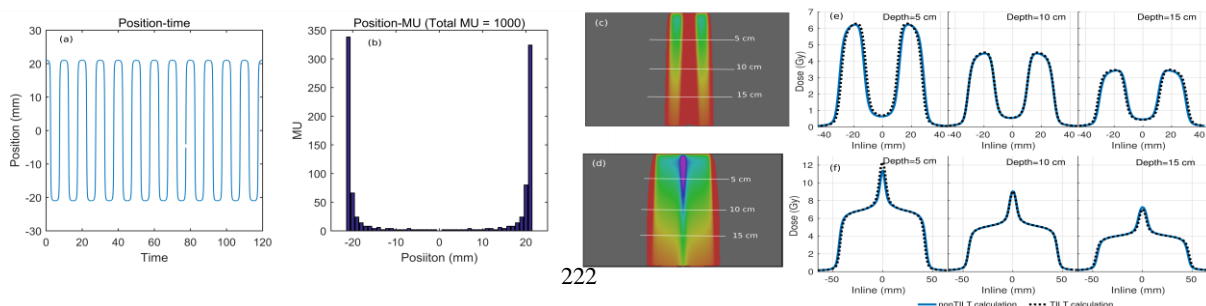


Fig. 1. The breathing of the target (a), the MUs distributions (b) for the dose calculation within the TPS, the calculated dose distributions (c, d) and the dose profile comparison between dose calculation with- and without- the tilt rotation (e, f) for field sizes 2 cm x 2 cm and 5 cm x 5 cm.

## **DOSIMETRIC COMPARISON OF RAPIDPLAN AND MANUALLY OPTIMIZED PLAN IN VOLUMETRIC MODULATED ARC THERAPY FOR PROSTATE CANCER PATIENTS**

Kazuki Kubo<sup>1</sup>, Hajime Monzen<sup>1</sup>, Mikoto Tamura<sup>1</sup>, Kentaro Ishii<sup>2</sup>, Ryo Ogino<sup>2</sup>, Ryu Kawamorita<sup>2</sup>, Wataru Okada<sup>2</sup>, Ryuta Nakahara<sup>2</sup>, Shun Kishimoto<sup>2</sup>, Kotoko Imai<sup>2</sup>, Toshifumi Nakajima<sup>2</sup>, Yasumasa Nishimura<sup>1</sup>

<sup>1</sup> Kinki University, Japan

<sup>2</sup> Tane General Hospital, Japan

### **Purpose**

RapidPlan (Varian Medical Systems, Palo, Alto, CA) is a commercially available knowledge-based planning software that uses a model library consisting of previous plans. The purpose of this study is to evaluate the performance of RapidPlan in volumetric modulated arc therapy (VMAT) for prostate cancer.

### **Methods**

Fifty-one prostate VMAT plans, which optimized sparing of the rectum and bladder doses, were used to train the RapidPlan model. Thirty consecutive patients with clinically treated localized prostate cancer were enrolled. For each patient, a VMAT plan was generated using RapidPlan and compared with a manually optimized clinical plan (MOCP) using dose-volume parameters of the rectum and bladder. All the plans were normalized by setting the target volume mean dose.

### **Results**

The mean absolute differences between the plans generated with RapidPlan and the MOCPs were 0.3%, 1.2%, 0.1%, 0.6%, and 2.1% at rectal mean dose (Dmean), V50Gy, V70Gy, V75Gy, and V78Gy, respectively, and 1.5%, 1.5%, 1.3%, 0.8%, and 1.0% at bladder Dmean, V50Gy, V70Gy, V75Gy, and V78Gy, respectively. Plans generated using RapidPlan resulted in statistically significant low values at the rectum V50Gy and bladder Dmean, V50Gy, V70Gy, and V75Gy ( $p < .05$ ).

In contrast, the MOCPs resulted in statistically significant low values at rectum V75Gy, rectum V78Gy and bladder V78Gy ( $p < .05$ ).

### **Conclusions**

The RapidPlan-based plans were comparable to the MOCPs in terms of rectal and bladder doses even though slightly higher doses were observed at rectum V75Gy, rectum V78Gy and bladder V78Gy.

### **Key words**

RapidPlan, VMAT, knowledge-based planning

## **ESTIMATION OF INTERPLAY BETWEEN RESPIRATORY MOTION AND DYNAMIC BEAM DELIVERY IN STEREOTACTIC BODY RADIOTHERAPY USING TREATMENT LOG FILES**

Yuichi Akino<sup>1</sup>, Hiroya Shiomi<sup>2</sup>, Ryoong-Jin Oh<sup>3</sup>, Shintaro Maruoka<sup>4</sup>, Junichi Sasaki<sup>4</sup>, Kazuhiko Ogawa<sup>2</sup>

<sup>1</sup> Suita Tokushukai Hospital, Japan

<sup>2</sup> Osaka University Graduate School Of Medicine, Japan

<sup>3</sup> Miyakojima Igrt Clinic, Japan

<sup>4</sup> Suita Tokushukai Hospital, Japan

### **Purpose**

For stereotactic body radiotherapy (SBRT), intensity-modulated radiotherapy (IMRT) technique often improves treatments in terms of conformal dose distribution and shortened treatment time. For moving targets, dynamic beam delivery will cause degradation of dose distribution. Here, we developed a technique to estimate such interplay effects using treatment log files.

### **Methods**

Dynamic (DMLC) and static (SMLC) IMRT plans were created for 6 patients who received SBRT for hepatocellular carcinoma. Prescribed dose was tentatively 10 Gy / fraction. The beams were irradiated in air using 'QA-mode' of TrueBeam STx (Varian Medical Systems) linac. In treatment log files, which are automatically generated after irradiation, delivered MU and geometric information are recorded every 20 ms. For each period, a fluence map was generated using an in-house software. The fluence maps were translated with sinusoidal motion mimicking respiration. The amplitude and frequency of the motion were derived from cine-MRI of each patient. Fluence maps were summed for each beam and compared with the original maps summed without translation.

### **Results**

Blurring effects were observed at superior and inferior edges of the dose distribution. Therefore, dose difference was calculated in area overlapping with internal target volume (ITV). For criteria of 2% of maximum, passing rate of the dose differences were  $86.1 \pm 7.0\%$  and  $90.2 \pm 8.3\%$  for DMLC and SMLC plans, respectively.

### **Conclusions**

The interplay effects between target motion and IMRT beams were estimated using log files. With the system developed in this study, the effects can be easily simulated without additional devices such as motion phantoms.

### **Key words**

respiratory motion | SBRT | IMRT

## **EVALUATING CORRELATION BETWEEN GEOMETRICAL RELATIONSHIP AND DOSE DIFFERENCE CAUSED BY RESPIRATORY MOTION USING STATISTICAL ANALYSIS**

Dong-Seok Shin, Seong-Hee Kang, Dong-Su Kim, Tae-Ho Kim, Kyeong-Hyeon Kim, Min-Seok Cho, Yu-Yun Noh, Tae Suk Suh

Department of Biomedical Engineering, and Research Institute of Biomedical Engineering, College of Medicine, The Catholic University of Korea, Korea

### **Purpose**

Dose differences between three-dimensional (3D) and four-dimensional (4D) dose could be varied according to geometrical relationship between a planning target volume (PTV) and an organ at risk (OAR). The purpose of this study is to evaluate correlation between overlap volume histogram (OVH), which quantitatively shows the geometrical relationship, and the dose difference.

### **Methods**

Four-dimensional computed tomography (4DCT) were acquired for ten liver cancer patients. Internal target volume based treatment planning was performed. Three-dimensional dose was calculated on a reference phase (end- exhale). Four-dimensional dose was accumulated using deformation vector fields between the reference and other phase images of 4DCT from deformable image registration. OVH was calculated to quantify geometrical relationship between a PTV and selected OAR. The statistical analysis was performed to verify correlation with the OVH and the dose difference for OAR, and the OVH and center-of-mass distance between the PTV and OAR.

### **Results**

On the basis of specific points that correspond to 10%, 20%, 30%, 40%, and 50% of OAR volume overlapped with expanded PTV, respectively, the correlation between the OVH and the dose difference for duodenum was verified. Correlation coefficients range was -0.691 to -0.679, and R-square range by regression analysis was 0.461 to 0.488 (p-value range from 0.025 to 0.031). However, the distance did not correlate with the dose difference (p-value =0.181).

### **Conclusions**

The correlation between the OVH and the dose difference was verified. In potentially, the OVH can be an indicator that predicts the dose difference between 4D and 3D dose.

### **Key words**

4D dose, overlap volume histogram, respiratory motion

## COMMISSIONING OF RADIOTHERAPY TREATMENT PLANNING SYSTEM BY USING CIRS (002LFC) LIKE LOCALLY DEVELOPED INHOMOGENEOUS PHANTOM

Md. Anwarul Islam<sup>1</sup>, Asim Kumar Paul<sup>2</sup>, Golam Abu Zakaria<sup>3</sup>

<sup>1</sup> Jahangirnagar University, Bangladesh

<sup>2</sup> Gono University, Bangladesh

<sup>3</sup> Gummersbach, Academic Teaching Hospital of The University of Cologne, Germany

### Purpose

To commissioning the radiotherapy treatment planning system by using locally developed inhomogeneous wax phantom.

### Methods

A locally developed inhomogeneous wax phantom have been used which is incorporated with animal's bone (hole-4) as bone equivalent, cork sheet (hole-1) and plastic bottle with cotton (hole-3) as lung equivalent and wax (hole-2) as body tissue equivalent materials. Four individual scans have been taken for each hole and chamber. Seven different treatment plans have been made using the Eclipse treatment planning system (version 8.6) on the wax phantom following TECDOC-1583 protocol. Each of those plans has been delivered by Varian Clinac DHX-4526 (6MV photon energy). The differences between the measured and calculated dose have been reported and agreement of criterions have been mentioned in the first bracket individually.

### Results

Percent of deviation between calculation and measurement dose for case-1 in hole-1, hole-2, are 7.424%(4%),3.896%(2%), case-2 in hole-1, 14.16%(4%), case-3 in hole-2, 2.44%(3%), case-4 in hole-1, hole-2, hole-3, 3.38%(4%),0.249%(3%), 0.68%(4%) case-5 in hole-1, hole-2, 0.69%(4%), 0.99%(2%), case-6 in hole-2, hole-4, 4.16%(3%),2.82%(4%) and case-7 in hole-2 from different angle 2.04%(3%), 5.26%(3%), 2.68%(3%) respectively.

### Conclusions

Most of the cases have been obtained very good agreement with the agreement criterion and for a very few cases incongruity due to exact placement of ionization chamber, air gap and effective point of measurement of the ionization chamber in the measuring hole. If the above mentioned problem could be resolved, this locally developed phantom could be used to verify the treatment planning system in our country.

### Key words

Treatment Planning, Wax Phantom

## **DOSIMETRIC ANALYSIS FOR FLATTENING FILTER FREE BEAMS IN RAPIDARC AND INTENSITY MODULATED RADIOTHERAPY FOR HEAD AND NECK CANCER**

Girigesh Yadav, Manindra Bhushan, Lalit Kumar, Kothanda Raman, Mahammood Suhail, Ravindra Shende, Gourav Kumar, Parveen Ahlawat, Munish Gairola  
Medical Physics Division, Rajiv Gandhi Cancer Institute And Research Centre, Sector-5, Rohini, Delhi, India

### **Purpose**

To study the dosimetric impact of flattening filter free beams (FFFB) in RA and IMRT for Head and Neck cancer.

### **Methods**

Varian True Beam linear accelerator was operated in FFF mode to generate the beam data for TPS (Eclipse version 11.0) commissioning. For ten cases, RA and dynamic IMRT planning were generated using 6MV photon beam for flatten beam (FB) and FFFB. Plan quality were analyzed in terms of target coverage, homogeneity, conformity, organ at risk (OAR) sparing, Monitor units and integral dose to normal tissue.

### **Results**

It was observed that, FFFB shows comparable target coverage ( $p > 0.05$ ) and slight reduction in mean doses to OAR's ( $p > 0.05$ ) as compared to FB in both modalities. Although FFFB delivers less homogenous dose distribution in comparison to FB in RA and IMRT. Conformity Index also does not deviate much in any modality. FFFB delivers lesser integral dose to normal tissues but difference was significant for RA (IMRT  $p > 0.05$  and RA  $p < 0.05$ ). There were significant ( $p < 0.05$ ) reduction in low dose volumes of 2Gy and 5 Gy for FFFB in both modalities. FFFB requires significantly ( $p < 0.05$ ) higher MU's to deliver same dose distribution compare to FB in both RA and IMRT.

### **Conclusions**

FFFB reduces doses to OAR's for similar target coverage, but it generate lesser homogeneous dose distribution in compare to FB for both modalities. It also requires more number of MU's to deliver the same dose in RA and IMRT.

### **Key words**

RapidArc, IMRT, flattening filter free beams, flatten beam

## **DEVELOPMENT OF THREE-DIMENSIONAL RESPIRATORY CURVE MONITORING SYSTEM USING KINECT V2 CAMERA**

Atsuyuki Ohashi<sup>1</sup>, Teiji Nishio<sup>1</sup>, Daiki Hashimoto<sup>2</sup>, Masato Tsuneda<sup>1</sup>, Akito Saito<sup>1</sup>, Makiko Suitani<sup>2</sup>, Hidemasa Maekawa<sup>2</sup>, Shuichi Ozawa<sup>1</sup>, Koji Ikenaga<sup>3</sup>, Yasushi Nagata<sup>1</sup>

<sup>1</sup> Hiroshima University Department of Radiation Oncology, Graduate School of Biomedical & Health Science and Ashiya Radiotherapy Clinic Nozomi

<sup>2</sup> Mizuho Information & Research Institute, Inc., Japan

<sup>3</sup> Ashiya Radiotherapy Clinic Nozomi, Japan

### **Purpose**

In radiation therapy, variable type respiration monitoring system is used principally for treatment of lung cancer and liver cancer. Most of those systems have only measurement function of one or two dimensional location of respiratory curve monitoring. Therefore, development of simplified system with measurement of three dimensional location is important for high precision of radiation therapy. The purpose of our study is to develop construct and verify of the 3-D respiratory curve monitoring system using near infrared radiation.

### **Methods**

Respiratory curve monitoring system was constructed by Kinect v2 (Microsoft Corporation) and special software developed for determination of the location. The system can detect maximum 30 circle markers of RGB with about 15 - 30Hz. 3-D locational detection precision of our system was verified by tracking of 5 blue circle markers with step

of 7 cm. Also, the location measurement of 10 seconds was conducted with several distances of every 5 cm between the system and the marker.

### **Results**

The location resolution (fluctuation) of marker detection of 10 seconds was 0.3 mm. Each location of 5 markers was determined within 2 mm in three axes. And the location of each 5 markers with several distances of every 5 cm between the system and the marker was measured by precision within 2 mm in three axes.

### **Conclusions**

We developed prototype 3-D respiratory curve monitoring system using Kinect v2 and verified resolution of 3-D location. It was indicated that this developed system was useful for high precision of radiation therapy.

### **Key words**

near infrared measurement, respiratory curve monitoring

## **BASIC PHOTON BEAM DATA OF LINEAR ACCELERATOR INPUT INTO TREATMENT PLANNING SYSTEM AND VERIFY THE RESULTING DATA WITH PHOTON BEAM DATA ACCORDING TO TRS-398 AND TG-53 PROTOCOL**

Md. Sharafat Hossain<sup>1</sup>, Md. Sharafat Hossain<sup>1</sup>, Hasin Anupama Azhari<sup>1</sup>, Golam Abu Zakaria<sup>2</sup>, S.M. Enamul Kabir<sup>3</sup>

<sup>1</sup> Department of Medical Physics and Biomedical Engineering (MPBME) of Gono Bishwabidyalay, Savar, Dhaka, Bangladesh

<sup>2</sup> Department of Medical Radiation Physics, Gummersbach Academic Teaching Hospital, University of Cologne, Germany

<sup>3</sup> Department of Radiation Oncology, North East Medical College, Sylhet, Bangladesh

### **Purpose**

The purpose of the study is to verify the accuracy of the dose calculation method using a comprehensive set of measurements, to create a new data set from the TPS for accurate dose distribution and to notify that the depth dose and beam profile are under the tolerance level and clinical situation.

### **Methods**

Dose distributions from a linear accelerator were measured using an ion chamber in a water phantom (blue phantom). Photon beam data set includes - open square fields' Percentage Depth Dose's (PDDs) and profiles, wedged fields' Percentage Depth Dose's (PDDs) and profiles and output factor. The data set has inputted in the TPS algorithm and obtained a new data set. This procedure was TRS-398 and TG-53 protocol based.

### **Results**

As a result of that comparison, the calculated PDDs, profiles and output factor was in excellent agreement with the measured data set. The monitor unit tests revealed that the 6MV open square fields and wedged field meet the TG-

53 criteria all the time. The calculations of dose agreed with actual measurements to within  $\pm 5\%$  for both open and wedge fields.

### **Conclusions**

The main purpose of us is to obtain a maximum cure rate and without getting accurate data from TPS, it is totally impossible to obtain this. So, this type of study may help to more develop the treatment.

### **Key words**

Percentage Depth Dose, Beam Profile, Output, Treatment Planning System.

## **PREDICTION OF RADIATION PNEUMONITIS USING FOUR-DIMENSIONAL COMPUTED TOMOGRAPHY-BASED IMAGING TO IDENTIFY POORLY VENTILATED LUNG REGIONS**

Masakazu Otsuka<sup>1</sup>, Noriyuki Kadoya<sup>2</sup>, Hajime Monzen<sup>1</sup>, Kenji Matsumoto<sup>1</sup>, Mikoto Tamura<sup>1</sup>, Masahiro Inada<sup>3</sup>, Tamaki Nishi<sup>4</sup>, Kenta Sakaguchi<sup>4</sup>

1 Department of Medical Physics, Graduate School of Medical Science, Kindai University, Japan

2 Department of Radiation Oncology, Tohoku University School of Medicine, Japan

3 Kindai University Faculty of Medicine Department of Radiation Oncology, Japan

4 Department of Central Radiology Kindai University Hospital, Japan

### **Purpose**

Prediction of radiation pneumonitis using four-dimensional computed tomography-based imaging to identify poorly ventilated lung regions

### **Methods**

Pretreatment 4D-CT data were used to compute ventilation images for 40 lung cancer patients. Ventilation images were calculated from 4D-CT data using a deformable image-registration and Jacobian-based algorithm. We normalized each ventilation map by converting it to percentile images. 4D-CT based ventilation images can be provided quantitative indication by percentile. Lung and poorly ventilated areas of the 0–10th, 0–20th, 0–30th, 0–40th, and 0–50th percentiles were estimated from the mean lung dose (MLD), V 20, and V 5. The utility of dose volume and ventilation-based dose volume (poorly ventilated areas) for prediction of severe ( grade 2) radiation pneumonitis was assessed using the area under the curve (AUC).

### **Results**

The highest MLD AUC values were observed in the 0–30th percentiles (0.809) of ventilated lung areas. For V20, the highest AUC values were found in ventilated lung areas of the 0–30th percentiles (0.774), and for V5 they were in ventilated lung areas of the 0–20th percentiles (0.843). The highest AUC values for MLD, V20, and V5 were obtained in poorly ventilated areas.

### **Conclusions**

The highest V 5 and MLD AUC values were obtained in the 0–30th percentiles of poorly ventilated areas, while for V 20 they were obtained in the 0–20th percentiles. Our data suggest that avoidance of poorly ventilated areas (for the 20th and 30th percentiles) can be useful to decrease the risk of severe radiation pneumonitis.

### **Key words**

deformable image registration, pulmonary ventilation, lung cancer, treatment planning

## PLANEVALUATION OF INTENSITY MODULATED RADIATION THERAPY AND VOLUMETRIC MODULATED ARC THERAPY IN BILATERAL BREAST IRRADIATION WITH 3 ISOCENTERS TECHNIQUE

Puntiwa Oonsiri<sup>1</sup>, Kitwadee Saksornchai<sup>1</sup> and Sivalee Suriyapee<sup>2</sup>

<sup>1</sup>Department of Radiology, King Chulalongkorn Memorial Hospital, Bangkok, Thailand

<sup>2</sup>Department of Radiology, Faculty of Medicine, Chulalongkorn University, Bangkok, Thailand

**Key words:** Bilateral breast irradiation, IMRT, VMAT, DVH parameter

**Introduction:** Bilateral breast irradiation needs a sophisticated treatment planning due to the large treated volume and the concern regarding the low dose volume of normal lungs and heart irradiated. The VMAT technique is investigated to be feasible for breast irradiation in many clinical cases [1]. The limitation of gantry rotation has made VMAT planning in bilateral breast irradiation limited. The aim of this study was to compare the dosimetric parameter between intensity modulated radiation therapy (IMRT) and volumetric modulated arc therapy (VMAT) plan with 3 isocenters technique for bilateral breast irradiation.

**Methods:** The retrospective of 5 bilateral breast cancer cases were reviewed. The CT data was acquired with Siemens Somatom Definition 64 slices (Siemens Healthineers, Erlangen, Germany) as 2 mm slice thickness. The eclipse treatment planning version 11.0.31 was used for IMRT and VMAT optimization. The prescribed dose was 50 Gy in 25 fractions. 3 isocenters were used for the setup position; left, middle and right of PTV volume while the longitudinal and vertical were the same. The isocenter setup and beam angles are shown in Fig. 1. PTV volume of D<sub>95%</sub>, Conformity index ( $V_{\text{Prescribed}}/V_{\text{PTV}}$ ) and homogeneity (D<sub>5%</sub>-D<sub>95%</sub>), mean lung dose (MLD) and volume receiving 20Gy (V<sub>20Gy</sub>), mean heart dose, maximum dose of left anterior descending coronary artery (LAD) and the number of MU per fraction were compared for both techniques.

**Results:** The mean±SD of D<sub>95%</sub> for PTV volume was 48.7±0.2 for IMRT and 48.7±0.8 Gy for VMAT. The mean CI for both technique was the same (0.97). The IMRT plans showed significantly better for homogeneity of dose distribution in PTV volume than VMAT, 5.6±0.7 Gy for IMRT and 7.6±1.1 Gy for VMAT. The MLD was 16.2±0.6 Gy (IMRT) and 16.6±0.9 Gy (VMAT). Mostly, the two tails

student t-test showed no significant dose differences between IMRT and VMAT for PTV volume and organs at risk. The ratio of MU<sub>IMRT</sub> to MU<sub>VMAT</sub> = 3.0.

**Discussion:** Our study shows that IMRT and VMAT technique for bilateral breast irradiation were comparable for DVHs analysis which is consistent with the results from Giorgia et al [2]. we used 3 isocenters for IMRT and VMAT plan which was changed only the lateral direction, as the longitudinal and vertical direction was fixed. These positions can make its easily to setup by the technologist. The delivery time of VMAT plan was lesser than IMRT technique.

**Conclusion:** The 3 isocenters technique of VMAT plan for bilateral breast irradiation showed comparable plan quality with IMRT with shorter treatment delivery time.

### References:

1. Singla R, King S, Albuquerque K, Creech S, Dogan N: **Simultaneous integrated boost intensity modulated radiation therapy (SIB-IMRT) in the treatment of early stage left side breast carcinoma.** Med Dosim 2006, 31:190-196
2. Nicolini G, Clivio A, Fogliata A, Vanetti E, Cozzi L: **Simultaneous integrated boost radiotherapy for bilateral breast: a treatment planning and dosimetric comparison for volumetric modulated arc and fixed field intensity modulated therapy.** Radiation Oncol 2009, 4: 27: 1-12.

Corresponding author email: nim\_1000d@hotmail.com

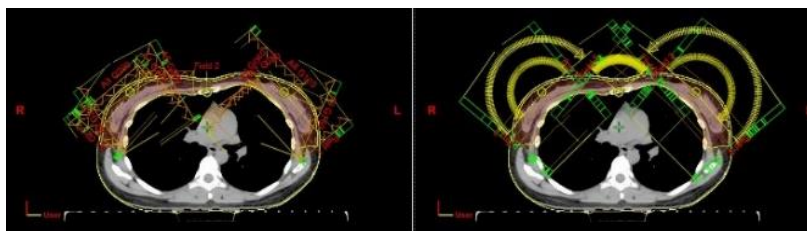


Figure 1. The isocenter setup and beam angles for IMRT (left) and VMAT (right) planning

## DEFINITION OF TARGET MARGINS TO INTERNAL TARGET VOLUME IN DYNAMIC TRACKING IRRADIATION

Naoki Hayashi<sup>1</sup>, Yuma Takada<sup>2</sup>, Tsutomu Mizuno<sup>2</sup>, Shingo Tanahashi<sup>2</sup>, Hiroki Nakae<sup>2</sup>, Taro Murai<sup>3</sup>

<sup>1</sup> Kisk0224, Japan

<sup>2</sup> Department of Radiology, Ogaki Tokushukai Hospital, Japan

<sup>3</sup> Department of Radiology, Nagoya City University, Japan

### Purpose

The VERO-4DRT system can provide dynamic tracking irradiation (DTI) for the target with respiratory motion. The radiotherapy planning of DTI requires suitable target margins to internal target volume (ITV). The purpose of this study is to define the suitable target margins to ITV in DTI.

### Methods

We defined ITV through four-dimensional computed tomography (4DCT) with specific gating window in each patient. For definition of target margins to ITV and to make sure the accuracy of DTI, we performed several contents in commissioning of DTI: the accuracy of absorption dose at isocenter in DTI, the field size and penumbra of DTI, the accuracy of 4D modeling in DTI. These contents were compared the results between static irradiation and DTI. The sine and irregular shaped waves were used for demonstrative respiratory motion.

### Results

As the comparison of the absorbed dose, the average dose error at isocenter was less than 0.5%. As the result of relative dose distribution, the field size (defined by 50% dose line) was not significantly differences in all respiratory patterns. However, the penumbra was larger in greater respiratory motion (up to 4.1 mm). From these data, target margins to ITV should be defined by respiratory motion patterns. The 4D modeling coincidence between actual and created waves was within 1%.

### Conclusions

We evaluated the characteristics of DTI by phantom-based commissioning. The target margins to ITV should be defined by patient specific quality assurance.

### Key words

Dynamic tracking irradiation, respiratory motion, target margins, radiotherapy planning

## **A TECHNIQUE FOR PEDIATRIC TOTAL BODY ELECTRON IRRADIATION**

Tomas Kron, Grace Donahoo, Peta Lonski, Maria Portillo, Sam English, Greg Wheeler  
Peter MacCallum Cancer Centre, Melbourne

### **Purpose**

Total Body Electron Irradiation (TBEI) is a technique to treat cutaneous lymphomas. While TBEI is rarely required in pediatric patients it poses particular problems for the delivery. It was the aim of the present work to develop a method to deliver TBEI to young children requiring anesthetics during treatment.

### **Methods**

A customized couchtop with a Mylar base and Perspex frame was built and the patient treated in supine position. Two times six fields of 6MeV electrons spaced by 60 degree gantry angles were used without electron applicator and a jaw defined field size of 36 x 36cm<sup>2</sup>. Electron energy was degraded using a 12mm Perpex block on the gantry. Focus to skin distance was maximized by displacing the patient in opposite direction of the beam using both vertical and lateral couch adjustments. FSD was carefully monitored as each field was delivered at a different couch position.

The two sets of six fields were matched at approximately 65% dose at skin by displacing them in sup/inf direction by 60cm.

### **Results**

A two year old patient was treated in 12 fractions of 1.5Gy over 2.5weeks. Dose to skin was verified daily using thermoluminescence dosimetry and radiochromic film. The treatment parameters were adjusted slightly based on in vivo dosimetry resulting in a dose distribution for most of the treatment volume within +/- 20% of the prescribed dose. Six areas were boosted using conventional electron therapy.

### **Conclusions**

TBEI can be delivered to pediatric patients positioned supine using a conventional linear accelerator.

### **Key words**

Radiotherapy, Skin, Electrons, Total Body

# **STUDY OF UNFLATTENED BEAM OVER FLATTENED BEAM USING DIFFERENT PHOTON ENERGIES AND DOSE CALCULATION ALGORITHMS ON DIFFERENT VENDORS DELIVERY SYSTEMS IN BILATERAL CARCINOMA OF BREAST**

Suresh Tamilarasu<sup>1</sup>, Madeswaran Saminathan<sup>2</sup>, Sk Sharma<sup>1</sup>, Anjali Pahuja<sup>1</sup>, Abhinav Dewan<sup>1</sup>

<sup>1</sup> Rajiv Gandhi Cancer Hospital and Research Center, India

<sup>2</sup> Vit University, India

## **Purpose**

To evaluate the quality of plans of three different photon energies and two dose calculation algorithms and compare the unflattened (UF) to flattened beam (FB) in VMAT and IMRT.

## **Methods**

Thirty plans were generated for bilateral carcinoma of breast and the dose prescribed to PTV was 50.4Gy in 28 fractions. Six different plans were made for each patient using 4MV FB, 6MV FB and 6MV UFB and AAA & Monte Carlo dose calculation algorithms. Plans were generated on Eclipse and Monaco TPS and capable to be delivered on True beam STx and Synergy platform. The Homogeneity index (HI), conformity index (CI), normal tissues integral dose (NTID), effect of low dose volume on normal tissue and monitor units (MU) were noted.

## **Results**

All the plans were clinically acceptable. The HI and CI of 6MV UF Rapid Arc (RA) plans were higher compared to other plans  $1.16\pm 0.05$  and  $0.12\pm 0.00$  respectively. There is no huge difference observed in OAR's doses. The mean NTID and low dose volume was significantly low in Varian 6MV RA FB and UFB plans compared to other plans. 6MV RA UFB needs 20-30% higher MU compared to other plans ( $p<0.05$ ).

## **Conclusions**

RA plan generated with UFB in Eclipse, achieved the target coverage and preserved OAR's almost similar to 6MV RA FB, 4MV and 6MV FB of Elekta IMRT/VMAT plans. However RA plans generated in Varian Eclipse of FB and UFB were superior in lesser mean NTID and lower low dose volumes in normal tissue.

## **Key words**

Flattened and Unflattened beam, Rapid Arc and Volumetric Arc Therapy

## **1.6 Brachytherapy**

## COMPARISON OF TG43 AND TG186 DOSIMETRY FOR AN INFLATABLE MULTICHANNEL HDR ESOPHAGEAL APPLICATOR

Allan Wilkinson, Anzi Zhao, Shengqiang Gao, John Greskovich

Cleveland Clinic, USA

**Key words:** HDR brachytherapy dose calculations heterogeneity corrections TG186

### **Purpose**

To compare dosimetric distributions calculated using TG43 and TG186 with measured distributions under different inflation conditions of an esophageal applicator.

### **Methods**

A 6-channel inflatable esophageal applicator designed in our institution was used in a water phantom under various inflation conditions (water vs air, different volumes) with an Elekta microSelectron v3 HDR afterloader to irradiate EBT-3 films. The films were scanned using an Epson Perfection 4990 flatbed scanner and the data exported into Omnipro software. Planar dose distributions were calculated using TG43 formalism and recalculated using TG186 and sent from the Oncentra TPS (v 4.5) to Omnipro for analysis.

### **Results**

Dose distributions were measured and calculated for 2 planes--abetting the applicator and 1 cm from it. For the water filled inflations, both TG43 and 186 calculations agreed well with the measured values (gamma values of  $> 99\%$  (3%, 3mm) ). When air was used to inflate the applicator, the TG 186 calculation was significantly better than the TG43 (gamma values of 99% and 81% respectively (3%,3mm) ).

### **Conclusions**

As expected, the TG43 dose calculation compared well with the film dosimetry when the inflation material was water. However, the presence of air in the applicator produced perturbations in the dose distribution that were modeled well only when using an advanced algorithm such as ACE (TG186 calculation).

## **BRAZIL RADIOACTIVE SOURCES PRODUCTION FOR CANCER TREATMENT**

Maria Elisa Rostelato, Carla D. Souza, Carlos A. Zeituni, João A. Moura, José R. O. Marques, Osvaldo L. Costa, Anselmo Feher, Bruna T. Rodrigues, Daiane C. B. De Souza, Fernando S. Peleias Junior, Anderson Sorgatti, Rodrigo Mosca, Eduardo S. De Moura, Rodrigo T. Abreu, Rachel V. De Souza, Beatriz N. De Souza

IPEN-CNEN/SP, Brazil

### **Purpose**

The modality, known as brachytherapy, was performed in Brazil by only a handful of hospitals at an extremely high cost. For producing new sources, five major areas must be considered: 1) source production: nuclear activation and/or radiochemical reaction; 2) welding; 3) Quality control: leakage tests; 4) Dosimetry and metrology; 5) Operational procedures; 6) validation studies. To perform all steps, a multidisciplinary team works together to overcome difficulties. - Iridium-192 pellets: In Brazil there are 140 machines with pellets that replacement every 5 years. Our new production line has assembly, welding and quality control hot cells. - Iridium-192 wires: Produced since 1999. The wire is activated at IPEN's IEA-R1 reactor for 30 hours with  $5 \times 10^{13}$  n/cm<sup>2</sup>.s<sup>-1</sup> neutron flux resulting in 192 mCi maximum activity. - Iridium-192 seed: New seed for ophthalmic cancer treatment. The irradiation device presented 90% activity homogeneity. We are still testing in-vivo. - Iodine-125 seeds: Largely used in low dose brachytherapy. I-125 binding yield achieved with our new reaction was 80%; Laser welding presented 70% efficiency. Approved in all leakage tests. - Other ongoing projects: Veterinary brachytherapy, Waste management, Radionecrosis healing with laser, calibrations sources production, linear accelerator calculations for hospitals, sources with polymeric matrix Our Iodine-125 seeds will be available in 2018. All other projects are advancing. We will continue to develop new products hoping to help the Brazilian population fight against cancer. For producing new sources, five major areas must be considered: 1) source production: nuclear activation and/or radiochemical reaction; 2) welding; 3) Quality control: leakage tests; 4) Dosimetry and metrology; 5) Operational procedures; 6) validation studies. To perform all steps, a multidisciplinary team works together to overcome difficulties

### **Methods**

For producing new sources, five major areas must be considered: 1) source production: nuclear activation and/or radiochemical reaction; 2) welding; 3) Quality control: leakage tests; 4) Dosimetry and metrology; 5) Operational procedures; 6) validation studies. To perform all steps, a multidisciplinary team works together to overcome difficulties.

### **Results**

- Iridium-192 pellets: In Brazil there are 140 machines with pellets that replacement every 5 years. Our new production line has assembly, welding and quality control hot cells.  
- Iridium-192 wires: Produced since 1999. The wire is activated at IPEN's IEA-R1 reactor for 30 hours with  $5 \times 10^{13}$  n/cm<sup>2</sup>.s<sup>-1</sup> neutron flux resulting in 192 mCi maximum activity.  
- Iridium-192 seed: New seed for ophthalmic cancer treatment. The irradiation device presented 90% activity homogeneity. We are still testing in-vivo.  
- Iodine-125 seeds: Largely used in low dose brachytherapy. I-125 binding yield achieved with our new reaction was 80%; Laser welding presented 70% efficiency. Approved in all leakage tests.  
- Other ongoing projects: Veterinary brachytherapy, Waste management, Radionecrosis healing with laser, calibrations sources production, linear accelerator calculations for hospitals, sources with polymeric matrix

### **Conclusions**

Our Iodine-125 seeds will be available in 2018. All other projects are advancing. We will continue to develop new products hoping to help the Brazilian population fight against cancer.

## THE “CLAWS” – A UNIQUE GOLD APPLICATOR LOADED WITH I-125 SEEDS FOR WHOLE-EYE RADIOTHERAPY

C Trauernicht<sup>1</sup>, ER Hering<sup>1</sup>, FCP du Plessis<sup>2</sup>, GJ Maree<sup>1</sup>

<sup>1</sup>Groote Schuur Hospital and University of Cape Town, South Africa; <sup>2</sup>University of the Free State, Bloemfontein, South Africa

**Key words:** Claws, I-125, whole-eye radiotherapy

**Introduction:** The “Claws” is a specially designed gold applicator that is loaded with I-125 seeds for localised whole-eye radiotherapy [1]. The applicator is mainly used to treat retinoblastoma, a childhood cancer of the eye.

**Methods:** Under general anaesthesia, a pericorneal ring is attached to the 4 extraocular muscles, and 4 appendages, each loaded with I-125 seeds, are inserted beneath the conjunctiva in-between each pair of muscles and attached anteriorly to the ring. The applicator has an inside diameter of 22 mm. This study aims at improving the dose calculations in the “Claws” from the current point source approximation of each seed to a Monte Carlo based method [2]. Spectra of the seed at different angles were measured using a silicon drift detector. Seed measurements in specially designed phantoms were done using thermoluminescent dosimeters and gafchromic film. A CAD model of the “Claws” was designed [3] and used to manufacture a PVC model in a milling machine, which was then micro-CT scanned at a 20 µm resolution. The CAD model was also cut into 20 µm slices; these will be edited and used as input for Monte Carlo simulations.

**Results:** The applicator irradiates the eye with minimal dose to the surrounding bony orbit, extraocular optic nerve, eyelids and lacrimal gland. Certain seeds may be omitted to reduce the dose to the unaffected parts of the eye. A typical treatment prescription is 40 Gy given over

4 days to the centre of the eye. General anaesthesia is also required for the removal of the applicator.

**Conclusion:** The applicators are cost-effective because they can be re-used, and the I-125 seeds are regularly used for other eye plaques and implants. Cosmesis is excellent. The Monte Carlo simulations will take into account the gold shielding of the applicator and the anisotropic dose distribution around the I-125 seeds, which will give a better estimation of the dose to the organs at risk.

### References:

1. Stannard, C *et al.*: Localized whole eye radiotherapy for retinoblastoma using a I-125 applicator, “claws”; *Int. J. Radiation Oncology Biol. Phys.*, Vol.51, No.2, 2001, pp 399-409
2. Trauernicht, CJ *et al.*: The „Claws“ – A gold applicator loaded with I-125 seeds for localized whole eye radiotherapy; *RadiotherOncol* Vol 103, Supplement 2, S151-2, May 2012
3. Trauernicht, CJ *et al.*: Improved dose calculations in the “Claws”; *PhysicaMedica*: Vol. 31, S13, Sep 2015



Figure 1: Model of the “Claws” loaded with I-125 seeds

## DEVELOPMENT OF IR-192 SOURCE POSITION MONITORING SYSTEM BY USING A PIN-HOLE CAMERA

Shinji Kawamura<sup>1</sup>, Masahiro Koike<sup>2</sup>, Shotaro Takahashi<sup>3</sup>, Takehiro Shiinoki<sup>3</sup>, Hideki Hanazawa<sup>3</sup>, Yoshinori Tanabe<sup>2</sup>, Keiko Shibuya<sup>3</sup>

<sup>1</sup>Teikyo University, Japan

<sup>2</sup>Yamaguchi University Hospital, Japan

<sup>3</sup>Department Of Radiation Oncology, Graduate School Of Medicine, Yamaguchi University, Japan

**Key words:** Ir-192, pin-hole camera, source position, quality assurance

### Purpose

In recent years, several medical events related source position error of brachytherapy have been reported in Japan. Source position detection during treatment is one of the most important QA of brachytherapy. We developed stereo-type pin-hole camera for detecting source positions during treatment. The purpose of this study is to evaluate the accuracy of source monitoring system and usefulness as a QA tool.

### Methods

We developed stereo-type pin-hole camera which have been shielded entire circumference by lead plate and can insert imaging plate as a photon detecting device. First we implemented phantom study to evaluate image quality and accuracy of 3-dimensional source coordinates by using image analysis software. Next, we applied this system to clinical treatment of cervical cancer to compare the coordinate of source position that calculated by pin-hole images to the coordinates from TPS data. The estimate equation of position differences  $D_n$  describe below:

$$D_n = \sqrt{((P_{pin}(x) - P_{tps}(x))^2 + (P_{pin}(y) - P_{tps}(y))^2 + (P_{pin}(z) - P_{tps}(z))^2)}$$

Where:  $n$ : number of source point,  $P_n, pin(x)$ : x coordinate from pin-hole camera,  $P_n, TPS(x)$ : x coordinate from TPS, 'y' and 'z' as well.

### Results

We could get pin-hole images which can analyze the coordinate of source positions. The average value of difference of source coordinate almost within 1 mm.

### Conclusions

Pin-hole camera is one of the most preferable QA tools for source position detection during brachytherapy treatment.

## **DESIGN AND DEVELOPMENT OF MULTICHANNEL BRACHYTHERAPY APPLICATOR USING INDIGENOUSLY DEVELOPED 3D PRINTING MACHINE**

Senthil Kumar

Madurai Medical College, India

**Key words:** Brachytherapy, multichannel applicator, 3D-printer

### **Purpose**

The purpose of this study was to develop multichannel Brachytherapy applicator and compared with the commercially available applicators by using the indigenously developed 3D Printing machine.

### **Methods**

3D Brachytherapy concept uses the benefits of 3D printing by using steerable needle motion that precisely threads radioactive sources through printed channels to cancer areas. We have successfully indigenously developed the 3D printing machine. Which contain the 3 dimensional motion platform, Heater unit, base plate, ect... To fabricate the Brachytherapy multichannel applicator the 3D design were developed in the computer as virtual design and a 3D modeling program.

### **Results**

The multi channel applicators were printed on a indigenously developed 3D printer using polylactic acid (PLA) material. The same dimensions were used to develop the applicators in the acrylic material also for the comparative study. Applicator was then scanned to confirm the placement of multiple catheter position. Finally dose distributions with rescanned CTs were compared with those computer generated applicator.

### **Conclusions**

The applicators were sterilized multiple times without damage. As of submission 2 types of unique cylinders have been designed, printed and compared dosimetrically. Inverse planning simulated annealing optimization was applied to ensure >99% target coverage and minimal dose to OARs. Statistical significance was evaluated and no difference between the reference plan vs the other catheter combinations in terms of target coverage and doses to OAR. Although this study was specific to polylactic acid, the same setup can be used to evaluate other 3D-printing materials.

## **DOSIMETRIC COMPARISON BETWEEN MANUAL AND INVERSE OPTIMIZATION IN BRACHYTHERAPY PLANNING FOR CERVICAL CANCER**

Pornsuree Chaiyarith, Ekkasit Tharavichitkul, Somsak Wanwilairat

Division of Therapeutic Radiology and Oncology, Faculty of Medicine, Chiang Mai University, Chiang Mai, Thailand

**Key words:** Manual optimization, Inverse optimization, CT-based brachytherapy

### **Purpose**

To evaluate dosimetric parameters between manual and inverse planning simulated annealing (IPSA) optimization in CT-based brachytherapy for cervical cancer

### **Methods**

Total 44 fractions CT images of 11 cervical cancer patients were enrolled to this study. All patients were treated by 50Gy in 25 fractions of teletherapy plus 7Gy x 4 fractions of intracavitary brachytherapy to the D90 of HR-CTV. The dosimetric parameters D90, D100, V100, V200 to HR-CTV and D2cc to bladder, rectum and bowels were evaluated in both manual and IPSA optimization plans. The optimized planning time were evaluated.

### **Results**

The mean D90, D100 and V200 per fraction of HR-CTV in Manual vs IPSA optimized plan were  $7.005 \pm 0.005$  Gy vs  $7.007 \pm 0.004$  Gy,  $4.556 \pm 0.429$  vs  $4.718 \pm 0.456$  Gy and  $0.330 \pm 0.043$  vs  $0.311 \pm 0.041\%$ , respectively ( $p < 0.05$ ). The mean V100 in both optimized method was not significantly. Inverse optimize planning yielded the higher bladder and rectum dose than manual (D2cc Manual vs IPSA:  $5.554 \pm 0.986$  vs  $5.832 \pm 0.831$  and  $3.711 \pm 0.923$  vs  $3.970 \pm 0.906$  Gy, respectively;  $p < 0.05$ ) while lower in bowels and sigmoid (D2cc Manual vs IPSA:  $3.879 \pm 1.573$  vs  $3.459 \pm 1.361$  and  $4.078 \pm 1.331$  vs  $3.804 \pm 1.211$  Gy, respectively;  $p < 0.05$ ). The planning time was lower in inverse optimized planning (Manual vs IPSA;  $5.62 \pm 1.710$  vs  $4.59 \pm 2.970$ ;  $p < 0.05$ )

### **Conclusions**

The result show inverse optimize planning yield lower dose to bowels and sigmoid in the planning. IPSA optimization time is significant faster than manual optimization.

## **DOSIMETRIC COMPARISON BETWEEN CO60 AND IR192 HDR INTRACAVITARY BRACHYTHERAPY IN UTERINE CERVICAL CARCINOMA: TREATMENT PLANNING STUDY**

Rosarin Sintuprom<sup>1</sup>, Puangpen Tangboonduangjit<sup>1</sup>, Nuanpen Dumrongkitudom<sup>2</sup>

<sup>1</sup>Medical Physics School, Department of Radiology, Faculty of Medicine Ramathibodi Hospital, Mahidol University

<sup>2</sup>Department of Radiological Technology, Faculty of Medical Technology, Mahidol University, Thailand

**Key words:** Intracavitary brachytherapy; Co60 source; Ir192 source; dose volume parameters

### **Purpose**

This research aimed to study the difference of dose volume parameters in treatment planning between Co60 and Ir192 HDR intracavitary brachytherapy in uterine cervical carcinoma.

### **Methods**

This retrospective study made by collecting computed tomography (CT) images and treatment planning of patients that were treated by Ir192 source at Ramathibodi Hospital and re-planning by using Co60 source at Bhumibol Adulyadej Hospital. The sample group was 10 cases of tandem and ovoids technique and 10 cases of Cylindrical technique. Research instruments included 2 treatment planning systems which are Oncentra Brachy v 4.3 for Ir192 source calculation and HDR plus 3.0 for Co60 source calculation. Dose volume parameters collected includes V100%, D100, D90 of HR-CTV and D0.1cc, D1cc, D2cc of bladder and rectum. In addition, dose at 0.5 cm. and 1 cm. from tip of cylindrical applicator were also compared. Data was analyzed using Paired t-test.

### **Results**

For preliminary result, it was found that there is no significant difference of HR-CTV V100% ( $p=0.489$ ), HR-CTV D100 ( $p=0.354$ ), HR-CTV D90 ( $p=0.864$ ), bladder D0.1cc ( $p=0.526$ ), bladder D1cc ( $p=0.892$ ), bladder D2cc ( $p=0.957$ ), rectum D0.1cc ( $p=0.796$ ), rectum D1cc ( $p=0.902$ ) and rectum D2cc ( $p=0.956$ ) in Cylindrical technique.

### **Conclusions**

The Co60 and Ir192 source used for uterine cervical carcinoma treatment has no different findings of dose volume parameters in intracavitary brachytherapy treatment planning in initial technique despite a different radial dose function and anisotropy function between two sources.

## IMAGING LIGHT FROM WATER IRRADIATED WITH AN IR-192 SOURCE FOR QUALITY ASSURANCE OF HDR BRACHYTHERAPY

Akihiro Matsushita<sup>1</sup>, Katsunori Yogo<sup>1</sup>, Takahiro Shimo<sup>2</sup>, Tsuyoshi Terazaki<sup>3</sup>, Yoshiki Fujisawa<sup>1</sup>, Takumi Narusawa<sup>1</sup>, Yuya Tatsuno<sup>1</sup>, Kohei Kamada<sup>1</sup>, Nobuaki Syuto<sup>3</sup>, Hiromichi Ishiyama<sup>4</sup>, Kazushige Hayakawa<sup>4</sup>

<sup>1</sup>Kitasato University, Graduate School of Medical Sciences, Japan

<sup>2</sup>Tokyo Nishi Tokushukai Hospital, Japan

<sup>3</sup>Kitasato University Hospital, Japan

<sup>4</sup>Kitasato University, School of Medicine, Japan

**Key words:** HDR, Ir-192, QA

### Purpose

We aimed to develop a quality assurance (QA) tool for high dose-rate (HDR) brachytherapy using light from pure water irradiated with Ir-192 source. The source position measured using light captured from water was compared with that measured by the conventional film method.

### Methods

The Ir-192 source was placed in a water tank and transported with the HDR brachytherapy unit. Light from pure water irradiated with Ir-192 was reflected with a mirror and captured with a camera in a black box. The Ir-192 source was stopped 4 points at 10 mm intervals for 1, 10, 60 and 180 seconds. The source position was recorded at the midpoint of full width at half maximum (FWHM) of light profile from water. The recorded source positions of the light were compared with those measured with radiochromic films.

### Results

We succeeded in imaging light from pure water irradiated with an Ir-192 source. Percentage standard deviations of brightness were within 1.3% stopped for 10-180 seconds, and 5.2% stopped for 1 second. The source position interval measured with our QA tool was  $10.1 \pm 0.4$  mm stopped for 180 seconds. These values were comparable with  $10.0 \pm 0.3$  mm measured with the films.

### Conclusions

Source position intervals measured with light from pure water were comparable to those measured with the films, indicating that our QA tool can be used to accurately measure source intervals. Further development of the tool would enable us to measure shorter source intervals that cannot currently be resolved using films.

## **A MEASUREMENT OF THE TRANSIT DOSIMETRY IN BRACHYTHERAPY**

Sun Young Moon<sup>1</sup>, Dong Wook Kim<sup>2</sup>, Myonggeun Yoon<sup>1</sup>, Weon Kuu Chung<sup>2</sup>, Mijoo Chung<sup>2</sup>

<sup>1</sup>Korea University, Republic of Korea

<sup>2</sup>Kyung Hee University Hospital at Gangdong

**Key words:** Brachytherapy, Scintillator, Glass Dosimeter

### **Purpose**

Confirming the dose delivered to a patient is important to make sure the treatment quality and safety of the radiotherapy. Measuring a transit dose of the patient during the radiotherapy could be an interesting way to confirm the patient dose. In this study, we evaluated the feasibility of the transit dosimetry with a glass dosimeter and scintillating fiber in brachytherapy.

### **Methods**

We made a phantom that inserted the glass dosimeters and placed under patient lying on a couch for cervix cancer brachytherapy. And we placed a scintillating fiber under patient's phantom. A point putting 1cm vertically from the source was prescribed as 500 cGy with glass dosimeter. And A-point was prescribed as 500 cGy with scintillating fibers. Solid phantoms of 0, 2, 4, 6, 8, 10 cm were placed between the source and the glass dosimeter. The transit dose was measured each thickness using the glass dosimeters and compared with a treatment planning system (TPS).

### **Results**

When the transit dose was smaller than 10 cGy, the average of the differences between measured values and calculated values by TPS was 0.50 cGy and the standard deviation was 0.69 cGy. If the transit dose was smaller than 100 cGy, the average of the error was  $1.67 \pm 4.01$  cGy. The error to a point near the prescription point was -14.02 cGy per 500.00 cGy of the prescription dose.

### **Conclusions**

The results of this preliminary study showed the probability of the glass dosimeter and scintillating fibers as the transit dosimeter in brachytherapy.

## **DOSIMETRIC CHARACTERIZATION OF OPTICALLY STIMULATED LUMINESCENCE DOSIMETER UNDER COBALT-60 HIGH DOSE RATE BRACHYTHERAPY SYSTEM.**

Munira Mohd Rejab<sup>1</sup>, Zulaikha Jamalludin<sup>1</sup>, Wei Loong Jong<sup>2</sup>, Jeannie Hsiu Ding Wong<sup>2</sup>, Ngie Min Ung<sup>2</sup>

<sup>1</sup>University of Malaya Medical Centre, Malaysia

<sup>2</sup>University of Malaya

**Key words:** Optically stimulated luminescent dosimeters, Co-60 HDR brachytherapy, in-vivo dosimetry.

### **Purpose**

- (i) To investigate the physical characteristics of optically stimulated luminescence dosimeter (OSLD) for application in Cobalt-60 High Dose Rate (HDR) brachytherapy and
- (ii) To evaluate the suitability of OSLD for dosimetric verification for HDR brachytherapy.

### **Methods**

The OSLDs were characterized for linearity, reproducibility, angular dependence, depth dependence, signal depletion, annealing rate and cumulative dose measurement. A dosimetric verification exercise was conducted using OSLDs and other dosimeters namely in-vivo diodes and Farmer ionization chamber. The results were compared with the calculated dose by the treatment planning system (TPS).

### **Results**

OSLD signal indicated supralinear response ( $R^2 = 0.9998$ ). The reproducibility standard deviation were intraday (0.06 Gy), interday (0.01 Gy) and weekly (0.01 to 0.04 Gy). OSLD agreed with inverse square law (ISL) and exhibited depth independent trend after a steep dose gradient. The signal depletion per readout was negligible (0.017%) with expected deviations for angular dependence ranged from 1% to 16%. The signal decreased from 99.5%, 99.13% and 98.58% within one day of annealing rate for 18 Gy, 10 Gy and 5 Gy respectively. The accumulated and annealed OSLD gave a standard deviation of 0.78 Gy and 0.18 Gy correspondingly. The measured doses overestimated the calculated dose from TPS with deviations of 5.9%, 17.2%, 6.5% and 7.6% for OSLD, Farmer ionization chamber, bladder and rectal probe respectively.

### **Conclusions**

OSLD can be an alternative for in-vivo measurements under Co-60 HDR brachytherapy environment with high consideration of possible positional uncertainty in the high dose gradient region.

## **2 Radiobiology**

## **RADIATION-INDUCED STOCHASTIC EFFECTS FROM PHOTON-BEAM RADIOTHERAPY FOR BONE HEMANGIOMAS OF THE LUMBAR SPINE**

Michalis Mazonakis<sup>1</sup>, Antonis Tzedakis<sup>2</sup>, Efrossyni Lyraraki<sup>2</sup>, John Damilakis<sup>3</sup>

<sup>1</sup>University of Crete, Greece

<sup>2</sup>University Hospital Of Heraklion

<sup>3</sup>University Of Crete

**Key words:** bone hemangiomas, radiotherapy, stochastic effects

### **Purpose**

Bone hemangiomas are benign neoplasms which often appear in lumbar vertebrae and may cause pain and/or neurological deficits. This study determined the risk of stochastic effects after radiotherapy of this benign disease.

### **Methods**

Photon-beam radiation therapy to 36 Gy for bone hemangiomas of the lumbar spine was simulated with a Monte Carlo model. Computational humanoid phantoms were employed to calculate the radiation dose to gonads and critical out-of-field organs. The probabilities of developing heritable effects and out-of-field cancer were estimated with the risk coefficients of the ICRP-103 and BEIR-VII reports, respectively. The organ equivalent dose (OED) to in-field tissues was found by analyzing differential dose-volume histograms derived from patients' conformal radiotherapy plans. The OEDs were used to estimate the in-field cancer risks with an approach accounting for dose fractionation and tissue repopulation.

### **Results**

The radiation doses to organs excluded from the treatment volume were 2.6-28.9 cGy. These peripheral doses increased the baseline risks of cancer induction up to 5.8 % by assuming typical 40-year-old patients with bone hemangiomas. The probability for the appearance of heritable effects in the offspring of irradiated patients was below 0.11 %. The maximum OED was 317.8 cGy. The in-field organ doses from radiotherapy of male patients were found to elevate the baseline cancer risks by 5.4-38.0 %. The corresponding increase in females exceeded 13.8 %.

### **Conclusions**

The presented risks associated with the development of stochastic effects from radiation therapy for benign bone hemangiomas may be of value in the patient's treatment planning and follow-up.

## **IRON OXIDE NANOPARTICLES (IONPS) AS RADIATION DOSE ENHANCER FOR PHOTON BEAM RADIOTHERAPY**

Rosmazihana Binti Mat Lazim<sup>1</sup>, Wan Nordiana Rahman<sup>1</sup>, Khairunisak Abdul Razak<sup>1</sup>, Norhayati Dollah<sup>2</sup>, Raizulnasuha Rashid<sup>1</sup>, Moshi Geso<sup>3</sup>, Binh Pham<sup>4</sup>

<sup>1</sup>Universiti Sains Malaysia

<sup>2</sup>Hospital Universiti Sains Malaysia

<sup>3</sup>Rmit University,

<sup>4</sup>University of Sydney

**Key words:** iron oxide nanoparticles, dose enhancement, megavoltage photon beam radiotherapy

### **Purpose**

Iron oxide nanoparticles that are commonly used as contrast agents for magnetic resonance imaging (MRI) have potential to be applied as radiosensitizer in radiotherapy. The aim of this study is to investigate the dose enhancement effects by IONPs for megavoltage photon beam radiotherapy.

### **Methods**

T24 bladder cancer cells were irradiated with 6 and 10 MV photon beams at different doses with and without 1 mMol of IONPs. Standard clonogenic assay were used to determine the cell survival. The experimental data were then fits to the LQ model using OriginPro 9.2 software.

### **Results**

Dose enhancement factors (DEF) were calculated from the fitting curve generated from the LQ model. Fitting curve of photon beam for cell survivals with and without IONPs was found to be close to the experimental data. The LQ model was found to be in good agreement with the experimental cell survival especially for the cell survival with IONPs. DEF calculated at 90% survival for 6 and 10 MV photon beams are 1.71 and 2.5 respectively showing radiosensitizing effects by IONPs. The results show that the presence of IONPs influenced the dose enhancement effects. The enhancement could be link to the interaction that induced free radical and reactive oxygen species (ROS) that enhanced the cell death.

### **Conclusions**

The investigation on the dose enhancement effects by IONPs were found to be effective as a dose enhancer for cancer radiotherapy using megavoltage photon beam radiotherapy.

# RADIOBIOLOGICAL EVALUATION OF RADIOSENSITIZATION EFFECTS BY GOLD NANOPARTICLES FOR HDR BRACHYTHERAPY

R.Abd Rashid<sup>1</sup>, R. Abdullah<sup>1</sup>, K. Abdul Razak<sup>2</sup>, M. Geso<sup>3</sup>, W. N. Rahman<sup>1</sup>

<sup>1</sup>School of Health Sciences, Universiti Sains Malaysia, Health Campus, 16150 Kota Bharu, Kelantan, Malaysia.

<sup>2</sup>School of Material and Mineral Resources Engineering, Engineering Campus, Universiti Sains Malaysia, 14300 Nibong Tebal, Penang, Malaysia.

<sup>3</sup>Division of Medical Radiation, School of Health & Biomedical Sciences, RMIT University, Bundoora, Victoria, 3083 Australia.

**Keywords:** gold nanoparticles, radiosensitization, radiobiological model, brachytherapy

**Introduction:** Radiosensitization effects by gold nanoparticles (AuNPs) have been proven to potentially increase the effectiveness of radiotherapy. In this study, the radiosensitization effects for High Dose Rate (HDR) brachytherapy were analyzed using radiobiological models and correlations between the models' parameters were investigated.

**Methods:** HeLa cells were irradiated with different radiation doses and AuNPs concentration using Iridium-192 HDR Brachytherapy source. Standard clonogenic assay were used to determine the cell survival. The experimental data were then fits to the Linear Quadratic (LQ), Multi Target (MT) and Repairable Conditionally Repairable (RCR) models. The sensitization enhancement ratio (SER) were obtained in each models fitted.

**Result:** The fitting curves of the cells survivals indicate that MT model were found to be close to the experimental data compare to LQ and RCR model. Quantification of the SER between different models and AuNPs concentration provides value ranges from 1.13 to 2.80 (Fig.1). The radiobiologic parameters showed a larger  $\alpha$  (0.04-0.19) and a lower quasi-threshold dose  $D_q$  (1.10-6.21) as well as the increment for all the RCR model parameters in regard to the increase of the radiosensitization effects induced by AuNPs (Fig. 1).

**Discussion:** The SER increased with the AuNPs concentrations which described the multiple reactions both primary and secondary radiations occurred with the higher accumulation of dose at the cells targeted [1]. All the parameters in each model are found to compliment with the quantified radiosensitization effects.

**Conclusion:** The LQ, MT and RCR models proved it capability for describing the radiosensitization effects

by AuNPs. MT model was found to be more accurate in describing the cell survival in the presence of AuNPs compare to LQ and RCR models. Parameterization of the models also found to be correlated with the increase in radiosensitization effects.

**References:**

1. Rahman, W. N., Bishara, N., Ackerly, T., He, C. F., Jackson, P., Wong, C, Davidson, R., & Geso, M. (2009). Radiation Oncology Enhancement of radiation effects by gold nanoparticles for superficial radiation therapy. *Nanomedicine: Nanotechnology, Biology, and Medicine*, 5, 136–142.
2. Iwata, H., Matsufuji, N., Toshito, T., Akagi, T., Otsuka, O., & Shibamoto, Y. (2012). Compatibility of the repairable-conditionally repairable, multi-target and linear-quadratic models in converting hypofractionated radiation doses to single doses. *Journal of Radiation Research*, 54, 367–373.
3. Fertil, B. & Malaise E. P. (1985). Intrinsic radiosensitivity of human cell lines is correlated with radioresponsiveness of human tumors: Analysis of 101 published survival curves. *Int. J. Radiation Oncology Biol. Phy.*, 11,1699-1707.

Corresponding author email: [wandiana@usm.my](mailto:wandiana@usm.my)

**INFORMATION ABOUT THE ABSTRACT**

LQ model was considered applicable to doses per fraction of 1 to 10 Gy. However it continuously bending curve due to the  $\beta$  cell kill component does not reflect experimental data which most likely to show a linear relationship. MT model known as the classical model are able to fit the empirical data, especially in the range of high doses. Meanwhile RCR model explained the low dose hypersensitivity were fitted nicely with data collected [2]. LQ model show steep initial slope and small shoulder of the cell survival curves. Therefore larger  $\alpha$  value, smaller  $\beta$  and larger  $\alpha/\beta$  ratio are observed. MT model indicate increasing radiosensitization correlate with the parameters of lower  $D_1$ , smaller  $D_0$  and  $n$  values [3]. Meanwhile increment of all  $a$ ,  $b$  and  $c$  parameters values in RCR model, explained radiosensitization effects produced by AuNPs.

| Irradiation             | AuNPs Concentrations (mMol/L) |                  |                      | Sensitization Enhancement Ratio (SER) |         |         |        |         |        |        |
|-------------------------|-------------------------------|------------------|----------------------|---------------------------------------|---------|---------|--------|---------|--------|--------|
|                         |                               |                  |                      | LQ                                    | MT      | RCR     |        |         |        |        |
| 0.38 MeV<br>(Gamma-Ray) | 1 mMol/L                      |                  |                      | 1.24                                  | 1.13    | 1.31    |        |         |        |        |
|                         | 2 mMol/L                      |                  |                      | 1.48                                  | 1.43    | 1.77    |        |         |        |        |
|                         | 3 mMol/L                      |                  |                      | 2.80                                  | 2.65    | 2.30    |        |         |        |        |
| Radiobiological models  | LQ                            |                  |                      | MT                                    |         |         |        | RCR     |        |        |
| Parameters              | Alpha ( $\alpha$ )            | Beta ( $\beta$ ) | $\alpha/\beta$ ratio | $D_1$                                 | $D_0$   | $D_q$   | $n$    | $a$     | $b$    | $c$    |
| Control                 | 0.0311                        | 0.0289           | 1.07                 | 6.5738                                | 32.3762 | 30.3762 | 8.7823 | 1.4065  | 1.1736 | 0.5369 |
| 1 mMol/L                | 0.1622                        | 0.0269           | 6.03                 | 5.6536                                | 7.9213  | 6.2051  | 6.0722 | 0.9675  | 0.7725 | 0.4701 |
| 2 mMol/L                | 0.0392                        | 0.0648           | 0.60                 | 4.6151                                | 2.9598  | 2.1027  | 5.1338 | 3.9599  | 2.0707 | 0.8367 |
| 3 mMol/L                | 0.1946                        | 0.0852           | 2.29                 | 3.5215                                | 2.2050  | 1.1034  | 3.1653 | 39.0749 | 1.9899 | 1.0272 |

Table 1: SER values and radiobiological parameters of LQ, MT and RCR Models

## PLATINUM NANODENDRITES AS NOVEL RADIOSENSITIZER FOR MEGAVOLTAGE RADIOTHERAPY: IN VITRO STUDY

Muhammad Afiq K.A.<sup>1</sup>, R. Abd Rashid<sup>1</sup>, R. Mat Lazim<sup>1</sup>, N. Dollah<sup>1</sup>, K. Abdul Razak<sup>2</sup>, W. N. Rahman<sup>1</sup>

<sup>1</sup>School of Health Sciences, Universiti Sains Malaysia, Health Campus, 16150 Kota Bharu, Kelantan, Malaysia.

<sup>2</sup>School of Material and Mineral Resources Engineering, Engineering Campus, Universiti Sains Malaysia, Nibong Tebal, Penang, Malaysia.

**Key words:** platinum nanoparticles, platinum nanodendrites, radiosensitization, megavoltage radiotherapy

**Introduction:** High atomic number characteristic of metal based nanoparticles such as gold nanoparticles (AuNPs) have been widely exploited to induce radiosensitization in cancer cell, in order to enhance radiotherapy efficacy [1]. In this study, the feasibility of platinum nanodendrites (PtNDs) to induce radiosensitization in conjunction with megavoltage photon beam was investigated.

**Methods:** PtNDs of sizes 29 nm, 36 nm, 42 nm and 52 nm were synthesized using chemical reduction method [2]. The study was conducted in-vitro using HeLa cell line incubated with PtNDs. The cytotoxic effect of PtNDs without irradiation was evaluated using Prestoblue® assay. Samples containing 0.1 mMol/L of PtNDs were then irradiated using 6 MV photon beam with dose ranging from 0 to 10 Gy. Clonogenic assay were used to study the cell survival. The sensitization enhancement ratios (SER) were extrapolated from cell survival curve at 50% survival fraction.

**Results:** The cytotoxicity evaluation shows that PtNDs poses minor cytotoxicity (>70% cell viability). Quantification of the SER for PtNDs of sizes 29 nm, 36 nm, 42 nm and 52 nm provides SER value of 2.02, 2.32, 2.29 and 1.78 respectively.

**Discussion:** The slight cytotoxicity of PtNDs observed in this study might be caused by the formation of platinum ions produced in the media during incubation period, as suggested in previous study [3]. The dose enhancements by PtNDs are found to increase around two folds. Several factors were suggested to be the mechanism behind the radiosensitization: (a) the radiosensitization was contributed by the increase in radiation interaction due to the presence

of PtNDs and production of secondary electron, and (b) the radiosensitization effect were caused by multiple complex biological mechanisms that determine the cell death [4]. The PtNDs concentration used in this study (0.1 mmol/mL) are low compared to AuNPs concentration used in many previous studies and yet PtNDs give considerably higher SER value. Hence, PtNDs could potentially be effective radiosensitizer for megavoltage photon beam. The unique shape and size of PtNDs might play important role in the radiosensitization process.

**Conclusion:** This study demonstrates the potential of PtNDs as radiosensitizer for megavoltage radiotherapy. The increase in radiosensitization effects due to PtNDs could be attributed to many factors such as size, shape and concentration of PtNDs. The mechanism of radiosensitization may closely similar to AuNPs but further investigation is required to fully understand multiple factors that involve in the radiosensitization process.

### References:

1. Kwatra, D., Venugopal, A., & Anant, S. (2013). Nanoparticles in radiation therapy: a summary of various approaches to enhance radiosensitization in cancer. *Translational Cancer research*, 2(4), 330-342.
2. Ridhuan, N. S., Muzafaruddin, N. I., Khairunisak, A. R., & Aw, K. (2014). Formation of Platinum Nanodendrites Embedded Organic Insulator for Memory Application. *Advanced Materials Research*, 1024, 44-47.
3. Gehrke, H., Pelka, J., Hartinger, C. G., Blank, H., Bleimund, F., Schneider, R., ... & Marko, D. (2011). Platinum nanoparticles and their cellular uptake and DNA platination at non-cytotoxic concentrations. *Archives of toxicology*, 85(7), 799-812.
4. McMahon, S. J., Hyland, W. B., Muir, M. F., Coulter, J. A., Jain, S., Butterworth, K. T., ... & Prise, K. M. (2011). Nanodosimetric effects of gold nanoparticles in megavoltage radiation therapy. *Radiotherapy and Oncology*, 100(3), 412-416.

Corresponding author email: wandiana@usm.my

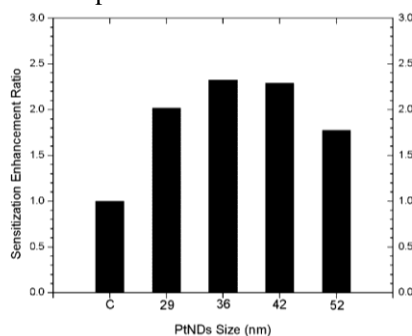


Fig.1 SER comparison between control sample (C) and PtNDs of size 29 nm, 36 nm, 42 nm and 52 nm

## **ISOBIO SOFTWARE: THE BIOLOGICAL DOSE DISTRIBUTION AND BIOLOGICAL DOSE VOLUME HISTOGRAM FROM PHYSICAL DOSE CONVERSION USING LINEAR QUADRATIC LINEAR MODEL**

Tanwiwat Jaikuna , Patchareewan Khadsiri , Ekkasit Tharavichitkul , Suwit Seakho , Nisa Chawapun

Chiang Mai University, Thailand

**Key words:** Biological dose, LQL model, EQD2 software

### **Purpose**

To develop an in-house software program able to calculate and generate the biological dose distribution and biological dose volume histogram by physical dose conversion using Linear Quadratic Linear (LQL) model.

### **Methods**

The Isobio software was developed using MATLAB version 2014b to calculate and generate biological dose distribution and biological dose volume histogram. Physical dose from each voxel in treatment planning was pulled out through Computational Environment for Radiotherapy Research (CERR) and the accuracy was verified by the differentiation between dose volume histogram from CERR and treatment planning system, Equivalent dose in 2 Gray fraction (EQD2) was calculated using BED based on LQL model. Software and manual calculation were compared for EQD2 verification with pair t-test statistical analysis using IBM SPSS statistic version 22 (64bit).

### **Results**

Biological dose distribution and biological dose volume histogram was display correctly by Isobio software in 2- and 3 -dimentional. Physical dose different between CERR and TPS was found in Oncentra with 3.33, 0.56 and 1.74% when determine D90% and D2cc in HR-CTV, bladder and rectum respectively and less than 1% in Pinnacle. The EQD2 between software and manual calculation was not significantly different with 0.000-0.002% as p-value 0.820, 0.095, and 0.593 for External Beam Radiation Therapy (EBRT) and 0.240, 0.320, and 0.849 for Brachytherapy (BT) in HR- CTV, bladder and rectum respectively.

### **Conclusions**

The Isobio software are feasible to generate biological dose distribution and biological dose volume histogram for treatment plan evaluation in both EBRT and BT.

# TEMPERATURE-DEPENDENT AC IMPEDANCE AND DIELECTRIC SPECTROSCOPY OF COMPOSITE BIOMATERIALS FOR BONE TISSUE REPAIR AND ENGINEERING BASED ON CHITOSAN AND NANOCRYSTALLINE HYDROXYAPATITE

Ivo Petrov<sup>1</sup>, Oksana Kalinkevich<sup>2</sup>, Maksym Pogorielov<sup>2</sup>, Aleksei Kalinkevich<sup>2</sup>, Aleksandr Stanislavov<sup>3</sup>, Anatoly Sklyar<sup>4</sup>, Sergei Danilchenko<sup>3</sup>, Temenuzhka Yovcheva<sup>5</sup>

<sup>1</sup>University Hospital – Pleven, Bulgaria

<sup>2</sup>Sumy State University, Sumy, Ukraine

<sup>3</sup>Institute of Applied Physics, Sumy, Ukraine

<sup>4</sup>Sumy State Pedagogical University, Sumy, Ukraine

<sup>5</sup>Department of Experimental Physics, Physics Faculty, University of Plovdiv, Bulgaria

**Key words:** Dielectric spectroscopy; Chitosan; Hydroxyapatite; Nanocomposite

## Purpose

We present our utilization of temperature-dependent impedance/dielectric spectroscopy and equivalent circuits modelling to study chitosan/nano-hydroxyapatite composites and discuss the results' implications in the materials' biomedical applications context.

## Methods

Chitosan/hydroxyapatite nanocomposites were synthesized by one-step coprecipitation method. Physicochemical studies showed that the materials contained nanosized hydroxyapatite with structural features similar to biogenic apatites. Impedance spectra  $|Z|(f)$ ,  $(f)$  in the range  $f=20\text{Hz}-1\text{MHz}$  at different temperatures ( $25^{\circ}\text{C}-100^{\circ}\text{C}$ ) were measured with a modified dielectric spectroscopy system. Data analysis was performed with Microsoft Excel and EC- Lab.

## Results

Nyquist plots  $Z(Z)$ , Bode plots  $Z(f)$  and  $(f)$ , frequency dependencies  $(f)$  and  $(f)$ ,  $|Z|(T)$  at different frequencies, as well as tabulated data of interest were obtained. Further data analysis was performed, including equivalent circuit modelling. Our best fit empirical model for  $37^{\circ}\text{C}$  is presented and its implications and limitations are discussed.

## Conclusions

The studied nanocomposites show behavior quite different from that of chitosan alone and hydroxyapatite alone. Permittivity data are of particular interest and the values observed at physiological temperature in frequency ranges applied in electrostimulation procedures are similar to data available from dielectric spectroscopy of bone tissues. The abrupt and irreversible changes in materials' properties at high temperatures are attributed to chitosan degradation and provide basis for application of DS as nondestructive method for the evaluation of chitosan's stability and preservation in composites for biomedical application. The Warburg element in the presented equivalent circuit represents a RC transmission line behavior that is to be expected with such heterogenous nanocomposites.

# AN INTEGRATED MONTE-CARLO MODEL FOR HETEROGENEOUS GLIOBLASTOMA MULTIFORME TREATED WITH BORON NEUTRON CAPTURE THERAPY

Leyla Moghaddasi<sup>1</sup>, Eva Bezak<sup>2</sup>

<sup>1</sup>The University of Adelaide, Australia

<sup>2</sup>The University of South Australia

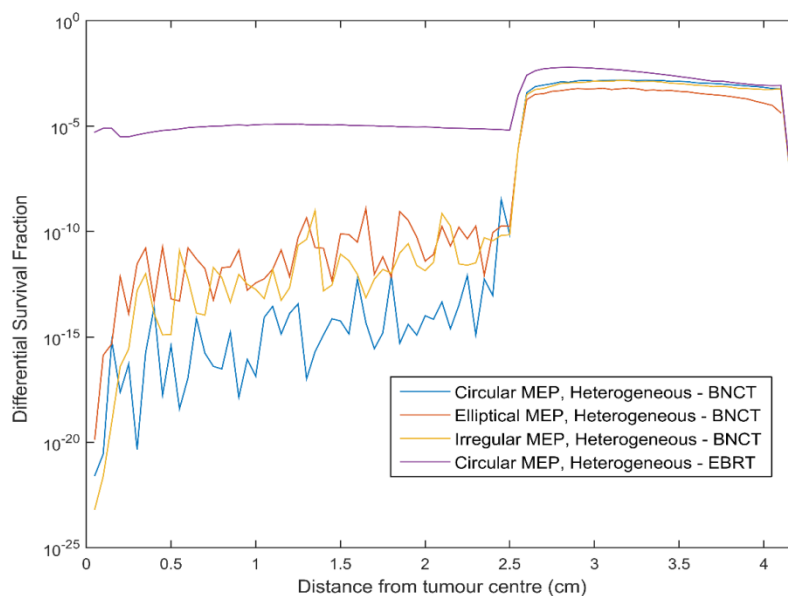
**Key words:** BNCT, glioblastoma

**Purpose:** Boron Neutron Capture Therapy (BNCT), a biochemically-targeted radiotherapy based on thermal neutron capture by <sup>10</sup>B atoms, represents an alternative therapy for Glioblastoma (GBM). The objective of the current work is to develop a BNCT GBM treatment model to investigate the efficacy of BNCT in terms of cell Survival Fraction (SF) following a treatment.

**Methods:** The BNCT GBM model developed is a cell-based dosimetry model using GEANT4.9.6.p02, integrated with in-house developed Microscopic Extension Probability (MEP) and epithermal neutron beam models. The system was defined as a cubic phantom divided to 20 μm side voxels and irradiated with an epithermal neutron beam. Typical <sup>10</sup>B concentrations in GBM and normal brain cells were obtained from literature. Each cell was assigned a material composed of a brain material and a <sup>10</sup>B concen-

tration depending on its MEP status. Heterogeneous radiosensitivity was simulated using a range of  $\alpha/\beta$  values associated with different GBM cell lines. Results from the cell-based dosimetry model and the *in-silico* GBM model were combined to evaluate treatment efficacy in terms of cell SF for CTV margins of 2.0 & 2.5cm. Calculated SFs were compared with those obtained for 6 MV x-ray radiotherapy (XRT).

**Results & Conclusion:** Following BNCT treatment of heterogeneous-hypoxic GBM, SFs within the beam region were smaller by more than two orders of magnitude as compared to XRT. However, compared to XRT, the change in SF as a result of CTV extension was lower by ~2 times using BNCT. Hence, while BNCT results in more efficacious cell kill, extension of the CTV margin may not increase the treatment outcome significantly.



## **3 Diagnostic Imaging**

## EXPERIMENTAL STUDIES FOR MEASURING SLICE THICKNESS IN A TOMOSYNTHESIS SYSTEM

Taku Kuramoto<sup>1</sup>, Junji Morishita<sup>2</sup>, Yutaka Yoshida<sup>2</sup>, Takeshi Shiomi<sup>3</sup>, Toyoyuki Kato<sup>4</sup>, Yasuhiko Nakamura<sup>4</sup>

<sup>1</sup>The Doctoral Course of Health Science, Department of Health Sciences, Kyushu University, Japan

<sup>2</sup>Department of Health Sciences, Faculty of Medical Sciences, Kyushu University, Japan

<sup>3</sup>Medical Systems Division, Shimadzu Corporation, Japan

<sup>4</sup>Division of Radiology, Department of Medical Technology, Kyushu University Hospital, Japan

**Key words:** tomosynthesis, slice thickness, center of rotation (COR)

### Purpose

Acquisition settings, such as height from an imaging table and/or height setting of the center of rotation (COR) in a tomosynthesis system, may affect the slice thicknesses during tomosynthesis imaging. The aim of this study is to quantitatively evaluate the effects of various height settings on the slice thicknesses during tomosynthesis imaging.

### Methods

This study was performed using a tomosynthesis system. A metal bead (diameter, 0.3 mm) was used to measure the slice thicknesses under various conditions. The height of the bead from the imaging table was varied from 50 to 200 mm with the same COR height. In addition, the COR were set at 50 to 250 mm from the heights of the bead. In this study, the slice thickness was defined at the complete full width at half maximum of the bead profile curve.

### Results

Increase in the bead position led to a decrease in the slice thickness with same height settings of the bead and COR. If the height setting of the bead was different from the COR, the slice thickness tended to be increased by approximately 5–10% when the height setting and the COR was higher than the bead. Similarly, the slice thickness decreased when the height settings of the COR were lower than the bead.

### Conclusions

Our preliminary results quantitatively indicated that the slice thickness on tomosynthesis imaging varied depending on the relationship between the height settings of the bead and the COR.

## **A PROPOSAL ON A LAYERED SLIT COLLIMATOR FOR RADIOGRAPHIC IMAGING**

Ippei Kusakari<sup>1</sup>, Koichi Ogawa<sup>1</sup>, Hiroaki Suzuki<sup>1</sup>, Keisuke Usui<sup>2</sup>

<sup>1</sup>Hosei University, Japan

<sup>2</sup>Juntendo University, Japan

**Key words:** collimator, Monte Carlo simulation

### **Purpose**

In the case of x-ray imaging, a collimation is performed with thin lead foils and materials to fill up the spaces between the foils. The filling up materials reduce the number of primary photons passing through the collimator. The purpose of our research is to develop a new layered slit collimator for x-ray imaging.

### **Methods**

We propose a collimator with thin tungsten plates with a thickness of 0.1mm, and insert these plates to a collimator frame with a guide. A thin tungsten plate has some hardness, and so we can make a slit collimator easily. And if we stack these slit collimators alternatively in x- and y-directions, we can eliminate scattered photons without losing the primary photons entering a collimator hole. Performance of the proposed layered slit collimator was confirmed by Monte Carlo simulations. We assumed a water slab phantom with the thickness of 20cm. The tube voltage was 120kV (Al:10mm filter). The distance of the phantom-source and phantom-detector was 75cm. The height of a single slit collimator was 9mm and the perfect parallel hole collimator was 18mm.

### **Results**

The results of simulations showed that the ratio of scatter/primary photons was 0.49 (without a collimator), 0.27 (with a perfect rectangular collimator), and 0.30 (with layered slit collimators in the direction of x and y.)

### **Conclusions**

The performance of the proposed layered slit collimator was almost equivalent to that of the true parallel hole collimator, even though the structure of the collimator was simple, and easy to make.

## DUAL-ENERGY X-RAY COMPUTED TOMOGRAPHY SCANNER UTILIZING AN LSO-MULTIPIXEL PHOTON DETECTOR

Y Sato<sup>1</sup>, E Sato<sup>2</sup>, S Yamaguchi<sup>3</sup>, S Ehara<sup>3</sup>, O Hagiwara<sup>4</sup>, H Matsukiyo<sup>4</sup>, T Enomoto<sup>4</sup>, M Watanabe<sup>4</sup>, S Kusachi<sup>4</sup>

<sup>1</sup>Central Radiation Department, Iwate Medical University Hospital, Japan; <sup>2</sup>Department of Physics, Iwate Medical University, Japan; <sup>3</sup>Department of Radiology, School of Medicine, Iwate Medical University, Japan; <sup>4</sup>Department of Surgery, Toho University Ohashi Medical Center, Japan

**Key words:** high-speed photon counting, high-speed I-V amplifier, dual-energy counting, LSO-MPPC detector, X-ray CT

**Introduction:** Recently, we have developed several energy-dispersive computed tomography (ED-CT) scanners [1-3] with cadmium telluride (CdTe) detectors to perform K-edge imaging using iodine and gadolinium contrast media. However, it is not easy to reduce the exposure time for CT because the maximum count rate of the fairly available CdTe detector for measuring X-ray spectra is approximately 5 kilocounts per second (kcps).

In our research, major objectives are as follows: to develop dual-energy (DE) counter using three comparators, to improve the spatial resolution, to increase the count rate, and to perform DE-CT. Therefore, we developed a high-count-rate DE-CT scanner and confirmed the image-contrast variations with changes in the threshold energy.

**Methods:** DE photon counting was performed using a high-count-rate detector, consisting of lutetium oxyorthosilicate (LSO) crystal and a multipixel photon counter (MPPC) [4]. The DE counter is used to determine two energy ranges for CT and consists of three comparators (COMs) and two microcomputers (MCs). The three threshold energies are determined using three COMs, respectively, and the MC counts X-ray photons between two threshold energies.

**Results:** The energy resolution of the LSO-MPPC detector was approximately 50% at 59.5 keV, and DE-CT was accomplished at a tube voltage of 100 kV and a current of 0.15 mA. The spatial resolutions were 0.5×0.5 mm<sup>2</sup>, and the exposure time for CT was 9.8 min. Using iodine media, coronary arteries were observed at high contrast.

**Discussion:** To improve the spatial resolution, we set a 0.5-mm-diameter lead collimator attached to the detector. Thus, the spatial resolutions were 0.5×0.5mm<sup>2</sup>, and the image quality improves with increasing the photon count per measuring point. In the DE-CT, the maximum count rate was 35 kcps, and the count rate can be increased easily to beyond 100 kcps by improving the counting electronics between two thresholds.

**Conclusion:** We developed a high-count-rate DE-CT scanner with an LSO-MPPC detector. The DE-CT was accomplished at two energy ranges of 33-50 and 50-70 keV, and two-different-energy tomograms were obtained simultaneously.

### References:

1. Sato E, Oda Y, Abudurexiti A, Hagiwara O, Matsukiyo H, Osawa A, Enomoto T, Watanabe M, Kusachi S, Sato S, Ogawa A, Onagawa J, (2012), Demonstration of enhanced iodine K-edge imaging using an energy-dispersive X-ray computed tomography system with a 25 mm/s-scan linear cadmium telluride detector and a single comparator, *Appl. Rad. Isot.* 70, 831-836.
2. Chiba H, Sato Y, Sato E, Maeda T, Matsushita R, Yanbe Y, Hagiwara O, Matsukiyo H, Osawa A, Enomoto T, Watanabe M, Kusachi S, Sato S, Ogawa A, Onagawa J, (2012), Investigation of energy-dispersive X-ray computed tomography system with CdTe scan detector and comparing-differentiator and its application to gadolinium K-edge imaging, *Jpn. J. Appl. Phys.* 51, 102402-1-5.
3. Hagiwara O, Sato E, Watanabe M, Sato Y, Oda Y, Matsukiyo H, Osawa A, Enomoto T, Kusachi S, Ehara S, (2014), Investigation of dual-energy X-ray photon counting using a cadmium telluride detector and two comparators and its application to photon-count energy subtraction, *Jpn. J. Appl. Phys.* 53, 102202-1-6.
4. Oda Y, Sato E, Wada K, Momokawa H, Kataoka D, Otani R, Yamaguchi S, Ehara S, Hagiwara O, Matsukiyo H, Watanabe M, Kusachi S, (2015), Dual-energy X-ray computed tomography using a YAP(Ce)-multipixel-photon detector and an energy-selecting device, *Med. Imag. Inform. Sci.* 32, 71-76.

Corresponding author email: dresato@iwate-med.ac.jp

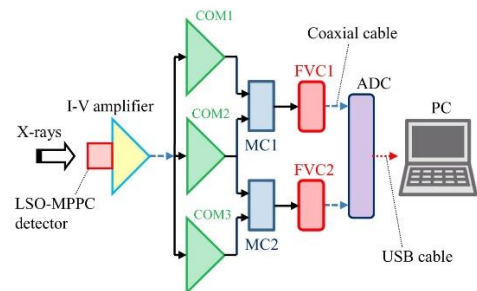


Fig. 1 Block diagram for counting using an LSO-MPPC detector and DE photon counter. The MC performs photon-count energy subtraction in the photon-energy range between two threshold energies.

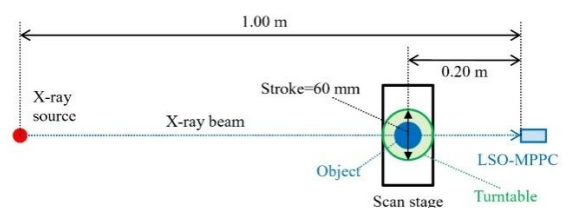


Fig. 2 Experimental setup of the main components in the DE-CT scanner. The DE-CT is performed by repeated linear scans and rotations of the object using an LSO-MPPC linear scanner.

## **A FEASIBILITY STUDY OF BREAST CANCER DETECTION WITH COMPUTER AIDED DIAGNOSIS SYSTEM BASED ON MACHINE LEARNING**

Donghoon Lee, Ye-seul Kim, Hyemi Kim, Sunghoon Choi, Haenghwa Lee, Byungdu Jo, Seungyeon Choi, Dohyeon Kim, Hee-Joung Kim

Yonsei university, Republic of Korea

**Key words:** Breast cancer, mammography, Computer-aided diagnosis

### **Purpose**

The breast cancer is one of the most critical cancer types that are found in women and early detection of breast cancer is significantly important. For years, mammography has been considered as a gold standard for detecting breast cancer and reading mammograms is a significant demanding job for radiologists. In this aspect, computer-aided diagnosis(CAD) is becoming an increasingly important tool to assist radiologists. The purpose of this study is to classify normal and breast cancer lesion with gabor filter texture analysis and machine learning process.

### **Methods**

The 20 normal breast and 10 abnormal breast cases in mini-MIAS database were used for data mining process and gabor filter with four scales, six orientations, and frequencies in the range of 0.05 and 0.4 (mm/lp) were used. After selecting breast cancer and normal tissue features with gabor filter, supervised classification method with linear regression was conducted.

### **Results**

The results of breast cancer CAD system with machine learning showed the ability of cancer classification. For example, the presence or absence of cancer in randomly selected breast mammograms was effectively predicted with developed machine learning CAD system. However it has several limitations: accurate cancer boundary was not perfectly predicted and cancer type such as benign and malignant was not be able to be classified at this time.

### **Conclusions**

In conclusion, breast cancer can be classified with feature analysis and machine learning, although further studies are required to overcome several limitations.

## SPECTRAL X-RAY COMPUTED TOMOGRAPHY SCANNER USING A CADMIUM TELLURIDE DETECTOR

E Sato<sup>1</sup>, Y Oda<sup>1</sup>, S Yamaguchi<sup>2</sup>, T Ishii<sup>3</sup>, O Hagiwara<sup>3</sup>, H Matsukiyo<sup>3</sup>, T Enomoto<sup>3</sup>, M Watanabe<sup>3</sup>, S Kusachi<sup>3</sup>

<sup>1</sup>Department of Physics, Iwate Medical University, Japan; <sup>2</sup>Department of Radiology, School of Medicine, Iwate Medical University, Japan; <sup>3</sup>Department of Surgery, Toho University Ohashi Medical Center, Japan

**Key words:** X-ray CT, photon counting, quad-energy dispersion, spectral CT, CdTe detector, K-edge imaging

**Introduction:** To perform quasi-monochromatic X-ray computed tomography (CT), we developed an energy-selecting device (ESD) [1] for determining an energy range for photon-counting energy-dispersive CT (ED-CT)[2,3]. Using this ED-CT, K-edge imaging using iodine and gadolinium media was performed. In our research, we have developed a spectral CT (SP-CT) scanner with a quad-energy photon counter for obtaining four tomograms with four different photon energy ranges simultaneously.

**Methods:** Figure 1 shows the quad-energy X-ray photon counter, consisting of four sets of comparators, microcomputers (MCs) and frequency-voltage converters (FVCs). X-ray photons are detected using a cadmium telluride (CdTe) detector with an energy resolution of 1% at 122 keV, and the event pulses from a shaping amplifier are sent to four comparators simultaneously to regulate four threshold energies of 20, 33, 50 and 65 keV.

The CdTe detector with the charge-sensitive amplifier oscillates on the scan stage with a velocity of 25 mm/s and a stroke of 60 mm. The X-ray projection curves for tomography are obtained by repeated linear scans and rotations of the object, and the scanning is conducted in both directions of its movement (Fig. 2). Two step values of the linear scan and rotation are selected to be 0.5 mm and 1.0°, respectively. Using this CT scanner, the exposure time is 9.8 min.

**Results:** Using this counter, the energy ranges are 20-33, 33-50, 50-65 and 65-100 keV; the maximum energy corresponds to the tube voltage. Four tomograms were obtained simultaneously at four energy ranges. The maximum count rate was 9.2 kilo-counts per second with energies ranging from 10 to 100 keV, and the exposure time for tomography was 9.8 min.

**Discussion:** In the SP-CT, we used an oscillation-type CdTe linear scanner and cone beams. To improve the spatial resolution, because a 1.0-mm-diameter lead pinhole was used, the resolutions were approximately 1×1 mm<sup>2</sup>. Next, the scan velocity was a maximum value of 25 mm/s, and the image quality improves with reducing the velocity to increase the total photon count per measuring point.

**Conclusion:** We developed a SP-CT scanner with a quad-energy counter, and K-edge imaging using iodine and gadolinium media was carried out utilizing two energy ranges of 33-50 and 50-65 keV, respectively. To reduce the exposure time for CT, the count rate should be maximized under the pileup-less condition.

### References:

1. Watanabe M, Sato E, Oda Y, Sagae M, Sato Y, Yamaguchi S, Hagiwara O, Matsukiyo H, Kusachi S, Ehara S, (2015), Quasi-monochromatic X-ray photon counting using a silicon-PIN detector and an energy-selecting device and its application to iodine imaging, *Med. Imag. Inform. Sci.* 32, 38-43.
2. Sato E, Oda Y, Abudurexiti A, Hagiwara O, Matsukiyo H, Osawa A, Enomoto T, Watanabe M, Kusachi S, Sato S, Ogawa A, Onagawa J, (2012), Demonstration of enhanced iodine K-edge imaging using an energy-dispersive X-ray computed tomography system with a 25 mm/s-scan linear cadmium telluride detector and a single comparator," *Appl. Rad. Isot.* 70, 831-836.
3. Hagiwara O, Sato E, Watanabe M, Sato Y, Oda Y, Matsukiyo H, Osawa A, Enomoto T, Kusachi S, Ehara S, (2014), Investigation of dual-energy X-ray photon counting using a cadmium telluride detector and two comparators and its application to photon-count energy subtraction, *Jpn. J. Appl. Phys.* 53, 102202-1-6.

**Corresponding author email:** dresato@iwate-med.ac.jp

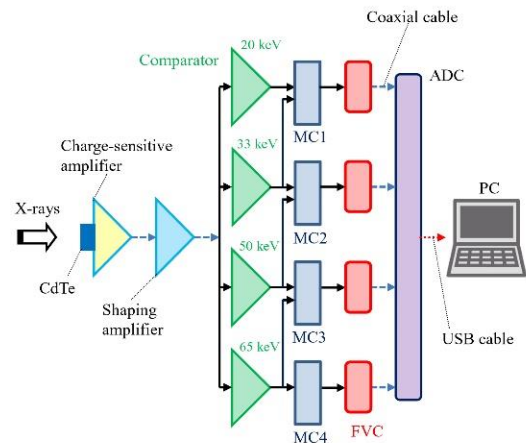


Fig. 1 Block diagram of quad-energy photon counting using a CdTe detector and four sets of comparators, MCs and FVCs. The MC performs photon-count energy subtraction in the photon-energy range between two threshold energies.

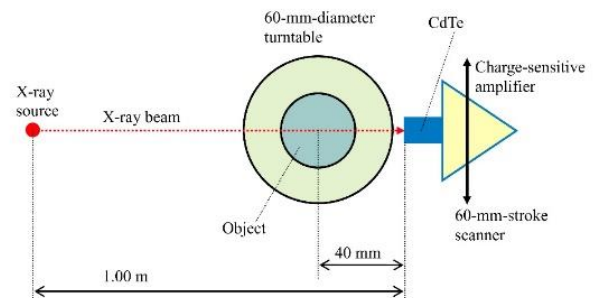


Fig. 2 Experimental setup of the main components in the SP-CT scanner. The SP-CT is performed by repeated linear scans and rotations of the object using a CdTe linear scanner.

## **TRIPLE-ENERGY X-RAY COMPUTED TOMOGRAPHY SCANNER USING A SMALL PHOTOMULTIPLIER TUBE AND AN LSO CRYSTAL**

Satoshi Yamaguchi , Eiichi Sato

Iwate Medical University, Japan

**Key words:** High-speed photon counting, X-ray CT, energy dispersion, triple-energy CT, LSO-PMT detector

### **Purpose**

Cadmium telluride (CdTe) detectors are useful for measuring X-ray spectra, and we developed several photon-counting energy-dispersive computed tomography (ED-CT) scanners. Using this ED-CT, we performed K-edge imaging using iodine and gadolinium media. However, it is difficult to increase the photon count rate of the CdTe detector. Therefore, we have developed a high-count-rate detector and applied this to triple-energy computed tomography (TE-CT).

### **Methods**

X-ray photons are detected using a lutetium oxyorthosilicate (LSO) single-crystal scintillator with a decay time of 40 ns and a small-sized photomultiplier tube (SPMT). The negative output pulse from the SPMT is amplified by a high-speed inverse amplifier, and the event pulses are sent to a multichannel analyzer to measure X-ray spectra. The energy resolution of the spectrometer is 15% at 59.5 keV. TE-CT is carried out using contrast media with a maximum rate of approximately 500 kilo counts per second.

### **Results**

In the TE-CT, the tube voltage and current were 100 kV and 0.5 mA, respectively. The energy ranges were 20-33, 33-50 and 50-65 keV. The X-ray photons with an energy range of 33-50 keV were useful for performing iodine K-edge CT, and gadolinium K-edge CT was accomplished using a range of 50-65 keV.

### **Conclusions**

We developed a TE X-ray photon counter using a SPMT and a short-time-constant amplifier. With changes in the photon-energy range, we confirmed the image contrast variations. Using this TE-CT, we obtained both the iodine and gadolinium K-edge tomograms simultaneously.

## AN IMPROVED METHOD OF EFFECTIVE DOSE ESTIMATION USING SIZE-SPECIFIC CONVERSION FACTOR IN CORONARY COMPUTED TOMOGRAPHY ANGIOGRAPHY (CCTA)

Sock-Keow Tan<sup>1,2</sup>, Chai-Hong Yeong<sup>1,2</sup>, Jeannie Hsiu-Ding Wong<sup>1,2</sup>, Yang Faridah Abdul Aziz<sup>1,2</sup>,  
Zhonghua Sun<sup>3</sup>, Kwan-Hoong Ng<sup>1,2</sup>

<sup>1</sup>Department of Biomedical Imaging, Faculty of Medicine, University of Malaya, 50603 Kuala Lumpur, Malaysia.

<sup>2</sup>University of Malaya Research Imaging Centre (UMRIC), Faculty of Medicine, University of Malaya.

<sup>3</sup>Department of Medical Radiation Sciences, Curtin University, Perth, WA 6845, Australia.

**Keyword:** Coronary computed tomography angiography, effective dose, size-dependent conversion factor.

**Introduction** This paper presented an improved method of effective dose ( $H_E$ ) estimation in coronary computed tomography angiography (CCTA) by applying the size-specific  $k$ -conversion factor ( $k_{size}$ ) in air kerma-length product ( $P_{KL}$ )-to- $H_E$  conversion.

**Methods** Prospectively ECG-gated CCTA were performed using 64-detector-row single source CT (SSCT),  $2 \times 32$ -detector-row-dual source CT (DSCT),  $2 \times 64$ -detector-row DSCT and 320-detector-row SSCT system and recommended clinical protocol. Absorbed organ doses were measured using optically stimulated luminescence dosimeters (OSLD) placed inside an anthropomorphic female phantom.  $H_E$  were estimated using three methods: 1) summing up all the organ doses measured by OSLDs (“measured  $H_E$ ”); 2) multiplying  $P_{KL}$  with the  $k$ -conversion factor, 0.014 mSv/mGy.cm recommended by the European Commission for chest (“computed  $H_E$ ”); 3) multiplying  $P_{KL}$  with the size-specific  $k$ -conversion factor ( $k_{size}$ ) suggested in this study (“size-specific  $H_E$ ”). The “computed  $H_E$ ” and “size-specific  $H_E$ ” were then compared with the “measured  $H_E$ ” (gold standard).

**Results** The  $k_{size}$  of 0.028 mSv/mGy.cm was obtained by multiplying the size-dependent conversion factor of 1.65 determined from Tables 1D AAPM TG-204 (2012)[1]. The “computed  $H_E$ ” were lower than “measured  $H_E$ ” by 38.3 to 53.2%. The difference between “size-specific  $H_E$ ” and “measured  $H_E$ ” were ranged from 0.7 to 22.7%.

**Conclusion** This study suggests an improved method in estimating  $H_E$  from CCTA examination by applying the size-specific  $k$ -conversion factor ( $k_{size}$ ) during  $P_{KL}$ -to- $H_E$  conversion. It provides  $H_E$  estimation with improved accuracy by accounting for differences in body habitus.

**References:**

1. AAPM Task Group 204, Size Specific Dose Estimates (SSDE) in Pediatric and Adult CT Examinations. 2012.

**Corresponding author email:** [ngkh@um.edu.my](mailto:ngkh@um.edu.my)

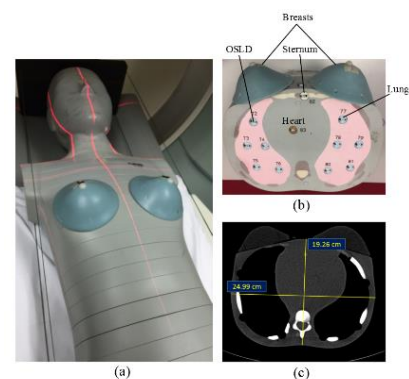


Fig 1. (a) Positioning of phantom according to the clinical CCTA settings; (b) Axial view of the phantom's sectional slab showing the lungs, spine, heart, sternum and breasts; (c) Antero-posterior and lateral distance measurements at the centre of the scanned volume.

Table 1 Estimated effective doses obtained from prospectively ECG-triggered CCTA using different generations CT scanners and protocols.

| Parameter                                       | Protocol A        | Protocol B             | Protocol C                     | Protocol D               | Protocol E         |
|---|-------------------|------------------------|--------------------------------|--------------------------|--------------------|
| Scanner model                                   | Optima CT 660     | Ingenuity 128          | Somatom Definition Dual Source | Somatom Definition Flash | Aquilion ONE       |
| Detector-row                                    | 64                | 64                     | $2 \times 32$                  | $2 \times 64$            | 320                |
| Acquisition technique                           | Snapshot Pulse    | Step and Shoot Cardiac | Adaptive Cardio Sequence       | Flash Spiral             | Volumetric Cardiac |
| Tube current-time (mAs)                         | 197               | 180                    | 218                            | 169                      | 15                 |
| Total exposure time (s)                         | 1.76              | 1.96                   | 3.04                           | 0.45                     | 1.22               |
| $P_{KL}$ (mGy.cm)                               | $193.40 \pm 2.52$ | $168.10 \pm 3.44$      | $204.00 \pm 3.30$              | $83.00 \pm 3.01$         | $57.90 \pm 1.21$   |
| Measured $H_E$ (mSv)                            | $5.60 \pm 0.68$   | $5.02 \pm 0.73$        | $6.06 \pm 0.72$                | $1.88 \pm 0.25$          | $1.34 \pm 0.48$    |
| Computed $H_E$ (mSv)                            | $2.71 \pm 0.04$   | $2.35 \pm 0.05$        | $2.86 \pm 0.05$                | $1.16 \pm 0.04$          | $0.81 \pm 0.02$    |
| Size-specific $H_E$ (mSv)                       | $4.47 \pm 0.06$   | $3.88 \pm 0.08$        | $4.71 \pm 0.08$                | $1.92 \pm 0.07$          | $1.33 \pm 0.03$    |
| % difference (Measured $H_E$ - Computed $H_E$ ) | 51.6%             | 53.2%                  | 52.8%                          | 38.3%                    | 39.6%              |

## **DOES THE MPR IMAGE OF THE CT HAVE AN ISOTROPIC RESOLUTION? (SPATIAL RESOLUTION OF X-Y DIRECTION AND Z- AXIS DIRECTION)**

Yuta Goto

Fujita Health University School Of Health Sciences Faculty of Radiological Technology, Japan

**Key words:** MPR image, Isotropic resolution, Reconstruction kernel

### **Purpose**

The MPR image of the CT is used by many diagnoses. In addition, various image reconstruction kernels are used to improve spatial resolution in the CT. We measured the spatial resolution of the MPR image by the change of the image reconstruction kernel in the CT.

### **Methods**

Copper wire of 0.2mm in diameter was used for an experiment. Because there was it to an MPR image perpendicularly, the wire was installed radially. MPR images were made by scanned data set. We measured the LSF about X-Y direction, Z-axis direction and 45 degrees oblique. Then we calculated MTF.

### **Results**

The reconstruction kernel was for a soft tissue, the spatial resolution of X-Y direction and Z-axis direction were equal. However, the reconstruction kernel was for lung or bone, X-Y direction had the higher spatial resolution with Z-axis direction.

### **Conclusions**

The spatial resolution of X-Y direction changes by the reconstruction kernel. However, it does not depend on the Z- axis direction. The spatial resolution of the Z-axis direction depends on the slice thickness and the image interval. The achievement of the isotropic resolution is difficult only by the control of the reconstruction kernel with the MPR image. The high resolution soft tissue kernel and very thin slice thickness lead to the achievement of the true isotropic resolution.

## **REDUCTION OF CT RING ARTIFACTS USING EDGE DETECTION METHOD BASED ON IMAGE-DOMAIN**

Zhen Chao, Haenghwa Lee, Sunghoon Choi, Dohyeon Kim, Pil-hyun Jeon, Hee-Joung Kim

Yonsei University, Republic of Korea

**Key words:** Ring artifacts Remove Image-domain CNR

### **Purpose**

Ring artifacts can be caused by mis-calibration or defective detector elements which results in degradation of diagnostic quality of CT images. Therefore reducing or removing ring artifacts becomes a necessity to improve image quality. In this study, we developed a novel ring artifact correction method and evaluated its performance.

### **Methods**

Firstly, we did filter processing by Shepp-Logan (S-L) filter for enhancing identification of artifacts. Next we transformed ring artifacts from cartesian coordinate to polar coordinate to make artifacts into line shape. The line artifacts were then extracted through Laplace operator and bwlabel function. Finally, a cubic spline interpolation was performed to compensate artifact region and we inversely transform it to original Cartesian coordinate to acquire corrected image. In this experiment, we used SL computerized phantom, physical chest phantom, and 3 different sections of patients' head data from a CBCT scanner. Contrast-to-noise ratio (CNR) was used to quantitatively compare among other two conventional methods (low-pass method and adaptive smoothing method).

### **Results**

The low pass method and adaptive smoothing method generated similar results, where the eliminations of artifacts were not realistic by showing low CNR values. On the contrary, the reduction for artifacts based on edge detection method presented much better than the other methods.

### **Conclusions**

The edge detection method can reduce artifacts compared with the other two conventional methods, although, our proposed method can cause the image edge distortion slightly because of coordinate transformation.

## PERFORMANCE EVALUATION OF ART AND ML METHODS FOR PROTOTYPE CHEST DIGITAL TOMOSYNTHESIS

Haenghwa Lee

Yonsei University, Republic of Korea

**Key words:** Chest digital tomosynthesis, Algebraic reconstruction technique, Maximum-likelihood-expectation-maximization

### Purpose

We studied feasibility of the limited-angle cone-beam reconstruction methods for newly developing chest digital tomosynthesis (CDT) and compared two methods including reconstruction parameters such as relaxation parameter, number of iteration and initial guess

### Methods

A prototype CDT system consisted of a CsI(Tl) scintillator flat panel digital detector (Pixium RF 4343, Thales, France) and X-ray tube (TE-E7869X, Toshiba, Japan). The LUNGMAN phantom (Kyoto Kagaku, Japan) including grand-glass opacity (GGO) tumors was positioned in a posterior-anterior (PA) view mode, and acquired the 41 projection views with a 40 angular range. To investigate comparison of tomosynthesis algorithms for CDT system, the projection views were reconstructed using algebraic reconstruction technique (ART) and maximum-likelihood (ML) methods. We evaluated the quality of reconstructed images with contrast-to-noise ratio (CNR) and artifact spread function (ASF).

### Results

To acquire better image quality from same projection data, we calculated relaxation parameter =0.4 for uniform (UI) initial guess and =0.6 for back-projection (BP) initial guess in this study. We found that BP initial guess for ART and ML methods could provide better CNR values with a faster speed, and also improve ASF curves. With a properly selected relaxation parameter, initial guess and number of iteration, ART method could provide better CNR and ASF than ML method.

### Conclusions

We compared two iterative algorithms and investigated the effect of reconstruction parameters. The results may show the possibility that key imaging parameters could provide better image quality for detection of lung nodules in CDT system.

## **EVALUATION OF EFFECTIVE DETECTIVE QUANTUM EFFICIENCY IN PROTOTYPE DIGITAL BREAST TOMOSYNTHESIS SYSTEM**

Seungyeon Choi, Ye-Seul Kim, Sunghoon Choi, Haenghwa Lee, Donghoon Lee, Hee-Joung Kim

Yonsei University, Republic of Korea

**Key words:** Prototype DBT system, effective DQE

### **Purpose**

Digital breast tomosynthesis (DBT) system is a system which rotates in a limited angle and acquires image through compressed breast. This makes the system strongly depend on the performance of the detector regarding whole X-ray system. In recent years, effective detective quantum efficiency (eDQE) has been introduced to measure the detector's efficiency of a total X-ray system containing the effects of focal spot size, scattered radiation and magnification. The purpose of this study is to evaluate eDQE in a prototype DBT system with different tube voltages.

### **Methods**

In this study, we used the prototype DBT system with CsI(Tl) scintillator/CMOS flat panel digital detector (2923MAM, Dexela Ltd.) developed by Korea Electrotechnology Research Institute. For the eDQE evaluation, effective modulation transfer function (eMTF) and effective normalized noise power spectrum (eNNPS) according to the frequency compensated by magnification factor were acquired in different tube voltages with 5 cm breast equivalent phantom. Scatter fraction and the transmission fraction were also acquired for eDQE.

### **Results**

The eMTF was independent with increasing X-ray tube voltage, while maintaining average glandular dose of 3 mGy. On the other hand, the eNNPS was decreased, but X-ray beam transmission fraction was increased with increasing tube voltage. Consequently, eDQE increased with increasing tube voltage in high frequency, although it showed small deviations.

### **Conclusions**

In this study, we evaluated eDQE in different tube voltages to measure detector's efficiency in the whole prototype DBT system. These results showed that the system efficiency can be measured by eDQE in clinical applications.

## **FAST IMPLEMENTATION OF IMAGE RECONSTRUCTION WITH 2-POINT STEP SIZE GRADIENT PROJECTION METHOD USING GPU ACCELERATION IN A PROTOTYPE CHEST DIGITAL TOMOSYNTHESIS SYSTEM**

Sunghoon Choi<sup>1</sup>, Ye-Seul Kim<sup>1</sup>, Haenghwa Lee<sup>1</sup>, Donghoon Lee<sup>1</sup>, Seungyeon Choi<sup>1</sup>,  
Jungwook Shin<sup>2</sup>, Woojin Jang<sup>2</sup>, Hee-Joung Kim<sup>1</sup>

<sup>1</sup>Yonsei University, Republic of Korea

<sup>2</sup>Listem Corporation, Republic of Korea

**Key words:** chest tomosynthesis, GP-BB, CUDA

### **Purpose**

Chest digital tomosynthesis (CDT) has an advantage of low radiation dose compared to conventional computed tomography (CT) by utilizing small number of projections (~80) acquired from limited angle range. The most widely used filtered back-projection (FBP) method is a generic solution that works for any types of imaging modalities. However, iterative reconstruction enables a higher quality of image although we have small number of projections by solving a convex problem until converges to certain degree. In this study, we implement total-variation (TV) minimization image reconstruction based on the compressed sensing (CS) theory by using a single graphic processor unit (GPU) card.

### **Methods**

We acquired total 41 projection images with 1° angle step using our recently developed prototype CDT system (LISTEM corporation, Wonju, Korea) in  $\pm 20^\circ$  angle range. For fast convergence of TV minimization based reconstruction, we utilized the Barzilai-Borwein (BB) 2-point step size gradient projection method (GP-BB). The entire programming was coded in C++ with CUDA toolkit (Ver. 7.5) to utilize the parallel computation to accelerate our algorithm.

### **Results**

The reconstructed physical phantom images using GP-BB method showed the contrast to noise ratio (CNR) of 36.18 by comparing between the Teflon target and its background materials, whereas conventional FBP presented 20.23. The total reconstruction times of GP-BB algorithms for producing total 100 axial slices using our GPU card was 71.2 sec.

### **Conclusions**

We proposed a fast TV based iterative CDT reconstruction algorithm. The proposed algorithm could produce images within a clinically reasonable time while presenting higher image quality.

## FIRST-GENERATION NEAR-INFRARED-RAY COMPUTED TOMOGRAPHY SCANNER

E Sato<sup>1</sup>, Y Oda<sup>1</sup>, Y Sato<sup>2</sup>, T Ishii<sup>3</sup>, O Hagiwara<sup>3</sup>, H Matsukiyo<sup>3</sup>, T Enomoto<sup>3</sup>, M Watanabe<sup>3</sup>, S Kusachi<sup>3</sup>

<sup>1</sup>Department of Physics, Iwate Medical University, Japan; <sup>2</sup>Central Radiation Department, Iwate Medical University Hospital, Japan; <sup>3</sup>Department of Surgery, Toho University Ohashi Medical Center, Japan

**Key words:** NIR CT, first-generation CT, NIR LED, NIR phototransistor, monochromatic NIR rays

**Introduction:** Recently, we have developed several energy-dispersive X-ray computed tomography (ED-CT) scanners [1-3] to perform molecular imaging including K-edge CT using iodine and gadolinium media. To perform biomedical CT without the absorbed dose, we are constructing visible- and infrared-ray CT (NIR-CT) scanners. For this research, we introduce an NIR-CT scanner as a teaching tool for the medical-physics experiment.

**Methods:** Figure 1 shows the block diagram of the NIR-CT scanner. The NIR rays are produced from a light-emitting diode (LED) and detected using an NIR phototransistor (PT). The wavelengths of the LED peak intensity and the PT high sensitivity are both 940 nm. The photocurrents flowing through the PT are converted into voltages using a cathode-follower circuit, and the output voltages are sent to a personal computer through an analog digital converter. The X-ray projection curves for tomography are obtained by repeated linear scans and rotations of the object, and the scanning is conducted in both directions of its movement (Fig. 2). Two step values of the linear scan and rotation are selected to be 0.5 mm and 1.0°, respectively. Using this CT scanner, the exposure time is 9.8 min.

**Results:** In the measurement of NIR spectra, the peak wave length was 940 nm, and the spectral intensity decreased with increasing density of the food colors. In the NIR-CT, the image density decreased with increases in the color density.

**Discussion:** The NIR photons easily penetrate a transparent object at a small incident angle, and the photons reflect around the objects at a large incident angle to the object. In addition, the photons also refracted, and only penetrating photons should be detected using a small-diam long collimator for the PT.

The pixel dimensions of the reconstructed CT image were 0.5×0.5 mm<sup>2</sup> because the scan step was 0.5 mm. However, the original spatial resolution was primarily determined by both the diameter(1.5 mm) and the length (10 mm), and the spatial resolutions were approximately 2×2 mm<sup>2</sup>.

**Conclusion:** We developed a first-generation NIR-CT scanner as a teaching tool for the physical experiment using a set of readily available LED and PT. Using the LED, although the photons hardly penetrated the objects, the penetrating photons may be detected by an extremely high-sensitivity detecting device or by increasing LED intensity.

**References:**

1. Sato E, Oda Y, Abudurexiti A, Hagiwara O, Matsukiyo H, Osawa A, Enomoto T, Watanabe M, Kusachi S, Sato S, Ogawa A, Onagawa J, (2012), Demonstration of enhanced iodine K-edge imaging using an energy-dispersive X-ray computed tomography system with a 25 mm/s-scan linear cadmium telluride detector and a single comparator," Appl. Rad. Isot. 70, 831-836.
2. Hagiwara O, Sato E, Watanabe M, Sato Y, Oda Y, Matsukiyo H, Osawa A, Enomoto T, Kusachi S, Ehara S, (2014), Investigation of dual-energy X-ray photon counting using a cadmium telluride detector and two comparators and its application to photon-count energy subtraction, Jpn. J. Appl. Phys. 53, 102202-1-6.
3. Watanabe M, Sato E, Oda Y, Sagae M, Sato Y, Yamaguchi S, Hagiwara O, Matsukiyo H, Kusachi S, Ehara S, (2015), Quasi-monochromatic X-ray photon counting using a silicon-PIN detector and an energy-selecting device and its application to iodine imaging, Med. Imag. Inform. Sci. 32, 38-43.

Corresponding author email: dresato@iwate-med.ac.jp

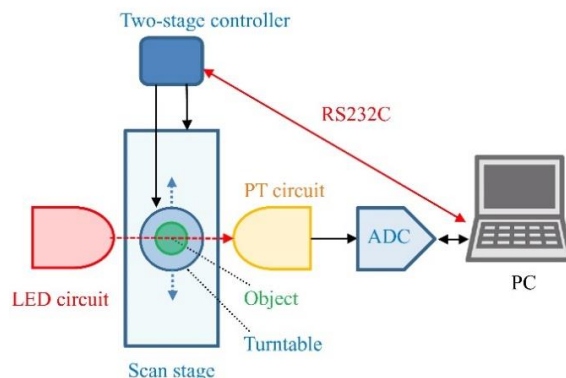


Fig. 1 Block diagram of the NIR-CT scanner utilizing LED and PT circuits.

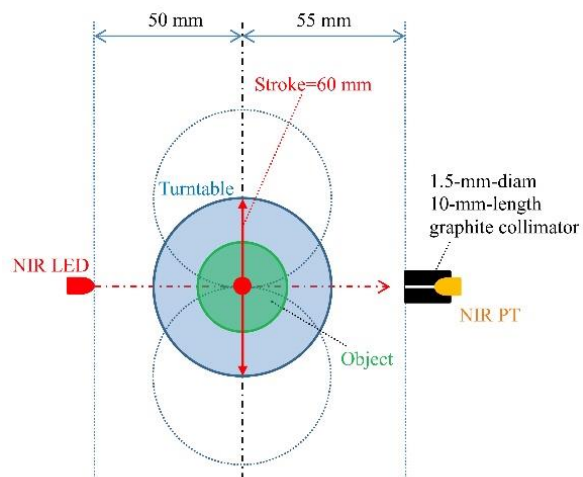


Fig. 2 Experimental setup of the main components in the NIR-CT scanner. The CT is performed by repeated linear scans and rotations of the object.

## OPTIMIZATION OF RADIATION DOSE AND IMAGE QUALITY IN ABDOMINAL RADIOGRAPHY USING MOBILE X-RAY SYSTEM

S Suwan-o-pas<sup>1</sup>, P Suwanpadit<sup>1</sup>, K Khamwan<sup>1</sup>

<sup>1</sup>Medical Imaging, Department of Radiology, Faculty of Medicine, Chulalongkorn University, Bangkok, Thailand

**Key words:** Digital mobile x-ray system, Abdominal Radiography, Entrance surface air kerma, Exposure Index (EI), Optimization

**Introduction:** The abdominal radiography using digital mobile x-ray system is commonly requested for immobilized patient. Most of patient wards are not designated for radiation protection. Moreover, there is no AEC mode for most of digital mobile x-ray systems. Therefore, the selection of the exposure parameters needs the experience of the operator for radiation dose and image quality optimization. Since the mobile digital radiography (DR) was introduced at King Chulalongkorn Memorial Hospital in September 2013. [1] we have found that some radiographers still used exposure parameters as same as CR system especially in abdominal radiographic images. The optimal parameter will provide the good image quality with low radiation dose to patient. The purpose of this study was to optimize the radiation dose and image quality for abdominal radiography utilizing digital mobile x-ray system in phantom.

**Methods:** GE digital mobile x-ray system coupled with image receptor, and the Kyoto Kagaku model PBU-50 with 21 cm of thickness abdominal anthropomorphic phantom were used. The ionization chamber dosimeter was used to measure the ESAK at the surface over the phantom in each parameter. Totally 60 experimental exposure parameters including 3 times repetition were performed. The clinical parameter setting was done to compare the radiation dose and image quality with optimal parameter. The determination of image quality based on IAEA protocol and qualitative noise were scored by three observers. The exposure index (EI) was recorded for each image.

**Results:** The ESAK for abdominal radiography in both experimental and clinical setting at different exposure parameters in this study, were between 0.23 – 3.08mGy. The EI ranged 91.72 – 2,252.88 were obtained. The image quality scoring was greater than or equal to 50% (4-7), and the qualitative noise scoring was between 1 and 2 was obtained from 3 observers.

**Discussion:** In this study, The ESAK in each parameter was not exceeded the DRL recommended by IAEA at 10 mGy. The image quality and noise scoring assessed by three observers were used for optimization as well as ESAK and exposure index. According to Aldrich JE, et al. [2], the average ESAK of abdominal radiography using DR system was 1.86 mGy which is also used for the reference level in this study. For ESAK, the exposure parameter using 75, 80, 85, 90 kVp with 25 mAs were 2.05, 2.38, 2.72 and 3.08 mGy respectively and clinical exposure using 75 kVp 32 mAs was 2.63 mGy. It is found that the ESAK from the

parameters were higher than the ESAK investigated by Aldrich JE, et al study [2]. For the image quality and qualitative noise scoring by using 70, 75, 80, 85, 90 kVp with 3.2 mAs, we found that the image quality does not meet the criteria for the interpretation. DR image receptor system is different from screen–film radiography system as it has a different energy response and does not require a fixed detector dose [3]. For this study, we found that at 75 kVp, 6.3 mAs can be used as the lower ESAK. However, the exposed image was too noisy. Finally, the optimal parameter of 80 kVp 6.3 mAs can provide the patient dose of 0.61 mGy with the exposure index of 381.73. The image quality and qualitative noise scoring were 5.5 and 1, respectively

**Conclusion** The optimal ESAK at 21 cm thickness of the phantom in this study was 0.61mGy. The proper exposure parameter was 80 kVp, 6.3 mAs at 100 cm of SID. The ESAKs of optimal parameter were 78% and 67% lower than the clinical parameter and reference study whilst the image quality is within the acceptable limit.

### References:

1. Sangdao, P., Krisanachinda, A. and Khamwan, K. (2014) Optimization of radiation dose and image quality in chest radiography using digital mobile x-ray system at King Chulalongkorn Memorial Hospital. In proceeding of 14th Asia-Oceania Congress of Medical Physics & 12th South East Asia Congress of Medical Physics. Vietnam, 2014, pp. 235-238.
2. Aldrich JE, et al. (2006) Optimization of dose and image quality for computed radiography and digital radiography. *Journal of digital imaging* Journal 19:126-131.
3. Jones A, Ansell C, Jerrom C, Honey ID (2015). Optimization of image quality and patient dose in radiographs of paediatric extremities using direct digital radiography. *Br J Radiol Journal* 88 DOI 2014060.

Corresponding author email:kitiwat.k@chula.ac.th

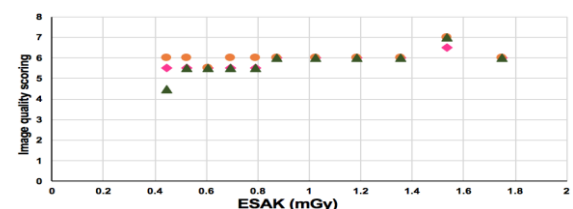


Figure 1. The scatter plot between ESAK and image quality scoring after image analysis.

Table 1. The comparison between clinical and optimal parameter based on ESAK, image quality and image noise.

| Parameters     | ESAK (mGy) | Image Quality | Image Noise |
|----------------|------------|---------------|-------------|
| 70 kVp 32 mAs  | 2.627      | 7             | 1           |
| 80 kVp 6.3 mAs | 0.608      | 5.5           | 1           |

## QUANTITATIVE AND QUALITATIVE METRICS IN ASSESSING MASS AND MICROCALCIFICATION DETECTION ON 2D DIGITAL MAMMOGRAPHY

Mutia Muharani Putri, Lukmanda Evan Lubis, Kristina Tri Wigati

Department of Physics, Faculty of Mathematics and Natural Sciences, University of Indonesia

**Key words:** The 3D structured phantom, image quality, contrast, 4-AFC

### Purpose

To perform and correlate the quantitative and qualitative metrics for mass and microcalcification detection in 2D digital mammography.

### Methods

The 3D structured phantom by Cockmartin et al. has been used for performance assessment on Siemens Mammomat Inspiration system. Thirty images were acquired under 3 dose settings (Half AEC dose, AEC dose, and double AEC dose). Signal to noise difference ratio (SDNR), contrast (C), non-prewhitened with eye filter model observer ( $d'$ ) and percentage correctly detected (PC) from four alternative forced choices (4-AFC) study were used as metrics of image quality performance. A logistic function-based psychometric curve was applied for determining the correlation of qualitative metric (PC) with the other quantitative metrics, as well as determining the threshold values according to 62.5% of PC.

### Results

At AEC dose setting, the threshold values obtained for SDNR, C, and  $d'$  were respectively  $1.44 \pm 0.11$ ,  $4.23\% \pm 0.45\%$ , and  $3.94 \pm 0.41$  for spiculated mass;  $1.11 \pm 0.35$ ,  $3.24\% \pm 0.94\%$ , and  $3.00 \pm 0.86$  for non-spiculated mass; and  $1.91 \pm 0.00$ ,  $5.37\% \pm 0.00\%$ , and  $0.15 \pm 0.00$  for microcalcification detection. We found that changing the dose mode has more effect on microcalcification detection than on mass detection. Contrast were found to have good correlation with PC, with  $R^2$  from the fitted curve of C – PC was 0.92 for spiculated mass, 0.83 for non-spiculated mass, and 1.00 for microcalcification detection.

### Conclusions

Detection of mass and microcalcification by using the 3D structured phantom for 2D digital mammography has been successfully performed in terms of quantitative and qualitative metrics. The results can be recommended as baseline values for the image quality assessment.

## **TECHNICAL SPECIFICATIONS OF CT SCANNERS FOR CARDIAC IMAGING**

Cornelius Lewis

King's Technology Evaluation Centre, King's Collage London, UK

**Key words:** cardiac, CT, image quality

### **Purpose**

CT imaging of the heart is perhaps one of the most difficult applications for this technology particularly when there are significant challenges, including for example, high calcium score, high heart rate, arrhythmia and patient obesity. Selecting a CT scanner always requires detailed examination of performance parameters and this is particularly important for cardiac imaging.

### **Methods**

Technical performance parameters for CT scanners were reviewed to identify those which were considered to be particularly important for imaging of the coronary arteries. This included a consideration of parameters which would affect the ability of the scanner to provide suitable diagnostic image quality in patients presenting with significant challenges to cardiac imaging. Technical parameters of particular interest were determined to be temporal resolution, spatial resolution, longitudinal (z-axis) coverage, x-ray output and dose efficiency.

### **Results**

A thorough analysis of technical performance parameters and their impact on image quality provided an 'ideal' scanner specification for cardiac imaging. This indicated that the 'ideal' scanner would have the highest temporal resolution, spatial resolution and x-ray output as well as enabling full coverage of the cardiac volume in a single gantry rotation at the lowest absorbed dose.

### **Conclusions**

A review of current scanner models from various manufacturers showed that none had the highest specification in all the parameters considered to be important. Selection of the most appropriate CT scanner for cardiac imaging requires an understanding of the effect of technical performance on image quality and detailed comparison of performance parameters.

## **SCATTERED RADIATION - A NOVEL SOURCE OF IMAGE QUALITY IMPROVEMENT IN CT AND PET**

Stephen Pistorius

University Of Manitoba, Canada

**Key words:** Scattered Radiation, CT, PET, Reconstruction, Simulation

### **Purpose**

In imaging, scattered radiation is an unwanted by-product, reducing image quality and producing artifacts. By coupling, high spatial- and energy-resolution detectors with advanced reconstruction algorithms, we have shown that scattered photons can be turned into useful signals.

### **Methods**

Analytical and Monte Carlo (MC) simulation was used to investigate and develop advanced algorithms, capable of reconstructing CT images with a limited number of projections, lower x-ray dose and improve image quality. In PET enhanced functional image quality and more accurate attenuation corrections, were obtained without CT or MRI. This presentation will describe the theory behind the spectroscopic Compton CT scatter approach and the Generalized Maximum Likelihood Expectation Maximization approach used in PET. MC simulated data was used to demonstrate the dependence of the Modulation Transfer Function (MTF), Contrast to Noise Ratio (CNR), and the Contrast Recovery Coefficient (CRC) on the detector size, energy resolution, and (for CT) the number of projections.

### **Results**

The CNR for Scatter CT, is a function of the number of projections and the fluence. The MTF was independent of the projection number, but strongly dependent on detector energy-resolution. For PET, the inclusion of scatter enhances the CRC and simultaneous reconstruction of the radionuclide activity distribution and an attenuation map is feasible.

### **Conclusions**

With suitable detectors and appropriate algorithms, scattered photons can be harnessed to improve the image quality, reducing dose and artifacts and providing diagnostic information that was hitherto unavailable.

## BASIC STUDY FOR MATERIAL IDENTIFICATION TOWARD DEVELOPMENT OF A NEXT GENERATION TYPE X-RAY DIAGNOSIS

N. Kimoto<sup>1</sup>, H. Hayashi<sup>1</sup>, T. Asahara<sup>1</sup>, Y. Mihara<sup>1</sup>, Y. Kanazawa<sup>1</sup>,  
T. Yamakawa<sup>2</sup>, S. Yamamoto<sup>2</sup>, M. Yamasaki<sup>2</sup>, M. Okada<sup>2</sup>

<sup>1</sup>Tokushima University, Japan; <sup>2</sup>Job Corporation, Japan

**Key words:** material identification, photon counting technique, X-ray spectrum, CdTe single-probe-type detector

**Introduction:** Currently, X-ray imaging based on a photon counting technique has attracted attention in medical diagnosis [1]. This system has the ability to discriminate energy [1], therefore it is expected to obtain information which leads to material identification. In this study, we propose a novel material identification method and demonstrate the accuracy of the method.

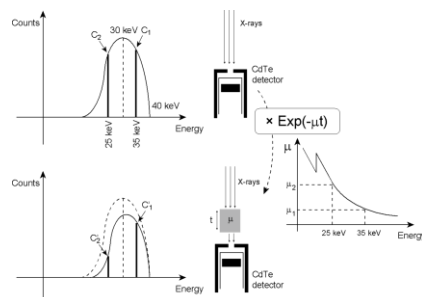


Fig.1 Schematic drawing for deriving linear attenuation factors using X-ray spectra at 40 kV.

**Methods:** Figure 1 shows a schematic drawing for deriving a normalized linear attenuation coefficient. First, we prepared an experiment for the upper X-ray spectrum at 40 kV using a CdTe detector. Here, we focused our attention on the counts of  $C_1$  and  $C_2$  which correspond to monochromatic energies of 35 keV and 25 keV, respectively. Next, when a sample having thickness “ $t$ ” is placed in front of detector, the penetrating X-ray spectrum is obtained by multiplying counts by  $\text{Exp}(\mu t)$  [2]. Then, a new vector  $\vec{P}$  is defined as

$$\vec{P} = \{\mu_{35 \text{ keV}} \times t, \mu_{25 \text{ keV}} \times t\} = \left\{ \ln \left( \frac{C_1}{C_1'} \right), \ln \left( \frac{C_2}{C_2'} \right) \right\}. \quad (1)$$

where  $C_1'$  and  $C_2'$  represent the counts of the penetrating X-ray spectrum, and  $\mu_{35 \text{ keV}}$  and  $\mu_{25 \text{ keV}}$  are linear attenuation coefficients corresponding to 35 keV and 25 keV, respectively. In order to eliminate the material thickness variable, we normalize the vector  $\vec{P}$  and a normalized linear attenuation coefficient is derived as

$$\frac{\vec{P}_x}{\sqrt{\vec{P}_x^2 + \vec{P}_y^2}} = \frac{\mu_{35 \text{ keV}}}{\sqrt{\mu_{35 \text{ keV}}^2 + \mu_{25 \text{ keV}}^2}}. \quad (2)$$

Here, because the linear attenuation coefficient is strongly related to the effective atomic number  $Z$ , we define the following relation,

$$\left\{ \frac{\mu_{35 \text{ keV}}}{\sqrt{\mu_{35 \text{ keV}}^2 + \mu_{25 \text{ keV}}^2}}, Z \right\}. \quad (3)$$

Then, substituting the linear attenuation coefficient listed in database [3] to equation (3), reference data can be determined. If we measure unknown material, the effective

atomic number can be derived by comparing it with the reference data. In order to demonstrate our method, we performed an experiment using four different phantoms (soft tissue equivalent, bone equivalent, acrylic and aluminum). In this analysis, we used whole X-ray spectra and corrected for beam hardening effect [4].

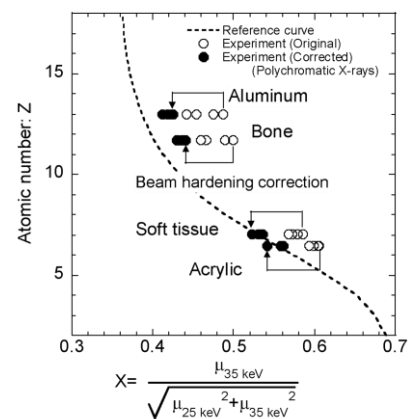


Fig.2 Result of material identification

**Results and discussion:** Figure 2 shows the result of the relationship between the normalized linear attenuation coefficient and atomic number. The broken line represents the reference curve. The circles show typical experimental data in which four different materials having different thickness were measured at 600 mAs. The open circles are original data and closed circles are the data corrected for beam hardening effect. The corrected data of the soft tissue equivalent phantom and acrylic agree with the reference curve. On the other hand, the data of aluminum and bone equivalent phantom do not agree with the reference curve. This figure indicates that our material identification method can work properly for materials in the range of 6.0-8.0 in effective atomic number.

**Conclusion:** We proposed a novel material identification method. Using our method, materials which provide the same digital value during conventional X-ray imaging system can be differentiated.

**References:**

1. Taguchi K., Iwanczyk J. S., (2013) Medical Physics 40: 100901-1-19 DOI 10.1118/1.4820371
2. Knoll G. F., (2000) Radiation Detection and Measurement third edition 1-802 John Wiley & Sons, Inc, New York.
3. Johnson T.E., Birky, B.K. (2012) Health physics and radiological health, 4th edition, 1-1281, a Wolters Kluwer business, Lippincott Williams & Wilkins, Philadelphia.
4. Brooks R. A., Chiro G. D., (1976) Physics in Medical and Biology 21: 390-398

**Corresponding author email:** hayashi.hiroaki@tokushima-u.ac.jp

## DENTAL IMAGE FUSION WITH A KINECT

Kohei Kawai<sup>1</sup>, Koichi Ogawa<sup>1</sup>, Tatsumasa Fukui<sup>2</sup>, Akitoshi Katsumata<sup>2</sup>

<sup>1</sup>Hosei University, Japan

<sup>2</sup>Asahi University, Japan

**Key words:** dental panoramic x-ray imaging, KINECT, image fusion, face image

### **Purpose**

The objective of this study was to develop a new practical method to make a fusion image combined with a face image and pseudo three dimensional jaw-bone image reconstructed with a panoramic x-ray data.

### **Methods**

We proposed a system with a KINECT to make a face image, and the KINECT was attached to the dental panoramic x-ray system (QRmaster-P, Telesystems, Japan). In order to measure the distance between the face of a patient and infrared image sensor in the KINECT, we used a mirror which was located on the x-ray tube. After the conventional panoramic x-ray study of a patient, we rotated the gantry around the patient again, and acquired the face image data with the KINECT. The pseudo three dimensional image of the jaw bones was made with the software of the QRmaster-P. The registration of two images was performed with tungsten rubber makers.

### **Results**

The face image of a volunteer was reconstructed using the KINECT data, and the quality of the image was acceptable for the clinical use. And the fusion image of the face and jaw bones were successfully performed using the tungsten rubber markers.

### **Conclusions**

The results of experiment showed that our proposed system could make a fusion image of a patient with a low cost.

## **4 Imaging Dosimetry**

## **THE IAEA/WHO TLD POSTAL DOSE AUDIT OF EXTERNAL BEAM RADIOTHERAPY IN B.P.KOIRALA MEMORIAL CANCER HOSPITAL (BPKMCH), BHARATPUR, NEPAL**

Chaurasia P.P., Chand S.B, Adhikari M.P., Yadav R.N., Jha A.K.

B.P.Koirala Memorial Cancer Hospital, Nepal

**Key words:** External beam radiotherapy, beam calibration, external quality audit, Thermoluminescence.

### **Purpose**

The study involved determining the variation across the measured output dose of megavoltage Cobalt and linear accelerators photon beams using IAEA postal TLD.

### **Methods**

Clinically calculated 2 Gray dose is delivered to TLD in 10cm depth in water phantom in 10cmx10cm field following SSD technique. IAEA TRS 398 absolute dosimetry performed details supplied.

### **Results**

A table of results of postal TLD irradiation tests from 2007 to 2015 of Cobalt-60, 6MV photon of Varian 600 C/D and 6 MV photon and 20 MV photon beams 2300 C/D machines, mean dose (standard deviation  $2.056 \pm 0.043$ ,  $2.018 \pm 0.040$ ,  $2.056 \pm 0.041$  and  $2.04 \pm 0.056$ ) respectively in a total of 18 runs performed against machines output variation checked and adjusted. It helped to correct and rectify new Cobalt output measured dose -5.1%, urgently to be validated with postal TLD within -1.4% next month.

### **Conclusions**

The result of the TLD postal dose audits indicated high levels of accuracy of dose determination in audited radiotherapy beams in subsequent audit runs in BPKMCH. It is assured that the basic dose calibration is accurate and within tolerance here to treat patients with more confidence that the patients are being treated safely. Its importance and impact is clearly recognized and its encouragement of the links to other wider radiotherapy audits has been significant.

## **2D/3D REGISTRATION-BASED FRAMEWORK FOR ESTIMATING FOUR-DIMENSIONAL DOSE DISTRIBUTIONS ACCORDING TO DYNAMIC IMAGES OF AN ELECTRONIC PORTAL IMAGING DEVICE DURING STEREOTACTIC BODY RADIOTHERAPY FOR LUNG CANCER**

Takahiro Nakamoto<sup>1</sup>, Hidetaka Arimura<sup>1</sup>, Taka-aki Hirose<sup>2</sup>, Ken'ichi Morooka<sup>1</sup>, Saiji Ohga<sup>1</sup>, Yoshiyuki Umezu<sup>2</sup>, Yasuhiko Nakamura<sup>2</sup>, Hiroshi Honda<sup>1</sup>, Tomonari Sasaki<sup>1</sup>

<sup>1</sup>Kyushu University, Japan

<sup>2</sup>Kyushu University Hospital, Japan

**Key words:** 4D dose distributions, SBRT, EPID dynamic image

### **Purpose**

The aim of this study was to develop a 2D/3D registration-based framework for estimating four-dimensional (4D) dose distributions according to dynamic images of an electronic portal imaging device (EPID) during stereotactic body radiotherapy (SBRT) for lung cancer.

### **Methods**

The 4D dose distributions during treatment time were estimated by applying a dose calculation algorithm to computed tomography (CT) images with patients' consecutive variabilities during treatment time. The "treatment" 4D-CT images were calculated by deforming planning CT images using affine transformation matrices so that planning portal dose images (PDIs) can be similar to dynamic clinical PDIs for all frames of the EPID dynamic images. Parameters of the affine transformation matrices were optimized using an adaptive transformation parameter approach with a Levenberg-Marquardt algorithm. The planning PDIs were calculated by applying the dose calculation algorithm to the planning CT images. The dynamic clinical PDIs were estimated from the EPID dynamic images for all frames. Gamma pass rates (3 mm/3%) were calculated for evaluating a similarity of the dose distributions between the dynamic clinical PDIs and dynamic "treatment" PDIs, which were calculated from "treatment" 4D-CT images, for all frames.

### **Results**

The framework was applied to ten lung cancer patients who were treated with the SBRT. Mean gamma pass rate between the dynamic clinical PDIs and the dynamic "treatment" PDIs for all cases was  $96.1 \pm 2.2\%$ .

### **Conclusions**

The proposed framework might be able to physically verify the quality of the SBRT by estimating the 4D dose distributions during treatment time.

## **A REAL-TIME ERROR DETECTION USING TRANSIT EPID DOSIMETRY IN RADIATION THERAPY**

Todsaporn Fuangrod<sup>1</sup>, John Simpson<sup>2</sup>, Peter Greer<sup>2</sup>

<sup>1</sup>Calvary Mater Newcastle, Australia

<sup>2</sup>Calvary Mater Newcastle, Radiation Oncology, Australia

**Key words:** Real-time patient safety tool, transit EPID dosimetry, Quality assurance

### **Purpose**

A real-time EPID-based patient dose monitoring system for clinical implementation was developed as an advanced patient safety tool. The aim of this study is to investigate the use of this system for real-time error detection in IMRT and VMAT, system performance and limitation.

### **Methods**

The system compares measured cumulative transit EPID image frames to cumulative predicted image frames in real-time during treatment using chi-comparison with 4%, 4mm criteria. To determine the body site-specific threshold levels (%pass-rate) for real-time error detection, a statistical process control (SPC) technique has been applied based on real-time verification results of 82 prostate IMRT, 37 head and neck (HN) IMRT, 18 rectum IMRT, and 10 HN VMAT. A random sample of 20 patients (5 prostate IMRT, 5 HN IMRT, 5 rectum IMRT, and 5 HN VMAT) were analysed in post-processing for error classification.

### **Results**

The threshold levels were 76%, 71%, 71%, 60% for prostate IMRT, HN IMRT, rectum IMRT, and HN VMAT respectively. Regarding the sample 20 patients, the system detected approximately 3.5% of entire treatment course as patient related delivery errors, 2.8% of system errors, 0.6% of EPID acquisition errors, and 1.2% of user errors.

### **Conclusions**

The real-time EPID-based patient dose monitoring for IMRT and VMAT has been demonstrated that aims to prevent major mistreatment in real-time for radiation therapy.

# SIZE-SPECIFIC DOSE ESTIMATES FOR THORACIC IMAGING IN 320 ROW DETECTOR COMPUTED TOMOGRAPHY

S.Yoykaew, A.Krisanachinda

Medical Imaging, Department of Radiology, Faculty of Medicine, Chulalongkorn University, Bangkok, Thailand

**Key words:** Multi-detector computed tomography, Size-specific dose estimates, Thoracic CT examination.

**Introduction:** Computed Tomography is the best modality for low contrast imaging. Thoracic region has several sensitive organs to radiation with high risk of fatal cancer such as lung and breast. AAPM Report no.204 [1] introduced in 2011 and AAPM Report no.220[2] introduced in 2014 on the size-specific dose estimates (SSDEs) for CT examination in order to provide more accurate on radiation dose to the patient. The purpose of this study is to determine the patient dose using size-specific dose estimate (SSDE) for thoracic imaging in 320 row detector computed tomography and the parameters influenced SSDE.

**Methods:** This study is retrospective analysis with 230 patients (115 male and 115 female) of the age range from 18 to 93 years old, the weight range from 40 to 70 kg. They underwent thoracic contrast enhancement with venous phase protocol scanned by 320 MDCT from September 2015 to December 2016. The patient data with thoracic MDCT scan from the image DICOM header at King Chulalongkorn Memorial Hospital and the CT scanner was operated with automatic exposure control system. The patient radiation dose was calculated in terms of SSDE, the product of conversion factor,  $f_{size}$  and the  $CTDI_{vol}$ . The  $f_{size}$  is displayed in AAPM Report no. 204. AAPM Report no.220, SSDE is the product of  $f_{Dw}$  and  $CTDI_{vol}$  and calculated from the slice at the middle of scan range and middle of organ (chest).

**Results:** When SSDEs were measured from middle of organ (chest), the  $SSDE_{AP+LAT}$  was 8.05-24.58mGy.  $SSDE_{effective\ diameter}$  was 8.09-24.45 mGy and the  $SSDE_{Dw}$  was 9.30-26.83mGy. When the slice at the middle range was selected, the range of  $SSDE_{AP+LAT}$  was 8.14-24.85mGy. The range of  $SSDE_{effective\ diameter}$  was 8.15-24.70 mGy and the range of  $SSDE_{Dw}$  was 9.39-31.20mGy while the range of  $CTDI_{vol}$  was 5.10-19.20mGy.

- The correlation coefficient,  $R^2$  between SSDE/ $CTDI_{vol}$  and AP+LAT were measured from middle of organ (chest) was 0.52 and 0.75 respectively (Fig.1). The correlation coefficient,  $R^2$  between SSDE/ $CTDI_{vol}$  and AP+LAT were measured from middle of scan range was 0.50 and 0.74 respectively (Fig.2).

- The percentage difference for estimate SSDE between slice middle of scan range and slice middle of organ (chest) is less than 0.02%.

**Discussion:** Christner.J.A .et al [3] showed the patient dose(as indicated by SSDE) was independent of size. Our study, SSDE increases when patient size increases because

of sum AP and LAT dimension is less than 72 cm, SSDE will increase when the conversion factor is greater than 1.  $SSDE_{Dw}$  depends on the composition of substance in the thoracic such as air, tissue and lung disorders such as nodules and lesion. The location to determine SSDE such as at the middle of scan range and the middle of the organ(chest) has been selected suitably for the measurement from CT transverse-axial image.

**Conclusion:** SSDE can be applied as the patient dose further from  $CTDI_{vol}$  and provide higher accuracy especially in patients of different sizes. SSDE (Dw) should be applied in patients of different attenuations with higher accuracy.

**References:**

1. American Association of Physicists in Medicine. (2011). Size-Specific Dose Estimates (SSDEs) in Pediatric and Adult Body CT Examinations (Task Group 204). College Park, MD: American Association of Physicists in Medicine.
2. American Association of Physicists in Medicine. (2014). Use of water-equivalent diameter for calculating patient size and size-specific dose estimates (SSDEs). In: CT (task group 220). College Park, MD: American Association of Physicists in Medicine.
3. Christner JA, Braun NN, Jacobsen MC, Carter RE, Kofler JM, McCollough CH. Size-specific dose estimates for adult patients at CT of the torso. *Radiology* 2012;265(3):841-847.

Corresponding author email: anchali.kris@gmail.com

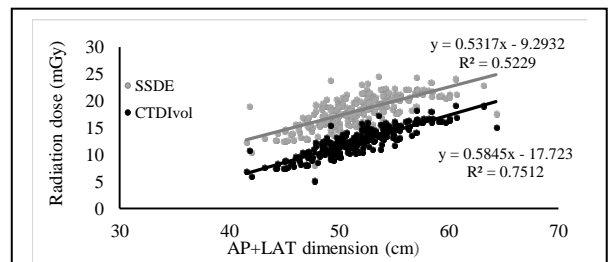


Fig.1 The relationship between SSDE/ $CTDI_{vol}$  and AP+Lateral dimension were measured at middle of organ (chest).

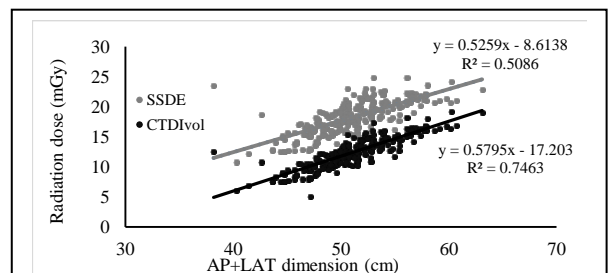


Fig.2 The relationship between SSDE/ $CTDI_{vol}$  and AP+Lateral dimension were measured at middle of scan range.

## WHICH PATIENT DOSE INDEX IS APPROPRIATE FOR CONE-BEAM COMPUTED TOMOGRAPHY?

Hidemi Kamezawa<sup>1</sup>, Hidetaka Arimura<sup>1</sup>, Noboru Kameda<sup>2</sup>

<sup>1</sup>Kyushu University, Japan

<sup>2</sup>Fujimoto General Hospital, Japan

**Key words:** Cone-beam computed tomography, Patient dose index

### Purpose

We have several dose indices to measure patient doses from cone-beam computed tomography (CBCT) used for interventional radiology or radiation therapy. However, there have been no studies on comparison among five dose indices, i.e. CTDI(CT dose index)<sub>100</sub>, CTDI<sub>IEC</sub>, CTDI<sub>∞</sub>, two types of midpoint doses f(0)PMMA, and f(0)Phan. Therefore, the purpose of this study was to reveal which patient dose index is appropriate for CBCT scanning.

### Methods

The CTDI<sub>100</sub>, CTDI<sub>IEC</sub> and CTDI<sub>∞</sub>, which were employed as the dose indices on CBCT, were derived from CTDI approaches proposed by International Electrotechnical Commission (IEC). The midpoint dose f(0)PMMA, which was adopted as the dose index with another concept, was proposed by American Association of Physicists in Medicine (AAPM), and it was measured for a CTDI phantom (effective diameter: 32.0 cm) made of polymethyl methacrylate (PMMA). Moreover, the midpoint dose was employed to take into account the object size as f(0)Phan for an anthropomorphic phantom (effective diameter: 22.7 cm). All dose indices were obtained based on the doses measured with a 100-mm ionization chamber and a CTDI phantom.

### Results

The percentages of CTDI<sub>100</sub>, CTDI<sub>IEC</sub>, CTDI<sub>∞</sub> and midpoint dose f(0)PMMA to the midpoint dose f(0)Phan for the anthropomorphic phantom were 15%, 32%, 52%, and 57%, respectively.

### Conclusions

These preliminary results suggested that the dose indices were affected by the measurement approach.

# A NEW METHOD FOR DETERMINING THE HALF-VALUE LAYER IN DUAL-SOURCE CT: APPLICATION TO DUAL ENERGY ACQUISITION

K Matsubara<sup>1</sup>, H Nagata<sup>2</sup>, A Aizu<sup>1</sup>, K Nishikori<sup>1</sup>

<sup>1</sup>Kanazawa University; <sup>2</sup>Kanazawa Medical University Hospital, Japan

**Key words:** computed tomography, half-value layer, dual-energy

**Introduction:** Determination of the half-value layer (HVL) in computed tomography (CT) is difficult because the assistance of service engineers is required to fix the X-ray tube. Our previous study indicated that a lead-covered case method, which uses X-rays from a rotating X-ray tube, could give reasonable accuracy for the HVL measurement [1]. We proposed a new method applying the lead-covered case method for determining HVL in dual-source dual-energy CT without fixing the X-ray tubes.

**Methods:** A third-generation dual-source CT system (SOMATOM Force; Siemens Healthineers, Erlangen, Germany) was used. A custom-made lead-covered case and an ionizing chamber (10X6-3CT; Radcal, Monrovia, CA, USA) connected with a multi-function digitizer module (Accu-Gold; Radcal) were used. The chamber was placed in the center of the case, and aluminum or copper filters were placed above the aperture surface (Fig.1). First, HVL was measured using aperture widths of 1.0, 2.0, and 3.0 cm for tube voltages of 80, 120, 150 kV, calculated from the peak air kerma rate (peak method) and the accumulative air kerma (accumulation method), and compared with those of the conventional nonrotating method. Second, HVL was measured using an aperture widths of 1.0 cm for tube voltages of 100/Sn150 and 70/Sn150 kV (dual-energy acquisitions) and calculated with the peak method.

**Results:** The combination of 1.0-cm aperture and the peak method was adequate, because of its small differences in the HVL (0.02 to 0.08 mm Al) in the conventional nonrotating method (Table 1). In dual-energy acquisitions, the differences in the HVL were 0.09 mmAl for 70 kV, 0.02 mm Al for 100 kV, and 0.3 mm Al and 0.01 mm Cu for Sn150 kV (Table 2).

Table 1 Results of the HVLs at different tube voltage settings in single-energy CT

| Method       | Aperture width (cm) | HVL           |                |                |
|--------------|---------------------|---------------|----------------|----------------|
|              |                     | 80 kVp (mmAl) | 120 kVp (mmAl) | 150 kVp (mmAl) |
| Nonrotating  | ---                 | 5.63          | 7.89           | 9.19           |
| Peak         | 1.0                 | 5.71          | 7.84           | 9.26           |
|              | 2.0                 | 5.80          | 7.91           | 9.40           |
|              | 3.0                 | 5.91          | 8.18           | 9.50           |
| Accumulation | 1.0                 | 5.86          | 8.35           | 9.88           |
|              | 2.0                 | 5.86          | 8.26           | 9.98           |
|              | 3.0                 | 5.91          | 8.30           | 9.92           |

**Discussion:** When absorbed organ doses are estimated, the mass energy coefficient ratio of each organ to air would be required. Because the coefficient changes according to the photon energy [2,3], the photon energy has to be estimated from the HVL when calculating the absorbed organ dose. The lead-covered case can adjust the aperture width by sliding the two lead plates. Our previous study showed that the appropriate aperture width was 2.0 cm. However, the previous study calculated HVL based on the accumulation method. This study showed that the peak method was more appropriate than the accumulation method when calculating HVL. When the peak method is applied, the aperture width of 1.0-cm is adequate because of its small differences in the HVL in the conventional nonrotating method.

**Conclusion:** Although our proposed method demonstrated slightly larger or smaller HVL compared to those of the conventional nonrotating method, it can determine HVL in dual-source dual-energy CT with good accuracy without fixing X-ray tubes.

**References:**

1. Matsubara K, Ichikawa K, Murasaki Y, et al. (2014) Accuracy of measuring half- and quarter-value layers and appropriate aperture width of a convenient method using a lead-covered case in X-ray computed tomography, J Appl Clin Med Phys. 15(1) 309-316
2. International Commission on Radiation Units and Measurements (1989) Tissue substitutes in radiation dosimetry and measurement, ICRU Report 44, Bethesda, MD, USA.
3. International Commission on Radiation Units and Measurements (1992) Photon, electron, proton and neutron

Table 2 Results of the HVLs at different tube voltage settings in dual-energy CT

| Method                 | HVL          |               |                 |                 |
|------------------------|--------------|---------------|-----------------|-----------------|
|                        | 70 kV (mmAl) | 100 kV (mmAl) | Sn150 kV (mmAl) | Sn150 kV (mmCu) |
| Nonrotating            | 4.84         | 6.79          | 14.9            | 1.62            |
| Peak (1.0-cm aperture) | 4.93         | 6.77          | 15.2            | 1.63            |

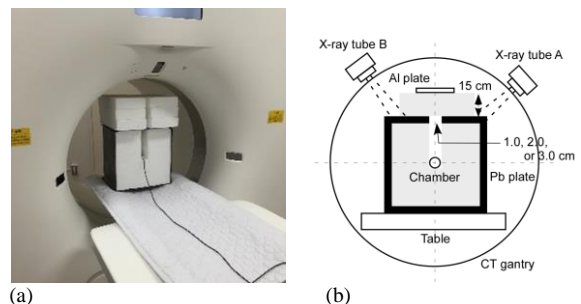


Fig.1 Experimental setup for the lead-covered case method. The case was manufactured from polystyrene foam and covered with 4 mm thick lead plates. The size of the case was 30 × 30 × 15 cm. Photograph (a) and projection view (b) of the experimental setup.

## EVALUATION OF EFFECTIVE DOSES IN CT SIMULATION USING CTDI<sub>w</sub> CALCULATION

Watcharaphawn Sanklaa<sup>1</sup>, Taweap Sanghangthum<sup>2</sup>, Thanaphat Chongsan<sup>1</sup>

<sup>1</sup>Thammasat University, Thailand

<sup>2</sup>Chulalongkorn University, Thailand

**Key words:** CT simulator, effective dose, CTDI

### Purpose

Computed Tomography (CT) simulator is used for primary imaging in the radiation therapy department. It is also the leading standard of treatment planning because it directly measures the electron densities needed for dosage computation. However, it is known to deliver more radiation dose to patients and hence, the purpose of this study is to determine the effective dose for cancer patients undergoing the CT simulator.

### Methods

An ionization chamber was used to measure CTDI<sub>air</sub> in the CT simulator (Siemens, Somatom Definition AS, Germany) and the measurement of CTDI<sub>w</sub> was done by placing the Pencil Ionization Chamber (Radcal, USA, SN:05-0340) in the PMMA head and body phantoms to measure CTDI<sub>100</sub> for the head and abdomen region respectively. Subsequently, 10 cases each for head cancer, breast cancer, and pelvic cancer were recorded. CTDI<sub>vol</sub>, DLP, Scan length, kV, mAs, Pitch, Rotation time were collected in each patient for CTDI<sub>w</sub> dose calculation to obtain the effective dose.

### Results

The dose index in air (CTDI<sub>air</sub>) was 8.84 mGy and CTDI<sub>w</sub> in PMMA head and body phantom were 16.67 and 10.33 mGy respectively. The effective doses in head, thorax, and abdomen cases were shown to be 2.63±1.88, 7.78±5.32, 10.26±7.88 mSv, respectively.

### Conclusions

The effective doses are different in each region. Although, these doses are less than the recommended dose reference level, it should still be taken into consideration because it might possibly induce secondary malignancy in the future.

## **RADIATION DOSES AND RISKS INVOLVED IN RADIOGRAPHY OF NEONATAL CHEST (ANTERIOR-POSTERIOR) EXAMINATIONS-A HOSPITAL BASED STUDY**

Jibon Sharma, Jogesh Sarma, Sushant Agarwal, Gautam Goswami

Gauhati Medical College & Hospital, India

**Key words:** Neonatal Intensive Care Units, chest X-ray, PCXMC, radiation doses, radiation risks.

### **Purpose**

Radiological imaging is an important modality of today's overall practicum. Imaging can begin as early as the first day of life. Neonates are 3-4 times more sensitive to radiation than adults. The purpose of the work was to assess the diagnostic reference level(DRL), radiation organ dose and risk arising to neonates for both sexes from chest(AP) radiograph, which is the most common radiographic examination performed at the neonatal intensive care unit(NICU) of Gauhati Medical College Hospital.

### **Methods**

The incident air kerma (EAK) was measured using a solid state PIN type detector and the value was used as the input factor to PCXMC-2.0 software to calculate the entrance surface air kerma, patient specific organ dose and risk of death due to radiation cancer incidence originated from chest (AP) examinations of neonates at NICU. The mean value of ESAK is taken as dose reference level (DRL) for neonates (both male and female).

### **Results**

The mean entrance surface air kerma (ESAK) value of male neonates is  $(79.6 \pm 1.4)$   $\mu\text{Gy}$  and for female is  $(79.9 \pm 1.9)$   $\mu\text{Gy}$ , and the institutional dose reference level (DRL) is  $80.35$   $\mu\text{Gy}$  for male and  $81.2$   $\mu\text{Gy}$  for female (i.e. third quartile value). A statistical dependency (correlation) between Neonates BMI (body mass index) and ESAK was defined for both the sexes. Significant positive correlation were found between ESAK per patient with respect to body mass index (BMI) of both male ( $R=0.83$ ,  $p=1E-05$ ) and female ( $R=0.72$ ,  $p=0.00055$ ) neonates. The results of our study reveal that for male and female neonates, the corresponding risk ranges were found to be 4.39-5.13 and 8.61-11.7 per million respectively. In case of female it is almost twice that of male.

### **Conclusions**

The results for neonatal dose in NICU were agreed and compatible with the literature. The result presented well serve as a baseline data for selection of technical parameters in neonatal chest (AP) X-ray examination.

## **5 Interventional Radiology**

## DEVELOPMENT OF SCINTILLATOR WITH OPTICAL FIBER DOSIMETER FOR PATIENT SKIN DOSE MEASUREMENT

Masayori Ishikawa<sup>1</sup>, Keiji Nakagawa<sup>2</sup>, Toshiyuki Igarashi<sup>2</sup>, Yu Furuhashi<sup>3</sup>, Yusuke Sakuhara<sup>4</sup>

<sup>1</sup>Hokkaido University, Japan

<sup>2</sup>Taiho Denshi Electronics Corp., Japan

<sup>3</sup>Acrobio Corp., Japan

<sup>4</sup>Department of Radiology, Hokkaido University Hospital, Japan

**Key words:** SOF dosimeter, Interventional Radiology, Skin dose measurement, Radiation protection

### Purpose

X-ray exposure in medicine is increasing with concerning to radiation damage of patient's skin due to long-period X-ray exposure. Conventional ionization chamber for diagnostic X-ray is not small due to less efficiency. To overcome this issue, we have developed scintillator with optical fiber dosimeter (called 'SOF dosimeter') dedicated for diagnostic X-ray dosimetry. In this presentation, we will report basic concept and properties of the SOF dosimeter.

### Methods

The SOF dosimeter consists of a monomer-based scintillator coupled with a plastic optical fiber, photomultiplier tube, discriminator and counter. As a basic property of the SOF dosimeter for diagnostic X-rays, dose linearity, dose rate linearity, energy dependency and angular dependency were evaluated. The beam quality of RQR2 (40kV) ~ RQR10 (150kV) was used for the X-ray exposure and a shadow free chamber was used for reference dosimeter.

### Results

The dose dependency is linear at ranging from 4 to 2,800 uGy, and the dose rate dependency is linear at ranging from 5~1,700 mGy/min, however, slight fluctuation was observed over 1,200 mGy/min. The energy dependency for conventional probe was 0.84 (@40kV)~1.02 (@110kV) respect to the 80 kV. Moreover, the energy dependency from 60 to 120 kV is within  $\pm 3\%$ , quite small energy dependency was achieved.

### Conclusions

The new SOF dosimeter dedicated for diagnostic X-ray dosimetry is not only invisible in fluoroscopic image, but also having good properties concerning to dose dependency, dose rate dependency and energy dependency.

## PATIENT DOSE MEASUREMENT IN TRANSARTERIAL CHEMOEMBOLIZATION PROCEDURES USING SCINTILLATION WITH OPTICAL FIBER DOSIMETER

S. Teankreu<sup>1</sup>, A. Krisanachinda<sup>1</sup>, M. Ishikawa<sup>2</sup>

<sup>1</sup>Chulalongkorn University, Bangkok, Thailand; <sup>2</sup>Hokkaido University, Sapporo, Japan

**Key words:** patient skin dose, interventional radiology, scintillation with optical fiber dosimeter

**Introduction:** Interventional radiology is an essential part of patient treatment using fluoroscopically guided procedure for more than 10 years. Radiation-induced skin injury in interventional procedure patients has also been increasingly reported in the literature and received growing attention among the medical community. Therefore; it is important to estimate the patient skin dose and try to reduce it. Trans arterial chemo embolization, TACE, is one of the high exposure procedures for both patients and staff in routine clinical service at King Chulalongkorn Memorial Hospital (KCMH). Radiation skin injuries to patient can be occurred by this interventional procedure[1].

**Objective:** To determine patient skin doses from TACE procedures using Miniature Invisible Dosimeter using Scintillator with Optical Fiber, MIDSOF and to identify parameters influence the patient skin dose in TACE procedures.

**Material and Methods:** During TACE procedure using Angiographic and CT systems, manufactured by Toshiba at Interventional Radiology Unit, King Chulalongkorn Memorial Hospital, the patient skin dose was measured by MIDSOF dosimeter [2]. The patient data, the air kerma area product (KAP) and DLP had been recorded. The effective dose was calculated from DLP values displayed on CT console[3],[4].

**Results:** Thirty patients (8 women and 22 men) with the mean  $\pm$  SD of age, height, weight and BMI were  $65 \pm 10$  years,  $163 \pm 8.4$  cm,  $64 \pm 10.2$  kg and  $24.13 \pm 3.8$  kg/m<sup>2</sup> respectively. The mean  $\pm$  SD of fluoroscopic time, total number of radiographic frames were  $2113.7 \pm 909$  and  $220 \pm 194$  respectively (Table 1). The mean  $\pm$  SD of patient skin dose was  $1.78 \pm 1.3$  Gy. The mean  $\pm$  SD of patient dose determined by KAP was  $26.18 \pm 14.1$  Gy<sup>2</sup>. The correlation, r between the air kerma area product, KAP (Gy<sup>2</sup>) and patient skin dose determined by MIDSOF (Gy) is 0.76 as shown in figure 1.

The mean effective dose with range of fluoroscopic and CT procedures were 87.59 (20.30 - 182.78) and 6.96(3.32-12.38) mSv respectively as shown in figure 2.

**Discussion:** The scintillator dosimeter is most suitable for skin dose measurement for its small size of detector, easily use and there was no need to estimate the surface area expose. However, scintillator detector could identify the result in limited area because of the small size of detector. During the procedure to identify the selected vascular supply tumor, the CT was used in patients which increasing the surface dose. The resultson KAP readout were compared with Sitthibhan [1] of 22.5-537.5 Gy<sup>2</sup>[1],

while our KAP readout was 10.3 – 70.3 Gy<sup>2</sup> which is lower than [1] **Conclusion:** The mean  $\pm$  SD with range of TACE procedure for patient skin dose measured by MIDSOF dosimeter was  $1.78 \pm 1.3$  (0.68-5.48) Gy. The maximum skin dose can produce skin injury as the level is higher than the threshold. The mean  $\pm$  SD with range of effective dose for fluoroscopy and CT procedures were 87.59 (20.30 - 182.78) and 6.96(3.32- 12.38) mSv respectively.

**References:**

1. Sitthiphan, P. The determination of patient effective dose in transarterial oily chemo embolization (TOCE) procedure using digital flat-panel system. Master Degree, Thesis (M.Sc) Chulalongkorn University. (2009).
2. Ishikawa, M. Development of a wavelength-separated type scintillator with optical fiber (SOF) dosimeter to compensate for the cerenkov radiation effect. Journal of Radiation Research, 2015,56 372-381.
3. National Council on Radiation Protection & Measurements: REPORT NO.160, 2009.
4. American Association of Physicists in Medicine: REPORT NO. 96, 2008: 13.

Corresponding author email: anchali.kris@gmail.com

Table 1. The factors affecting patient dose in TACE procedure

| Factors                           | Mean $\pm$ SD    | Range    |
|-----------------------------------|------------------|----------|
| Fluoroscopic Time (s)             | 2113.7 $\pm$ 909 | 832-4257 |
| Number of Frames                  | 229.6 $\pm$ 189  | 104-1128 |
| Number of procedures              | 2.9 $\pm$ 2.5    | 1-10     |
| Experience of radiologist (Years) | 4 $\pm$ 1        | 3-5      |

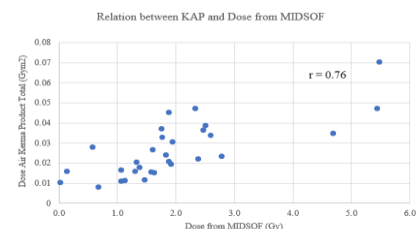


Fig 1. The relation between the air kerma area product, KAP(Gy<sup>2</sup>) and patient skin dose determined by MIDSOF (Gy) from 30 cases in TACE procedure with r=0.76.

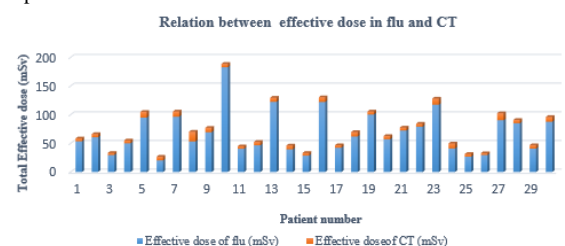


Fig.2 Effective dose (mSv) in TACE from fluoroscopy and CT procedures

## **MEASUREMENT OF EYE LENS DOSES RECEIVED BY OCCUPATIONAL STAFF FOR VARIOUS CARDIAC INTERVENTIONAL PROCEDURES**

Gourav Kumar Jain<sup>1</sup>, Arun Chougule<sup>2</sup>, Anoop Jain<sup>3</sup>, Vijay Pathak<sup>3</sup>

<sup>1</sup>SMS Medical College & Hospitals Jaipur, India

<sup>2</sup>Department of Radiological Physics, SMS Medical College & Hospital, India

<sup>3</sup>Department of Cardiology, SMS Medical College & Hospital, India

**Key words:** Interventional procedure, OSLD, DAP

### **Purpose**

Eye lens is a radiation sensitive organ and recent change in ICRP dose limits for eye lens drawn attention for its protection and dosimetry. The present study deals with measurement of eye lens doses received by occupational staff for various cardiac interventional procedures.

### **Methods**

A sample of 40 cardiac interventional procedures was observed for the study including cardiac angiography and angioplasty. The measurements were performed on two machines Siemens Axiom Artis and Siemens Artis Zee. After completion of each procedure, fluoroscopy time and Dose Area Product (DAP) reading for patient Entrance skin Dose (ESD) were recorded. The eye lens doses were measured for occupational staff including cardiologist, technologist. The measurement of eye lens dose was performed using optically stimulated luminescence dosimeters (OSLD). Further, appropriate correction factors were applied to calculate dose.

### **Results**

The average fluoroscopic time and DAP reading were found to be 3.62 minutes and 31 Gy.cm<sup>2</sup> for angiography procedure. However, the average fluoroscopic time and DAP reading were found to be 17.69 minutes and 75 Gy.cm<sup>2</sup> for angioplasty procedure. The most common value for overall time to complete the procedure was found to be 15 Minutes and 40 minutes for angiography and angioplasty procedures respectively. The eye lens doses for cardiologist and technologist for angioplasty procedure was about 2 to 3 times higher than an angiography procedure.

### **Conclusions**

The observed fluoroscopy time and DAP meter reading were found lesser than the European Union data.

## **6 Radiation Protection**

## UNIVERSAL DOSE CALIBRATION OF THE SMALL-TYPE OSL DOSIMETER FOR DIAGNOSTIC X-RAYS - DIRECT, SCATTERED AND PENETRATING X-RAYS

Tohru Okazaki<sup>1</sup>, Mary Ann Kaila A. Reginaldo<sup>2</sup>, Hiroaki Hayashi<sup>3</sup>, Yoshiki Mihara<sup>3</sup>, Natsumi Kimoto<sup>3</sup>, Yuki Kanazawa<sup>3</sup>, Kousaku Higashino<sup>3</sup>, Kazuta Yamashita<sup>3</sup>, Kazuki Takegami<sup>4</sup>, Takuya Hashizume<sup>1</sup>, Ikuo Kobayashi<sup>1</sup>

<sup>1</sup>Nagase Landauer, Ltd., Japan

<sup>2</sup>Nagase Philippines Corp., Philippines

<sup>3</sup>Tokushima University, Japan

<sup>4</sup>Yamaguchi University Hospital, Japan

### Key words

OSL dosimeter, Dose calibration, Eye lens dose, Diagnostic X-ray.

### Purpose

The small type optically stimulated luminescence dosimeter, nanoDot is expected to apply to the evaluation of eye lens dose. Dose calibration of nanoDot is carried out by the air kerma of the X-ray, however the main component of eye lens exposure is scattered X-ray in the medical field. Therefore we evaluated the reliability of the dose calibration of nanoDot dosimeter in different quality of X-rays.

### Methods

The main calibration curve was determined by the air-kerma of 83 kV X-rays in dose range of 4 microGy to 2 mGy. In addition, to evaluate the reliability of the calibration curve in different X-ray qualities, the response of nanoDots were compared with the air kerma of scattered X-ray and penetrated X-ray, and/or entrance skin dose. In the same manner, 55 and 108 kV X-rays were irradiated. Then the differences between the main calibration and other data were evaluated.

### Results

The measured data of each conditions were in good agreement with the main calibration curve derived by the air kerma of 83 kV X-ray. Even in 4 Gy irradiated dosimeters, most of the results were in inside of +/-15% deviations from the calibration curve.

### Conclusions

In this study, we evaluated the reliability of the calibration of the small-type OSL dosimeter, nanoDot. The nanoDot calibrated by the air kerma of 83 kV X-ray can be applied to the air kerma of scattered X-ray and penetrated X-ray and/or entrance skin dose of diagnostic X-rays when we adopt 15% systematic uncertainty.

## **CALCULATION OF ENERGY AND ANGULAR DEPENDENCES OF THE SMALL-TYPE OSL DOSIMETER IN THE DIAGNOSTIC AND NUCLEAR MEDICINE REGIONS USING THE MONTE-CARLO SIMULATION CODE**

Tohru Okazaki<sup>1</sup>, Hiroaki Hayashi<sup>2</sup>, Hiroki Okino<sup>2</sup>, Yoshiki Mihara<sup>2</sup>, Natsumi Kimoto<sup>2</sup>, Yuki Kanazawa<sup>2</sup>, Kazuki Takegami<sup>3</sup>, Takuya Hashizume<sup>1</sup>, Ikuo Kobayashi<sup>1</sup>

<sup>1</sup>Nagase Landauer, Ltd., Japan

<sup>2</sup>Tokushima University

<sup>3</sup>Yamaguchi University Hospital

### **Key words**

OSL dosimeter, Monte-Carlo simulation, Angular dependence, Energy dependence, Diagnostic X-ray.

### **Purpose**

The International Commission on Radiation Protection (ICRP) reviewed the threshold of the cataract, and recommended the new dose limits as 100 mSv / 5 y and 50 mSv / y. To estimate the eye lens dose, the small type optically stimulated luminescence dosimeter, nanoDot is expected to be used. The aim of this study is to evaluate the angular and energy dependences of the nanoDot OSL dosimeter for the precise measurement of the eye lens dose.

### **Methods**

Using the Monte-Carlo simulation code (electron gamma shower ver. 5: EGS5), the simplified OSL dosimeter was modeled. Then, taking account of the secondary electron equilibration, angular dependence of 0-360 degrees and energy dependence of 10 keV-2 MeV were calculated. Moreover, we performed experiments using the diagnostic X-ray equipment, and the obtained results were compared with the simulation.

### **Results**

In the diagnostic X-ray region, angular dependences were found to be almost flat except for 90 and 270 degrees (side directions), and these trends were in good agreement with the experiments. The energy dependence was defined as measured value divided by air-kerma. In this definition, rapid change was not observed in the energy region of 20 keV-2 MeV.

### **Conclusions**

In this study, we simulate the response of the small-type OSL dosimeter, nanoDot, using the Monte-Carlo simulation code. The nanoDot dosimeter was expected to be a proper dosimeter for the evaluation of the eye lens dose, especially caused by the scattered radiations in the medical diagnosis.

## CALCULATION OF RADIATION SHIELDING FOR MEGAVOLTAGE GAMMA RAY FACILITY USING MONTE

Nguyen Thi Cam Tu<sup>1</sup>, Nguyen Ngoc Anh<sup>1</sup>, Nguyen Tan Chau<sup>2</sup>, Nguyen Dong Son<sup>3</sup>

<sup>1)</sup> Oncology & Nuclear Medical Department –115 People's Hospital, Vietnam;

<sup>2)</sup> Unit of PET/CT & Cyclotron, Cho Ray Hospital, Vietnam;

<sup>3)</sup> University of Technology, HCMC, Vietnam.

**Introduction** This research applies the Monte Carlo simulation method EGSnrc Electron Gamma Shower (EGSnrc) Code with two code is dedicated: BEAMnrc code is used to simulate the beam emitted from the accelerator head and DOSXYZnrc code is used to calculate the dose emitted from the accelerator. From there, beam attenuation of radiation emitted from the accelerator through the layers of shielding material at staff area and public area is evaluated.

**Methods**

**Declaring Accelerator Head Simulation**

Accelerator in this study is Primus linear accelerator, emit photon beam energy 6MV. Accelerator Head includes 9 parts: Vacuum envelope, Target, Filter, Chamber, Mirror, the Collimator (Jaw X, Jaw Y), Mica and Air layer. Use BEAMnrc code, declare the components of the engine speed. (Fig.1)

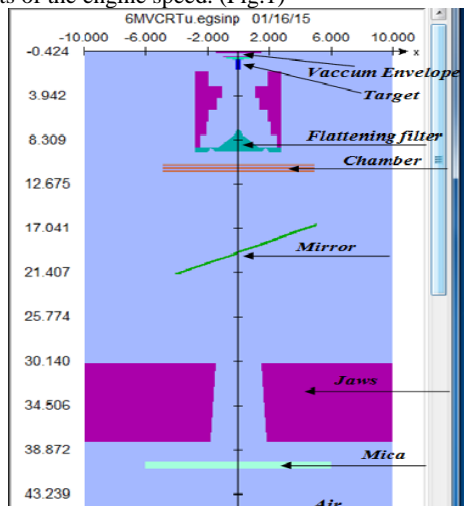


Fig 1: Simulation results accelerator head

**Region dose calculation dose (Phantom)**

Phantom used in this study is the accelerator room with water phantom (dimensions 50x50x50cm<sup>3</sup>) located at distance 100cm from source to Phantom surface. Accelerator room size in the x, y, z coordinates are 1100x1007x708cm<sup>3</sup>. Use DOSXYZnrc code, declare the components of the engine speed. Phantom is divided into 11x11x11 voxels are presented.

**Results and Discussion**

**Case 1: Dose at the area staff**

Table 1: Dose array at staff area

| Position (cm) | Dose value (Gy) | Error  |
|---------------|-----------------|--------|
| -5 → 5        | 1.10E-14        | 0.00%  |
| 5 → 25        | 4.93E-18        | 0.00%  |
| 25 → 390      | 7.54E-19        | 0.10%  |
| 390 → 445     | 1.37E-19        | 0.00%  |
| 445 → 520     | 4.45E-22        | 0.40%  |
| 520 → 550     | 1.23E-24        | 59.60% |

From Table 1, equivalent dose at staff area is

$$D_{Staff} = \frac{1.23E-24}{1.10E-14} * 1000 = 0.11 \left(\frac{mSv}{week}\right)$$

**Case 2: Dose at the public**

Table 2: Dose array at public area

| Position (cm) | Dose value (Gy) | Error |
|---------------|-----------------|-------|
| -5 → 5        | 3.97E-18        | 0.0%  |
| 5 → 25        | 1.43E-18        | 0.0%  |
| 25 → 390      | 4.05E-21        | 1.0%  |
| 390 → 445     | 8.41E-23        | 0.6%  |
| 445 → 520     | 1.44E-24        | 3.0%  |
| 520 → 550     | 9.05E-26        | 5.0%  |

From Table 2, equivalent dose at public area is

$$D_{public} = \frac{9.05E-26}{3.97E-18} * 1000 = 1.1 \left(\frac{mSv}{week}\right)$$

Table 3: Comparison of measured and simulated results

| Area   | Simulation by EGSnrc | Measurement at 115 People's Hospital |
|--------|----------------------|--------------------------------------|
| Public | 1.1 (mSv/year)       | < 1 (mSv/year)                       |
| Staff  | 5.5 (mSv/year)       | < 6 (mSv/year)                       |

Radiation dose in the public area of simulation case is higher than 10% compared with the actual results in the 115 People's Hospital, which is explained as follows:

- The presence of radiation leakage.
- The radiation scattered from the patient, angle, direction of the slide projector, ...

**Conclusion** In this work, the author and colleagues have successfully applied EGSnrc simulation program with two dedicated codes BEAMnrc and DOSXYZnrc. The initial results of the study showed that the dose limit in the area is 0.11 staff mSv/ week (5.5 mSv/year) and at public area is 0.022 mSv/ week (1.1 mSv/year). This result is lower than 8.3% in staff area and in the public area is 10% higher than the regulations of the IAEA, the ICRP [2]. However, these results need to be verified further through further research.

**Acknowledgements** I would like to thank the following people for their assistance and support: Dr.Nguyen Ngoc Anh and Msc.Nguyen Tan Chau for sharing their knowledge and advice. A special note of thanks to Dr.Nguyen Dong Son, professor of medical physics at University of Technology, HCMC for his expert guidance.

**References**

1. Mayles P., Nahum A., Rosenwald J.C. (2007), Handbook of radiotherapy physics, Taylor & Francis.
2. National Council on Radiation Protection and Measurements (2005), "Structural Shielding Design and Evaluation for Megavoltage X and Gamma Ray Radiotherapy Facilities", NCRP Report No.151, NCRP.
3. Podgorsak E.B. (2005), Radiation oncology physics: A handbook for teachers and students,IAEA.
4. Reynaer N., Van der Marck S., Schaart D., Van der Zee W., Tomsej, Van Vliet-Vroegindewij C., Jansen J., Coghe M., De Wagter, Heijmen B. (2006), Monte Carlo Treatment Planning: An introduction, Report 16 of the Netherlands Commission on Radiation Dosimetry, NCS, Delft, The Netherlands.
5. Rogers D.W.O., Walters B., and Kawrakow I. (2002), "BEAMnrc Users Manual", National Research Council of Canada Report PIRS-0509a, Ottawa.

**Corresponding author email:**Nguyen Thi Cam Tu [Oncology & Nuclear Medical Department, 115 People's Hospital, 88 Thanh Thai, Ward 12, Distrist 10, HCMC, Vietnam]. tu.nguyenthicam1985@gmail.com

## **DETERMINING RADIATION DOSE TO MEDICAL STAFF AND MEMBERS OF THE PUBLIC FOR ZIRCONIUM-89 IMMUNO-PET: A COMPARISON STUDY WITH INDIUM-111 CONVENTIONAL SPECT RADIOTRACER**

Krisanat Chuamsaamarkkee<sup>1</sup>, Putthiporn Charoenphun<sup>1</sup>, Philip J. Blower<sup>2</sup>, Lefteris Livieratos<sup>2</sup>

<sup>1</sup>Nuclear Medicine, Ramathibodi Hospital, Thailand

<sup>2</sup>Imaging Sciences and Biomedical Engineering, King's College London, UK

### **Key words**

Zirconium-89, Indium-111, Radiation Protection, Immuno-PET

### **Purpose**

Immuno-PET with Zirconium-89 has been appealing in nuclear medicine. However, the high energy photon (909 keV with 99% abundance) might raise a number of questions with regard to radiation protection and radiation safety. Therefore, the aim of this study is to determine the radiation safety aspect of using Zirconium-89 compared with conventional immuno-SPECT Indium-111.

### **Methods**

This research used the published pharmacokinetic Indium-111 labelled polyclonal-IgG combined with the measurement of the dose-rates of both radionuclides in an anthropomorphic Torso chest phantom. The pharmacokinetic of Zirconium-89 was obtained by decay correcting indium data by assuming that changing radionuclide does not alter the compound bio-distribution. The cumulated activities together with time spent in several circumstances of the previously published data, were used to calculate the radiation dose to the public, family members and technologists.

### **Results**

The calculated effective half-life of Zirconium-89-polyclonal IgG was 81.30 h while the published Indium-111 was 69.32 h. Interestingly, the estimated doses to family, technologists and public members in several conditions of Zirconium-89 were 3 - 4 times higher than those observed for Indium-111. The dose to the patient's partner can be as high as  $19.92 \pm 0.31$   $\mu\text{Sv}/\text{MBq}$  for Zirconium-89 whereas it was only  $5.22 \pm 0.17$   $\mu\text{Sv}/\text{MBq}$  for Indium-111.

### **Conclusions**

Patients injected with Zirconium-89 should have further advice about the restrictions when travelling on public transport, going to public places, and should also limit close contact with family members and their partner.

## OCCUPATIONAL RADIATION DOSIMETRY SERVICE AT RADIOLOGICAL FACILITIES

Buddha Ram Shah<sup>1</sup>, Bipin Rijal<sup>1</sup>

<sup>1</sup>Nepal Academy of Science and Technology, Nepal

### Key words

Radiation worker, Dosimetry service, TLD,

### Purpose

Ionizing radiation is being used for both diagnostic and therapy purposes. However, dosimetry service for radiation workers is yet not available in the country. Only 3-4 hospitals having radiotherapy facility monitor their personnel by sending TLD badges in India. So, Government of Nepal has assigned Nepal Academy of Science and Technology (NAST) to provide dosimetry service to all radiation workers in the country.

### Methods

TLD 100 LiF:TiMg phosphor is used in the form of TLD cards. A TLD card is worn by a radiation worker during duty hours for a period of three months. After this period, these cards are collected back for the exposure to be read out by Harshaw 6600 Plus TLD Reader installed at NAST through an assistance of IAEA TC Project. Then, a new set of TLD cards are provided to the workers for the process to continue.

### Results

At the initial phase, one hospital has been chosen under a test service, where 22 TLD cards were provided and about one and a half month report issued last March 2016 shows significant radiation dose absorbed by some personnel. The maximum values of both Hp(10) and Hp(0.07) for the personnel recorded were 5.18 mSv and 7.34 mSv for the duration from 24 January to 15 March 2016.

### Conclusions

The first dosimetry report for a hospital shows some alarming radiation absorbed dose values by radiation workers. According to the ILO requirement, every radiation worker receiving 10% dose of MPD limit set by ICRP must be monitored.

## **DEVELOPMENT AND IMPLEMENTATION OF IN-HOUSE WIRELESS & WIRED LAST MAN OUT SWITCH IN RADIOTHERAPY MACHINES**

Senthilkumar Kumar<sup>1</sup>

<sup>1</sup>Madurai Medical College, India

### **Key words**

Wireless, Radiotherapy, LMOS, Radiation Safety

### **Purpose**

The purpose of this work was to develop indigenously both the wireless and wired Last Man Out Switch (LMOS) to fulfill and satisfy the Regulatory requirements.

### **Methods**

Both the wireless and the wired LMOS have been developed successfully. To install the LMOS in the radiotherapy rooms, wire has to be brought from the door interlock to treatment room. To avoid the wiring in the existing radiotherapy room, we have used the latest RF technology to develop the wireless LMOS. So, there is no need of any wire connection between machine and LMOS.

### **Results**

Both LMOS switches were connected with the door interlock. The machine cannot be operated without pressing the LMOS and closing the door thereafter. After completion of patient set-up, the operator needs to press the last man out switch after ensuring that nobody is present in the treatment room. Once the LMOS is pressed, it activates an Audio Alarm and red light flashing for 20sec. Subsequently the operator needs to close the door within 20Sec. However, if the door is opened, either before switching ON the beam or during treatment, the operator needs to press once again the LMOS in order to switch ON the beam.

### **Conclusions**

Developed devices fulfill and satisfy the regulatory requirements and are also successfully installed and tested in many Radiotherapy machines. Accidental exposure to radiation workers due to operator mistakes is prevented, using this device, as it enables protection from unwanted irradiation from Radiotherapy machines.

## **ESTIMATION OF ENTRANCE SKIN DOSE USING A DICOM RADIATION DOSE STRUCTURED REPORT FOR PATIENTS UNDERGOING ANGIOGRAPHIC PROCEDURES**

Tokitaka Ueno<sup>1</sup>, Junji Morishita<sup>2</sup>, Toshioh Fujibuchi<sup>2</sup>, Tadahisa Uemura<sup>3</sup>, Minoru Tanaka<sup>3</sup>

<sup>1</sup>Ph.D Course in Department of Health Sciences, Graduate School of Medical Sciences, Kyushu University, Japan

<sup>2</sup>Department of Health Sciences, Faculty of Medical Sciences, Kyushu University

<sup>3</sup>Department of Radiological Technology, Fukuoka University Hospital

### **Key words**

Radiation Dose Structure Reporting RDSR entrance skin dose

### **Purpose**

It is important to accurately estimate the entrance skin dose (ESD) for patients undergoing angiographic procedures, to prevent radiation damage. The purpose of this study was to develop a system that estimates ESD for each radiologic procedure by utilizing tags of Digital Imaging and Communication in Medicine (DICOM) Radiation Dose Structure Reporting (RDSR) files, and to examine the estimation accuracy.

### **Methods**

ESD was estimated using the McParland's formula published in the British Journal of Radiology. Dose area product, irradiation area on image sensor, focus-to-image distance, focus-to-skin distance, tube voltage, and copper filter thickness were obtained from an RDSR file. The estimated ESD was corrected for back-scattering factor, ratio of tissue absorbed dose conversion factor to skin, and corrected value of absorbed dose on a bed. The estimated ESDs were compared with actual measurements.

### **Results**

The ESD estimated by our system based on information obtained from the RDSR was 1.07% to 22.9% lower than the actual measurements. These results were below the acceptable error range for a dose area product meter ( $\pm 25\%$ ). Therefore, our system seems to be clinically useful in the determination of ESD.

### **Conclusions**

Our study indicated the usefulness of a method for estimation of ESD during angiographic procedures.

## **INFORMATION-BASED IMPLEMENTATION OF RADIATION MANAGEMENT AND ASSESSMENT OF RADIATION PROTECTION IN A MOLECULAR IMAGING AND THERAPY FACILITY**

Sylvia J.Gong<sup>1</sup>, Graeme J. O'Keefe<sup>1</sup>

<sup>1</sup>Department of Molecular Imaging And Therapy, Austin Health, Melbourne, Australia

### **Key words**

Radiation safety and protection, Information system, Molecular imaging and therapy

### **Purpose**

In compliance with the key aspects of ARPANSA statutory and regulatory in protecting patients, workers, and the public against hazards of ionising radiation, the aims of this study were to develop an information system framework in supporting the implementation of radiation safety management and the assessment of radiation protection in our molecular imaging and therapy facility.

### **Methods**

The information system design incorporated the configuring and maintenance of multiple databases with user-friendly interfaces. The database layouts included: library of international guidelines, national regulations, institutional policies and departmental procedures of radiation safety and precaution; registration of departmental radiation sources and monitoring apparatus; update of optimised dose levels corresponding to diagnostic imaging procedures; log of reported radiation incidents; record keeping of occupational radiation exposure dose history; map of area and radioactive waste dose rates, etc. Application modules were also developed to perform the data analysis, risk notification, and periodic reporting.

### **Results**

The relational database and application modules were successfully integrated using FileMaker Pro. The main functions included the timely notification of dose exceedances; charting of occupational radiation doses of individuals and critical groups along time; in-advance schedule of source licensing, apparatus servicing and compliance testing; data sorting for patient internal dose assessment; reporting of compliance test, area survey, and radiation experiment results; and summarizing radiation management activities in a defined period, etc. The radiation safety training module is under construction.

### **Conclusions**

The system is useful to facilitate and enhance the information sharing and efficient communication of radiation risks and envisaged protective measures; and to potentially expedite assessment and audit of radiation events for recommending correction actions.

## **ANALYSIS OF A PRACTICAL CASE OF MEDICAL FACILITIES SHIELDING**

Franco Milano<sup>1</sup>

<sup>1</sup>University of Florence, Italy

### **Key words**

Shielding, Scattering, Medical radiation

### **Purpose**

The goal of radiation shielding is to limit radiation exposure to members of staff and public to an acceptable level. There are many National and International Protocols and Codes of Practice related with recommendations and technical information to design and install structural shielding for facilities using ionizing radiations for medical imaging. The purpose of the presentation is to analyse the shielding planning in a practical case and its robustness.

### **Methods**

The knowledge of the radiation field in the examination room, during patient exposure, is essential in order to reach the shielding goal. Most of the Protocols consider the primary and secondary radiation where the latter consists of x-ray scattered from patient and other objects including the leakage radiation from the protective housing of the x-ray tube. Different shielding Protocols are examined.

### **Results**

The Author presents the outcomes of acceptance tests performed on two medical x-ray imaging facilities: a Computed Tomography installation and a dedicated chest installation where the shielding goals failed to meet the user specifications. When the shielding calculations were performed, it appears a series of requirements were not fulfilled, resulting in a complete inadequacy of the installed shielding. The outcomes of the measurements performed during the acceptance tests are presented.

### **Conclusions**

The Author analyses all the steps of the planning of shielding which caused the failure of any shielding design goal. The intention of the presentation is to point out limitations of the particular shielding planner and, at the same time, to discuss and comment the main shielding Protocols to permit their full application.

## **RADIATION DOSE FOR PATIENTS UNDERGOING DIAGNOSTIC CT: FOLLOW-UP BREAST CANCER**

L.C.G.Oliveira<sup>1</sup>, M.A.Pinto<sup>1</sup>, S.K.Renha<sup>1</sup>, L.T. Dauer<sup>2</sup>

<sup>1</sup>Institute of Radiation Protection and Dosimetry (IRD/CNEN), Rio de Janeiro, Brazil.

<sup>2</sup>Department of Medical Physics, Memorial Sloan-Kettering Cancer Center, New York, EUA.

### **Key words**

Computed Tomography, Breast Cancer and Dosimetry

### **Purpose**

Breast cancer is the most frequent type of cancer among women. Computed tomography (CT) is not routinely used as diagnostic tool for screening breast cancer. It can help in planning radiotherapy treatment and follow-up of breast cancer patients. However, it can be useful to identify the augment of lesions close to thoracic wall, and possible metastasis. As a result, such patients should be submitted more than once to CT throughout their lives, in order to check for possible reappearance of cancer. The aim of the present study is to estimate the total radiation dose for patients undergoing thorax CT in the follow up breast cancer.

### **Methods**

Total radiation dose for thorax CT procedures have been reported, surrounding a total of 50 CT examinations conducted in one oncology hospital in Rio de Janeiro. In each woman-patient, technical parameters and radiation dose were supported by database. Radiation doses were verified using the ImPaCT CT dosimetry calculator.

### **Results**

Patients ranged in age between 38 and 90 years with a mean age of 54 years. 90% of breast cancer of patients were classified in an infiltrating ductal carcinoma. During 2 years in the follow up of breast cancer, the women were submitted to mean of 6 thorax CT. Therefore, the mean values of CTDIvol and DLP were equal to 86.41mGy and 2774 mGy.com, respectively.

### **Conclusions**

These results indicate the importance of justification and optimization and the necessity of developing Optimization Programs.

## **7.1 Diagnostic Radiology QA**

## **A CLOUD BASED PLATFORM FOR AUTOMATED DIGITAL MAMMOGRAPHY QUALITY CONTROL : MammoQC**

Rasika Rajapakshe

BC Cancer Agency, Canada

**Key words:** quality control, digital mammography, image quality, SDNR

### **Purpose**

Develop a cloud based platform for automating quality control testing of digital mammography systems across multiple sites.

### **Methods**

We have developed a cloud based software platform, MammoQC, which takes advantage of a province-wide image transfer network to facilitate automated quality control measurement, recording, and tracking for digital mammography centers. Technologists acquire the appropriate phantom exposure and send the resulting image to the transfer network. MammoQC automatically identifies, downloads, and processes the test images. The test results are housed in a centralized database and made available via a website which includes functionalities of report generation, graphing of results, and the ability to review test images. This entire process occurs over the span of a few minutes and allows a center to perform and review QC tests for multiple units with minimal time.

### **Results**

Cloud based MammoQC digital mammography QC platform was deployed within the province of British Columbia in Canada since 2010 and is currently being utilized by 29 digital mammography centers with 39 FFDM units. More than 4200 weekly SDNR data points have been accumulated representing 81 unit years of QC data with an average of 108 SDNR data points per unit.

### **Conclusions**

The cloud based automated digital mammography quality control system minimizes the time spent by technologists performing routine QC, efficiently consolidates test data and provides a visualization platform for both individual units and a population based screening mammography program for quality assurance purposes.

## THE SIZE-SPECIFIC DOSE ESTIMATE (SSDE) FROM TRUNCATED COMPUTED TOMOGRAPHY IMAGES

Choirul Anam<sup>1</sup>, Freddy Haryanto<sup>1</sup>, Rena Widita<sup>1</sup>, Idam Arif<sup>1</sup>, Geoff Dougherty<sup>2</sup>

<sup>1</sup>Bandung Institute of Technology (ITB), Indonesia

<sup>2</sup>California State University Channel Islands (CSUCI), USA

**Key words:** SSDE, CTDI, Dw, truncated axial CT image

### Purpose

The purpose of this study is to investigate truncated axial CT images in the clinical environment and to produce correction factors for abdomen, thoracic and head regions based on clinical data, in order to accurately predict the water-equivalent diameter (DW) and size-specific dose estimate (SSDE).

### Methods

We investigated axial images of 75 patients who underwent CT examinations. Truncated axial images were characterized by the truncation percentage (TP). Correction factors were calculated by using the value of DW for a certain TP (truncated image) divided by the value of DW for TP 0% (non truncated image).

### Results

Most of the thorax images acquired for this study were truncated images (86.20%), while in the abdomen region, about a half of images were truncated (48,07%), and in the head region only a small portion were truncated (9.10%). In the thorax region, the value of TP for the truncated images varied up to almost 50%, in the head region, it varied up to almost 35%, while for the head region, it was smaller than 10%. The correction factors increased exponentially with the increasing of TP. The corrected DW and SSDE regarding this truncated image were important in the thoracic region, however it was not important in the abdomen and head regions.

### Conclusions

An accurate estimation of DW is essential for an accurate estimation of SSDE. We have shown how to accurately estimate DW and SSDE by applying a correction factor to truncated images.

## **AN OBJECTIVE APPROACH TO EVALUATE TEMPORAL CHANGES IN LUMINANCE UNIFORMITY OF MEDICAL DISPLAY DEVICES**

Keishin Kawamoto<sup>1</sup> Junji Morishita<sup>2</sup>

<sup>1</sup>Department Of Health Sciences, Graduate School Of Medical Sciences, Kyushu University, Japan

<sup>2</sup>Department Of Health Sciences, Faculty Of Medical Sciences, Kyushu University, Japan

**Key words:** Liquid-crystal displays, luminance uniformity, digital camera

### **Purpose**

The aim of this study is to propose an objective method to evaluate deterioration of liquid-crystal displays (LCDs) by detecting temporal changes in luminance uniformity using a digital camera.

### **Methods**

Monochrome LCDs (GS310, EIZO Corporation) with different operating hours (0 - 24,994 h) and original test patterns for evaluating luminance uniformity were used in this study. One of the LCDs could not be calibrated at recommended maximum luminance due to prolonged use. Digital driving level corresponding to the background of test patterns was determined to be 204. Each test pattern displayed on the LCDs was captured using a digital camera. Captured images of long-term used LCDs were subtracted from that of the LCD use at initial condition with a constant pixel value to detect temporal changes in luminance uniformity. The relative decreasing rate of luminance uniformity was evaluated for subtraction images obtained with the digital camera.

### **Results**

The results showed temporal changes in luminance uniformity could be visually detected by subtraction images using the digital camera. The relative decreasing rate of luminance uniformity was increased as operation hours of LCDs became long. The relative decreasing rates of luminance uniformity in subtraction images of LCDs ranged from 2.58 to 8.11 (5,381 - 24,994 h).

### **Conclusions**

Proposed evaluation technique based on subtraction images by a digital camera was useful to detect temporal changes in luminance uniformity. Deterioration of LCDs could be quantitatively evaluated by comparing the luminance performances before and after using the LCDs.

## **AUTOMATIC SEGMENTATION OF BREAST DENSITY AND LESIONS BY USING K-MEANS CLUSTERING ALGORITHM**

Hyemi Kim, Haenghwa Lee, Byungdu Jo, Dohyeon Kim, Donghoon Lee, Hee-Joung Kim

Yonsei University, Republic of Korea

**Key words:** segmentation, K-means clustering algorithm

### **Purpose**

Mammography has been the most widely used modality for early detection of breast cancer. In a dense breast, the sensitivity of mammography for the detection of breast cancer is reduced due to the difficulty of detecting ill-defined lesions. We have proposed a segmentation technique based on appropriate k-means clustering algorithm for breast cancer evaluation in the early stage.

### **Methods**

We used the K-means clustering algorithm for quantitative evaluation of breast density and lesion feature extraction. K-means clustering algorithm is one of the segmentation methods to classify a given data set according to the number of cluster. This method aims to minimize the sum of the distance of each point in the cluster to the K center. First, in order to quantitatively measure the breast density, the breast region is segmented from the surrounding background by boundary detection algorithm. Breast density is calculated as the ratio of segmented density region according to breast region. Second, automatic segmentation for detecting breast lesions are performed.

### **Results**

This study demonstrated the feasibility of segmentation technique for evaluation of breast density and lesion detection. Similar results were obtained between calculated densities the actual densities in breast image. In addition, breast lesions (masses and microcalcifications) were well extracted by using segmentation algorithm.

### **Conclusions**

The results indicate that segmentation technique based on appropriate k-means clustering algorithm is useful for automated estimation of breast density and breast lesion. Therefore, the accuracy of the breast cancer diagnosis in the early stage can be further improved.

## **7.2 Radiation Therapy QA**

## **QUALITY ASSURANCE OF ABSORBED DOSE DELIVERY FOR BREAST CANCER PATIENTS USING IN-VIVO MEASUREMENTS**

Muhammad Asghar<sup>1</sup>, Saeed Ahmad Buzdar<sup>2</sup>, Shahab Fatmi<sup>3</sup>

<sup>1</sup> Bahawalpur Institute of Nuclear Medicine and Oncology (BINO), Bahawalpur, & Medical Physics Research , Pakistan

<sup>2</sup> Medical Physics Research Group, Department of Physics, The Islamia University of Bahawalpur , Pakistan

<sup>3</sup> Bahawalpur Institute of Nuclear Medicine and Oncology (BINO), Bahawalpur , Pakistan

### **Purpose**

In vivo dosimetry (IVD) is an important technique in quality assurance (QA) of delivered dose to patients undergoing radiation therapy. The current study was exclusively aimed to verify the absorbed dose delivered to breast cancer patients.

### **Methods**

Diode IVD system has been used as a QA tool for breast cancer treatment. Cobalt-60 radiotherapy machine has been used for characterization of IVD system and for the treatment of breast cancer patients. Entrance and exit dose has been measured and compared with the calculated dose for each radiation field. During current investigation, two hundred and twenty six (226) patients with one thousand, three hundred and sixty six (1366) radiation fields have been monitored over two year.

### **Results**

The action level has been set to  $\pm 5\%$ . The mean percentage difference between calculated and measured dose remained within  $\pm 1.087\%$  with standard deviation of  $\pm 2.680$ . Out of 1366, only 57 (4.17%) measurements have been noticed that were out of tolerance i.e.  $\pm 5\%$ . One systemic error has been detected during this study. In breast fields, the positioning of diode has been a challenging task.

### **Conclusions**

Diode IVD system is a valuable and effective tool to measure entrance & exit doses in radiotherapy. This study has enhanced the quality of radiotherapy dose delivery and reliability of the system.

### **Key words**

External Beam Radiation Therapy, Quality Assurance, In Vivo Dosimetry, Diodes

## QUALITY CONTROL OF THE JAWS-ONLY- IMRT PLANS FOR HEAD-AND-NECK CANCER

D.T. Tai<sup>1,3</sup>, N.D. Son<sup>2</sup>, T.T.H. Loan<sup>3</sup>, N.T.H. Trang<sup>3</sup> and H. P. W Anson<sup>4</sup>

<sup>1</sup>Depart Dong Nai General Hospital, Vietnam; <sup>2</sup>Chi Anh Medical Technology Co.,Ltd, Vietnam; <sup>3</sup>University of Science, Vietnam; <sup>4</sup>PTW-Asia Pacific Ltd, Hong Kong;

**Key words:** Intensity modulated radiation therapy (IMRT), Jaw Only (JO).

**Introduction:** Intensity Modulated Radiation Therapy (IMRT) is a type conformal radiation therapy used to treat cancer and noncancerous tumors with linear accelerator (LINAC). In most oncology centres, this advanced technique is facilitated by a multi-leaf collimator (MLC) [1]. However, the use of MLC is not necessarily mandatory. Several authors [1, 2, 3] have investigated and developed algorithms for IMRT using the integrated jaws of Linacs instead of the MLC, the so called JO-IMRT technique [1]. Most recently, the JO-IMRT has been implemented in a commercial system (Panther Treatment planning system, Prowess Inc.). This Panther Treatment planning system, version 4.6 has been installed in Dong Nai Hospital, Vietnam in 2009, where one of the authors of this report is working.

Only a few reports were found regarding quality assurance of JO-IMRT. G Mu and Ping Xia performed the JO-IMRT plans for head and neck cancer and prostate cancer on the Panther Treatment Planning System [1, 2]. Their study aimed at the evaluation of treatment planning parameters and was not including quality assurance. In this report we present the results of the application of this Jaws-Only-IMRT (JO-IMRT) technique in treating nasopharyngeal carcinoma (NPC) patients including the quality control of the planning following the instructions of AAPM [4] for conventional (with MLC) IMRT.

**Methods:** Twenty-five plans of nasopharyngeal patients were randomly chosen. For each patient, a JO-IMRT plan was generated and a series of pre-treatment verifications were performed including (1) point dose measurement with a ion chamber (Farmer FC65-P, IBA), (2) plane dose measurement with a 2D-array detector (MapCHECK2, Sun Nuclear Corporation) and (3) 4-dimension dose measurement using a rotatable phantom with a 2D-array detector (Octavius 4D 1500, PTW).

### Results:

#### Point measurement using ionization chamber

Table 1 the relative differences of the measured and TPS-calculated

| Plan QA | Calculation (mGy) | Measurement (mGy) | Rel. difference (%) |
|---------|-------------------|-------------------|---------------------|
| Plan 1  | 860.8             | 849.0             | -1.37               |
| Plan 2  | 853.0             | 851.9             | -0.13               |
| Plan 3  | 880.0             | 913.8             | 3.84                |
| Plan 4  | 848.3             | 840.3             | -0.94               |
| Plan 5  | 953.2             | 940.6             | -1.32               |
| Plan 6  | 942.9             | 984.9             | 4.45                |
| Plan 7  | 1060.0            | 1024.0            | -3.40               |

The results of the point measurements were summarized in table 1. The relative differences between measured and

calculated doses among 25 head and neck plans were within 2.2 %.

#### Detector array measurements

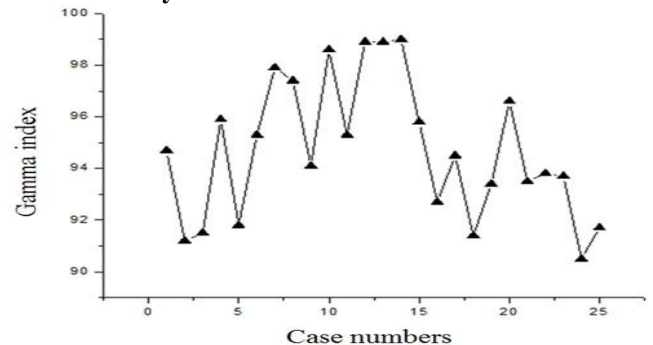


Fig 8 The gamma pass rate for the Octavius 4D

The average percentage of gamma passed rate among 25 IMRT plans was 94.7% with 3%/3mm pass criteria. 11 samples (44%) dropped into the range of 95-99% pass rate. 14 sample (56%) was in the range 90-94.7%. Cases pass rate below 90% were treated as fail referred to AAPM task group 119. No samples from this study resulted in below 90% pass rate.

**Discussion:** All the 3 pre-treatment measurements: point dosimetry; 2D check with MapCHECK 2 and 4D check with Octavius for quality control of our JO-IMRT plans shown that they have uncertainty within the tolerance and meet the criteria need for conventional IMRT treatment plans.

**Conclusion:** The JO-IMRT technique is new, not popular and not commonly used for clinic as MLC-IMRT. The pre-treatment verification is very important to consider the feasibility of application of this technique before treatment. Our measurements, done with MapCHECK 2 and Octavius 4D showed that the dose distributions planned on our JO-IMRT treatment planning system for H&N patients are accurate enough for treatment delivery.

#### References:

1. G Mu and P Xia (2009), A feasibility study of using conventional jaws to deliver complex IMRT plans for head and neck cancer, Phys. Med. Biol, 54, 5613–5623
2. Kim Y, Verhey L J and Xia P (2007), A feasibility study of using conventional jaws to deliver IMRT plans in the treatment of prostate cancer Phys. Med. Biol, 52, 2147–56.
3. M. A. Earl, D. M. Shepard (2007), Jaws only IMRT using direct aperture optimization, Medical physics, 34(1), 21201-1595.
4. Young K Lee, Anthony T Kim, Peiying Zhao, Aliaksandr Karotki (2015), Practical dose delivery verification of craniospinal IMRT, Journal of Applied Clinical Medical Physics, 16(6).

Corresponding author email: thanhtai\_phys@yahoo.com

## **CLINICAL IMPLEMENTATION OF 6MVFFF AND 10MVFFF BEAMS ON ELEKTA AGILITY HEAD TO TREAT VMAT SABR FOR LUNG TUMOURS**

Mahesh Mundayadan Chandroth

Mid North Coast Cancer Institute, Port Macquarie, NSW, Australia

### **Purpose**

As part of the agility head retrofit upgrade, MNCCI Port Macquarie purchased the 6MVFFF and 10MVFFF photon beams in November 2015. The beam data collection was performed in December 2015 and the beam model was received back from Elekta in January 2016. We performed extensive validation tests on the beam model for 3DCRT, IMRT/VMAT and DCAT delivery for SABR treatments.

### **Methods**

The beam data was collected using various radiation detectors including small volume ion chambers and diodes. Special consideration was given to small fields. A new formalism was introduced for absolute output determination pertaining to IAEA/AAPM standards. Various tests in homogenous and heterogeneous phantoms were performed. Various delivery methods like 3DCRT/IMRT/VMAT/DCAT were tested. ACDS Level 1B audits performed. Extensive pre-treatment QA performed for treating VMAT SABR bilateral Lung tumours. Film dosimetry, point dose measurement and Gamma Analysis using ArcCHECK were employed for plan QA.

### **Results**

The various beam specific parameters like depth dose, output factors, off axis and extended SSD calculations are all within tolerance for the TPS calculation and independent measurement. ACDS level 1B audits passed for reference dosimetry. 3DCRT/IMRT/VMAT/DCAT plans within departmental and internationally accepted tolerances. Excellent results were obtained for the pre-treatment QA of the plans. A significant reduction in treatment time was observed using 6MVFFF compared to 6MV flat beam plans.

### **Conclusions**

Beam models are now ready for clinical use and treated a bilateral lung tumour patient using VMAT SABR successfully.

### **Key words**

Flattening Filter Free (FFF), Volumetric Modulated Arc Therapy (VMAT), Stereotactic Body Radiation Therapy (SBRT), lung tumour.

# VALIDATION OF FLUENCE-BASED 3D VMAT DOSE RECONSTRUCTION SYSTEM USING A NEW TRANSMISSION DETECTOR ON A HETEROGENEOUS ANTHROPOMORPHIC PHANTOM

Y Nakaguchi<sup>1</sup>, T Oono<sup>2</sup>, R Onizuka<sup>2</sup>

<sup>1</sup>Kumamoto University Hospital, Kumamoto, Japan; <sup>2</sup>Kumamoto University, Kumamoto, Japan

**Key words:** quality assurance, on-line verification, transmission detector, VMAT, 3D reconstruction.

**Introduction:** In this study, we evaluated the performance of the three dimensional (3D) dose verification system, COMPASS (IBA Dosimetry, Schwarzenbruck, Germany), which has a dedicated beam model and a dose calculate engine. It is possible to reconstruct 3D dose distributions on the patient anatomy based on measured fluence using a new transmission detector (Dolphin, IBA Dosimetry, Schwarzenbruck, Germany).

**Methods:** The COMPASS system was compared with Monte Carlo simulation (MC), glass rod dosimeter (GRD), and treatment planning system (TPS) using an anthropomorphic phantom for volumetric arc therapy (VMAT) dose verification in a clinical neck case.

**Results and Discussion:** The GRD measurements were in agreement with the MC within 5% in most measurement points (table 1). Besides, most points for COMPASS and TPS were also in agreement with the MC within 5%. The COMPASS system showed better results than TPS in dose profiles due to the accuracy of a calculate engine (see Fig. 1). As for the dose-volume-histograms, there was not a large difference between MC, Analytical Anisotropic algorithm (AAA) in Eclipse TPS, and the COMPASS system. Especially, the COMPASS showed good agreement with MC (see Fig. 2).

**Conclusion:** These results indicated that the COMPASS system had high accuracy in 3D dose calculation for clinical VMAT quality assurance. Also, the COMPASS system has the feasibility of a new QA technique using fluence-based 3D dose reconstruction.

Corresponding author email: nakaguchi@fc.kuh.kumamoto-u.ac.jp

| Points | MC    | GRD   | TPS    |       | COMPASS |       |            |
|--------|-------|-------|--------|-------|---------|-------|------------|
|        | cGy   | cGy   | GRD/MC | cGy   | TPS/MC  | cGy   | COMPASS/MC |
| 1      | 118.6 | 116.2 | 0.98   | 114.5 | 0.97    | 122.0 | 1.03       |
| 2      | 35.9  | 37.2  | 1.04   | 34.9  | 0.97    | 37.0  | 1.03       |
| 3      | 208.6 | 207.1 | 0.99   | 201.2 | 0.96    | 201.4 | 0.97       |
| 4      | 199.0 | 198.5 | 1.00   | 197.0 | 0.99    | 196.1 | 0.99       |
| 5      | 99.8  | 101.1 | 1.01   | 114.3 | 1.15    | 95.1  | 0.95       |
| 6      | 219.7 | 221.1 | 1.01   | 198.6 | 0.90    | 225.6 | 1.03       |
| 7      | 201.9 | 206.8 | 1.02   | 199.6 | 0.99    | 207.2 | 1.03       |
| 8      | 200.1 | 203.5 | 1.02   | 203.8 | 1.02    | 204.8 | 1.02       |
| 9      | 200.7 | 198.4 | 0.99   | 198.6 | 0.99    | 196.4 | 0.98       |
| 10     | 30.0  | 28.4  | 0.95   | 29.9  | 1.00    | 28.3  | 0.94       |

Table 1. Comparison of point doses in anthropomorphic Rando-Alderson phantom between MC, GRD, TPS, and COMPASS at measurement points 1–10.

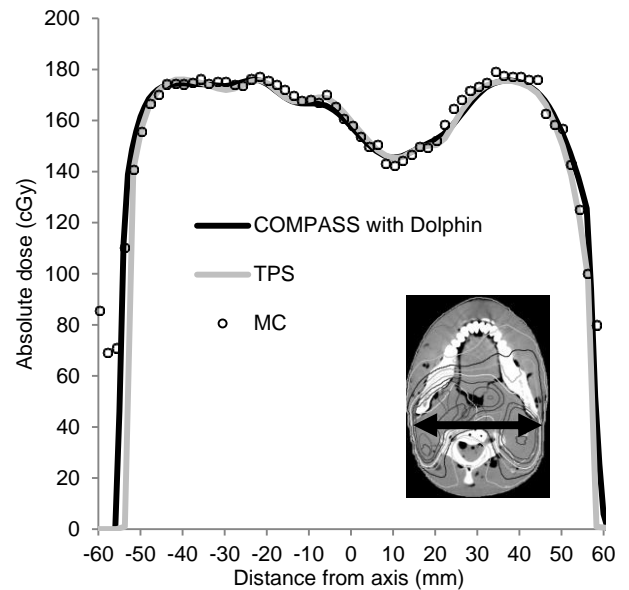


Fig. 1. Comparison of VMAT dose profiles between TPS, COMPASS, and MC calculations at a lateral direction on the axial image at the isocenter.

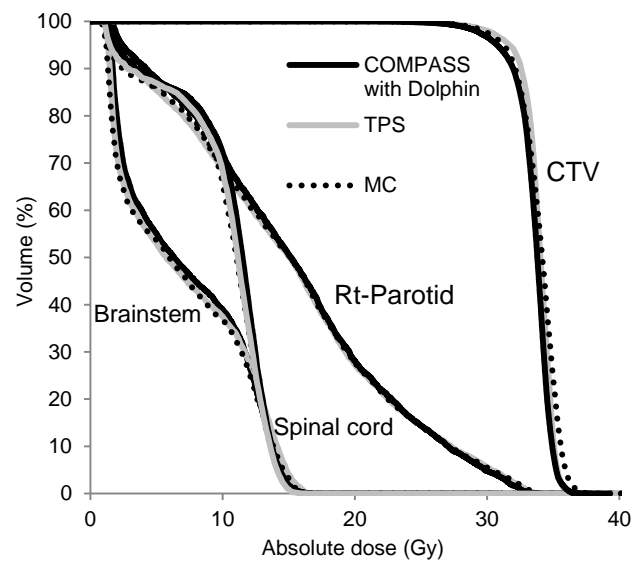


Fig. 2. Comparison of DVHs in anthropomorphic Rando-Alderson phantom between COMPASS, TPS and MC for a neck plan.

## EARLY EXPERIENCE OF GAMMA KNIFE ICON™ QUALITY ASSURANCE

HT Chung<sup>1</sup>, YK Joo<sup>1,2</sup>, JH Kim<sup>1,2</sup>

<sup>1</sup>Department of Neurosurgery, Seoul National University College of Medicine, Seoul, Korea

<sup>2</sup>Department of Neurosurgery, Seoul National University Hospital, Seoul, Korea

**Keywords:** Gamma Knife Icon, Quality assurance

**Introduction** Quality assurance results of a recently introduced Gamma Knife Icon™ (GKI) were analyzed. The stability of the image quality and positional accuracy of the cone-beam CT (CBCT) of the GKI were assessed. The accuracy of the coregistration procedure with CBCT for single and/or multiple session frameless Gamma Knife surgery was evaluated with patient image data.

**Methods** During the commissioning procedure, the global gamma index pass rates (GIPR) of single shot dose distributions were obtained with GafChromic® EBT3 films at the center of a vendor provided solid water phantom. The positional accuracy of the irradiation point was measured at the mechanical center (x=100, y=100, z=100) and an extreme position (x=40, y=160, z=100) with EBT3 films and a specific vendor provided phantom. After starting clinical operation, deviation of the radiological center was measured daily using a diode detector for six months. The positional accuracies of four ball bearings of the CBCT quality assurance phantom were also assessed daily. The image quality of the CBCT was measured biweekly with Catphan® 503 phantom for the same period. The differences in pixel coordinates, maximum and minimum absorbed doses to the targets, target coverage ratio (TCR), and Paddick conformity index (PCI) between stereotactic fiducial marker based MR images and MR images co-registered to the CBCT images were evaluated using MR images of 28 patients.

**Results** The GIPR of the 4 mm, 8 mm, and 16 mm single shot distributions was 99.9 +/- 0.2 %, 100.0 +/- 0.0%, and 100 +/- 0.0 % under 3% / 1 mm criteria, respectively. The radiological center of the GKI coincided with the mechanical center with 0.12 +/- 0.06 mm accuracy. The positional accuracy at the extreme position was 0.04 +/- 0.04 mm. The mean deviation of the radiological center

was 0.1 +/- 0.0 mm for six months. The mean value of positional deviation of a single ball bearing was 0.04 +/- 0.02 mm and the mean value of the maximum deviation of four ball bearings was 0.06 +/- 0.02 mm for the same period (Fig. 1). For images taken with a pre-defined protocol of weighted computed tomography dose index (CTDI<sub>w</sub>) 6.3 mGy, line pair per centimeter was 8 +/- 0, contrast to noise ratio was 1.77 +/- 0.8, and uniformity was 14.5 +/- 0.7%. For 2.5 mGy CTDI<sub>w</sub> images, they were 7 +/- 0, 1.12 +/- 0.04, and 14.6 +/- 0.7%, respectively (Fig. 2). After co-registration of MR images to CBCT images for 28 patients, the mean value of the maximum deviation of target coordinates was 0.88 +/- 0.37 mm. The ratio of D<sub>max</sub>, D<sub>min</sub>, TCR, and PCI were 0.89 +/- 0.14, 1.00 +/- 0.01, 0.96 +/- 0.04, and 0.93 +/- 0.07, respectively. Because treatment planning was based on pre-defined MR images, target dosimetry with CBCT images showed worse values in dose-volume histogram parameters.

**Discussion** All CBCT accuracy and image quality related parameters stayed well within the criteria for six months. The co-registration procedure of CBCT images to MR images needs more sophisticated and thorough verification because the positional accuracy of the co-registered images depended on the choice of co-registration range and MR image distortion. Co-registration accuracy evaluation with distortion free images such as clinical CT images are mandatory.

**Conclusion** Radiological and mechanical accuracy of GKI and CBCT were found to be acceptable for stereotactic radiosurgery. The largest error was found in image co-registration procedure between CBCT and MR images so that more sophisticated study is mandatory to assess this error.

**Corresponding author email:** htchung@snu.ac.kr

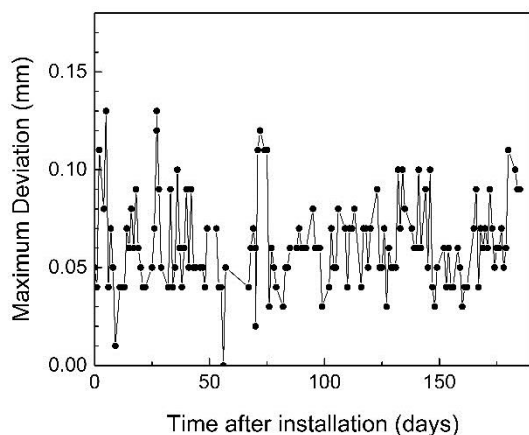
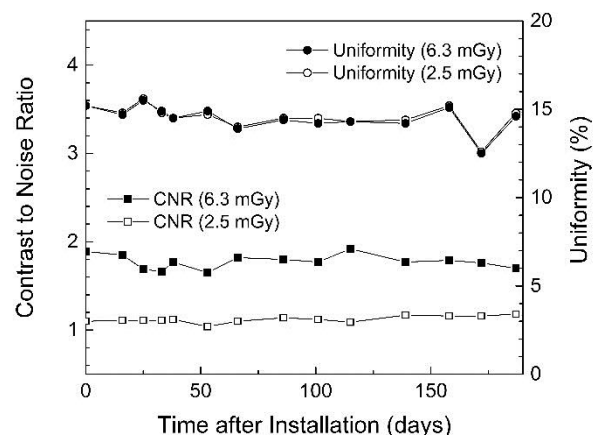


Fig. 1 Variation of maximum deviation of four ball bearings in time after installation



## **ERRORS IN RADIOTHERAPY-EXPERIENCES AND ISSUES IN NEPAL**

Matrika Prasad Adhikari, B.P.Koirala  
Memorial Cancer Hospital, Nepal

### **Purpose**

Radiotherapy has been an essential component of the treatment of cancer for many years. Approximately half of all cancer patients require radiotherapy at some time in their illness. Radiotherapy is a complex, multi-step process that requires the involvement of different staff groups such as Radiation Oncologist, Medical Physicist and Radiotherapy Technologist and Nurses in the planning and delivery of the treatment. Though errors are rare, but when they do occur the consequences can be significant for the patient.

### **Methods**

We have tried to gather the information both by prospective and retrospective way. Some errors are found on the spot and some are found at the middle of treatment and some are at the end.

We have attempted to collect the errors, near misses, faulty data, miscalculation, wrong planning in different modalities Cobalt-60, High Dose Rate (HDR), Brachytherapy, Linear accelerators and Treatment Planning System (TPS)

### **Results**

About 10 types of errors were detected in beam data configuration in TPS, Beam data output printing, planning in 2Dimensional and 3Dimensional Conformal Radiotherapy (3DCRT), Calculation, Brachytherapy planning and treatment in Linear accelerator and Co-60.

### **Conclusions**

Majority of the errors are hidden and not brought forward for discussion hence they are repeated and could not be minimized. Lack of radiation act, lack of manpower, external QA and monitoring system and lack of consumer right and awareness, poorly trained or untrained manpower, fear of being accused etc. are the issues to be addressed. Many errors can be corrected if proper recording and reporting culture is encouraged.

### **Key words**

## **CHARACTERISATION AND APPLICATION OF SH EPR-ALANINE PELLET DOSIMETERS FOR PRE-TREATMENT VERIFICATION IN STEREOTACTIC ABLATIVE RADIOTHERAPY**

Nsikan Esen<sup>1</sup>, Prabhakar Ramachandran<sup>2</sup>, Clare Smith<sup>3</sup>, Moshi Geso<sup>3</sup>

<sup>1</sup> RMIT University, Melbourne, Australia

<sup>2</sup> Peter McCullum Cancer Centre, Victoria, Australia, RMIT University Melbourne, Australia

<sup>3</sup> RMIT University, Melbourne, Australia

### **Purpose**

The aim is to study the characteristics of the Synergy Health (SH) Electron Paramagnetic Resonance (EPR)-Alanine pellet dosimeters and explore the feasibility of using these dosimeters for pre-treatment verification of the dose delivered to patients undergoing stereotactic ablative radiotherapy.

### **Methods**

Prior to the application of SH EPR-alanine dosimeter for Pre-treatment verification of Stereotactic Ablative Radiotherapy (SABR) plans, the dosimeter was studied for dose linearity, angular dependence, energy dependence and dose rate dependence of megavoltage x-rays beams. The Bruker EleXsys E500 EPR spectroscopy of 9.5MHz was used to read the EPR signals. The alanine pellet dosimeters were placed inside a phantom made of Perspex that simulates the human body to perform the pre-treatment verification. Five different SABR cases including Lung, Liver, Scapula, Sternum and Spine were considered in this study. The measured dose from SH EPR-alanine dosimeters were then compared to the dose calculated from eclipse treatment planning system. In addition to this, we also used the ArcCheck and Ionization chamber to compare the measured dose.

### **Results**

The relationship between dose and the alanine-EPR signal followed a linear curve ( $R^2 = 0.998$ ) and no significant difference with dose rate and energy was observed. The differences between the measured and the TPS (Treatment Planning System) computed dose was less than 2%.

### **Conclusions**

Our study shows that the SH EPR-Alanine dosimeter is consistent and provides good agreement between the measured and the calculation dose and proved to be a valuable dosimeter for hypo-fractionated radiotherapy pre-treatment quality assurance.

### **Key words**

Alanine-EPR, SABR, ArcCheck, treatment planning system, Quality Assurance

## AVAILABILITY OF APPLYING DIAPHRAGM MATCHING WITH THE BREATH-HOLDING TECHNIQUE IN SBRT FOR LIVER TUMORS

Daisuke Kawahara<sup>1</sup>, Shuichi Ozawa<sup>2</sup>, Akito Saito<sup>3</sup>, Teiji Nishio<sup>3</sup>, Tatsuhiko Suzuki<sup>3</sup>, Shintaro Tsuda<sup>4</sup>, Yusuke Ochi<sup>4</sup>, Takuro Okumura<sup>4</sup>, Takeo Nakashima<sup>4</sup>, Yoshimi Ohno<sup>4</sup>, Yasushi Nagata<sup>3</sup>

<sup>1</sup> Hiroshima University, Japan

<sup>2</sup> Hiroshima High-Precision Radiotherapy Cancer Center, Japan

<sup>3</sup> Department of Radiation Oncology, Institute of Biomedical & Health Sciences, Hiroshima University, Japan

<sup>4</sup> Radiation Therapy Section, Department of Clinical Support, Hiroshima University Hospital, Japan

### Purpose

Image-guided radiotherapy (IGRT) based on bone matching can produce large target-positioning errors because of expiration breath-hold reproducibility during stereotactic body radiation therapy (SBRT) for liver tumors. Therefore, the feasibility of diaphragm-based 3D image matching between planning computed tomography (CT) and pretreatment cone-beam CT was investigated.

### Methods

In 59 liver SBRT cases, Lipiodol uptake after transarterial chemoembolization was defined as a tumor marker. Further, the relative isocenter coordinate that was obtained by Lipiodol matching was defined as the reference coordinate. The distance between the relative isocenter coordinate and reference coordinate, which was obtained from diaphragm matching and bone matching techniques, was defined as the target positioning error. Furthermore, the target positioning error between liver matching and Lipiodol matching was evaluated.

### Results

The positioning errors in all directions by the diaphragm matching was significantly smaller than those obtained by using by the bone matching technique ( $p < 0.05$ ). Further, the positioning errors in the A-P and C-C directions that were obtained by using liver matching were significantly smaller than those obtained by using bone matching ( $p < 0.05$ ). Liver matching The estimated PTV margin calculated by the formula proposed by van Herk for diaphragm matching, liver matching, and bone matching were 5.0 mm, 5.0 mm, and 11.6 mm in the C-C direction; 3.6 mm, 2.4 mm, and 6.9 mm in the A-P direction; and 2.6 mm, 4.1 mm, and 4.6 mm in the L-R direction, respectively.

### Conclusions

Diaphragm matching-based IGRT may be an alternative image matching technique for determining liver tumor positions in patients.

### Key words

SBRT, IGRT, diaphragm matching

## **EVALUATION OF DELIVERY UNCERTAINTIES OF RAPIDARC AND DYNAMIC IMRT PLANS FOR NPC PATIENTS USING ARCCHECK**

Yoke Lim Soong, Joseph Tien Seng Wee, James Cheow Lei Lee  
National Cancer Centre, Singapore

### **Purpose**

The purpose of this study is to evaluate delivery of uncertainties of RapidArc and intensity modulated radiation therapy (IMRT) in the treatment of Nasopharyngeal Carcinoma (NPC) using the quality assurance (QA) performance metric, gamma passing rate (%GP)

### **Methods**

9 Nasopharyngeal Carcinoma (NPC) patients were planned retrospectively using the Eclipse Treatment Planning System (Version 10.0.42) with RapidArc and sliding window IMRT (SW IMRT) technique. Pretreatment verifications were performed for all patients' plans by a diode array phantom, ArcCHECK. Measured dose distributions were compared with the calculated ones using the gamma index (GI) method applying global maximum (Van Dyk). The passing rate ranging from 1%-1 mm up to 5%-3mm were measured. MATLAB programme was used to calculate the mean of the segment gaps for all the plans

### **Results**

The mean %GP of RapidArc is higher compared to IMRT for all the criteria, except for 1%-1mm. The mean %GP of RapidArc is significantly (p-value < 0.01) better than IMRT for criteria 3%-1mm, 5%-1mm and 2%-2mm, with  $94.7 \pm 1.9$  %,  $99.4 \pm 0.3$  % and  $92.0 \pm 2.4$  % for RapidArc respectively and  $84.7 \pm 5.1$  %,  $95.1 \pm 2.7$  % and  $86.1 \pm 4.1$  % for SW IMRT. The mean leaf gap of the RapidArc is significantly bigger than IMRT (p-value < 0.01), with  $28.7 \pm 4.2$  mm and  $9.5 \pm 1.0$  mm respectively for RapidArc and SW IMRT. The wider leaf gap may be one of the main factors for the higher %GP of RapidArc Plans.

### **Conclusions**

The higher %GP of RapidArc showed that this technique has less delivery uncertainties and more robust for treating NPC cases

### **Key words**

IMRT, Uncertainties, RapidArc

## DETERMINATION OF PERCENTAGE DEPTH DOSES, BEAM PROFILES AND OUTPUT FACTORS IN SMALL PHOTON FIELD 6 MV USING THREE DETECTORS

S Mamesa, S Suriyapee, T Sanghangthum, S Oonsiri

Medical Imaging Program, Department of Radiotherapy Faculty of Medicine Chulalongkorn University, Bangkok, Thailand

**Keywords:** Small photon field dosimetry, PDDs& Beam Profiles, Output Factors (OPF), Ionization Chamber, Silicon Diode Detector.

**Introduction:** Small photon field is widely used in radiotherapy application. However, performing dosimetry in small photon field are still challenging to be observed[2,5].

**Methods:** The observation was performed in 6MV Varian TrueBEAM Linac by varying field sizes into some sizes from 10x10 cm<sup>2</sup> to 0.5x0.5 cm<sup>2</sup>. Reference depth& reference field size were 10cm and 10x10cm<sup>2</sup>, respectively. We began the observation by measuring PDDs&beam profiles and were continued to OPF measurement. Each measurement used three different detectors (CC01, PFD Diode and EDGE Detector) subsequently. In particular, we varied CC01 into two directions towards radiation beam; parallel & perpendicular direction in order to observe any directional dependence related to OPF measurement. For percentage depth doses&beam profiles measurement, CC01 was only employed in perpendicular direction.

**Results:** (A) In PDDs for fields size of 10x10cm<sup>2</sup> to 2x2cm<sup>2</sup>, the results showed CC01 in a good agreement with PFD & EDGE within average difference of 0.9%. When the field size was decreased smaller than 2x2cm<sup>2</sup>, the percentage difference increased significantly. However, PFD & EDGE showed a good agreement in all fields size within 0.5% of the average differences. (B) In Beam Profiles measurement for all fields size, CC01 produced a good agreement in field width half maximum (FWHM) analysis compared to PFD and EDGE detector within difference of 0.4mm. Meanwhile, PFD and EDGE detector showed a small percentage difference of 0.06mm. For penumbra measurement (80-20), there were two trends occurred in this work: the first trend occurred when the field size were increased from 2x2cm<sup>2</sup> to the largest field 10x10cm<sup>2</sup>, the trend of percentage difference was increasing significantly. The second trend occurred when the field size was set smaller than 2x2cm<sup>2</sup>. The percentage differences were increasing as we decreased the field size. (C) In OPF comparison, CC01 in parallel direction was giving a higher reading compared to the perpendicular direction. On the other hand, PFD and EDGE were constantly giving a higher OPF reading compared to CC01 in both directions.

**Discussion:** Higher result in PDDs obtained by CC01 may occur due to the effect of volume averaging. Wider penumbra result from CC01 was due to the higher electron range in the air cavity than in water[1]. A large penumbra reading from CC01 in this work was also fit with Gersh et

al[3]. In OPF measurement, when CC01 was set in parallel direction, the probability of photon beam to interact with the steel material in the central electrode is also higher, which could lead into the over-response of dosimeter reading[4]. PFD and EDGE detector showed a higher reading in OPF measurement compared to CC01 in any directions. This can occur due to the interaction between radiation with Silicon material (Silicon,  $\rho=2.3\text{gr/cm}^3$ ) as the main component of PFD and EDGE detector. Other high-density materials surrounding the sensitive volume such as the encapsulating material also contribute in the higher reading of OPF measurement from PFD & EDGE detector [1,3,6].

**Conclusion:** CC01 showed a good agreement with PFD and EDGE in PDDs & FWHM measurement, but larger penumbra region. In parallel direction, CC01 was found delivering a higher OPF measurement compared to the perpendicular direction. This result has showed that CC01 is directional dependence. Henceforth, special consideration of CC01 direction is required when performing small field dosimetry. PFD and EDGE were constantly giving a higher OPF measurement compared to CC01 in any directions. Moreover, PFD and EDGE showed an excellent agreement for every measurements in this research, thus both detectors may be utilized interchangeably. Further studies shall be performed on this possibility.

### References

1. Godson HF, Ravikumar M, Sathiyam S, Ganesh K M, Ponmalar Y R, Varatharaj C. Analysis of small field percent depth dose and profiles: Comparison of measurements with various detectors and effects of detector orientation with different jaw settings. *J Med Phys* 2016;41:12-20.
2. Hamza Benmakhlouf, Josep Sempau, Pedro Andreo. Output Correction factors for nine small fields detectors in 6 MV radiation therapy photon beams: A PENELOPE Monte Carlo Study. *Medical Physics* Vol.41, No 4, April 2004.
3. Jacob A. Gersh, Ryan C.M. Best, Ronald J.Watts. The Clinical Impact of Detector Choice for Beam Scanning. *Journal of Applied Clinical Medical Physics*, Volume 15, Number 4, 2014.
4. Muir BR and Rogers DW. The Central electrode correction factor for high Z electrodes in small ionisation chambers. *Med Phys* .2011;38(2):1081-88.
5. S.D Sharma. Challenges of Small photon field dosimetry are still challenging. *Journal of Medical Physics*, July-September 2014; 39(3): 131-132.
6. Tyler M, Liu PZ, Chan KW, Ralston A, McKenzie DR, Downes S, et al. Characterization of small-field stereotactic radiosurgery beams with modern detectors. *Phys Med Biol* 2013;58:7595-608.

**Corresponding email author:** ssvalee@yahoo.com

## **DEVELOPMENT OF A NOVEL QUALITY ASSURANCE METHOD OF RADIATION STANDARD DOSIMETRY BASED ON FAILURE MODE AND EFFECTS ANALYSIS**

Yusuke Ochi<sup>1</sup>, Akito Saito<sup>2</sup>, Teiji Nishio<sup>2</sup>, Shuichi Ozawa<sup>3</sup>, Daisuke Kawahara<sup>4</sup>, Tatsuhiko Suzuki<sup>2</sup>, Masato Tsuneda<sup>5</sup>, Sodai Tanaka<sup>6</sup>, Yoshimi Ohno<sup>4</sup>, Yasushi Nagata<sup>2</sup>

<sup>1</sup> Hiroshima University, Japan

<sup>2</sup> Department of Radiation Oncology, Institute of Biomedical & Health Sciences, Hiroshima University, Japan

<sup>3</sup> Hiroshima High-Precision Radiotherapy Cancer Center, Japan

<sup>4</sup> Radiation Therapy Section, Department of Clinical Support, Hiroshima University, Japan

<sup>5</sup> Medical and Dental Sciences Course, Graduate School of Biomedical & Health Sciences, Hiroshima University, Japan

<sup>6</sup> Department of Nuclear Engineering and Management, School of Engineering, University of Tokyo, Japan

### **Purpose**

Output of the linear accelerator (linac) is the one of the most important quality assurance (QA) in radiotherapy. However, there is no quantitative rationale for frequency and tolerance. The purpose of this study is to develop a novel QA method based on Failure Mode and Effects Analysis (FMEA).

### **Methods**

Standard dosimetry data based on Japanese guideline and the daily measurement data in Hiroshima University Hospital were analyzed. The analysis involved the number of patients per year for five types of fractionations. Risk Priority Number (RPN) is defined as a product of Occurrence (O), Severity (S) and Detectability (D) in the standard FMEA. In addition, we introduced Severity due to drift (output change per day) (S') and the number of patients per year for five types of fractionations (W). We calculated the RPN  $O \times S \times D \times S' \times W$  and quantitatively evaluated the risk in standard dosimetry.

### **Results**

Lower number of fractionations and measurement frequency resulted in the higher RPN. Since the standard dosimetry data has drifting effect which is missing in human processes, it was essential to use S' in addition to the standard FMEA. The parameter W was important to evaluate interinstitutional QA of standard dosimetry.

### **Conclusions**

We developed a novel index that can quantitatively evaluate the risk in standard dosimetry based on FMEA. The suggested RPN could quantitatively evaluate the risk in standard dosimetry of each facilities and machines.

### **Key words**

Standard Dosimetry, FMEA

## **APPLICATION OF FAILURE MODE EFFECT ANALYSIS (FMEA) IN RADIOTHERAPY: A PROACTIVE APPROACH TO CONTINUOUS QUALITY IMPROVEMENT AND PATIENT SAFETY**

Gopinath Mamballikalam

Aster Medcity, India

### **Purpose**

The project is basically aimed to prevent/ reduce the errors reaching the patient by assessing the risk for patient's undergoing Radiotherapy treatment and to redefine the process thereby maximizing the benefits of Radiotherapy by controlling the cancer and improving the quality of life. Also the project is aimed to increase the overall patient satisfaction & continuous quality improvement by enhancing safety measures and improving clinical care.

### **Methods**

The project takes care of all steps in Radiation treatment understanding the processes and sub processes and predict the potential failure modes that can happen in each steps. The effect of each failure and causes of failure are evaluated and a Risk Priority Number (RPN) is assigned for each failure depending on the severity, Occurrence and detectability of the failure. A set of actions to minimize the RPN score for each event is implemented to achieve the desired result of treatment.

### **Results**

The data analysed after a year of total 524 patients, 71 cases (13.5%) showed errors which has been identified and prevented before transferring to the patients. These are

- 1) Prescription Error - 12
- 2) Contouring error - 10
- 3) Body Contour error - 18
- 4) Couch Insert error - 16
- 5) Planning error - 08
- 6) Simulation error - 03
- 7) QA and Collision test failed - 04

### **Conclusions**

A total of 15 processes (Fig 1) and 76 sub processes (Fig 2) are identified for the entire Radiotherapy. 27 Failure Modes are identified from Simulation till the completion of treatment. A two-step FMEA is carried out. The project redefined the entire Radiation Oncology process. The major changes carried out are

- Complete NO to Verbal orders
- Follow evidence based practice and clinical review
- Define TAT for Planning process
- Proper scheduling of Daily Treatment
- Implementation of peer review mechanism
- Patient Identification & risk assessment
- Staff Training and Competency

### **Key words**

## COMMISSIONING OF THE PATIENT-SPECIFIC QA OF VMAT PLAN CALCULATED BY ACUROS® XB ALGORITHM

Minoru Nakao

Hiroshima High-Precision Radiotherapy Cancer Center, Japan

### Purpose

Acuros® XB (AXB) algorithm on Eclipse requires the correct mass densities and elements of medium for accurate dose calculation. However, the data for polymethylmethacrylate (PMMA) that consists of ArcCHECK® is different from the PMMA data registered on Eclipse. The purpose of this study is to propose the appropriate mass density and elements for the material of ArcCHECK® on AXB

### Methods

The material of ArcCHECK® was replaced by several alternative materials and arbitrary density on AXB, and absolute doses at the center of ArcCHECK® were calculated by with 10cm×10cm fields of 4X, 6X, 8X, 10X, 6XFFF and 10XFFF beams by Varian TrueBeam STx. The suitable material and density was determined based on the comparison between dose calculation by AXB and measured dose at the center of ArcCHECK® by PinPoint® ionization chamber (PTW 31016). After the determination of material and density for ArcCHECK®, patient-specific QA by ArcCHECK® had done for 10 patient plans with VMAT technique to valid the material and density assigned for ArcCHECK®.

### Results

Water with the density of 1.105 g/cm<sup>3</sup> gave the minimum difference for calculation and measurement with 10cm×10cm field. The average and 1SD of the difference between calculation and measurement for 10cm×10cm field and VMAT QA were  $0.1 \pm 0.5$  % and  $1.7 \pm 0.6$  %. The average and 1SD of gamma analysis (3mm/3%, threshold 10%) was  $96.6 \pm 2.5$  %.

### Conclusions

This study proposed the appropriate material for the QA with ArcCHECK® and showed the commissioning procedure and limitation for AXB.

### Key words

ArcCHECK, Acuros XB, Patient-specific QA, VMAT

## **KOMPEITO-SHOT: DEVELOPMENT OF A NOVEL VERIFICATION SYSTEM FOR 3D BEAM ALIGNMENT**

Masato Tsuneda<sup>1</sup>, Teiji Nishio<sup>1</sup>, Akito Saito<sup>1</sup>, Kazunari Hioki<sup>2</sup>, Takuro Okumura<sup>2</sup>, Yusuke Ochi<sup>2</sup>, Daisuke Kawahara<sup>1</sup>, Keiichiro Matsushita<sup>1</sup>, Tatsuhiko Suzuki<sup>1</sup>, Sodai Tanaka<sup>3</sup>, Shuichi Ozawa<sup>1</sup>, Yasushi Nagata<sup>1</sup>

<sup>1</sup> Hiroshima University, Japan

<sup>2</sup> Hiroshima University Hospital, Japan

<sup>3</sup> The University Of Tokyo, Japan

### **Purpose**

The purpose of this study is the development of high-resolution irradiation position measurement system for 4D radiation therapy. Firstly, we designed and developed a prototype system for 3D beam alignment (3D Isocentricity) including the sag of gantry head. This system enables to verify directly and quantitatively gantry rotation axis as angle information (the sag of gantry head). We examined the concept of this system.

### **Methods**

The system composed of a plastic scintillator (PS), a truncated cone-shaped mirror, a plane mirror and a CCD camera. The PS was separated two shape (Column type and Barrel type). We inserted the shading film between Column type PS and Barrel type PS. The system was irradiated with a 6-MV photon beam and the scintillation light was measured using the CCD camera. The gantry angle was set from 270 to 300 degrees to mimic the sag of the gantry head for evaluating the accuracy of this system.

### **Results**

Entrance and exit areas in the measurement images were visualized clearly. The relation between the calculated gantry angle and the irradiated gantry angle had good linearity. We evaluated the mean and standard deviation of the histogram showed the difference between the calculated gantry angle and the irradiated gantry angle. Mean and standard deviation of this system was -0.26 and 0.33, respectively.

### **Conclusions**

We developed the prototype system for 3D beam alignment and evaluated the accuracy of the system. The basic concept works for the verification of 3D isocentricity.

### **Key words**

4D Radiation Therapy, 3D Isocentricity, Plastic Scintillator

## **VMAT PLAN AND DELIVERY VERIFICATION OF ELEKTA VERSA HD USING MOBIUS SYSTEM**

Hooi Yin Lim, Lip Teck Chew  
Farrer Park Hospital, Singapore

### **Purpose**

To implement Mobius system as a comprehensive radiotherapy plan check and every fraction QA check.

### **Methods**

50 patients (15 SRT Brain) were planned with Monaco® and treated with Elekta Versa HD™ using VMAT. Patients' full DICOM-RT plans were sent to Mobius server for independent plan check (Mobius3D). The delivery log files were acquired with MobiusLog. They were sent back to Mobius server for independent QA (delivery) check (MobiusFX) on the same DICOM-RT dataset. All Mobius3DFX results were tabulated. For 20 plans randomly selected, pre-treatment QA was carried out using point dose measurement and FilmQA™ Pro in 20 cm RW3 phantom. The results were compared to Monaco® and Mobius3D. The criteria used for gamma analysis were 3%/3mm for general and 3%/2mm for SRT cases.

### **Results**

All point dose results were within 3% compared to Monaco® and Mobius system in phantom. The FilmQA™ Pro results were above 95%. The average Mobius 3D-gamma results for plan check and QA check were above 98% for both general and SRT cases.

### **Conclusions**

Mobius System is a comprehensive and efficient Patient Specific QA for a modern radiation oncology department. It serves as an independent verification of DICOM-RT file integrity, radiotherapy plan check and QA check for every individual patient.

### **Key words**

Patient Specific Quality Assurance, Delivery Verification, Mobius, VMAT, Versa HD™

## **QUALITY ASSURANCE PROCESSES IN FRAMELESS VMAT-BASED FRACTIONATED STEREOTACTIC RADIOTHERAPY WITH NO INTRA-FRACTION MOTION MONITORING**

Sergei Zavgorodni<sup>1</sup>, Isabelle Gagne<sup>1</sup>, Reid Townson<sup>2</sup>, Will Ansbacher<sup>1</sup>

<sup>1</sup> BC Cancer Agency, Vancouver Island Center, Canada

<sup>2</sup> University of Victoria, Canada

### **Purpose**

To establish patient-specific quality assurance (QA) program for frameless VMAT-based stereotactic radiotherapy (SRT) without intra-fraction motion monitoring

### **Methods**

Patient immobilization at CT and treatment is performed with a locally modified full mask. CT slice thickness of 1.25mm is used. Plans with two coplanar arcs are produced with Eclipse AAA calculations at 1.25mm resolution and verified against a clinical protocol to ensure compliance of all dosimetric indices. Two pre-treatment CBCT acquisitions with 6D followed by 4D-couch corrections are performed; post-treatment CBCT is also taken and reviewed off-line. For two patients off-line review detected loosening of the mask and prompted corrections. Dosimetry QA includes Monte Carlo verification of the dose distribution on patient CT data, 3D EPID-based verification in a virtual cylinder phantom, and iso-cal verification of MV and kV beams' congruence. In-phantom point dose measurements have been performed for the first thirty patients and are now performed only as required.

### **Results**

Forty one patients were treated during the first year in our program. Mean point dose difference between MC and microDiamond detector was 0.3% (1.6%SD). Mean PTV dose difference between MC and AAA calculations was 0.4% (1.2%SD). For EPID verification, mean point dose difference was -0.6% (1.4%SD), mean 3%/1mm pass rate was 97.7% (4.9%SD). Mean radial treatment setup error was 0.2mm (0.2mm SD), mean radial treatment error was 0.4mm (0.2mm SD)

### **Conclusions**

Rigorous QA through each step of SRT is essential. Pre-and-post treatment CBCTs allowed accurate patient positioning while MC calculations and EPID-based 3D dosimetry allow efficient 3D dose verification.

### **Key words**

Stereotactic radiotherapy, VMAT, Quality Assurance

## DOSIMETRIC COMPARISON OF PATIENT SPECIFIC QA IN LUNG SBRT USING UNFLATTENED BEAMS BETWEEN TWO DOSIMETER SYSTEMS

S Maknitikul<sup>1</sup>, S Suriyapee<sup>1</sup>, T Sanghangthum<sup>1, 2</sup>, S Oonsiri<sup>2</sup>

<sup>1</sup>Medical Imaging program, Department of Radiology, Faculty of Medicine, Chulalongkorn University, Bangkok, Thailand

<sup>2</sup>Division of Therapeutic Radiology and Oncology, Department of Radiology, King Chulalongkorn Memorial Hospital, Bangkok, Thailand

**Keywords:** Stereotactic body radiation therapy (SBRT), Flattening filter free (FFF), Dosimetry system, Patient specific quality assurance

**Introduction:** Nowadays, Stereotactic Body Radiation Therapy (SBRT) is widely used, because the benefits are high dose delivery in a few fractions, short treatment time, conformation of high doses to the target and minimize the normal tissue toxicity [1, 3]. To increase capability, flattening filter free (FFF) is applied with the SBRT technique. The advantages of flattening filter free are high dose rate, high dose per pulse reduced lateral changes in beam hardening, reduce leakage and out-of-field dose [1]. For this high dose technique, the accuracy of dose delivery is important that can verify by patient specific quality assurance. The aim of this study is to compare the patient specific QA tool between ArcCHECK and Gafchromic film in Lucy phantom for VMAT in lung SBRT using unflattened photon beams.

**Methods:** The fifteen lung VMAT SBRT plans using 6MV FFF beams with prescribed dose of 4-30 Gy/fraction were selected for this study. The Varian TrueBeam™ linear accelerator with 1,400 MU/min maximum dose rate were employed. Varian Eclipse treatment planning (version 11.0.3) and Acuros XB algorithm (version 11.0.31) were used for calculation of reference dose and dose distribution. For point dose, the first system was IBA CC13 ionization chamber in ArcCHECK. The second system was IBA CC01 and CC13 ionization chamber in Lucy phantom. The isodose distribution was measured by ArcCHECK and Gafchromic EBT3 film in Lucy phantom. Before measuring with EBT3 films, the films were calibrated in virtual water slab phantom for 10×10 cm<sup>2</sup> field size at 7 cm depth, 100 cm. SAD and 15 cm backscatter with several 6MV FFF beams doses. The criteria for comparison of measured dose and calculated dose (treatment plan) was  $\pm 3\%$  point dose difference and the gamma criteria 3% dose difference and 3 mm distance to agreement for isodose distribution.

**Results and discussion:** The mean percentage point dose difference between measured dose and calculated dose of IBA CC13 ion chamber in ArcCHECK and IBA CC01, CC13 in Lucy phantom were  $-1.25 \pm 2.25\%$ ,  $-1.37 \pm 1.74\%$  and  $-0.68 \pm 2.27\%$ , respectively. The mean percentage gamma pass between measured dose and calculated dose of ArcCHECK and Gafchromic EBT3 film in Lucy phantom were  $94.89 \pm 1.88\%$  and  $92.59 \pm 5.87\%$ , respectively.

**Conclusion:** The selection of patient specific QA tool was important for advance technique such as SBRT. This study was the comparison of patient specific QA tools in lung SBRT using unflattened photon beams. The point dose difference and gamma pass between two dosimeter systems were agreeable.

### References:

1. Rasmus Lübeck Christiansen, Olfred Hansen, Jonathan B. Sykes, et al. (2015) Plan quality and delivery accuracy of flattening filter free beam for SBRT lung treatments. *Acta Oncologica*, 54: 422–432
2. Guangjun Li, KuiWu, M.Sc., Guang Peng, Yingjie Zhang, et al. (2014) A retrospective analysis for patient-specific quality assurance of volumetric-modulated arc therapy plans. *Medical Dosimetry*
3. Stanley H. Benedict et al. (2010) Stereotactic body radiation therapy: The report of AAPM Task Group 101. *Medical Physics*, volume 37, number 8

Corresponding author email: ssivalee@yahoo.com

## **EXTERNAL DOSE AUDIT OF HIGH ENERGY RADIOTHERAPY PHOTON BEAMS IN JAPAN**

Suoh Sakata

Association for Nuclear Technology in Medicine, Japan

### **Purpose**

Nine years have passed since the Association for Nuclear Technology in Medicine (ANTM) launched the external dose quality audit (EDQA) of high energy radiotherapy photon beams for radiotherapy departments in Japan. When EDQA was started, the object was limited to beams of reference condition (10cm square field size, 10cm depth in water) and was expanded to non-reference conditions of field size changes and wedge filter insertions in 2010. In this study we report the results of this EDQA and the present status of dose estimation in Japan evaluated from EDQA.

### **Methods**

In the EDQA by ANTM, radiophotoluminescent glass dosimeter (RGD) is used as the detector. ANTM send RGD elements and solid phantom to radiotherapy departments and RGD are returned to ANTM after the irradiation of a specified dose. The dose delivered to RGD is measured at Dose Calibration Center of ANTM and is compared to the dose stated by radiotherapy department.

### **Results**

Until March 2016, 3,351 beams of 784 therapy units from 629 departments have been audited. The numbers of beams are classified into 1,663 of reference condition, 1,103 of field size change and 585 wedge filter insertion. The averages of difference between measured and stated dose were 0.39% in reference condition, 0.19% in field changes and 0.17% in wedge filter insertions. The standard deviations were around 1% for all conditions.

### **Conclusions**

The external dose QA by ANTM shows that the status of dosimetry at radiotherapy departments in Japan is in satisfying level.

### **Key words**

External dose audit, High energy photon beam, Dosimetry, Radiotherapy

## **EVALUATION OF THE DOSIMETRIC LEAF GAP EFFECT ON THE IMRT VERIFICATION OF PATIENT SPECIFIC QUALITY ASSURANCE BY USING OCTAVIUS 2D ARRAY DOSIMETER**

Swe Swe Lin, Sivalee Suriyapee, Taweap Sanghangthum  
Chulalongkorn University, Thailand

### **Purpose**

The complexity of IMRT treatment delivery need the patient specific quality assurance (QA) to achieve the dose distribution goal. Dosimetric leaf gap (DLG) is an important role to module accurately the MLC characteristics defined in treatment planning system (TPS). The objective of this study is to evaluate the effect of DLG on IMRT verification patient specific QA by using Octavius dosimeter.

### **Methods**

The five highly modulated Head and Neck cases, the four moderately modulated esophageal cases and the five minimally modulated brain cases IMRT plans from the Eclipse treatment planning system were employed to observe the relation between the DLG and the patient specific QA by Octavius. The DLG value of -0.1551 mm measured from the Varian Clinac iX was used as the reference and then changing the DLG 0.1 mm apart started from 1.0 mm to 2.0 mm for the dose calculation in TPS.

### **Results**

The gamma pass for 2D measurement in Octavius dosimeter ranged from 78.90% to 100% at 3%,3mm criteria in Octavius 2D array detector. When the DLG was change from the reference value, the gamma pass rate also changed in the range from 2-20%. Decreasing the DLG will increase the gamma pass rate and vice visa.

### **Conclusions**

DLG is effect to the patient specific QA of high modulated IMRT plan. However, it shows no effect for the moderate and minimal modulated cases.

### **Key words**

patient specific QA, DLG, gamma pass, IMRT, intentional error

## **THREE DIMENSIONAL IMRT PATIENT-SPECIFIC QA USING INCIDENT FLUENCE OF EPID**

Sangutid Thongsawad  
Chulabhorn Hospital, Thailand

### **Purpose**

The aim of the study was to provide a method for three dimensional IMRT patient-specific QA by using EPID.

### **Methods**

The method includes first step to convert integrated electronic portal image to incident fluence. The incident fluence was generated with deconvolution between integrated electronic portal image and kernel of EPID. In these studies, the kernel of EPID was modeled with a proper method. The secondary step, the incident fluence was imported to TPS (Eclipse V13.00, AAA algorithm) for dose distribution calculations in CT images. The accuracy of method was evaluated in three head and neck IMRT plans by comparing between the incident fluence calculation using EPID and TPS fluence map with gamma index ( $\gamma$ ) criteria of 2 %, 2 mm. These studies also investigated the capability of EPID for three dimensional IMRT patient-specific QA by comparing between three dimensional dose reconstructions using EPID and TPS in tumor coverage (D95%) and normal organ.

### **Results**

The comparing between incident fluence calculation using EPID and TPS fluence map have been shown the gamma passing rate more than 98% for IMRT plans. The disagreement between three dimensional dose reconstruction using EPID and TPS was less than 2.2 % for tumor coverage (D95%), less than 1.5% for parotid (mean dose) and less than 2.3% for spinal cord (max. dose).

### **Conclusions**

The method can provide a simply and accurate procedure for three dimensional IMRT patient-specific QA.

### **Key words**

IMRT, EPID, Thee dimensional IMRT patient-specific QA

## COMPARISON OF ACTUAL RADIOTHERAPY INCIDENT DATA AND RISK EXPECTATION THROUGH EXPERT GROUP SURVEY

Jihye Koo<sup>1</sup>, Myeonggeun Yoon<sup>1</sup>, Weonkuu Chung<sup>2</sup>, Mijoo Chung<sup>2</sup>, Dongwook Kim<sup>2</sup>

<sup>1</sup> Korea University, Kopea

<sup>2</sup> Kyung Hee University Hospital at Gangdong, Kopea

### Purpose

To evaluate the reliability of RPN (Risk Priority Number) decided by expert group and to provide preliminary data for adapting FMEA in Korea.

### Methods

1163 Incidents reported in ROSIS were used as a real data to be compared with, and were categorized into 146 items. The questionnaire was composed of the 146 items and respondents had to evaluate 'occurrence (O)', 'severity (S)', 'detectability (D)' of each item on a scale from 1 to 10 according to the proposed AAPM TG-100 rating scales. 19 medical physicists in Korea had participated in the survey.

### Results

The average O,S,D were 1.77, 3.50, 2.13, respectively and the item which had highest RPN(32) was 'patient movement during treatment' in the survey. When comparing items ranked in the top 10 of each survey(O) and ROSIS database, two items were duplicated and 'Simulation' and 'Treatment' were the most frequently ranked RT process in top 10 of survey and ROSIS each. When comparing O\*D, the average difference was 1.4.

### Conclusions

This work indicates the deviation between actual risk and expectation. Considering that the respondents were Korean and ROSIS is mainly composed of incidents happened in European countries and some of the top 10 items of ROSIS cannot be applied in radiotherapy procedure in Korea, the deviation could have been came from procedural difference. Moreover, if expert group was consisted of experts from various parts, expectation might have been more accurate. Therefore, further research on radiotherapy risk estimation is needed.

### Key words

Radiotherapy, Risk Assessment, FMEA

## **INTERLOCKS AS A MEASURE OF LINEAR ACCELERATOR HEALTH: TRENDS OVER THREE YEARS**

Tomas Kron, Gerrard Janson, Brad Shilling, Li Zhu  
Peter MacCallum Cancer Centre, Melbourne, Australia

### **Purpose**

Linear accelerators (linacs) are the most important tool for external beam radiotherapy delivery. They feature many interlocks that indicate faults to ensure safe patient treatment. We analyzed the frequency and type of interlocks observed on 15 linacs in a single institution over three years.

### **Methods**

All interlocks that require engineering or medical physics intervention are recorded at Peter MacCallum Cancer Centre using an in-house developed software tool, Track to Treat (T2T). We studied frequency of interlocks on 15 Varian Clinac 21 type machines (two 21ex, eleven 21iX, 2100CD, Trilogy) over 5 campuses. All linacs are serviced in house. Interlock type and frequency was linked to machine age and use as identified by the presence of an on-board image (OBI).

### **Results**

From Nov 2012 until Nov 2015 more than 7000 thousand interlocks were recorded with 85% of them specified in the database. The most common interlock was 'Hardware' (HWFA,  $n = 1152$  or 16%) followed by dose interlocks XDRS and DS12 (11% and 10%, respectively). Nine machines have on-board imaging and cone beam CT. These linacs featured typically more interlock occurrences than the non-OBI machines but this was not evident for MLC type interlocks despite the fact that IMRT is usually delivered on these machines. They also showed a trend for increasing number of interlocks with age of the machine ( $r^2 = 0.35$ ).

### **Conclusions**

Interlocks report important functionality, safety and reliability issues. Analysing their frequency and type can assist with linac maintenance, quality assurance and replacement strategies.

### **Key words**

Radiotherapy, Quality Assurance, Linacs, Interlocks

## **STATISTICAL METHODS TO ASSESS AGREEMENT OF RESULTS FROM DIFFERENT PRE-TREATMENT QA DEVICES, STABILITY OF EACH QA PROCESS AND THE APPROPRIATE ACTION LEVEL**

Yun Inn Tan<sup>1</sup>, Taweap Sanghangthum<sup>2</sup>, Leong Yuh Fun<sup>1</sup>, Teh Mun Woan<sup>1</sup>, Sháun Baggarley<sup>1</sup>

<sup>1</sup> National University Cancer Institute, Singapore

<sup>2</sup> Chulalongkorn University, Thailand

### **Purpose**

There are many commercial options available to perform patient-specific pre-treatment QA. The aims of this study are: (1) to assess the agreement of gamma analysis results from two commercial systems and (2) to assess the process performance of each system using control chart and derive individual action limit.

### **Methods**

Two groups of IMRT fields were investigated in this study: 6 MV head and neck (HnN) and 10 MV prostate. Each IMRT field was measured with ArcCHECK (AC, Sun Nuclear) and Portal Dosimetry (PD, Varian) in the same session. Absolute global gamma comparisons were done with the respective software using the same settings (threshold 10%, criterion 3%/3mm).

### **Results**

Results showed that the AC and PD percentage gamma pass rates were statistically comparable for the 6 MV HnN group ( $p=0.552$ ) but not for the 10 MV prostate group ( $p=0.000$ ). Control chart revealed that the QA process for the 10 MV prostate group with PD was not in control, with a process capability index ( $C_{pml}$ ) of only 0.71 ( $<1$ ). Other QA processes were stable and in control ( $C_{pml} >1$ ). The poor performance of PD for the 10 MV group was due to improper calibration of the device. Individual action limits, derived for processes that were in control, ranged from 92.9% to 94.8%.

### **Conclusions**

In conclusion, a framework to qualitatively assess and compare QA processes was demonstrated in this study. Control chart was found to be useful in highlighting problem in a QA process and for setting individual action limit instead of a generic limit.

### **Key words**

Statistical process control, pre-treatment QA

## **TUMOR AND CRITICAL ORGAN'S DOSE IN CRANIOSPINAL RADIOTHERAPY WITH PHOTON AND ELECTRON**

Hamid Gholamhosseinian

Mashhad University of Medical Sciences, Iran

### **Purpose**

Surgery is the main treatment technique of cerebrospinal tumors. But due to the tumor location (posterior cranial fossa brain), complete removal of the tumor is difficult, Therefore; adjuvant therapies such as radiotherapy of spinal cord with electron or photon beams are required. the present study aimed to compare RT two techniques, a) with a single photon beam b) with a combination of photon and electron beams.

### **Methods**

CT-Scan of brain and spine of a Rando Phantom were obtained. The Two techniques were planned. In the first technique, both brain and spinal cord were irradiated with 6 MV photon). In the second technique, brain was irradiated with 6 MV photons and spinal cord with on 18 MeV electron beam. To compensate the dose deficiency in lumbar, an anterior field of 15 MV photon beam was also applied.

The dose to target volume and OARs were measured by TLD and compared by TPS the value corresponding calculated.

### **Results**

OARs included heart, mandible, thyroid and lungs received lower dose from technique 2 compared with technique 1, kidneys were exceptions which received more dose in the technique 2. Finally based on the TRS-430 protocol, the accuracy of Isogray in dose calculation was confirmed.

### **Conclusions**

thyroid, heart and lungs received lower dose in technique 2, while kidneys received higher dose in technique 2, this was caused by using the anterior 15 MV photon beam. Therefore, when the patient is a child it is wiser to use electron for irradiation spine.

### **Key words**

Critical Organs, Craniospinal, Radiotherapy, Tumor

## **VALIDATION OF PERFRACTION 3D EPID BASED PATIENT SPECIFIC QA SOFTWARE**

Abdul Aziz Sait A<sup>1</sup>, Freedom Hliziyo<sup>1</sup>, Jason Figueredo<sup>2</sup>, Thomas McGowan<sup>1</sup>, Glenn Jones<sup>1</sup>, Rhonda Sealey Thomas<sup>3</sup>, Henry Hazel<sup>1</sup>, Ramani Ramaseshan<sup>4</sup>

<sup>1</sup> The Cancer Centre Eastern Caribbean

<sup>2</sup> Sun Nuclear Corporation

<sup>3</sup> Ministry Of Health

<sup>4</sup> BC Cancer Agency

### **Purpose**

To validate the PerFRACTION software by comparing its performance against a standard 2D array MapCHECK system as well as ionization chamber measurements.

### **Methods**

Two phantoms were constructed to evaluate the point dose and fluence. The first phantom was made of 1 cm PMMA slabs with total thickness of 10 cm with an ionization chamber positioned at 5 cm depth. The second phantom was constructed with combination of 2D array and 1cm PMMA slabs to create radiological equivalent thickness of 10 cm while maintaining the diode array at 5 cm depth. Volumes resembling a prostate, bladder, rectum and the femoral heads were created on a PMMA slab using copper wire and placed on the slab above and below the measuring devices. Both phantoms were scanned and planned with VMAT. Initial measurements were made without any phantom and set as Fraction0, directly irradiating onto the EPID. Fraction1 to 15 were delivered on both phantoms separately and exit doses were recorded and reconstructed to calculate the 3D dose and fluence. Subsequent evaluation included comparison between phantom measurements, PerFRACTION reconstructed doses and planning system.

### **Results**

Initial data analysis showed that the ionization chamber point doses were not significantly different from

PerFRACTION reconstructed dose at  $P < 0.05$ . Mean  $\pm$  sd of ionchamber point dose  $1.980 \pm 0.01$  versus PerFRACTION  $1.966 \pm 0.04$ .

### **Conclusions**

The outcome of the validation process is expected to establish the accuracy of PerFRACTION in-vivo dosimetry software in daily treatment for the direct assessment of treatment quality through monitoring errors involving machine delivery, patient anatomical changes, and setup variations on a daily or periodical basis and missing patient specific attachments.

### **Key words**

In-vivo dosimetry, EPID, PerFRACTION

## **7.3 Nuclear Medicine QA**

## COMPARATIVE STUDY OF RADIOLYTIC STABILIZERS FOR RADIOLABELING DOTA-BOMBESIN CONJUGATES WITH <sup>68</sup>GA

Sarinya Wongsanit, Wiranee Sriwiang

Thailand Institute of Nuclear Technology, Thailand

**Key words:** <sup>68</sup>Ga-DOTA- Bombesin, radiolytic oxidation, radiochemical purity, radiolytic stabilizers

### **Purpose**

The aim of the present work was to obtain stabilized <sup>68</sup>Ga-labeled bombesin conjugates for preclinical evaluations. In the labeling experiment, the radiolytic stabilizers were added in order to decrease impurities which caused by radiolytic oxidation by-products of <sup>68</sup>Ga-DOTA-Bombesin that were observed in the chromatogram of the analytical radio-HPLC.

### **Methods**

DOTA-[Pro1, Tyr4]-bombesin was labeled with <sup>68</sup>Ga. Labeling conditions were optimized by adjusted the amount of peptide, pH and buffer. A set of various concentrations ranged from 0 to 30 milligram w/w or 10% w/v of gentisic acid, sodium thiosulfate, ascorbic acid and ethanol were added during the labeling. The effect of stabilizers on radiopeptides stability at room temperature was systematically categorized applying chromatography techniques.

### **Results**

The addition of gentisic acid, sodium thiosulfate, ascorbic acid or ethanol to the reaction mixture showed significant improvement on the radiochemical purity of <sup>68</sup>Ga-DOTA-Bombesin and they was achieved in avoided the radiolysis and significantly increased the stability.

### **Conclusions**

Results from our study will be further analyzed in conjunction with other chemical and HPLC method performed on the same type of samples.

## ABSOLUTE STANDARDIZATION METHODS OF <sup>153</sup>SM FOR NUCLEAR MEDICINE IN INDONESIA

Gatot Wurdianto<sup>1</sup>, Agung Agusbudiman<sup>1</sup>, Hermawan Candra<sup>1</sup>

<sup>1</sup>Center for Technology of Radiation Safety and Metrology – National Nuclear Energy Agency of Indonesia (PTKMR – BATAN)

**Key words :** Standardization, 4phi beta(LS)-gamma coincidence, dose calibrator, short half-life, <sup>153</sup>Sm

**Introduction:** The Standardization absolutely of radioactive sources <sup>153</sup>Sm, to calibrate the nuclear medicine equipment, has been carried out in PTKMR-BATAN. This is necessary because the radioactive sources used in the field of nuclear medicine have a very short half life in other that to obtain a quality measurement results require special treatment. Besides that, the use of nuclear medicine techniques in Indonesia develops rapidly [1].The purpose of this study is to determine the standardization methods of <sup>153</sup>Sm for calibrating nuclear medicine instruments more accurately, precisely and traceable to International System Unit.

**Methods :**The <sup>153</sup>Sm source used in this experiment is produced by the neutron bombardment of isotopically enriched <sup>152</sup>Sm<sub>2</sub>O<sub>3</sub> in nuclear reactor, multi purpose Siwabessy reactor, Serpong-Indonesia. The source was prepared by gravimetric method. Three sets of <sup>153</sup>Sm samples were prepared from the initial stock solution. The first set is used for the absolute activity measurement using a 4πβ(LS)-γ coincidence counting method [2]. The second set of samples are used for the impurities test using a gamma spectrometer system. For the last set, two samples were prepared in ampoules to calibrate the dose calibrator unit.The 4πβ(LS)-γcoincidence counting method was used to determine the activity of <sup>153</sup>SmThe general equation is shown below:

$$\rho_{\beta} = A \left[ \varepsilon_{\beta} + \frac{(1-\varepsilon_{\beta})(\alpha\varepsilon_{ce} + \varepsilon_{\beta\gamma})}{1+\alpha} \right] \quad (1)$$

$$\rho_{\gamma} = A \frac{\varepsilon_{\gamma}}{1+\alpha} \quad (2)$$

$$\rho_{\beta\gamma} = A \left[ \frac{\varepsilon_{\beta}\varepsilon_{\gamma}}{1+\alpha} \right] + (1 - \varepsilon_{\beta})\varepsilon_{c} \quad (3)$$

where A is the activity of radionuclide,  $\rho_{\beta}$ ,  $\rho_{\gamma}$ , and  $\rho_{\beta\gamma}$  are the count rate for beta, gamma, and beta-gamma coincidence, respectively. The efficiency of beta, gamma, and beta gamma coincidence are represented respectively as  $\varepsilon_{\beta}$ ,  $\varepsilon_{\gamma}$ , and  $\varepsilon_{c}$ . The impurity of <sup>153</sup>Sm were measured by gamma spectrometry method's.

**Result :**Efficiency calibration curve, founded the efficiency, y is = -2E-12x<sup>4</sup> + 2E-09x<sup>3</sup> - 7E-07x<sup>2</sup> + 0.0001x - 0.0028.The nuclide impurity is 0.001% of <sup>155</sup>Eu in <sup>153</sup> Sm at initial time. The result of absolutely activity measurement was 88.48 kBq/g.with uncertainty 1.36% at k=2.

**Tabel 1.** Uncertainty components for the R-value determined dose calibrator for <sup>153</sup>Sm

| Source of uncertainty    | Std.Uncert. (%) |
|--------------------------|-----------------|
| Standard                 | 0.68            |
| Half-life of sample      | 0.02            |
| Statistics of counting   | 0.40            |
| Detector response        | 1.155           |
| Accuracy of reading      | 1.732           |
| Repeatability            | 0.577           |
| Non-linearity            | 0.35            |
| Mass                     | 0.05            |
| Combine standard uncert. | 2.31            |
| Expanded Uncert. (k = 2) | 4.62            |

**Discussion :** The energy used to make efficiency calibration curve as much as six of energies, respectively 59.54, 80.99, 121.78, 244.70, 344.28, and 356.01 keV[3]. Efficiency calibration curve, estimated by fourth polynomial equation, which is done to improve the quality measurements for more accurate, precision and traceable. The activity of <sup>153</sup>Sm was determined from efficiency extrapolation taking a plot the  $\rho\beta\gamma/\rho_c$  as a function of  $(\rho\gamma/\rho_c - 1)$ . The extrapolation curves were obtained from the measurement at 103 keV gamma gate. The efficiency range of 80% - 90% shows a very linear trend and was used to extrapolate to 100% β-counting efficiency. A final activity results of 88.48 kBq/g at reference time was obtained with uncertainty 1.36% at k=2.

**Conclusion :** The radionuclide <sup>153</sup>Sm has been standardized using the 4πβ(LS)-γ coincidence counting with digital sampling method. The result was used as primary standard to calibrate the secondary standard instrument at PTKMR-BATAN, and we found the calibration factor for Capintec CRC-7BT dose calibrator is 1.05with4.62 % of the expanded uncertainties.

### References :

1. Gatot Wurdianto and Hermawan C., The standard. meth. of radioact. sources (<sup>125</sup>I, <sup>131</sup>I, <sup>99m</sup>Tc, and <sup>18</sup>F) for calibrating nucl. medicine equip. in Indonesia, Journ. of Physic : Conf. Series 694 (2016) 012060.
2. K.B. Lee et al., Application of digital sampling techniques for 4πβ(LS)-γ coincidence counting. Nucl. Instrum. Methods, 626-627(2011), p. 72-76.
3. Bé et al., Table of radionuclides , Monographie BIPM-5 Vol. 1 – A=1 to 150, Bureau International des Poids et Mesures, Sèvres, 2004.

## FABRICATION OF A 3D PRINTING THYROID PHANTOM FOR IMAGE QUALITY EVALUATION IN NUCLEAR MEDICINE.

M Alssabbagh<sup>1</sup>, A A Tajuddin<sup>2</sup>, M A Manap<sup>1</sup>, R Zainon<sup>1</sup>

<sup>1</sup>Advanced Medical and Dental Institute, Universiti Sains Malaysia, Malaysia; <sup>2</sup>School of Physics, Universiti Sains Malaysia, Malaysia

**Key words:** Thyroid, Phantom, 3D printing, mass attenuation coefficients.

**Introduction** Gaining attention in the late 1990s, the 3D printing innovation technology is utilized generally these days as a part of numerous enterprises. 3D printing technology in medical field is now widespread. Anatomical structures can be printed from 3D images using computed tomography (CT) and magnetic resonance imaging (MRI) scanners to meet the accurate organ geometry. The 3D printer utilizes an arrangement of three-dimensional images or any 3D modelling software to develop the fancied three-dimensional model which is layered by the 3D printing material [1]. Generally, most of the phantoms today have basic geometric forms [2–4]. The polycarbonate 3D printing material used in this research is cost-effective and commercially available.

**Methods** The elemental composition of polycarbonate material was used to feed the XCOM photon cross-section database to obtain its mass attenuation coefficients [5]. The results were compared with the attenuation coefficient values of the human thyroid that were published by the International Commission on Radiation Units and Measurements – ICRU no. 44. A healthy thyroid of young children of 10 years old was designed with an average size of the thyroid lobe of 2.5 cm in length, 0.8 cm in thickness, and 1.25 cm in width [6,7] using the 3Ds Max software to design the model from scratch. The model was then 3D printed with a 3D Pursa i3 printer using the polycarbonate material. The Scintigraphy images were obtained after injection of Tc-99 inside the thyroid phantom.

**Results:** As illustrated in Figure 1.a, the 3D printed thyroid was effectively made. Since the thyroid size is changing naturally with the age, the dimension of the 3D thyroid model can be altered conferring to the target age and gender prior printing the phantom. The time taken to print out the paediatric thyroid phantom using the 3D printing technology was approximately 50 minutes. Figure 1.b, displays the scintigraphy image of the 3D thyroid phantom as being similar to normal thyroids. The imaging system will be assessed using a suitably acquired image of the phantom.

**Discussion:** The presented research has had polycarbonate evaluated in order to mimic the

human thyroid gland. The mass attenuation coefficients of the polycarbonate and thyroid show a match. The mean ratio and the standard deviation of the attenuation values of polycarbonate and the thyroid was  $0.9 \pm 0.03$ . This shows that the polycarbonate has good agreement with the human thyroid, which is very close to 1. The 3D printed thyroid phantom simulates the real human thyroid in terms of the shape, size and tissue equivalence. The quality of the images in nuclear medicine was evaluated, where the images are similar to the images of a healthy human thyroid. This means the radioisotope is distributed uniformly in the fabricated phantom.

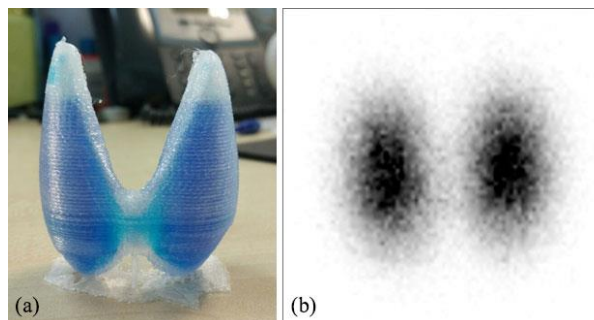


Fig.1(a) The 3D printed thyroid (b) The Scintigraphy image of the 3D printing phantom.

**Conclusion:** The result shows that the polycarbonate material can be used as a tissue-equivalent substitute for the human thyroid. An original three-dimensional thyroid phantom was designed from scratch. Apparently, at least 95% of the real human thyroid can be simulated. Additionally, the accommodation of different gender and age categories is possible through the 3D printing technology. The distribution of the Tc-99 in the phantom is uniform, and hence the phantom can be used for testing the quality of the images in nuclear medicine. The 3D printing technology shortens the time of phantom fabrication and it shows good results to mimic the real geometry of the human thyroid.

### References:

1. 3ders. Website: [www.3ders.org/3d-printing.html](http://www.3ders.org/3d-printing.html)
2. Kramer, G. H., Gamarnik, K., et al. (1996). The BRMD Thyroid-Neck Phantom: Design and Construction. *Health Physics*, 71(2), JOUR.
3. Cerqueira, R. A. D., & Maia, A. F. (2014). Development of thyroid anthropomorphic phantoms

## **8 Nuclear Medicine**

## **A MASS INDEPENDENT, UPTAKE BASED REGIMEN FOR ABSORBED DOSE TO THE THYROID IN I-131 TREATMENTS FOR BENIGN THYROID DISEASE**

Daniel Fakhry-Darian, Richard T. Meades, Kuldip S. Nijran  
Imperial College Healthcare NHS Trust, UK

### **Key words**

Thyroid, Dosimetry

### **Purpose**

The implementation of the European EURATOM BSS Directive in the UK requires dosimetry and planning for all radiotherapies. I-131 for benign thyroid disease is often prescribed based on activity and not dose. The aim of this project was to develop a simple method to estimate absorbed dose to the thyroid.

### **Methods**

An adapted version of the MIRD formulation was developed using a prior pertechnetate uptake scan as a predictor of I-131 uptake 24 hours post administration. A review of published literature suggests that single exponential decay of I-131, with a disease dependent effective half-life, is a sufficient model for benign thyroid disease. An equation incorporating these parameters was developed to allow for dosimetry based prescription, or retrospective dose audit, of I-131 for a range of benign thyroid diseases.

### **Results**

Doses were retrospectively calculated for 59 female Graves' patients receiving fixed activity therapy (600MBq, n=48; 800MBq, n=11) and compared with the EANM target of 300Gy. For 600MBq administrations, mean±SD administered activity and calculated dose were 597±20MBq and 511±106Gy respectively; for 800MBq administrations, mean±SD administered activity and calculated dose were 799±27MBq and 508±125Gy.

### **Conclusions**

A wide range of high doses are administered using a fixed activity approach. Reduction of fixed activity, or a dosimetric approach, could reduce the range of absorbed doses. This method provides an easy to implement formula that could be adopted in a clinical nuclear medicine department to demonstrate compliance with EURATOM in Europe. However errors should be understood and, where possible, optimised before application.

## THE IMPACT OF RECONSTRUCTION ALGORITHMS ON THE EVALUATION OF THE HETEROGENEITY IN 18F-FDG PET

Keishin Morita<sup>1</sup>, Toshiki Takeshita<sup>2</sup>, Yusuke Matsunobu<sup>1</sup>, Akira Maebatake<sup>3</sup>, Go Akamatsu<sup>4</sup>, Yuji Tsutsui<sup>5</sup>, Kazuhiko Himuro<sup>5</sup>, Shingo Baba<sup>5</sup>, Masayuki Sasaki<sup>1</sup>

<sup>1</sup>Department of Health Sciences, Graduate School of Medical Sciences, Kyushu University, Japan

<sup>2</sup>Department of Radiology, Teikyo University Hospital, Mizonokuchi

<sup>3</sup>Department of Radiology, Juntendo University Hospital

<sup>4</sup>Division of Radiological Technology, Institute of Biomedical Research and Innovation

<sup>5</sup>Department of Radiology, Kyushu University Hospital

### Key words

Heterogeneity, Reconstruction algorithms, Texture analysis

### Purpose

The purpose of this study was to examine the influence of reconstruction algorithms on the evaluation of heterogeneity of FDG uptake as assessed by texture analysis.

### Methods

A 5×5 cm box phantom, consisting of 25 wells (8×8 mm) was filled with different concentrations of 18F solution and placed in a NEMA IEC body phantom to simulate a homogeneous (HOMO) tumor and seven heterogeneous (HETERO 1-7) tumors. The radioactivity ratio of HETERO 1-3 was 8:4:2:1, while that of HETERO 4-7 was 8:4:1. PET data were acquired using a Biograph mCT scanner and reconstructed with the ordered-subsets expectation maximization (OSEM) algorithm, the OSEM+point-spread function (PSF) model, the OSEM+time-of-flight (TOF) model, and the OSEM+PSF+TOF model. The heterogeneity of the 18F distribution was evaluated according to ten texture features on a co-occurrence matrix.

### Results

In the OSEM algorithm, seven features showed differences between the HOMO and HETERO group. Seven features showed differences between HETERO 1-3 group and HETERO 4-7 group. Seven features showed differences among HETERO 1-3 and among HETERO 4-7. Among images reconstructed using 4 different algorithms, five features did not show any differences. In comparison with images using OSEM, those using PSF improved differentiation between the HOMO and HETERO in 3 features, those using TOF in 1 features and those using PSF+TOF in 2 features. Images using PSF+TOF improved differentiation among HETERO 1-3 and among HETERO 4-7 in 5 features.

### Conclusions

The PSF+TOF algorithm improved the evaluation of the heterogeneity using texture analysis on PET images.

## **A STUDY ON THE ACCURACY OF THE PARTITION MODEL IN ESTIMATING ABSORBED DOSE FOR YTTRIUM-90 RADIOEMBOLIZATION**

Nurul Ab. Aziz Hashikin<sup>1</sup>, Chai-Hong Yeong<sup>1</sup>, Susanna Guatelli<sup>2</sup>, Basri Johan Jeet Abdullah<sup>1</sup>, Kwan-Hoong Ng<sup>1</sup>, Alessandra Malaroda<sup>2</sup>, Anatoly B. Rosenfeld<sup>2</sup>, Alan Christopher Perkins<sup>3</sup>

<sup>1</sup>Department of Biomedical Imaging, Faculty of Medicine, University of Malaya, Malaysia

<sup>2</sup>Centre for Medical Radiation Physics, Faculty of Engineering and Information Sciences, University of Wollongong

<sup>3</sup>Medical Physics and Clinical Engineering, Medical School, University of Nottingham

### Key words

The partition model; Yttrium-90; Geant4 Monte Carlo; Hepatocellular carcinoma

### Purpose

To study of the partition model (PM) accuracy in estimating the absorbed doses to tumour (DT), normal liver (DNL) and lungs (DL), when cross-fire irradiations between these compartments are being considered.

### Methods

MIRD-5 phantom with various tumour involvement (TI), tumour-to-normal liver uptake ratio (T/N) and lung shunting (LS) were simulated using Geant4 Monte Carlo toolkit.  $10^8$  histories were generated for each scenario to obtain the absorbed dose per activity to each compartment. Using PM, the administered activities to achieve either maximum DNL or DL (70 or 30 Gy, respectively) were estimated. The activities were multiplied with the absorbed dose per activity attained by Geant4, to obtain the actual dose to each compartment.

### Results

PM overestimates DL by 11.7 % for all scenarios, due to PM estimation of DL based on energy deposition of  $^{90}\text{Y}$  in soft tissue, rather than in lung tissue (as applied in the Geant4 simulations). DT and DNL by Geant4 were largely affected by T/N, which was not considered by PM due to cross-fire exclusion at tumour-normal liver boundary. When maximum DNL was estimated via PM, Geant4 showed significantly higher DNL for scenarios with higher T/N and lower LS, by surprisingly up to 124 Gy. All DL and DT were overestimated by PM, hence maximum DL were never exceeded.

### Conclusions

PM is adequate for estimations of DT. However, for DNL, caution should be taken for scenarios with higher TI and T/N, and lower LS. For DL, different correction factor for dose calculation should be used for better accuracy.

## **PHYSICAL CHARACTERISTICS OF NOVEL EVALUATION METHOD USING TRACEABLE POINT-LIKE GE-68/GA-68 SOURCE COMBINED WITH CYLINDRICAL PHANTOM FOR PET SCANNERS**

Koyama Shoji<sup>1</sup>, Tomoyuki Hasegawa<sup>1</sup>, Hrioki Miyatake<sup>1</sup>, Kei Kikuchi<sup>1</sup>, Yusuke Inoue<sup>1</sup>, Kei Wagatsuma<sup>2</sup>, Keiichi Oda<sup>3</sup>, Yasushi Sato<sup>4</sup>, Kazuya Sakaguchi<sup>1</sup>

<sup>1</sup>Kitasto Univercity

<sup>2</sup>Tokyo Metropolitan Institute of Gerontology

<sup>3</sup>Hokkaido University of Science

<sup>4</sup>AIST

### **Key words**

Traceable point-like source, PET, calibration

### **Purpose**

We have developed a practical and reliable calibration and evaluation method using traceable point-like sources. The purpose of this study is to analyze the physical characteristics of experimental data measured using a traceable point-like Ge-68/Ga-68 source together with a specially designed cylindrical phantom.

### **Methods**

A traceable point-like Ge-68/Ga-68 source with a spherical acrylic absorber was used in this study. The cylindrical acrylic phantom was 20 cm in diameter and had a small cavity, in which the point-like source can be inserted. The point-like source, without or with the phantom, was placed at the central field-of-view position of a clinical PET/CT scanner (Biograph mCT Flow, Siemens). Circular region of interests (ROIs) were defined in reconstructed images, and the total ROI values and recovery curves were obtained as functions of ROI radius. The obtained data were analyzed in detail.

### **Results**

Some scatter background was observed in the recovery curves obtained from scatter-corrected images. It was possible to estimate an inherent constant component using a fitting method although the plateau region was not clearly observed. The scatter component was also observed in the plane-number dependence of the ROI values. Based on a detailed analysis of the data, it was found that the uncertainty in attenuation and scatter correction can be evaluated as a response to the point-like source in the medium.

### **Conclusions**

The proposed method using a traceable point-like Ge-68/Ga-68 source together with a spherical acrylic absorber and cylindrical phantom is expected to be useful for calibrating and evaluating PET scanners.

## **PRIMARY STANDARDIZATION AND MEASUREMENT TRACEABILITY OF $^{18}\text{F}$ IN INDONESIA**

Agung Agusbudiman, Gatot Wurdianto, Hermawan Candra

PTKMR – BATAN, Indonesia

### **Key words**

$^{18}\text{F}$  Standardization, Measurement Traceability,  $4\pi\beta(\text{LS})-\gamma$  coincidence counting method, Digital counting technique

### **Purpose**

The primary standardization of  $^{18}\text{F}$  was conducted to establish new standard and national traceability chain for measurement of  $^{18}\text{F}$  in Indonesia.

### **Methods**

The standardization of  $^{18}\text{F}$  was performed by means of  $4\pi\beta(\text{LS})-\gamma$  coincidence counting method using the digital sampling technique. Activity of  $^{18}\text{F}$  was determined based on three parameters obtained from experiment, the  $\rho_\beta$ ,  $\rho_\gamma$ , and  $\rho_c$ . The final activity result was used to establish new secondary standard by calibrating the standard dose calibrator to obtain its calibration factor. Impurities of  $^{18}\text{F}$  solution used in experiment were examined using gamma-ray spectrometry.

### **Results**

Final activity result from measurement with  $4\pi\beta(\text{LS})-\gamma$  coincidence counting system is found to be  $286.39 \text{ kBq/g} \pm 3.43 \text{ kBq/g}$  at reference time. As comparison, final result was compared to the previously  $^{18}\text{F}$  standard value determined by gamma-ray spectrometry system which gave uncertainty level of 3.8% at  $k=2$ . The new standard provide a better result with quoted uncertainty level of 1.2% at  $k=2$ .

### **Conclusions**

Primary standardization of  $^{18}\text{F}$  has been done by  $4\pi\beta(\text{LS})-\gamma$  coincidence counting and the secondary standard for  $^{18}\text{F}$  established through the Capintec CRC-7BT dose calibrator with better uncertainty value compared to existing value.

## **DIGITAL IMAGING AND COMMUNICATIONS IN MEDICINE (DICOM) INFORMATION CONVERSION PROGRAM FOR COMPATIBILITY USED BY MEASURING STANDARDIZED UPTAKE VALUE (SUV) IN DIFFERENT PET SCANNERS**

Han-Back Shin<sup>1</sup>, Do-Kun Yoon<sup>1</sup>, Tae Suk Suh<sup>1</sup>, Heesoon Sheen<sup>2</sup>, Ho-Young Lee<sup>3</sup>

<sup>1</sup>The Catholic University of Korea, Republic of Korea

<sup>2</sup>GE Healthcare Korea & School of Medicine, Sungkyunkwan University

<sup>3</sup>Seoul National University Bundang Hospital

### **Key words**

DICOM, SUV, PET

### **Purpose**

In nuclear medicine, standardized uptake value (SUV) is the most widely used for semi-quantitative factor based on the FDG-PET images. We founded that the DICOM header file of Philips Allegro PET scanner was differently stored compared with other scanners. Thus, the purpose of this study was to develop the DICOM information conversion program for compatibility between Allegro and other equipment.

### **Methods**

The NEMA IEC Body phantom was scanned using the Allegro PET scanner. For the measurement and comparison of SUV values using conversion data, we were measured using the commercially software and were calculated using the self-developed program. This program was composed of the three parts; input part can be loaded regardless of the number of DICOM images. The conversion part and output part is used to converted DICOM header information and stored in order of slice. The conversion procedure is used to convert units from pixel intensity to activity within the region of interest (ROI). And then, it should be calculated the actual activity at the scan time.

### **Results**

The results of calculation data had a good agreement with measurement data within the 12 circular ROI. The error rate caused by ROI between the calculation data and measurement data was lower than the 1 %.

### **Conclusions**

In conclusion, this study suggested the simple and convenient method to solve the incompatibility problem. This study would give the physician more accurate information for diagnosis and treatment.

## **THE EFFECT OF RESOLUTION RECOVERY ON TUMOR VOLUME ESTIMATION ACCURACY IN RADIOTHERAPY PLANNING WITH SPECT-CT**

Albert Guvenis<sup>1</sup>, Sultan Damgaci<sup>1</sup>, Bilal Kovan<sup>2</sup>, Leyla Poyraz<sup>2</sup>

<sup>1</sup>Bogazici University, Turkey

<sup>2</sup>Capa NM Department Istanbul University

### **Key words**

Radiotherapy Planning, Nuclear Medicine, SPECT-CT

### **Purpose**

The purpose of this study is to evaluate the effectiveness of resolution recovery correction in SPECT imaging during the estimation of tumor metabolic volume for therapy planning purposes.

### **Methods**

A Jaszack phantom (NEMA 2012/IEC 2008) and a SPECT/CT camera (General Electric Discovery NM/670) were used for the study. Sphere 1 (26.52 mL), sphere 2 (11.49 mL), sphere 3 (5.56 mL), sphere 4 (2.57 mL), sphere 5 (1.15 mL), sphere 6 (0.52 mL) were inserted into a Jaszack phantom (9700 mL) in order to represent small tumors. Activities for phantoms were calculated according to standard clinical situations covering an injection of 185 MBq <sup>99m</sup>Tc-MAA in a liver of 1500 mL. 74 MBq <sup>99m</sup>Tc activity was selected for the spheres. SPECT/CT acquisition was performed with 30 projections, 128\*128 matrix, and 20 s/projection. Image processing was carried out with Xeleris Workstation and volume measurements were performed with Osirix software manually by three medical physicists. The relative volume measurement errors, which were defined as follows:  $(\text{measured volume} - \text{real volume}) \div \text{real volume} \times 100$  were calculated and averaged.

### **Results**

Initial results indicated high volume estimation errors both before and after resolution recovery for simulated lesions of diameter of 22 mm or less. For sphere 1 and sphere 2 decrease in volume estimation errors was calculated as 43.28 % while the largest error was less than 20%.

### **Conclusions**

Resolution Recovery improves tumor volume estimation accuracy. However algorithm optimization and further image processing are needed. Potential solutions will be discussed.

## ESTIMATION OF EFFECTIVE DOSE TO PATIENTS UNDERGOING MYOCARDIAL PERFUSION SPECT/CT

H. Nitar<sup>1</sup>, A. Krisanachinda<sup>1</sup>, P. Pasawang<sup>2</sup>, K. Khamwan<sup>1</sup>

<sup>1</sup>Medical Imaging, Department of Radiology, Faculty of Medicine, Chulalongkorn University;

<sup>2</sup>King Chulalongkorn Memorial Hospital, Bangkok, Thailand

| MPI                                 | Our study                      |                                | Tootell et al [18]             |                                |
|-------------------------------------|--------------------------------|--------------------------------|--------------------------------|--------------------------------|
|                                     | SPECT/CT                       |                                | SPECT/CT                       |                                |
|                                     | Rest                           | Stress                         | Rest                           | Stress                         |
| Injected activity ( MBq )           | 900                            | 900                            | 800                            | 800                            |
| s-value                             | Asian reference man            |                                | based on ICRP reference man    |                                |
| CT parameters                       | 20 mAs<br>5 mm slice thickness | 20 mAs<br>5 mm slice thickness | 30 mAs<br>5 mm slice thickness | 30 mAs<br>5 mm slice thickness |
| $\Gamma_E^{MIBI}$ ( mSv / MBq )     | 0.013                          | 0.01                           | 0.009                          | 0.008                          |
| <sup>99m</sup> Tc-MIBI dose ( mSv ) | 11.7                           | 9                              | 7.2                            | 6.4                            |
| CT dose ( mSv )                     | 1.5                            | 1.4                            | 3                              | 3                              |
| Total effective dose ( mSv )        | 13.2                           | 10.4                           | 10.2                           | 9.4                            |

**Key words:** SPECT/CT, Effective dose, <sup>99m</sup>Tc-MIBI.

**Introduction:** Single-photon emission CT SPECT/CT has become widely used in Myocardial Imaging [1]. Role for CT in myocardial perfusion SPECT/CT is the attenuation correction and anatomical correlation of functional SPECT. This results in better quality corrected SPECT imaging and higher patient exposure than SPECT alone [2].

**Methods:** The biodistribution and dosimetry of <sup>99m</sup>Tc-MIBI have been evaluated in 20 patients, 10 at rest and 10 under stress study of myocardial perfusion SPECT/CT at King Chulalongkorn Memorial Hospital. After injection of <sup>99m</sup>Tc-MIBI, whole-body planar imaging was performed at 15min, 2h and 4h with conjugate counting method. The absorbed dose and effective dose from radiopharmaceutical were calculated by MIRD method with the “S” tables modified for the organ masses of the Asian reference man to obtain more realistic estimation of absorbed doses. The absorbed dose and effective dose from CT scan were determined by using ImPACTSCAN dose spreadsheet. The effective dose received was expressed in relation with Background Equivalent Radiation Time (BERT).

**Results:** Average dose coefficients from administration of <sup>99m</sup>Tc-MIBI were 12.5±1.5 μSv / MBq in rest study and 11.2±0.5 μSv / MBq in stress study of myocardial perfusion imaging. Average <sup>99m</sup>Tc-MIBI activities of 900 MBq was injected for each study, resulted average effective dose from SPECT scan of 11.7±2.1 mSv in rest and 9±1.5 mSv in stress study. The average effective dose from CT was 1.5±0.2 mSv in rest and 1.4±0.4 mSv in stress study. The average effective

dose from rest of MPI was 13.2±1.1 mSv and BERT was 4.4 years and for stress study was 10.4±0.9 mSv and BERT was 3.5 years.

Table 1 Comparison of effective dose, and related parameters with our study and Totell

**Discussion:** <sup>99m</sup>Tc-MIBI was mainly eliminated through the hepatobiliary system and some was excreted via the urinary tract. Therefore, the organs involved in excretory pathway of MIBI (GB, ULI,

LLI and kidneys) receive the highest absorbed dose as shown in Fig-1. There was also specific uptake in thyroid and so receiving relatively high absorbed dose.

Due to different injected activities, techniques, physiology and sizes of study population, there may be variations in dose estimation between studies. The mean injected activity used for this study was higher due to the use of implementation with gated ECG which required more injected activity. As “S” tables were modified based on organ masses of Asian reference man of smaller organ masses, the dose estimated from present study were higher than literature that used “S” tables based on ICRP reference man. The results of our study and parameters utilized were compared with typical literature in Table-1.

**Conclusion:** The dosimetric and biokinetics distribution of MIBI in this study provide the dose coefficient of <sup>99m</sup>Tc-mibi which can be used for determination of patient radiation dose from myocardial perfusion imaging. These values can be used as reference for Asian population. Furthermore, the specific dosimetric information assists in justification of risk and optimization of myocardial perfusion imaging.

### References:

- Hendel RC, Corbett JR, Cullom SJ, DePuey EG, Garcia EV, Bateman TM. The value and practice of attenuation correction for myocardial perfusion SPECT imaging: a joint position statement from the American Society of Nuclear Cardiology and the Society of Nuclear Medicine. J Nucl Med 2002; 43: 273–80.
- Hesse B, Lindhardt TB, Acampa W, Anagnostopoulos C, Ballinger J, Bax JJ, et al. EANM/ESC guidelines for radionuclide imaging of

## **TECHNETIUM-99M CARDIAC SPECT IMAGE QUALITY ENHANCEMENT USING MATERIAL FILTER TECHNIQUE: PHANTOM STUDY**

Inayatullah Shah Sayed<sup>1</sup>, Mohd Zamzuri Che Daud<sup>1</sup>, Nurul Farizan Mohd Zulkele<sup>1</sup>, Nazifah Abdullah<sup>2</sup>, Norhanna Sohaimi<sup>1</sup>, Muhammad Shahrir Abdul Rahim<sup>1</sup>

<sup>1</sup>International Islamic University Malaysia

<sup>2</sup>Universiti Sultan Zainal Abidin, Malaysia

### **Key words**

Image Quality, Tc-99m Cardiac SPECT, Material Filter, Scatter Correction

### **Purpose**

Myocardial perfusion SPECT with Tc-99m is most commonly performed for the assessment of patients with a suspected or known coronary artery disease (CAD). However, registration of scattered gamma photons in projection data degrades the quality of the reconstructed image, which in turn leads to inaccuracy in the diagnosis. The objectives of this study were to improve the image quality and enhance the accuracy in the measurement of the size of cold defect.

### **Methods**

A new technique, which uses a flat sheet of material i.e., aluminium 0.1mm thick and 550mm x 440mm in size as pre-filter for scattered gamma photons was applied. Carlson's phantom with cardiac insert which mimics the left ventricle was scanned using GE Infinia dual head gamma camera with LEHR collimator. Myocardial cold defect made from polystyrene was placed at the anterior side of the myocardial wall chamber. SPECT data acquisition parameters were selected similar to those which are applied in clinical myocardial perfusion studies. Data was acquired with and without the material filter. Images were reconstructed with filtered back projection selecting Butterworth filter of a 0.40/cm cut off frequency and order 10. Chang's attenuation correction was applied.

### **Results**

SA views were visually analyzed and cold defect size was measured. Our findings showed that image quality and accuracy in defect size improved significantly ( $p < 0.05$ ) with material filter.

### **Conclusions**

It is concluded that the filter technique may be applied in clinical myocardial perfusion studies. However, this requires more studies with other phantoms which simulate the human heart closely, e.g., Heart/Thorax Anthropomorphic Phantom.

## **CO-57 ROD FORM STANDARD SOURCE FOR GAMMA COUNTER CALIBRATING IN NUCLEAR MEDICINE**

Hermawan Candra, Gatot Wurdianto, Agung Agusbudiman,

Center For Technology Of Radiation Safety And Metrology - National Nuclear Energy Agency, Indonesia

### **Introduction:**

Making of Co-57 standard source for Rod form has been carried. Co-57 standard source of Rod form is used for calibrating nuclear instrumentation in nuclear medicine is Gamma Counter with well type NaI(Tl) scintillation detector. Gamma Counter with well type NaI(Tl) scintillation detector is nuclear instrumentation have high sensitivity for radioactive contamination level.

### **Method:**

Co-57 standard source of Rod form consists of a lucite rod measuring 127 mm x 12.7 mm diameter. The half-life of Co-57 standard source is 271.80(5) days and gamma emission of gamma energy is 122.06065(12) keV and 136.47356 (29) keV. Co-57 standard source preparation of solution geometry form in ampoule and solid geometry form in point source and Rod form. Radioactivity measurement of Co-57 Radionuclide use gamma spectrometer counting system with High Purity Germanium detector is using Eu-152 multi gamma standard source with wide energy range of gamma energies 121keV to 1408keV and  $4\pi\gamma$  ionization chamber counting system.

### **Result:**

The result of activity measurements of Co-57 standard source of solution geometry form in ampoule without dilution is  $(5434.12 \pm 4\%)$  kBq/g, solution geometry form in ampoule with dilution is  $(5432.67 \pm 4\%)$  kBq/g, solid geometry form in point source is  $(5423.95 \pm 2.72\%)$  kBq/g and Rod form is  $(5414.46 \pm 2.72\%)$  kBq/g at reference time 1 April 2014.

### **Conclusion:**

From the research carried out it can be concluded that PTKMR BATAN have been able to make Co-57 rod form standard source used for Gamma Counter nuclear instrumentation calibrating in nuclear medicine with uncertainty measurement of 3.06%

## **10 Magnetic Resonance**

# PROPOSAL OF AN APPROPRIATE ECHO TIME-INPUT FUNCTION FOR QUANTITATIVE SUSCEPTIBILITY MAPPING

Y Matsumoto<sup>1</sup>, Y Kanazawa<sup>1</sup>, Nikemitsu<sup>1</sup>, TSasaki<sup>1</sup>,  
 HHayashi<sup>1</sup>, K Takegami<sup>2</sup>, T Matsuda<sup>3</sup>, MHarada<sup>1</sup>  
<sup>1</sup>Tokushima University, Japan; <sup>2</sup>GE Healthcare Japan Corp., Japan

**Key words:** quantitative susceptibility mapping (QSM), echo time (TE),  $T_2^*$  mapping

**Introduction:** Quantitative susceptibility mapping (QSM) is possible to get magnetic properties from phase images by several post-processing. QSM is performed using a three-dimensional GRE sequence with multiple echoes (1-12 echoes). Then, the signal-to-noise ratio of the phase image ( $SNR_\theta$ ) can be represented as follows:

$$SNR_\theta = \frac{2\pi f t M_0 e^{-\frac{t}{T_2^*}}}{\sigma^\theta}$$

where,  $f$  is the frequency offset,  $t$  is the TE,  $M_0$  is the transverse magnetization,  $\sigma^\theta$  is the standard deviation of the phase [2]. Because  $SNR_\theta$  is dependent on TE and  $T_2^*$ , an appropriate TE setting is necessary. For material having strong susceptibility and short  $T_2^*$  it is necessary to detect phase accumulation before dephasing, this is accomplished by setting a short TE dataset. On the other hand, the material having weak susceptibility and long  $T_2^*$  it is necessary to detect phase accumulation sufficiently, this is accomplished by setting a long TE dataset [1]. For instance, since intracranial calcifications have short  $T_2^*$ , a short TE derives good susceptibility distribution which is more advantages than a long TE when carrying out QSM. For that reason, when performing QSM, it is necessary to obtain a good  $SNR_\theta$ . We aim to improve susceptibility distributions for each material, and to develop an appropriate TE-input method for QSM.

**Methods:** On a 3.0 T MR system (GE Healthcare), we performed a phantom study using an in-house constructed cylindrical phantom. Our phantom was composed of six tubes; three tubes filled with different concentrations (0.1, 0.2, and 0.5 wt%) of gadopentetate dimeglumine (Gd-DTPA; Bayer Pharma), and three others filled with different concentrations (100, 200, and 350 mg/mL) of calcium hydroxyapatite ( $3Ca_3(PO_4)_2 \cdot Ca(OH)_2$ ; Kishida

Chemical). Post-processing for QSM was divided into several steps. First, it is necessary to estimate the off-set frequency of each voxel from phase images (field map estimation). After the field map estimation is computed for each voxel, the appropriate TE dataset input method was developed using  $SNR_\theta$ . Figure 1 shows schematic illustrations of the method to determine the appropriate TE dataset.

**Results:** Figure 2 shows QSM and the relationship between the measured susceptibility value and the concentration of Gd-DTPA and hydroxyapatite. The upper row (Fig. 2a, b, and c) shows the results for the 1-12 dataset, and the lower row (Fig. 2d, e, and f) shows the results using the appropriate TE dataset.

**Discussion:** In this study, to improve susceptibility distributions of QSM, we developed an appropriate TE data input method focusing on  $SNR_\theta$ . For hydroxyapatite, the maximum  $SNR_\theta$  was reached within the set TE. On the other hand, for Gd-DTPA, maximum  $SNR_\theta$  was not reached within the set TE. As a result, when hydroxyapatite, QSM is derived from an appropriate TE dataset there is good linearity when compared with the 1-12 TE dataset (0.74 vs 1.00).

**Conclusion:** Using appropriate TE dataset, QSM make it possible to obtain more accurate susceptibility distribution

**References:**

1. Wang Y and Liu T. Quantitative susceptibility mapping (QSM): Decoding MRI data for a tissue magnetic biomarker. *Magn Reson Med*. 73;82-101, 2015.
2. Wu B, Li W, Avram AV, Gho SM, Liu C. Fast and tissue-optimized mapping of magnetic susceptibility and T2\* with multi-echo and multi-shot spirals. *Neuroimage*. 59;297-305, 2012.

**Corresponding author email:** yk@tokushima-u.ac.jp

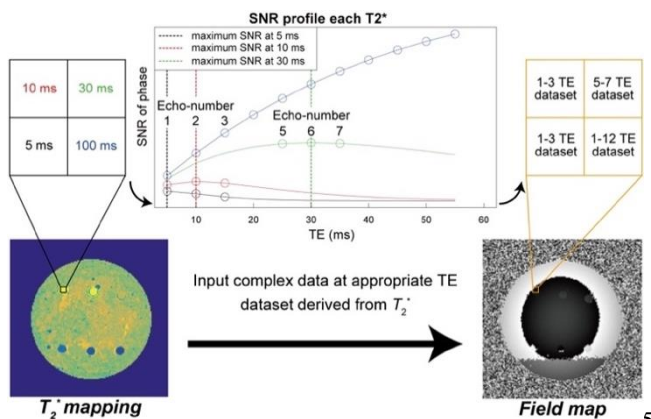


Fig. 1 Schematic illustrations of method of the appropriate TE dataset.

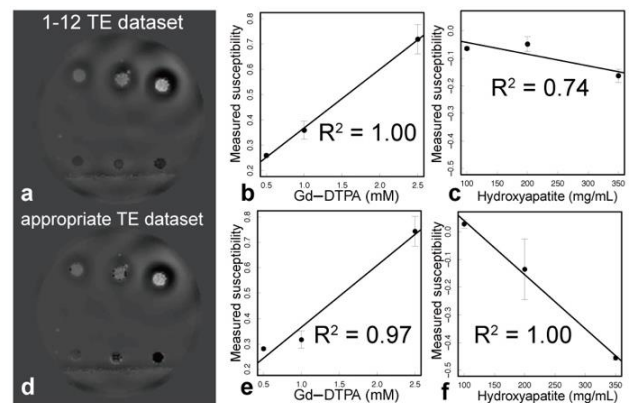


Fig. 2 Result of the measured susceptibility derived from QSM.

# THE EFFECT OF REPETITION TIME DURING THE MEASUREMENT OF MUSCLE T<sub>2</sub> FOR INVESTIGATING MUSCLE ACTIVITY AT 1.5 TESLA MRI

P. Polharn<sup>1</sup>, A. Krisanachinda<sup>1</sup>, N. Tawara<sup>1,3</sup>, K. Ponkanist<sup>2</sup>

<sup>1</sup>Chulalongkorn University, <sup>2</sup>King Chulalongkorn Memorial Hospital, Bangkok, Thailand.

<sup>3</sup>Faculty of Health Sciences, Japan Health Care College, Sapporo, Japan.

**Key words:** transverse relaxation time, repetition time, muscle functional MRI

**Introduction** The evaluation of muscle function by T<sub>2</sub> mapping is important in sports medicine and rehabilitation [1]. Repetition time (TR) is the one most important parameter for calculating T<sub>2</sub> and affects the accurate T<sub>2</sub> measurements. Almost previous study used SE or MSE to calculate T<sub>2</sub>, there are few reports about the extensive comparative evaluation of the imaging parameters. Thus, the our goals were 1) to evaluate the effect of TR to decrease scan time for T<sub>2</sub> measurement in the pulse sequences at 1.5 Tesla MRI and, 2) to investigate the feasibility of shortening scan time of T<sub>2</sub> measurement to detect the muscle activity that induced by exercise.

**Materials** A PVA-gel phantom and the right lower legs of eight male subjects were scanned using a 1.5tesla MR scanner with an extremity coil. MSE and SE-EPI were performed with TR 1000, 2000,., 4000 ms, TE 15, 30,., 390 ms. Regarding exercise study, to evaluate the feasibility of SE-EPI to detect muscle activity. All subject performed ankle plantar flexion of the right leg 200 times. MR images were acquired at rest and after exercise. ROIs were placed on PVA-gel and muscle images. T<sub>2</sub> was calculated by mono-exponential linear least-squares of TE 30, 45, 60, 75 ms.

**Results:** Phantom and in vivo studies showed the result in the same way. For MSE, relaxation curve of TR 2000 ms or more is likely be the same MR signal. As for SE-EPI, all relaxation curve showed approximately the same, and all MR signals of SE-EPI were lower than the signals of MSE. However, when all T<sub>2</sub> were compared. Those values have no significant difference between TR and sequences (Table 1). Regarding exercise study, T<sub>2</sub> of the m. gastrocnemius at after exercise was significantly higher than the T<sub>2</sub> value at rest (Table 2) and the other observed values.

**Discussion** As for MSE in phantom and muscle, MR signal of TR = 1000 ms is lower than the other TR signals. The reason is that the effect of low SNR in a short TR because of incomplete recovery of longitudinal magnetization. When all T<sub>2</sub> were compared. All value is no significant difference between TR and sequences. In this study, the results of T<sub>2</sub> comparison exceeding 10 percent of the T<sub>2</sub> were assumed to be significant [4]. Regarding exercise study, the stimulated muscle differ from the previous studies [2], the exercise protocol had not made the strict settings when compared to the other's reports. Therefore, the cause was suggested that it was possible to have been under load in addition to the target muscle. It is the limit of this study.

**Conclusion:** MR images with a short TR (TR 1000 ms) under suitable condition are possible to calculate muscle T<sub>2</sub> on mfMRI to reduce the scanning time dramatically. Calculating T<sub>2</sub> using SE-EPI can be applied to detect the

muscle activity that induced by exercise with the shortening acquisition time of approximately 1/17 of the previous method and can be acquired on the muscles of the trunk in a single breath-hold.

**References:**

1. Tawara N, Nitta O, Itoh A. (1997) Comparison of pulse sequences for T<sub>2</sub> measurement of human skeletal muscle. Japan J Magn Reson 38:759–768 [Japanese]
2. Tawara N, Nitta O, Kuruma H, Hoshikawa A, Kawahara A. (2013) Complications related to repetition time during the measurement of muscle T<sub>2</sub> in 3.0 Tesla. In Proceedings of the 18th Annual Scientific Meeting of Korea Society for Magnetic Resonance in Medicine 18 207-207.
3. Tawara N, Nitta O, Kuruma H, Niitsu M, Itoh A. (2011) T<sub>2</sub> mapping of muscle activity using ultrafast imaging. Magn Reson Med Sci. 10:85–91
4. Schneiders NJ, Post H, Brunner P, Ford J, Bryan RN, Willcott MR. Accurate T<sub>2</sub> NMR images. Med Phys 1983; 10(5):642-5

**Corresponding author email:** anchali.kris@gmail.com

Table 1. Comparison of T<sub>2</sub> of PVA-gel phantom and in tibialis anterior muscle [TA] between MSE and SE-EPI.

|         | TR (ms)     | 1000     | 2000     | 3000     | 4000     |
|---------|-------------|----------|----------|----------|----------|
| Phantom | MSE (ms)    | 75.8±0.2 | 75.8±0.1 | 78.6±0.1 | 78.9±0.3 |
|         | SE-EPI (ms) | 82.4±0.2 | 83.6±0.3 | 85.2±0.4 | 83.5±0.4 |
| TA      | MSE (ms)    | 32.5±2.0 | 32.3±2.3 | 32.0±2.5 | 32.0±2.3 |
|         | SE-EPI (ms) | 32.2±2.4 | 33.0±1.2 | 30.6±2.0 | 31.8±1.4 |

Table 2. The muscle T<sub>2</sub> values at rest and after exercise of tibialis anterior muscle [TA] and gastrocnemius muscle [GA] muscles.

| Muscle         | T <sub>2</sub> relaxation time (ms) |          |
|----------------|-------------------------------------|----------|
|                | TA                                  | GA       |
| rest           | 31.4±1.8                            | 30.0±2.4 |
| after exercise | 32.2±1.9                            | 39.8±2.2 |

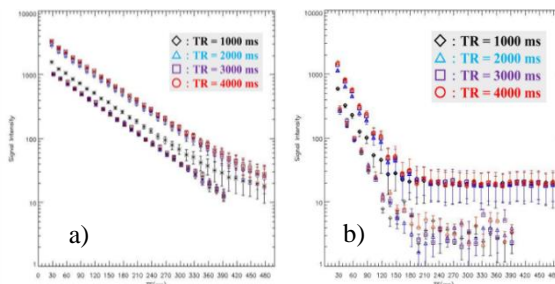


Figure 1. Comparison of T<sub>2</sub> relaxation curve between MSE and SE-EPI of a) PVA-gel phantom b) tibialis anterior muscle [TA].

## **FAT QUANTIFICATION IN HUMAN LIVERS: A COMPARATIVE STUDY BETWEEN MAGNETIC RESONANCE IMAGING, MAGNETIC RESONANCE SPECTROSCOPY, QUANTITATIVE IMAGE ANALYSIS AND CONVENTIONAL HISTOPATHOLOGY METHODS**

Thomas Greig<sup>1</sup>, Leon Adams<sup>2</sup>, Michael House<sup>2</sup>, Mike Bynevelt<sup>1</sup>, Bastiaan DeBoer<sup>3</sup>, Lincoln Codd<sup>1</sup>, Anne Winsor<sup>1</sup>, Rogern Price<sup>1</sup>, Janette Atkinson<sup>1</sup>

<sup>1</sup>Sir Charles Gairdner Hospital, Australia

<sup>2</sup>University of Western Australia

<sup>3</sup>Anatomical Pathology

### **Purpose**

This work compares the current gold standard for the assessment of liver fat (histopathology assessment by a pathologist) with image morphometry of biopsy samples and non-invasive techniques such as, three-point Dixon imaging (3PD) and magnetic resonance spectroscopy (MRS). The main objective of this comparison was to observe the correlation and relationship between different quantification techniques to determine the viability of routine clinical implementation of the non-invasive quantification methods for the diagnosis/grading of hepatic steatosis.

### **Methods**

30 patients diagnosed with hepatic steatosis and that were undergoing liver biopsy assessment as part of their routine clinical treatment were recruited. These patients were sent for MRI and MRS on the morning before their biopsy. A multi-echo in-phase/out-phase sequence was used for 3PD quantification and a point-resolved spectroscopy sequence was used for MRS quantification. Biopsy samples were visually assessed by a reporting pathologist and were also digitally scanned for image morphometry analysis.

### **Results**

The 3PD and MRS estimations of fat fraction show a very strong correlation/agreement with the more objective image morphometry assessment of the biopsy slides ( $R > 0.9$ ). In comparison to the gold standard it was found that all of these methods significantly 'underestimated' the fat fractions by a factor greater than 3.

### **Conclusions**

These preliminary results are promising in that there is strong agreement between the image morphometry and the non-invasive quantification techniques, however, the sensitivity and specificity of these methods when compared to the gold standard needs to be investigated further to determine whether or not non-invasive techniques can be implemented clinically.

## **12 Computer Aided Diagnostic and Therapy**

## **SEX CLASSIFICATION IN EACH AGE GROUP BY COMBINED INFORMATION OBTAINED FROM A THORACIC VERTEBRA AND RIBS**

Shun Tsubaki<sup>1</sup>, Junji Morishita<sup>2</sup>, Yusuke Matsunobu<sup>1</sup>, Yusuke Kawazoe<sup>3</sup>, Yosuke Usumoto<sup>4</sup>, MikiOkumura<sup>5</sup>, Noriaki Ikeda<sup>5</sup>

<sup>1</sup>Department of Health Sciences, Graduate School of Medical Sciences, Kyushu University, Japan

<sup>2</sup>Department of Health Sciences, Faculty of Medical Sciences, Kyushu University

<sup>3</sup>Department of Health Sciences, School of Medicine, Kyushu University

<sup>4</sup>Department of Legal Medicine, Yokohama City University Graduate School of Medicine and Department of Forensic Pathology And Sciences, Graduate School of Medical Sciences, Kyushu University

<sup>5</sup>Department of Forensic Pathology and Sciences, Graduate School of Medical Sciences, Kyushu University

**Key words:** Sex classification, Thoracic vertebra, Rib, Chest radiograph

### **Purpose**

The purpose of this study is to investigate the accuracy of sex classification in each age group by a combination of geometric properties obtained from the 10th thoracic vertebra and 6th and 7th ribs.

### **Methods**

The Internal Review Board approved the 300 chest radiographs (from 150 males and 150 females) used in this study. These images were randomly selected from patients belonging to six age groups (20s, 30s, 40s, 50s, 60s, and 70s). Each group included 50 images (from 25 males and 25 females). Various features, including 7 measured lengths for the vertebra, 5 indices including 4 ratios of widths or heights, area of the vertebra, and 2 widths for the ribs, were analyzed to classify the sex. Dominant features contributing to sex classification were selected by applying stepwise discriminant analysis after checking the variance inflation factor for multicollinearity. The accuracies of sex classification in each age group were calculated from the selected features by stepwise discriminant analysis.

### **Results**

The accuracy of sex classification showed high performances from 88% in the 60s to 98% in the 20s and 30s. Selected features by stepwise discriminant analysis included some features of the vertebra and rib width in all age groups. These results indicate the usefulness of combined information obtained from the thoracic vertebra and ribs.

### **Conclusions**

Sex classification through a combination of geometric properties obtained from the thoracic vertebra and ribs indicated high accuracy, especially in patients in their 20s and 30s.

## REDUCTION OF ARTIFACTS IN SIMILAR IMAGE SUBTRACTION TECHNIQUES BY ADJUSTING THE IMAGE CONTRAST

Hitomi Nakamura<sup>1</sup>, Junji Morishita<sup>2</sup>, Yoichiro Shimizu<sup>3</sup>, Shigehiko Katsuragawa<sup>4</sup>, Hidetake Yabuuchi<sup>2</sup>

<sup>1</sup>Kyushu University, Japan

<sup>2</sup>Department of Health Sciences, Faculty of Medical Sciences, Kyushu University

<sup>3</sup>Department of Health Sciences, Graduate School of Medical Sciences, Kyushu University

<sup>4</sup>Faculty of Fukuoka Medical Technology, Teikyo University

**Key words:** Chest radiographs, Computer-aided diagnosis (CAD), Similar subtraction images

### Purpose

The aim of this study was to improve the image quality by reducing artifacts around subtle nodules on subtraction images obtained from similar chest radiographs of different patients.

### Methods

An institutional review board approved the use of 24 chest radiographs with lung nodules as target images. Images similar to the target images were searched from our database (36,212 patients). Matrix size was normalized to  $512 \times 512$  pixels for all images. Our preliminary study indicated that the histograms of the pixel values in the regions of interest (ROIs) with a matrix size of  $128 \times 128$  pixels were not significantly impacted by the contrast and diameters of simulated nodules, which were deduced from the nodules in the target images. The  $128 \times 128$  pixels ROIs were selected on the target and similar images, and the histograms in the ROIs of similar images were matched with those in the target images using histogram-matching techniques. Similar subtraction images were obtained by subtracting the target images from similar images. Quantities of artifacts caused by the subtraction were evaluated using coefficient of variation (CV) values in the ROIs.

### Results

The artifacts in the subtraction images were effectively reduced by the histogram-matching techniques. The CV values of 96% (23/24) cases with histogram-matching techniques were lower than those without the histogram-matching techniques.

### Conclusions

The image quality of the subtraction images obtained from similar chest radiographs of different patients was improved due to reduction of artifacts using the histogram-matching techniques.

## **A USEFUL PRE-PROCESSING FOR AUTOMATED EXTRACTION OF BIOLOGICAL FINGERPRINTS ON CHEST IMAGING**

Yoichiro Shimizu<sup>1</sup>, Junji Morishita<sup>2</sup>

<sup>1</sup>Kyushu University, Japan

<sup>2</sup>Department of Health Sciences, Faculty of Medical Sciences, Kyushu University

**Key words:** digital chest radiograph, patient recognition, biological fingerprints

### **Purpose**

The purpose of this study is to propose effective method for determining the image orientation and automated extraction of five biological fingerprints (BFs), i.e., whole lung field, lung apex, superior mediastinum, cardiac shadow, and right lower lung.

### **Methods**

Two hundred digital chest radiographs, were used in this study as hypothetically misfiled images, were randomly selected from our image database (36,212 patients). The orientations of the misfiled images were randomly rotated in four directions (upright, left rotated, upside down, and right rotated) before starting our experimental study. Average images for male and female were produced by averaging the pixel value of 100 chest radiographs for each gender. Image orientations of the misfiled images were analyzed by computer and were corrected by using the average images. The BF templates were extracted from each average image. The normalized cross-correlation value (C value) was used to evaluate the similarity between the BFs in templates and the corresponding BFs in misfiled images. BFs were extracted from the location having the highest C values. If extracted region of interest (ROI) included in each BF, we considered correctly extracted.

### **Results**

The image orientations of misfiled images were automatically recognized and modified correctly. Further, 100% (200/200) of the five BFs that were extracted automatically by using the average images for each gender were included with extracted ROIs.

### **Conclusions**

Our method, based on average images was able to detect and modify image orientation. Five BFs were automatically and correctly extracted by using proposed method.

## **DEVELOPMENT OF PERSONAL IDENTIFICATION SYSTEM BY USING PROJECTED BONE IMAGES FROM X-RAY COMPUTED TOMOGRAPHY IMAGING IN FORENSIC CASES**

Yusuke Matsunobu<sup>1</sup>, Junji Morishita<sup>2</sup>, Yosuke Usumoto<sup>3</sup>, Miki Okumura<sup>4</sup>, Masayuki Sasaki<sup>2</sup>, Noriaki Ikeda<sup>4</sup>

<sup>1</sup>Kyushu University, Japan

<sup>2</sup>Department of Health Sciences, Faculty of Medical Sciences, Kyushu University

<sup>3</sup>Department of Legal Medicine, Yokohama City University Graduate School of Medicine, and Department of Forensic Pathology And Sciences, Graduate School of Medical Sciences, Kyushu University

<sup>4</sup>Department of Forensic Pathology and Sciences, Graduate School of Medical Sciences, Kyushu University

**Key words:** personal identification, computed tomography, forensic radiology, image matching

### **Purpose**

The aim of this study was to examine the usefulness of projected bone images for personal identification in forensic cases.

### **Methods**

Projected bone images were obtained from X-ray computed tomography (CT) imaging. The CT images of 10 forensic cases (5 male, 5 female) were used in this study. Each case had ante-mortem and post-mortem CT images. The projected bone images were reconstructed from chest CT images using a threshold method and the ray-sum projection technique. These bone images consisted of the ribs, sternum, and vertebrae. The similarities between ante-mortem and post-mortem bone images of the same person and different people were evaluated in terms of the normalized cross-correlation (NCC) value using the image matching technique. NCC values range from -1.0 to 1.0. An NCC value close to 1.0 indicates greater similarity between two images.

### **Results**

The accuracy of identification of the same person (rank-one identification rate) was 100% (10/10) in this study. The average of the NCC values for projected bone images of the same person (0.770) was higher than that of the different people (0.547).

### **Conclusions**

Our preliminary study indicated that the projected bone image would be useful for personal identification in the field of forensic medicine. This system has the potential to identify a large number of dead bodies automatically within a short period of time in a large-scale disaster.

## **EVALUATION OF HOUNSFIELD UNIT FROM VARIOUS HIGH DENSITY MATERIALS FOR RADIOTHERAPY**

Jayapramila Jayamani, Mohd Zahri Abdul Aziz, Noor Diyana Osman, Abdul Aziz Tajuddin

Universiti Sains Malaysia

**Key words:** High density material, Hounsfield Unit

### **Purpose**

This study investigates the relationship between Hounsfield Unit (HU) and density of high Z material on single energy CT and dual-energy CT

### **Methods**

HU for single energy and dual energy computed tomography (CT) was investigated by using CT calibration phantom for low density material and various high density materials (titanium, lead, cerrobend, amalgam, and gold) for different photon energy range. Reconstructed image was evaluated by using fixed area margin to determine HU for each material. Further analyses were conducted to study the relationship between HU and density of high Z material. Calculated density was determined from equation derived from plotted graph and comparison was made with the actual density of the materials.

### **Results**

Dual energy CT images was observed to display all high density materials at 3071 HU due to machine default setting for DICOM type image storage was set to be 12 bit per image. Meanwhile single energy CT which store images using 16 bit was able to display extended HU scale for high density materials. The lowest HU among high density materials was observed to be titanium with value of 8,736 HU, and the highest HU was exerted by gold materials with value of 21,416 HU. Generally density of low Z materials was able to be predicted using derived equation (approximately less than 2% percentage error) while in high density materials higher percentage error was observed between calculated density and actual density (as high as 43% percentage different)

### **Conclusions**

Considering the fact of HU as an important aspect in radiotherapy treatment planning, physicist need to be aware about CT HU value limitation when high density material present in patient especially for 12 bit image. Further investigation on high density material need to be added in HU to density conversion table for accurate dose delivery in radiotherapy treatment.

**13 e-Learning, Networking and IT**  
**14 Education and Training**

## PIONEERING, DEVELOPMENT AND FUTURE OF E-LEARNING IN MEDICAL PHYSICS

S Tabakov<sup>1,2</sup>, F Milano<sup>3</sup>, M Stoeva<sup>2,4</sup>, C Lewis<sup>1,5</sup>, S Keevil<sup>1</sup>, V Tabakova<sup>1</sup>

<sup>1</sup>King's College London, UK; <sup>2</sup>IOMP; <sup>3</sup>Florence University, Italy; <sup>4</sup>Medical Univ. Plovdiv, Bulgaria; <sup>5</sup>King's College Hospital, UK

**Key words:** e-learning, education, training

**Introduction** The presented results are based on 7 International projects, developed over 20 years (1994-2014) [1], the first to develop and introduce e-learning in medical physics. The projects are described in detail in the new book "The Pioneering of e-Learning in Medical Physics" (www.emerald2.eu/e-learning) [2].

**Methods** The paper presents briefly the e-learning methods used by these projects; the development process; the testing/ implementation of e-learning in the profession. It also includes the feedback from the users and views for the future implementation of e-learning in medical physics.

**Results:** The outcomes of the 7 international educational projects can be summarised as:

- Five e-books based on the above Workbooks (including 250 training tasks) [3]
- Five CD-ROMs with Image Databases for Medical Physics training (3100 images) [3]
- Three Educational web sites in Medical Physics
- A Multilingual Dictionary of Medical Physics Terms (translated in 29 languages) [4]
- An on-line Encyclopaedia of Medical Physics [4]

**Discussion:** The paper highlights the challenges of the development and introduction of e-learning in medical physics. The method of application of computer simulations in the teaching process is discussed. Currently the described e-learning materials are used worldwide (by almost 4000 colleagues per month – Fig.1). Part of the discussion will include the current update of these materials, with emphasis on EMITEL Encyclopaedia and its Multilingual Dictionary.

**Conclusion:** e-Learning is imperative for a dynamic profession as medical physics. It is based on large team work and requires regular updates. Possible ways for improving the longevity of e-learning products are recommended.

### References:

1. Tabakov S, Sprawls P, Krisanachinda A, Lewis C, (2011), Medical Physics and Engineering Education and Training – part I, ISBN 92-95003-44-6, ICTP, Trieste, Italy
2. Tabakov, S, V Tabakova, (2015), The Pioneering of e-Learning in Medical Physics, London, ISBN 978-0-9552108-3-9
3. EMERALD, EMIT web site: www.emerald2.eu
4. EMITEL Web site: www.emitel2.eu

### GLOBAL USE OF THE DESCRIBED E-LEARNING PROJECTS

The described e-learning projects (EMERALD, EMIT, EMERALD - INTERNET ISSUE, EMITEL, etc) are now used globally for some 20 years by thousands of colleagues each month (over Internet). The EMITEL e-Dictionary and e-Encyclopedia alone have about 5000 users per month (the Encyclopedia was also published on paper by CRC Press). These projects triggered other excellent e-learning projects, web sites and activities in the profession.

Looking at the global growth medical physicists in the world, we can see that during the first three decades after the formation of IOMP (1965-1975; 1975-1985; 1985-1995) the number of medical physicists globally has increased at a rate of about 2,000 per decade. However the following two decades (1995-2005; 2005-2015) the number of medical physicists globally has increased, respectively, at a rate of about 4,000 and 6000 per decade. This more than double growth is linked to various factors, but an important one of these is certainly the introduction of e-learning in the profession after 1995. IOMP is a major supporter of this trend of new delivery of teaching materials. To facilitate the exchange of information in the field of Education and Training in medical physics, it initiated in 2013 a new Journal Medical Physics International. This open-source publication (available free through www.mpijournal.org) is dedicated to educational and professional development in medical physics and has regularly about 6000 readers per month.

The 7 projects described in the presentation were also a clear proof of the success of international cooperation in this field – the projects included hundreds of leading specialists from 44 countries (the e-Encyclopedia and Dictionary EMITEL included more than 300 specialists from 36 countries). These and other similar educational projects created a name of medical physics as a profession firmly linked to e-learning.

**Corresponding author email:** slavik.tabakov@emerald2.co.uk



Fig.1 Global use (web site visits) of e-learning materials EMERALD and EMIT in the period 2010-2016

## INVESTIGATION OF DOSE PREDICTION ACCURACY OF PENCIL BEAM CONVOLUTION ALGORITHM IN A INHOMOGENEOUS PHANTOM

Devi Prasad Pandey

Shyam Shah Medical College, India

**Key words:** Pencil Beam Convolution ; Heterogeneity Correction; PDD Calculation

### Purpose

Dose prediction accuracy of dose calculation algorithms is important in external beam radiation therapy. This study investigated the effect of air gaps on depth dose calculations computed by pencil beam convolution algorithm (PBC) algorithm

### Methods

A computed tomography (CT) scan of inhomogeneous phantom ( $30 \times 30 \times 30$  cm<sup>3</sup>) containing rectangular solid- water blocks and two 5 cm air gaps was used for central axis dose calculations computed by PBC in Oncentra treatment planning system. Depth dose measurements were taken using a cylindrical ionization chamber for identical beam parameters and monitor units as in the depth dose computations. The calculated and the measured percent depth dose (PDDs) were then compared. The data presented in this study included 6 MV photon beam and field sizes of  $3 \times 3$  cm<sup>2</sup>,  $5 \times 5$  cm<sup>2</sup>,  $10 \times 10$  cm<sup>2</sup>, and  $15 \times 15$  cm<sup>2</sup>.

### Results

The results of PBC were within  $\pm 1.7\%$  in the first water medium. However, upon traversing the first air gap and re- entering the water medium, in comparison to the measurements, the PBC over-predicted the dose, with difference ranged from -1.8% to -3.5% for  $3 \times 3$  cm<sup>2</sup>, from -2.6% to -4.4% for  $5 \times 5$  cm<sup>2</sup>, from -2.5% to -6.9% for  $10 \times 10$  cm<sup>2</sup>, and from -1.7% to -6.5% for  $15 \times 15$  cm<sup>2</sup>. After the second air gap, the PBC continued to under-predict the dose, and the difference ranged from -3.3% to -3.9% for  $3 \times 3$  cm<sup>2</sup>, from -2.6% to -5.6% for  $5 \times 5$  cm<sup>2</sup>, from -2.5% to -6.0% for  $10 \times 10$  cm<sup>2</sup>, and from -1.6% to -5.6% for  $15 \times 15$  cm<sup>2</sup>.

### Conclusions

The PBC overpredicted the dose in water medium after the photon beam traversed the air gap. Special attention must be given during the patient set-up since large air gap between the patient body and immobilization devices may lead to unacceptable dose prediction errors

## **DEVELOPMENT OF A TECHNOLOGY ENHANCED FRAMEWORK FOR MEDICAL PHYSICS LEARNING AND TEACHING**

Andrew Fielding, Iwona Czaplinski

Queensland University of Technology, Australia

**Key words:** Medical Physics Education, Technology-Enhanced Learning, Authentic Learning.

### **Purpose**

The authors undertook the development of a technology-enhanced framework for the Radiation Therapy unit, part of a medical physics Masters course. The project aimed to enhance students learning experience by creating a blended learning environment encouraging active engagement with the study material by exposing students to diverse and complex practical techniques within an in-campus environment.

### **Methods**

The framework encompassed online components including high quality interactive, multimedia-based educational resources (videos) and face-to-face, in-class learning and teaching activities. The specifically developed educational videos demonstrated important clinical procedures and practice, as well as a series of questionnaires and quizzes that tested students' understanding of the video content and provided connection with the in-class activities. The in-class component included authentic active learning activities, and the use of a Virtual Reality Radiotherapy simulation environment (VERT).

### **Results**

The specific benefits of the project included: (1) increased students' awareness and understanding of 'real world' clinical practice, (2) improved practical skills, (3) increased student engagement by encouraging clinically relevant active learning, (4) development of more attractive, technology-enhanced, flexible approaches to learning, and (5) strengthened links with clinical departments.

### **Conclusions**

Overall, the findings indicate that the blended learning model resulted in improved student engagement measured in terms of both satisfaction and progression. In addition, based on the preliminary results, the researchers identified the potential for a move to an online delivery model that better suits the educational needs of the Medical Physics profession in the Asia-Pacific Region.

## **TRAINING OF MEDICAL PHYSICISTS TO CONDUCT PERFORMANCE TEST OF RADIOGRAPHY/FLOUROSCOPY, MAMMOGRAPHY AND CT**

Marlon Raul Tecson, Jake Ryan Oliganga, Roujahn Durante

Medical Physics & Health Physics Services, Inc., Philipinnes

**Key words:** Medical Physicist, Performance Test, ACR Accreditation Phantom, Quality Manual

### **Purpose**

To describe the training for newly-hired medical physics graduates in the conduct of performance test of radiography/fluoroscopy, mammography and CT.

### **Methods**

Newly hired Master in Medical Physics graduate undergoes apprenticeship-type training. The medical physicist of Medical Physics and Health Physics Services, Inc. (MPHPS) is expected to be knowledgeable in performing acceptance -, QA-, and performance tests, in preparing reports, and in reviewing, interpreting, and approving all data measurements indicated in the tests. In the Philippines, the Medical Physicist must possess either a BS degree in Physics or in Engineering, and a Master's degree in Medical Physics from the University of Santo Tomas Graduate School (USTGS) - the only school offering Medical Physics program in the country. Medical physicists hired by MPHPS are either graduates of the USTGS Master in Medical Physics program or are current students working on their research to fulfil the requirements for graduation; however, graduates of the program do not necessarily possess the ability to conduct performance test of x-ray, mammography and CT.

### **Results**

Medical physicist trained by MPHPS gain competence through the apprenticeship-type training that is a blend of theory and practice; undergo on-site witnessing by the Philippine Accreditation Bureau (PAB) under PNS ISO/IEC 17020:2012 assessment and in due time will be responsible in teaching incoming new hires.

### **Conclusions**

MPHPS provide a training that is an excellent supplement to the M.Sc Medical Physics training at the University of StTomas Graduate School.

## THE CAPE TOWN ACCESS TO CARE COURSE: BRIDGING THE AFRICAN RADIOTHERAPY TRAINING GAP

C Trauernicht<sup>1</sup>, J Parkes<sup>1</sup>, H Burger<sup>1</sup>, B Wyrley-Birch<sup>2</sup>, J-M Valentim<sup>3</sup>, J Groll<sup>3</sup>

<sup>1</sup>Groote Schuur Hospital and University of Cape Town, South Africa; <sup>2</sup>Cape Peninsula University of Technology, South Africa; <sup>3</sup>Varian Medical Systems, Switzerland

**Key words:** 3D conformal radiotherapy training, VERT, Eclipse, teaching platform

**Introduction:** The World Health Organization's GLOBOCAN 2012 project data indicate that 56.4% of the world's cancer patients had access to only 31.7% of the global teletherapy units, with an increase in cancer incidence of 23.9% expected by 2020. [1] Forty countries in Africa have no access to radiotherapy at all, with the majority of the units located in Egypt and South Africa [1, 2]. Where linear accelerators are available, centres are faced with the challenge of moving from 2D radiotherapy to computerized 3D Conformal Radiotherapy (3DCRT) techniques. The challenge not only relates to equipment, but to the appropriate skills required by Radiation Oncologists (RO), Medical Physicists (MP) and Radiation Therapists (RTT) required to safely operate the equipment to deliver good quality 3DCRT treatment in a safe and efficient manner. Training programmes in first world countries often focus on advanced radiotherapy techniques, and may not be appropriate to bridge the gap between 2D and 3DCRT radiotherapy. The Cape Town Access to Care training project aims at providing an innovative technology based teaching platform to teach teams of developing country ROs, MPs and RTTs to allow for the safe transition from 2D to 3DCRT. It is a joint collaborative training initiative between Varian Medical Systems, the University of Cape Town (UCT) and the Cape Peninsula University of Technology (CPUT), creating a program that links with the global Varian Access to Care program.

**Methods:** Two workshops were held in 2014 to develop an appropriate training programme focusing on the training needs in the African context, legal and contractual implications of a multi-party cross-discipline training platform, the infrastructure required,

technological alternatives to allow for remote access to training material and learning approaches required to teach the Millennium generation.

An integrated course was created consisting of three weeks at the training facility in Cape Town, followed by a three month email mentorship programme. Four teams (RO, MP& RTT per team) can attend each course and learn the skills required to create and execute clinical and quality assurance protocols at their own facilities by the end of the mentorship programme. Teaching is done in a "teaching by trying" environment, using the Vertical Seminar Vert<sup>TM</sup> system and a Varian Eclipse<sup>TM</sup> Treatment Planning System laboratory, which is linked via optic fibre to servers in Switzerland.

**Results:** The first full course was hosted in August 2015 and attended by teams from Ghana and Zimbabwe. Pre and post course surveys were done to assess participants' skills levels and improvements. Post-course surveys indicated a 25% improvement in familiarity with immobilization devices, imaging and localisation skills improved by 41% and 3D planning skills by 30%. The technology, Eclipse and VERT was found to enhance the learning process. Teams from Cameroon and Ethiopia, as well as local teams, attended the course in 2016.

**Conclusion:** The Cape Town Access to Care programme has created a platform to allow teams from developing countries to successfully transition from 2D to 3DCRT.

### References:

1. Datta NR, Samiei M, Bodis S. Radiation therapy infrastructure and human resources in low-and middle-income countries: present status and projections for 2020. *International Journal of Radiation Oncology\* Biology\* Physics*. 2014;89(3):448-57.
2. Abdel-Wahab M, Bourque J-M, Pynda Y, Iżewska J, Van der Merwe D, Zubizarreta E, et al. Status of radiotherapy resources in Africa: an International Atomic Energy Agency analysis. *The Lancet Oncology*. 2013;14(4):e168-e75.

## **CLINICAL TRAINING OF RADIOPHARMACEUTICAL SCIENTISTS IN AUSTRALIA: DESIGNING AND LAUNCHING A NEW TRAINING, EDUCATION AND ASSESSMENT PROCESS**

Jennifer Guille<sup>1</sup>, Jacob Pearce<sup>2</sup>, Andrew Katsifis<sup>3</sup>

<sup>1</sup>ACPSEM, Australia

<sup>2</sup>Australian Council for Educational Research

<sup>3</sup>Department of Nuclear Medicine, Royal Prince Alfred Hospital

**Key words:** Education, Training, Radiopharmaceutical Science, Nuclear Medicine

### **Purpose**

Radiopharmaceutical Science (RPS) is a small and critical workforce, with specialist knowledge, skills and attributes required to deliver safe and effective diagnostic and therapeutic radiopharmaceutical products and services to nuclear medicine.

Professional standards needed to be articulated, and an effective program of clinical training and assessment developed, in order to train competent professionals.

### **Methods**

A framework of essential knowledge and skills for the safe practice of RPS was developed, using established ACPSEM programs as models. The group then worked with educational experts to incorporate contemporary theory and practice in training, education and assessment to develop the RPS TEAP.

### **Results**

The program design incorporates assessment as a driver of the formative learning process using programmatic and progressive assessment, not isolated assessment instruments. Key competencies were identified requiring a mixture of low and high stakes assessments that provide useful experience and information for trainees, supervisors and assessors. Rather than assign assessors to exams or specific assessment events, each competency area has an appointed assessor to ensure consistency, quality and validity of assessment.

### **Conclusions**

RPS TEAP is a new model which will support future development of ACPSEM medical physics programs. Strategies were developed to overcome the challenges of a small profession lacking workforce to support the teaching, training and assessment requirements, and enable the safer practice and growth of a complex discipline. The development has been strongly supported by the Australian Government Department of Health. The RPS TEAP had its first enrolments in May 2016.

## MEDICAL PHYSICS EDUCATION IN SOUTH ASIA: PROBLEMS AND PERSPECTIVES

Hasin Anupama Azhari

Gono Bishwabidyalay (University), Savar Dhaka, Bangladesh

The working field areas of medical physicists are radiation oncology, diagnostic imaging and nuclear medicine. The qualification of this profession is a MSc /PhD in medical physics. This study covers Medical Physics education and especially for female students in the south Asian region especially in **Bangladesh, India, Nepal and Pakistan.**

While incidence rates for all cancers combined in economically developed countries are nearly twice as high as in economically developing countries in both males and females, mortality rates for all cancers combined in developed countries are only 21% higher in males and only 2% higher in females. Such disparities in incidence and mortality patterns between developed and developing countries will reflect, for a given cancer, regional differences in the prevalence and distribution of the major risk factors, detection practices, and/or the availability and use of treatment services. On the other hand researchers estimate that at least 2 percent of all future cancers in the U.S. - approximately 29,000 cases and 15,000 deaths per year - will stem from CT scans alone. Even some standard X-rays which seem to expose much smaller amounts of radiation, can pose risks if one undergoes multiple ones. Without medical physicist professionals the patient cannot be protected from the deterministic effect of radiation.

The educational status and with this the opportunity of medical physics courses in these four countries are slowly emerging. As in most of the developing countries, this is a new subject. In **Bangladesh** only Gono University has offered this subject since 2000. Though 2 or 3 other universities tried to start medical physics courses, but due to shortage of faculty members, these universities could not run this subject. In Gono University presently about 10% of total students (currently 250 students) are female. In **Nepal** no formal MSc in medical physics course is yet established. M.Sc. Physics studies started in 1969 at the Tribhuvan University, Kathmandu, Nepal. In 1998, biomedical physics as a special paper was introduced in the second year and some students are assigned with thesis related to radiation physics in radiology, nuclear medicine, radiotherapy and radiation protection in different institutions and hospitals under supervision of physicists. In Nepal there are 39-40% female students up to higher secondary education but in higher education in MSc in physics there are only 5% women. In **Pakistan** an institute, the Pakistan Institute of Engineering and Applied Sciences (PIEAS), run by the Pakistan Atomic Energy Commission (PAEC) has a 2-year MS degree program for MP. Among these countries **India**

has progressed furthest in the MP education. Seventeen universities in different provinces are offering this course as diploma (1 year), MSc degree (2 years). 20% of all students are female in India.

The current number of the cancer hospitals is increasing in each country to meet the demand required by the WHO for cancer treatment. The number of medical physicists is yet far below the requirement. Reduced job opportunities in MPs have led to discourage the students. In a world where just 30% of researchers are women, the reasons are manifold, ranging from the challenge of balancing family life and career to a lack of childcare support and role models. The number of female students is still remarkably low in science subjects compared to social subjects. Nowadays, gender inequalities in women's academic careers are in progression intersecting with other structures of inequality such as social class, caste, religion, ethnicity and language. Backgrounds and beliefs were reported as significant constraints to women pursuing academic careers. The primary identification of women was typically thought to be with the private, domestic sphere, in association with caring/nurturing extended family roles. In developing countries females are always considered for house hold work and early marriage. Although most governments have made female education mandatory up to class ten, it usually happens that after the 10<sup>th</sup> form parents are not interested in further education. So it is obvious that females never succeed to a career as medical physicist or in higher academic posts in medical physics or pure science. Also the problems mostly lie with the social stigma about hiring or employing a female physicist. The unavailability of suitable career opportunities at feasible distances or the increased responsibility of family and children keeps potential female physicists from pursuing their careers. In some places, the societies are concerned about occupational radiation hazards forcing females to discontinue their careers. Whatever the problems are, we need to start working as teams to change the social beliefs regarding female education. Different approaches need to be adopted for overcoming the present situation. This paper proposes some solutions, e.g. institutes can exempt or reduce study fees to female students. Certain institutes can give preference to female students in particular quota system. Public awareness is needed and through media it can be circulated. With encouragement, professional development, financial support for the education in medical physics, we can solve the obstacles for females.

## **15 Professional Development**

## **IOMP JOURNAL *MEDICAL PHYSICS INTERNATIONAL* RESULTS AND STATISTICS AFTER 3 YEARS**

Slavik Tabakov, Perry Sprawls

IOMP President, MPI Co-Editor, King's College London, UK  
Emory University, MPI Co-Editor, USA

**Key words:** Educational publication, Journal

### **Purpose**

IOMP launched a new Journal in 2013 - MEDICAL PHYSICS INTERNATIONAL (MPI) - a free access e-publication ([www.mpijournal.org](http://www.mpijournal.org)). The statistics for MPI usage shows the need of the Journal for the profession. Currently MPI has more than 5000 readers per month.

### **Methods**

The presentation is based on the original statistics from the MPI web server, related to number of visits, downloads and geographical distribution.

### **Results**

Since 2013 MPI issued 6 e-Journals with 380 pages of articles and 840 pages of Conference abstracts. Initially the Journal had about 4000 users per month. Currently the number increased with more than 50%. By May 2016y MPI has 204,000 visits, and 75% of these are direct entries. About 30% of the papers published papers have more than 1000 downloads (five papers have above 10,000 downloads). The global use of the last issue of the MPI Journal (December 2015) is indicative for the development of the profession – as per the server statistics the number of downloads are: Asia: 5508; Europe: 4178; North America: 3779; Africa: 421; Oceania: 323; Latin America: 267. The 45 professional and educational papers published in MPI have c.35,000 downloads. Specific interest attract also the papers describing technological innovations for educational purposes (some papers are directly from the industry) - they have c.52,000 downloads. The feedback from all readers is very encouraging.

### **Conclusions**

The IOMP Journal MPI has already found a steady place in the profession, describing and encouraging a number of new professional activities and enriching the educational process.

## **CODES OF CONDUCT AND CODES OF ETHICS IN MEDICAL PHYSICS**

Howell Round

University of Waikato, New Zealand

**Key words:** Ethics, conduct, professionalism

### **Purpose**

Many organizations and societies that represent professional groups have a Codes of Conduct or Codes of Ethics that their members commit to abide by. The Asia-Oceania Federation of Organizations for Medical Physics (AFOMP) has decided to produce a Code of Ethics to act as a model for its national member organizations to adopt.

### **Methods**

A survey was made of a number of medical physics professional societies and organizations to obtain their codes of conduct or ethics. This was initially done by searching on-line for such statements, and later most of the IOMP member organizations were approached individually for copies of their codes of conduct or ethics.

### **Results**

It was clear that very few such statements have been developed by medical physics professional societies or organizations. Those that had been developed ranged from short outlines that covered a couple of pages to in-depth statements running to a dozen pages that set out complaint and disciplinary procedures.

### **Conclusions**

As AFOMP is an umbrella organization for approximately 20 medical physics national member organizations from different countries, it needs to develop a code of ethics that is acceptable to all of its members taking into consideration the different cultures involved. This does not mean that it should set low expectations for the ethical conduct of the medical physicists in those countries, but it must still specify standards that are internationally acceptable.

## SYNERGETIC EFFECT OF MEDICAL PHYSICS WITH MEDICAL ENGINEERING AND MEDICAL INFORMATICS

Kiyonari Inamura

Professor Emeritus Osaka University

**Key words:** medical engineering, information sciences

**Introduction:** The purpose of the presentation is to provide young researchers of medical physics with topics on the cultivation of new horizon of investigation and development cooperating with medical engineering and medical informatics. Especially, to bring synergetic effect with fruitful results.

**Method:** To raise titles of research fields and focus them onto concrete method of development. Close reviews and analyses of papers, presentations and related articles from AAPM journals, IJCARS (International Journal of Computer Assisted Radiology and Surgery), IJBME, AJMI (American Journal of Medical Informatics), BIIJ, and PRT (Radiological Physics and Technology) were done. Also experiences of author in these three fields are retrospectively presented and future prospect is sought logically.

**Result:** 1 New modality for diagnoses and therapy such as portable CT for disaster ambulance in earthquake [1], 2. Predictive, preventive and personalized medicine [2][3][4][7], 3. Information processing in computer assisted interventions [3][4], 4. Application of big data and cloud computing [5], 5. Multiscale digital patient [6], 6. Medical decision support, 7. Quantitative imaging biomarkers, 8. Medical robotics and manipulators and deep brain stimulation 9. Smart cyber operating theater[1], and 10. BNCT

**Conclusion:** Breakdown of above each item into specific detail is presented in this lecture. Coming World Congress in 2018 and 2021 where both International Congresses of Medical Physics and International Federation of Medical Biology and Engineering are held at the same time and in the same place will be good opportunity for young investigators to present synergetic results of R&D. World Congress 2022 hopefully in Japan is the final target of harvesting fruitful results of cooperated R&D.

### References

- 1) Int. J. of CARS 10, Suppl.1, June 2015, Springer
- 2) Final Program of CARS 2015 June 24-27,2015, Barcelona, Spain,
- 3) www.cars-int.org
- 4) Lemke and Golubnitschaja The EPMA Journal 2014, 5 : 8 <http://www.epmajournal.com/content/5/1/8>
- 5) Int. J. of CARS 10, No.6, June 2015, 6th IPCAI 2015 Special Issue, Springer
- 6) Banerjee .I, et al. Semantic annotation of 3D anatomical models to support diagnosis and follow-up analysis of musculoskeletal pathologies. Int. J. of CARS First online: 28 November 2015 1-14.

- 7) Lemke and Golubnitschaja The EPMA Journal 2014, 5: 8

**Corresponding author email:** [ina-kiyo@mue.biglobe.ne.jp](mailto:ina-kiyo@mue.biglobe.ne.jp)

INFORMATION ABOUT THE ABSTRACT.

### **Predictive, preventive and personalized medicine[4]:**

Co-morbidities and complex clinical situations in elderly populations should be considered as the persistent challenge that requires new strategies in healthcare. Integrative medical approaches are strongly desirable to analyze common risk factors as well as their individual and synergistic effects. Frequent versus rare co-morbidity profiles in cardiovascular disease patient cohorts should be created for advanced treatment regiments.

At the international EPMA (European Association for Predictive, Preventive and Personalized Medicine) Summit carried out in the EU Parliament (September 2013), the main challenges in Predictive, Preventive and Personalized Medicine have been discussed and strategies outlined in order to implement scientific and technological innovation in medicine and healthcare utilizing new strategic program such as 'Horizon 2020' [4][7].

Personalization in healthcare urgently needs innovation in design of PPPM-related medical services, new products, research, education, didactic materials, propagation of targeted prevention in the society and treatments tailored to the person. For the paradigm shift from delayed reactive to predictive, preventive and personalized medicine, anew culture should be created in communication between individual professional domains, between doctor and patient, as well as in communication with individual social (sub)groups and patient cohorts. This is a long-term mission in personalized healthcare with the whole spectrum of instruments available and to be created in the field.

### **CARS (Computer Assisted Radiology and Surgery)[1]:**

CARS emphasizes the consolidate position of the leading experts who are aware of the great responsibility of being on a forefront of predictive, preventive and personalized medicine. Both societies of CARS and EPMA consider long-term international partnerships and multidisciplinary projects to create PPPM relevant innovation in science, technological tools and practical implementation in healthcare.

### **BNCT (Boron neutron capture therapy) by means of accelerator:**

More than 14 research institutes have installed facility of BNCT in Europe, USA, Asia and South America. Among them 8 facilities are pursuing possibilities of generating neutron by accelerator instead of nuclear reactor of expensive initial investment cost. Especially in Japan, at least 8 new projects of BNC using different type of accelerator have started to search most appropriate method by different way of investigation.

## 150 YEARS WOMEN IN MEDICAL PHYSICS

Magdalena Stoeva

IOMP MPW Board Chair, Medical University Plovdiv, Bulgaria

**Key words:** Medical physics, women, IOMP, IOMP-W

### Purpose

Medical physics is among the leading contemporary sciences with important contribution to the development of healthcare, patient, staff and public safety. Although for centuries the scientific world was dominated by men, women have always played a key-role in Medical physics.

### Methods

Following the recent demands of our professional society, IOMP formed IOMP-W - the Women Subcommittee (1, 2). IOMP-W is dedicated to development, implementation and coordination of tasks and projects, related to the role of females in medical physics scientific, educational and practical aspects.

### Results

Whilst discussing the role of women in science, this is indisputably dominated by Marie

Skłodowska-Curie – the brilliant physicist and chemist, the first woman to win a Nobel Prize, the first person to win two Nobel Prizes and the only person to win Nobel Prizes in multiple scientific disciplines.

Many other brilliant women have made their contribution to science – some of them with a direct relation to Medical Physics - Irène Joliot-Curie, Goepfert-Mayer, Rosalyn S. Yalow, Harriet Brooks, Chien-Shiung Wu.

### Conclusions

As an appreciation of the role of women in medical physics, IOMP recently shared the initial plans for 2017, when all medical physicists will celebrate the 150th birthday of Marie Curie: the IDMP theme will be dedicated to women and a New Award will be introduced to recognize major contributions by female medical physicists.

### References

1. [www.iomp.org](http://www.iomp.org)
2. [www.iomp.org/IOMP-W](http://www.iomp.org/IOMP-W)

## ICMP 2016



## POSTER PRESENTATIONS

## **CORRELATION ANALYSIS OF DOSE ESCALATION IN PROTON BORON FUSION THERAPY (PBFT) AND BORON NEUTRON CAPTURE THERAPY (BNCT)**

Joo-Young Jung<sup>1</sup>, Do-Kun Yoon<sup>1</sup>, Tae Suk Suh<sup>1</sup>

<sup>1</sup>Catholic University of Korea

**Key words:** Proton boron fusion therapy, boron neutron capture therapy, Monte Carlo simulation, Bragg-peak

### **Purpose**

Proton boron fusion therapy (PBFT) based on using the characteristics of alpha particles on which occur with proton and boron particle. The PBFT technique is similar to the boron neutron capture therapy (BNCT) technique at the part of using boron particle. The aim of this study is to compare between PBFT and BNCT and analysis a dose escalation in the PFBT perspective using a Monte Carlo simulation code.

### **Methods**

We set that the proton beam passed through the water including boron. The variation and influence about the alpha particle was observed from the percent depth dose (PDD) and lateral dose profile of both the neutron and proton beam.

### **Results**

The peak value in the maximum dose level when the boron particle was accurately labelled at the region was 192.4% among the energies.

### **Conclusions**

We confirmed the dramatic effectiveness of the alpha particle, especially in PBFT. The utility of PBFT was verified using the simulation, it has sufficient worth of application for the radiotherapy.

## **QUANTITATIVE ANALYSIS OF PROTON BORON FUSION THERAPY (PBFT): BEYOND BNCT**

Joo-Young Jung<sup>1</sup>, Do-Kun Yoon<sup>1</sup>, Han-Back Shin<sup>1</sup>, Moo-Sub Kim<sup>1</sup>, Sun-Mi Kim<sup>1</sup>, Tae Suk Suh<sup>1</sup>

<sup>1</sup>Catholic University of Korea

**Key words:** PBFT, boron, maximal proton dose, Monte Carlo simulations

### **Purpose**

The proton-boron nuclear reaction produces three alpha particles which may be useful in radiotherapy applications. We performed simulation studies to determine the effectiveness of the proton boron fusion therapy (PBFT) under various conditions.

### **Methods**

Boron uptake regions (BURs) of different widths and densities were implemented in Monte Carlo n-particle extended (MCNPX) simulation code. The effect of proton beam energy was considered for different BURs. Four simulation scenarios were designed to calculate the dose enhancement that was observed due to the proton boron reaction. The simulations considered several variables including proton beam energy, BUR size, location, and concentration.

### **Results**

Proton dose amplification was confirmed for all proton beam energies considered (< 96.62%), the threshold for the range in which proton dose amplification occurred was estimated as 0.3 cm. Effective proton boron reaction requires boron concentration to be at least 14.4 mg/g.

### **Conclusions**

We simulated PBFT and quantified the dose enhancement under various treatment conditions. These results provide a PBFT dose enhancement database.

## STABILITY EVALUATION OF WATER EQUIVALENT TYPE MULTI-LAYER IONIZATION CHAMBER

Hiroyuki Kobayashi<sup>1</sup>, Shigekazu Fukuda<sup>1</sup>, Soma Iwata<sup>1</sup>, Hiroki Arai<sup>1</sup>

<sup>1</sup>Chiba University, Japan

<sup>1</sup>Chiba University, QST NIRS

<sup>1</sup>Chiba University, AEC

**Key words:** MLIC, Carbon Therapy, Water Equivalent, QA/QC

### Purpose

We examined the cause of the short-term and long-term output instability of the water-equivalent type multi-layer ionization chamber developed for the carbon therapy. The short-term instability was that there was 2% difference between the first and subsequent measurements after continuous irradiation. We observed the correlation between the relative humidity and the measured values over long periods.

### Methods

We measured the outputs under condition the readout pattern was shielded or unshielded, and compared them. In addition, the measurement was performed in a dry state using silica gel, and the correlation to be expected was verified.

### Results

There was observed 2% difference between the first and the fifth measurements when the pattern wasn't shielded. On the other hand, when the pattern was shielded it produced only 0.2% difference. Despite the expectation that the measured value rises when the relative humidity falls, the measurements was resulted in 20% decrease compared with the previous data of the same irradiation conditions.

### Conclusions

The short-term instability problem was due to the beam hit the reading pattern. To improve the stability the readout pattern should be narrower. For the long-term instability problem the cause was not clear. However, we found that signal substrate made from PMMA which has hygroscopicity was shrunken by drying and the sensitive volume had decreased. Therefore, this suggested the signal substrate should be made of a low-hygroscopic substance.

## **DEPENDENCE OF DOSE-MONITOR CALIBRATION FACTOR ON BEAM CONDITIONS IN BROAD BEAM THERAPY**

Manabu Mizota<sup>1</sup>

<sup>1</sup>Ion Beam Therapy Center, Saga Himat Foundation, Japan

**Key words:** calibration factor, output factor, monitor-unit, wobbling method, carbon therapy

### **Purpose**

Generally in the particle beam therapy, we should perform dose calibration measurement in order to convert the prescribed dose at a reference point of a target to a monitor count value for each irradiation. At SAGA-HIMAT (Saga Heavy Ion Medical Accelerator in Tosu) facility, we have introduced a precise calculation method for deriving the monitor unit for radiotherapy with carbon beam. In this derivation method semi-empirical computation is used with linear functions based on measurements in various range shifter thickness under each irradiation condition for each individual port. We are now trying to derive these functions considering the configuration of the irradiation devices.

### **Methods**

In our irradiation system, there are four ports (1 vertical, 1 oblique and 2 horizontal). As the arrangement of the irradiation device are the same, an identical irradiation field is expected when using the same parameters. We had investigated whether there are differences among these ports focusing on the dose in calibration depth.

### **Results**

The results of measurement for each condition commonly used for the treatment irradiation were compared and we found that differences among 4 ports were all within 1%.

### **Conclusions**

It was found that individual differences in terms of the dose output among the ports is very small. These results showed the possibility of calculating dose output if taken into consideration only the irradiation devices. So we attempt to express the output using the irradiation condition parameters or a simple modeling.

## **DEVELOPMENT OF SPOT PROFILE MEASUREMENT FOR PROTON PENCIL BEAM USING CHERENKOV RADIATION IN TWO DIMENSIONAL OPTICAL FIBER ARRAYS**

Jaeman Son<sup>1</sup>, Dongho Shin<sup>2</sup>, Sanghyeon Song<sup>2</sup>

<sup>1</sup>Korea University, S Korea

<sup>2</sup>National Cancer Center, S Korea

**Key words:** Proton therapy; Pencil beam scanning; Cherenkov radiation

### **Purpose**

Proton therapy aims to deliver a high dose in a well-defined target volume while sparing the healthy surrounding tissues thanks to their inherent depth dose characteristic (Bragg peak). In proton therapy, several techniques can be used to deliver the dose into the target volume. The one that allows the best conformity with the tumor, is called PBS (Pencil Beam Scanning). The measurement of the proton pencil beam spot profile (spot size) and position is very important for the accurate delivery of dose to the target volume with a good conformity.

### **Methods**

We have developed detector array to monitor the PBS. A prototype beam monitor using Cherenkov radiation in clear plastic optical fibers (cPOF) has been developed for continuous display of the pencil beam status during the therapeutic proton Pencil Beam Scanning mode operation. Spot profiles of various pencil beam energies(100 MeV to 226 MeV) are measured. Two dimensional Gaussian fit is used to analyze the beam width and the spot center. The results are compared with that of Lynx(Scintillator-based sensor with CCD camera) and EBT3 Film.

### **Results**

The measured Gaussian widths using fiber array system changes from 13 to 5 mm for the beam energies from 100 to 226 MeV. The results agree well with Lynx and Film within the systematic error.

### **Conclusions**

The results demonstrate good monitoring capability of the system. Not only measuring the spot profile but also monitoring dose map by accumulating each spot measurement is available.

## **EXTERNAL-BEAM RADIOTHERAPY FOR PIGMENTED VILLONODULAR SYNOVITIS OF THE KNEE: IS THE PROBABILITY OF RADIATION-INDUCED CARCINOGENESIS TRIVIAL?**

Michalis Mazonakis<sup>1</sup>, Antonis Tzedakis<sup>2</sup>, Efrossyni Lyraraki<sup>2</sup>, John Damilakis<sup>1</sup>

<sup>1</sup>University of Crete

<sup>2</sup>University Hospital of Heraklion

**Key words:** radiation therapy, benign diseases, PVNS, carcinogenesis

### **Purpose**

Pigmented villonodular synovitis (PVNS) is a non-malignant disorder which may involve the synovium of the knee joint. This disorder usually appears in individuals of reproductive age. Adjuvant irradiation is often required to prevent disease recurrence. This study estimated the risk of carcinogenesis from external-beam radiotherapy for PVNS.

### **Methods**

A previously validated Monte Carlo model of a medical linear accelerator producing 6 MV X-rays was used. Knee irradiation for PVNS was simulated on an androgynous mathematical phantom with equally weighted anteroposterior and posteroanterior treatment fields giving 35 Gy to the target site. The phantom represented the dimensions of the average adult patient. Twenty-two F6-type tallies were positioned inside the phantom to calculate the radiation dose to critical organs having a strong predilection for carcinogenesis. The lifetime attributable risk (LAR) of developing any organ-specific malignancy was estimated for typical 30-year-old male and female patients by using the BEIR-VII methodology.

### **Results**

The organ doses varied widely by the organ location in respect to the treatment volume. The urinary bladder received the highest radiation dose of 0.9 cGy. The LAR of cancer induction was estimated to be (0.0004-0.007) % depending upon the organ of interest and the patient's gender. Radiation therapy in male and female patients increased the nominal cancer risks for the unexposed population up to 0.2 % and 0.6 %, respectively.

### **Conclusions**

The probability of radiation-induced carcinogenesis attributable to radiotherapy for PVNS in the knee region should be considered as trivial.

## **FEASIBILITY STUDY OF PARALLEL MONTE CARLO PHOTON TRANSPORT USING LOW-RESOLUTION VOXEL ALGORITHM ON THE GPU**

Masatsugu Hariu<sup>1</sup>

<sup>1</sup>Tokyo Metropolitan University

**Key words:** graphics processing units, parallel computing, photon transport, low-resolution voxels

### **Purpose**

Fast Monte Carlo (MC) photon transport is attempted by parallel computing on graphics processing units (GPU). Woodcock tracking is one of representative photon transport algorithm for GPU. In Woodcock algorithm, iterative calculation is time-consuming when small high-density material exists within low-density volume. On the other hand, MC algorithm using low-resolution voxels (called macrocells) has been proposed. This algorithm provides higher efficiency of photon tracking than Woodcock algorithm. However, reliability of MC simulation using macrocells has not been assessed in detail yet. Therefore, MC simulation code using macrocells was developed and the reliability of photon energy spectrum was investigated by comparison with EGS5 in this report.

### **Methods**

30 cm×30 cm×30 cm heterogeneous phantom and sampling plane were arranged. In the MC simulation, mono-energetic photon pencil beam was impinged on the surface of the phantom and energy spectra of photons passed from the phantom were sampled by concentric regions. The MC simulations were performed with several sizes of macrocells. Energy spectra and computing time by own code and EGS5 were compared.

### **Results**

Photon energy spectrum of each sampling region shows good agreement with that by EGS5 for all incident energies and several sizes of macrocells. Additionally, by adjusting the size of macrocells optimally, speedups of 100 to 300 times were achieved against EGS5.

### **Conclusions**

Consequently, reliability and high efficiency of the MC code using macrocells was confirmed.

## **PROBABILITY ESTIMATION OF RADIATION-INDUCED DNA DOUBLE-STRAND BREAKS IN THE CELL NUCLEUS**

Ryosuke Mori<sup>1</sup>, Yusuke Matsuya<sup>1</sup>, Yuji Yoshii<sup>2</sup>, Hiroyuki Date<sup>3</sup>

<sup>1</sup>Graduate School of Health Sciences, Hokkaido University, Japan

<sup>2</sup>Education and Instrumentation Center, Sapporo, Japan

<sup>3</sup>Faculty of Health Sciences, Hokkaido University, Japan

**Key words:** DNA amount of cell cycle, DNA double-strand breaks (DSBs), Monte Carlo simulation

### **Purpose**

To estimate the probability distribution of the number of DNA double-strand breaks (DSBs) in a cell nucleus based on the amount of DNA per nucleus and the non-uniformity of radiation energy deposition.

### **Methods**

We measured the DNA amount depending on the cell cycle by flow cytometry with Propidium Iodide (PI) and the number of DSBs per nucleus after irradiation (200 kVp X-rays with 0.5 mmCu0.5 mm Al filtration) with H2AX immunofluorescent staining for CHO-K1 cells. Next, to determine the absorbed dose per nucleus, we calculated the energy distribution of the secondary electrons produced by X-rays with the EGS5 code. Thus, the probability of DSB induction was deduced based on the absorbed dose and the DNA amount per nucleus, to make comparison with the measured number of DSBs (H2AX) per nucleus.

### **Results**

We obtained the distribution of DNA amount per nucleus and the number of DSBs corresponding to two cell phases: one for the logarithmic phase and the other for the plateau phase of the growth curve. The results show that the number of DSBs deduced with the two phases is in good agreement with the measured values.

### **Conclusions**

Our results suggest that the consideration of the DNA amount depending on the cell cycle and the probability density of energy deposition by X-ray irradiation are essential to estimate the number of DSBs accurately.

## **VERIFICATIONS OF GPU-BASED FAST RECONSTRUCTION ALGORITHM FOR NUCLEAR MEDICINE IMAGE UNDER POOR CONDITIONS USING THE MONTE CARLO SIMULATION**

Moo-Sub Kim, Do-Kun Yoon, Joo-Young Jung, Han-Back Shin, Sunmi Kim, Tae Suk Suh

The Catholic University of Korea, Republic of Korea

**Key words:** GPU, image reconstruction, Monte Carlo simulation, SPECT, PET

### **Purpose**

Purpose of this study is to develop a graphic processing unit (GPU) based fast reconstruction algorithm for a nuclear medicine image under poor conditions. And verifications of the developed algorithm are involved to achieve the purpose of this study.

### **Methods**

Simple pattern water phantoms including isotopes were designed using Monte Carlo simulation. And then SPECT and PET scanning processes are simulated to acquire the projection data. The image reconstruction was performed using the developed algorithm with GPU. After the acquisition of images, in order to verify the performance of algorithm, the analysis of image profile, SNR, contrast and reconstruction time were investigated through the comparison with reconstructed image including each different conditions.

### **Results**

The developed the GPU based fast iterative reconstruction algorithm for nuclear medicine image in order to provide fast computing process as well as good quality image in spite of poor condition such as low projection and low effective event number. The contrast and SNR results in each three RURs of the image using the GPU based fast iterative reconstruction algorithm was clearly better than the CPU based FBP algorithm.

### **Conclusions**

We confirmed the good performance of the developed GPU-based algorithm in that image reconstruction can be conducted in significantly short time and with relatively good image quality, compared with that using a conventional CPU-based algorithm under the same conditions.

## **EVALUATION OF THE ANALYTICAL ANISOTROPIC ALGORITHM IN LUNG CANCER FOR VMAT 6MV PHOTON BEAM USING MONTE CARLO SIMULATION**

Dian Nuramdiani<sup>1</sup>, Sitti Yani<sup>1</sup>, M Fadhillah Rhani<sup>2</sup>, Freddy Haryanto<sup>1</sup>

<sup>1</sup>ITB, Indonesia

<sup>2</sup>Tan Tock Seng Hospital

**Key words:** AAA, MC, VMAT delivery technique, DVH

### **Purpose**

In radiation therapy it is important to minimize the uncertainties in the treatment. Therapy requires accurate planning, dose calculations and radiotherapy techniques in order to provide the maximum dose for cancer tissue and minimum dose for healthy tissue. VMAT delivery technique is one of the radiotherapy technique developed to achieve the main goal of radiotherapy. The purpose of this study was to investigate the accuracy of AAA in lung cancer for VMAT delivery technique 6MV photon beam.

### **Methods**

The accuracy of AAA was evaluated by compared relative dose distribution with Monte Carlo. Simulation of VMAT with the MC algorithm performed using software EGSnrc/ BEAMnrc and DOSXYZnrc program. Parameters data reading from rtplan.dicom has been done to determine MLC leaf position, isocentre coordinate, the angles of gantry rotation, collimator angle, and amount of fraction dose given during treatments. The phantom is derived from CT data image in dicom format. It changed to phantom that can be read by DOSXYZnrc with using ctcreate. Simulations done using history of one billion particles are delivered through 114 control point.

### **Results**

Dose distributions difference between AAA and MC for VMAT delivery technique in lung cancer expressed by a deviation of DVH less than 5 %

### **Conclusions**

The results of this study suggest that AAA showed a good accuracy overall especially for volumetric modulated arc therapy technique.

## **ESTIMATION OF CONTAMINANT ELECTRON IN VARIAN TRILOGY CLINAC IX 10 MV PHOTON BEAM BASED ON MONTE CARLO SIMULATION**

Sitti Yani<sup>1</sup>, Mohamad Fahdillah Rhani<sup>2</sup>, Roger C.X. Soh Nanyang<sup>3</sup>, Freddy Haryanto<sup>1</sup>, Idam Arif<sup>1</sup>

<sup>1</sup>Institut Teknologi Bandung, Indonesia

<sup>2</sup>National University Cancer Institute Singapore

<sup>3</sup>Technological University, Indonesia

**Key words:** Monte Carlo, EGSnrc, Electron Contamination

### **Purpose**

The purpose of this study was to investigate the contaminant electron of Varian Trilogy Clinac iX 10 MV photon beam for field size 6x6, 10x10 and 20x20 cm<sup>2</sup> based on Monte Carlo (MC) simulation.

### **Methods**

The simulation studies have been performed using MC EGSnrc code system. The linac head calibrated by comparing the dose distribution calculated from MC and the measurement data in a water phantom. The particles released from linac stored in phase space (phsp) file. The phsp file after MLC was analyzed to characterize the characteristics of particles stored either photons or electrons. The water phantom with dimension 40x40x40 cm<sup>3</sup> was used to investigate the effect of contaminant electron. This effect was evaluated by subtracting the relative absorbed dose from all particles and photons in 0-5 cm depth for field size 6x6, 10x10 and 20x20 cm<sup>2</sup> in a water phantom. Moreover, the fluence, angular and spectral distribution of all particles, photons and electrons in phsp files quantified.

### **Results**

The presence of this contaminant electron in phase space (phsp) file contributed the dose distribution in the water phantom, especially on the phantom surface. These results reveal that the amount of electron increased with increasing of field size. The calculated relative dose distribution between all particles and photons show the difference more than 5%.

### **Conclusions**

This study demonstrated the accuracy of MC code in simulating the contaminant electrons of 10 MV photon beam. The electron doses in the phantom surface in the treatment planning cannot be ignored.

## **DOSE DISTRIBUTION OF TREATMENT ROOM FOR CARBON ION THERAPY**

Sungho Cho

KIRAMS, Republic of Korea

**Key words:** Electronic device failures, neutron dose, carbon ion therapy

### **Purpose**

In the treatment room for carbon ion therapy, there are many electronic devices like a sliding CT or other imaging hardware. In the case of ion beam therapy, the incident particle is primarily a ion and the emitted particles can essentially be any light or heavy particle such as photons, neutrons or alpha particles. But electronic systems are sensitive to radiation and may suffer a loss of function if exposed. So, our purpose is to investigate the dose distribution of treatment room for carbon ion therapy.

### **Methods**

The simulation was conducted using Fluka (version 2011.2b), a system to provide Monte Carlo particle transmission. The simulation model was built using PRECISIO parameters, the default provided in Fluka. Fluence and equivalent particle dose were calculated using the Fluka USRBIN card and DOSE-EQ parameters. Equivalent dose was estimated as the AMB74 parameter, calculated using the AUXSCORE card

### **Results**

Neutron dose for treatment room is approximately 0.002mSv to 0.1mSv per treatment Gy. Also, error is less than 0.3%. (we will attach dose map for treatment room)

### **Conclusions**

Electronic device is very sensitive for radiation dose. So, physicists should monitor it and shield if it is necessary.

## **A STUDY OF THE ELECTRON GRID THERAPY WITH A NOVEL TUNGSTEN FUNCTIONAL PAPER**

Hajime Monzen, Mikoto Tamura, Kazuki Kubo, Makoto Hirata, Yasumasa Nishimura

Kindai University, Japan

**Key words:** Electron GRID therapy, Tungsten functional paper, Monte Carlo method

### **Purpose**

Electron GRID therapy is expected to be valid treatment for bulky superficial tumors. Tungsten functional paper (TFP) is a novel paper containing radiation shielding material based on tungsten (lead-free) and easy to process. In this study, we investigated whether TFP could be used for electron GRID therapy.

### **Methods**

Dose distributions were measured using 9-MeV electron GRID beams from a Cerrobend GRID collimator. For the simulation study, the same GRID irradiation fields were shaped using the TFP GRID collimator (thicknesses of 0.15, 0.3, 0.6, 0.9, and 1.2 cm) by laid on a phantom. We calculated the dose distributions using a Monte Carlo method and compared the Cerrobend and TFP electron GRID beams regarding dose distributions, including the depths of the maximum dose ( $d_{max}$ ), 90% dose ( $d_{90}$ ), and 80% dose ( $d_{80}$ ), and the ratios of doses in the areas with/without shielding (valley-to-peak ratios). We determined the equivalent dosimetric thickness obtained with the TFP GRID collimator.

### **Results**

For the Cerrobend GRID collimator,  $d_{max}$ ,  $d_{90}$ , and  $d_{80}$  were 1.0, 2.1, and 2.5 cm, respectively, and the valley-to-peak ratios at those depths were approximately 0.48, 0.66, and 0.73, respectively. The 0.52-cm-thick TFP GRID collimators had equivalent dose distributions, and  $d_{max}$ ,  $d_{90}$ , and  $d_{80}$  were 1.1, 1.9, and 2.3 cm, respectively, and the valley-to-peak ratios at those depths were approximately 0.49, 0.63, and 0.71, respectively.

### **Conclusions**

The TFP GRID collimator could deliver excellent dose distributions flexibly and be used in the electron GRID therapy instead of the Cerrobend GRID collimator.

## **ESTIMATION OF EXTREMELY SMALL FIELD RADIATION DOSE FOR BRAIN STEREOTACTIC RADIOTHERAPY USING THE VERO4DRT SYSTEM**

Shinichi Nakayama<sup>1</sup>, Hajime Monzen<sup>2</sup>, Yutako Oyama<sup>1</sup>, Yuichi Onishi<sup>1</sup>, Hirofumi Enomoto<sup>1</sup>, Miharuru Oshima<sup>1</sup>, Soichiro Kaneshige<sup>2</sup>

<sup>1</sup>Division of Clinical Radiology Service, Okayama Central Hospital, Japan

<sup>2</sup>Department of Radiation Oncology, Kindai University Graduate School of Medicine

### **Key words**

Small field; Stereotactic radiotherapy; Vero4DRT

### **Purpose**

The purpose of this study was to estimate the adequacy of dose verification for an extremely small field regarding brain stereotactic radiotherapy (SRT) using the Vero4DRT system.

### **Methods**

The Vero 4DRT linear accelerator and treatment planning system (TPS) (iPlan Ver.4.5.1; algorithm XVMC) were used. We compared measurement data with calculation data, such as percentage depth dose (PDD), dose profile and absorbed dose in a small square field using an ionization chamber (0.01 cc or 0.04 cc). We performed dose verification for the extremely small field with the ionization chamber and radiochromic film (EBT3) (the equivalent field sizes used were 0.95, 0.82, 0.89, 1.29 and 0.87 cm<sup>2</sup>) using five brain SRT cases that were irradiated using two to four dynamic conformal arcs.

### **Results**

The PDD and dose profile were in good agreement when the data were compared. Slice thickness was observed to have a slight influence on the in-line dose profile. The dose differences concerning the absorbed dose in a small square field of 3x3, 2x2 and 1x1 cm<sup>2</sup> were 0.45, 1.0 and -1.6%, respectively. In the dose verification for the brain SRT plan, the dose differences between the calculated dose and the measured dose were -1.55% (range, -2.73 to -0.83%), and the average pass rates for the gamma index under the 3%/2 mm criterion were 96.71%, 93.37% and 97.58% in coronal, sagittal and axial plane, respectively.

### **Conclusions**

The Vero4DRT system has a feature that can be used to deliver accurate radiation doses to extremely small fields for brain SRT.

## Temperature characteristics of a Farmer ionization chamber in routine dosimetry of absorbed dose to water

Yuichi Kato<sup>1</sup>, Hiraku Fuse<sup>2</sup>, Yuki Doukawa<sup>2</sup>, Kazuya Shinoda<sup>1</sup>, Katsumi Miyamoto<sup>1</sup>, Shinji Abe<sup>2</sup>, Tatsuya Fujisaki<sup>2</sup>

<sup>1</sup> Tsukuba Medical Center Hospital, Tsukuba City, Japan; <sup>2</sup> Ibaraki Prefectural University of Health Sciences, Ami Town, Japan

**Key words:** Farmer Ionization Chamber, Thermal Equilibration Time, Temperature Characteristic

**Introduction:** A Farmer ionization chamber of waterproof type PTW 30013 is most widely used dosimeter for accurate dose determinations in external therapeutic beam. The aim of the present study were to measure the thermal equilibrium time by direct temperature measurement in the cavity air of a Farmer ionization chamber type PTW 30013 and verifies the validity of the temperature correction to the electric charge changing inside a cavity for various water temperatures.

**Methods:** The Farmer ionization chamber's electrode was replaced by a thin thermocouple for measuring the air temperature inside a cavity of a chamber that called "Created chamber" in this study. The thermal equilibration time of a chamber were taken in a homemade water bath phantom which provides changing a water temperature. The equipment was placed in a water phantom as indicated in Fig.1. Ionization produced inside a chamber was also measured to clarify the variation of absorbed dose by changing inside a cavity temperature.

**Results:** The thermal equilibration time of the chamber in a water phantom is shown in Fig.2. This study presents the thermal equilibrium time depends on the initial temperature difference that was shown to be between 30 s to 50 s. The Farmer chamber response is shown in Fig.3. The temperature characteristic of a Farmer chamber was under 0.1 % from the ideal response by difference of 8 °C.

**Discussion:** Giessen and Tailor et al. had measured the thermal equilibrium time using rubber sleeve having a thickness of approximately 2 mm for waterproofing the Farmer chamber [1] [2]. This experiment yields that the thermal equilibrium time in a water was up to 78 s. It is thought that in the heat conduction between in the rubber sleeve and the waterproofing materials. The measurement results at room temperature 22 °C, 25 °C and 28 °C are showed strong correlation. Therefore, a cavity temperature is hardly affected by the difference of the room temperature. Corrected response of the environment range of routine dosimetry measurements were substantially the same as the previous study [3].

**Conclusion:** We were investigated that the thermal equilibrium time by direct temperature measurement in the air cavity of a chamber and the validity of the temperature correction using Farmer chamber with a photon beam. Thermal equilibrium time was up to 50 s for the various initial temperature difference. The validity of the temperature correction using Farmer chamber was different about 0.1% from the ideal response.

### References:

1. van der Giessen PH. About the rate of temperature changes in a thimble chamber. *Radiat Oncol* 1986; 7(3): 287-291.
2. Tailor RC, Chu C, Followill DS, Hanson WF. Equilibration of air temperature inside the thimble of a Farmer-type ion chamber. *Med Phys*, 1998; 25(4): 496-502.
3. AlMasri HI, Funyu A, Kakinohana Y, Murayama S. Investigation of thermal and temporal responses of ionization chambers in radiation dosimetry. *Radiol Phys Technol* 2012; 5(2):172-177

Corresponding author email: ykato0906@yahoo.co.jp

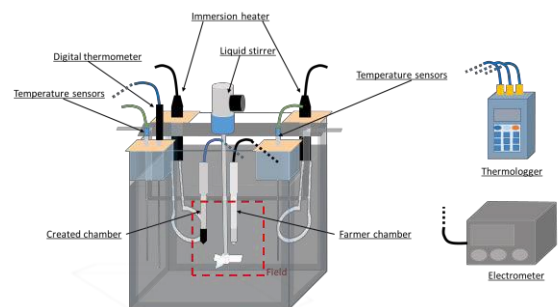


Fig. 1 Picture of the experimental set-up layout.

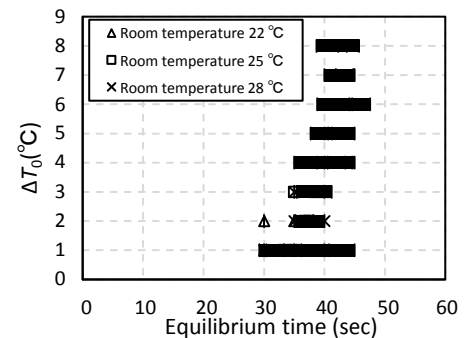


Fig. 2 The data represent thermal equilibrium time of Farmer chamber r in a water. Errors bars represent one standard deviation.

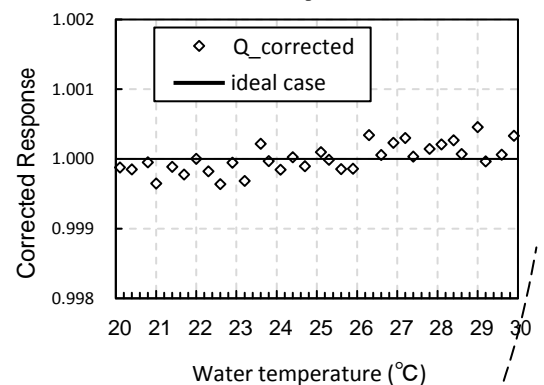


Fig. 3 The data represent responses of the ionization chamber from the ideal gas law after temperature and pressure correction and normalizing at 22 °C.

## **A NEW FABRICATION METHOD FOR SECONDARY SKIN COLLIMATION USING 3D SCANNER AND 3D PRINTER**

Joo-Young Jung<sup>1</sup>, Bo Lu<sup>2</sup>, Chihray Liu<sup>2</sup>, Tae Suk Suh<sup>1</sup>

<sup>1</sup> Catholic University of Korea, Republic of Korea

<sup>2</sup> University of Florida, US

### **Key words**

Secondary skin collimator, Orthovoltage treatment, 3D printing, 3D scanning

### **Purpose**

Using secondary skin collimator (SSC) to protect the critical organ surrounding the tumors is always desirable for electron and/or ortho-voltage treatments. The aim of this study is to develop a new SSC fabrication method using 3D scanning and 3D printing technologies in order to largely decrease the human labor involvement and fabrication time, also improve the fabrication accuracy.

### **Methods**

First, the patient surface was scanned with a 3D scanner. The raw scan data was subsequently transferred to a 3D modeling software. The tumor contour was then digitized and shielding region was determined by clinicians in the same software. The corresponding SCC conformed to the skin surface was then automatically generated by the software with the proper shielding thickness. The shell of the SCC (with hollow inside) was consequently printed by a 3D printer using plastic material. Finally, the hollow mold of SCC was filled up with a melted cerrobend alloy.

### **Results**

The results indicated the proposed method can achieve a much shorter time on making a SCC compared with tradition fabrication method. The processes of making a skin contour model for patients have been eliminated with the new method. SCC created by the new method possessed better accuracy and better conformality to patient's skin contours.

### **Conclusions**

In this study, we have demonstrated a new method for the SCC fabrication. It is anticipated that our method can be an alternative way to replace conventional manual-based methods for electron and/or ortho-voltage SCC fabrication.

## **INVESTIGATION OF AAA AND ACUROSXB ALGORITHMS FOR THREE DIFFERENT STEREOTACTIC ABLATIVE RADIOTHERAPY TECHNIQUES (SABR): VOLUMETRIC MODULATED ARC THERAPY (VMAT), INTENSITY MODULATED RADIATION THERAPY (IMRT) AND 3D CONFORMAL RADIOTHERAPY (3D-CRT)**

Abdulrahman Tajaldeen

Rmit University, Melbourne Australia

**Key words:** Anisotropic Analytical Algorithm (AAA) AcurosXB; Volumetric Modulated Arc Therapy (VMAT); Intensity modulated radiation therapy (IMRT); 3D Conformal Radiotherapy (3D-CRT)

### **Purpose**

To investigate the dosimetric changes between three different SABR techniques: volumetric modulated arc therapy (VMAT), intensity modulated radiation therapy (IMRT) and 3D conformal radiotherapy involving non-coplanar beams (3D-CRT) by using two different algorithms: Anisotropic Analytical Algorithm (AAA) and AcurosXB.

### **Methods**

This study was performed for twelve patients undergoing lung cancer radiotherapy. Three different plans viz: VMAT, IMRT, SABR were generated for all these patients. The tumour volume ranged from 5.15 cc to 47.39 cc (mean: 23.55 cc  $\pm$  12.90). One of the main criteria during planning was to ensure 99% of the tumour volume received 100% of the prescription dose (26 Gy). Dose calculation was performed using anisotropic analytical algorithm (AAA) and AcurosXB in Eclipse treatment planning system. The following dosimetric indices were used to compare the treatment plans: Conformity, homogeneity, dose fall off index, D5, D95, V20 for lung, dose maximum to heart, oesophagus and spinal cord.

### **Results**

We observed significant variation among the three different techniques for most of the dosimetric parameters. The mean conformity indices for VMAT, IMRT and 3D-CRT techniques for AAA calculation and AcurosXB algorithms were 1.21 $\pm$ 0.08, 1.28 $\pm$ 0.12, 1.38 $\pm$ 0.22 and 1.17 $\pm$ 0.07, 1.26 $\pm$ 0.13, 1.36 $\pm$ 0.15 respectively.

### **Conclusions**

The VMAT technique provides better conformity and homogeneity index as compared to the IMRT and 3D-CRT techniques. Also, this study proves that the Acuros XB algorithms can provide better results in the planning process for different techniques, especially when treating heterogeneous medium-like lungs.

## ANALYSIS OF THE SPATIAL DOSE DISTRIBUTION IN TSEB THERAPY

**Dilvoi Maria, Patatoukas George, Kouloulis Vassilis, Georgakopoulos John, Kypraiou Eyfrosini, Kougioumtsoyopoulou Andromachi, Trogkanis Nikolaos, Efstathopoulos Efstathios, Platoni Kalliopi.**

2<sup>nd</sup> Department of Radiology, University General Hospital ‘Attikon’, School of Medicine, National and Kapodistrian University of Athens. Athens, Greece

**Key words:** TSEB, Electron, TLD, Dosimetry

**Purpose:** The purpose of the current work is to present a basic statistical analysis of the spatial distribution of the over- and under- dosage areas in Total Skin Electron Beam (TSEB) patients treated in our Radiotherapy Department.

**Methods:** Since its initial implementation in our department’s clinical routine, 12 patients diagnosed with cutaneous T-cell lymphoma (CGTL) have been treated using the ‘SIX DUAL FIELD’ or ‘STANFORD TECHNIQUE’ tailored to our department’s needs. Our clinical therapeutic protocol incorporates a two-day irradiation scheme, yielding a total session skin dose of 2Gy. Our dosimetry protocol introduces LiF –based TLD dosimetry at various pre-defined points on the patient’s body for dosimetry-based patient position verification. Dosimetry is always performed in the first two fractions and at various randomly selected time points during the course of the therapy to ensure adequate dose coverage. Emphasis is given to areas that receive less than 80% (under-dose) or more than 120% (over-dose) of the dose prescribed by the physician.

**Results:** Our analysis indicates that under-dose and over-dose areas are obtained in all patients regardless of age and sex. In more than 50 % of the cases ‘under-dose’ regions, in both upper extremities, and ‘over-dose’ regions, in both lower extremities, were observed.

Table1. Average over-dose and under-dose in upper and lower extremities.

| PATIENTS | AVERAGE OVER-DOSE AT UPPER EXTREMIT IES(Gy) | AVERAGE OVER-DOSE AT LOW EXTREMIT IES(Gy) | AVERAGE UNDER-DOSE AT UPPER EXTREMIT IES(Gy) | AVERAGE UNDER-DOSE AT LOW EXTREMIT IES(Gy) |
|----------|---|---|--|--|
| 1        | 2,8   | 2,6                                       | 1,5  | 1,6  |
| 2        | 2,4   | -   | 1,3  | 1,3  |
| 3        | 2,9   | 2,7                                       | -  | -  |
| 4        | 3,5   | 2,5                                       | 1,4  | 1,4  |
| 5        | -   | 2,6                                       | 1,6  | -  |
| 6        | 2,4   | 2,4                                       | 1,5  | -  |
| 7        | -   | -   | 1,5  | 1,6  |
| 8        | -   | 2,7                                       | 1,5  | 1,6  |
| 9        | -   | 2,9                                       | 1,6  | 0,7385                                     |
| 10       | -   | -   | 1,4  | 1,1  |
| 11       | 2,6   | 2,9                                       | 1,6  | 1,5  |
| 12       | 2,7   | 3   | 1,6  | 1,6  |

**Discussion:** No significant differences were obtained along the patients’ lateral or central AP-PA axis.

**Conclusion:** Dose recording and analysis of the spatial distribution of the under-dose and over-dose areas in patients treated with TSEB is vital in providing feedback regarding the radiation treatment procedure and eventually affecting the therapeutic outcome.

**References:**

- [1] Diamantopoulos S, Platoni K, Dilvoi M, Nazos I, Geropantas K, Maravelis G, Tolia M, Beli I, Efstathopoulos E, Pantelakos P, Panayiotakis G, Kouloulis V. Clinical implementation of total skin electron beam (TSEB) therapy: a review of the relevant literature. *Phys Med.* 2011 Apr;27(2):62-8
  - [2] Platoni K, Diamantopoulos S, Panayiotakis G, Kouloulis V, Pantelakos P, Kelekis N, Efstathopoulos E. First application of total skin electron beam irradiation in Greece: setup, measurements and dosimetry. *Phys Med.* 2012 Apr;28(2):174-82.
  - [3] Diamantopoulos S, Platoni K, Kouloulis V, Pantelakos P, Dilvoi M, Papadavid E, Antoniou C, Efstathopoulos E. First treatment of mycosis fungoides by total skin electron beam (TSEB) therapy in Greece. *Rep Pract Oncol Radiother.* 2013 Aug 13;19(2):114-9.
- Corresponding author email:** dilbomar@yahoo.gr

## EVALUATION OF THE SCANNING AND MICRO IONIZATION CHAMBERS FOR STANDARD DOSIMETRY IN PHOTON BEAM

Tetsuro Katayose<sup>1</sup>, Toru Kawachi<sup>1</sup>, Hidetoshi Saitoh<sup>2</sup>, Weishan Chang<sup>2</sup>, Eri Iriyama<sup>2</sup>

<sup>1</sup>Chiba Cancer Center, Japan

<sup>2</sup>Tokyo Metropolitan University

### Key words

Standard dosimetry, Micro ionization chamber

### Purpose

Scanning or micro ionization chamber are useful for standard dosimetry of flattening filter free beam or CyberKnife beam. In this report, characteristic of scanning and micro chamber was evaluated for the standard dosimetry.

### Methods

The scanning (31021, PTW) and micro (A26, Standard Imaging) ionization chamber are new designed small type chambers. Characteristics of the 31021 and A26 were evaluated based on specification of the addendum to the AAPM TG-51. The stabilization, leakage current, ion recombination and polarity effect of these chambers were evaluated in megavoltage photon beams (from 4 to 10 MV).

### Results

Reciprocal of reading  $\langle I \rangle M \langle I \rangle$  ( $1/\langle I \rangle M \langle I \rangle$ ) varied linearly with reciprocal of polarizing voltage  $\langle I \rangle V \langle I \rangle$  ( $1/\langle I \rangle V \langle I \rangle$ ) range from 50 V to 250 V for 31021, and from 50 V to 200 V for A26. When polarizing voltage was set to 200V, 31021 satisfied specification of the addendum. However, initial recombination of A26 exceeded specification of the addendum (1.002). In some cases, stabilization time ( $\pm 0.1\%$  of saturation current) of A26 exceeded 5 minutes which is recommended by the addendum.

### Conclusions

The 31021 satisfied specification of the addendum. If A26 were used for standard dosimetry, it is necessary to pay attention to stabilization time and consistency of ion recombination between  $^{60}\text{Co}$  calibration and user beam. Since long-term stability was not evaluated in this report, further investigation is needed.

## COMPARISON OF CARDIAC AND LUNG DOSES FOR BREAST CANCER PATIENTS WITH FREE BREATHING AND BREATH HOLD TECHNIQUE - A DOSIMETRIC STUDY

Suresh Poudel<sup>1</sup>, Hasin Anupama Azhari<sup>2</sup>, Karthick Raj Mani<sup>3</sup>, Golam Abu Zakaria<sup>2</sup>

<sup>1</sup>Nepal Cancer Hospital and Research Center, Nepal

<sup>2</sup>Gono University

<sup>3</sup>United Hospital

### Purpose

To investigate the cardio-pulmonary doses to assess change in morbidity between Deep Inspiration Breath Hold and Free Breathing technique in left sided breast irradiation

### Methods

DIBH CT and FB CT were acquired for 10 Ca-breast patients who underwent whole breast irradiation. Three fields and two tangential fields with single iso-center techniques were used for patients in node positive and node negative patients respectively. All the critical structures were delineated in both DIBH & FB scan. Both scans with same dicom coordinates were fused. The critical structures of the FB scan were transferred to DIBH dataset with reference to dicom origin. Plans were created in the DIBH scan for a dose range between 50Gy in 25 fractions. Critical structures doses were recorded from the DVH for both the DIBH and FB data set for evaluation.

### Results

DIBH average mean heart dose as compared to FB reduced (13.18 Gy vs 6.97 Gy,  $p=0.0063$ ) significantly. Relative V5 (34.42Vs19.72; $p=0.0080$ ), V10(27.79vs13.96; $p=0.0073$ ), V20(24.54vs11.35; $p=0.0069$ ), & V30(22.27vs9.89; $p=0.0073$ ) reduced significantly with DIBH as compared to FB. Compared to FB, DIBH average mean left lung dose reduced slightly by 1.43 Gy (13.73 Gy vs 12.30 Gy; $p=0.4599$ ) but insignificantly. Relative V5(37.95Vs36.69; $p=0.0798$ ), V10(30.20vs27.49; $p=0.0539$ ), V20(26.05 vs 22.91; $p=0.4451$ ), V30(23.75vs20.85; $p=0.4585$ ) decreased but insignificantly with DIBH as compared to FB.

### Conclusions

DIBH shows a substantial reduction of cardiac doses but slight and insignificant reduction of pulmonary doses as compared with FB technique. Using the simple DIBH technique, we can effectively reduce the cardiac morbidity and at the same time radiation induced lung pneumonitis is unlikely to increase.

## **DOSE DISTRIBUTION OF THE INFIELT AND OUTFIELD BY USING WEDGE FILTER**

Yon-Lae Kim

Choonhae College of Health Sciences, Republic of Korea

### **Key words**

Metal wedge, Enhanced dynamic wedge, Gafchromic EBT3 film, Surface dose, Build up region dose

### **Purpose**

Wedge filter could be used to increase the dose distribution at the hot dose regions. We evaluated dose discrepancy at surface and build up region in the infield and outfield where Metal Wedge (MW) and Enhanced Dynamic Wedge (EDW) were interacting with photon.

### **Methods**

In this paper, we used Gafchromic EBT3 film that had excellent spatial resolution, composed the water equivalent materials and changed the optical density without development. The set up conditions of linear accelerator were fixed 6 MV photon, 100 SSD, 10×10 field size and were irradiated 400 cGy at Dmax. The dose distribution and absorbed dose were evaluated when we compared the open field with 15°, 30°, 45° metal wedge and enhanced dynamic wedge.

### **Results**

A 15° metal wedge could increase the surface and build up region dose more than using a 15° enhanced dynamic wedge. A 30° metal wedge could decrease the surface and build up region dose more than using a 30° enhanced dynamic wedge. A 45° metal wedge could decrease by large deviation the surface and build up region dose than using a 15° enhanced dynamic wedge. The dose of penumbra region at outfield was increased on the thick side but was decreased on the thin side.

### **Conclusions**

It is possible to reduce the surface dose and build up region dose, if the metal wedge filters were properly used to make a good dose distribution and if not at close distance to the surface.

## **IMRT COMMISSIONING OF THE ELEKTA VERSAHD LINEAR ACCELERATOR AND MONACO TREATMENT PLANNING SYSTEM**

Dahl Park<sup>1</sup>, Haryung Park<sup>2</sup>, Yongho Kim<sup>2</sup>, Won Taek Kim<sup>2</sup>, Yongkan Ki<sup>2</sup>, Donghyun Kim<sup>2</sup>, Jinsook Bae<sup>2</sup>

<sup>1</sup>Medical Research Institute, Pusan National University Hospital, South Korea

<sup>2</sup>Pusan National University Hospital

### **Key words**

IMRT, commissioning, VersaHD, Monaco

### **Purpose**

The purpose of this study is to assess the accuracy of planning and delivery of IMRT treatments. Monaco treatment planning system (TPS) with Monte Carlo dose calculation algorithm was used for the IMRT planning. Elekta VersaHD linear accelerator with 6 MV, 10 MV, 15 MV, 6 MV FFF, 10 MV FFF x-rays and the Agility MLC which has leaf width of 5 mm at the isocenter was used for the IMRT delivery.

### **Methods**

We performed the verification using the process proposed in AAPM TG119 report. A set of IMRT cases was planned using the CT images of rectangular phantom for each x-ray energy. The planned doses and measured doses were compared. Ion chamber CC13 was used for the point dose comparison in high and low dose regions. EBT3 films were used for the comparison of coronal planar doses with all fields delivered. Two-dimensional ion chamber array MatriXX was used for the field-by-field verification with the gantry angle zero. The gamma-index analysis with criteria 3%/3 mm was used for the comparison of planar doses. Confidence limits were calculated for each test results and compared with the values reported in TG119.

### **Results**

Average confidence limits for high dose, low dose, film and MatriXX measurements were 0.024, 0.025, 95.54 and 99.07, respectively. The results showed that the accuracy of test IMRT cases was better than the one reported in TG119.

### **Conclusions**

IMRT commissioning of the Elekta VersaHD linear accelerator and Monaco TPS was successfully performed for all the photon energies.

## **SPINE SBRT DOSIMETRIC VERIFICATION USING MOSKIN DETECTORS**

Wei Loong Jong<sup>1</sup>, Ngie Min Ung<sup>1</sup>, Jeannie Hsiu Ding Wong<sup>1</sup>, Kwan Hoong Ng<sup>1</sup>, Anatoly Rosenfeld<sup>2</sup>

<sup>1</sup>University Of Malaya, Malaysia

<sup>2</sup>University Of Wollongong

### **Key words**

Stereotactic, MOSFET, Dosimetry, Quality assurance,

### **Purpose**

To investigate the feasibility of the MOSkin detectors for dosimetric verification in the steep dose gradient regions during spine stereotactic body radiotherapy (SBRT).

### **Methods**

Ten clinical approved spine (cervical, thoracic and lumbar) SBRT plans were selected for dosimetric verification in an anthropomorphic phantom. These plans were delivered using either volumetric-modulated arc therapy (VMAT) or intensity-modulated radiotherapy (IMRT). The detectors were positioned around the target and spinal cord inside the phantom. All MOSkin measurements were compared against film measurements and treatment planning calculations.

### **Results**

The position of the MOSkin detectors was verified using cone-beam computed tomography before the dose delivery. For the dose inside the target, the MOSkin measurements were in good agreement with film measurement and treatment planning calculations. For the dose around the spinal cord, despite of the very high dose gradient region, the MOSkin measurements were in acceptable agreement with film measurement and treatment planning calculations.

### **Conclusions**

This work shows that the MOSkin detectors are a suitable tool for dosimetric verification in the steep dose gradient regions during spine SBRT.

## **MEASUREMENT OF PHANTOM SKIN DOSE ASSOCIATED WITH DIFFERENT THICKNESS OF BOLUS FOR BREAST CANCER HELICAL TOMOTHERAPY USING OPTICAL STIMULATED LUMINESCENCE DOSIMETER**

P. Khanngoon<sup>1</sup>, D. Tippanya<sup>1</sup>, W. Nopnop<sup>1</sup>, S. Wanwilairat<sup>1</sup> and I. Chitapanarux<sup>1</sup>

<sup>1</sup>Department of Radiology, Faculty of Medicine, Chiang Mai University, Chiang Mai, Thailand

**Key words:** Helical tomotherapy, Tissue equivalence material, OSL.

### **Purpose**

To measure radiation dose of the Rando phantom skin with different tissue equivalent material thicknesses using OSL dosimetry for breast cancer helical tomotherapy application.

### **Methods**

Breast cancer treatment plans of 6MV photon irradiated 2.65 Gy in 16 fractions were generated using Helical Tomotherapy (HT) treatment planning system. The CT images of Rando phantom chest wall without bolus and bolus thickness 0.5, 1.0, 1.5, 2.0 cm were used for HT planning. The OSL dosimeters were placed at different three points on the phantom's surface to measure the skin dose. The planned doses were delivered to the phantom on HT unit. The OSL measurement doses were compared to the TPS calculation doses and the planning target volume dose.

### **Results**

The average skin dose measurement using OSL dosimeters at three different positions on phantom chest wall had a standard deviation between 0.54 – 3.95%. The average percentage dose difference between the OSL measurement and TPS calculation were 3.66%, 5.14%, 1.87%, 3.20% and 4.17% for no bolus and bolus thickness 0.5, 1.0, 1.5 and 2.0 cm, respectively. The average percentage of OSL dose normalize to PTV fraction dose (2.65 Gy) were 78.12%, 94.75%, 94.06%, 93.64% and 97.44% for no bolus and bolus thickness 0.5, 1.0, 1.5 and 2.0 cm, respectively.

### **Conclusions**

The skin dose measurement using OSL dosimeter in HT had accuracy between 1.87% - 5.14% compared to the treatment planning calculation. The tissue equivalent material of thickness more than 0.5 cm can provide skin dose more than 90% in HT breast cancer irradiation.

## PROPOSAL FOR THE GAMMA-RAY POSITION MEASURING SYSTEM USING $e^+ / e^-$ PAIR PRODUCTION EVENTS

Shota KIMURA, Yusaku EMOTO, Kento FUJIHARA, Hiroshi ITO, Naomi KANEKO, Hideyuki KAWAI, Atsushi KOBAYASHI, Takahiro MIZUNO  
 Dept. Of Physics, Chiba University, JAPAN

**Key words:** pair production, position measuring, Geant4

**Introduction:** In the region of particle beam therapy, to identify dose points, PET detectors or Compton cameras have been studied. However, these systems haven't got competent performance yet. We propose the system which measures pair production events occurred in the system by gamma-rays over 20 MeV come from exposed points. This system can define incidence points and directions.

**Methods:** This system consists of 20 layers of detectors at 10 mm distances. Each layer is composed of wavelength shifting fibre (WLSF) sheets and a GAGG scintillation board of 1.0 mm thickness. An area of each board is  $300 \times 300 \text{ mm}^2$ . Sheets are made by ordering WLSF with a diameter of 0.2 mm. The board is sandwiched in sheets, and directions of the sheets are in orthogonal (an illustration is on Fig.1). Gamma-rays which energy is over 7 MeV are more likely to create an  $e^+ / e^-$  pair than being scattered [1]. The light yield at the pair produced layer is unstable, but at following layers, particles consume 1.8 MeV of energy on average. In case Compton scattering has occurred the energy loss in following layers are 0.8 MeV in average. Sometimes a pair annihilated gamma-ray loses energy at a former layer, but such energy loss is under 511 keV. Therefore, we can extract pair production events if there is 1.3-2.3 MeV loss of energy at few layers continually.

Monte Carlo simulations were performed by Geant4. First, gamma-rays were shot to the system, then counted events that  $e^+$  are found on scintillation boards. Data of total energy deposit on scintillation boards was taken, as well as their positions. If there is some energy deposit over 511 keV, and 1.3-2.3 MeV at following 2 layers, it was judged that the event is a pair production event. The

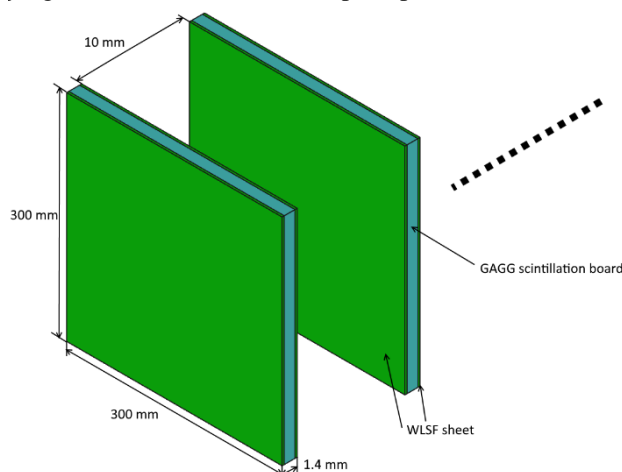


Fig.1 The illustration of our system.

gamma-rays' energy was changed in the range of 10-51 MeV.

**Results:** It was confirmed that our system can define pair production events over 70% accuracy when gamma-rays' energy are 20 MeV (Fig.2). Our team is now in the process of calculating deviations from gamma-rays' expected trajectories. We are expecting that our detector can distinguish 2 particles passing from 1 particle passing.

**Discussion:** The ratio of events that is found  $e^+$  on scintillation boards are lower than expected. This ratio may improve by changing thicknesses of scintillation boards.

Non-expensive and high performance scintillation boards can serve the purpose and therefore, we estimate the cost will be very low.

**Conclusion:** This system has a potential to be a high resolution gamma-ray position measuring system. It could be useful in many regions of Physics.

### References:

- Olive, K. A., Agashe, K., Amsler, C., et al. (Particle Data Group), REVIEW OF PARTICLE PHYSICS, CHINESE PHYSICS C, 38, 9, (2014)

Corresponding author email: shota\_kimura@hepburn.s.chiba-u.ac.jp

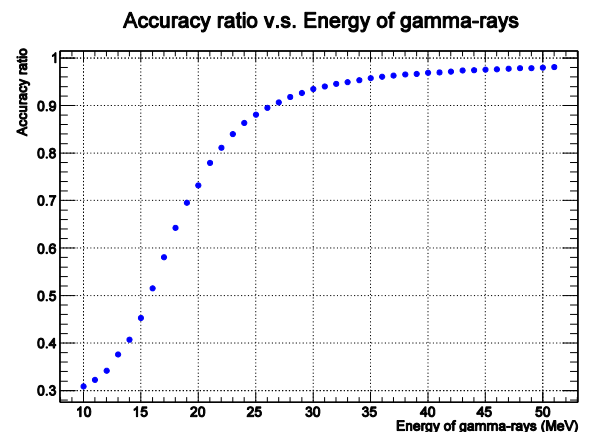


Fig.2 Energy dependency of our system's accuracy ratio that is the ratio of well-judged events to events that are judged as pair production events. When gamma-rays' energy is 20 MeV, over 70% of judges are collect.

## **CLINICAL IMPLEMENTATION AND ASSESSMENT OF RAYSTATION ELECTRON MONTE CARLO (EMC)**

Dayan Loria

Auckland Radiation Oncology, New Zealand

### **Key words**

Raystation, Electron Monte Carlo

### **Purpose**

This study aims to assess the Electron Monte Carlo beam model in Raystation Treatment Planning System.

### **Methods**

A number of tests were performed for 6, 9, and 12 MeV for 3 matched Elekta machines at 100 cm and 110 cm SSD. The calculated output factors, PDDs and profiles for open, irregular fields, and oblique incidence were compared to water tank measurements using the in-house 1D gamma spreadsheet. The dose calculated for in-homogeneity, different bolus thicknesses, and clinical plans were compared to chamber or diode measurements. The calculated 2D planes at  $d_{max}$  in solid water and for in-homogeneity assessment were compared to MatriXX 2D array measurements and the photon-electron junctions were compared using film dosimetry.

### **Results**

The output factors and other dose comparison at  $d_{max}$  were within 5%. The result using 1D gamma criterion 3%/3mm for PDD and profiles for open, irregular fields, and oblique incidence were satisfactory. However some profiles, particularly for large fields needs improvement due to penumbral mismatches. All 2D gamma analyses (3%/3mm) were >95%.

### **Conclusions**

The dose to irregular surface that resembles to body contour was not evaluated. Thus the beam model is acceptable for clinical use with certain restrictions to cases where the number of MUs is more than 3% compared to the measured MUs in flat phantom. These cases were reviewed for the amount of missing tissue, obliquity and tissue variation to be used for further development.

# Reduction in Imaging Doses with CyberKnife Using a New Real-time Monitoring System for Intracranial Treatments

HInata<sup>1</sup>, Y Nakaguchi<sup>2</sup>, Y Kuribayashi<sup>1</sup>, N Sodeoka<sup>1</sup>, S Nakayama<sup>1</sup>

<sup>1</sup>SaiseikaiImabari Hospital, Japan; <sup>2</sup> Kumamoto University Hospital, Japan

**Key words:** real-time monitoring, CyberKnife, imaging dose, intracranial

**Purpose:** Although the CyberKnife system accurately detects head displacement with the Target Locating System (TLS), it cannot adequately adjust for abrupt and fluctuating motion without an imaging dose. The purpose of this study was to retrospectively estimate the reduction ratio of the imaging dose for the combination of our real-time monitoring system [1] and TLS.

**Methods:** Our system has the ability to continuously monitor head motion during treatments without an imaging dose. When head displacement is detected beyond the threshold value by our system during every interval of TLS acquisition, the head position is reconfirmed by TLS. We analyzed 33 patients, 159 plans, and 5435 head displacements and assumed that the probability distribution of head displacement detected by the TLS is nearly identical with that of the actual head displacement. Head displacement was divided by a threshold value of 1 mm using a 2 × 2 confusion matrix [2]. The reduction ratio of the imaging dose was then estimated for the combination of our system and TLS in proportion to the broadening interval of TLS acquisition.

**Results and Discussion:** The reduction ratio of the imaging dose was estimated to be 24-73% in proportion to 1-10-minute intervals of TLS acquisition by the combination of our new system and TLS. Errors in the detection of head displacement beyond 1 mm were reduced by the combination of our new system and TLS.

**Conclusion:** The combination of our system and TLS may reduce the imaging dose to 24-73% with high positioning accuracy in CyberKnife treatments.

**References:**

1. Inata H, Araki F, Kuribayashi Y, Hamamoto Y, Nakayama S, Sodeoka N, Kiriyama T, &Nishizaki O. Development of a real-time monitoring system for intra-fractional motion in intracranial treatment using pressure sensors. *Physics in Medicine and Biology*. 2015, 60(18): 7229-7243.
2. Edward L N. *Applications of Statistics to Medicine and Medical Physics*. Medical Physics Publishing. 2011, Madison, WI.

Corresponding author email: inata.hiroki@gmail.com

**Key Methods and Results**

Table 1 shows a 2 × 2 confusion matrix to divide head displacements with a threshold value of 1 mm. TLS acquisition was performed every TLS interval (1-10minute) and additional TLS acquisition was performed when displacement detected by our new system was beyond 1 mm (True Positive and False Positive). The displacement was reset to “zero” position at every TLS acquisition in the Cyberknife treatment. Errors in the detection of head displacement beyond 1 mm also were related to False Negative. Therefore reduction ratio of imaging dose and errors in the detection of head displacement beyond 1 mm were calculated by following equations.

$$\text{Reduction ratio of imaging dose} = \frac{1}{\frac{\text{Number of TLS acquisitions for the combination of our system and TLS}}{\text{Total number of TLS acquisitions}}} \quad (1)$$

$$\text{Errors} = \frac{\text{Number of False Negative}}{\text{Total number of TLS acquisitions}} \quad (2)$$

Table 2 shows the result of reduction ratio of the imaging dose and errors in the detection of head displacement beyond 1 mm for the combination of our new system and TLS.

Table 1. Confusion matrix to divide head displacements with a threshold value of 1 mm.

| Test Result    | Target Locating System (reference) |                        |
|----------------|------------------------------------|------------------------|
|                | Positive: more than 1 mm           | Negative: 1 mm or less |
| Our new System | True Positive (TP)                 | False Positive (FP)    |
|                | False Negative (FN)                | True Negative (TN)     |

Table 2. Reduction ratio of the imaging dose and errors in the detection of head displacement beyond 1 mm for the combination of our new system and TLS in proportion to 1-10-minute intervals of TLS acquisition.

| Interval of TLS acquisition (minute) | Reduction ratio of the imaging dose | Errors  |
|--------------------------------------|-------------------------------------|---------|
| 1                                    | 24 %                                | 0.4 %   |
| 2                                    | 48 %                                | 0.5 %   |
| 3                                    | 58 %                                | 0.6 %   |
| 5                                    | 67 %                                | 0.7 %   |
| 7                                    | 71 %                                | 0.9 %   |
| 10                                   | 73 %                                | 1.0 %   |
| (50)                                 | (74 %)                              | (1.3 %) |

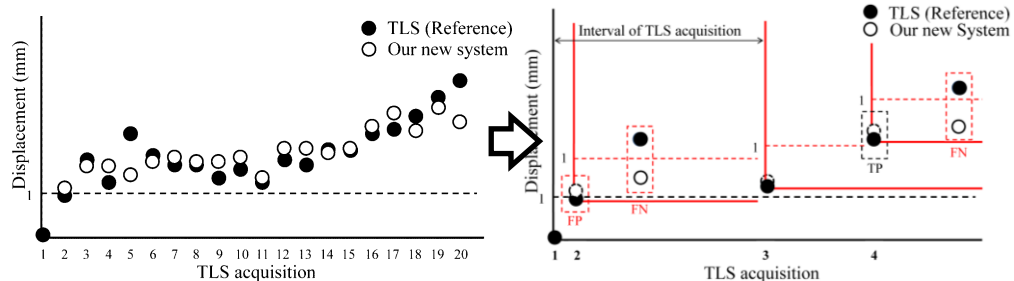


Fig.1 Small section of a recorded motion pattern of a patient. The primary goal of the analysis is to count a number of TLS acquisitions for the combination of our new system and TLS. In this case, a total number of TLS acquisitions was reduced from 20 to 4 times. TLS = Target Locating System, TP = True Positive, FP = False Positive, FN = False Negative.

## **AN IMAGE RECONSTRUCTION METHOD USING ELECTRON BEAM MODE OF LINEAR ACCELERATOR**

Atsushi Myojoyama, Hidetoshi Saitoh, Takahito Chiba, Masatsugu Hariu  
Tokyo Metropolitan University, Tokyo, Japan

### **Purpose**

Megavoltage portal images are used to verify the proper positioning of the patient in image-guided radiation therapy (IGRT). However, portal images are not used in electron therapy. To reduce patients unnecessary absorption dose, we designed the portal imaging method using the electron beam mode of linear accelerator.

### **Methods**

The copper and aluminum filters were arranged on EPID surface. Using this method, patient images could be acquired during electron beam treatment. The quality of the images acquired by electron beam were improved using a wavelet analysis. We developed the portal image reconstruction system by using Qt 5.6 (C++), OpenCV3.0 library and CUDA (NVIDIA).

### **Results**

The image which the filter was arranged on EPID was similar to the image which the target was arranged at the front of patient. The image acquired by 4MeV was high contrast and noisy. The image acquired by 9MeV was the smallest noise and low contrast. Therefore, the image acquired by 6MeV was the best result.

### **Conclusions**

When the filter was arranged on EPID, the portal images could be acquired during electron therapy. The portal images could be acquired every electronic energy, but the weight of the filter was considered, and we assumed that 6 MeV was most suitable.

### **Key words**

electron therapy, portal imaging, GPGPU, realtime reconstruction

## **BASIC VERIFICATION OF RESPIRATORY-GATED INTENSITY MODULATED RADIATION THERAPY USING A REAL-TIME TUMOR- TRACKING RADIOTHERAPY SYSTEM**

Shigetoshi Noda<sup>1</sup>, Yusuke Watanabe<sup>2</sup>, Nobuaki Syuto<sup>1</sup>, Yui Akimoto<sup>3</sup>, Tomoya Fukumitsu<sup>3</sup>, Kou Eguchi<sup>3</sup>, Hiromichi Ishiyama<sup>4</sup>, Kazushige Hayakawa<sup>4</sup>

<sup>1</sup> Department of Radiology, Kitasato University Hospital, Japan

<sup>2</sup> School of Allied Health Sciences, Kitasato University, Japan

<sup>3</sup> Graduate School of Medical Science, Kitasato University, Japan

<sup>4</sup> School of Medicine, Kitasato University, Japan

### **Purpose**

We have developed a system of intensity modulated radiation therapy (IMRT) using TrueBeam (Varian) equipped with a real-time tumor-tracking radiotherapy (RTRT) system. In this study, we evaluated the reproducibility of the dose distribution in dynamic multileaf collimator (MLC) IMRT (dIMRT) using the RTRT system.

### **Methods**

We used SyncTraX (Shimadzu) as the RTRT system. We used a dynamic phantom, changed the speed of movement of the MLC from 0.5 to 2.5 cm/sec, and obtained fluence images using an EPID. We compared the fluence images with those of the dynamic phantom when it was at rest using gamma analysis (2 mm/2%). We also analyzed the physical characteristics of the position of MLC from trajectory log files. The X-ray energies used for the verification were 6 MV, 10 MV, and 10 MV flattening-filter-free. The dynamic phantom simulated a general respiratory cycle, and the internal margin (IM) of the respiration synchronizing irradiation was  $0 \pm 3$  mm.

### **Results**

The leaf gap size and the mean leaf location error obtained from trajectory log files were both less than 0.04 mm. Gamma analysis results from fluence images were  $97.3 \pm 2.3\%$ ,  $95.6 \pm 1.6\%$ , and  $91.6 \pm 2.2\%$  for  $\pm 1$  mm,  $\pm 2$  mm,  $\pm 3$  mm of IM, respectively. Thus, the gamma passing rate decreased as the IM increased.

### **Conclusions**

The reproducibility of dose distribution in dIMRT using SyncTraX was evaluated using a dynamic phantom. No position error of MLC was detected, but the gamma passing rate was affected by the IM of the respiration synchronizing irradiation.

### **Key words**

## STUDY OF THE GATING WINDOWS IN THE RESPIRATORY GATED RADIOTHERAPY USING THE VISIBLE GUIDING SYSTEM

Se An Oh<sup>1</sup>, Ji Woon Yea<sup>1</sup>, Jae Won Park<sup>1</sup>, Heon Bo Park<sup>2</sup>, Sung Kyu Kim<sup>1</sup>

<sup>1</sup> Department of Radiation Oncology, Yeungnam University Medical Center, Korea

<sup>2</sup> Konkuk University Medical Center, Korea

### Purpose

Respiratory-gated radiation therapy (RGRT) is used to minimize the radiation dose to normal tissue in lung-cancer patients. Although determining the gating window in the respiratory phase of patients is important in RGRT, it is not easy. We aim to determine the optimal gating window with a visible guiding system in RGRT.

### Methods

Between April and October in 2014, the breathing signals of 23 lung-cancer patients were recorded with a real-time position management (RPM) respiratory gating system (Varian, USA). We performed statistical analysis with breathing signals to find the optimal gating window for guided breathing in RGRT.

### Results

On comparing breathing signals before and after breathing training, 19 of the 23 patients showed statistically significant differences ( $p < 0.05$ ). The standard deviation of respiration signals after breathing training was the lowest for phases of 30%–70% ( $p < 0.05$ ). Statistical analysis showed that the optimal gating window in RGRT is 40% (30%–70%) with respect to repeatability for breathing after respiration training with the visible guiding system.

### Conclusions

RGRT with the RPM system confirmed the usefulness of the visible guiding system. Respiratory regularity improved with the RPM system and our visible guiding system; therefore, the accuracy and efficiency of RGRT would improve.

### Key words

Respiratory gated radiation therapy (RGRT) Real-time position management (RPM) Visible guiding system Gating window

## **A FEASIBILITY STUDY ON THE USE OF TOMOTHERAPY FOR URGENT PALLIATIVE PATIENT TREATMENT**

Yunfei Hu<sup>1</sup>, Mikel Byrne<sup>2</sup>, Ben Archibald-Heeren<sup>2</sup>

<sup>1</sup> Radiation Oncology Centres, Gosford, Australia

<sup>2</sup> Radiation Oncology Centres, Wahroonga, Australia

### **Purpose**

Tomotherapy uses Megavoltage fan-beam computed tomography (MV-FBCT) as the imaging guidance technique to correct patient setup before each treatment. Compared to conventional KV x-rays, it shows poorer visualisation of lower-density materials but also produces less artefact and image distortion when high-density material is present. In this study, the authors assessed the possibility of using Tomotherapy MV-FBCT for urgent palliative patient planning.

### **Methods**

To verify dose calculation accuracy on MV-FBCT, a CT-ED table was created from a CT-ED phantom. A CIRS phantom was used for end-to-end verification measurements to assess accuracy of the calculation based on the MV-FBCT. The imaging dose was measured both on the surface and at the centre of the CIRS phantom. The image quality was also assessed in terms of spatial resolution, noise, contrast and uniformity.

### **Results**

The end-to-end test revealed that the dose calculation based on Tomotherapy MV-FBCT were within  $\pm 3.0\%$  to the measurement. MV-FBCT images also had larger noises compared to KV x-rays but the noise introduced negligible uncertainty to the calculation. Daily imaging dose accounted for about 0.3% to 1.0% of the therapeutic dose. The prolonged scan time brought the problem of imaging artefact from patient inter-fraction motion. Image quality in terms of spatial resolution, contrast and uniformity was comparable to that of conventional KV x-rays.

### **Conclusions**

Tomotherapy MV-FBCT provides reasonable image quality and dose calculation accuracy for palliative treatments of certain areas but due to the lengthy scan time and large noise it should not be used solely for treatment scans of curative plans.

### **Key words**

## **DOSE DIFFERENT BETWEEN ORIGINAL TREATMENT PLANNING AND PLANNED ADAPTIVE CALCULATION IN HELICAL TOMOTHERAPY FOR NASOPHARYNGEAL CANCER**

Suwapim Chanlaor, Imjai Chitapanarux, Somsak Wanwilairat, Ekkasit Tharavichitkul, Wannapa Nopnaob

Department of Radiology, Faculty of Medicine, Chiang Mai University, Chiang Mai, Thailand

### **Purpose**

Changing anatomic and volumetric occur in Nasopharyngeal cancer (NPC) patients during fractioned radiotherapy cause the delivered dose considerably different from the original plan. The purpose of this study is to evaluate the different between original plan dose and calculated dose from planned adaptive software during the course of radiotherapy in NPC patients treated on the Tomotherapy HiArt system.

### **Methods**

Three NPC patients treated with helical tomotherapy underwent daily positional correction using megavoltage CT. Both parotid glands and spinal cord were recontoured on the MVCT images and the dose distribution were recalculated for all 33 fractions by planned adaptive software.

### **Results**

The percent difference between original plan and planned adaptive dose of the PTV70 (D95%), left and right parotid glands (D50%) were statistically significant ( $p < 0.05$ ) since 2nd, 8th and 7th fraction, respectively. (mean  $\pm$  SD =  $1.74\% \pm 0.32\%$ ,  $35.19\% \pm 12.67\%$  and  $24.60\% \pm 15.21\%$ , respectively). The percentage of spinal cord dose (D2%) difference between original plan and planned adaptive was not statistically significant (mean  $\pm$  SD =  $8.76\% \pm 10.15\%$ ). The decrease percentage of PTV70, left and right parotid glands volumes compare to original plan were 9.43%, 29.00% and 27.29%, respectively. The volume of spinal cord did not change during all the treatments.

### **Conclusions**

There were significant anatomic and volumetric changes in the target and both parotid glands of nasopharyngeal cancer patients. Adaptive radiotherapy should be considered to correct for the delivery dose.

### **Key words**

Adaptive planning, MVCT, NPC, Helical tomotherapy

## OPTIMIZING FOUR-DIMENSIONAL DIGITAL TOMOSYNTHESIS ACQUISITION BASED ON RESPIRATORY GUIDANCE

Dong-Su Kim<sup>1</sup>, Seungwan Lee<sup>2</sup>, Siyong Kim<sup>3</sup>, Seong-Hee Kang<sup>1</sup>, Tae-Ho Kim<sup>1</sup>, Kyeong-Hyun Kim<sup>1</sup>, Min-Seok Cho<sup>1</sup>, Dong-Seok Shin<sup>1</sup>, Yu-Yun Noh<sup>1</sup>, Do-Kun Yoon<sup>1</sup>, Tae Suk Suh<sup>1</sup>

<sup>1</sup> The Catholic University of Korea, Korea

<sup>2</sup> Konyang University, Korea

<sup>3</sup> Virginia Commonwealth University, Korea

### Purpose

Patient breathing-related sorting method of projections in 4D digital tomosynthesis (DTS) can be suffered from severe artifacts due to non-uniform angle distribution of projections and noncoplanar reconstructed images for each phase. In this study, we propose a method for optimally acquiring projection images in 4D DTS.

### Methods

Depending on scan parameters such as the number of acquisition points per cycle, total scan angle and projections per acquisition amplitude, acquisition sequence is pre-determined. A simulation study for feasibility test was performed. To mimic actual situation closely, a group of volunteers were recruited and breathing data were acquired both with/without biofeedback. Then, x-ray projections for a humanoid phantom were virtually performed following (1) the breathing data from volunteers without guide, (2) the breathing data with guide and (3) the planned breathing data (i.e., ideal situation). Images from all of 3 scenarios were compared.

### Results

Scenario #2 showed significant artifact reduction compared to #1 while did minimal increase from the ideal situation (i.e., scenario #3). We verified the performance of the method with regard to the degree of inaccuracy during respiratory guiding. Also, the scan angle dependence-related differences in the DTS images could reduce between using the proposed method and the established patient breathing-related sorting method.

### Conclusions

Through the proposed 4D DTS method, it is possible to improve the accuracy of image guidance between intra/inter fractions with relatively low imaging dose.

### Key words

4D Tomosynthesis, respiratory guidance

## **LINEAR TOMOSYNTHESIS WITH FLAT-PANEL DETECTOR FOR IMAGE GUIDED RADIATION THERAPY**

Dong-Su Kim<sup>1</sup>, Tae-Ho Kim<sup>1</sup>, Seong-Hee Kang<sup>1</sup>, Kyeong-Hyeon Kim<sup>1</sup>, Min-Seok Cho<sup>1</sup>, Dong-Seok Shin<sup>1</sup>, Yu-Yun Noh<sup>1</sup>, Siyong Kim<sup>2</sup>, Do-Kun Yoon<sup>1</sup>, Tae Suk Suh<sup>1</sup>

<sup>1</sup> The Catholic University Of Korea, Korea

<sup>2</sup> Virginia Commonwealth University, Korea

### **Purpose**

In this study, we propose a novel imaging technique using linear tomosynthesis with flat-panel detector that can produce tomographic images at arbitrary anterior-posterior depth position for image guided radiation therapy.

### **Methods**

To verify the usefulness of the imaging performance, we performed systematic simulation studies for simple linear movement of a couch with digital phantoms in several layers along the coronal direction. Projections were acquired at specific position through the calculated proper shift amounts for particular or multi-focal level imaging. The linear tomosynthesis images were reconstructed by shift-and-add (SAA) method. Furthermore, to increase blurring effect of out-focal objects in the image, we investigated a subsidiary technique that used sections of extra detector pixels along the anatomical axis.

### **Results**

According to our preliminary results, a designed specific coronal plane was well focused with good image sharpness and multi-focal image layers were realized with the proposed method. We have also derived the thicknesses of the focused image layer as functions of the number of pixels used in focal or out-focal section of the pixel array.

### **Conclusions**

Our results showed that defined plane-of-interests were well focused with image sharpness and the position of image layer center was adjusted precisely with proper shift amounts in the linear motion tomosynthesis. We expect that the proposed method will be very useful for accurate localization with less dose than other imaging modality such as cone-beam computed tomography.

### **Key words**

linear tomosynthesis, flat-panel detector, IGRT, shift-and-add

## **COMMISSIONING AND CLINICAL IMPLEMENTATION OF 4D-CBCT FOR LUNG SBRT**

Richard Sims

Auckland Radiation Oncology

### **Purpose**

Geometric verification of the tumour for free-breathing lung SBRT patients is challenging due to limitations of CBCT imaging. This can be overcome by using novel tools to produce a 4D-CBCT dataset that can be acquired before (inter-fraction) and during (intra-fraction) treatment.

The commissioning and clinical experience of such a commercial system will be presented.

### **Methods**

An anthropomorphic phantom was used to investigate system efficacy for identifying changes in reconstructed motion for a variety of clinical situations. The sensitivity of the system was compared to baseline 4DCT imaging with image quality and absorbed dose being quantified using suitable phantoms. The use of the system during treatment was then investigated and compared to baseline imaging, with system performance being assessed in terms of image registration accuracy.

### **Results**

The system identifies amplitude motion to within  $\pm 2$ mm of baseline and is sensitive to image artefacts with different/irregular respiratory cycles and number of image projections. The absorbed was  $23.0 \pm 1.6$ mGy with a registration accuracy of  $\pm 0.4$ mm. There is a reduction in image quality when using the system during treatment owing to the dependence on VMAT delivery and presence of MV scatter.

The 4D matching algorithm was influenced by image noise depending on VMAT arc parameters, causing a reduction in the measured amplitude of tumour motion. Nevertheless the accuracy of automatic registration was within  $\pm 0.9$ mm (2SD) when compared to baseline imaging.

### **Conclusions**

4D-CBCT imaging has been implemented successfully at our clinic and is now mandated for all lung SBRT patients.

### **Key words**

Radiation Therapy, Cone-Beam CT, Imaging, Geometric Verification

## **CLINICAL RULE BASED ALGORITHM TO DETECT VERY SMALL BRAIN LESIONS IN MRI SCANS PRECEDING STEREOTACTIC RADIOSURGERY**

Joseph Barbieri  
HUMC

### **Purpose**

Present an algorithm that automatically detects very small brain lesions on high resolution MRI scans for patients undergoing Stereotactic Radiosurgery (SRS) thereby assisting in speedy throughput with reduced observer dependence.

### **Methods**

A MATLAB algorithm was created that incorporates standard clinical rules and patient specific guidelines to optimize performance depending on the individual MRI parameters. For this work very small targets are characterized by three basic criteria: (1) one pixel in the target is significantly higher than the adjacent pixels, (2) the pixel intensity is in a select range above normal tissue but below higher intensities in normal structures or contrast, and (3) the high intensity is only present on one 1mm transaxial slice. The algorithm also accounts for small registration differences between adjacent slices. The procedure is analogous to looking at the starry night sky and picking out only the stars that twinkle. Three patients previously diagnosed for SRS treatment were analyzed and compared with expert opinion after lengthy review by neuroradiologist, neurosurgeon, and radiation oncologist.

### **Results**

All targets delineated for SRS treatment were automatically detected using the algorithm. Several false positives were easily eliminated by the observer due to their physical location or characteristics.

### **Conclusions**

Though many algorithms exist for automated target delineation we present a unique clinically oriented procedure to specifically detect very small lesions which are highly observer dependent. Early detection can lead to improved outcome and lower normal tissue exposure in SRS.

### **Key words**

SRS, algorithm, MRI

## REPRODUCIBILITY EVALUATION OF ABC-ASSISTED DIBH LEFT-SIDED BREAST RADIOTHERAPY

Chih Chieh Chang, Jo Ting Tsai

Department Of Radiation Oncology, Shuang Ho Hospital, Taipei Medical University, New Taipei City, Taiwan

### Purpose

The heart dose received from the left-sided breast radiotherapy increased the cardiac toxicity. Using active breathing control (ABC)-assisted deep-inspiration breath-hold (DIBH) technique during the treatment can minimize the exposure to the heart. This study assessed the reproducibility of ABC-assisted DIBH left-sided breast radiotherapy.

### Methods

Nine left-sided breast cancer patients were acquired ABC-assisted DIBH CT images for hybrid-IMRT planning in Pinnacle3 version 9.2. The dose description to the PTV was 5000cGy/25fx. After 20 fractions (about after one month), all patients were received another ABC-assisted DIBH CT simulation. The treatment plan from the first image set was copied to the second image set and recalculated the dose. The paired t-test was used to compare volumes and dose metrics in the ipsilateral lung (mean dose, V30Gy, V20Gy, V10Gy, V5Gy), heart (mean dose) and PTV (Dmax, V47.5Gy) between two image sets.

### Results

Volumes and dose metrics in the ipsilateral lung and heart all showed no significant difference ( $p > 0.09$ ) between two image sets. The PTV coverage (V47.5Gy) and Dmax in the second image set (V47.5Gy =  $96.7 \pm 2.1$  %, Dmax =  $55.2 \pm 0.70$  Gy) were both different from the first image set (V47.5Gy =  $98.6 \pm 0.6$  %, Dmax =  $54.6 \pm 0.26$  Gy) with  $p = 0.011$  and  $p = 0.033$ , respectively.

### Conclusions

The dosimetry results showed slight instability in PTV using ABC-assisted DIBH radiotherapy technique in left-sided breast. We recommended that routine image-guided therapy with 4D cone-beam CT during DIBH breast treatment course to insure the coverage and avoid the hot spot in the target.

### Key words

ABC-assisted DIBH, breast cancer

## **CLINICAL ADVANTAGES OF A ROBOTIC RADIOSURGERY SYSTEM EQUIPPED WITH A MULTI-LEAF COLLIMATOR IN PROSTATE STEREOTACTIC BODY RADIATION THERAPY**

Masashi Tomida<sup>1</sup>, Junji Suzuki<sup>1</sup>, Hironori Takahashi<sup>1</sup>, Kyohei Hamajima<sup>1</sup>, Takeshi Kamomae<sup>2</sup>, Yoichi Ohashi<sup>1</sup>, Hiroshi Oguchi<sup>2</sup>, Takahito Okuda<sup>1</sup>

<sup>1</sup> TOYOTA Memorial Hospital, Japan

<sup>2</sup> Nagoya University Graduate School of Medicine, Japan

### **Purpose**

The robotic radiosurgery system equipped with multi-leaf collimator (MLC) has been introduced recently and has been shown capable of providing clinical benefits. This study aims to find out the advantages of MLC when compared to other existing collimators used for prostate stereotactic body radiation therapy (SBRT).

### **Methods**

Six prostate cancer patients underwent treatment planning for prostate SBRT (36.25 Gy/5 fr) using each different type of collimator (i.e., fixed collimator, variable collimator, and MLC). Setting the same dose-volume goals for the three different types of collimators, we compared their dose-volume histograms as well as other parameters (e.g., treatment-time). For the quality assurance of the delivery of the dose to the patient, the irradiated radiochromic films were evaluated using Gamma-Index analysis with 3% dose difference/2 mm distance-to-agreement criteria.

### **Results**

For a prescription dose covering 95% of the planning target volume, the required average normalization to the isodose line was  $82\pm 2\%$  for the fixed collimator,  $83\pm 4\%$  for the variable collimator, and  $82\pm 3\%$  for the MLC. The average treatment-times per fraction were  $46\pm 5$  min with the fixed collimator,  $41\pm 3$  min with the variable collimator, and  $34\pm 4$  min with the MLC. For what concern patient quality assurance, the average Gamma-Index pass rates were high ( $> 95\%$ ) with all collimators.

### **Conclusions**

When compared with other collimators used for prostate SBRT, a robotic radiosurgery system equipped with a MLC has the distinctive advantages of treatment-time reduction and high consistency between planned and delivered dose distribution.

### **Key words**

prostate cancer, robotic radio surgery system, dose distribution, patient quality assurance

## **3D-TBI PLANNING AND TLD STUDY FOR HEAD AND NECK REGION USING AN ANTHROPOMORPHIC PHANTOM**

James Cheow Lei Lee

Division of Radiation Oncology, National Cancer Centre Singapore, Singapore

### **Purpose**

Total body irradiation (TBI) involves irradiating the whole body to prepare patient for bone marrow transplant. The irregular shape and sudden variations of body thicknesses challenges homogeneous distribution of prescribed dose. The dose objective for 3D-TBI is 90%-110% coverage of the prescribed dose calculated on a supine patient CT data set at extended SSD (450cm). Only the H&N and lower limbs are non-planned and compensated for their smaller separation by the use of Perspex and bolus materials assuming an average separation value. This study seeks to extend 3D-TBI planning to the H&N region and verified by TLD measurement.

### **Methods**

A 3D-TBI-H&N plan was developed with the addition of multi-leaf collimator (MLC), inhomogeneity correction and simulated Perspex to limit doses to H&N organs-at-risk (OARs) and to meet the dose objective. A H&N anthropomorphic phantom and plastic water was used for the study. In-vivo and external TLD measurements were performed to validate the plan's accuracy.

### **Results**

By using the Eclipse TPS with AAA algorithm (Varian Medical Systems Inc., USA), a good 3D-TBI-H&N dose plan was achieved. Result of in-vivo TLD measurement showed good overall agreement of  $\pm 2.93\%$  average within the head. Neck and back of head had close to 5% deviation. High deviations were noted, for instance, along the external shoulder areas (18.3%). These high slope areas generally pose challenges for dose verification.

### **Conclusions**

Overall in-vivo results show that 3D-TBI-H&N planning is within accuracy, therefore clinically feasible. Surface verification challenges posed by high slope areas (e.g. shoulder) exist.

### **Key words**

TBI, head and neck, anthropomorphic phantom, TLD

## **ANALYSIS OF TUMOUR CONTROL PROBABILITY, NORMAL TISSUE COMPLICATION PROBABILITY AND ISOTOXIC EFFECTS FOR PROSTATE CANCER**

Nurnada Syahrain Mohd Fauzee, Wan Nordiana Wan Abd. Rahman, Reduan Abdullah  
Universiti Sains Malaysia, Malaysia

### **Purpose**

to analyse the Tumour Control Probability (TCP), Normal Tissue Complication Probability (NTCP) and isotoxic effect for prostate cancer

### **Methods**

Eight prostate treatment plans with Collapsed Cone algorithm were evaluated in term of TCP, NTCP and isotoxic effect using BioSuite and BIOPLAN software. The treatment plans were then recalculated using Pencil Beam algorithm and similar TCP, NTCP and isotoxic effects were evaluated. Evaluation of all the treatment planning were conducted based on the DVH data from Oncentra MasterPlan (OMP) transferred to the both software.

### **Results**

NTCP value of rectum is higher for LKB model while for bladder; the value is higher using RS model. For all plans, the TCP values are 100% and isotoxic effect of organs are below the isotoxic level (5%). Pencil Beam shows a slightly higher than Collapsed Cone in total dose of target volume for most of plans. NTCP value obtained from BIOPLAN is greater than NTCP value from BioSuite. Total dose calculation of target volume for DVH from OMP is varied from BioSuite.

### **Conclusions**

In summary, there is no significant different between Pencil Beam and Collapsed Cone algorithm in TCP, NTCP and isotoxic effects. The dissimilarity in dose calculation using different algorithm is influenced by anatomical position of organ, tumour volume and treatment planning system. Variation in evaluation method will not give similar findings even same data is used. Software development between BioSuite and BIOPLAN indicates a larger difference in NTCP values between two different softwares.

### **Key words**

BioSuite, TCP, NTCP, isotoxic

## EFFECT OF GRID SIZE ON DOSE CALCULATION IN LUNG SBRT WITH FLATTENING FILTER FREE BEAMS

K Sakda<sup>1</sup>, S Taweap<sup>2</sup>, A Sawwanee<sup>1</sup>, A Lukkana<sup>3</sup>

<sup>1</sup>Mahidol Univ. Ramathibodi Hospital, Bangkok; <sup>2</sup>Chulalongkorn University, Bangkok; <sup>3</sup>Chulalongkorn University, Bangkok

**Key words:** grid size, flattening filter free (FFF), stereotactic body radiation therapy (SBRT)

**Introduction** To investigate the impact of grid resolution on dose calculation of ACUROS XB algorithm for lung Stereotactic Body Radiation Therapy (SBRT) considering both dosimetric impact and computational efficiency

**Methods** Dose distributions for lung SBRT plans with varying grid size (1.5, 2, and 2.5 mm) were calculated by ACUROS XB algorithm on Eclipse treatment planning system (TPS). The 13 lung SBRT patient data were retrospectively selected to estimate the dose variation as a function of grid size on TrueBeam linac with 6X-FFF and 10X-FFF beams. For all patients, the planning target volume (PTV) was smaller than an equivalent diameter of 7 cm. The quality of planned dose distribution can be evaluated from target coverage, conformity index (CI), homogeneity index (HI), and organ at risk (OAR) doses. The calculation time using each grid size was compared for clinical practice.

**Results:** Compared with 2-mm grid size, the 1.5-mm and 2.5-mm grid sizes caused PTV mean dose increases of less than 1% for both 6X-FFF and 10X-FFF beams, while the HI and CI values is similar. For OARs, the 1.5-mm grid size caused a dose increase up to 7% for the spinal cord. The 2.5-mm grid size produced lower dose in spinal cord and slightly higher dose in lung. The calculation time was reduced by average of 57.2±6% and 51.6±8% using the 2-mm and 2.5-mm grid sizes, respectively.

**Conclusion:** Dose analysis of target coverage showed no clinically significant in dose. The reducing in calculation time caused by increased grid resolution was more than half lung SBRT using FFF beams.

### References:

1. Low DA, Harms WB, Mutic S et al. (1998) A technique for the quantitative evaluation of dose distributions. *Med Phys* 38(3):1314-1338
2. Stanley HB, Kamil MY, David F et al. (2010) Stereotactic body radiation therapy: The report of TG101. *Med Phys* 37(8):4079-4101
3. Park JY, Kim S, Park HJ et al. (2014) Optimal set of grid size and angular increment for practical dose calculation using the dynamic conformal arc technique: a systematic stereotactic body radiation therapy. *Radiat Oncol* 9:5 DOI 10.1186/1748-717X-9-5
4. Huang B, Wu L, Lin P et al. (2015) Dose calculation of Acuros XB and Anisotropic Analytical Algorithm in lung stereotactic body radiotherapy treatment with flattening filter free beams and the potential role of calculation grid size. *Radiat Oncol* 10:53 DOI 10.1186/s13014-015-0357-0

## **OPTIMIZATION OF THE IRRADIATION SCHEME IN RADIOTHERAPY FOCUSING ON THE DOSE AND DOSE RATE TO THE TUMOR AND ORGANS AT RISK**

Ryota Yamada<sup>1</sup>, Yusuke Matsuya<sup>1</sup>, Takaaki Kimura<sup>1</sup>, Masahiro Mizuta<sup>2</sup>, Hiroyuki Date<sup>3</sup>

<sup>1</sup> Graduate School of Health Sciences, Hokkaido University, Japan

<sup>2</sup> Laboratory of Advanced Data Science, Information Initiative Center, Hokkaido University, Japan

<sup>3</sup> Faculty of Health Sciences, Hokkaido University, Japan

### **Purpose**

The fractionated irradiation scheme is currently performed for the treatment of solid tumors in order to minimize the damage to organs at risk (OARs). However, the optimal parameters (i.e., the number of fractions and dose per fraction) are not easy to determine. In this study, we utilize a graphical method to minimize the damage effect on an OAR under the constraint of a certain degree of tumor damage for planning the optimal scheme.

### **Methods**

We adopted the Microdosimetric-kinetic (MK) model for continuous irradiation to describe the radiation damage to the tumor and an OAR because this model can consider radiation quality and dose rate effects. On the assumption that the fractionated irradiation is given with 6 MV Linac X-rays with 2.5 Gy/min, we minimized the damage effect on the OAR under a fixed radiation effect on the tumor using a 2D plot of the damage to the tumor vs. OAR, to obtain the optimal number of fractions and dose per fraction.

### **Results**

The optimization scheme was constructed in the MK model frame, in which we incorporated the dose rate. It was found that the optimal number of fractions and dose per fraction are slightly different from those in the conventional schemes obtained with the universal survival curve and the linear-quadratic model.

### **Conclusions**

We determined the optimal parameters of fractionated irradiation for radiotherapy by the use of the MK model considering the effects of radiation quality and dose rate.

### **Key words**

Optimal number of fractions, Fractionated scheme, Microdosimetric-Kinetic model

## **DEVELOPMENT OF PHOTON TRANSPORT CALCULATION METHOD USING VOXEL-BASED BOLTZMANN TRANSPORT EQUATION**

Takahito Chiba, Hidetoshi Saitoh, Atsushi Myojoyama

Tokyo Metropolitan University, Japan

### **Purpose**

Dose calculation method of solving the Linear Boltzmann Transport Equation deterministic is accurate in the heterogeneous region. However, the dose calculation time is longer than other methods in simple irradiation conditions. Therefore, in order to develop a fast dose calculation method at all irradiation conditions, we developed photon transport calculation method using voxel-based Boltzmann transport equation.

### **Methods**

We combined Lattice Boltzmann Method with the existing method. The lattice points were considered as the coordinate of photon transport destination. The photon transport destination is specified in three dimensions by the kernel-shaped fluence distribution. The numbers of directions of the transported photon were limited to 18. The photon transport simulation was processed in parallel by dividing the region. The information of transported photons such as the fluence, energy and direction were exchanged between the lattice points of the divided regions.

### **Results**

The proposed method enabled dividing the calculation area for parallel computing, and speed up photon transport calculation.

### **Conclusions**

We developed optimal photon transport calculation method for parallel computation using a voxel-based Boltzmann transport equation. It should be possible to more speed up with implementing to GPU. And we would develop electron transport calculation in a similar method and calculate absorbed dose.

### **Key words**

Boltzmann Transport Equation, Lattice Boltzmann Method, photon transport simulation, parallel computation

## **DOSIMETRIC COMPARISON BETWEEN ACUROSXB (AXB) AND ANISOTROPIC ANALYTICAL ALGORITHM (AAA) DOSE CALCULATION FOR VOLUMETRIC MODULATED ARC THERAPY (VMAT) LUNG PLAN**

Rattapol Rangseevijitprapa, Puangpen Tangboonduangjit, Nuanpen Dumrongkijudom  
Medical Physics School, Department Of Radiology, Faculty Of Medicine Ramathibodi  
Hospital, Mahidol University, Bangkok, Thailand

### **Purpose**

To verify dose calculated by the AcurosXB (AXB) algorithm and Analytical Anisotropic Algorithm (AAA) version 11.0.31 in predicting air/tissue interface doses in VMAT technique.

### **Methods**

The dose computation was performed within Eclipse TPS and CC13 ionization chamber was used for point dose measurement. Open single field in a homogeneous and inhomogeneous phantom, and volumetric arc therapy (VMAT) plans for lung cancer in CIRS thorax phantom were performed with 6 MV photon beams. Both algorithms were normalized using the same monitor unit.

### **Results**

The calculated central axis depth dose in a homogeneous phantom for open field shows good agreement with measurement to within 1.5%. Calculations on inhomogeneous interfaces with different densities such as titanium ( $=4.5 \text{ g.cm}^{-3}$ ), bone ( $=1.85 \text{ g.cm}^{-3}$ ), soft tissue ( $=0.92 \text{ g.cm}^{-3}$ ), and lung ( $=0.26 \text{ g.cm}^{-3}$ ) were found to agree with measurement to within 1.5% in bone, soft tissue, and lung except in titanium, the dose differences was up to 9.37%. And below the air cavity for open field showed that the discrepancies for AXB were ranged from -0.54 to 1.08% and for AAA were between 1.63% to 4.61%. For VMAT lung plan, the AXB plans provided lower coverage to PTV by about 20% than the AAA plans. The percentage of ipsi-lung volume receiving at least (V20) and contra-lung volume V5 were higher in the AXB plans than in the AAA plans by 13% and 6.9% respectively.

### **Conclusions**

The AXB algorithm provides slightly better accuracy compared to AAA for inhomogeneous media.

### **Key words**

AcurosXB (AXB); Analytical Anisotropic Algorithm (AAA); volumetric modulated arc therapy (VMAT); Lung cancer

## **EVALUATION OF TUMOR CONTROL PROBABILITY AND NORMAL TISSUE COMPLICATION PROBABILITY FOR 3-DIMENSIONAL CONFORMAL RADIATION THERAPY TREATMENT PLANNING**

Sukainah Suhana Abdullah, Wan Nordiana Wan Abd Rahman, Reduan Abdullah,  
Rosmazihana Mat Lazim  
Universiti Sains Malaysia, Malaysia

### **Purpose**

The evaluation of tumor control probability (TCP) and Normal Tissue Complication Probability (NTCP) for 3 Dimensional Conformal Radiation Therapy (3D CRT) treatment planning as one of treatment planning evaluation tools provide more consideration in term of probability for local tumor control and probability of complication to normal tissue.

### **Methods**

TCP was calculated using Poisson model while NTCP was calculated using radiobiological model of Lyman-Kutcher- Burman (LKB) and Relative Seriality (RS) models using BioSuite software. The calculation was conducted with DVH (Dose Volume Histograms) information from Oncentra MasterPlan (OMP). The evaluation was done on 5 different types of cancer: Bladder, Brain, Breast, Prostate and Thorax cancers. The effects of multiple beams arrangement were also investigated for bladder and prostate cancers.

### **Results**

TCP calculated for all types of cancer were found to be maximum at 100%. NTCP-LKB value for bladder cancer had 0.1% probability to be diagnosed for rectum stricture-bleeding. NTCP-LKB was 0.3% for spinal cord necrosis in brain cancer while highest for left breast cancer with NTCP-LKB value of 12.3% for left lung pneumonia. Prostate cancer had NTCP-LKB 2.0% for rectum while NTCP-LKB in thorax cancer plans was 13.4% for lung pneumonia. Multiple beam present significant effects on dose distribution and hence alter the NTCP value.

### **Conclusions**

The TCP and NTCP value are influenced by factors such as multiple beams arrangement, location of tumor and amount of peripheral dose received by normal tissue. Therefore, better estimation of prognosis for cancer patient by radiobiological evaluation is crucial and necessary.

### **Key words**

TCP and NTCP, 3D CRT, Treatment Planning

## COMPARISON OF DOSE DISTRIBUTIONS CALCULATED BY THREE GOLD MODELS FOR HELICAL TOMOTHERAPY

T Isomura<sup>1</sup>, H Shimizu<sup>1</sup>, K Sasaki<sup>2</sup>, K Sugi<sup>3</sup>, T Nakabayashi<sup>4</sup>, H Fukuma<sup>5</sup>, Y Takaishi<sup>6</sup>, M Uchida<sup>7</sup>,  
K Nakashima<sup>1</sup>, T Kodaira<sup>1</sup>

<sup>1</sup>Department of Radiation Oncology, Aichi Cancer Center hospital, Japan;

<sup>2</sup>Graduate School of Radiological Technology, Gunma Prefectural College of Health Sciences, Japan;

<sup>3</sup>Hitachi, Ltd. Healthcare Business Unit, Japan;

<sup>4</sup>Customer Support & Area Operation Headquarters, Physics & Clinical Support, Accuray Japan K.K, Japan;

<sup>5</sup>Department of Radiology, Nagoya City University hospital, Japan;

<sup>6</sup>Narita Memorial Hospital, Japan;

<sup>7</sup>Kasugai Municipal Hospital, Japan

**Key words:** tomotherapy, gold model

**Introduction** We have ever reported that the variation in beam outputs of tomotherapy in multiple facilities was a little difference [1]. The outputs are adjusted to match a common beam model (gold model) within the tolerance in the commissioning of the tomotherapy; therefore, the outputs of all tomotherapies seem to be even. However, there are three kinds of the gold models (legacy, TP, TP1) by timing of the introduction. If the difference of the gold model gives the effect for the dose distribution, we need to classify the data from multiple facilities such as that of a clinical trial in each beam model for the analysis. If not so, three gold models can be even. It means that the analysis of treatment data would be made easy. The aim of this study was to clarify the difference between the dose distributions which calculated by each gold model.

**Methods** The dose profiles of the gold models were obtained from vendor and compared. These profiles were three direction per one model; x and y profiles for off center ratio (OCR) and percent depth dose (PDD), for three kind of field width (10, 25 and 50 mm). First, field width half maximum (FWHM), field width quarter maximum (FWQM), dose difference (DD), and gamma index were used for the comparison of each model. As a reference of the tolerance, we adopted for AAPM task group 148 [2] which described about the method of QA/QC for the tomotherapy; 1% of field width for FWHM, 1 mm for FWQM, 1% for DD, 1 for gamma index. Second, the treatment plan was designed under same condition for each gold model. The dose profiles were obtained from designed treatment plans. The DD was used for the comparison of the result. The agreement between the models was evaluated with error bars of 3 mm/3%.

**Results:** For the comparison of the profile of the gold models, the FWHM of legacy, TP, and TP1 were 10.7, 10.8, 10.8 mm for 10 mm field width (FW), 25.4, 25.5, 25.6 mm for 25 mm FW, and 51.1, 51.4, 51.4 mm for 50 mm FW, respectively, the FWQM were 411.4, 410.9, 410.6 mm for 10 mm FW, 411.6, 411.0, 410.7 mm for 25 mm FW and 411.7, 411.2, 410.9 mm for 50 mm FW. The average 4DDs ( $\pm$  standard deviation) between legacy and TP, legacy and TP1, TP and TP1 were  $0.17\% \pm 0.55\%$ ,  $0.29\% \pm 0.66\%$  and  $0.11\% \pm 0.25\%$ , respectively. The gamma indexes were 0.17

$\pm 0.17$ ,  $0.22 \pm 0.12$  and  $0.07 \pm 0.10$ , respectively. All indexes (FWHM, FWQM, DD and gamma index) were within the tolerance in the beam core region, which was the ranges of 25% dose, 50% dose and beyond build-up region for x profile, y profile and PDD, respectively. For the comparison of the dose distributions of the treatment plan, the DDs for x direction of 10 mm FW between legacy and TP, legacy and TP1, TP and TP1 were  $0.1 \pm 0.5\%$ ,  $0.0\% \pm 0.5\%$  and  $-0.1\% \pm 0.6\%$ , respectively. Others profiles were almost the same tendency except profile for y direction of 50 mm FW. In the evaluation of error bars, most profiles were agreed with tolerance. However, profile of y direction for 50 mm FW was out of tolerance as well as the results of the DDs.

**Discussion:** The difference in all indexes was in tolerance level. It was indicated that the difference between gold models would be very small. This result suggested that we would be able to unify the gold models. The error bar for the profile of y direction for 50 mm FW was out of tolerance as well as the results of the DDs. We believe that the parameters registered in treatment planning system (TPS) of the tomotherapy could be an important factor [3] as well as the number of the dose optimized calculation.

**Conclusion:** In this study, we concluded that we would be able to make the gold models unify. However, the difference had occurred to result of the dose optimized calculation. The investigation of its cause was needed.

### References:

1. H Shimizu, K Sasaki, K Sugi, et al.: The variation in beam outputs of tomotherapy: investigation in multiple facilities, Japan Social Medical Physics, 35(3), 79
2. Katja M Langen, Niko Papanikolaou, John Balog et al.: QA for helical tomotherapy: Report of the AAPM Task Group 148
3. Tomotherapy training manual: 1d Beam Model and Machine Setting

Corresponding author email: t.isomura.k@gmail.com

## **DEVELOPMENT OF MONITOR UNIT CALCULATION PROGRAM FOR INTEGRATION TO RADIATION THERAPY INFORMATION SYSTEM**

Damrongsak Tippanya<sup>1</sup>, Somsak Wanwilairat<sup>2</sup>, Ekkasit Tharavichitkul<sup>2</sup>

<sup>1</sup> Chiang Mai University, Thailand

<sup>2</sup> Division of Therapeutic Radiology and Oncology, Faculty of Medicine, Chiang Mai University, Thailand

### **Purpose**

To develop a Monitor Unit (MU) calculation program for integration with an in-house Radiation Therapy Information System (RTIS). The program is used for 6MV photon MU calculation in 2D technique teletherapy.

### **Methods**

The MU calculation program is based on the Clarkson's integration method and divided into two parts. The first part is scatter sector radius determination from 2D simulation images. This part was programming in JAVA language. The second part is MU calculation using Clarkson's irregular field method. The later part was programming in Microsoft visual Foxpro language. The calculated MU are verified by dose measurement following the test cases (1a, 1b, 1c, 2a, 2b and 7) of the IAEA-TECDOC-1540. After the dose different between the calculation and the measurement are within the acceptance criteria, the program is integrated to the RTIS.

### **Results**

The scatter sector radius determination program workflow are the selection the angle between each radius, the image distance calibration, the defining of isocenter and field size edge defining. The program will generate radius distance and export to a file. The MU calculation part workflow are the input of field size (width, length) and tumor depth. Following TECDOC-1540 the dose different range between the calculation and the measurement is -1.98% to 1.40% for test case 1a, 1b, 1c, 2a and 2b and the range is -3.02% to 0.99% for test case 7. This program is integrated to the dosimetry menu in the RTIS. Then the RTIS can calculate the MU for each field size of each patient and record to the patient database.

### **Conclusions**

The MU calculation computer program is developed, verified and integrated to the RTIS. The program is used for 6MV photon monitor unit calculation in 2D technique irradiation.

### **Key words**

Clarkson's integration method, IAEA-TECOC-1540, Monitor Unit, Programing.

## FEASIBILITY STUDY OF PLANNING PHASE OPTIMIZATION USING PATIENT GEOMETRY-DRIVEN INFORMATION

Seong-Hee Kang<sup>1</sup>, Siyong Kim<sup>2</sup>, Dong-Su Kim<sup>3</sup>, Tae-Ho Kim<sup>3</sup>, Dong-Suk Shin<sup>3</sup>, Min-Suk Cho<sup>3</sup>, Kyung-Hyun Kim<sup>3</sup>, Yu-Yun Noh<sup>3</sup>, Tae-Suk Suh<sup>3</sup>

<sup>1</sup> Catholic Univ. of Korea, Korea

<sup>2</sup> Department of Radiation Oncology, Virginia Commonwealth University, USA

<sup>3</sup> Department of Biomedical Engineering, The Catholic University of Korea College of Medicine, Korea

### Purpose

To propose a simple and effective cost value function to search optimal planning phase (gating window) and demonstrated its feasibility for respiratory correlated radiation therapy.

### Methods

We acquired 4DCT of 10 phases for 10 lung patients who have tumor located near OARs such as esophagus, heart, and spinal cord (i.e., central lung cancer patients). A simplified mathematical optimization function was established by using overlap volume histogram (OVH) between the target and organ at risk (OAR) at each phase and the tolerance dose of selected OARs to achieve surrounding OARs dose-sparing. For all patients and all phases, delineation of the target volume and selected OARs (esophagus, heart, and spinal cord) was performed (by one observer to avoid inter-observer variation), then cost values were calculated for all phases.

### Results

A simplified mathematical cost value function showed noticeable difference from phase to phase, implying it is possible to find optimal phases for gating window. The lowest cost value which may result in lower mean/max dose to OARs was distributed at various phases for all patients. The mean doses of the OARs significantly decreased about 10% with statistical significance for all 3 OARs at the phase with the lowest cost value.

### Conclusions

It is demonstrated that optimal phases (in dose distribution perspective) for gating window could exist differently through each patient and the proposed cost value function can be a useful tool for determining such phases without performing dose optimization calculations.

### Key words

Respiratory correlated radiation therapy, overlap volume histogram (OVH), Treatment planning optimization

## FABRICATION OF A 3D-PRINTED SHIELDING BLOCK WITH HIGH ACCURACY FOR TOTAL BODY IRRADIATION

A Sawada<sup>1</sup>, Nitoh<sup>1</sup>, YImataki<sup>1</sup>, MShintani<sup>1</sup>, M Sueoka<sup>2</sup>, STaniuchi<sup>2</sup>, MKokubo<sup>2,3</sup>

<sup>1</sup>Kyoto College of Medical Science, JP; <sup>2</sup>Kobe City Medical Center General Hospital, JP; <sup>3</sup>Institute of Biomedical Research and Innovation, JP

**Key words:** Shielding block, 3D printer

**Introduction** In total body irradiation (TBI), lead shielding blocks are employed to control the irradiation dose to OARs such as lungs. The shielding blocks are separately fabricated for each patient.

The purpose of this study was to fabricate a shielding block with high accuracy using a 3D printer device.

**Methods** The lung contour was delineated on the lateral fluoroscopic image (1760x2140 pixels, 0.2 mm/pixel) and was labeled inside with 1 as a 2D lung model. By adding thickness in 10 mm along a perpendicular direction to the 2D lung model, 3D lung model was created and saved as a STL formatted file.[1] Then, using MeshLab [2] software, unstructured 3D triangular meshes were edited to delete unnecessary meshes. Subsequently, the above 3D lung model was imported to a 3D printer device (da Vinci 1.0 AiO, XYZprinting, Inc.). In order to avoid a difficulty in shearing the printed lung model from the surface in the 3D printer device, the 3D lung model was rotated to make the area on the printed surface as small as possible. After the 3D lung model was printed, the printed lung model was put into a rectangle container surrounded by the Lego blocks and then, silicone gel was poured inside it to create a mold of the shielding block. Finally, the low melting alloy containing Pb was poured inside the mold.

**Results:** Fig. 1 shows the printed 3D lung model, the silicone mold, and the shielding block made of low melting alloy.

The difference between the computed and the printed 3D lung model was 0.0, 0.0 mm on x-y plane in fig. 1 while the difference was 1.05 mm in the perpendicular direction (z) to the plane. On another hand, the difference between the printed 3D lung model and the shielding block made of Pb was 1.8 (18%), -0.6 mm (-0.9%) on x-y plane while the difference was 0 mm (0%) in z direction.

### Discussion:

The difference in length between the computed and the printed 3D lung model was larger along z direction. It may be because of the weight of the stacked filaments while the platform moved down along the z direction.

Fig. 2 shows a photograph of the enlarged shielding block. The stacked filament was represented as streak lines on the surface of the shielding block; however, the influence on TBI may be negligible.

The printed time was approximately 120 minutes. However, extra 24 hours were needed to harden silicone gel while the burden of creation of the lung model became lightened.

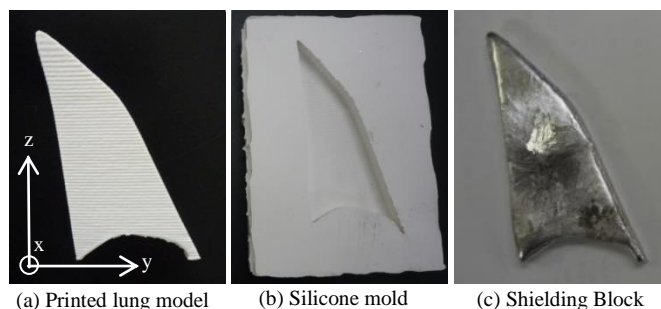


Fig. 1 Photographs of (a) Printed lung model, (b) Silicone mold, and (c) Shielding Block



Fig. 2 Photograph of the enlarged shielding block

**Conclusion:** The preliminary result has demonstrated that a 3D-printed shielding block for TBI has geometrically high accuracy although further improvement such as processing time is required.

### References:

1. Selva3D Web site: selva3d.com
2. MeshLab Web site: meshlab.sourceforge.net

Corresponding author email: sawada@kyoto-msc.jp

## **EVALUATION OF HYBRID-DYNAMIC CONFORMAL ARC THERAPY FOR RADIOTHERAPY OF LUNG CANCER**

Sung Joon Kim<sup>1</sup>, Jae-Chul Kim<sup>2</sup>, Min Kyu Kang<sup>2</sup>, Jeong Won Lee<sup>1-2</sup>, In Kyu Park<sup>1</sup>, Seong-Jun Lee<sup>1</sup>, Soo Ho Moon<sup>1</sup>, Byoung Soo Ko<sup>1</sup>, Shin-Hyung Park<sup>1</sup>, Mi Young Kim<sup>1</sup>, Bong Kyung Bae<sup>1</sup>, Jun Hee Park<sup>1</sup>

1 Department of Radiation Oncology, Kyungpook National University Hospital, Daegu, Korea

2 Department of Radiation Oncology, Kyungpook National University School Of Medicine, Daegu, Korea

### **Purpose**

We developed a hybrid-dynamic conformal arc therapy (HDCAT) technique which permits concurrent delivery of static field-in-field beam and dynamic conformal arc beam in a single arc (half rotation). The aim of this study was to evaluate the dosimetric benefits of HDCAT plans for lung cancer.

### **Methods**

This study was performed in 10 lung cases treated with HDCAT by VERO system (BrainLab, Germany). Dosimetric parameters of HDCAT were compared to those of 3-dimensional conformal radiotherapy (3D-CRT) plans in terms of target volume coverage, dose conformity, and sparing of organs at risk.

### **Results**

When compared to 3DCRT, HDCAT plans offered better dose conformity (median CI: 0.79 vs. 0.65;  $p=0.012$ ). HDCAT technique reduced the lung volume receiving above 30 Gy (median V30: 12% vs. 14.6%;  $p=0.005$ , V50: 5.2% vs.6.6%;  $p=0.008$ ) and the maximum spinal cord dose (median Dmax: 31.6 Gy vs. 43.2 Gy;  $p=0.005$ ) when compared to 3D-CRT. Regarding lung volume receiving below 20 Gy, HDCAT spared the lung with a marginal significance (median V20: 19.4% vs. 22.8%;  $p=0.093$ ).

### **Conclusions**

Compared to 3D-CRT, HDCAT was shown to have dosimetric advantages for the radiation treatment of lung cancer.

### **Key words**

Hybrid-dynamic conformal arc therapy, 3D-CRT, VERO system

## **FUNDAMENTAL STUDY OF HEAVY ION CT USING INTENSIFYING SCREEN AND EMCCD CAMERA FOR HUMAN HEAD IMAGING**

Mamoru Yokose<sup>1</sup>, Hiroshi Muraishi<sup>1</sup>, Hidetake Hara<sup>1</sup>, Tohoru Takeda<sup>1</sup>, Takara Watanabe<sup>2</sup>, Shinji Abe<sup>3</sup>, Yusuke Koba<sup>4</sup>, Shigekazu Fukuda<sup>4</sup>

<sup>1</sup> Kitasato University, Japan

<sup>2</sup> Tokyo Metropolitan University, Japan

<sup>3</sup> Ibaraki Prefectural University of Health Sciences, Japan

<sup>4</sup> National Institute of Radiological Sciences, Japan

### **Purpose**

The objective of this study was to evaluate the fundamental feature of the heavy ion CT (IonCT) using an intensifying screen and Electron Multiplying CCD (EMCCD) camera for human head imaging from the point of view of the data acquisition time as well as the spatial resolution.

### **Methods**

We developed a new calculation method to estimate the relative residual range for each projection line by fitted with reference curves measured by the full experiment for one projection. We carried out the evaluation of the spatial resolution by applying the radial-edge method for the reconstructed PMMA rod image that was acquired by the IonCT system using the Heavy Ion Medical Accelerator in Chiba (HIMAC) at the National Institute of Radiological Sciences (NIRS). We also designed a new broad beam of <sup>12</sup>C generated by spreading out the pencil beam using a scatterer without wobbler magnets.

By using a new online system that can take 10 images within 1 s while the rotation phantom rotates continuously, a fast CT data acquisition around 10 min is possible.

### **Results**

The reconstructed image of an object with a water equivalent thickness of 18cm was achieved with the spatial resolution of 1 mm. Performance test with regard to the fast CT data acquisition will be performed in June 2016.

### **Conclusions**

This IonCT technique would be worth applying to the heavy-ion treatment planning for head and neck cancers from the point of view of the spatial resolution and the data acquisition time.

### **Key words**

Heavy ion CT, Spatial resolution

## **DOSIMETRIC COMPARISON BETWEEN DIFFERENT PLANNING TECHNIQUES IN POST MASTECTOMY RADIOTHERAPY TO LEFT CHEST WALL**

Wai Lwin Lwin Kyaw<sup>1</sup>, Swe Swe Lin<sup>2</sup>, Sivalee Suriyapee<sup>3</sup>, Taweap Sanghangthum<sup>3</sup>

<sup>1</sup> SEAFOMP

<sup>2</sup> Department of Radiation Oncology, Pinlon Cancer Center, Yangon, Myanmar

<sup>3</sup> Department of Radiology, Faculty of Medicine, Chulalongkorn University, Bangkok, Thailand

### **Purpose**

The purpose of this study is to compare Homogeneity Index (HI) and Conformity Index (CI) in different planning techniques of post mastectomy radiation therapy to left chest wall.

### **Methods**

This study was performed the dose comparison of HI and CI with seven planning techniques; which are Tangential Open Field (OPEN), standard wedged tangent (SWT), electronic compensator (E-Comp), Field in Field (FinF), Tangential IMRT(T-IMRT), Coplanar IMRT(Co-IMRT), and Non-Coplanar IMRT(NC-IMRT), in three cases post- mastectomy radiation therapy to left chest wall treated in Varian Clinic iX. The doses of D2%, D50% and D98% were recorded to calculate HI according to ICRU 83. For the CI, calculated of treated volume (TV) and planning target volume (PTV) were used.

### **Results**

In comparison of 7 planning techniques, IMRT is a novel technique that can deliver a more homogeneous dose of radiation throughout the breast. The HI was significantly improved in Co-IMRT ( $0.07\pm 0.02$ ) as well as NC-IMRT( $0.07\pm 0.01$ ), while E-Comp ( $0.14\pm 0.06$ ), FinF( $0.16\pm 0.04$ ) and SWT( $0.16\pm 0.04$ ) was comparable in HI with OPEN ( $0.17\pm 0.04$ ). The CI showed the best result in Co-IMRT( $1.28\pm 0.07$ ) and NC-IMRT( $1.29\pm 0.07$ ), while SWT( $2.55\pm 1.51$ ) was the worse result in CI due to no beam modulation in 3D breast shape. The E-Comp ( $1.84\pm 0.34$ ) and FinF( $1.49\pm 0.55$ ) showed better results in CI than SWT.

### **Conclusions**

It is concluded that all IMRT based techniques show very good HI and CI, while E-Comp and FinF give the good result and faster to create than IMRT based.

### **Key words**

conformity index, homogeneity index, IMRT, Left breast

## **DOSIMETRIC COMPARISONS OF STATIC NON-COPLANAR IMRT AND RAPIDARC FOR STEREOTACTIC RADIOSURGERY**

Pornpirom Laojunun, Chumpot Kakanaporn, Siwadol Pleanarom, Porntip Iampongpaiboon  
Siriraj Hospital, Thailand

### **Purpose**

To evaluate the dosimetric study of the static non-coplanar intensity modulated radiation therapy (NCP-IMRT) and volumetric modulated arc therapy (VMAT) or Varian RapidArc, linear accelerator based stereotactic radiosurgery (SRS) for the treatment of cerebral arteriovenous malformation (AVM)

### **Methods**

The NCP-IMRT plans performed on Brainlab iPlan were compared with RapidArc plans performed on Varian Eclipse V.10.0 system. In order to evaluate the treatment plans, several dosimetric evaluation parameters such as Paddick's conformity index (PCI), homogeneity index (HI) and dose gradient index (DI) in the plans are calculated and compared for each of the plans. Eight AVM patients are retrospectively selected for this study. All treatment plans were calculated with a Varian True Beam STx with 2.5 mm central leaf width multileaf collimator (MLC)

### **Results**

The PCI was found to be superior with NCP-IMRT plans. Both techniques produced plans with comparable homogeneity. During this study it was observed that the NCP-IMRT had shown better dose gradient and conformity as compared to the RapidArc technique. And also the NCP-IMRT can produce homogeneous plans.

### **Conclusions**

The results of this study showed the superiority of NCP-IMRT when compared to 2 coplanar arcs from RapidArc treatment plans. The NCP-IMRT technique was surprising in that it delivered quite homogeneous plans and also had steep dose gradients comparable to the RapidArc technique. The process of extending this retrospective study with non-coplanar RapidArc technique and comparing will be studied.

### **Key words**

NCP-IMRT, RapidArc, conformity index, homogeneity index

## **INFLUENCE OF JAW TRACKING IN IMRT AND VOLUMETRIC MODULATED ARC RADIOTHERAPY FOR HEAD AND NECK CANCERS- A DOSIMETRIC STUDY**

Sagar Upadhayay<sup>1</sup>, Karthick Raj Mani<sup>2</sup>, Hasin Anupama Azhari<sup>3</sup>, Golam Abbu Zakaria<sup>4</sup>

<sup>1</sup> Kathmandu Cancer Center

<sup>2</sup> United Hospital , Dhaka , Bangladesh

<sup>3</sup> Dept. Of Medical Physics And Biomedical Engineering, Gono University, Dhaka, Bangladesh

<sup>4</sup> Dept Of Medical Radiation Physics, Gummersbach Hospital, Academic Teaching Hospital Of The University Of Cologne, Gummersbach, Germany

### **Purpose**

To Study the dosimetric advantage of the Jaw tracking technique in IMRT & VMAT for Head and Neck Cancers.

### **Methods**

We retrospectively selected ten previously treated H&N cancer patients stage (T1/T2, N1, M0) in this study. All the patients were planned for IMRT and VMAT with SIB technique to deliver a differential dose per fraction to the high, intermediate and low risk volume using a single plan. We intend to deliver 70Gy to the high risk volume, 63Gy to the intermediate risk volume and 56Gy to the low risk volumes in 35 fractions. All the plans were planned with 6MV photons using Millennium 120 MLC

### **Results**

For all patients, the V5, V10, V20, & V30 mean dose (Dmean) for the whole body and OARs in all patients in the jaw tracking (IMRT/VMAT) plans were significantly less than the corresponding values of the without jaw tracking (IMRT/VMAT) plans. In all patients V5 typically showed the largest improvement and V20 the least improvement. The mean doses reductions for these OARs ranged from 1.40% to 7.64% for IMRT and 0.5% to 2.0%.

### **Conclusions**

Jaw tracking resulted in decreased dose to critical structures in IMRT and VMAT plans. But significant dose reductions were observed for critical structure in the IMRT with jaw tracking compared to IMRT without jaw tracking. In VMAT with jaw tracking technique the dose reduction to the critical structure were not significant.

### **Key words**

Jaw Tracking, IMRT, VMAT, Simultaneous Integrated Boost (SIB)

## **DOSE-SPARING EFFECTS OF A RECTAL BALLOON IN PROTON THERAPY OF THE PROSTATE**

Doo Hyun Lee

National Cancer Center, Korea

### **Purpose**

The normal organ (bladder, rectum) sparing is very important for radiation therapy of the pelvis. Many people are studying with the effort for rectal and bladder sparing, however the actual circumstances to be satisfied which can not find the method. In this study, the decrease used the balloon to order the rectal dose. The aim of the study was to investigate the dose volume effects of a water-filled rectal balloon in the rectum.

### **Methods**

We inserted the balloon(100cc water filled, 10cm length, 3cm diameter ) in rectum for 10 proton therapy patients with prostate cancers. The systems were loaded with Eclipse proton planning system(Ver. 7.5) and Two sets of CT images before and after ballooning were acquired. Rectum and bladder volumes were delineated on 3-mm-thick CT images. A comparison between dose volume histogram(DVH) with and without balloon in rectum for proton therapy of the prostate cancers.

### **Results**

More organ and target volume changes with shape because inserted the balloon in rectum. Mean dose of rectal difference between with and without balloon was about 20%, because volume of rectum escape from a radiation area due to the balloon. Mean dose of bladder difference between with and without balloon was about 6%.

### **Conclusions**

The rectal balloon is very useful for bladder and rectal sparing with proton therapy of the prostate cancers. This research is believed to be sufficiently accurate and clinically useful.

### **Key words**

rectal balloon, proton therapy, dose volume histogram(DVH)

## **DEVELOPMENT OF MONITOR UNIT CALCULATION PROGRAM FOR INTEGRATION TO RADIATION THERAPY INFORMATION SYSTEM**

Damrongsak Tippanya<sup>1</sup>, Somsak Wanwilairat<sup>2</sup>, Ekkasit Tharavichitkul<sup>2</sup>, Sumbhat Wanwilairat<sup>3</sup>, Thanit Chaiwiang<sup>4</sup>

<sup>1</sup> Chiang Mai University

<sup>2</sup> Division Of Therapeutic Radiology And Oncology, Faculty Of Medicine, Chiang Mai University

<sup>3</sup> Thailand's Petroleum Exploration And Production Company

<sup>4</sup> Datasoft Company

### **Purpose**

To develop a Monitor Unit (MU) calculation program for integration with an in-house Radiation Therapy Information System (RTIS). The program is used for 6MV photon MU calculation in 2D technique teletherapy.

### **Methods**

The MU calculation program is based on the Clarkson's integration method and divided into two parts. The first part is scatter sector radius determination from 2D simulation images. This part was programming in JAVA language. The second part is MU calculation using Clarkson's irregular field method. The later part was programming in Microsoft visual Foxpro language. The calculated MU are verified by dose measurement following the test cases (1a, 1b, 1c, 2a, 2b and 7) of the IAEA-TECDOC-1540. After the dose different between the calculation and the measurement are within the acceptance criteria, the program is integrated to the RTIS.

### **Results**

The scatter sector radius determination program workflow are the selection the angle between each radius, the image distance calibration, the defining of isocenter, field size edge defining and the equivalent square field. The program will generate radius distance and export to a file. The MU calculation part workflow are the input of prescription dose and tumor depth. Following TECDOC-1540 the dose different range between the calculation and the measurement is -1.98% to 1.40% for test case 1a, 1b, 1c, 2a and 2b and the range is -3.02% to 0.99% for test case 7. This program is integrated to the dosimetry menu in the RTIS. Then the RTIS can calculate the MU for each field size of each patient and record to the patient database.

### **Conclusions**

The MU calculation computer program is developed, verified and integrated to the RTIS. The program is used for 6MV photon monitor unit calculation in 2D technique irradiation.

### **Key words**

Clarkson's integration method, IAEA-TECOC-1540, Monitor Unit, Programing.

## **INTRODUCTION OF THE RESPIRATORY TRAINING AND GUIDING SYSTEM USING THE BIOFEEDBACK ALGORITHM**

Eunhyuk Shin, Hee-Chul Park, Jungsuk Shin, Youngyih Han, Sanghoon Chung, Sungkoo Cho, Seyjoon Park, Doohoon Lim  
Samsung Medical Center, Korea

### **Purpose**

The tumor and surrounding organ movement caused by breathing have a change on reducing target dose or increasing surrounding organ dose. In order to reduce this effects in respiratory synchronized radiation therapy, we was developed a respiration training and management system and its clinical feasibility was evaluated.

### **Methods**

Our developed system was programmed in Labview. First, some various marker images located patient abdomen site were acquired using a commercial camera. After several edge enhance image process conducted to convert to binary image by applying a threshold values, a moving target was tracked by matching pre-defined tracking pattern. During the matching of image, the coordinate of tracking point was recorded for analysis of post treatment. Also, because gating and Breath hold tech. was mainly used in recent clinical respiratory synchronized radiation therapy, our system was designed to be implemented in both techniques. In the gating treatment option, Modeled respiratory guiding signal was displayed through the patient head mounted goggle system for improve regularity. In breath hold treatment option, pre-defined breath hold position in simulation stage was guided through same system for reproducibility.

### **Results**

The system had no problem in applying the patients in receiving with both treatment techniques. All patient were improved regularity (standard deviation reduction) received in gating 4DRT and reproducibility in breath-hold RT compared to without this management system.

### **Conclusions**

The developed respiratory training system is capable of improving the regularity or reproducibility in respiratory gating or breath holding treatment.

### **Key words**

4DRT, Biofeedback, Breathing management, Gating and Breath hold tech.

## A dual-pinhole imaging system for in vivo tracking of a high-dose-rate source for cervical cancer brachytherapy

Yusuke Watanabe<sup>1</sup>, Hideyuki Takei<sup>2</sup>, Hidetake Hara<sup>1</sup>, Hiroshi Muraishi<sup>1</sup>, Tsutomu Gomi<sup>1</sup>, Tsuyoshi Terazaki<sup>3</sup>, Nobuaki Shuto<sup>3</sup>, Katsunori Yogo<sup>4</sup>, Hiromichi Ishiyama<sup>5</sup>, Kazushige Hayakawa<sup>5</sup>

<sup>1</sup>School of Allied Health Sciences, Kitasato University, Japan; <sup>2</sup>Proton Medical Research Center, Tsukuba University, Japan; <sup>3</sup>Department of Radiology, Kitasato University Hospital, Japan; <sup>4</sup>Graduate School of Medical Science, Kitasato University, Japan; <sup>5</sup>Kitasato University School of Medicine, Japan

**Key words:** High-dose-rate (HDR) brachytherapy, dual-pinhole imaging system, *in vivo* source tracking

**Introduction** In high-dose-rate (HDR) brachytherapy, a remote after-loading system is used to transport a high activity Ir-192 source directly inside or near the tumor. The accuracy of the source position and dwell time directly affect the safety and quality of HDR brachytherapy. Verification of the actual dose delivered to the tumor and normal tissue requires real-time information on the actual source movement during the treatment. Our aim was to develop a dual-pinhole imaging system for *in vivo* source tracking.

**Methods** The system consists of a GOS scintillator (PI-200, Mitsubishi chemical), CCD camera, and dual-pinhole collimator, which enabled us to measure three-dimensional positions of the source based on a triangulation method (Fig.1). Dwell time was measured from the movie by counting the number of scintillation frames and the frame rate. Measurements were performed on microSelectron-HDR V3 (Nucletron, an Elekta company) using Ir-192, which is a diameter of 0.6 mm and a length of 3.5 mm. The source was transported in a water bath using a tandem and ovoid applicators to simulate a clinical case of cervical cancer brachytherapy. The source positions and dwell times were measured with the system and compared to the predefined positions and times.

**Results:** The accuracy of three-dimensional measurement of the source positions with our system depended on the accuracy of the two-dimensional measurement of the positions of the scintillation emission. The scintillation image quality was particularly affected by the radiation shielding capability of the collimator. The mean differences between the measured and predefined source positions and dwell times were  $1.0 \pm 0.4$  mm and  $0.2 \pm 0.1$  s, respectively (Fig.2). The measurement accuracy of the source positions was improved by choosing the most suitable direction of the field of view.

**Discussion:** The brightness decreased so that distance increased from the level of the pinhole. It is caused by the square of distance from the source and the attenuation of the gamma rays by the pinhole shape. It is necessary to decide the pinhole shape that accepted a treatment area appropriately. In future studies, the optimal choice of a pinhole shape that defines the field of view, would be necessary depending on the treatment area. Next development of an integrated system should improve the

geometric-installation accuracy of each component and the measurement accuracy of the system.

**Conclusion:** We demonstrated that a dual-pinhole imaging system can provide clear scintillation images for verification of dwell positions and dwell times of the Ir-192 source. The imaging system has a potential to track the *in vivo* Ir-192 source in real time and to be a useful tool for quality assurance in HDR brachytherapy under clinical use.

### References:

1. Duan J, et al. Real-time monitoring and verification of in vivo high dose rate brachytherapy using a pinhole camera. *Med Phys.* 2001 Feb;28(2):167-73.
2. MatejBatic, et al. Verification of High Dose Rate 192Ir Source Position During Brachytherapy Treatment Using Silicon Pixel Detectors. *IEEE Trans. Nucl. Sci.* 2011;58(5):2250-6.

Corresponding author email: y-nabe@kitasato-u.ac.jp

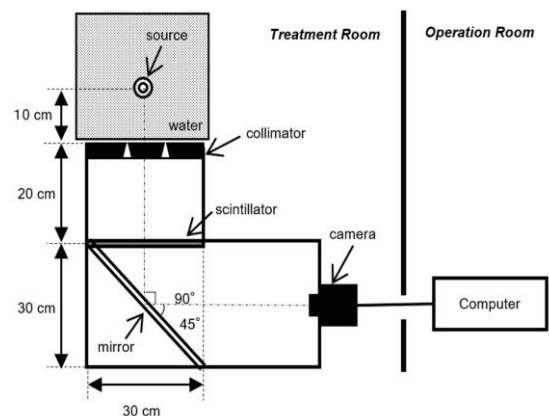


Fig.1 Schematic of the setup for Ir-192 source movement tracking system.

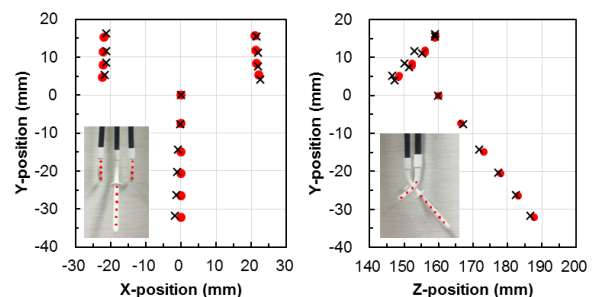


Fig.2 The differences in the measured (×) and planned (●) values for source positions. (a) X-Y plane. (b) Z-Y plane.

## **DOSE COMPARISON BETWEEN VARIABLE ANGLE AND SEMI-ORTHOGONAL RECONSTRUCTION TECHNIQUES OF THE FLETCHER APPLICATOR IN 2D-BASED BRACHYTHERAPY**

Chotika Jumpangern<sup>1</sup>, Taweap Sanghangthum<sup>2</sup>, Jaruek Kanphet<sup>1</sup>, Siriporn Promwan<sup>1</sup>

<sup>1</sup>King Chulalongkorn Memorial Hospital, Thailand

<sup>2</sup>Department of Radiology, Faculty of Medicine, Chulalongkorn University, Thailand

**Key words:** variable angle, semi-orthogonal, 2D brachytherapy, dose comparison

### **Purpose**

The applicator reconstruction in brachytherapy treatment planning system (TPS) is important. The uncertainties in the applicator position reconstruction lead to an incorrect dose distribution in the patient. In this study the variable angle (VA) reconstruction technique of the Fletcher applicator is compared with the semi-orthogonal (SO) reconstruction technique in 2D-based brachytherapy.

### **Methods**

The applicator, tandem and tandem with ovoid set, in water equivalent in-house phantom with localization jig were exposed at 0° and 90° gantry angles from conventional simulator. The applicator was set at center, 4 cm shifted in right, left, in and out directions. The images were exported to brachytherapy TPS, OncentraBrachy v. 4.3. The applicators were reconstructed using VA and SO techniques. The dwell position and dwell time were identical defined for both techniques. The dose at 4 reference points at right, left, anterior, and posterior around the applicator were compared between VA and SO reconstruction techniques.

### **Results**

The tandem reconstruction showed dose differences in right-left shifted of  $1.49 \pm 1.00\%$ , in-out shifted of  $1.35 \pm 2.02\%$ , while tandem with ovoids showed dose differences in right-left shifted of  $2.32 \pm 1.10\%$ , in-out shifted of  $4.07 \pm 3.97\%$ . The tandem alone presented the lesser dose differences ranging from  $-1.47$  to  $4.93\%$ , while the tandem with ovoid set displayed the deviation in range of  $-1.91$  to  $8.97\%$ .

### **Conclusions**

The different reconstruction methods plays an important role to the dose distribution. The applicator at right-left shifted showed the small dose deviation between VA and SO technique than longitudinal shifted. The experience of the planner is another factor to the reconstruction of the images.

## MONTE CARLO-BASED GAMMA ANALYSIS OF IMPACT OF TISSUE HETEROGENEITY ON DOSE DISTRIBUTIONS IN CERVICAL CANCER INTRACAVITARY BRACHYTHERAPY

Takahiro Iwasaki<sup>1</sup>, Hidetaka Arimura<sup>2</sup>, Tran Thi Thao Nguyen<sup>1</sup>, Yoshifumi Oku<sup>3</sup>, Takashi Yoshiura<sup>4</sup>

<sup>1</sup>Graduate School of Medical Sciences, Kyushu University, Japan

<sup>2</sup>Faculty of Medical Sciences, Kyushu University, Japan

<sup>3</sup>Kagoshima University Hospital, Japan

<sup>4</sup>Graduate School of Diagnostic Radiotherapy, Kagoshima University, Japan

**Key words:** Cervical cancer intracavitary brachytherapy, Tissue heterogeneity, Monte Carlo simulation, Gamma pass rate

### Purpose

The purpose of this study was to investigate the impact of tissue heterogeneity on dose distributions in intracavitary brachytherapy for uterine cervical cancer using high dose rate (HDR) 192-Ir with a Monte Carlo (MC) simulation.

### Methods

A computed tomography (CT) image of a cervical cancer patient and a water phantom were employed in this simulation. Fifteen 192-Ir sources were positioned within a tandem and two ovoids according to a clinical setting of dwell positions, and the same procedure was applied to the water phantom. Then, dose calculations were calculated using the MC simulation with PHITS (Particle and Heavy Ion Transport code System). The discrepancy between two dose distributions in the CT image and water phantom was evaluated by using a gamma pass rate in sagittal, coronal, and axial regions. The regions covered with 10% and 1% of a prescribed dose were evaluated by using the gamma pass rate.

### Results

A gamma pass rate in a region covered by a 10% isodose of a prescribed dose was 100%. Gamma pass rates in a region with heterogeneous normal tissue covered by 1% isodose were  $89.9 \pm 9.15$  for an axial plane,  $93.8 \pm 7.06$  for a sagittal plane, and  $74.8 \pm 8.95$  for a coronal plane.

### Conclusions

The impact of tissue heterogeneity on dose distributions could not be negligible within a region covered by 1% of a prescribed dose.

## **SURFACE DOSE MEASUREMENTS USING GAFCHROMIC EBT2 FILMS FOR HIGH DOSE RATE BRACHYTHERAPY**

Wan Nordiana Rahman

Universiti Sains Malaysia

**Key words:** Film dosimetry, Gafchromic EBT2, Brachytherapy, Surface dose

### **Purpose**

To evaluate the feasibility of Gafchromic EBT2 films for surface dose measurements using High Dose Rate (HDR) Brachytherapy Methods Surface dose measurements were conducted with dose prescription of 5 Gy at 1 cm using Gafchromic EBT2 films for HDR Brachytherapy with Iridium-192 source. Measurements were done at various step size sources of 0.25, 0.5 and 1 cm using single and double catheters. The films were position at 5 cm and 1 cm depth from the source. The results were then compare to treatment planning data.

### **Results**

The results show that the dose profiles have better uniformity at smaller step size at the middle of the source distance along the catheter. Double catheters also present better dose distribution compare to the single catheter due to smaller hot spot. Comparison with the treatment planning data indicate percentage differences up to 10%.

### **Conclusions**

In conclusion, surface dose measured using Gafchromic EBT2 films were found to be more uniform when double catheters and smaller step size sources were employed. Gafchromic EBT2 films have clinical potential for further application in brachytherapy dosimetry.

## **RADIOBIOLOGICAL MODEL APPLICABILITY IN RADIOTHERAPY: SINGLE AND FRACTIONATED IRRADIATION**

Nurul Akmal Ariffin ,Wan Nordiana , Rahman , Norhayati Dollah , Raizulnasuha Abd Rashid

Universiti Sains Malaysia

**Key words:** Linear Quadratic model, Multi-Target model, Single Irradiation, Fractionated Irradiation

### **Purpose**

Cell survival described by radiobiological models could be used to predict the radiosensitivity and sublethal damage repair of cells to radiation. In this study, the linear quadratic (LQ) and multi-target (MT) cell survival curve models were used to describe the cell survival with single and fractionated irradiation.

### **Methods**

HeLa cells were irradiated using 6 MV photon beam with 10×10 cm<sup>2</sup> field size, 100 cm SSD at different doses. Standard clonogenic assay was performed to determine the cell survival. The experimental data were fitted to the LQ and MT model using OriginPro 9.2 software. Radiobiological parameters were evaluated from the fitting curves generated from these models.

### **Results**

Fitting curve of the LQ and MT models for cell survival with single irradiation were found to be close to the experimental data. The survival curves fitted with LQ and MT model for single irradiation displayed steep initial slope and small shoulder. The sublethal damage repair was better for fractionated irradiation with wider shoulder. The parameters of LQ model showed a larger  $\alpha/\beta$  ratio whereas for MT model showed a smaller  $n$ ,  $D_0$  and  $D_q$ .

### **Conclusions**

MT model seems to be more accurate in describing the radiosensitivity of the cells especially at high dose for both single and fractionated irradiation because the experimental data plotted fitted closely to the curve. The most commonly used model, LQ seem to provide unsatisfactory fitting at high dose. Both models were applicable in analysing single and fractionated irradiation.

## **IN-VITRO INVESTIGATION OF OUT-OF-FIELD CELL SURVIVAL FOR PHOTON BEAM RADIOTHERAPY**

Nurhikmah Azam , Wan Nordiana Rahman , Mohd Reduan Abdulllah , Norhayati Dollah, Raizulnasuha Rashid , Rosmazihana Lazim

Universiti Sains Malaysia

**Key words:** intercellular communication, out-of-field, infield, cell survival fraction, photon beam, radiosensitivity

### **Purpose**

to determine the effect of out-of-field photon beam radiotherapy to the cell survival

### **Methods**

Two different types of cells were prepared which are HeLa and T24 cancer cells. Cells were irradiated in two different conditions, one with intercellular communication with the infield cell and one without the communication. Irradiations were done using 6 MV and 10 MV of photon beam energies. Cells survival was determined by clonogenic assay

### **Results**

The data showed that when intercellular communication was present, the cell death was increased thus decrease in survival fraction. However, this effect only demonstrated at 10 MV rather than 6 MV. 6 MV of energy was insufficient to produce the effect of intercellular communication towards the cell survival with 300 cGy doses delivered to the cell. In a comparison of cell type, higher cell death was exhibited by HeLa as compared to T24 cells.

### **Conclusions**

In a nutshell, it appeared that the communication status and photon energy level was the determinant of survival difference. Since the effect is not solely based on scattered radiation, thus, the intercellular communications become a significant issue. Inhibition of intercellular communication will increase the cell survival. Although the cell survival was reduced when using 6 MV compared to 10 MV of photon energy but it was insufficient to prove the effect of intercellular communication. For the cell comparison, T24 was said to be more radioresistant since higher survival fraction from HeLa cells.

## **DOSE ENHANCEMENT EFFECTS WITH DIFFERENT SIZE OF GOLD NANOPARTICLES FOR 6 MV PHOTON BEAM**

Mahfuzah Muhammad , Wan Nordiana W Abd. Rahman , Raizulnasuha Abdul Rashid ,  
Norhayati Dollah

Universiti Sains Malaysia

**Key words:** Size AuNPs, survival curve, DEF

### **Purpose**

Gold nanoparticles (AuNPs) have been widely investigated as radiation dose enhancer for radiotherapy due to its intriguing potential in increasing radiotherapy therapeutic efficiency. The applicability of AuNPs depends on many factors including nanoparticles size. In this study, the effects of nanoparticle size on the AuNPs dose enhancement effects were investigated.

### **Methods**

AuNPs of 5nm and 15 nm were used in this study. The efficacy of both sizes of AuNPs was tested in-vitro using HeLa cell lines. The cells were incubated with the AuNPs and irradiated at different doses with 6 MV photon beam at 100 cm SSD and 10 cm x 10 cm field size. Cell survival curves were obtained from standard clonogenic assay and fitted to the Linear Quadratic (LQ) model using OriginPro 9.2 software. Dose enhancement factor (DEF) and radioparameters were extrapolated and evaluated from the cell survival curve.

### **Results**

The results show that 15 nm AuNPs produce better dose enhancement compare to 5 nm of AuNPs. DEF for 15 nm are found to be around 2.2 meanwhile for 5 nm is 1.75. The curves also demonstrate steepest slope and small shoulder for larger size AuNPs which indicate increase in biological effects. The LQ parameters such as alpha, beta and alpha/beta ratio are in agreement with the DEF results.

### **Conclusions**

Larger size AuNPs produce higher dose enhancement compare to small size of AuNPs which conclude that nanoparticles size is important factor that need to be taken into account for AuNPs to be applied in radiotherapy.

## **BIOPHYSICAL MODELING FOR TARGETED AND NON-TARGETED EFFECTS ON CELLS AFTER IRRADIATION**

Yusuke Matsuya<sup>1</sup>, Kohei Sasaki<sup>2</sup>, Yuji Yoshii<sup>3</sup>, Hiroyuki Date<sup>4</sup>

<sup>1</sup>Graduate School of Health Sciences, Hokkaido University, Japan

<sup>2</sup>Faculty of Health Sciences, Hokkaido University of Science, Japan

<sup>3</sup>Biological Research, Education and Instrumentation Center, Sapporo Medical University, Japan

<sup>4</sup>Faculty of Health Sciences, Hokkaido University, Japan

**Key words:** Targeted and Non-targeted effects, Cell surviving fraction, Integrated Microdosimetric-Kinetic model

### **Purpose**

Radiosensitivity of cells after low-dose irradiation is affected by not only targeted effects but also non-targeted effects. The purpose of this study is to quantify the surviving fraction (SF) of cells in consideration of both these effects.

### **Methods**

To establish a biophysical model for both targeted and non-targeted effects, we customized the Microdosimetric-Kinetic (MK) model, calling it the "Integrated MK (IMK) model." The IMK model was applied to fit the experimental SF data reported by B. Marples, et al. Next, we made a further modification of the model to include medium transfer non-targeted (MTNT) effects, and compared the resultant SF with the experimental data by Z. Liu, et al. The adequacy of the model was evaluated with the chi-square value and Akaike's Information Criterion (AIC).

### **Results**

It was shown that the IMK model illustrates low-dose hyper-radiosensitivity (HRS) and MTNT effects in good agreement with the experimental data, where the values of chi-square and AIC are smaller than those in the conventional MK model.

### **Conclusions**

We developed the IMK model by incorporating both targeted and non-targeted effects. The model can describe the low-dose SF properly and even the medium transfer non-targeted effects.

## **BIOLOGICAL EFFECT CONSIDERATIONS WHEN COMPARING FRACTIONATED AND SINGLE-DOSES OF HELICAL TOMOTHERAPY ON HUMAN CERVICAL CANCER CELLS**

Kochakorn Phanthawong<sup>1</sup>, Satit Inta<sup>1</sup>, Nahathai Dukaew<sup>2</sup>, Damrongsak Tippanya<sup>1</sup>, Somsak Wanwilairat<sup>1</sup>, Ekkasit Tharavichitkul<sup>1</sup>, Sittiruk Roytrakul<sup>3</sup>, Ariyaphong Wongnoppavich<sup>2</sup> and Narongchai Autsavapromporn<sup>1</sup>

<sup>1</sup>Division of Therapeutic Radiology and Oncology, Department of Radiology

<sup>2</sup>Department of Biochemistry, Faculty of Medicine, Chiang Mai University, Chiang Mai, 50200, Thailand

<sup>3</sup>Proteomics Laboratory, Genome Institutes, National Center for Genetic Engineering and Biotechnology, Thailand Science Park, Pathumthani, 12120, Thailand

**Key words:** Cervical Cancer, Fractionation, Helical Tomotherapy, Biological Effects

### **Purpose**

Cervical cancer is the leading cause of cancer for Northern Thai women and radiotherapy remains a common treatment. However, to improve treatment of cervical cancer, there is a need to better understanding how cancer cells respond to the fractionated-dose in comparison with single-dose irradiations and explicate new specific biomarker for predict treatment outcome. In this study was conducted to determine biological effects of human cervical cancer cells (HeLa cells) after fractionation and single doses of Helical Tomotherapy

### **Methods**

HeLa cells were exposed with fractionation (2 Gy/day for 3 days) and single doses (6 Gy/day) with HT. After irradiation, cells were assessed by colony formation for determined ability of cell proliferating and micronucleus formation, which detection tool of radiation-induced DNA DSB damage.

### **Results**

Relative to non-irradiated HeLa cells, fractionated irradiation show HeLa cells exhibited increased colony formation (45.3%) than a single-dose irradiation (2.7%), and consistent with decreased micronucleus formation in fractionation (9.5%) by comparison with single dose (29.7%). Therefore, the overall treatment time allow the repopulation of surviving cancer cells, which occur in the observed effects.

### **Conclusions**

These finding provide that HT are given in multiple doses, which are spaced out to allow the repair of damage in survival cancer cells between treatments than a single dose and this process of repopulation is an important factor for treatment failure. Additional research is needed to focus on new strategies to a specific inhibit the repopulation of survival cervical cancer cells that could potentially further improve clinical outcomes.

## The effects of different treatment schedule with immunological aspects in radiotherapy

M Oita<sup>1</sup>, K Nakata<sup>2</sup>, H Aoyama<sup>3</sup>, M Sasaki<sup>4</sup>, M Tominaga<sup>5</sup>, H Honda<sup>6</sup>, Y Uto<sup>7</sup>

<sup>1</sup> Okayama University Graduate School of Health Sciences, Japan; <sup>2</sup> Tokyo University of Science, Japan; <sup>3</sup> Okayama University Hospital, Japan; <sup>4</sup> Tokushima University Hospital, Japan; <sup>5</sup> The Tokushima University, Department of Radiological Technology, Japan; <sup>6</sup> Ehime University Hospital, Japan; <sup>7</sup> The Tokushima University, Department of Life System, Japan

**Key words:** Immuno-radiotherapy, radiobiology, TCP/NTCP

**Introduction:** Recent advances in immunotherapy make possible to combine with radiotherapy. Hypoxia, intrinsic radioresistance, and cellular proliferation of the tumor cells are known to induce genetic and molecular biological changes. Applying biophysical models for treatment planning in radiotherapy could improve both tumor responses and tissue toxicities [1,2]. Nevertheless, there are some uncertainties surrounding radiosensitivity due to many biological factors, which are still under investigation [3-6]. The aim of this study was to assess the TCP/NTCP model with immunological aspects in different treatment schedule (5fr/week and 6fr/week).

**Methods:** In the clinical 3D-RTPS (Eclipse ver.11.0, Varian medical systems, US), biological parameters can be set as any given values to calculate the TCP/NTCP. Using a prostate cancer patient data with VMAT commissioned as a 6 MV photon beam of Novalis-Tx (BrainLab, US) in clinical use, the fraction schedule in this analysis were hypothesized as 70-78Gy/35-39fr, 72-81Gy/40-45fr, 52.5-66Gy/16-22fr, 35-40Gy/5fr of 5-7 fractions in a week. The effects of the TCP/NTCP variation of repair parameters of the immune system as well as the intercellular uncertainty of tumor and normal tissues have been evaluated.

**Results:** Regardless of the difference of the  $\alpha/\beta$ , the TCP/NTCP had increased in conventional fractionation protocols in the 6fr/week rather than 5fr/week arm, or in hypo-fractionation protocols. For tumor, if the repopulation parameters such as  $T_{pot}$  and  $T_{start}$  could immunologically work as elongation of those time, the TCP improved in the 6fr/week rather than 5fr/week arms. However, the elongation

of repair half-time (long) increased the NTCP in the case of 6fr/week arms with conventional fractionation protocols.

**Discussion:** Our study suggested that the TCP/NTCP should have considered not only the general biological parameters such as the  $\alpha/\beta$  ratio,  $D_{50}$ ,  $\gamma$ , but also repair, repopulation and other parameters for complicated cellular responses. We also have found that the optimal fractionation and dose fraction protocol relates to those factors and uncertainties would improve the tumor responses and tissue toxicity in immune-radiotherapy.

**Conclusion:** We have shown the variety and difference of biological parameters of the tumor and normal tissues. Conventional fractionation protocols could improve in the 6fr/week. Farther improvements are required for the RTPS, which incorporated with complicated biological optimization.

### References:

- Hayes M, Lan C, Yan J, et al., (2011) ERCC1 expression and outcomes in head and neck cancer treated with concurrent cisplatin and radiation. *Anticancer Res* 31:4135-4139
- Gluck I, Vineberg KA, Ten Haken RK et al., (2009) Evaluating the relationships between rectal normal tissue complication probability and the portion of seminal vesicles included in the clinical target volume in intensity-modulated radiotherapy for prostate cancer. *Int J Radiat Oncol Biol Phys* 73:334-340
- Dasu A, Toma-Dasu I, and Fowler JF, (2003) Should single or distributed parameters be used to explain the steepness of tumour control probability curves? *Phys Med Biol* 48:387-397
- Gong J, Dos Santos MM, Finlay C et al., (2013) Are more complicated tumour control probability models better? *Math Med Biol* 30:1-19
- Hall EJ, Astor M, Bedford J et al., (1988) Basic radiobiology. *Am J Clin Oncol* 11:220-252
- Harada H, (2011) How can we overcome tumor hypoxia in radiation therapy? *J Radiat Res* 52:545-556

Corresponding author email: oita-m@cc.okayama-u.ac.jp

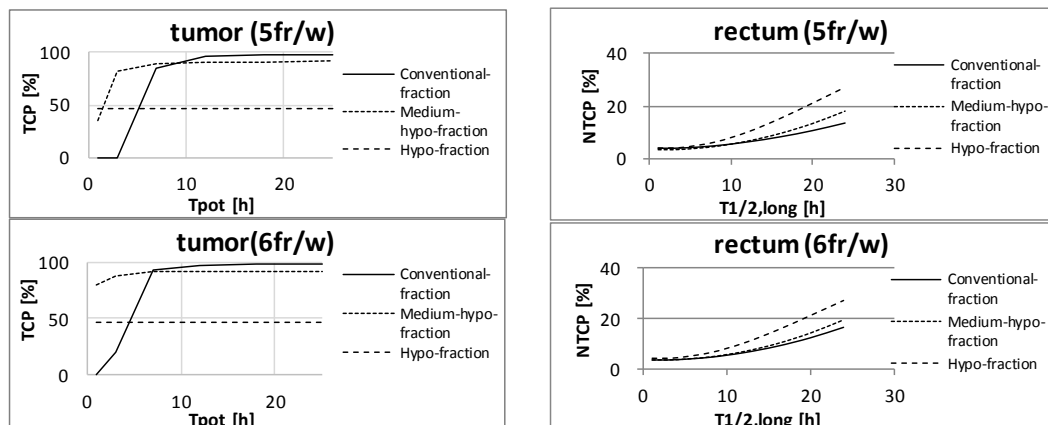


Fig.1 The differences of TCP/NTCP changes by repopulation/repair between five and six fractions per week in various dose fraction protocols.

## What We Know About the Biological Effects after Single-and Fractionated Doses of Helical Tomotherapy on Human Lung Cancer-and Normal Lung Cells

S Inta, K Phanthawong, D Tippanya,  
S Wanwilairat, P Klunklin and N Autsavapromporn\*

Division of Therapeutic Radiology and Oncology, Department of Radiology, Faculty of Medicine, Chiang Mai University, Chiang Mai, 50200, Thailand

**Key words:** Lung cancer, Normal lung fibroblasts, Fractionated doses, Helical tomotherapy

**Purpose:** Radiobiological effects have been concerned in their biological responses on human tumors and normal tissues during and after fractionated radiation treatment. However, little is known about the effects of Helical Tomotherapy (HT) that delivers radiation therapy with a spiral delivery, which travels around the patient [1]. The aim of the current study was to investigate the biological effects in lung cancer-and normal lung cells after single-and fractionated-doses of HT.

**Materials and methods:** Confluent normal lung fibroblasts (MRC5) and human pulmonary adenocarcinoma (A549) cells cultured in 25 cm<sup>2</sup> cell culture flasks. The flasks were filled up medium and placed into hole of virtual water phantom then exposed to HT at a single dose of 6Gy in 1 fraction and fractionate doses of 6Gy in 3 fractions given at three consecutive days (2 Gy × 3 days). Immediately after irradiation, cells were assayed for different endpoints consisting of colony formation, micronucleus formation and protein oxidation.

**Results:** Percentage of viable MRC5 cells exposed to fractionation irradiation reduced to 29.33%, compared with the control group, while single dose had lowest survival fraction (2.49%). Similarly, fractionated irradiation of A549 cells (52.83%) showed more survival rate than single dose (4.3%). The responses of two cell lines in the same regimen revealed that the fractionated doses induced increase of cell viability more than single dose. In addition, the relative rate of repair (RRR) compares survival rate of fractionated-to single dose were found increased higher in A549 cells (12.28) than MRC5 cells (11.78).

Moreover, the study of DNA damage at the chromosome levels showed a good correlation with the colony formation assay. As shown in figure 1, the frequency of micronuclei in both normal fibroblasts and lung cancer cells increased in single dose more than fractionated dose.

**Acknowledgments:** This work is funded by National Research Universities-Chiang Mai University (Gynecologic Oncology) and Chiang Mai University.

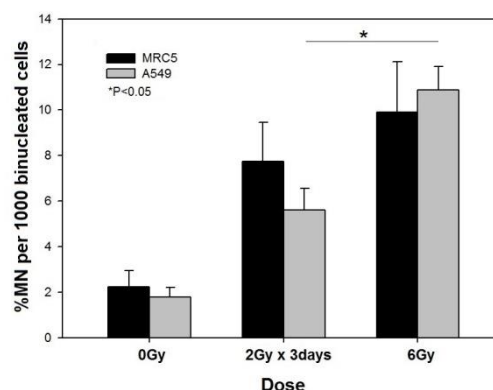


**Figure 1:** Frequency of micronuclei in MRC5-and A549 cells after single-and fractionated doses of HT (n=5).

We further confirmed those result using Protein oxidation was shown that reactive oxygen species (ROS) levels increased in single dose than in fractionated doses.

**Discussion:** Our study first compared the radiobiological effects of single-and fractionated doses of HT on human lung cancer and normal lung cells. Both cell lines exhibited decreased cloning efficiency with single dose irradiation more than those induced by the fractionated irradiation of HT [2]. Interestingly, normal human lung cells proliferate relatively more slowly compared to lung cancer cells, which were found to be correlated with the levels of DNA double strand breaks damage and ROS.

**Conclusions:** Our finding support the role of repair and repopulation of survival lung cancer cells during radiotherapy. They highlight the importance role of fractionated irradiation in the irradiated cells, may have potential implication in the risk of second cancer among survival patients after treatment. Further studies are needed to investigate the biological effects cross-talk between lung cancer and normal lung cells.

### References:

1. Welsh JS, Patel RR, Ritter MA, (2002), Helical Tomotherapy: An Innovative Technology and Approach to Radiation Therapy. *Technol Cancer Res Treat.* 1(4):311-16.
2. Carsten N. and Michael B. Fractionation Concepts. In: C. CarstenNieder, J.A. Langendijk, editors. *Re-irradiation: New frontiers.* Springer, Berlin, 2011: p. 13-26.

\*Corresponding author email: narongchai.a@cmu.ac.th

## Evaluation of the effect of ionizing radiation on the elastic properties of human erythrocytes cytoskeleton

E. Spyratou<sup>1</sup>, K. Platoni<sup>1</sup>, M. Dilvoi<sup>1</sup>, M. Makropoulou<sup>2</sup>, A.Serafetinides<sup>2</sup>, E. P. Efstathopoulos<sup>1</sup>

<sup>1</sup>2<sup>nd</sup> Department of Radiology, Medical School, National and Kapodistrian University of Athens, 12462 Athens, Greece.

<sup>2</sup> Physics Department, Faculty of Applied Mathematical and Physical Sciences, National Technical University of Athens, Zografou Campus, 15780 Athens, Greece.

**Keywords:** Erythrocytes, elasticity, ionizing radiation, Atomic Force Spectroscopy

**Introduction:** The biomechanical behavior of the erythrocyte's membrane skeleton is an important predictor of circulation efficiency and cell's health. In this work the effect of ionizing radiation at different doses on the morphology and the elastic properties of human erythrocytes were studied after radiation treatment. The dose threshold at which no erythrocyte's alteration is indicated was also evaluated. The erythrocyte's changes were probing by using Atomic Force Microscopy which is ideally suited for single cell measurements providing simultaneously information about the morphology and the mechanical properties of the cells in nanoscale.

**Methods:** Whole human blood was drawn by venipuncture and subjected to the minimum possible treatment which can be induced morphological alterations. The blood samples were irradiated in the range of 0.2Gy -2.0 Gy doses and with a dose rate of 240 cGy/min. The morphology and the elastic modulus of the erythrocytes were examined in comparison with non-irradiated erythrocytes by using AFM and just few drops of whole blood without any special preparation.

**Results:** No morphological changes appeared according to the shape of the erythrocytes. However, the roughness of the erythrocyte cytoskeleton was increased as the irradiation dose was increased. According to the quantitative analysis of the AFM force curves, the elasticity modulus of the irradiated sample was reduced with the increasing of radiation dose.

**Discussion:** AFM appears a powerful tool and accurate technique for probing cytomorphology and biomechanical properties of the erythrocytes. Changes in the membrane elasticity were found with a strong correlation of the irradiated. The roughness of the cytoskeleton membrane is correlated with any redistribution of lipid molecules or proteins in the membrane bilayer and can indicate any rearrangement of the bilayer structure induced by external factors such as ionizing irradiation.

**Conclusions:** The elastic modulus and the membrane roughness of the erythrocytes could be an index to assess the damage caused by irradiation.

### References:

1. O'Reilly M, McDonnella L, O'Mullane J, (2001), Ultramicroscopy 86:107-112.
2. Thomas G, Burnham N A, Camesano T A, Wen Q, (2013), J. Vis. Exp. 76: e50497.
3. Zhang B, Liu B, Zhang H, Wang J, (2014), Plos One 9: e112624

**Corresponding author email:** spyratouellas@gmail.com

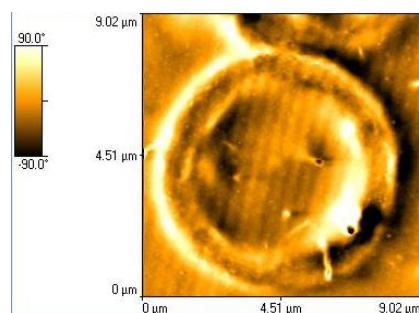


Figure 1. AFM topographic image of a single erythrocytes irradiated with 2 Gy.

## **PERFORMANCE EVALUATION OF TOTAL VARIATION (TV) TECHNIQUE FOR NOISE REDUCTION IN DIGITAL SUBTRACTION ANGIOGRAPHY (DSA)**

Youngjin Lee, Kanghyen Seo, Seung Hun Kim, Se Young Bae, Jong Seok Kim, Seong Hyeon Kang, Dong Jin Shin

Eulji University, Republic of Korea

**Key words:** Digital subtraction angiography (DSA), Total variation (TV), Noise reduction

### **Purpose**

The edge is the identifying point where gray value is changing rapidly in image. Not only exact segmentation of this point but also noise reduction methods can improve image performance in the field of the digital angiography. The purpose of this study was to quantitatively evaluate image performances using contrast to noise ratio (CNR) and normalized noise power spectrum (NNPS) with respect to the various noise reduction techniques in digital subtraction angiography (DSA) images.

### **Methods**

As a highly accurate edge preservation and noise reduction, we can consider many denoising techniques. Among these techniques, total variation (TV) is very useful and powerful technique for noise reduction. In the following, we applied the median filter, Rudin-Osher-Fatemi (ROF), Anscombe and TV and evaluated a quantitative result of the simulation and experimentation. The projection image and simulation phantom image were acquired and we calculated the CNR and NNPS.

### **Results**

The measured CNR of the noisy image, median filter, ROF, Anscombe and TV was about 28.41, 126.38, 109.26, 134.94 and 294.82, respectively in simulation. The result of NNPS using the used techniques showed that the highest noise reduction was acquired by using a TV in both simulation and experimentation.

### **Conclusions**

In conclusion, our results demonstrated that TV is the best denoising technique because of the highest CNR value and NNPS at all frequencies in DSA images.

## **COMPARATIVE STUDY OF IMAGE QUALITY BETWEEN GOLD NANOPARTICLES AND IODINE CONTRAST MEDIA USING MOBILE AND GENERAL X-RAY**

Nooriedayu Mohd Said, Wan Nordiana Rahman, Ahmad Zaky Harun, Raizulnasuha Abd Rashid

University Sains Malaysia

**Key words:** Contrast media, AuNPs, Iodine

### **Purpose**

To comparatively investigate the effects of Iodinated contrast media (CM) and Gold nanoparticles as potential contrast media to increase the image quality in general radiography.

### **Methods**

AuNps and Iodine were prepared in 3mMol, 5mMol, 10mMol, 15mMol, 20mMol, 30mMol and 40mMol. Those samples were exposed under digital radiography (DR) and computed radiography (CR) techniques from 50 kVp to 110kVp and 5 mAs. The regions of interests (ROIs) were drawn on the image to obtain the mean pixel value (MPV). Signal-to- Noise Ratio (SNR), Contrast-to-Noise Ratio (CNR) and Mean Pixel Contrast (MPC) then were calculated from MPV.

### **Results**

The SNR value of AuNPs and Iodine contrast media were dependent on the tube potential used. The SNR value increase linearly with tube potential for CR and for DR the linear increase stop at 70 kVp and remain constant. The CNR value also show similar pattern for AuNPs and iodine but show significant different at higher kVps. The MPC also found to be higher in DR compared to CR. The study found that 40 mMol produce the best image quality for CR and 3 mMol is enough to obtain similar results with DR.

### **Conclusions**

This study indicates the potential of AuNPs as contrast agent. However, more optimization on the nanoparticles concentration and characteristic as well as the tube potential is necessary to translate the application of AuNPs into clinical practice.

## PRECISION IMPROVEMENT OF THE CA-SCORING IN THE EXERCISING HEART

Toshihiko Yamagiwa<sup>1</sup>, Katsumi Tsujioka<sup>2</sup>, Masayoshi Niwa<sup>3</sup>, Yoichi Tomita<sup>4</sup>, Yujiro Doi<sup>5</sup>, Ryoichi Katou<sup>2</sup>

<sup>1</sup>Fujita Graduate School of Health Sciences, Fujita Health University, Japan

<sup>2</sup>Fujita Health University School of Health Sciences Faculty of Radiological Technology, Japan

<sup>3</sup>Department of Radiology, Yokkaichi Municipal Hospital, Japan

<sup>4</sup>Department of Radiology, Meitetsu Hospital, Japan

<sup>5</sup>Department of Radiology, Fujita Health University Hospital, Japan

**Key words:** Ca-scoring, Partial volume effect, Volume measurement

### Purpose

The Ca-scoring becomes the important information of the examination of heart. However, it is not measured definitely by cardiac movement. We developed the new method of the Ca-scoring to solve this problem. Our method is satisfied by two of the TPVE (temporal partial volume effect) method and the Ring-ROI method. The TPVE method increased the time element in conventional PVE (partial volume effect). The Ring-ROI method supports the neighboring CT level change at the volume calculation.

### Methods

The disk of hydroxyapatite of 5mm in diameter and 2mm thickness was used for the experiment. Around this disk was filled with agar and oil. The ratio of agar and oil were changed with 0:100, 25:75, 50:50, 75:25 and 100:0. This phantom exercises at speed same as heart by a robot. We performed Ca-scoring using the TPVE method and the Ring-ROI method with scanned data set.

### Results

In the case of a conventional method, the result of the measurement changed by phantom motion. And the measured volume was always less than 50% of hydroxyapatite disk. According to our new method, the measurements were constant without depending on the movement of the phantom, and the measurement error was less than 8%.

### Conclusions

Ca-scoring is the important measurement by clinical practice. However, results of measurements are change by heart movement. And we cannot stop heart movement. The TPVE method and the Ring-ROI method that we developed can solve these problems.

## **EFFECTS OF GOLD NANOPARTICLES SIZE AND CONCENTRATION ON IMAGE CONTRAST IN CT IMAGING**

Siti Nor Shikha Othaman<sup>1</sup>, Moshi Geso<sup>2</sup>, Wan Nordiana Rahman<sup>1</sup>, Ahmad Zaky Harun<sup>1</sup>, Raizulnasuha Rashid<sup>1</sup>

<sup>1</sup>Universiti Sains Malaysia

<sup>2</sup>RMIT University, Australia

**Key words:** AuNPs, CT imaging, Contrast enhancement, Hounsfield unit, CNR, size AuNPs, Concentration AuNPs

### **Purpose**

To investigate the effects of gold nanoparticles (AuNPs) size and concentration on image contrast in computed tomography (CT) imaging. Influence of CT parameters such as tube voltage and kernel reconstruction was also evaluated.

### **Methods**

The sizes of AuNPs investigated were 1.9nm, 15nm, 20nm, and 40nm prepared in different concentration from 1mMol to 40 mMol. The AuNPs samples were scanned under CT SOMATOM Definition AS scanner at tube voltages from 80 kVp to 140 kVp at 410 mAs and different types of kernel reconstruction modes. The Hounsfield Unit (HU) for each sample was analysed and the contrast to noise ratio (CNR) were calculated

### **Results**

The results indicate contrast enhancement by AuNPs with the AuNPs of 15 nm size provide highest CNR value compared to smaller AuNPs. Different concentration of AuNPs also influence the contrast with highest CNR obtained at 15 mMol for 1.9 nm meanwhile the 15 nm provided highest CNR at 20 mMol concentration. The standard deviations (SD) of different kernel modes used indicate lower SD for the head protocol compared to abdomen protocol. The choice of tube voltage could alter the contrast as the CNR value dependent on the attenuation level proportion to the kVp.

### **Conclusions**

AuNPs sizes and concentration has significant influence on CT contrast enhancement as well as CT tube voltage and kernel reconstruction mode. As a conclusion, AuNPs have clinical potential as contrast agent for CT imaging with details characterization on the AuNPs and CT parameters.

## DEVELOPMENT OF AN ULTRA-SMALL ANGLE X-RAY SCATTERING IMAGING USING LAUE CASE ANALYZER

D Shimao<sup>1</sup>, N Sunaguchi<sup>2</sup>, T Yuasa<sup>3</sup>, S Ichihara<sup>4</sup>

<sup>1</sup>Hokkaido University of Science, Japan; <sup>2</sup>Gunma University, Japan; <sup>3</sup>Yamagata University, Japan; <sup>4</sup>Nagoya Medical Center, Japan

**Key words:** ultra-small angle X-ray scattering, Laue case analyzer, synchrotron, breast cancer

**Introduction:** Ultra-small angle x-ray scattering (USAXS) imaging using Bragg case analyzer has been proved to be good at depicting objects with weak x-ray absorption but exhibiting strong USAXS[1-3]. The purpose of this study is to develop a novel USAXS imaging by “Laue case” wafer as an analyzer crystal[4].

**Methods:** A symmetrically cut Si (111) Laue case analyzer was utilized for the USAXS imaging. The imaging experiment was performed using synchrotron radiation (KEK Photon Factory, BL14B) of 19.8 keV (Fig. 1). The imaging object was breast cancer specimen embedded in paraffin. The rotation angle range of Laue case analyzer was  $-2.4^\circ$  to  $+2.4^\circ$  at  $0.02^\circ$  step during image acquisition by CCD camera. The exposure time of the each projection image was 2 sec. The degree of ultra-small x-ray scatter was estimated from the expanse of the intensity curve of the each local pixel during Laue case wafer rotated within the range. Then fusion image of refraction contrast image and USAXS image was made.

**Results:** High sensitivity USAXS image of breast cancer specimen by Laue case analyzer was acquired and the area with large USAXS was indicated as brighter area. Refraction contrast image and USAXS image of the same area, and their fusion image were shown in Fig. 2.

**Conclusions:** It was revealed that we could acquire some new internal information of breast cancer specimen on USAXS image, which are different from that on refraction contrast image, with greater sensitivity than that using conventional Bragg case analyzer. Although we need to compare findings on USAXS image with pathological ones,

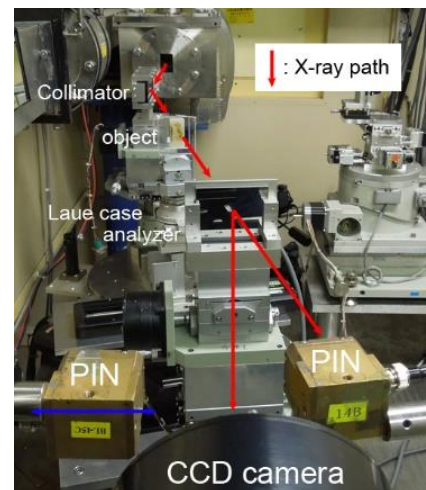


Fig.1 Imaging apparatus constructed at KEK PF BL14B.

USAXS imaging using Laue case analyzer may have a potential for a novel image diagnosis method.

### References:

1. Wernick MN, Wirjadi O, Chapman D, et al. (2003), Phys. Med. Biol. 48, 3875-3895
2. Khelashvili G, Brankov JG, Chapman D, et al. (2006), Phys. Med. Biol. 51, 221-236
3. Suhonen H, Fernandez M, Bravin A, et al. (2007), J. Synchrotron. Radiat. 14, 512-521
4. Shimao D, Kunisada T, Sugiyama H, et al. (2007), Jpn. J. Appl. Phys. 46, L608-L610

Corresponding author email: shimao-d@hus.ac.jp

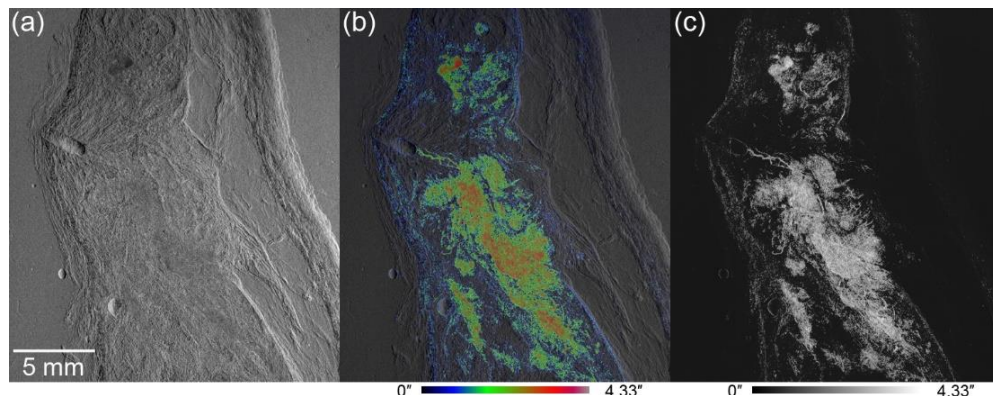


Fig.2(a): Refraction contrast image, (b): fusion image of (a) and (c), (c): USAXS image.

## **EEG COHERENCE IN ALZHEIMER'S DISEASE (AD) AND MILD COGNITIVE IMPAIRMENT (MCI) PATIENTS**

Nita Handayani, Idam Arif, Siti Nurul Khotimah, Freddy Haryanto, Warsito Purwo Taruno

Institut Teknologi Bandung, Indonesia

**Key words:** EEG, Alzheimer's Disease, Coherence, Mild Cognitive Impairment

### **Purpose**

This paper presents a EEG study for interhemispheric and intrahemispheric coherence in Alzheimer's Disease (AD) and Mild Cognitive Impairment (MCI) patients. EEG coherence is a statistical measure of correlation signals from electrodes spatially separated on the scalp.

### **Methods**

Brain signals recorded using the Emotiv EPOC 14 channel (AF3, AF4, F3, F4, F7, F8, FC5, FC6, T7, T8, P7, P8, O1, O2) and 2 channels reference (CMS and DRL) with a sampling frequency of 128 Hz. Subjects consisted of 5 MCI patients, 5 AD patients and 10 healthy subjects as controls. Coherence of each electrode pair are calculated for all frequency bands (delta, theta, alpha and beta).

### **Results**

In AD patients, the value of coherence is generally lower than MCI patients and healthy subjects. The decline of intra-hemispheres coherence value in AD patients occurred in the left temporo-parietal-occipital region. A pattern of decline in AD coherence is associated with decreased cholinergic connectivity along the path that connects the temporal, occipital, and parietal to the frontal area of the brain. The decreased of this brain connectivity is caused by the formation of beta amyloid plaques and tau protein tangles in the brain of AD patients.

### **Conclusions**

The study of EEG coherence has the potential to distinguish between potential AD patients in the early stages from healthy elderly subjects. Coherence can be used as a mathematical and physiological markers in the EEG for early detection of AD.

## **UNMATCHED SYSTEM MODEL-BASED ITERATIVE RECONSTRUCTION IN COMPUTED TOMOGRAPHY**

Seungwan Lee, Sooncheol Kang, Jisoo Eom

Konyang University, Republic of Korea

**Key words:** Unmatched system model, Iterative reconstruction, Computed tomography

### **Purpose**

A projector is an essential component for iterative reconstruction because the projector determines the characteristics of a system model and reflects system geometry as well as imaging physics. Although several projectors were proposed with their benefits, each projector has limitations in forward- or back-projection. The purpose of this study is to perform iterative reconstruction using unmatched system models in computed tomography (CT) and evaluate the quality of reconstructed images.

### **Methods**

Unmatched system models were designed by using pixel-driven, ray-driven, and distance-driven projectors. 180 projections of a simulated phantom were obtained during a 360 degree rotation. The projections were reconstructed by using the maximum-likelihood expectation maximization (MLEM) algorithm, which was modified to allow the use of unmatched system models, with 30 iterations. The reconstructed images were analyzed by using coefficient-of-variation (COV), full-width at half-maximum (FWHM) and normalized root-mean-square error (NRMSE) for evaluating noise, spatial resolution and artifacts.

### **Results**

The unmatched system models with the distance-driven back-projector decreased the COV by factors of 0.06-0.32 for the other back-projectors. The NRMSE of the images reconstructed with the distance-driven forward-projector were 0.53-0.95 times smaller than those reconstructed with the other forward-projectors. The ray-driven back- projector decreased the FWHM by factors of 0.86-0.89 for the other back-projectors.

### **Conclusions**

The unmatched system models for iterative reconstruction affect noise, spatial resolution, and artifacts. The optimal combination of forward- and back-projectors can be determined in consideration of image quality improvement.

## CR VS. DR VS FILM-SCREEN COMPARISON OF DOSE REDUCTION AND IMAGE QUALITY

Magdalena Stoeva<sup>1</sup>, Alexander Georgiev<sup>2</sup>

<sup>1</sup>IOMP Medical Physics World Board

<sup>2</sup>Department of Imaging Diagnostics, Medical University – Plovdiv, Bulgaria

**Key words:** CR, DR, SFR, Diagnostic Imaging

### Purpose

Following the latest EU requirements and trends in the diagnostic imaging, an extensive campaign is being held in the country to introduce digital imaging techniques in conventional diagnostic radiology.

### Methods

Most hospitals and diagnostic centers in the country have already installed or are in the stage of transition to CR or DR systems, while few of them have both. A certain number of hospitals have not yet chosen the type of digital system they want installed, or even whether they need one at all. The present study is a retrospective analysis of data from diagnostic imaging departments and covers 2000 patients that have undergone frontal chest X-ray.

### Results

We defined the surface and absorbed dose, and performed a randomized double-blind evaluation of the quality of the images with 10 physicians with acquired specialty in imaging diagnostics.

Analysis is made of the patient dose with different imaging techniques, as well as classification based on various criteria - patient dose, price, options for post processing, applicability.

Reducing radiation exposure in the area of the chest in DR is 60% compared to the FS.  $P < 0.001$ .

The reduction of the radiation dose in the region of the thorax in CR is 35% less than that in the SF.  $P < 0.001$ .

DR compared with CR enables the realization of x-rays of the thorax with nearly 50% lower radiation exposure.  $P < 0.001$ .

According to the data from the survey: to achieve the same image quality with CR, we have to use approximately 2/5 of the dose compared to the SF.  $P < 0.001$

When DR is required: 1/5 of the dose for SF can be used to obtain an image with similar or identical quality.  $P < 0.001$

According to the data from our study the highest sum dose is obtained from X-rays done by film - screen combination.

We found that the highest radiation dose, that patients received, was related to repetition of X-rays due to incorrectly selected data or etc. Repetition of radiographs directly leads to doubling of the patients and staff dose.

In terms of price systems are arranged as follows: CR; DR; SF.

With respect to The exploitation systems ranks as follows: DR; CR; SF.

Undoubtedly the quality of x-rays is directly dependent on the ability of the person that is performing it. Or in other words, the so-called human factor that is always present.

The only way to reduce it is through adequate training of the staff.

### Conclusions

Moving to one of the digital methods is something that will contribute to a good dose reduction for the patients and the staff in the diagnostic imaging departments, will contribute to the optimization of the diagnostic process and improving the informativeness of the diagnostic image.

### References

1. P. Palin ,B. Heaton. *Physics for Diagnostic Radiology, Third Edition ISBN: 13: 978-14398-9692-1 p 105-133*
2. C. Prokop, U. Neitzel, H Venema "Digital chest radiography: an update on modern technology, dose containment and control of image quality" *Eur Radiol. 2008 Sep; 18(9): 1818–1830*
3. Uffmann M, Prokop M, Eisenhuber E et al (2005) *Computed radiography and direct radiography: Influence of acquisition dose on the detection of simulated lesions. Invest Radiol 40(5):249–56*
4. Koerner M, Treilt M, Schaetzing R et al (2006) *Depiction of low contrast detail in digital radiography: comparison of powder and needle-structured storage phosphor systems. Invest Radiol 41(7):593–599*
5. Metz S, Damoser P, Hollweck R et al (2005) *Chest radiography with a digital flat-panel detector: experimental receiver operating characteristic analysis. Radiology 234(3):776–784*

## **CAN PSEUDOCOLOR IMPROVE PERFORMANCE OF PORTABLE AND MOBILE DEVICES DISPLAYS FOR HIGH DETAIL, LOW CONTRAST MEDICAL IMAGES AT DAYLIGHT CONDITIONS?**

Albert Guvenis<sup>1</sup>, Nuran Ozturk<sup>1</sup>, Hıdır Kaygusuz<sup>2</sup>

<sup>1</sup>Bogazici University, Turkey

<sup>2</sup>A Yurtaslan Oncology Hospital

**Key words:** Medical Displays, Mobile Computing

### **Purpose**

The objective of this study is to assess the potential use of pseudocolor for improving the performance of displays used in portable and mobile devices at daylight conditions with varying radiologist experience levels for high detail low contrast studies.

### **Methods**

The Japanese Society of Radiological Technology (JSRT) database has been used for this investigation. The images were digitized with a 0.175 mm pixel size, a matrix size of 2048 by 2048, and 4096 gray levels. As a preliminary study, 30 chest x-ray images with nodules of different contrast levels have been selected and presented to the radiology department staff on a laptop of type HP Pavilion dv6 and having a resolution of 1366 x 768 and the number of detected nodules was noted. The study has been repeated after two weeks with the pseudocolor images being presented in addition to the original grey level images. Pseudocolor was produced by using the MATLAB ind2rgb (image, jet(300) function).

### **Results**

19 nodules have been detected with the grey level images alone. With the use of pseudocolor, the number of detected nodules were 24, corresponding to an increase of 17% ( $p=0.02$ , McNemar chi-squared test).

### **Conclusions**

The preliminary study shows that the use of pseudocolor may be useful in improving the performance of sub-optimal portable computer and mobile computer displays at daylight conditions for low contrast high detail studies. Further investigations are needed and currently continuing for estimating both sensitivity and specificity in comparison with a medical monitor.

## **DIRECT MEASUREMENTS OF EYE LENS DOSES IN PEDIATRIC BRAIN COMPUTED TOMOGRAPHY EXAMINATIONS**

Agapi Ploussi<sup>1</sup>, Ioannis Stathopoulos<sup>1</sup>, Vasileios Syrgiamiotis<sup>2</sup>, Triantafillia Makri<sup>2</sup>, Christiana Hatzigiorgi<sup>2</sup>, Eleftheria Carinou<sup>3</sup>, George Sakellaropoulos<sup>4</sup>, George Panayiotakis<sup>4</sup>, George Panayiotakis<sup>4</sup>, Kalliopi Platoni<sup>1</sup>, Efstathios Efstathopoulos<sup>1</sup>

<sup>1</sup>2nd Department of Radiology, University General Hospital 'Attikon', School of Medicine, National and Kapodistrian University of Athens, Greece

<sup>2</sup>Children's Hospital Agia Sophia, CT-MRI Department, Greece

<sup>3</sup>Greek Atomic Energy Commission, Greece

<sup>4</sup>Department of Medical Physics, Faculty of Medicine, University of Patras, Greece

**Key words:** pediatric CT; TLD; lens dose

### **Purpose**

In Brain Computed Tomography (CT), the lens of the eye is of great concern since recent studies support that the threshold for cataract formation is much lower than the previously considered dose level. The goal of the study is to estimate eye lens dose during pediatric brain CT examinations using in vivo dosimetry.

### **Methods**

The cohort study included 35 pediatric patients who underwent brain CT examinations on a 16-slice CT scanner. The patients were categorized in 3 age groups: 0-18 mo (group A), 18 mo-5 yr (group B) and 5-15 yr (group C). All examinations were performed using iterative reconstruction algorithm, axial mode and automatic exposure technique. Gantry tilt was used in all scans to keep eyes outside the primary radiation beam. For each patient, 4 TLDs were placed on the center of both eyes.

### **Results**

The measurements show that the absorbed dose to the lens of the eye is  $10.5 \pm 3.3$ ,  $29.9 \pm 8.6$  and  $34.2 \pm 14.9$  mGy for groups A, B and C respectively. To our knowledge, up to now, there are no literature reports concerning the evaluation of eye lens dose in pediatric brain CT using gantry tilting. However, other studies have shown that direct exposure to eye during CT delivers dose to the lens ranging from 19.1-94.6 mGy.

### **Conclusions**

Eye lens dosimetry is of significant importance in pediatric CT. The use of TLD is an accurate method to estimate dose in the lens of the eye. Gantry angulation is the one of the most efficient tools to reduce dose to the eye lens.

## **SURFACE DOSE MEASUREMENTS FOR CT: COMPARISON BETWEEN PARALLEL-PLATE IONIZATION CHAMBER, MOSFET AND OSLD**

Md Nurul Amin, Bern Norrlinger, Robert Heaton

Princess Margaret Cancer Centre, Canada

**Key words:** MOSFET, OSLD, CT, Surface dose

### **Purpose**

CT and CBCT are essential tools for radiology and radiotherapy practice for accurate diagnosis and precision treatment delivery. TLDs, MOSFETs and OSLDs are the detectors of choice for surface dose measurements. The present study investigates the performance of MOSFETs and OSLDs for surface dose measurement for CT and CBCT.

### **Methods**

The nanoDots dosimeter with the InLight MicroStar reader, high sensitivity MOSFETs with the mobileMOSFET reader and parallel plate chamber (PPC) of volume 0.5ml were used for this investigation. The detector energy response was studied from 75 kV to 320kV for OSLDs and 40 kV to 220 kV for MOSFETs. Calibration and energy response for each detector were determined through comparisons to the measured dose from a calibrated ion-chamber (NE2571) under reference conditions. Surface doses for different presets of 80kV, 100kV and 120kV were measured using MOSFET and OSLD for CT and CBCT scans of a Rando phantom and were compared to the dose measured by PPC.

### **Results**

Both MOSFET and OSLD were found to be dependent of energy in the kV range. Dose measurements in CBCT and CT using the MOSFET system differed by  $(30.9\pm 3.9)\%$  and  $(13.0\pm 3.2)\%$  respectively, compared to the PPC measurements. An average dose variation of  $(5.3\pm 5.1)\%$  and  $(4.2\pm 3.7)\%$  were observed between PPC and OSLDs for CBCT and CT scan respectively. Measurements were repeated three times to confirm the results.

### **Conclusions**

The results of this study indicate that OSLD gives better agreement than MOSFET in comparison with PPC for surface dose measurements of CT and CBCT.

## **INTERVENTIONAL CARDIOLOGY PROCEDURES: EIGHT YEARS PATIENT RADIATION TRENDS IN A LARGE HOSPITAL IN GREECE**

Virginia Tsapaki, N Fotos, S Patsilinakos

Konstantopoulio General Hospital, Greece

**Key words:** Interventional cardiology, patient dose

### **Purpose**

To analyze patient radiation data from interventional cardiology (IC) procedures in a large hospital of Greece performed the last 8 years, investigate trends and compare with national and international reference levels (RL).

### **Methods**

Patient radiation metrics in terms of Kerma-Area Product (KAP) in Gy $\cdot$ cm<sup>2</sup>, cumulative dose (CD) in mGy, fluoroscopy time (T) in min and total number of frames (F) were analyzed from a pool of data ranging from January 2009 to May 2016. Coronary Angiography (CA) and Percutaneous Coronary Intervention (PCI) were included in the sample. The procedures were carried out with a Philips Integris Allura Xper FD20 fully digital monoplane machine with flat detector (FD) (Philips Medical Systems, Best, The Netherlands). Using appropriate conversion factors, Peak Skin Dose (PSD) and effective dose (E) were estimated.

### **Results**

The sample included 8286 IC procedures performed by 2 interventional cardiologists with more than 10 years of experience; 5469 were CAs (66 %) and 2817 were PCIs (34 %). Median values of KAP, CD, T, and F ranged from 27.0-30.5 Gy $\cdot$ cm<sup>2</sup>, 444.5-446.6 mGy, 2.03-3.6 min and 436-514 for CA and 85.6-103.7 Gy $\cdot$ cm<sup>2</sup>, 1542-1942 mGy, 12.7-14.8 min and 1082-1294 for PCI. Results were within national, European and International RLs. Median PSDs were lower than the 2 Gy dose threshold for the first skin radiation effects and none of patients reported any skin effect.

### **Conclusions**

The radiation dose trends in IC procedures for the last 8 years suggest that patient radiation doses in our hospital are optimized.

## **PATIENT AND STAFF RADIATION EXPOSURE ENDOSCOPIC RETROGRADE CHOLANGIOPANCREATOGRAPHY: EIGHT YEARS OF DOSE MONITORING**

Virginia Tsapaki, N Fotos, K.D. Paraskeva, N Angelogiannakopoulou, J.A Karagiannis

Konstantopoulio General Hospital, Greece

**Key words:** ERCP, patient dose, staff dose

### **Purpose**

To analyze 8 years of patient and staff radiation exposure data during endoscopic retrograde cholangiopancreatography (ERCP).

### **Methods**

Data were analyzed for the last 8 years (January 2009-May 2016). Patient data included age in years (Y), radiation exposure in terms of Kerma-Area Product (KAP, in Gy $\cdot$ cm<sup>2</sup>), fluoroscopy time (T) in min and total number of films (F). The procedures were carried out with a Philips Essenta X-ray system with the X-ray tube over the patient table (Philips Medical Systems, Best, The Netherlands) by a single operator with more than 15 years of experience. TLD badges were provided by the radiation protection authorities every month.

### **Results**

The sample included 1235 therapeutic ERCP procedures showing an increasing trend in annual numbers, starting from 85 ERCPs to 246 per year. Patient age did not change significantly through the years, ranging from 70-78.5 years. Median values of KAP and T revealed a decreasing trend during the 8 years of monitoring. For staff, the radiation exposure values provided by the authorities were always close to 0 Sv. It should be noted that all staff used their own lead apron (2 piece front and back protection 0.25 mm Pb, collar, lead protective glasses and 2 lead equivalent articulated screens 90cm wide during the whole procedure).

### **Conclusions**

The 8 years evaluation of patient and staff radiation exposure shows that both patient and staff exposure is reduced year by year. Routine monitoring proved a valuable tool for reducing both patient and staff radiation levels.

## **PAEDIATRIC INTERVENTIONAL CARDIOLOGY RADIATION EXPOSURE; ARE WE MISSING SOMETHING?**

Virginia Tsapaki<sup>1</sup>, N Kollaros<sup>2</sup>, C Plemmenos<sup>2</sup>, I Mastorakou<sup>2</sup>, S C Apostolopoulou<sup>2</sup>

<sup>1</sup>Konstantopoulio General Hospital, Greece

<sup>2</sup>Onassis Cardiac Surgey Center, Greece

**Key words:** Paediatric patients, radiation dose

### **Purpose**

To evaluate paediatric interventional cardiology radiation doses in dedicated cardiology center in the context of optimisation.

### **Methods**

Patient data included age in years (Y), radiation exposure in terms of Kerma-Area Product (KAP, in Gy $\cdot$ cm<sup>2</sup>), fluoroscopy time (T) in min and total number of frames (F). The procedures were carried out by operators with more than 15 years of experience. The types of IC procedures included were: Diagnostic normal and complex exams, Aortic Angioplasty, Pulmonary Angioplasty, Pulmonary Angioplasty and stent, Atrial septum device (ASD), Aortic valvuloplasty, Pulmonary valvuloplasty, patent ductus arteriosus (PDA) closure cell, PDA closure device, electrophysiology and ablation. Effective doses (ED) were calculated using suitable conversion factors.

### **Results**

The sample included 1020 diagnostic and therapeutic paediatric IC procedures. Large range of patient doses were observed with median values of KAP, T and F being: 9.0 Gy $\cdot$ cm<sup>2</sup>, 6.6 min and 1107 frames. Our radiation dose values were comparable to literature. However, the lack of paediatric IC diagnostic reference levels (DRLs) was identified which prohibited the identification of good practices.

### **Conclusions**

Our study reports data from over 1000 patients and contributes significantly to the international literature. It shows that age has immense influence on radiation dose and that ED levels are comparable to recently published data. Radiation dose monitoring proves to be an important element of an up-to-date paediatric interventional cardiology laboratory. Paediatric DRLs should be established in the near future to further optimize radiation dose

## **ESTIMATION OF RADIATION DOSE FOR RADIATION WORKER STAFF IN NUCLEAR MEDICINE AND MOLECULAR IMAGING CENTER**

Hanan Aldousari<sup>1</sup>

<sup>1</sup>Jaber Alahmad Center For Nuclear Medicine And Molecular Imaging, Qatar

### **Purpose**

The aim of this study was to estimate the radiation dose for the radiation workers staff in Nuclear medicine department (Jaber Al Ahmad center for Nuclear medicine & molecular imaging center) in order to determine whether rotation of the radiation workers staff is necessary and if the staff need more training about the ALARA principle.

### **Methods**

The effective radiation dose was measured for Radiation workers staff (Physician –Medical Physicist –Technologist - Nurse) in Nuclear medicine department, using (Thermoluminescent dosimeter TLD); the data was collected annually - month by month from (January to December 2015). The total staff was 24, including 3 Physicians, 2 Medical Physicists, 8 Technologists and 11 Nurses.

### **Results**

The results show the values of annual reading radiation dose for 28 radiation workers in nuclear medicine department, the results obtained are between 2.624 msv to 0.979 msv for the staff. This result was compared with the annual dose recommended from the IAEA - 20 msv per year. (13.12% - 4.895%). Physicians received the highest dose (2.624 msv – 2.401 msv – 2.310 msv) – (13.12% - 12.005% - 11.55%) from the recommended dose from IAEA and 2 of the Technologists also received high dose (2.48 msv – 2.311 msv) – (12.4% - 11.56%) from the recommended dose from IAEA.

### **Conclusions**

This study showed that effective radiation doses to the radiation workers staff were within the annual dose recommended by IAEA. The highest dose was received by the physicians because they regularly performed radionuclide injection using the butterfly technique with a syringe without shielding. The technologists receive high dose from the patients during the scan acquisition and when handling the radionuclide dose from hot lab to the scan room. The two technologists work in both camera PET/CT and SPECT/CT. All the staff have high awareness of radiation safety and ALARA Principle

### **Key words**

Radiation dose, Thermoluminescent dosimeter TLD, Nuclear medicine department, Radiation safety, ALARA Principle.

## **COMPARING CT DOSE FOLLOWING THE INTRODUCTION OF NATIONAL DIAGNOSTIC REFERENCE LEVELS**

Kam Shan Mong<sup>1</sup>

<sup>1</sup>Austin Health, Australia

### **Purpose**

In 2011 the Australian Radiation Protection and Nuclear Safety Agency (ARPANSA) introduced National Diagnostic Reference Levels (NDRL) for CT which highlighted the importance of radiation dose optimisation. An audit was conducted at a major teaching hospital in Melbourne, Australia, to assess the impact of NDRL.

### **Methods**

A retrospective analysis of 14,608 scans was conducted, which included the following non-contrast procedures: CT brain, CT chest, CT abdomen/pelvis and CT chest/abdomen/pelvis scans. Data was collected across 6 scanners. A one-way ANOVA test was used to detect the differences in the means across the data from 6 years. A Tukey post-hoc analysis was used to identify which years were significantly different.

### **Results**

A significant difference was present in the years pre-implementing NDRLs (2009 and 2010) and post (2011 onwards) NDRLs. No significant dose reduction was detected between subsequent years. In general, the CTDIvol decreased over time, with CT brain scans being the most apparent compared to other types of scans.

### **Conclusions**

A significant radiation dose reduction was detected following the introduction of NDRL in 2011. Although machine upgrades play a role in dose optimisation, the NDRLs ensured all machines were optimised to remain under the suggested NDRLs. Furthermore, regular CT dose audits are useful in managing dose trends and dose optimisation.

### **Key words**

Computed tomography, Diagnostic reference levels, Dose audit

## UNCERTAINTY ESTIMATION OF DOSE MEASURED WITH A SMALL-TYPE OSL DOSIMETER DURING CT SCANNING

H Hayashi<sup>1</sup>, T Okazaki<sup>2</sup>, Y Mihara<sup>1</sup>, K Yamada<sup>3</sup>, N Kimoto<sup>1</sup>, K Takegami<sup>4</sup>, Y Kanazawa<sup>1</sup>, K Higashino<sup>1,3</sup>, K Yamashita<sup>1,3</sup>, T Hashizume<sup>2</sup>, I Kobayashi<sup>2</sup>, MAKA Reginaldo<sup>5</sup>

<sup>1</sup>Tokushima University, Japan; <sup>2</sup>Nagase Landauer, Ltd., Japan; <sup>3</sup>Tokushima University Hospital, Japan; <sup>4</sup>Yamaguchi University Hospital, Japan; <sup>5</sup>Nagase Philippines, Corp., Philippines

**Key words:** OSL dosimeter, CT, dose

**Introduction:** Computed tomography (CT) scanning is widely used for clinical diagnosis. However exposure doses caused by the CT scan are increasing to measurable levels [1] and researchers recognize the risk of getting cancer [2]. We have developed small-type OSL dosimeter [3-6] for direct measurement of patients' doses. In this study, we performed fundamental study for using the OSL dosimeter, and evaluated the uncertainty of our procedure.

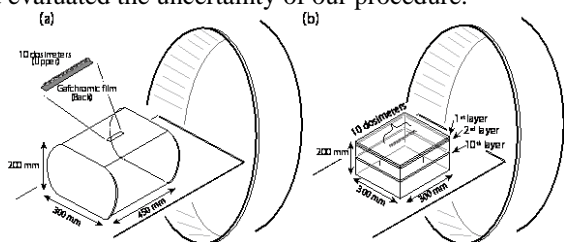


Fig. 1 Schematic drawing of experimental setup.

**Methods:** Figure 1 shows a schematic drawing of the experiments; left (a) and right (b) figures show the experiments for measuring the ESD (entrance-surface dose) and internal dose, respectively. We used a CT scanner having 320-rows of detectors (Aquilion ONE, Toshiba Medical Systems, Otawara, Japan).

First, ESD measurement was performed using the arrangement shown in Fig. 1 (a). A water phantom (JIS Z4915-1973) which was sized length 450 mm, width 300 mm and height 200 mm, was placed on the scanning bed. Both 10 nanoDot OSL dosimeters (Landauer, Glenwood, Illinois, U.S.A.) and Gafchromic film (XR-SP2, ASHLAND Ltd., New Jersey, U.S.A.) were placed on the phantom. The nanoDot OSL dosimeters were calibrated with ionization chambers. Using a microStar reader, the measurable value "Counts" were obtained, and they were converted to the dose using calibration curve [3-6]. The Gafchromic film was also calibrated using an ionization chamber. The irradiation conditions were as follows: 0.5 mm (detector size) × 16, 32 and 64 rows, tube current of 260-600 mA, PF (pitch factor) of 0.6-1.4. The tube current was determined so as to have the effective dose of 200 mAs.

Second, internal dose measurement was carried out using the setup shown in Fig. 1 (b). We made a phantom consisting of polycarbonate; the size of the phantom was 300 mm in length, 300 mm in width and 200 mm in height, and the upper region was separated into 10 layers. Each layer had a thickness of 10 mm. In the center region of the 10 layers, 10 nanoDot OSL dosimeters could be implanted. We set the phantom on the scanning bed, and CT examination was performed. The irradiation condition was as follows: 0.5

mm (detector size) × 64 rows of detectors, 120 kV, 600 mA, PF = 1.484 in helical scan mode.

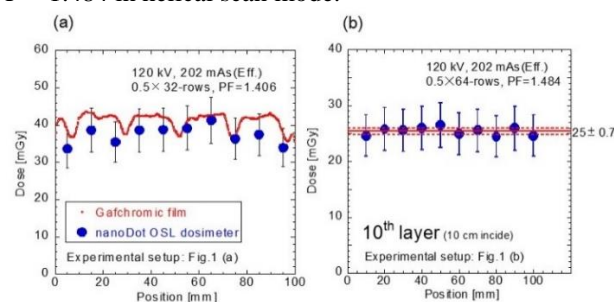


Fig. 2 Comparison of doses measured with the nanoDot OSL dosimeters for experiments in Fig. 1 (a) and (b).

**Results and discussion:** Figure 2 shows typical results of measured doses in this study; (a) and (b) represent results of experiments of Fig. 1 (a) and (b), respectively. In this graph, the OSL dosimeter has uncertainty of 15%, which includes error causes such as energy and angular dependences. Based on these results, we discussed the uncertainty when patients wear the OSL dosimeter on their bodies during the CT examination, and then we found that the parameter of PF plays an important role.

**Conclusion:** We studied the practicality of the nanoDot OSL dosimeters to measure patient exposure doses during a multi detector CT examination. For the ESD measurement, we found that the measured value of the nanoDot OSL dosimeter strongly depended on pitch factor. Therefore we suggested to use the dosimeter under the conditions of  $PF \leq 1.000$ . In this situation, the systematic uncertainty of our dosimetric method was estimated to be 25%, and with consideration of other contributing factors, the total uncertainty was estimated to be 30%. In addition, we preliminarily examined the deviations of internal dose measurements. The deviations were much smaller than those of the entrance skin dose.

### References:

- Gonzalez AB, Darby S (2004), Lancet 363: 345-351 DOI 10.1016/S0140-6736(04)15433-0
- John DM, Anna VF, Zoe B et al. (2013), BMJ 346:f2360 (18 pages) DOI 10.1136/bmj.f2360
- Takegami K, Hayashi H, Okino H et al. (2015), Radiological Physics and Technology 8: 286-294 DOI 10.1007/s12194-015-0318-1
- Hayashi H, Takegami K, Okino H et al. (2015), Medical Imaging and Information Science 32: 8-14 DOI 10.11318/mii.32.8
- Takegami K, Hayashi H, Okino H et al. (2016), Radiological Physics and Technology 9: 99-108 DOI 10.1007/s12194-015-0339-9
- Takegami K, Hayashi H, Okino H et al. (2016), Radiological Physics and Technology 9: 286-292 DOI 10.1007/s12194-016-0362-5

Corresponding author email: hayashi.hiroaki@tokushima-u.ac.jp

## **PHOTO-NEUTRON MEASUREMENTS FOR 15 MV PHOTON BEAM FROM MEDICAL LINAC UNDER DIFFERENT IRRADIATION GEOMETRIES**

Siji Cyriac<sup>1</sup>

<sup>1</sup>Apollo Hospitals, India

### **Key words**

Medical LINAC, Photo-neutrons tracks, CR-39 detector, TLD 600 and 700 detectors.

### **Purpose**

The photo-neutron dose equivalents of 15 MV Elekta precise accelerators were measured for different depths in phantom, for various field sizes, at different distances from the isocenter in the patient plane and for various wedged fields.

### **Methods**

Fast and thermal neutrons are measured using passive detectors such as CR-39 and pair of TLD 600 and TLD 700 detector from Elekta Medical Linear accelerator.

### **Results**

It is found that fast photo-neutron dose rate decreases as the depth increases, with a maximum of  $0.57 \pm 0.08$  mSv/Gy photon dose at surface and minimum of  $0.09 \pm 0.02$  mSv/Gy photon dose at 15 cm depth of water equivalent phantom with 10 cm backscatter. Photo neutrons decrease from  $1.28 \pm 0.03$  mSv/Gy to  $0.063 \pm 0.032$  when measured at isocentre and at 100 cm far from the field edge along the longitudinal in the patient plane. Fast and thermal neutron doses increase from  $0.65 \pm 0.05$  mSv/Gy to  $1.08 \pm 0.07$  mSv/Gy as the field size increases; from  $5 \times 5$  cm<sup>2</sup> to  $30 \times 30$  cm<sup>2</sup> for fast neutrons. With increase in wedge field angle from 0° to 60°, it is observed that the fast neutron dose increases from  $0.42 \pm 0.03$  mSv/Gy to  $0.95 \pm 0.05$  mSv/Gy.

### **Conclusions**

Measurements indicate the photo neutrons at few field sizes are slightly higher than the IEC standard specifications. Photoneutrons from Omni wedged fields are studied in details. These studies of the photo neutron energy response will enlighten the neutron dose to radiation therapy patients and are expected to further improve radiation protection guidelines

## **RADIATION SAFETY IN RENAL DIALYSIS PATIENT TREATED WITH IODINE-131**

Wirote Changmuang<sup>1</sup>, Putthiporn Charoenphun<sup>1</sup>, Arpakorn Kositwattanarerk<sup>1</sup>, Arkom Nongnuch<sup>2</sup>, Natthaporn Kamwang<sup>3</sup>, Jeerawat Esor Dosimetry<sup>4</sup>

<sup>1</sup>Division of Nuclear Medicine, Department of Diagnostic and Therapeutic Radiology, Faculty of Medicine Ramathibodi Hospital, Mahidol University, Bangkok, Thailand

<sup>2</sup>Nephrology unit, Department of Medicine, Faculty of Medicine Ramathibodi Hospital, Mahidol University, Bangkok

<sup>3</sup>Dosimetry Calibration Laboratory, Thailand Institute of Nuclear Technology (Public Organization), Bangkok

<sup>4</sup>Calibration Laboratory, Thailand Institute of Nuclear Technology (Public Organization), Bangkok

### **Key words**

Iodine-131, Renal Dialysis, Radiation Safety, Thyroid Disease

### **Purpose**

The study aimed to determine radiation dose from hemodialysis patient treated with I-131 in the surrounding of dialysis unit as well as dialysis working staff.

### **Methods**

Graves' disease patient with acute renal failure received 740 MBq I-131 for treatment and sent for hemodialysis post administration radioiodine for 8 hr. Over dialysis procedure, the radiation exposure of the surrounding area was measured using OSL dosimeter at 1 m and 3 m (nurse counter) apart from the treated patient. The radiation directly exposure to the nurse and nurse assistant who performed dialysis procedure was recorded by real-time dosimeters. The radioactive wastes generated during dialysis procedures must be segregated and measured the contamination levels using survey meter.

### **Results**

The radiation exposure at 1 m and 3 m distance from the patient was 85.0 and 8.3 Sv/h, respectively. The radiation dose to the nurse was 75.0 Sv for 55 min and 24.0 Sv for 45 min for the nurse assistant. All dialysis waste and the vomiting content were contaminated with radioactive for 0.8 and 2.5 Sv/h, respectively.

### **Conclusions**

Our results provide assurance in using 740 MBq I-131 treatment for patients who need hemodialysis for both occupational and public exposure.

## **EXAMINATION OF THE EFFECTIVE ACTIVATION REDUCTION MEASURES INSIDE 20 MEV UNSHIELDED COMPACT MEDICAL CYCLOTRON ROOM**

Takatoshi Toyoda<sup>1</sup>, Toshioh Fujibuchi<sup>2</sup>, Shingo Baba<sup>3</sup>, Yoshiyuki Umezu<sup>4</sup>, Isao Komiya<sup>4</sup>, Hiroshi Honda<sup>3</sup>

<sup>1</sup>Department of Health Sciences, Graduate School of Medical Sciences, Kyushu University, Japan

<sup>2</sup>Department of Health Sciences, Faculty of Medical Sciences, Kyushu University

<sup>3</sup>Department of Clinical Radiology, Graduate School of Medical Sciences, Kyushu University

<sup>4</sup>Department of Radiology, Kyushu University Hospital

### **Purpose**

With the use compact medical cyclotron, neutron was generated secondly. The neutron caused activation inside room, therefore measuring distribution of neutron fluence was essential to estimate the activation condition inside vault room. In this study, we measured distribution of thermal neutron fluence rate during  $^{18}\text{O}(p,n)^{18}\text{F}$  reaction by using gold foil activation method, and examined the effectiveness of activation reduction measures.

### **Methods**

We used HM-20 cyclotron with non-self-shielding type. Accelerated proton energy was 20 MeV, average beam current was 47.9  $\mu\text{A}$  and irradiation time was 45 minutes. Gold foils were positioned around wall and floor. Two gold foils set at each position, one was bare gold foils, the other was covered with cadmium plate. Activity of gold foils was measured by using CdZnTe semiconductor detector, and thermal neutron fluence rate was calculated.

### **Results**

The highest thermal neutron fluence rate was  $9.0 \times 10^6 \text{ cm}^{-2}\text{s}^{-1}$ , which occurred on the floor under the target. The lowest thermal neutron fluence rate inside cyclotron vault room was  $4.1 \times 10^5 \text{ cm}^{-2}\text{s}^{-1}$ . The highest fluence was an order of magnitude greater than the lowest fluence, and distribution of thermal neutron fluence inside vault room was heterogeneous. The neutron fluence became lower as the position moved away from the target.

### **Conclusions**

Monitoring of neutron distribution in a cyclotron room appears to be useful for not only obtaining an accurate estimate of the distribution of induced radioactivity, but also optimizing the shield design for radiation safety in preparation for decommissioning process. By intensively neutron shielding directly under the target, it can effectively reduce the activation.

# CREATING A COMPUTATIONAL THORACIC PHANTOM FOR EVALUATION OF THE ORGAN DOSE USING MONTE CARLO SIMULATION

Naoki Sato<sup>1</sup>, Toshioh Fujibuchi<sup>2</sup>

<sup>1</sup>Department of Health Sciences, Graduate School Of Medical Sciences, Kyushu University, Japan

<sup>2</sup>Department of Health Sciences, Faculty Of Medical Sciences, Kyushu University

## Key words

DICOM, Thoracic images, Voxel phantom, Monte Carlo simulation

## Purpose

To evaluate the radiation exposure for radiography by using Monte Carlo simulation, the DICOM (Digital Imaging and Communication in Medicine) data were implemented into the PHITS (Particle and Heavy Ion Transport code System), which is Monte Carlo code.

## Methods

The images of thorax were downloaded from the internet as a sample data, and the file format was exchanged in order to process the images. For these images, the region of bone, lung field and soft tissue were segmented respectively to modeling the surface of the organ. Due to this, the created computational phantom was anthropomorphic and realistic. After creating the phantom, the organ and the soft tissue data were integrated, which means voxel phantom was created, and implemented into the PHITS to calculate.

## Results

The organ and the soft tissue at the region of the thorax were segmented and modeled smoothly by using the image processing software. By using the PHITS, the data was made to the voxel phantom and implemented.

## Conclusions

A computational thoracic phantom was successfully created for dose evaluation of the radiography. Monte Carlo simulation was calculated. The data needs to be compared between the simulation and the measurement to confirm the reproducibility of the computational phantom.

## ESTIMATION OF RADIATION EXPOSURE OF EYE LENS DURING ENDOSCOPIC PROCEDURES WITH AN OVER-COACH X-RAY SYSTEM

YTakei<sup>1</sup>, K Matsubara<sup>2</sup>, I Kobayashi<sup>3</sup>, S Suzuki<sup>4</sup>, K Koshida<sup>2</sup>

<sup>1</sup>Hamamatsu University Hospital, JP; <sup>2</sup>Kanazawa University, JP; <sup>3</sup>Nagase Landauer Corporation, JP; <sup>4</sup>Fujita Health University,JP.

**Key words:** Radiation Exposure, Endoscopy, Eye Lens, Over-coach X-ray System

**Introduction:** The aim of this study was to determine the radiation exposure of the lens of the eye using the nanoDot optically stimulated luminescence dosimeter (OSLD) during diagnostic and therapeutic endoscopy procedures with an over-coach X-ray system.

**Methods:** This study was approved by our institute review board. During a five month period (November 2013, February, May, June and August 2014), 4 gastroenterologists and 16 nurses worn the radiation protection (RP) glass with lead equivalent of 0.07 mm attached the OSLDs on the inside and outside of glass for every month, we measured the Air Karma (AK) of staff members during diagnostic and therapeutic endoscopy procedures with an over-coach X-ray system. We calculated the equivalent dose of eye lens by multiplying the conversion coefficients<sup>1</sup> to AK.

**Results:** We measured eye lens dose of staff members about 51 cases of diagnostic and therapeutic endoscopic procedures. The Minimum, Median, 75th percentile and Maximum values of the equivalent dose of eye lens were 0, 0.1, 0.23 and 3.24 mSv for outside of RP glass, 0, 0.1, 0.23 and 1.07 mSv for inside of RP glass, respectively (Fig. 1). The equivalent dose of eye lens of outside of RP glass ranged 0 to 3.24 mSv for 16 nurses, and 0.11 to 2.99 mSv for 4 gastroenterologists (Fig.2). The estimated annual equivalent dose of eye lens of one gastroenterologist and two nurses were exceeded a revised equivalent dose limit for eye lens of 20 mSv. The RP glass with lead equivalent of 0.07 mm was able to reduce the equivalent dose of eye lens to one third.

**Discussion:** In April 2011, the International Commission on Radiological Protection (ICRP) revised the recommendation of an equivalent dose limit for eye lens of 20 mSv in a year, averaged over defined periods of 5 years, with no single year exceeding 50 mSv for the occupational exposure<sup>2</sup>. In our study, one gastroenterologist and two nurses were exceeded revised equivalent dose limit. To give nursing care to patient and to control the endoscope, their head positioned near X-ray tube as a higher scatter radiation area. But to wear the RP glass with lead equivalent of 0.07 mm, their equivalent dose of eye lens were decreased. We recommend the staff of endoscopic procedure with an over-coach X-ray system should be wear the RP glass.

**Conclusion:** The diagnostic and therapeutic endoscopy procedures with an over-coach X-ray system without RP shielding, the staff member received higher scatter radiation to eye lens. To avoid excess higher eye lens dose, medical

staff of diagnostic and therapeutic endoscopic procedures should wear the RP glass.

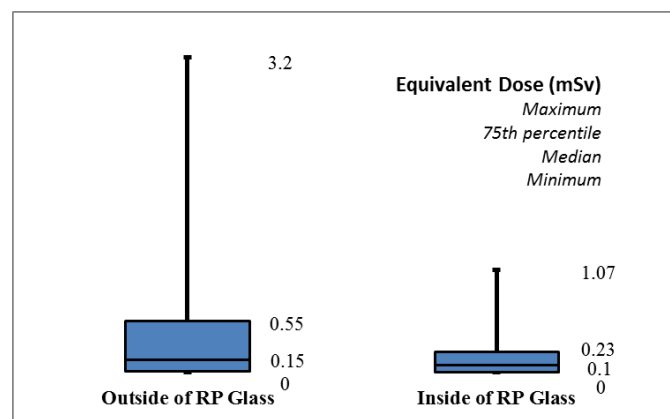


Fig.1 Equivalent Dose of Eye Lens on Inside and Outside of RP Glass.

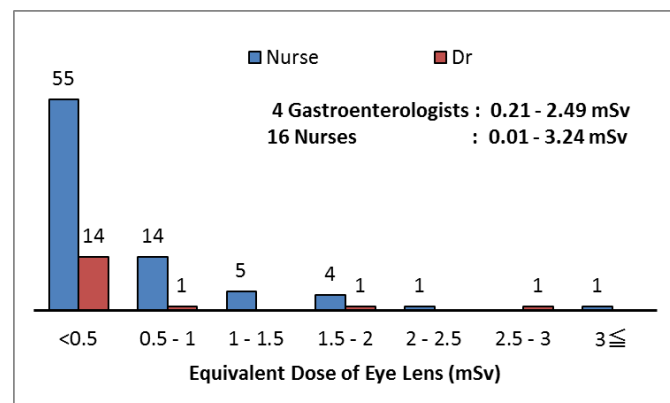


Fig. 2 Distribution of the Equivalent Dose on Outside of RP Glass

### References:

- Behren R, Air Karma to dose equivalent conversion coefficients not included in ISO 4037-3, Radiat. Prot. Dosimetry, (2011).
- Stewart FA, et al, ICRP Publication 118: ICRP statement on tissues and organs -threshold doses for tissue reactions in a radiation protection context, Ann ICRP;41(1-2):1-322, (2012)

Corresponding author email: ytakei-ham@umin.net

## **THE USE OF TUNGSTEN FUNCTIONAL PAPER TO RADIATION THERAPY ELECTRON BEAMS FOR DEMONSTRATED THE PRESENCE OF RADIATION REDUCTION AND CLEARLY SHARP PENUMBRA**

Morikazu Amano<sup>1</sup>, Hajime Monzen<sup>2</sup>, Yoshihiro Kawai<sup>1</sup>, Yasuhiko Matsuoka<sup>1</sup>, Makoto Sakashita<sup>1</sup>

<sup>1</sup>Department of Radiology, Fujieda municipal general hospital, Japan

<sup>2</sup> Graduate schools of medical sciences, Kinki University, Japan

**Key words:** TFP (Tungsten Functional Paper), Electron, Reduction effect, Penumbra

### **Purpose:**

When applying electron beams, shielding is extremely important to avoid organ risk. TFP has shielding ability to radiation with high atomic number; it is expected as a shielding material to replace lead. In this study, we have reported to evaluate the shielding effect of the electron beam (4, 6, 9 MeV), and to perform the penumbra shapes.

### **Materials and Methods:**

TFP is a sheet-form shielding material 0.3mm in thickness containing tungsten powder about 80% by weight. TFP placed on water or a water equivalent phantom. Percent depth ionization and transmission were measured for 4, 6 and 9 MeV electron beams, and measurements were performed by changing the thickness of TFP. The penumbra of 60 mm circle shape was compared with applicator (substantially 60mmdiameter lead) and TFP (contact of surface) by GafChromic film.

### **Results:**

The electron doses were reduced to measure the practical range by to addition of TFP thickness. In transmissions, the dose values were increased surface and that to confirm the build-up dose each electron beam, to measure on surface, 5mm depth and 1.5 mm depth by Marcus chamber. It was shown that developed shape the penumbra within applicator and TFP. The applicators of penumbras were 8.8 mm (4MeV), 6.5 mm (6MeV) and 5.6 mm (9MeV) by 80 – 20 % penumbra. Therefore, the TFPs were 1.1mm (4MeV), 1.7 mm (6MeV) and 2.3mm.

### **Conclusions:**

The study has demonstrated that TFP was proven to reduce radiotherapy electron beams. The penumbra is clearly sharp that using TFP on contact to surface as tertiary collimator.

## **ESTIMATION OF ACTIVITY DISTRIBUTION IN HEAD COMPONENTS OF MEDICAL LINEAR ACCELERATOR USING MONTE CARLO SIMULATION**

Toshioh Fujibuchi, Saaya Hirayama, Takatoshi Toyoda, Ryosuke Hatano

Kyushu University, Japan

### **Key words**

Activation, Medical linear accelerator, Monte Carlo simulation

### **Purpose**

Photonuclear reactions generate neutrons in the head of the linear accelerator. Therefore, some parts of the linear accelerator can become activated. Such activated materials must be handled as radioactive waste. Activated materials are non-uniform, therefore evaluation of activity is difficult. We attempted to investigate the distribution of induced radioactivity and concentration using Monte Carlo simulation.

### **Methods**

The results of the radioactive contaminants obtained by the measurement were compared with the calculated result by PHITS code. Configured components are target, flattening filter, primary collimator, upper jaw, lower jaw, and multi- leaf collimator. We evaluated by calculation the neutron amount and activity for each component.

### **Results**

The relative ratio of the neutrons generated from each part, accounted for the primary collimator majority. Jaws were activated only surface. MC simulation could be evaluated some nuclides. To improve the accuracy of simulation, selection of appropriate nuclear data is necessary.

### **Conclusions**

In this study, radioactive nuclides and radioactivity concentration of linear accelerator could be simulated. These data are important for the safety regulations of activated materials in linear accelerator dismantle. In the future, the construction of general-purpose and simple radioactivity concentration evaluation system is desired.

## **STAFF RADIATION DOSES IN INTERVENTIONAL CARDIOLOGY PROCEDURES AT HAMAD MEDICAL CORPORATION HOSPITALS IN QATAR**

Huda Al-Naemi, Mohamad Kharita, Antar Aly

Hamad Medical Corporation, Qatar

### **Key words**

Occupational effective dose, Interventional cardiology, Radiation dose

### **Purpose**

The number of interventional cardiology procedures performed in Hamad Medical Corporation (HMC) has increased rapidly over the last three years. Two HMC hospitals Hamad General Hospital (HGH) and Heart Hospital (HH) are performing interventional procedures for paediatric and adults respectively. This study focused on the evaluation of the dose received for 158 cardiologists, technologists and nurses during interventional cardiology procedures. The maximum annual effective dose was 2.7 mSv registered for cardiologist working in adult cath-lab. On the other hand the comparison between different categories for the two hospitals was also discussed. The objective of this study is to evaluate the dose received for 158 staff during interventional cardiology procedures performed in HMC hospitals

### **Methods**

The radiation dose was basically measured by thermoluminescence dosimeters (TLD) worn under the lead apron. Data on the exposure of interventional cath-lab staff, cardiologist, anesthetists, technologist and nurses have been analyzed.

### **Results**

The average effective dose over the last three years recorded by TLD for the monitored categories was as follow: -For HGH cath-lab, 0.58,0.85 and 0.49mSv for physicians, technologists and nurses respectively -For HH cath-lab, 0.89, 0.87and 0.95, for physicians, technologists, nurses, respectively.

### **Conclusions**

This study concluded that the effective radiation doses for all the staff during the last three years were well controlled and lower than the national dose limit. The low doses registered during the last three years may be due to using on dosimeter. Therefore two dosimeters should be used to give better estimation of the effective.

## **PREGNANCY AND MEDICAL PHYSICIST CAREER: COMPATIBLE OR NOT**

Kalliopi Platoni<sup>1</sup>, Agapi Ploussi<sup>2</sup>, Efi Koutsouveli<sup>3</sup>, Virginia Tsapaki<sup>4</sup>

<sup>1</sup>Attikon University Hospital, Greece

<sup>2</sup>2nd Department of Radiology, University General Hospital 'Attikon', School of Medicine, National And Kapodistrian University of Athens

<sup>3</sup>Medical Physics Department, Hygeia Hospital

<sup>4</sup>Medical Physics Unit, Konstantopoulou General Hospital

### **Purpose**

To investigate whether working as medical physicist with risk of radiation exposure can influence child bearing and how pregnancy can affect a medical physicist career.

### **Methods**

A bibliographic research was carried out in order to investigate if radiation exposure of women medical physicists during their duty can harm the health of the developing fetus and to present preconception and perinatal risks. Furthermore in order to determine whether pregnancy is a career negative factor for women medical physicists, a questionnaire was developed and a relevant literature review was performed.

### **Results**

Perinatal risks include deterministic and stochastic effects and dependent on the stage of gestation as well as the absorbed dose to the fetus. Threshold doses for fetal effects due to radiation exposure are presented. On the other hand pregnancy and the symptoms (psychological and physical sick imaging, maternity leave) seem to influence negatively women career. However there is a way to overcome this situation.

### **Conclusions**

Pregnancy and working as medical physicist are compatible. Proper use of radioprotection rules can lead to fetal doses well below the recommended limits. Women medical physicists can estimate the probable dose to the unborn child under their working environments and continue practicing their profession by minimizing all potential risks.

### **Key words**

Pregnancy, Radiation risk, Women medical physicist career

## **THE TRIAL PRODUCTION OF THE INNER TYPE RADIOLOGICAL PROTECTION CLOTHES USING DYEING TECHNOLOGY**

Hiroki Ohtani<sup>1</sup>

<sup>1</sup>Tokyo Metropolitan University, Japan

### **Key words**

Radiological protection clothes, Radiation shielding material, Dyeing technology

### **Purpose**

The purpose of this research is a trial production of inner type radiological protection clothes for personal use. A shield rate and the washing effect are examined by the technology of dyeing a fiber with the dye which is used in shield material.

### **Methods**

The dyeing technology of this research is the silk screen method. The number of meshes of the used silk screen is 600. Barium sulfate of diameter of particle 11.8  $\mu$ m was blended by 10 to 50% of mass ratio to the acrylic resin. This was made to adhere to cotton as dyeing material. X ray irradiation was performed on the dyed cotton, and the X ray decrease rate was calculated by the measurement using an ion-chamber. After washing in cold water for evaluation of the washing effect, the adhesion of dyeing material was measured.

### **Results**

The X ray decrease rate also increased, so that the mass ratio of barium sulfate to an acrylic resin was high. The decrease rate of 10% of the mass ratio was about 1.5%, and it was about 8% in 50% of the mass ratio. The reduction ratio of the acrylic resin by washing was 1 to 2%.

### **Conclusions**

Although data of the shield ratio was obtained, it is necessary to provide more detailed information. The shielding effect is preserved which was demonstrated by the resistance to washing.

## EVALUATION OF DIFFERENCES IN DISPLAY SLICE THICKNESS AND X-RAY BEAM WIDTH DUE TO DIFFERENCES IN X-RAY CT EQUIPMENT TYPES

S Suzuki<sup>1</sup>, Y Matsunaga<sup>2</sup>, A Kawaguchi<sup>2</sup>, K Minami<sup>1</sup>, M Kobayashi<sup>1</sup>, Y Takei<sup>3</sup>, Y Asada<sup>1</sup>, T Kuroda<sup>4</sup>

<sup>1</sup>Fujita Health University, Japan; <sup>2</sup>Tohoku University, Japan.; <sup>3</sup>Hamamatsu University Hospital, Japan; <sup>4</sup>Toyo Medic Co., Japan

**Key words:** computed tomography, beam width, tungsten ring

**Introduction:** Volume computed tomography dose index (CTDI<sub>vol</sub>) is commonly used to evaluate radiation doses in CT examinations. Evaluation methods usually calculate the dose by considering beam overlap and the nominal slice thickness that is displayed on the device [1]. The beam width must be wider than the nominal slice thickness. If there are differences between the nominal slice thickness and the actual beam width, they are typically evaluated via the film method, which is extremely complicated. An alternative is the simple measurement method, which is capable of a simple evaluation through the combined use of an ion-chamber dosimeter for CT and a tungsten mask.

**Methods:** Using a tungsten mask and an ion-chamber for CT, this evaluation method measures doses both with and without the mask. At the same time, we derived half widths using film measurements and subsequently calculated the beam widths. We used 64-row CT from five manufacturers (Hitachi, Toshiba, GE, Siemens, and Philips) and a 320-row CT (Toshiba). We performed our assessments using typical values of the specified nominal beam width for each device. For beam-width acquisition using the film method, we used a Gafchromic XR QA2 [2], while for the beam-width assessment, we used the image-processing software Image-J. For beam-width measurements via the W-ring method, we used a pencil-type CT ionization chamber (Radcal, 10X6-3CT). The W-rings we used were 8501-CT beam-width measuring tools (5, 10, 15 mm) (Fig. 1). We used the film method and W-ring method to perform measurements at the nominal slice width specified by the manufacturer of each CT.

**Results:** The discrepancy between the beam width determined from the dose efficiency shown on the monitors of 4 models and the beam width measured by the film method was less than 5% for all scanner models. We next computed the beam widths using our three sizes of W-ring, taking the beam widths determined by the film method as a standard.

For nominal slice widths between approximately 10 and 40 mm, measurements using the film method were matched with twice the width of the W-ring or greater were used. In the 5–10 mm, some discrepancies were present; the W-ring method yielded beam-width assessments with an accuracy of approximately 10%. For beam widths below 5 mm, the W-ring method did not yield adequate accuracy. For assessments using the 320-row CT, measurements using a 5 mm W-ring roughly agreed with nominal thickness of up to approximately 100 mm. For nominal thickness of 100, 120, 160 mm, beam widths measured using the W-ring were 7%, 27%, 58% lower than those measured using the film method, respectively. Upon varying the tube voltage, we found that the range of beam-width measurements increased as the tube voltage increased; however, for nominal thickness of 10 mm or above, the difference was of 5% or below (Table 1).

**Discussion:** The beam width in the CT is set wider than the nominal slice width to ensure that an effective radiation dose is delivered to the detector. Consequently, there is a portion of the actual radiation dose that is not used effectively, exposing the patient to excess radiation. In this study, we assessed this excess dose. The W-ring method used in this study employs a pencil ionization chamber, which is used to assess the dose delivered by X-ray CT scanners, of effective length 100 mm, and in which a W-ring may be placed. The beam width may be calculated by comparing the dose delivered with and without the W-ring present. The advantages of this method include high reproducibility for measurements made with the same configuration and the ability to obtain results rapidly by programming the relevant equations into spreadsheet software in advance.

**Conclusion:** The simple measurement method can evaluate beam thickness quickly and easily, and is therefore useful in clinical settings.

**References:**

1. IEC 60601-2-44 Amd.2 Ed. 3.0:2016 (b), Amendment 2 - Medical electrical equipment - Part 2-44: Particular requirements for the basic safety and essential performance of X-ray equipment for computed tomography
2. O. Rampado, E. Garelli and R. Ropolo, Computed tomography dose measurements with radiochromic films and a flatbed scanner, Med. Phys. 37, 189 (2010)

Table 1. Comparison of the beam width in dose measurement and film measurement

| Nominal [mm] | W-5mm |          | W-10mm |           | W-15mm |           | Gafchromic film [mm] | Dose efficiency [%] |
|--------------|-------|----------|--------|-----------|--------|-----------|----------------------|---------------------|
|              | CF-5  | W-5 [mm] | CF-10  | W-10 [mm] | CF-15  | W-15 [mm] |                      |                     |
| 40           | 0.219 | 44.9     | 0.220  | 44.7      | 0.251  | 39.2      | 44.76                | 44.59               |
| 20           | 0.214 | 25.2     | 0.218  | 24.8      | 0.215  | 25.1      | 24.39                | 24.10               |
| 15           | 0.214 | 20.0     | 0.217  | 19.7      | 0.213  | 20.1      | 19.39                | ---                 |
| 10           | 0.212 | 15.2     | 0.216  | 14.9      | 0.183  | 17.6      | 14.34                | 14.31               |
| 5            | 0.211 | 10.0     | 0.192  | 11.0      | 0.136  | 15.4      | 9.59                 | 9.26                |
| 1.25         | 0.151 | 5.9      | 0.087  | 10.3      | 0.052  | 17.3      | 4.75                 | 3.93                |

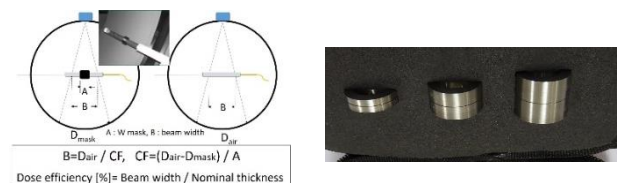


Fig. 1. Dose measurement arrangement and calculating formula (left), three types tungsten rings (right)  
Corresponding author email: ssuzuki@fujita-hu.ac.jp

## **EVALUATION OF NEUTRON DOSE BY PHOTONEUTRON PRODUCTION IN THE PRIMARY BARRIERS DURING TOTAL BODY IRRADIATION**

ChangHeon Choi, Jung-in Kim, So-Yeon Park, Jong Min Park, Minsoo Chun

Seoul National University Hospital, Republic of Korea

### **Key words**

Neutron Dose, Photoneutron, TBI, MCNP

### **Purpose**

To evaluate neutron dose equivalent of patient by photoneutron production in primary barriers during total body irradiation

### **Methods**

Monte Carlo simulations (MCNPX 2.7.0) were performed to simulate the production of photoneutrons and the neutron shielding effect. For two photon beam energies, 15 MV and 18 MV, we simulated to strike metal sheets which are used for primary barriers. The neutron dose was calculated at 50 cm distance from inner wall while delivering 3 Gy to the patient. The primary barrier was divided into the neutron shielding barrier, metal sheet shielding barrier and concrete wall. Borated polyethylene (5% boron weighted) and concrete were used as neutron shielding. Steel and lead were used as metal sheets.

### **Results**

When the primary barrier is composed of only concrete, the neutron ambient doses were 22.4 uSv and 2.3 uSv for 18MV and 15 MV, respectively. When the primary barrier was composed of a concrete wall and a one TVL lead sheet without neutron shielding, the neutron ambient doses were 358.5 uSv and 48.7 uSv for 18MV and 15 MV, respectively. The neutron dose was reduced by one-tenth using a 10 cm boron plate. For 22 cm thickness concrete, the neutron dose was decreased by a factor of 10-1.

### **Conclusions**

The laminated barrier composed of concrete and metal can be a good alternative as primary barrier design. Patients may be exposed to an unexpected neutron dose, which is not negligible. Neutron shielding should be considered at the wall. Neutron Dose, Photoneutron, TBI, MCNP

## **DETERMINATION OF NEUTRON DOSE AND RADIOACTIVITY DUE TO HIGH ENERGY X-RAY FROM MEDICAL LINEAR ACCELERATOR USING MONTE CARLO SIMULATION AND NESTED NEUTRON SPECTROMETER**

Siwapon Munsing<sup>1</sup>, Nuanpen Damrongkitudom<sup>2</sup>, Thiansin Liamsuwan<sup>3</sup>

<sup>1</sup>The School of Medical Physics, Faculty of Medicine Ramathibodi Hospital, Mahidol University, Thailand

<sup>2</sup>Department of Radiological Tecnology, Faculty of Medical Technology, Mahidol University, Bangkok

<sup>3</sup>Nuclear Research and Development Division, Thailand Institute of Nuclear Technology (Public Organization), Ongkharak, Nakorn Nayok

### **Key words**

High-energy X-ray, Neutron dose, Monte Carlo simulation, Neutron spectrometry

### **Purpose**

High-energy photons from medical linear accelerators are used for treating thick regions of patients and deep-seated tumors. Neutrons are unavoidably generated from photonuclear reactions between high-energy photons and high atomic number materials in the treatment head, shielding and walls of the treatment room. The purpose of this study was to determine neutron dose and radioactivity generated in a treatment room with 15 MV photon beams from Varian Clinac iX using Monte Carlo simulation and a cylindrically nested neutron spectrometer.

### **Methods**

The neutron spectrum and induced radioactivity were calculated using PHITS Monte Carlo code. In Monte Carlo calculations, target, flattening filter, collimator, ion chambers and walls of the treatment room were simulated. The quantified neutron production was measured using a neutron spectrometer, composed of a He3 proportional counter and multiple with multi-cylindrical polyethylene moderators.

### **Results**

The simulated photon beam was tuned until the difference between simulated and measured depth dose curves was smaller than 2%. Neutron spectrum and neutron dose equivalent were estimated from the simulation and the measurement. Radioactivity induced by nuclear reactions between neutrons and treatment head materials was followed using the Monte Carlo simulation.

### **Conclusions**

Since neutron dose and induced radioactivity can increase radiation dose to patients and radiation workers, the result of this work will help to find appropriate practices to avoid unnecessary radiation dose in radiotherapy using high-energy photons.

## **IMAGING OF RADIOACTIVE MATERIAL IN MEDICAL FACILITY BY USING ALL SKY GAMMA-RAY COMPTON CAMERA(GAMMA-I)**

Hiroshi Muraishi<sup>1</sup>, Ryoji Enomoto<sup>2</sup>, Takara Watanabe<sup>3</sup>, Shigekazu Fukuda<sup>4</sup>, Masahiro Fukushi<sup>3</sup>, Mika Kagaya<sup>5</sup>, Hideaki Katagiri<sup>5</sup>, Daisuke Kano<sup>6</sup>, Yusuke Koba<sup>7</sup>, Wataru Satoh<sup>5</sup>, Tohoru Takeda<sup>8</sup>, Manobu Tanaka<sup>9</sup>, Tomohisa Uchida<sup>9</sup>, Kiyoto Wada<sup>10</sup>, Ryo Wakamatsu<sup>5</sup>, Mamoru Yokose<sup>8</sup>

<sup>1</sup>Kitasato University, Japan

<sup>2</sup>ICRR, University of Tokyo

<sup>3</sup>Tokyo Metropolitan University

<sup>4</sup>National Institute of Radiological Sciences

<sup>5</sup>Ibaraki University

<sup>6</sup>National Cancer Center Hospital East

<sup>7</sup>National Institute of Radiological Sciences

<sup>8</sup>Kitasato University

<sup>9</sup>High Energy Accelerator Research Organization

<sup>10</sup>Fuji Electric

### **Key words**

Gamma-ray imaging, Radiation protection, Compton Camera

### **Purpose**

There are various low-level radioactive materials in a nuclear medicine facility and a radiation therapy facility. If the radiation sources are visualized in advance, it is possible to decrease the amount of occupational radiation exposure. In this study, we have developed a low-cost gamma-ray imaging Compton camera that has a high detection efficiency and is possible to visualize the gamma-ray sources over the all sky direction.

### **Methods**

The detector consisted of eleven CsI(Tl) scintillator cubes with a size of 3.5 cm, each of which readout by super-bialkali photomultiplier tubes. A flash ADC board operated at 2.5 MHz with SiTCP technology was adopted. Online program which was possible to operate on Windows was made with Visual C++ language and ROOT library. Image reconstruction was done by accumulating rings with the radius of theta degree which was calculated for each event.

### **Results**

The position of gamma-ray sources was successfully reconstructed in all sky direction with a wide energy range between 300 and 1400 keV. The angular resolution was found to be 18 degree. By using the developed system, we have done the field trials in nuclear medicine facility at the National Cancer Center hospital East, and in heavy ion treatment room at National Institute of Radiological Sciences in Japan, the results of which will be shown in this conference in detail.

### **Conclusions**

We developed the all sky RI imaging monitor. The experimental results show that our proposed detector would be suitable for a low-level radioactive material monitor.

## **EVALUATING OF SPATIAL DOSE RATE AND SURFACE CONTAMINATION AT RADIATION CONTROLLED AREA IN KIRAMS**

Bu-Hyung Lee<sup>1</sup>, Sung Ho Kim<sup>1</sup>, Soo Il Kwon<sup>2</sup>, Jae Seok Kim<sup>2</sup>, Jin-seong Jeong<sup>1</sup>, Young Hoon Ji<sup>1</sup>, Seung-UPark<sup>1</sup>, Mun-Sik Choi<sup>1</sup>, Gi-Sub Kim<sup>1</sup>, Min Seok Park<sup>1</sup>, Haijo Jung<sup>1</sup>

<sup>1</sup>Korea Institute of Radiological and Medical Sciences, Republic of Korea

<sup>2</sup>Kyonggi Univ.

### **Key words**

Radiation controlled area, Spatial dose rate, Surface contamination

### **Purpose**

The purpose of this study is providing information for managing exposure dose of radiation workers efficiently by evaluating on the basis of measurement results by radiation controlled area in KIRAMS (Korea Institute of Radiological and Medical Science, Seoul, South Korea).

### **Methods**

With their measurements: survey data of spatial dose rate and surface contamination of radiation controlled area in KIRAMS weekly from 2011 to 2015 is used. In measurement of spatial dose rate, portable radiation dosimeter for beta-gamma ray is used. Automatic low background alpha-beta counter is used in measurement of surface contamination activity. Each dose limit of these measurements is 10 Sv/h and 40 KBq/m<sup>2</sup>, respectively.

### **Results**

In case of exceeding the dose limit from 2011 to 2015, 2 cases were found in annual average for measurement of spatial dose rate and these were not found in the annual average for measurement of surface contamination.

### **Conclusions**

In radiation controlled area radiation exposure is inevitable, so it is essential to evaluate the dose values using dosimetry devices. The utilization of radioactive isotope will continuously increase for many years to come, thus the managing of radiation controlled area through regulation is definitely needed such as tightening access by controlling radiation workers, patients, and visitors entering radiation controlled area.

## THE CALCULATION OF CLEARANCE DAY FOR DISUSED AIR FILTERS IN RADIOISOTOPES PRODUCTION FACILITY

Sung Ho Kim<sup>1</sup>, Bu Hyung Lee<sup>1</sup>, Soo Il Kwon<sup>2</sup>, Jae Seok Kim<sup>2</sup>, Gi-Sub Kim<sup>1</sup>, Jin-seong Jeong<sup>1</sup>, Young Hoon Ji<sup>1</sup>, Seung U Park<sup>1</sup>, Mun-Sik Choi<sup>1</sup>, Min Seok Park<sup>1</sup>, Haijo Jung<sup>1</sup>

<sup>1</sup>Korea Institute of Radiological & Medical Sciences

<sup>2</sup>Kyonggi University

### Key words

radioactive waste, clearance day, air filter

### Purpose

To self-dispose disused air filters, we use Gamma Spectroscopy in analyzing nuclides and in measuring radioactivity of the air filters used in radioisotope facility at Korea Institute of Radiological Medical & Sciences (KIRAMS). With their measurements, the clearance days are calculated and these days define disposal method.

### Methods

There are several radioisotope facilities in KIRAMS, we changed the air filters of 30 MeV cyclotron accelerator room, 30 MeV radioiodine product room, and 30 MeV radioisotope (RI) product room. After air filters were changed, A piece of filters was collected in 90 ml plastic containers. Five specimens were collected at different positions in each filter and all the specimens were stored in 90 ml plastic containers. We used gamma spectroscopy for measurements of nuclide and radioactivity analyzed in accordance with the Genie-2000 (Canberra, USA). We used the maximum value of radioactivity to calculate clearance day from measured nuclide and radioactivity.

### Results

The maximum radiation concentration of I-123 generated in the radioiodine production room was 1,820 Bq/g, which can be disposed after 2 days. The maximum radiation concentration of Tl-202 generated in the radioisotope production room was 205 Bq/g, and this isotope must be stored for 53 days. The I-123 generated in the radioiodine production room had a maximum concentration of 1,530 Bq/g and must be stored for 2 days. The maximum radiation concentration of Na-22 generated in the radioisotope production room was 0.18 Bq/g and this isotope must be disposed after 827 days.

### Conclusions

To manage the air filters, we should determine the appropriate replacement time by examining the differential pressure through systematic measurements.

## OVERVIEW OF RADIATION PROTECTION WORLDWIDE

Magdalena Stoeva<sup>1</sup>, Richard Vetter<sup>2</sup>

<sup>1</sup>IOMP Medical Physics World Board

<sup>2</sup>Mayo Clinic, Rochester, MN

### Key words

Radiation protection, Diagnostic radiology, Nuclear medicine, Radiation oncology

### Purpose

Radiation Protection is a key discipline in medical physics, as well as in medicine and society in general. The purpose of this paper is to present and analyze the various radiation protection approaches that exist worldwide.

### Methods

The International Organization for Medical Physics (IOMP) and the International Radiation Protection Association (IRPA) have recently started an initiative to draw professionals' attention as well as to present important radiation protection information and advice to the members of our professional societies and the related disciplines (1).

Safety and quality assurance in the use of radiation in medicine aims to reduce unnecessary radiation risks while maximizing the benefits. Improvements in quality and safety in radiation medicine require a strong radiation safety culture. To better achieve the goals of strengthening radiation safety in healthcare and better protection of the patients from excessive or unnecessary radiation exposure, a concerted effort by all role players including the radiologists, referring practitioners, technologists, professional organizations, international bodies, and regulators is essential.

### Results

A unique analysis has been made of the professional, operational and regulatory aspects and approaches to radiation protection worldwide, based on the theoretical background and the

recommendations of the International Commission on Radiological Protection (ICRP).

Awareness of the need for emphasis on radiation protection contributes significantly to the safety of healthcare providers, patients, and the public. Contributions are most evident in facility design, in monitoring of personnel and the patient care environment, and in development of procedures and practices for proper handling and limitation of radiation exposure. Medical physicists are often challenged to maximize protection of personnel while minimizing the cost of resources necessary to keep radiation doses as low as reasonably achievable (ALARA). Advances in medical physics will continue to be based on evidence gathered through basic and applied research.

### Conclusions

Radiation protection is one of the leading and fastest developing areas of medical physics and society as evidenced by the emphasis hospitals and medical organizations are placing on radiation protection culture. The interdisciplinary nature of radiation protection makes it a key discipline in ensuring safety of the public.

Radiation protection in medical environments develops in 2 major branches – radiation protection from ionizing radiation and radiation protection from non-ionizing radiation. Strict and clear regulations exist in almost all areas of radiation protection from ionizing radiation, while non-ionizing radiation protection is still a field to explore and develop.

### References

1.Vetter R, M Stoeva, Radiation Protection in Medical Imaging and Radiation Oncology, CRC Press, Taylor & Francis Group, 2015, ISBN 978-148-224-537-0

## **DEVELOPMENT OF A MONTE CARLO BASED PROGRAM FOR ESTIMATION OF ORGAN DOSES IN CHEST RADIOGRAPHY (70KVP - 100KVP)**

Eden Vergado<sup>1</sup>, Agnette Peralta<sup>2</sup>, Augusto Morales<sup>2</sup>, Marvin Albao<sup>3</sup>

<sup>1</sup>Philippine Organization of Medical Physicists (POMP), Philippines

<sup>2</sup>Department of Health (DOH), Philippines

<sup>3</sup>IMSP, UPLB Philippines

### **Key words**

Monte Carlo, Organ doses, Photon transport

### **Purpose**

The internal patient doses received in radiology cannot easily be measured; however it is necessary that these doses be determined. Available computer simulation packages uses the ICRP Reference Man data incorporated in mathematical phantoms. In this study, a Monte Carlo simulation was used to estimate organ doses in chest radiograph (70 kVp to 100 kVp) using the ICRP Reference Man and the Reference Asian Man data incorporated in a mathematical phantom.

### **Methods**

The x-ray beam energy spectrum was generated using the Xertex 5.0 software. The energy values were used for the photon transport simulation of x-rays in the phantom. The organ doses were then estimated from the energy imparted in the mathematical phantom. Estimated organ doses were compared to those generated from the PCXMC version 2.0 software.

### **Results**

The heart and lung doses for both MCPDC and the PCXMC version 2.0 software were in good agreement but not for the other organs when the ICRP Reference Man data were used. The estimated doses differed greatly when the Reference Asian Man data were used because the PCXMC 2.0 had been developed using the ICRP Reference Man.

### **Conclusions**

There is a need for further study to determine the optimized number of simulation photons to be used to accurately estimate the doses using the MCPDC program.

## **INTERCOMPARISON 2016 FOR PERSONAL DOSE EQUIVALENT HP(10) AND HP(0.07) ON PHOTON AND BETA FIELDS IN SOUTHEAST AND SOUTH ASIA REGION**

Waraporn Sudchai<sup>1</sup>, Vithit Pungkun<sup>2</sup>, Jeelawat Esoa<sup>1</sup>, Waraporn Sudchai<sup>1</sup>, Ikuo Kobayashi<sup>3</sup>, Hiroshi Sekiuchi<sup>3</sup>, Hasnel Sofyan<sup>4</sup>, Ahmad Bazlie bin Abdul Kadir<sup>5</sup>, Ahmad Hafiz Bin Abdullah<sup>6</sup>, Kristine Marie D.Romallosa<sup>7</sup>, Jonathan Jerome Acuña<sup>8</sup>, Fang-Yhi Hsu<sup>9</sup>, Prachern Chettasingh<sup>10</sup>, Hguyen Van Hung<sup>11</sup>, Bui Duc Ky<sup>12</sup>, Sandar Aung<sup>13</sup>, Mary Ann Kaila A. Reginaldo<sup>14</sup>, Jung Won Kim<sup>15</sup>

<sup>1</sup>TINT, Thailand

<sup>2</sup>OAEP, Thailand

<sup>3</sup>Nagase Landauer, Ltd, Japan

<sup>4</sup>BATAN, Indonesia

<sup>5</sup>Nuclear Malaysia

<sup>6</sup>Asialab Malaysia

<sup>7</sup>PNRI, Philippines

<sup>8</sup>TUV Philippines

<sup>9</sup>National Tsing Hua University, Taiwan

<sup>10</sup>Bureau of Radiation and Medical devices, DMSc, Thailand

<sup>11</sup>NRI, Viet Nam

<sup>12</sup>INST, Viet Nam

<sup>13</sup>Radiation Protection Department, Myanmar

<sup>14</sup>Nagase Philippines Corporation-Dosimetry Laboratory.

<sup>15</sup>Hanil Nuclear Co. Republic of Korea

### **Key words**

Keywords: Personal dose equivalent, intercomparison, OSL system

### **Purpose**

OSL is one of the best technologies for passive personal dosimetry. The OSL system reporting in term of Hp(10), Hp(0.07) and Hp(3) is based on whole body dose algorithm accredited by National Voluntary Laboratory Accreditation Programme (NVLAP). In this intercomparison, OSL dose algorithm was verified by individual monitoring services (IMS) laboratory to reveal confidence between evaluated dose and delivered dose from the Secondary Standard Dosimetry Laboratory (SSDL), Office of Atoms for Peace (OAP). The standard doses are traceable to the Physikalisch-Technische Bundesanstalt (PTB) in Germany. The objective of this comparison is to improve OSL system for IMS laboratory in order to comply with ISO 17025.

### **Methods**

Fourteen laboratories from nine countries in Southeast and South Asia region participated in this programme. The programme had been designed for Inlight dosimeters in which the comparison of Hp(10) and Hp(0.07) from participants are included. The dosimeters were irradiated at beam qualities of Cs-137 for the deep dose (Hp(10)) and Sr-90 and the shallow dose (Hp(0.07)).

### **Results**

The results showed the performance of the evaluation quality for personal dose equivalent with regard to Hp(10) and Hp(0.07) in photon and beta fields in terms of compliance with the trumpet curve.

### **Conclusions**

The intercomparison programme will be continued on a regular basis to develop the quality management system and to develop the Personal Dosimetry Network of IMS laboratories in Southeast and South Asia region.

## **COMPARISON OF INCIDENT AIR KERMA (KI) FOR MOBILE X-RAY MACHINE (OPTIMA XR200) USING IONIZATION CHAMBER AND GAFCHROMIC FILMS**

Nurul Aishah Mohd Nasir, Siti Aishah Abdul Aziz, Nor Shazleen Ab Shukor, Norida Ahmad

Universiti Sains Malaysia

### **Purpose**

To determine the measurement of incident air kerma (Ki) for mobile unit x-ray Optima (XR200) using ionization chamber (IC) and Gafchromic films based on TRS457.

### **Methods**

The study begins with the study of dose response of the Gafchromic XR-QA2 and XR-RV3 films. The films irradiated with 70, 80, 90 and 100kVp for 20mAs. The films were scanned by using Epson 10000XL flatbed scanner after 24hours irradiation, to obtain the pixel value of the films. Then, the pixel value changed to optical density to plot the linear dose response graph. The study proceeded by irradiating the dosimeters with exposure parameters 83kVp/12.5 mAs, 85kVp/32.0 mAs and 85kVp/ 40mAs for abdomen examination, while for chest examination were 120kVp/5mAs, 125kVp/1.0 mAs and 125kVp/1.6mAs.

### **Results**

The study showed linear relationship for Gafchromic XR-QA2 film, but not for XR-RV3 films since the films were fluoroscopic-guided favour. The calibration curve for Gafchromic XR-QA2 films acquired to get the dose from the films. The dose for Ki calculation was obtained by manual calculation. Ki for films was higher than IC due to the high sensitivity of the films towards dose response. Range of percentage difference (%) for abdomen was 34% to 108%, while for chest was 32% to 350%. The large variations of percentage difference were due to the usage of out of range dose, properties of films and mishandling technique of the films.

### **Conclusions**

The significant difference of percentage between IC and Gafchromic films can be overcome by using the in range dose for future Gafchromic films study.

## **EVALUATION OF SIZE-SPECIFIC DOSE ESTIMATES (SSDE) IN PEDIATRIC BODY IMAGING USING 320-DETECTOR CT**

Saifhon Admontree

Ramathibodi Hospital, Thailand

**Key words:** Size-Specific Dose Estimates (SSDE), CTDIvol, pediatric CT, Diagnostic Reference Levels (DRLs).

### **Purpose**

To compare Volumetric Computed Tomography Dose Index (CTDIvol) and Size-Specific Dose Estimates (SSDE) in pediatric body CT image by using CT 320 slices.

### **Methods**

The quality control was performed prior to collect data. A retrospective consecutively analysis of 41 chest, 40 abdomen and 47 chest included abdomen pediatric CT examinations were categorized into four age groups: (A) 0-1, (B) 1-5, (C) 5-10 and (D) 10-15 years old. Using SSDE conversion factors for 32-cm-diameter CTDI phantom measurements derived from anteroposterior (AP) and lateral dimensions to estimate patient dose from scanner output indices (CTDIvol) for different patient sizes.

### **Results**

The average radiation dose in terms of displayed/SSDE CTDIvol in group A, B, C, D were 1.5/3.6, 1.7/4.2, 2.5/4.6, 3.1/4.3 mGy for pediatric chest CT, 1.7/3.7, 2.1/4.0, 2.3/4.3, 3.3/5.1 mGy for abdomen CT and 1.7/3.7, 1.9/3.9, 2.5/4.6, 3.1/4.7 for chest included abdomen CT, respectively. The percentage difference of displayed and SSDE CTDIvol in each group (A/B/C/D) for chest, abdomen and included abdomen were 140/147/84/39, 118/90/87/55 and 118/105/84/54, respectively.

### **Conclusions**

The highest percentage difference of displayed/SSDE CTDIvol was found in youngest age group (0-1 years old) with small patient size. Radiologists should be concerned and technologists have to estimate SSDE dose and adjust the scanning parameter prior to perform CT scan to ensure the radiation dose not excess the Diagnostic Reference Levels (DRLs).

## **DOSE VERIFICATION OF PROSTATE VMAT PLANS WITH DELTA4 PHANTOM**

Emmanuel Worlali Fiagbedzi  
National Cancer Institute, Cro

### **Purpose**

Complex radiotherapy treatment plans like volumetric modulated arc therapy (VMAT) for the prostate require dosimetric verification of a planned dose distribution to check for the agreement between the dose distribution calculated by the Treatment Planning System and the corresponding measured dose distribution before clinical delivery.

### **Methods**

Twenty Prostate cases were planned with the Eclipse 13.6 treatment planning system. The plans were recalculated in a three-dimensional measurement phantom Delta4 with the structures of every patient and accurate plan parameters. All plans were delivered and measured using the Delta4 phantom on a Varian Trilogy. All plans were analyzed using the three parameters %DA (limit 3%), DTA (limit 3%), (limit 3 mm), and Gamma-index with a 3% dose tolerance and 3 mm distance to agreement in relation to the treatment planning system. The gamma criterion was considered fulfilled if  $< 1$  in at least 90÷95% of the points.

### **Results**

Gamma maps comparison show that all three distributions mutually agreed to within a 3% (dose difference) and 3mm (distance-to-agreement) criteria. An averaged gamma pass ratio of 97.7% was obtained between the Delta4 measurement and Eclipse distributions with the 3mm/3% gamma criteria. The minimum gamma pass ratio was 90.3% and the maximum 100.0%.

### **Conclusions**

Results confirmed a good agreement between Eclipse calculation and Delta4 measurement for Prostate plans with high and conformed dose to the target and low dose to the organs at risk.

### **Key words**

Dose. verification, Prostate, Delta4

## **A QUALITY ASSURANCE PROGRAMME FOR 4DCT IMAGING OF LUNG TUMOUR**

Khong Wei Ang

National Cancer Centre, Singapore

### **Purpose**

Our aim is to develop & validate a systematic approach to quality assurance the entire imaging process of a free-breathing, retrospective phase binning 4DCT for lung radiation therapy.

### **Methods**

The Quasar Respiratory Motion Phantom, with a 3cm diameter acrylic sphere embedded in a cedar cylindrical insert, is driven at frequencies 4, 8, 10, 12 breathes/minute (BPM). A 6-point marker block placed on the Quasar is driven up & down. The acrylic sphere is adjusted to move in peak to peak range of 1cm in the in-out direction. The Varian RPM system will acquire a resultant sinusoidal breathing pattern. The set-up is imaged with a Siemens Somatom Definition AS 64-slice CT simulator, with 3 acquisition configurations, optimised to scan patients with breathing frequency > 6, 9, 12 BPM. For each breathing frequency & acquisition configuration, retrospective phase binning results in 10 phases of reconstructed volumes. Analysis of the power spectrum of the breathing pattern, & distortion of the reconstructed images for ideally driven, 5 patients coached to breath at 12 BPM, & 5 non-coached patients are performed to see if there are significant differences.

### **Results**

Maximum error in power spectrum analysis of ideally driven & coached frequency is 2.4% & 6.8%. Non-coached patients range from 10.986 to 16.845 BPM. Image reconstruction for coached patients is 10.6% better than non-coached.

### **Conclusions**

We have successfully validated that a chosen frequency & image acquisition configuration can be set as a reference for QA of our 4DCT imaging, in addition to established CT QA procedures.

### **Key words**

QA,RPM,4DCT

## **EVALUATION OF A Gd<sub>2</sub>O<sub>2</sub>S:Tb AS A QUALITY ASSURANCE TOOL FOR HIGH-DOSE-RATE BRACHYTHERAPY**

Takahiro Shimo<sup>1</sup>, Katsunori Yogo<sup>2</sup>, Msahiro Kato<sup>1</sup>, Hisato Nagano<sup>3</sup>, Jun Kubota<sup>1</sup>, Yoshinori Shimizu<sup>4</sup>, Yasuhiro Tashima<sup>1</sup>

<sup>1</sup> Tokyo Nishi Tokushukai Hospital, Japan

<sup>2</sup> Kitasato University, Japan

<sup>3</sup> Shonan Fujisawa Tokushukai Hospital, Japan

<sup>4</sup> Yamato Tokushukai Hospital, Japan

### **Purpose**

To use phosphor luminescence tracking for evaluating a rare-earth phosphor (Gd<sub>2</sub>O<sub>2</sub>S:Tb) and the complementary metal-oxide-semiconductor (CMOS) camera as a quality assurance (QA) tool.

### **Methods**

The distance from the Gd<sub>2</sub>O<sub>2</sub>S:Tb sheet to the CMOS camera was 80 cm. Each observation comprised five positioning steps at intervals of 2.5, 5.0, or 10 mm in space and 5 s in time. Iridium-192 was used as the radiation source. The CMOS camera recorded the phosphor luminescence at a fixed rate of 30 frames per second. Coordinates of the luminescence produced by the stepping source were obtained using a template-matching method on the recorded images. The coordinates, step distances, and dwelling times were estimated using an in-house program.

### **Results**

The phosphor luminescence position changed as the source moved. The accuracy of the source position (mean  $\pm$  standard deviation) acquired for each source step interval was  $0.16 \pm 0.11$ ,  $0.13 \pm 0.11$ , and  $0.13 \pm 0.11$  mm at the 10-, 5.0-, and 2.5-mm step intervals, respectively. The measurement range accuracy of the source position was  $0.14 \pm 0.10$  mm. The dwell time acquired for each source step interval was  $4.98 \pm 0.05$ ,  $4.97 \pm 0.02$ , and  $4.96 \pm 0.04$  s at the 10-, 5.0-, and 2.5-mm step intervals, respectively.

### **Conclusions**

Our procedure can provide real-time analysis of the source position with sufficient resolution time and is therefore useful as a simple QA tool for brachytherapy.

### **Key words**

Brachytherapy, quality assurance, phosphor luminescence

## **OUT-OF-FIELD DOSIMETRY ON PHOTON AND ELECTRON BEAMS USING GAFCHROMIC EBT3 FILM**

Nor Liyana Salim, Wan Nordiana Rahman, Reduan Abdullah, Norhayati Dollah,  
Raizulnasuha Abdul Rashid  
University Sains, Malaysia

### **Purpose**

To experimentally investigate the out of field dosimetry in the solid water phantom using Gafchromic EBT3 film.

### **Methods**

The study was carried out with 6 MV, 10 MV, 6 MeV and 15 MeV energy beams from Siemens Primus linear accelerator with constant dose rate of 200 monitor unit (MU). The measurements were performed using the 30x30x15 cm<sup>3</sup> solid water phantom at maximum depth dose (d<sub>max</sub>) with three field sizes, 5x5 cm<sup>2</sup>, 10x10 cm<sup>2</sup> and 15x15 cm<sup>2</sup> at lateral distances from 0,3,7,9,11,15 and 19 cm from the field edge.

### **Results**

The results for 6 MV photon beam show approximately 0.05% , 0.07% and 0.71% of the prescribed dose outside the field while for 10 MV photon beams, 0.68%, 0.30% and 0.56% was measured respectively for 5x5 cm<sup>2</sup>, 10x10 cm<sup>2</sup> and 15x15 cm<sup>2</sup> field size at 19 cm distance. For electron beam, an appearance of peak dose has been observed around 11-19 cm out of the field edge for all field sizes and energies. For 6 MeV electron beams, 4.7% of the prescribed dose appeared as highest peak dose for 5x5 cm<sup>2</sup> at 11 cm due to cerrobend usage and no peak dose was evidenced at the 10x10 cm<sup>2</sup> and 15x15 cm<sup>2</sup>. For 15 MeV electron beams, 1.93%, 4.11% and 2.13% of the prescribed dose resulted as the out of field dose for respectively 5x5 cm<sup>2</sup>, 10x10 cm<sup>2</sup> and 15x15 cm<sup>2</sup>.

### **Conclusions**

In summary, the out of field dose decrease with the increasing of distance out from the field edge and increase with increasing energy and field size for both photon and electron beams.

### **Key words**

Out-of-field dose, radiotherapy, Gafchromic EBT3 film, electron beam, photon beam, film dosimetry

## **EVALUATION OF SCANNER PARAMETERS ON EBT 2 AND EBT 3 FILM ANALYSIS**

Siti Nur Amirah Azhan, Wan Nordiana Rahman, Nor Shazleen Ab Shukor, Raizulnasuha  
Abd Rashid, Norhayati Dollah  
Universiti Sains Malaysia (USM), Malaysia

### **Purpose**

This study investigates the effects of scanner parameters properties to EBT 2 and EBT 3 films analysis irradiated with photon and electron beam energy.

### **Methods**

The EBT 2 and EBT 3 films were initially irradiated with photon and electron beams of different energies (6 MV, 10 MV, 6 MeV and 9 MeV) using Siemens Primus Linear Accelerator. After irradiation, the films were then scanned using Epson Expression 10000 XL flatbed using different scanning parameters.

### **Results**

As a result, the scanner flattening correction did not have any effects the optical density (OD) reading of EBT 2 and EBT 3 films. However, the interpretation section of scanner parameter did changes if invert 16-bit scan was used compared to similar reading obtained if invert 8-bit scan and standard parameter (no invert) were used. The OD of film type is significantly different than the standard parameter and the image type also affect the OD value. The different parameter of resolution flatbed scanner gives almost consistent OD value but changes to a higher resolution will increase the OD value.

### **Conclusions**

In conclusion, the scanning parameters have significant effects on the films OD analysis and hence affect the dose measured.

### **Key words**

films dosimetry, Epson Expression 10000 XL flatbed, parameters, photon beam, electron beam

## **COMPARISON OF BIOLOGICAL-BASED AND DV-BASED IMRT PLANS GENERATED BY A TREATMENT PLANNING SYSTEM**

Joseph Maria Das Koilpillai<sup>1</sup>, Senthilkumar K<sup>2</sup>, Balasubramanian K<sup>3</sup>, Deka AC<sup>3</sup>, Patil BR<sup>3</sup>

<sup>1</sup> Sanjay Gandhi Postgraduate Institute of Medical Sciences, India

<sup>2</sup> Research and Development Centre, Bharathiar University, Coimbatore, India

<sup>3</sup> Karnataka Cancer Therapy & Research Institute, Hubli, India

### **Purpose**

Nowadays most of the radiotherapy treatment planning systems uses dose or dose-volume (DV) based cost functions for intensity-modulated radiotherapy (IMRT) fluence optimization. Recently some of the treatment planning systems (TPS) incorporated biological-based cost function for IMRT optimization. Most of the previous studies compared IMRT plans optimized using biological-based and DV-based cost functions in two different treatment planning systems. Hence, the purpose of the study is to compare equivalent uniform dose (EUD)-based and DV-based IMRT plans generated using the same treatment planning system.

### **Methods**

Twenty patients with prostate cancer and twenty-two patients with head and neck cancer patients were retrospectively selected for this study. For each patient, two IMRT plans were generated using EUD-based cost function (EUD\_TP) and DV-based cost (DV\_TP) respectively. The generated IMRT plans were evaluated using both physical and biological dose evaluation indices.

### **Results**

Biological-based plans ended up with a highly inhomogenous target dose when compared to DV based plans. For serial organs, Dnear-max or D2% (Gy) of EUD-based plans showed significant difference with DV-based plans ( $p=0.003$ ). For parotid gland mean dose and V30Gy(%) of EUD-based plans showed significant difference with DV-based plans ( $p=0.004$ ). For both rectum and bladder, there was a significant difference in mean dose, D30% (Gy) dose between EUD-based plans and DV-based plans.

### **Conclusions**

In this study we estimated the influence of optimization parameters from the potential use of EUD-based cost functions on the plan quality by generating both the plans in the same TPS.

### **Key words**

Intensity-modulated radiotherapy (IMRT), Biological-based optimization, equivalent uniform dose (EUD), dose volume (DV)-based optimization

## **ESTIMATION OF PTV MARGIN BASED ON MARKER AND BONE MATCHING IN PROSTATE CANCER PATIENTS TREATED WITH IMAGE GUIDED RADIOTHERAPY**

Ajay Kumar, Pramod Kumar Gupta, Neeraj Rastogi, K J Maria Das, Shaleen Kumar  
Sanjay Gandhi Post Graduate Institute Of Medical Sciences (SGPGIMS), Lucknow, India

### **Purpose**

In prostate cancer (PC), Intensity modulated radiotherapy (IMRT) with image guidance (IGRT) is an established treatment. We analyzed 20 patients of PC treated by IGRT using either fiducial marker matching (MM) or anatomical bone matching (BM) to generate PTV margin.

### **Methods**

Patients were immobilized using knee rest. Three gold fiducial markers placed in prostate under transrectal ultrasonography. Radiotherapy volume was either whole pelvis to a dose of 50.4 Gy/28# followed by prostate boost 26Gy/13# by IGRT or prostate only RT (PORT) to a dose of 76Gy/38# by IGRT. Image guidance was done either by using MM or BM. Daily on board KV images (OBI) were taken and shifts were applied. Systematic error (SE), random error (RE) and PTV margin were calculated using Van Herk formula.

### **Results**

Population based PTV margin of 10 mm was given in all direction except posteriorly 5 mm in MM, 7 mm in BM. MM was done in 12(60%) and BM in 8(40%). Using MM; SE in ML (medio-lateral), CC (cranio-caudal), AP (ant-post) was 2.9, 3.5 & 2.3 mm and RE was 3.7, 3.6 & 2.7 mm and PTV margin required was 10.0, 11.2 & 7.6 mm respectively. Using BM; SE in ML, CC, AP was 2.1, 1.6 & 4.0 mm and RE was 5.1, 2.8 & 3.2 mm and PTV margin was 8.8, 6.0 & 12.3 mm respectively.

### **Conclusions**

Population based PTV margin may not be accurate for IGRT in PC. Every institute should generate its own PTV based on their immobilization and setup accuracy.

### **Key words**

Image guidance, prostate cancer, PTV

## **ESTIMATION OF PATIENT-SPECIFIC DOSE VERIFICATION USING LINEAR ACCELERATOR LOG FILES IN VOLUMETRIC MODULATED ARC THERAPY**

Kengo Kosaka<sup>1</sup>, Masao Tanooka<sup>2</sup>, Hiroshi Doi<sup>1</sup>, Hiroyuki Inoue<sup>2</sup>, Kazuo Tarutani<sup>1</sup>, Hitomi Suzuki<sup>1</sup>, Yasuhiro Takada<sup>1</sup>, Masayuki Fujiwara<sup>1</sup>, Norihiko Kamikonya<sup>1</sup>, Shozo Hirota<sup>1</sup>

<sup>1</sup> Department of Radiology, Hyogo College of Medicine, Japan

<sup>2</sup> Department of Radiological Technology, Hyogo College of Medicine College Hospital, Japan

### **Purpose**

The purpose of the present study was to estimate patient-specific dose verification results using linear accelerator (linac) log files in prostate cancer patients who undergo volumetric modulated arc therapy (VMAT).

### **Methods**

Twenty six prostate cancer patients who underwent VMAT were analyzed in this study. VMAT plans were created using Monaco (Elekta AB, Stockholm, Sweden) treatment planning system and were transferred to Synergy (Elekta AB, Stockholm, Sweden) linac. During the beam delivery, root mean square (rms) control errors and accelerations of the multi-leaf collimator and the gantry were recorded in the log files. Dose verification was also performed for all the plans using ArcCHECK (Sun Nuclear Corp., FL). The gamma index pass rates were evaluated under the criteria of 2 mm/2%. Subsequently, the correlation coefficients between the gamma index pass rates and each of the above rms values were calculated.

### **Results**

The correlation coefficients between the gamma index pass rates and the rms gantry angle errors were -0.64, whilst the correlation between the gamma index pass rates and the rms gantry accelerations were -0.68. On the other hand, the correlation coefficients between the gamma index pass rates and the rms leaf position errors were 0.31, whereas the correlation between the gamma index pass rates and the rms leaf acceleration were -0.17.

### **Conclusions**

We suggest that the VMAT quality assurance (QA) results can be directly estimated from the linac log files, and that there is a potential to simplify patient-specific prostate VMAT QA procedure.

### **Key words**

log file, patient-specific dose verification, volumetric modulated arc therapy

## THE EFFECT OF MLC LEAF MOTION CONSTRAINTS ON PLAN QUALITY AND DELIVERY ACCURACY IN VMAT

Jae-Yong Jung<sup>1</sup>, Dong-Jin Kang<sup>1</sup>, Seung-Chang Sohn<sup>1</sup>, Young-Joo Shin<sup>1</sup>, Yon-Lae Kim<sup>2</sup>, Jung-Whan Min<sup>3</sup>

<sup>1</sup> Department of Radiation Oncology, Inje University SangGye Paik Hospital, Korea

<sup>2</sup> Department of Radiological Technology, ChoonHae Health College, Korea

<sup>3</sup> Department of Radiological Science, ShinGu University College, Korea

### Purpose

Volumetric modulated arc therapy (VMAT) is very complex technique, which allows irradiation with simultaneous changing gantry speed, dose rates, control point, arc length, MLC speed and leaf motion constraint. Among these, particularly, the important parameters are MLC speed and leaf motion constraints. The purpose of this study is to evaluate the plan quality and delivery accuracy of VMAT under leaf motion constraints.

### Methods

VMAT plan were created for treatment of nasopharynx, pancreas, and prostate cancers. All treatment plans were optimized using 6 MV photon, single (pancreas and prostate) or dual arc (nasopharynx), 356° per arc, 2° gantry spacing and 90 sec per arc delivery time by Oncentra treatment planning system. But, MLC leaf motion constraints were optimized, using various parameters, between 0.1 and 2.0 cm/deg. Plan quality was performed by HI (Homogeneity index), CI (Conformity index), and QOC (Quality of coverage) at target and dose index (DI) at OARs, respectively. Evaluation of delivery accuracy was using the gamma analysis with 3%/3 mm and 2%/2 mm acceptance criteria by bi-planar diode array.

### Results

For all the plans, less restrictive leaf motion constraints were increased discrepancies of delivery accuracy but lead to superior plan quality. In contrast, more restrictive leaf motion constraints lead to inferior plan quality but discrepancies of delivery accuracy were decreased.

### Conclusions

Leaf motion constraints significantly affect plan quality and delivery accuracy in VMAT. Our studies showed that the optimal balance between plan quality and delivery accuracy indicate 0.3-0.8 cm/deg.

### Key words

VMAT, leaf motion, plan quality, delivery accuracy.

## **A STUDY OF THE IMPROVEMENT OF THE DOSE DISTRIBUTION VERIFICATION USING PORTAL DOSIMETRY**

Kazuo Tarutani<sup>1</sup>, Masao Tanooka<sup>2</sup>, Hiroshi Doi<sup>2</sup>, Hiroyuki Inoue<sup>2</sup>, Kengo Kosaka<sup>2</sup>, Masaki Miyashita<sup>3</sup>, Kazutoshi Abuta<sup>3</sup>, Hitomi Suzuki<sup>2</sup>, Yasuhiro Takada<sup>2</sup>, Masayuki Fujiwara<sup>2</sup>, Kazufumi Kagawa<sup>3</sup>, Norihiko Kamikonya<sup>2</sup>, Shozo Hirota<sup>2</sup>

<sup>1</sup> Hyogo College Of Medicine

<sup>2</sup> Department of Radiology, Hyogo College of Medicine

<sup>3</sup> Department of Radiology, Kansai Rousai Hospital

### **Purpose**

The accuracy of the field edge is unknown in the large field in the portal dosimetry (PD). The purpose of this study was to investigate the dose distribution verification accuracy of the PD by changing a diagonal dosimetry profile shape that was used for the correction of the profile.

### **Methods**

In this study, we assessed the diagonal dosimetry profile of each depth (at the maximum dose, 5, 10, and 20 cm). We made the test plans of the squares of 5, 10, 20, and 30 cm with each corrected file and performed the dose distribution verification in the PD. The qualitative evaluation confirmed the agreement degree of the profile visually. The quantitative evaluation was performed by a gamma analysis technique.

### **Results**

In the visual evaluation of the profile, the agreement degree of the large field edge was improved by the diagonal dosimetry profile of the depth of 10 cm. In the field size of 10cm the pass rate of the gamma analysis (tolerance; 2mm, 2%) was 100% in the profile of all evaluated depths. However, the pass rates were improved from (the depth of the maximum dose) 54.9% to 99.9% in the field size of 30 cm. In addition, the mean gamma value was improved from 1.04 (at the depth of the maximum dose) to 0.48 (at the depth of 10 cm).

### **Conclusions**

The verification accuracy of the PD in the large field (20 and 30 cm) was improved by changing the corrected file.

### **Key words**

portal dosimetry; dose distribution verification; gamma index

## **CONSTRUCTION AND MEASUREMENT OF OPTICAL CT SYSTEM FOR EVALUATION OF POLYMER GEL DOSIMETERS**

Hiraku Kawamura<sup>1</sup>, Takaoki Takanashi<sup>2</sup>, Yoshikazu Shimada<sup>1</sup>, Yuichi Sato<sup>1</sup>, Shinji Abe<sup>1</sup>

<sup>1</sup> Ibaraki Prefectural University of Health Sciences, Japan

<sup>2</sup> Riken, Japan

### **Purpose**

Polymer gel dosimetry, which utilizes chain polymerization that is proportional to radiation dose, is a new three-dimensional dosimetric tool for quality assurance. It could potentially be used to measure 3D doses in photon and proton radiotherapy.

We constructed Optical Computed Tomography (OCT) system for evaluation of polymer gel dosimeter. The reconstructed image from OCT is compared with R2 dose images with MRI scanner.

### **Methods**

The OCT was composed of He-Ne laser for light source, Photo diode for detector, rotation and linear motion stage and stage controller for stage operation. The detector in OCT was measured permeation light through gel dosimeter from light source. Acquired transmission data per angles was reconstructed using Filtered Back-Projection method. The tomographic images of polymer gels were done using OCT like X-ray CT. Irradiated PAGAT polymer gel samples were prepared. The samples were irradiated to 1, 2, 3, 4, 5 Gy respectively, with 10MV X-ray beams. The dose-response was executed using OCT of irradiated samples. The dose response curve using OCT was compared with dose R2 curve using MRI.

### **Results**

The reconstructed tomographic images of irradiated samples using reconstructed OCT were represented inner structure. In the results of dose response, when it was increased absorbed dose to gel samples, the response measured of reconstructed images of irradiated gels using the OCT was increasing likewise.

### **Conclusions**

We constructed original OCT system for evaluation of polymer gel dosimeter. The dose response was increased when the absorbed dose of the irradiated gels was increased.

### **Key words**

Polymer gel dosimeter, Optical Computed Tomography system

## EVALUATION OF DELIVERY ACCURACY QA FOR VMAT USING THE VARIAN DYNALOG FILES

Dong-Jin Kang<sup>1</sup>, Yon-Lae Kim<sup>2</sup>, Jung-Woo Lee<sup>3</sup>, Jung-Whan Min<sup>4</sup>, Young-Joo Shin<sup>5</sup>, Jae-Yong Jung<sup>5</sup>

<sup>1</sup> Inje University SangGye Paik Hospital, Korea

<sup>2</sup> Choonhae College of Health Sciences, Korea

<sup>3</sup> Department of Radiation Oncology, The Konkuk University Hospital, Korea

<sup>4</sup> Department of Radiological Science, The Shingu University College, Korea

<sup>5</sup> Department of Radiation Oncology, Inje University Sanggye Paik Hospital, Korea

### Purpose

For evaluating the treatment planning accurately, the QA for treatment planning is recommended when treated with VMAT. Recently, treatment plan QA software can be used to verify the delivered dose accurately before and after treatment. The purpose of this study is to evaluate the accuracy of beam delivery QA for VMAT plan with AAPM TG-119 protocol.

### Methods

Clinac iX with a built-in 120 MLC was used to acquire the MLC dynalog file be imported in MobiusFx. To establish VMAT plan, Oncentra RTP system was used target and organ structures were contoured in Im'RT phantom. For evaluation of dose distribution was evaluated by using gamma index, and the point dose was evaluated by using the CC13 ion chamber in Im'RT phantom.

### Results

For the evaluation of point dose, the mean of relative error between measured and calculated value was  $1.41 \pm 1.18\%$  (target) and  $0.89 \pm 0.80\%$  (OAR), the confidence limit were 3.21% (target) and 2.58% (OAR).

For the evaluation of dose distribution, in case of Delta4PT, the average percentage of passing rate were  $99.78 \pm 0.22\%$  (3%/3 mm),  $96.86 \pm 2.34\%$  (2%/2 mm). In case of MobiusFx, the average percentage of passing rate were  $99.90 \pm 0.1\%$  (3%/3 mm),  $97.98 \pm 1.72\%$  (2%/2 mm), the confidence limits were in case of Delta4PT, 0.62% (3%/3 mm), 6.60% (2%/2 mm), in case of MobiusFx, 0.38% (3%/3 mm), 5.88% (2%/2 mm).

### Conclusions

In this study, we performed VMAT QA method using dynamic MLC log file compare to binary diode array chamber. All analyzed results were satisfied with acceptance criteria based on TG-119 protocol.

### Key words

VMAT, Dynalog file, Gamma index, MobiusFx

## **DEVELOPMENT OF PATIENT POSITIONING GUIDANCE SYSTEM FOR ALIGNING THE PATIENT EASILY AND EXACTLY**

Hiraku Fuse<sup>1</sup>, Kenji Komatsu<sup>2</sup>, Hiroki Arakawa<sup>3</sup>, Takeji Sakae<sup>4</sup>, Tatsuya Fujisaki<sup>1</sup>

<sup>1</sup> Ibaraki Prefectural University of Health Sciences, Japan

<sup>2</sup> Hitachi General Hospital, Japan

<sup>3</sup> Seirei Sakura Citizen Hospital, Japan

<sup>4</sup> University of Tsukuba, Japan

### **Purpose**

Many studies were carried out to conduct patients positioning exactly and easily. These study were reported that developed devices were difficult to set the landmark at the same patient body surface exactly for every treatment. In this study, we aim to develop a positioning guidance system to determine patient position exactly and easily for the highly precise radiotherapy.

### **Methods**

We used six infrared (IR) cameras that placed by three in right and left of the treatment bed to acquire the position of the IR marker. The position guidance and monitoring system was calculated a displacement from reference position based on the position acquired by the IR camera and IR marker. Time shortening and alignment reproducibility were compared between the conventional line alignment and this system.

### **Results**

The conventional line alignment was up to 138 seconds for a minimum period of 70 seconds, and whereas this system was up to 73 seconds for a minimum period of 39 seconds. The conventional positioning was up to 332 seconds for a minimum period of 187 seconds, and whereas this system was up to 153 seconds for a minimum period of 90 seconds. The positioning time of this system was significantly shorter than a conventional line alignment ( $p < 0.0001$ ) in both parts.

### **Conclusions**

Positioning time of this system was shortened than a conventional line alignment method. Although, positioning reproducibility was no significant in the both methods

### **Key words**

patient positioning, alignment, IR marker, positioning time, positioning reproducibility, radiotherapy

## **RADIOPHOTOLUMINESCENT GLASS DOSIMETER APPLICATION TO THE DOSE AUDIT OF FLATTENING-FILTER-FREE LINEAR ACCELERATOR, TOMOTHERAPY AND CYBERKNIFE**

Hideyuki Mizuno<sup>1</sup>, Naoki Tohyama<sup>2</sup>, Akifumi Fukumura<sup>1</sup>, Shigekazu Fukuda<sup>1</sup>, Suoh Sakata<sup>3</sup>, Katsuhisa Narita<sup>3</sup>, Wataru Yamashita<sup>3</sup>, Nobuhiro Takase<sup>3</sup>, Masahiro Hoteida<sup>3</sup>, Yosuke Sasaki<sup>3</sup>, Hiroaki Okuyama<sup>3</sup>, Tota Ushiroda<sup>3</sup>

<sup>1</sup> National institute of Radiological Sciences, Japan

<sup>2</sup> Tokyo Bay Clinic, Japan

<sup>3</sup> Association for Nuclear Technology in Medicine, Japan

### **Purpose**

In Japan, postal dose audits have been performed on radiation therapy units using a radiophotoluminescent glass dosimeter (RGD), since 2007. The purpose of this study was to obtain a set of correction factors of the RGD output for reference condition for flattening-filter-free linear accelerator (FFF), Tomotherapy (Tomo) and Cyberknife (CK).

### **Methods**

Special phantom was designed in order to place 3 RGD elements in a tiny uniform region (dose gradient < 0.2%) at a field center around 3 mm. RGDs were irradiated by using this phantom for 1 Gy. Ionization chamber measurements using an A1SL chamber (Exradin) were done for same reference condition and monitor units for each modality. The response of RGD were evaluated by calculating the ratio between RGD and IC outputs. For every modality, at least 3 different machines were used and the results were averaged to derive final response of the RGD.

### **Results**

The response of the RGD was -0.1% (6 MV) and -0.6% (10 MV) for FFF, -0.8% (6 MV) for Tomo, and -0.1% (6 MV) for CK. The RGD showed good responses of less than 1% for the beam from every modality. For FFF beam, the difference could be attributed to the decrease of kQ for IC measurement of FFF beam that was mentioned in some published papers.

### **Conclusions**

RGD was proved to be useful to the modern treatment units. We will expand our audit application to such new modalities.

### **Key words**

Radiophotoluminescent glass dosimeter, dose audit, modern treatment unit, QA

## A multi-institutional study for the beam output of the tomotherapy in Japan

H Shimizu<sup>1</sup>, KSasaki<sup>2</sup>, T Kubota<sup>1</sup>, K Sugi<sup>3</sup>, H Fukuma<sup>4</sup>, T Nakabayashi<sup>5</sup>, T Isomura<sup>1</sup>,  
K Nakashima<sup>1</sup>, H Tachibana<sup>1</sup>, T Kodaira<sup>1</sup>

<sup>1</sup>Department of Radiation Oncology, Aichi Cancer Center Hospital, Japan;

<sup>2</sup>Graduate School of Radiological Technology, Gunma Prefectural College of Health Sciences, Japan;

<sup>3</sup>Hitachi, Ltd. Healthcare Business Unit, Japan;

<sup>4</sup>Department of Radiology, Nagoya City University Hospital, Japan;

<sup>5</sup>Customer Support & Area Operation Headquarters, Physics & Clinical Support, Accuray Japan K.K, Japan

**Key words:** tomotherapy, machine-specific reference field, beam output

**Introduction:** The investigation of the beam output is essential for the prevention of accidents and treatment misadministration. The aim of this study was to determine the variation in the beam output of the tomotherapy in multiple institutions.

**Methods:** Measurements of the beam output were conducted at 22-radiotherapy centers. The absolute dose to water in machine-specific reference field ( $f_{msr}$ ), which indicated a static field ( $5 \times 10 \text{ cm}^2$ ) in the reference conditions of the tomotherapy defined by the IAEA study group [1], were evaluated. According to a dosimetric protocol of Japan; the Standard Dosimetry of Absorbed Dose to Water in External Beam Radiotherapy (Standard Dosimetry 12) [2], the absolute dose to water in  $f_{msr}$  ( $D_{w,Q_{msr}}^{f_{msr}}$ ) has been defined as follows.

$$D_{w,Q_{msr}}^{f_{msr}} = M_{Q_{msr}}^{f_{msr}} N_{D,w,Q_0} k_{Q,Q_0} k_{Q_{msr},Q}^{f_{msr},f_{ref}} \dots (1)$$

Where,  $M_{Q_{msr}}^{f_{msr}}$  is a value that was multiplied the correction factors ( $k_s$ ,  $k_{pol}$ ,  $k_{TP}$  and  $k_{elec}$ ) on a reading value of an electrometer in  $f_{msr}$ . And,  $N_{D,w,Q_0}$  is a dose to water calibration coefficient for the reference beam quality ( $Q_0$ ), and  $k_{Q,Q_0}$  is a quality conversion factor from  $Q_0$  to the beam quality ( $Q$ ) of the conventional reference conditions ( $f_{ref}$ ), and  $k_{Q_{msr},Q}^{f_{msr},f_{ref}}$  is a quality conversion factor from  $Q$  to the beam quality of the reference conditions of the tomotherapy ( $Q_{msr}$ ).

Furthermore, the IMRT verification plans which were created by the vendor in the installation in order to adjust the beam output were compared.

**Results:** The mean value of the  $D_{w,Q_{msr}}^{f_{msr}}$  was 0.994 Gy  $\pm$  0.013 Gy (range; 0.974 Gy to 1.017 Gy).

The correlation coefficients of the  $D_{w,Q_{msr}}^{f_{msr}}$  and the mean value of percentage errors in the measurement for the IMRT verification were the following; the TomoDirect<sup>TM</sup> without the TomoEDGE<sup>TM</sup> modes, 0.795 (Pearson product-moment correlation,  $p < 0.05$ ); the TomoDirect with the TomoEDGE modes, 0.826 ( $p < 0.001$ ); the TomoHelical<sup>TM</sup> without the TomoEDGE modes, 0.443 ( $p = 0.13$ ); the TomoHelical with the TomoEDGE modes, 0.635 ( $p = 0.13$ ). If the error of the TomoDirect without the TomoEDGE modes in each institution was defined as the systematic error of the beam

output, the modified  $D_{w,Q_{msr}}^{f_{msr}}$  was 0.984 Gy  $\pm$  0.007 Gy (range 0.975 Gy to 0.997 Gy).

The mean errors in the IMRT verification by the TomoDirect mode and the TomoHelical mode, with the TomoEDGE mode, were 0.6% and -0.7%, respectively (Paired t-test,  $p < 0.001$ ). The mean errors in the IMRT verification by the TomoDirect mode and the TomoHelical mode, without the TomoEDGE mode, were 1.2% and 0.2%, respectively ( $p < 0.05$ ).

**Discussion:** Ost et al. reported that the mean static output of the tomotherapy in four institutions was 6.238 Gy  $\pm$  0.058 Gy (one standard deviation; 1 SD) for 60 s at a depth of 10 cm in water and 85 cm SAD[3]. In our results, the mean value of  $D_{w,Q_{msr}}^{f_{msr}}$  in multiple institutions was 0.994 Gy  $\pm$  0.013 Gy (1 SD) for 12 s at a depth of 10 cm in water and 85 cm SSD. If the exposure time and the distance of the measurement are revised by a calculation, our result could be 6.208 [= 0.994  $\times$  5  $\times$  (95 / 85)<sup>2</sup>]. Therefore, our result did not have the major difference in the output as compared with the report.

Our result showed the difference of the error between the measurement in the TomoDirect and the TomoHelical modes. In the current commissioning process, no beam modeling parameter to correct the difference of the error for the measurements between the different mode is exist. In the future, this difference may be canceled by the introduction of a new beam modeling parameter in the treatment planning station, such as the parameter to adjust a fluence of each mode. If the fluence of each mode is modified, the beam output will be able to lead to even.

**Conclusion:** It was evaluated that the variation of the beam output for the tomotherapy in multiple institutions were very low. The beam output is affected by the modes (e.g. TomoHelical); therefore, the beam output will be improved more by the introduction of a parameter for adjusting the fluence of each mode.

### References:

1. Alfonso R, Andreo P, Capote R, et al.: A new formalism for reference dosimetry of small and nonstandard fields, Med Phys. 35(11), 5179-5186, 2008.
2. Standard Dosimetry of Absorbed Dose to Water in External Beam Radiotherapy, 2012.
3. De Ost B, Schaecken B, Vynckier S, et al.: Reference dosimetry for helical tomotherapy: Practical implementation and a multicenter validation, Med Phys. 38(11), 6020-6026, 2011.

## **DEVELOPMENT OF REAL TIME ABDOMINAL COMPRESSION FORCE (ACF) MONITORING SYSTEM**

Tae Ho Kim<sup>1</sup>, Siyong Kim<sup>2</sup>, Dong-Su Kim<sup>1</sup>, Seong-Hee Kang<sup>1</sup>, Min-Seok Cho<sup>1</sup>, Kyeong-Hyun Kim<sup>1</sup>, Dong-Seok Shin<sup>1</sup>, Yu-Yun Noh<sup>1</sup>, Tae-Suk Suh<sup>1</sup>

<sup>1</sup> The Catholic University of Korea College of Medicine Department of Biomedical Engineering, Korea

<sup>2</sup> Department of Radiation Oncology, Virginia Commonwealth University, VA, USA

### **Purpose**

Abdominal compression is known to be effective, but no explicit method exists to quantify abdominal compression force (ACF) and maintain the proper ACF through the whole procedure. In this study, we developed and evaluated a system that both monitors ACF in real time and provides surrogating signal even under compression. The system can also provide visual-biofeedback.

### **Methods**

The system developed consists of a compression plate, an ACF monitoring unit and a visual-biofeedback device. The ACF monitoring unit contains a thin air balloon in the size of compression plate and a gas pressure sensor. The unit is attached to the bottom of the plate thus, placed between the plate and the patient when compression is applied, and detects compression pressure. For reliability test, 3 volunteers were directed to take several different breathing patterns and the ACF variation was compared with the respiratory flow and external respiratory signal to assure that the system provides corresponding behavior.

### **Results**

We could monitor ACF variation in real time and confirmed that the data was correlated with both respiratory flow data and external respiratory signal. Even under abdominal compression, in addition, it was possible to make the subjects successfully follow the guide patterns using the visual biofeedback system.

### **Conclusions**

The developed real time ACF monitoring system was found to be functional as intended and consistent. With the capability of both providing real time surrogating signal under compression and enabling visual-biofeedback, it is considered that the system would improve the quality of respiratory motion management in radiation therapy.

### **Key words**

abdominal compression

## **THE DEVELOPMENT OF SIMPLE METHOD FOR THE PBS BEAM ENERGY CHECK USING FILM BEFORE THE TREATMENT QA**

Sanghyeon Song, Luri Lee, Haksoo Kim, Eun Hee Jeang, Soonki Min, Jong Hwi Jeong, Se Byeong Lee, Yeong Kyeong Lim, Jeonghoon Park, Dongho Shin  
National Cancer Center, South Korea

### **Purpose**

In the PBS technique of the proton therapy, the beam range is very important parameter associated patient treatment directly. However, it is cumbersome and complex to check beam range unlike x-y position. Therefore we tried to develop for the simple method to check beam range which is visually verifiable using the photosensitive film.

### **Methods**

We have used that the dose amount varies depending on the variation of the depth by Bragg Peak curve. Normally, photo sensitivity of film is the highest in the Bragg peak depth area and diminished farther away from Bragg peak depth. Therefore we have made PMMA phantom formed like circular stair with 2 mm gap. it can be visually distinguished photosensitive degree of the film because of such phantom design. If the beam energy is changed the highest photosensitive region position will be changed. Thus, we can check the correct beam energy by using this changes.

### **Results**

The sensitivity difference of the photosensitive degree in the Bragg peak area and others was distinguished by visual observation. And the highest photosensitive position was changed when varied the depth compare with reference depth. It was consistent with the expected results.

### **Conclusions**

We tried to study for the simple beam range check method can be confirmed visually using the film. As the result, we can distinguish varying beam range by confirming degree of photosensitive visually in the film.

### **Key words**

PBS, QA, Beam Range

## INVESTIGATION OF WELL-BALANCED KV X-RAY IMAGING CONDITIONS BETWEEN SKIN DOSE AND IMAGE NOISE

T Nakai<sup>1</sup>, ASawada<sup>2</sup>, HTanabe<sup>3</sup>, MSueoka<sup>3</sup>, STaniuchi<sup>3</sup>, TShiinoki<sup>4</sup>, YIshihara<sup>5</sup>, MKokubo<sup>1,3</sup>

<sup>1</sup>Kobe City Medical Center General Hospital, JP; <sup>2</sup>Kyoto College of Medical Science, JP; <sup>3</sup>Institute of Biomedical Research and Innovation, JP; <sup>4</sup>Yamaguchi Univ., JP; <sup>5</sup>Kyoto Univ.,JP

**Key words:** dynamic tumor tracking, skin dose

**Introduction**In dynamic tumor tracking (DTT) irradiation using Vero4DRT, four dimensional correlation model (4D model) between positions of implanted gold markers and displacement of abdomen is used to predict the target position during beam delivery.[1] 3D positions of gold markers are calculated using 2D positions of markers in two orthogonal kV x-ray images. Therefore, it is of great importance of quantifying skin dose during acquisition of kV x-ray images.[2]On the other hand, image quality of kV x-ray images is greatly dependent on acquisition condition.

The purposes of this study were to estimate the accumulated kV x-ray imaging dose during DTT irradiation using water-equivalent phantoms and to address an analytical skin dose formula for investigating of well-balanced kV x-ray imaging conditions between skin dose and image noise.

**Methods**First, exposure dose to a flat panel detector (FPD) was measured using a single set of kV x-ray tube and FPD, a cylindrical ionization chamber, and water-equivalent phantoms during DTT irradiation. Next, half-value layer of aluminum was measured to estimate the effective energy and absorbed dose conversion factors of soft tissue. Then, the exposure dose to FPD was converted to the skin dose. We estimated imaging dose for six patients who were enrolled in the DTT treatment for lung cancers in our hospital using the system log file. Subsequently, variation of scattered dose to FPD was measured using the water-equivalent phantoms of 0-200 mm in thickness and the ionization chamber rigidly fixed at the midpoint between FPD and isocenter. For both a fully opened field and a field fitted to the whole chamber, the exposure doses to FPD as the amount of ionization were measured with tube voltage of 60, 80, 100, 120 kV. Then, the ratio of the amount of ionization between them was computed as the scattered dose ratio to FPD.

Image noise was computed from FPD images acquired for the fully opened field under a variety of x-ray tube voltage and thickness of the phantoms. The ratio of standard deviation to the mean pixel values within the predetermined region of interest with a size of 128×128 pixels in the FPD images was computed using Image-J as the image noise.

**Results:Skin dose:**From variations of skin dose for a single exposure as a function of x-ray tube current-time product (mAs), it has been observed that linear correlations between tube current-time product and skin doses for each tube voltage were high. Then, skin doses per mAs were calculated as the gradient of the regression lines, resulting in 0.034, 0.078, 0.130, 0.205 mGy for 60, 80, 100, 120 kV,

respectively. The skin dose in this study was a little greater by a factor of 1.4-1.6 than those in the Synergy system. **Scattered dose to FPD:**The difference in scattered dose to FPD for the phantom with the same thickness was insignificant with respect to x-ray tube voltage while the scattered dose to FPD became higher for thicker phantoms. **Image noise:**Image noise described as SD/MEAN of pixel values was linearly decreasing with entrance dose to FPD, independent of the tube voltage.

**Discussion:**Using tube voltage, tube current-time product, exposure time in the log file, and measured skin dose, the accumulated skin dose over DTT course (48Gy/4fr) was estimated for each kV x-ray tube. The average accumulated skin dose of kV x-ray tube #1 and #2 was 0.50 Gy while the maximum accumulated skin dose was 0.93 Gy.

From the acquired data, skin dose,  $D(N, t, v)$  (mGy) was formulated as  $(0.045/N)^{(1/0.479)} / Q_{FPD_{en}/mAs}(t, v) \times D_{/mAs}(v)$ , where  $N, t$  (mm),  $v$  (kV),  $Q_{FPD_{en}/mAs}(t, v)$  (pC), and  $D_{/mAs}(v)$  (mGy) denote image noise in the FPD, phantom thickness, tube voltage, entrance dose to FPD per mAs, and skin dose per mAs, respectively. From the above formula, it was indicated that the skin dose with tube voltage of 120 kV has become lower than that with any other tube voltage in this study.

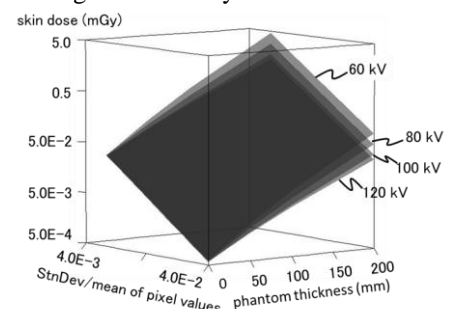


Fig. 1 Simulated skin dose using the above formula.

**Conclusion:**The accumulated skin dose during the dynamic tumor tracking irradiation for lung cancers was estimated as 0.50 Gy. Furthermore, the skin dose in kV x-ray imaging in the Vero4DRT system was described as a function of the image noise, the thickness of the phantom, and the x-ray tube voltage, suggesting that the image noise may be reduced with higher x-ray tube voltage.

### References:

1. N. Mukumoto, et al., "Positional accuracy of novel x-ray-image-based dynamic tumor-tracking irradiation," (2012) Medical Physics, doi: 10.1118/1.4754592
2. J. Valentin, "Radiological Protection in Medicine ICRP Publication 105," (2007) Ann. ICRP 37 -6

Corresponding author email:sawada@kyoto-msc.jp

## **IMPACT OF PHANTOM ROTATION ERROR AND DEGREE OF DOSE GRADIENT ON GAMMA EVALUATION RESULTS**

Kyeong-Hyeon Kim, Dong-Su Kim, Tae-Ho Kim, Seong-Hee Kang, Dong-Seok Shin, Min-Seok Cho, Yu-Yun Noh, Tae Suk Suh

Department of Biomedical Engineering, Research Institute of Biomedical Engineering, College of Medicine, The Catholic University of Korea, Seoul, Republic of Korea

### **Purpose**

A spatial uncertainty induced from phantom set-up inevitably occurs and gamma index that is used to evaluate IMRT plan quality can be affected differently by a combination of the spatial uncertainty and magnitude of dose gradient. In this study, we investigated the impacts of dose gradient and the phantom set-up error on both 2D and 3D gamma evaluation.

### **Methods**

Various dose distributions that have different dose gradients each other were designed to be used as calculation dose data in gamma evaluation, and three dose gradients that were used as measurement dose data were simulated by applying three different rotation errors that were pitch, roll, and yaw angle, to each calculation dose data. Both 2D and 3D gamma evaluation were performed between all of the calculation and measurement dose distributions, and the results of gamma evaluations were sorted according to the magnitude of dose gradient and the error rotation axis.

### **Results**

The 3D gamma showed relatively high tolerance to rotation error compared to 2D gamma. In the case of high dose gradient, both of two gamma evaluations were significantly affected contrary to low gradient case and gamma evaluations in roll angle error had similar results with those in pitch angle.

### **Conclusions**

In this study, we investigated the characteristics of gamma evaluation according to dose gradient and phantom rotation axis. As a result, 3D gamma had better performance than 2D gamma.

### **Key words**

IMRT QA, Gamma Evaluation, Dose Gradient, Phantom Set-up

## **GAMMA ANALYSIS WITH VARIOUS COMMERCIALIZED 2D MEASUREMENT DEPENDENCE ON SPECIFIED LOW-DOSE THRESHOLDS FOR VMAT QA**

Min-Joo Kim<sup>1</sup>, Sang-Won Kang<sup>1</sup>, Jin-Beom Chung<sup>2</sup>, Tae Suk Suh<sup>1</sup>

<sup>1</sup> Dept. of Biomedical Engineering, Research Institute of Biomedical Engineering, The Catholic Univ. of Korea College of Medicine, Korea

<sup>2</sup> Dept. of Radiation Oncology, Seoul National Univ. Bundang Hospital, Korea

### **Purpose**

Better interpretation and universal recommendation about low-dose threshold for gamma analysis was purposed by utilizing various commercialized 2D dosimetry tool as a further study of our previous research.

### **Methods**

A total of 60 VMAT treatment plans—20 head and neck, 20 brain, and 20 prostate cancer cases—were randomly selected from the Varian Eclipse treatment planning system (TPS). Various 2D dosimetry tool (MatrixX, MapCheck and EPID) using 20 cases (head and neck, prostate, brain) was applied. Then, the gamma analysis depending on three acceptance criteria (3%/3 mm, 2%/2 mm, and 1%/1 mm), four different low-dose thresholds (0%, 5%, 10% and 15%), and two normalization methods (Global normalization, Local normalization) was performed using each dosimetry software. Evaluation using percentage change and the significant difference determined by the non-parametric Kruskal-Wallis test and the Mann-Whitney analysis as a posteriori test was performed.

### **Results**

The gamma passing rate (%GP) for the global normalization decreased as the low-dose threshold increased, and all low-dose thresholds led to %GP values above 95% for both the 3%/3 mm and 2%/2 mm criteria.

### **Conclusions**

A close dependence of each 2D measurement tool and the selected low-dose threshold was observed. Our results suggest that detector dependence and the low-dose threshold level for local gamma analysis should be carefully considered for accurate analysis of treatment plan because the patient-specific QA result of the VMAT plan can vary depending on 2D measurement tool and the applied low-dose threshold level.

### **Key words**

Gamma Analysis, VMAT, Patient QA, 2D measurement, Low-dose threshold

## **DOSIMETRY CHARACTERISTICS AND GAMMA PASSING RATE OF ARCCHECK FOR HELICAL TOMOTHERAPY PLAN VERIFICATION**

Chalermchart Bunsong<sup>1</sup>, Imjai Chitapanarux<sup>2</sup>, Somsak Wanwilairat<sup>2</sup>

<sup>1</sup>Chonburi Cancer Hospital, Thailand

<sup>2</sup>Division Of Therapeutic Radiology and Oncology, Faculty of Medicine, ChiangMai University, Thailand

### **Purpose**

To study dosimetry characteristics of ArcCHECK and use to assess the gamma passing rate of Helical tomotherapy treatment planning

### **Methods**

ArcCHECK characteristics are evaluated including short term reproducibility, linearity and longitude profile comparison. Then the ArcCHECK is used to verify treatment planning of 30 patients who were irradiated with Helical Tomotherapy at Maharaj Nakorn Chiang Mai Hospital. The patients diagnosis were nasopharyngeal cancer, prostate cancer and lung cancer which had 10 cases in each group. Define gamma index equal to 3%/3 mm then evaluate the average gamma passing rate of each group. Determine the confidence limits and establish action level for tomotherapy treatment planning in department.

### **Results**

ArcCHECK has short term reproducibility when compare to an ionization chamber measurement is 0.4% with standard deviation 0.12. For linearity the dose measurement increase continuously with slope of a straight line. The longitude profile were measured at central axis and 5 cm jaw width, the profile show good agreement between ArcCHECK and ionization chamber. The average gamma passing rate was 98.40% with standard deviation 2.54 for gamma index 3%/3 mm.

### **Conclusions**

ArcCHECK show good dosimeter efficiency. We suggest the action level for acceptance criteria to evaluate treatment plan for the department is 93.43% passing rate with gamma index 3%/3 mm. Our result similar to the AAPM Task Group 148 which recommend gamma pass rate higher than 90% with gamma index 3%/3 mm for Helical Tomotherapy plan verification.

### **Key words**

Helical Tomotherapy, ArcCHECK, dosimetry characteristics, plan verification.

## **DOSE CALCULATION COMPARISON OF DIFFERENT INHOMOGENEITY PHANTOMS IN LINAC AND COBALT -60 EBRT**

Senthil Kumar<sup>1</sup>, Muthuvelu K<sup>2</sup>

<sup>1</sup> Madurai Medical College, India

<sup>2</sup> Rajiv Gandhi Government General Hospital, India

### **Purpose**

The main purpose of this study was to compare the dose calculation of the different inhomogeneity phantoms in EBRT for LINAC and Cobalt-60 machines.

### **Methods**

Three different type of indigenously developed phantoms PMMA slab phantom, cork slab phantom and water phantom were used for this study. All the phantoms were in same dimension and the dosimetric measurement were done with 0.6cc ion chamber. Ion chamber were inserted in the phantoms and irradiated for different field sizes for the different treatment conditions such as AP treatment, AP-PA treatment, 3 field oblique treatment, 4 filed treatment, Rotation treatment to analyses the dose difference in homogenous and inhomogeneous treatment condition.

### **Results**

Dosimetric measurements were performed using 6MV, 15MV Varian Clinac iX and cobalt-60 machines. The ion chamber measured values were the characteristic of those obtained for a range of field size, inhomogeneity thickness and positions chosen to represent typical geometric encountered in practice. The percentage of deviation for conventional treatment technique was observed for a maximum of 16.7% and minimum of 4.95%.

### **Conclusions**

The number of photons transmitted through Cork Phantom is higher than the Water Phantom and Acrylic Phantom, allowing more photons to reach a greater depth in the Cork Phantom and increasing dose to the chamber beyond the cork. Heterogeneity correction would definitely improve the cancer treatment of the heterogeneity region. This in- house phantom is inexpensive and easy to handle. This is a very reliable tool to measure the dose under heterogeneity condition.

### **Key words**

EBRT, inhomogeneity, Phantom

## Evaluation of correlations between percentage error of field width and error of output in IMRT verification plan for helical tomotherapy

KSasaki<sup>1</sup>, N Kasai<sup>2</sup>, N Yanagisawa<sup>2</sup>,

<sup>1</sup> Gunma Prefectural College of Health Sciences, Graduate School of Radiological Technology, Japan; <sup>2</sup>Aizawa Hospital, Japan

**Key words:** Helical tomotherapy, output test

**Introduction:** Helical tomotherapy is an intensity modulated radiation therapy (IMRT) modality that is capable of delivering highly conformal dose distributions [1]. In helical tomotherapy, radiation is delivered from a 6 MV linear accelerator, with an intensity modulated photon fan beam that rotates on a ring-style gantry, while the patient is simultaneously translated into the bore on a treatment couch. Flynn et al. suggested that linac output variations, for helical tomotherapy, be within  $\pm 2\%$  of the long-term average, for quality assurance purposes [2]. Francois et al. showed differences in static and rotational beam output delivery [3]. Quality assurance (QA) for helical tomotherapy is performed based on AAPM report-148 [4]. Among many QA items, stability of field width is an important item. Therefore, the relationship between the percentage error of field width and output in IMRT verification plan was evaluated.

**Methods:** Output tests, under static condition, and the stability tests of rotational output were performed. We compared variations of this data to a longitudinal profile test, which is a field width test. Furthermore, we changed the field width actively, and evaluated relationships between percentage error of field width and that of IMRT output.

**Results:** Daily change of the IMRT verification plan and static output measurement is shown in Fig.1. A time-course of adjustment of tomotherapy is shown in Table 1. The variation of static output was only 0.4%, whereas the variation of IMRT output was 2%. The correlation between percentage error of field width and error of output in IMRT verification plan is shown in Fig.2. There was a proportional relationship between the error of field width and the error of IMRT output. However, the gradient was different for every field width, and the variation was smaller for a large field width (5 cm). If the error of IMRT output in daily QA testing became larger than 1.4%, the error of field width would exceed 1% at 2.5 cm field width.

On the other hand, enhanced thread effect was present over 2.5% error of field width, but it was thought that the effect on dose distribution would be small.

**Discussion:** Only with quality assurance of output tests under static conditions, may we overlook a small output variation. Also, this may lead to overlooking a variation of field width.

**Conclusion:** In the daily output test of helical tomotherapy, measurement of at least one IMRT verification plan is desirable.

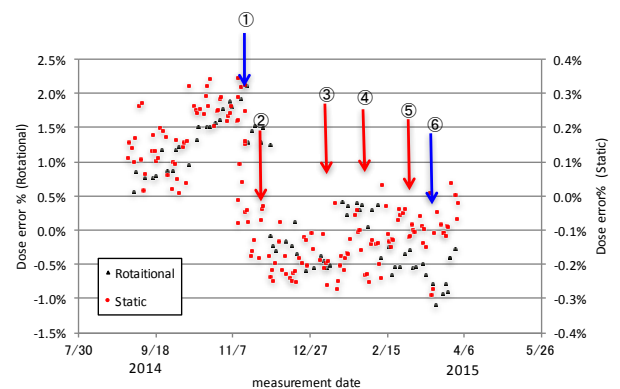


Fig. 1 Rotational and static output variation according to the elapsed time

Table 1 Description of the numbers in Fig.1, time-course of adjustment for tomotherapy

| No. | Date       | adjustment                           |
|-----|------------|--------------------------------------|
| ①   | 16/11/2014 | Error of rotational output exceed 2% |
| ②   | 01/12/2014 | Field width adjustment               |
| ③   | 17/01/2015 | Field width test                     |
| ④   | 11/02/2015 | MLC exchange                         |
| ⑤   | 16/03/2015 | Magnetron exchange                   |
| ⑥   | 28/03/2015 | Output conditioning                  |

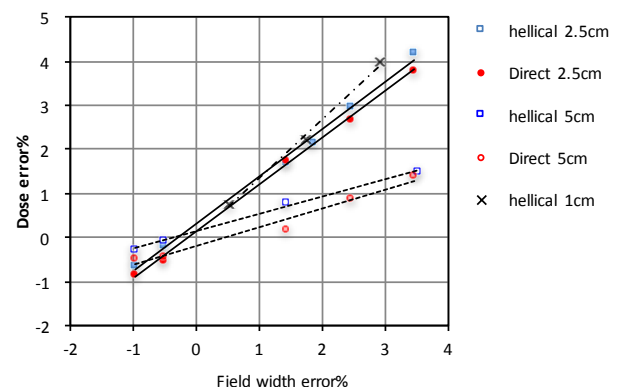


Fig.2 Relationship of field width error and dose error

### References:

1. T R Mackie, et al.: Tomotherapy: a new concept for the delivery of dynamic conformal radiotherapy Med. Phys. 20: 1709–19, 1993
2. Flynn R, et al.: The impact of linac output variations on dose distributions in helical tomotherapy. Phys. Med. Biol. 53: 417–430, 2008
3. Francois P and Mazal A.: Static and rotational output variation of a tomotherapy unit. Med. Phys. 36: 816–820, 2009
4. Katja M, et al.: QA for helical tomotherapy: Report of the AAPM Task Group 148. Med. Phys. 37: 4817–4853, 2010

## MULTI-INSTITUTIONAL QUALITY ASSURANCE ACTIVITY ON LINAC OUTPUT AND TREATMENT PLANNING SYSTEM

Shuichi Ozawa<sup>1</sup>, Minoru Nakao<sup>1</sup>, Fumika Hosono<sup>1</sup>, Kiyoshi Yamada<sup>1</sup>, Tohru Yoshizaki<sup>2</sup>, Yoshimi Morimoto<sup>3</sup>, Hiroshige Nozaki<sup>4</sup>, Kousaku Habara<sup>4</sup>, Daisuke Kawahara<sup>5</sup>, Yusuke Ochi<sup>5</sup>

<sup>1</sup> Hiroshima High-Precision Radiotherapy Cancer Center, Japan

<sup>2</sup> Hiroshima City Hiroshima Citizen Hospital, Japan

<sup>3</sup> Hiroshima Prefectural Hospital, Japan

<sup>4</sup> Hiroshima Red Cross Hospital & Atomic-bomb Survivor Hospital, Japan

<sup>5</sup> Hiroshima University Hospital, Japan

### Purpose

As the first step of multi-institutional quality assurance (QA) activity of regional cooperation group, we started the management of linac output and treatment planning system (TPS) for each institution. This study shows the determination of implementation and tolerance values for each parameter in this activity.

### Methods

Standard excel sheet and the implementation manual for the standard dosimetry protocol (JSMP12) measurement were prepared and sent to each institution. Not only the measured result under reference condition but also each factor for JSMP12 and the absolute dose setting under reference condition on TPS was required to enter in the excel sheet. Based on the accumulated data, tolerance of each parameter was decided. In this activity, measured results were compared to the absolute dose setting on TPS.

### Results

Measurement is required to repeat at least three times, and the tolerance of the coefficient of variation was set within 0.1%. The coefficients used in JSMP12 were allowed within  $1 \pm 0.005$ . Tolerance of beam quality conversion factors are within 0.5 % from the average of multi-institution for each energy with no linac-type dependence. The tolerance of the difference between measurement result and the setting value of TPS was decided within 2%.

### Conclusions

By comparing between the measured value and the absolute dose setting value of the TPS, it enables QA activity with practical conditions. As the next step, this activity is planned to expand the other QA item, for example, evaluation of CT calibration curve on planning system.

### Key words

quality assurance, linac output, standard dosimetry, treatment planning system

## **DOSIMETRY CHARACTERISTICS AND GAMMA PASSING RATE OF ARCCHECK FOR HELICAL TOMOTHERAPY PLAN VERIFICATION**

Chalermchart Bunsong  
Chonburi Cancer Hospital, Thailand

### **Purpose**

To study dosimetry characteristics of ArcCHECK and use to assess the gamma passing rate of Helical tomotherapy treatment planning.

### **Methods**

ArcCHECK characteristics are evaluated including short term reproducibility, linearity and longitude profile comparison. Then the ArcCHECK is used to verify treatment planning of 30 patients who were irradiated with Helical Tomotherapy at Maharaj Nakorn Chiang Mai Hospital. The patients diagnosis were nasopharyngeal cancer, prostate cancer and lung cancer which had 10 cases in each group. Define gamma index equal to 3%/3 mm then evaluate the average gamma passing rate of each group. Determine the confidence limits and establish action level for tomotherapy treatment planning in department.

### **Results**

ArcCHECK has short term reproducibility when compare to an ionization chamber measurement is 0.4% with standard deviation 0.12. For linearity the dose measurement increase continuously with slope of a straight line. The longitude profile were measured at central axis and 5 cm jaw width, the profile show good agreement between ArcCHECK and ionization chamber. The average gamma passing rate was 98.70% with standard deviation 1.76 for gamma index 3%/3 mm.

### **Conclusions**

ArcCHECK show good dosimeter efficiency. We suggest the action level for acceptance criteria to evaluate treatment plan for the department is 95.25% passing rate with gamma index 3%/3 mm. Our result similar to the AAPM Task Group 148 which recommend gamma pass rate higher than 90% with gamma index 3%/3 mm for Helical Tomotherapy plan verification.

### **Key words**

Helical Tomotherapy, ArcCHECK, dosimetry characteristics, plan verification.

## **GAMMA KNIFE RADIOSURGERY FOR INTRAOCULAR TUMOR TECHNIQUE ESTABLISHMENT**

Yi-Chieh Tsai

Taipei Medical University Shuang-Ho Hospital, Taiwan

### **Purpose**

Radiosurgery plays an important role in treating patients with intraocular tumor and retained visual function aiming at organ-conservation. We presented a new treatment protocol using GKRS to treat patient with intraocular tumor and evaluated the safety and precision of GKRS as a primary treatment for intraocular tumor.

### **Methods**

Two patients with uveal melanoma and one patient with breast cancer orbital metastasis treated with the Leksell Gamma Knife® Perfexion stereotactic radiosurgery in our hospital. Retrobulbar anesthesia following fixation of the treated eye by suturing two extraocular muscles to the stereotactic frame were performed in order to immobilize the eye in the whole treatment procedure. The dose to the tumor margin was 25-30Gy prescribed at 50-55% isodose line. CT scans were done after eye fixation, immediate before and after the GKRS to confirm the accuracy of tumor localization. We compared tumor volume, tumor and lens gravity point deviation, and tumor coverage in the 3 sets of CT scans to check the precision of immobilization and eye fixation.

### **Results**

The eye movement analysis revealed that the gravity point coordination deviation of the tumor and lens between CT-1 and CT-2, or CT-1 and CT-3 was less than 0.120mm. At least 95% of the tumor volume was covered by the prescription dose in the 3 sets of CT image.

### **Conclusions**

GKRS using our treatment protocol is a relatively non-invasive, organ-conserving, and less time-consuming single fraction treatment for intraocular tumor. Our eye fixation method reveals high accuracy.

### **Key words**

Leksell Gamma Knife® Perfexion, stereotactic radiosurgery, uveal melanoma, intraocular tumor

## **RADIOTHERAPY DOSE VERIFICATION ON A CUSTOMIZED ACRYLIC (PERSPEX) HEAD AND NECK PHANTOM**

Kae Yann Eng<sup>1</sup>, Sivamany Kandaiya<sup>2</sup>

<sup>1</sup> Ministry of Health, Malaysia

<sup>2</sup> Universiti Sains, Malaysia

### **Purpose**

This research is to verify the measured delivered dose to planned dose in radiotherapy.

### **Methods**

This dose verification procedure was done on a customized acrylic head-and-neck phantom using Gafchromic EBT2 film and metal-oxide-semiconductor-field-effect-transistor (MOSFET). Target volumes (TV) and organs-at-risk (OAR) which were previously contoured by oncologist on selected NPC patient was transferred to this phantom by image fusion procedure. Three radiotherapy plans were done: Plan1 7-field IMRT with prescribed dose 70Gy/33#; Plan2 7-field IMRT plan with 70Gy/35#; and Plan3 mid-plane-dose plan with 66Gy/33#.

### **Results**

The dose maps were first verified using MapCheck2 by SNC-PatientTM software. The passing rates from gamma analysis were 97.7% (Plan1), 93.1% (Plan2) and 100% (Plan3). Percentage difference between TPS calculated dose and MOSFET measured dose was comparatively higher than EBT2. Calculated dose and EBT2 measured dose showed difference of  $< \pm 3\%$  for TV and  $< \pm 10\%$  for OARs. Whereas MOSFET measured dose showed  $< \pm 6\%$  for TV and  $< \pm 10\%$  for OARs. An overdose treatment may occur as TPS calculated doses were lower than the measured doses as overall. This may be due to the effects of leaf leakage, leaf scatter and photon backscatter into the measuring tools (Pawlicki et al., 1999 and Ma et al., 2000). More IMRT plans have to be studied to validate this conclusion. However, the dose measurements were still within the 10% tolerance (AAPM Task Group 119).

### **Conclusions**

In conclusion, both Gafchromic EBT2 film and MOSFET are suitable for use in radiotherapy dosimetry.

### **Key words**

radiotherapy, IMRT, dose verification, MOSFET, EBT 2 film.

## **A MONTE CARLO SIMULATION OF RA-223 IMAGING FOR UNSEALED RADIONUCLIDE THERAPY**

Akihiko Takahashi<sup>1</sup>, Kazuhiko Himuro<sup>1</sup>, Shingo Baba<sup>2</sup>, Masayuki Sasaki<sup>1</sup>

<sup>1</sup>Kyushu University

<sup>2</sup>Kyusyu University Hospital

### **Key words**

Radium-223, Monte Carlo simulation, Radionuclide therapy, Bone scintigraphy

### **Purpose**

Radium-223(Ra-223), an alpha-emitting radionuclide, is used in unsealed radionuclide therapy for metastatic bone tumors. Our purpose is to investigate the feasibility and utility of Ra-223 imaging using an in-house Monte Carlo simulation code.

### **Methods**

A three-dimensional numeric phantom was installed in the simulation code. Ra-223 accumulated in a part of the spine, and 22 gamma rays between 80 and 450 keV were selected as the emitted photons. We also simulated technetium-99m(Tc-99m) imaging under the same conditions and compared the results.

### **Results**

The sensitivities of the three photopeaks were 147 counts per unit of source activity (cps/MBq; photopeak: 84 keV, full width of energy window: 20%), 166 cps/MBq (154 keV, 15%), and 158 cps/MBq (270 keV, 10%) for a low-energy general-purpose (LEGP) collimator, and those for the medium-energy general-purpose (MEGP) collimator were 33 cps/MBq, 13 cps/MBq, and 8.0 cps/MBq, respectively. In the case of Tc-99m, the sensitivity was 55 cps/MBq (141 keV, 20%) for LEGP and 52 cps/MBq for MEGP. The fractions of unscattered photons of the total photons reflecting the image quality were 0.09 (84 keV), 0.03 (154 keV), and 0.02 (270 keV) for the LEGP collimator and 0.41, 0.25, and 0.50 for the MEGP collimator, respectively.

### **Conclusions**

Our simulation study revealed that the most promising scheme for Ra-223 imaging is an 84-keV window using an MEGP collimator. The sensitivity of the photopeaks above 100 keV is too low for Ra-223 imaging.

## Kidney Depth Calculation By Anterior and Posterior Renal Scintigraphy Using Attenuation – Related Techniques

T Sontrapornpol<sup>1</sup>, T Chaiwatanarat<sup>2</sup>, C Kawinhammasak<sup>1</sup>, N Kamklon<sup>1</sup>, R Rattanamonrot<sup>1</sup>

<sup>1</sup>King Chulalongkorn Memorial Hospital, Thailand; <sup>2</sup>Chulalongkorn University, Thailand

**Keywords:** Kidney depth, renal scintigraphy, attenuation-related technique.

**Purpose:** To evaluate the more generalized and practical technique in calculation of kidney depth using the attenuation-related technique.

**Methods:** By using anterior and posterior images of the kidney phantom and known body phantom’s width, the kidney phantom depth is calculated using attenuation-related technique and compared with the actual value. The intra- and inter-operator variations are determined. The technique is applied in 98 patients of age  $32.75 \pm 23.20$  (average  $\pm$  SD) years old, including 30 children and in 68 adults. The kidney depth results(KD-dyn, KD-static)are compared with those using lateral view images measurement(KD-lat) and equation-derived kidney depth values(KD-Tonnesen[1], KD-Emory[2], KD-Itoh[3]).

**Results:** The phantom studies showed no significant intra-operator variations (deviation < 5%,  $p \geq 0.99$ ) and inter-operator variations ( $p = 0.9995$ ). The relationship of calculated kidney phantom depth and the actual value is close to ideal straight line ( $r > 0.99$ ). The studies in patient (Table1-3) show good correlation with other techniques ( $r^2 > 0.8099$ ) and no significant different values of the kidney depth calculated by this technique as compare with lateral view technique ( $p = 0.4414$ ). However, when compared with equation-derived values, there is no significant difference in the adult patients only, but significant difference in pediatric patients.

**Conclusion:** The kidney depth calculation using this technique is accurate, practical and can be used in most patient groups.

**References:**

1. Tonnesen KH, Munck O, Hald T, Mogensen P & Wolf H, 1974. Influence of the renogram of variation in skin to kidney distance and the clinical importance hereof.Presented at the Internation Symposium Radionuclides in Nephrology, Berlin.Cited by Schlegel JU &Hamway SA, 1976.Individual renal plasma flow determination in 2 minutes.J Urol, 116, 282-5.
2. Taylor A. Formulas to estimate renal depth in adults. J Nucl Med 1994;35:2054-5.
3. Itoh K, Arakawa M, Re-estimation of renal function with 99mTc-DTPA by the Gates' method. Kakuigaku 1987;24:389-96.

Table 1 shows means (cm), SD (cm) of kidney depths by each technique and the result of ANOVA or pair t-test for each technique comparison in all patients.

| KD method   | KD-dyn         | KD-static      | KD-lat         | KD-Tonnesen   | KD-Emory      | KD-Itoh |
|-------------|----------------|----------------|----------------|---------------|---------------|---------|
| Mean(cm)    | 5.5706         | 5.7675         | 5.7972         | 4.8991        | 5.3254        | 5.8888  |
| SD(cm)      | 1.9659         | 1.9096         | 1.7505         | 1.6599        | 2.3948        | 1.8018  |
| KD-static   | 0.9527<br>SNSD |                |                |               |               |         |
| KD-lat      | 0.9590<br>SNSD | 0.9419<br>SNSD |                |               |               |         |
| KD-Tonnesen | 0.9277<br>SSD  | 0.8999<br>SSD  | 0.9422<br>SSD  |               |               |         |
| KD-Emory    | 0.9254<br>SNSD | 0.9003<br>SSD  | 0.9320<br>SSD  | 0.9778<br>SSD |               |         |
| KD-Itoh     | 0.9302<br>SSD  | 0.9049<br>SNSD | 0.9418<br>SNSD | 0.9969<br>SSD | 0.9854<br>SSD |         |

SSD = statistically significant different at 0.05 level

SNSD = statistically not significant different at 0.05 level

Table 2 shows means (cm), SD (cm) of kidney depths by each technique and the result of ANOVA or pair t-test for each technique comparison in adult patients.

| KD method   | KD-dyn         | KD-static      | KD-lat         | KD-Tonnesen   | KD-Emory       | KD-Itoh |
|-------------|----------------|----------------|----------------|---------------|----------------|---------|
| Mean(cm)    | 6.5532         | 6.6721         | 6.6486         | 5.7707        | 6.6712         | 6.8525  |
| SD(cm)      | 1.2511         | 1.2475         | 1.1453         | 0.9773        | 1.1817         | 0.9663  |
| KD-static   | 0.8942<br>SNSD |                |                |               |                |         |
| KD-lat      | 0.8094<br>SNSD | 0.8703<br>SNSD |                |               |                |         |
| KD-Tonnesen | 0.9108<br>SSD  | 0.7476<br>SSD  | 0.8417<br>SSD  |               |                |         |
| KD-Emory    | 0.7932<br>SNSD | 0.7593<br>SNSD | 0.8393<br>SNSD | 0.9413<br>SSD |                |         |
| KD-Itoh     | 0.8063<br>SSD  | 0.7614<br>SNSD | 0.8453<br>SNSD | 0.9968<br>SSD | 0.9516<br>SNSD |         |

SSD = statistically significant different at 0.05 level

SNSD = statistically not significant different at 0.05 level

Table 3 shows means (cm), SD (cm) of kidney depths by each technique and the result of ANOVA or pair t-test for each technique comparison in pediatric patients.

| KD method   | KD-dyn        | KD-static      | KD-lat         | KD-Tonnesen   | KD-Emory      | KD-Itoh |
|-------------|---------------|----------------|----------------|---------------|---------------|---------|
| Mean(cm)    | 3.2774        | 3.8011         | 3.9364         | 2.8900        | 2.2235        | 3.6663  |
| SD(cm)      | 1.5548        | 1.5449         | 1.3022         | 1.0513        | 1.3784        | 1.2179  |
| KD-static   | 0.9108<br>SSD |                |                |               |               |         |
| KD-lat      | 0.9001<br>SSD | 0.8892<br>SNSD |                |               |               |         |
| KD-Tonnesen | 0.8732<br>SSD | 0.8336<br>SSD  | 0.9187<br>SSD  |               |               |         |
| KD-Emory    | 0.8641<br>SSD | 0.8411<br>SSD  | 0.8935<br>SSD  | 0.9539<br>SSD |               |         |
| KD-Itoh     | 0.8641<br>SSD | 0.8346<br>SNSD | 0.9135<br>SNSD | 0.9925<br>SSD | 0.9775<br>SSD |         |

SSD = statistically significant different at 0.05 level

SNSD = statistically not significant different at 0.05 level

## **THE EFFECT OF GEOMETRY ON THE MEASUREMENT OF AN ALPHA EMITTER RADIONUCLIDE, RADIUM-223**

Kittiphong Thongklam, Putthiporn Chareonphun

Division of Nuclear Medicine, Department of Diagnostic and Therapeutic Radiology, Faculty of Medicine Ramathibodi Hospital, Mahidol University, Thailand

### **Key words**

Radium-223, alpha emitter, geometry, dose calibrator, radionuclide therapy

### **Purpose**

Aims of this work are to investigate the influence of geometry on the measurement of Ra-223 and to receive suitable calibration factor for routinely use.

### **Methods**

Whole vial of Ra-223 was used to set up the initial calibration factor with decay correction at the time of measurement. The 1.0, 2.0, 3.0, 4.0 and 5.0 ml of Ra-223 solution was exactly dispensed into 5 ml syringe. Then the activity in filled syringe was measured with initial calibration factor and adjusted factors which were accordance with the actual activity calculation. Percentage of differences between measured activities with initial factor and adjusted factors of each volume was compared. Statistical significances were analysed by using pair T-test.

### **Results**

Initial dial factor of Ra-223 in the vial was 16.9 in Biodex and 269 in Capintec. The specific dial factors of 1.0, 2.0, 3.0, 4.0 and 5.0 ml were 13.5, 15.6, 15.7, 16.1 and 17.0 for Biodex and 350, 300, 295, 290, 269 for Capintec, respectively. The significant differences between measured activities of 1.0 to 4.0 ml but not in 5 ml Ra-223 solutions both in Biodex and Capintec dose calibrator were observed.

### **Conclusions**

The effect of geometry to the measurement of Ra-223 significantly occurred at the lower volume. In order to obtain accurate doses of Ra-223 used with the patients, appropriate calibration factor should be applied in specific volume especially with the small volume of Ra-223.

## **EVALUATION OF <sup>99m</sup>Tc IMAGE QUANTIFICATION USING ANTHROPOMORPHIC PHANTOMS FOR ESTABLISHING DOSIMETRY PROTOCOL IN INDONESIA**

Nur Rahmah Hidayati<sup>1</sup>, Diah Shanti Utaminingtiyas<sup>2</sup>, Djohan A.E Noor<sup>3</sup>, Prasetya Widodo<sup>4</sup>

<sup>1</sup>Center for Radiation Safety Technology and Metrology, Indonesia

<sup>2</sup>Magister Program of Physics, Brawijaya University, Indonesia

<sup>3</sup>Faculty of Mathematics and Science, Brawijaya University, Indonesia

<sup>4</sup>Center for Radiation Safety and Metrology Technology BATAN, Indonesia

### **Key words**

Anthropomorphic phantoms, Image quantification, Dosimetry protocol, MIRD 16

### **Purpose**

The authors aim to evaluate <sup>99m</sup>Tc image quantification using anthropomorphic phantoms regarding the need of standardization in internal dosimetry protocol in Indonesia and assess the technical aspects which is needed for developing the protocol. The comparison between measured activities in syringes and in the images are presented

### **Methods**

A series of anthropomorphic phantoms, which are kidneys, liver, bladder and heart, are constructed from a resin and being placed into a torso phantom which is filled with water. A pair of anterior and posterior images then were acquired from planar gamma camera images. Other parameters also are needed for supporting the image quantification process, namely the sensitivity factors and attenuation coefficient for <sup>99m</sup>Tc into the resin. With MIRD 16 method, all parameters were used for investigating the activity in the organs which has been acquired through the images

### **Results**

The results show that the activity of <sup>99m</sup>Tc in phantoms has been found less than the result from dose calibrator. The difference activities were varied, respectively, right and left kidney, liver, bladder and heart, at about 4.17%, 5.5%, 6.43%, 15.54%, and 18.74 %. Other previous studies have shown that the result of this study has less value difference.

### **Conclusions**

The authors have demonstrated the ability of the phantoms to be utilized for establishing dosimetry protocol using gamma camera planar images. The similar studies need to be done with other radionuclides to get more comprehensive results.

## **POINT-SPREAD-FUNCTION MODEL IMPROVED DETECTABILITY OF SUB-CENTIMETER HOT LESIONS USING CLINICAL PET/CT DEVICE**

Naoki Hashimoto<sup>1</sup>, Keishin Morita<sup>1</sup>, Yuji Tsutsui<sup>2</sup>, Kazuhiko Himuro<sup>3</sup>, Shingo Baba<sup>3</sup>, Masayuki Sasaki<sup>4</sup>

<sup>1</sup>Department of Health Sciences, Graduate School of Medical Sciences, Kyushu University, Japan

<sup>2</sup>Department of Radiology, Kyushu University Hospital and Department of Health Sciences, Graduate School of Medical Sciences, Kyushu University

<sup>3</sup>Department of Radiology, Kyushu University Hospital

<sup>4</sup>Department of Radiology, faculty of Medicine Kyushu University

### **Key words**

PET/CT, point-spread-function, sub-centimeter sphere

### **Purpose**

The aim of this study was to investigate the effect of the point-spread-function (PSF) correction on the detectability of sub-centimeter hot lesions using clinical PET/CT device.

### **Methods**

We used a Biograph mCT device to image a NEMA body phantom consisting six small spheres (inner diameters: 4, 5, 6, 8, 10 and 37 mm) containing 18F solution. The target-to-background ration of radioactivity was 8. The PET data acquired for 5 minutes were reconstructed using OSEM and OSEM+PSF with the voxel size of 2×2×2mm (2mm voxel) and 4×4×4mm (4mm voxel). The image quality was evaluated by visual assessment and by physical assessment of detectability index (DI) and recovery coefficients (RC).

### **Results**

By visual assessment, the 8-mm sphere was detected on images acquired for 5 minutes with 2-mm voxel reconstruction with OSEM+PSF, while 10-mm sphere with 4-mm voxel reconstruction. By physical assessment, the detectability of images between 6-mm sphere and 10-mm sphere with using OSEM+PSF was superior to those with OSEM on both 2-mm voxel and 4-mm voxel.

### **Conclusions**

The PSF model was proved to improve the detectability of sub-centimeter hot lesions in clinical PET/CT device.

## **RADIOEMBOLIZATION WITH SAMARIUM-153 MICROPARTICLES: A DOSIMETRIC STUDY**

Nurul Ab. Aziz Hashikin<sup>1</sup>, Chai-Hong Yeong<sup>1</sup>, Susanna Guatelli<sup>2</sup>,  
Basri Johan Jeet Abdullah<sup>1</sup>, Kwan-Hoong Ng<sup>1</sup>, Alessandra Malaroda<sup>2</sup>,  
Anatoly B. Rosenfeld<sup>2</sup>, Alan Christopher Perkins<sup>3</sup>

<sup>1</sup>Department of Biomedical Imaging, Faculty of Medicine, University of Malaya

<sup>2</sup>Centre for Medical Radiation Physics, Faculty of Engineering and Information Sciences, University of Wollongong

<sup>3</sup>Medical Physics and Clinical Engineering, Medical School, University of Nottingham

### **Key words**

153Sm-microparticles; Radioembolization, Geant4 Monte Carlo; Hepatocellular carcinoma

### **Purpose**

To study the dosimetry of 153Sm-microparticles for its feasibility in radioembolization as alternative to 90Y-microspheres

### **Methods**

MIRD-5 hermaphrodite phantom with various tumour involvements (TI), tumour-to-normal liver uptake ratio (T/N) and lung shunting (LS) were simulated using Geant4 Monte Carlo toolkit.  $10^7$  histories (correspond to 41.6Bq of 153Sm) were generated for each scenario to obtain the absorbed dose per activity (Gy.GBq-1) to the tumour, normal liver, lungs and other organs. These values were later integrated into an interactive excel spreadsheet. Using the spreadsheet, the highest possible tumour dose, DT were estimated by manipulating the administered activity so that the maximum dose to normal liver, DNL or lungs, DL (70 or 30Gy, respectively) were not exceeded. The corresponding dose to the other organs was evaluated for overexposure from gamma radiation. The results were compared with that of 90Y-microspheres using the partition model (PM) estimation.

### **Results**

Radioembolization with 153Sm-microparticles requires activities of approximately 4.42–4.60 fold higher than 90Y- microspheres. For smaller TI, 153Sm was able to deliver higher DT than 90Y, however for larger TI, opposite results were observed. For similar DT, 153Sm contributes to lower DNL but higher DL than 90Y. Organ absorbed doses by 153Sm were significantly larger than 90Y, however were far below 1Gy.

### **Conclusions**

153Sm-microparticles have shown to be feasible for radioembolization as alternative to 90Y-microspheres, as it able to deliver comparable DT, with lower DNL, slightly higher DL, and other organ doses far below 1Gy.

## **PREGNANCY POST RADIOIODINE I-131 ADMINISTRATION IN PENANG HOSPITAL**

Norsuraya Abdul Jabbar, Fatin Nadhirah A. Halim, Mohd Hizwan Mohd Yahya, Alex Khoo Cheen Hoe, Fadzilah Hamzah

Nuclear Medicine Penang Hospital, Malaysia

### **Purpose**

The aim of this study was to determine the prevalence of pregnancy post radioiodine I-131 administration for thyroid cancer in Malaysia.

### **Methods**

The data of all childbearing women receiving radioiodine treatment was collected from 2nd January 2011 until 31st March 2016. The interval between the last radioiodine administration (ranging from 5mCi to 200mCi) and conception ranged from day 16 to day 162 with the median of 56.4 days. Internal radiation dose calculations were done using ICRP 53 as the reference.

### **Results**

Total of 415 women patients, age ranging from 16 to 49 years old had undergone radioiodine administration. There were 10 patients (2.4%) becoming pregnant after receiving radioactive I-131 administration. For the 10 patients, the calculated absorbed doses were lower than the recommendation limit for termination of pregnancy. All the pregnant patients had uneventful pregnancies and delivered healthy babies with no congenital anomalies.

### **Conclusions**

Radioiodine administration up to 200mCi showed no untoward effects on pregnancies. However, larger studies are needed to confirm these findings.

## **COMPARISON OF ANALOG GEIGER MULLER AND IONIZATION CHAMBER FOR MEASURING EXPOSURE RATE IN RADIOACTIVE IODINE-131 THERAPY PATIENTS**

Fatin Nadhirah A Halim, Norsuraya Abdul Jabbar, Alex Khoo Cheen Hoe, Mohd Hizwan Mohd Yahya, Fadzilah Hamzah

Nuclear Medicine, Penang Hospital, Malaysia

### **Key words**

Analog Geiger Muller counter, Ionization Chamber counter, Iodine-131 therapy

### **Purpose**

The study aims to determine if Ionization Chamber (IC) counter can be used as an alternative to analog Geiger Muller (GM) counter for measuring exposure rate.

### **Methods**

A total of 62 patients receiving radioiodine therapy ranging 80 mCi to 200 mCi from 2nd January to 31st May 2016 were measured using analog GM and IC counter. The measurements were made on the skin surface and at 1 meter from patients at immediate, 1, 24, 48, 72 and 92 hours after Iodine-131 ingestion.

### **Results**

The analog GM counter was not able to measure the surface exposure rate from the first one hour until 48 hours of measurement whereas IC counter could. Thus comparisons for radiation exposure rate were made for measurements performed at 1 meter from patient. Paired T-test showed no significant difference between analog GM and IC counter ( $< 0.05$ ).

### **Conclusions**

Analog GM counters is not recommended for surface exposure rate measurement before 48 hours. Both analog GM and IC counter can be used for measuring patient exposure rate at 1 meter. IC counter is as good as analog GM counter in measurement of exposure rate Iodine-131 therapy patients.

## **SIMULATION STUDY ON A HIGH-RESOLUTION LYSO SCINTILLATION GAMMA CAMERA SYSTEM USING SINGLE-PINHOLE COLLIMATOR**

Youngjin Lee<sup>1</sup>, Se Young Bae<sup>1</sup>, Hee-Joung Kim<sup>2</sup>

<sup>1</sup>Eulji University, Republic of Korea

<sup>2</sup>Yonsei University

### **Key words**

Nuclear medicine, Gamma camera system, LYSO scintillation detector, Pinhole collimator

### **Purpose**

The purpose of this study was to design an optimized pinhole collimator to achieve appropriate sensitivity and spatial resolution in gamma camera system using LYSO scintillation detector.

### **Methods**

To evaluate image performances of proposed system, the sensitivity and spatial resolution were estimated. Both the sensitivity and spatial resolution were estimated when the pinhole diameter was varied from 0.2 to 2 mm by 0.2 mm increment at step for each magnification factor of 2, 3 and 6. Then, we plotted trade-off curves that express the relationship of sensitivity and spatial resolution to optimize collimator design with respect to the pinhole diameters and magnification factors. Finally, to confirm overall image performance, a hot-rod phantom was designed and acquired.

### **Results**

Compared to trade-off curves, regardless of changes in magnification factor, we found that the optimal pinhole diameter was approximately 1.4 mm. According to the phantom results, we found that the 0.5 mm rods were certainly resolved when magnification factor and the pinhole diameter were 6 and 0.2, respectively. Also, we found that the spatial resolution corresponds to between our proposed system and phantom image.

### **Conclusions**

In conclusion, we demonstrated optimum conditions of pinhole collimator with LYSO scintillation detector.

## **USING SIX DEGREES OF FREEDOM MOTION INFORMATION TO CORRECT MOTION INDUCED RECONSTRUCTED SPECT DATA WITH ALGORITHM**

Md. Nahid Hossain<sup>1</sup>, Kamila Afroj Quadir<sup>2</sup>, Adnan Kiber<sup>3</sup>, Roger Fulton<sup>4</sup>

<sup>1</sup>National Institute of Nuclear Medicine & Allied Sciences (NINMAS), Bangladesh Atomic Energy Commission (BAEC), Bangladesh

<sup>2</sup>Bio-Science Division, Bangladesh Atomic Energy Commission

<sup>3</sup>Department of Electrical & Electronic Engineering, University of Dhaka

<sup>4</sup>Department of Medical Physics, Westmead Hospital, Australia

### **Key words**

SPECT, Six degrees of freedom, Reconstructed data

### **Purpose**

In a SPECT study, the data acquisition is performed over a relatively long time. For longer period patient movement frequently occurs in clinical procedure. This movement causes misalignment of the projection frames, which degrades the image quality. In this work, six degrees of freedom (dof) motion information was used to correct motion induced reconstructed SPECT data with developed algorithm.

### **Methods**

Different data without motion were acquired by using a Trionix Triad triple-head SPECT camera and a Hoffman 3D brain phantom. The simulated data was produced by adding partial projection data to produce a new data set so that it simulates motion induced data. From two data set motion information could be estimated. Estimated six dof motion parameters were converted to a transformation matrix by using developed algorithm. After that the transformation was applied to the reconstructed data for correcting motion using another developed algorithm.

### **Results**

Estimating the six dof motion parameters; it was converted to a transformation matrix. A 4x4 transformation matrix was produced. This transformation was applied to the reconstructed data for correcting motion. After correcting motion the reconstructed image was shown with motion free.

### **Conclusions**

The field of motion detection and correction in SPECT is very open to future novel ideas especially software based improvement of motion estimation, characterization and compensation. The simulated data is very essential for examining the algorithm base methods.

## ***CONTRIBUTION OF HIGH RESOLUTION TRANSMISSION ELECTRON MICROSCOPY TO THE CHARACTERIZATION OF URINARY STONES***

Yuni Warty, Herman Herman, Freddy Haryanto

Institut Teknologi Bandung, Indonesia

**Key words:** Urinary stones, High resolution transmission electron microscopy

### **Purpose**

Urolithiasis is urinary tract disease that continues to increase globally. Location, depth and size of urinary stones depend on the composition. This study aimed to analyse characterization of microcrystalline in urinary stones.

### **Methods**

The stones collected from some patients with stones after surgery. Stones samples washed with distilled water and dried for one week at room temperature. Further, sample mixed ground in mortar to get fine powdered samples. Images analysis method used to analysis HR-TEM images

### **Results**

HR-TEM is the most detail tool that used to decide particle size and place of atoms in the sample. The detailed result of this study will be present in the meeting.

### **Conclusions**

HR-TEM can used to determine the particle size, morphology and crystal structure of urinary stones.

## DEVELOPMENT OF PET GAMMA-RAY DETECTORS WITH HIGH TIME RESOLUTION

A Kobayashi<sup>1</sup>, H Hiroshi, N Kaneko, HKawai<sup>1</sup>

<sup>1</sup>Graduate school of Science, Chiba University

**Key words:** PET gamma-ray detector, Plate scintillator, High time resolution, Silicon PMs

**Introduction** We are developing the hole-body PET detector with high position resolution (1mm) and low cost (\$3M). Scintillator plates, Wave Length Sifting Fibers and Silicon PMs are used. Fig.1 shows a structure of our detector. The size of each scintillator plate is 34 mm times 34 mm times 1 mm. In order to measure the incident position of gamma-ray, 160 Wavelength Shifting Fibers cover each 34 mm times 34 mm surface of each plate and all ends of each fiber are connected to SiPMs. To measure the energy and time of incident gamma-ray, SiPMs are attached on each side surface. We have already confirmed that this detector have the position resolution 1mm[1]. In this work, time resolution of our PET detector is measured.

**Methods** We made two detectors. These two are same detectors and these are consist of scintillator plate (34 mm times 34 mm times 1 mm), PMT attached on surface and 8 Silicon PMs (attached on each side surface). Fig.2 shows the setup of an experiment. When two 511keV gamma-rays from <sup>22</sup>Na incident scintillator, its deposit energy are measured by PMTs and its time is measured by SiPMs. We evaluate deference of time of each detector in the event of both of deposit energies are 511keV.

**Results:** At the preliminary experiments, we used 8 silicon PMs. The time resolution of each measurement is 300ps (RMS). The resolution of the average value of 8 silicon PMs is 110ps.

**Discussion:** It is well known that the resolution of the average value is inversely proportional to the square root of N, where N means a number of datas.

**Conclusion:** We will show that our gamma-ray detectors have the time resolution of 110ps.

**References:**

1. N.NAOMI, et al., Advancements in Nuclear Instrumentation Measurement Methods and their Applications, 220, Apr. 20-24 2015, Lisbon Convention Center, Portugal

**Corresponding author email:** koba@hepburn.s.chiba-u.ac.jp

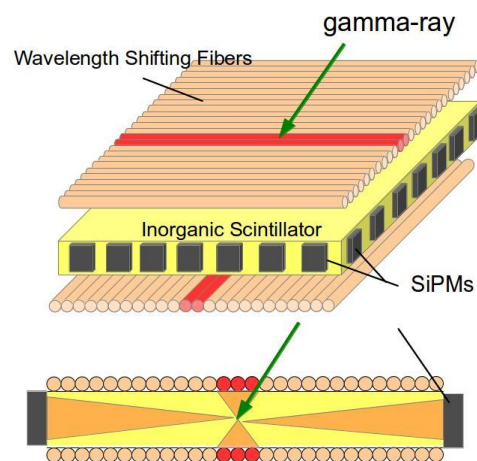


Fig.1 This figure is structure of our detector.

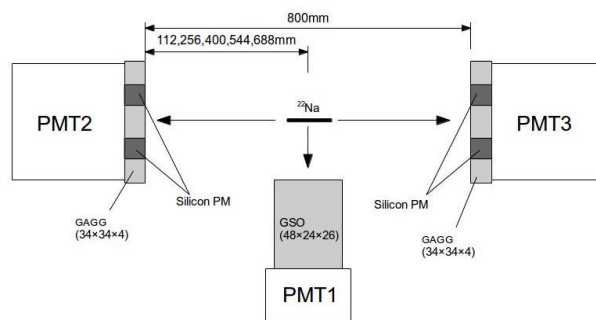


Fig.2 This figure is setup of an experiment.

## Development of gamma-detectors for PET with position resolution of 0.5mm

Y Emoto, K Fujihara, H Kawai, H Ito, N Kaneko, S Kimura, A Kobayashi, T Mizuno

Graduate School & Faculty of Science, Chiba University, Japan

**Key words:** PET, gamma-detector

**Introduction** In the conventional way of gamma imaging by PET, only photoelectric absorption events are used as the data and Compton scattering events are ignored. If you could completely distinguish photoelectric absorption events from Compton scattering events which occurred in the detectors, you will typically observe 5 events/mm<sup>3</sup> as the background and 10 events/mm<sup>3</sup> as the detection of cancer. It's not sufficient data for making the position resolution smaller than 1mm.

We are developing the gamma-ray detectors for detecting Compton events.

**Methods** We use plate-like(34mm×34mm× thickness of 3mm) GAGG scintillators of which sheets of wavelength-shifting fibers(Φ0.2mm) are attached on the top and bottom surfaces and 10 SiPM modules (3mm×3mm) are attached on each lateral side(Fig.1).We are evaluating the performance of this detector with the sodium-22 sealed gamma-sources. We also evaluated the performance of this detector using numerical calculation tool Geant4.

**Results:** 80% of the Compton scattering events in the detector were correctly determined as the Compton events. 50% of those events were determined the first Compton scattering position with the reliability of 95% despite Compton scattering would occur several times in one Compton event.

**Discussion:** See "Fig.2". This shows the result of our simulation by Geant4. When 10<sup>7</sup> positrons are created by radioactive decay of the ingredient of PET Drugs and the positrons caused the annihilation, how many times can we observe the pair of gamma rays? In "Fig.2", "double\_photoele" means the events which two gamma rays caused the photoelectric absorption in the detector. "double\_Comp(good)" means the events which two gamma rays caused the Compton scattering, but the first scattering positions are identified with 100% reliability because of the energy deposit. "photoele\_and\_Comp(good)" means the events which one gamma ray caused the photoelectric absorption and another gamma ray caused Compton scattering and the first scattering position is identified with 100% reliability. Generally, if the energy deposit was more than 340keV(=the Compton edge for 511keV gamma ray), it means that the photoelectric absorption has occurred at that position. Thus, in such case, first scattering position is identified with 100% reliability. So, the graph means that if we use the Compton events, we can observe the positron annihilation events at least 1.6 times as many as the events observed by conventional way of gamma imaging by PET which only uses photoelectric absorption events.

In the Compton events, most of the time the angle of the scattering is shallow. Considering it, the first scattering

position is inferred with 95% reliability in the events which are five times as many as the photoelectric absorption events.

**Conclusion:** When this detectors come into use for the PET devices, if energy threshold 426keV, you can observe 5 events/mm<sup>3</sup> as the background and 50 events/mm<sup>3</sup> as the detection of cancer. if energy threshold is 494keV, you can observe 2.5 events/mm<sup>3</sup> as the background and 40 events/mm<sup>3</sup> as the detection of cancer, and sufficient data can be acquired for making the position resolution 0.5mm.

**Corresponding author email:** yusaku\_emoto@hepburn.s.chiba-u.ac.jp

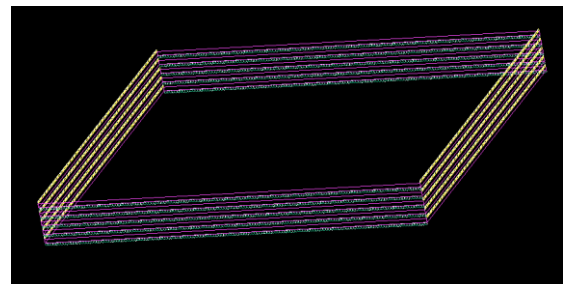


Fig.1 The image of our detectors.

In this illustration, the SiPM modules are not drawn. Five layers of GAGG scintillators and wavelength-shifting fibers are lined up in this illustration, but we may need eight layers or ten layers for getting sufficient data.

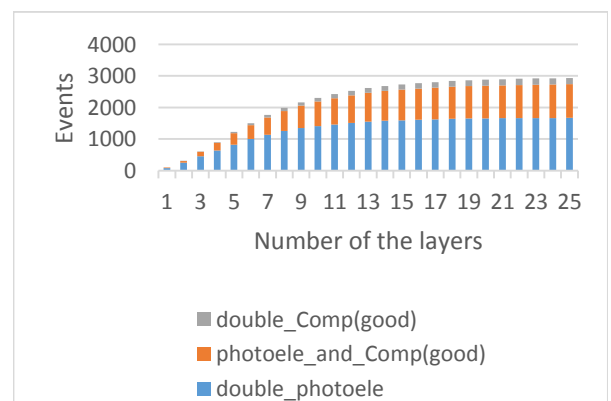


Fig2. Number of Compton events and photoelectron absorption events

## **DEVELOPMENT OF WHOLE-BODY PET SYSTEM WITH 3 MM RESOLUTION AND 1M\$**

Kento Fujihara, Yusaku Emoto, Hiroshi Ito, Naomi Kaneko, Hideyuki Kawai, Shota Kimura, Atsushi Kobayashi, Takahiro Mizuno

Chiba University, Japan

**Key words:** sintered-scintillator, PET, wavelength shifting fiber

### **Purpose**

We are developing low-cost gamma-ray detectors with plate-like sintered scintillator and Wavelength shifting fiber (WLSF) for whole-body PET system. This system will discover cancer with a diameter of 3 mm or more.

### **Methods**

We developed gamma-ray detectors. The effective area of the detector is 300 by 300 square mm. The detector consists of 20-30 layers. One layer consist of GAGG sintered scintillator of 1 mm thickness. Top and bottom surface of scintillator are covered by dual sheets of WLSF with a diameter of 0.2 mm. We measured the performance of this detector with Sodium-22 gamma-ray source.

### **Results**

We measured about 100 photoelectrons in 511 keV gamma-ray photoelectric absorption. Position resolution in photoelectric absorption was 0.2 mm, and minimum distance that this detector can recognize plural emission in Compton scattering was 1 mm.

### **Conclusions**

In PET, discernment of Compton scattering is essence of position resolution. We expect that whole-body PET system with this detector diagnose cancer with a diameter of 3 mm or more. Material cost of this system is, 0.2M\$ for sintered-scintillators, 0.03M\$ for WLSF, 0.03M\$ for 600 units of 6 by 6 mm SiPM's, 0.12M\$ for 12000 units of 1 by 1 mm SiPM's, and 0.09M\$ for 1800 channel of signal read-out circuits.

## HYBRID ASSESSMENT OF GADOPENTETIC ACID AND BONE STRUCTURE WITH ULTRASHORT ECHO TIME IMAGING

Y Kanazawa<sup>1</sup>, Y Matsumoto<sup>1</sup>, N Ikemitsu<sup>1</sup>, T Sasaki<sup>1</sup>,  
H Hayashi<sup>1</sup>, K Takegami<sup>2</sup>, T Matsuda<sup>3</sup>, M Harada<sup>1</sup>

<sup>1</sup>Tokushima University, Japan; <sup>2</sup>Yamaguchi University Hospital, Japan;  
<sup>3</sup>GE Healthcare Japan Corp., Japan

**Key words:** magnetic resonance image (MRI), ultrashort echo time (UTE), quantitative susceptibility map (QSM)

**Introduction:** Ultrashort echo time (UTE) magnetic resonance imaging (MRI) makes it possible to detect water proton existence in bone; also in collagenous connective tissues such as articular cartilage, tendon, ligaments, and bone, it has been proven to be effective [1]. In the near future, UTE imaging is expected to be useful in the diagnosis of bone tumors. The evaluation of activity for bone tumors has generally been performed using contrast-enhanced (CE)  $T_1$  weighted MRI with fat-suppression [2]. However, an evaluation of the effect of gadopentetic acid (Gd-DTPA) in CE-MRI with UTE could not be carried out in detail. In this study, to clarify the phase cycles of Gd-DTPA in UTE imaging, we evaluated the quantitative susceptibility map (QSM) for UTE imaging in a phantom experiment.

**Methods:** On a 3.0 T MR system (Discovery MR 750 3.0 T, GE Healthcare, Waukesha, WI, USA), we performed a phantom study using a three-dimensional dual UTE sequence, with an eight channel phased array HNS coil (as a receiver). The imaging parameters were 32  $\mu$ s and 3.2 ms dual TE, 40 ms repetition time, 12-degree flip angle,  $\pm 62.5$  kHz band width,  $256 \times 256$ , slice thickness 5.0 mm, 24 slices per slab. The imaging data for magnitude and phase images were acquired. The phantom components were made from different concentrations of a Gd-DTPA solution (0.1, 0.5, and 1 wt%) and calcium carbonate ( $\text{CaCO}_3$ ) sections (see Fig. 1). The samples were placed in pure water in an Acrylic case. Next, morphology enabled dipole inversion (MEDI) for QSM algorithm was applied to the dual UTE images; data procedures were Laplacian-based phase unwrapping, and projection onto dipole fields (PDF) for back ground removal [3]. Then, we set the region-of-interest (ROI) for each material section of the phantom on QSM images, and measured susceptibility values. The QSM

calculation and all data analysis were performed on MATLAB 2015b (Mathworks Inc., Natick, MA, USA).

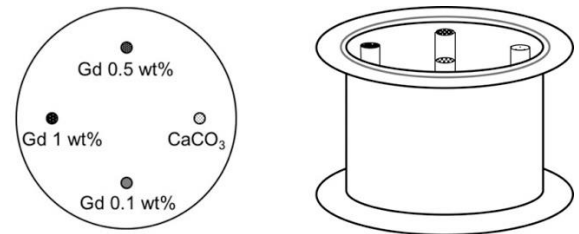


Fig.1 Schematic diagram of phantom component.

Table 1 The mean susceptibility values of each material obtained in the phantom.

| Imaging data for QSM calculation | Mean susceptibility (ppm) |                 |                 |                 |
|----------------------------------|---------------------------|-----------------|-----------------|-----------------|
|                                  | $\text{CaCO}_3$           | Gd-DTPA 0.1 wt% | Gd-DTPA 0.5 wt% | Gd-DTPA 1.0 wt% |
| 32 $\mu$ s                       | -39.44                    | -19.40          | -9.46           | -19.13          |
| 3.2 ms                           | 0.41                      | -0.93           | -0.87           | 0.16            |
| Dual-TE                          | 1.09                      | -0.14           | -0.61           | -1.24           |

**Results and discussion:** Table 1 shows mean susceptibility values of the Gd-DTPA solutions (0.1, 0.5, and 1 wt%) and  $\text{CaCO}_3$  obtained in the phantom. The susceptibility values were derived using the QSM from each single TE and dual UTE imaging. Figure 2 shows magnitude images, phase, unwrapped phase, and QSM images derived from each single TE (32  $\mu$ s and 3.2 ms), and the dual UTE imaging data. The mean susceptibility values of  $\text{CaCO}_3$  calculated from the dual UTE showed  $1.09 \pm 0.35$  ppm, i.e., a positive value. On the other hand, susceptibility values of 0.1, 0.5, and 1.0 wt% Gd-DTPA calculated from the dual UTE were  $-0.14 \pm 0.03$ ,  $-0.61 \pm 0.02$ , and  $-1.24 \pm 0.03$  ppm, i.e., all negative values. Based on these results, we discussed the usefulness of CE-MRI using dual-UTE sequence, and then we found the observation of Gd-DTPA depend on TE.

## CONNECTIVITY BETWEEN INFERIOR PARIETAL LOBE AND INFERIOR TEMPORAL GYRUS WHILE THE BRAIN IS AT REST

AN Yusoff<sup>1</sup>, K Abdul Hamid<sup>1,2</sup>, S Rahman<sup>1</sup>, SS Osman<sup>3</sup>, S Surat<sup>1</sup> & M Ahmad Marzuki<sup>3</sup>

<sup>1</sup>Universiti Kebangsaan Malaysia, Malaysia; <sup>2</sup>KPJ University College, Malaysia; <sup>3</sup>Universiti Kebangsaan Malaysia Medical Centre, Malaysia

**Key words:** resting state, Bayesian, DCM

**Introduction:** Inferior parietal lobule (IPL) and inferior temporal gyrus (ITG) are two important brain regions constituting a default mode network (DMN). They show a significant increase in neuronal activity and energy consumption as compared to other brain regions when the brain is at rest. These two regions are highly interconnected as determined from white matter and fiber tracking studies. However, little is known about the nature of connectivity between these two regions while the brain is at rest i.e. whether their connectivity can best be represented by linear, bilinear or nonlinear model.

**Methods:** Resting state functional magnetic resonance imaging (rsfMRI) data were obtained from 7 healthy male and female subjects (eyes open and fixed onto a fixation point 'x' with an empty mind). Data were analyzed using statistical parametric mapping (SPM12). Endogenous low frequency fluctuating (LFF) brain signals were modelled using Fourier basis set with frequencies 0.01, 0.02, 0.04 and 0.08 Hz. Fully connected linear (Fig. 1a), bilinear (Fig. 1b) and non-linear (Fig. 1c and 1d) models in both hemispheres were constructed and estimated by means of dynamic causal modelling (DCM12) and were compared using Bayesian Model Selection (BMS) for group studies.

**Results:** Fixed-effects (FFX) results indicated that bilateral IPL and ITG exhibited high neural activity at a corrected significant level ( $p_{FWE} < 0.05$ ). Neural activity was centered in left ITG (-32/2/-38) and right IPL (32/-38/50) respectively. Bayesian model selection (BMS) selected bilinear model (Fig. 1(i & ii)) as the winning model for both hemispheres (model posterior probability  $\sim 1.0$  and log-evidence  $> 1000$ ), whereas the minimum free energy ( $F$ ) =  $-4.41 \times 10^4$  and  $-4.09 \times 10^4$  for left and right hemisphere bilinear models respectively. IPL and ITG were found to be weakly but bi-directionally connected to each other.

**Discussion:** Parietal lobe and temporal gyrus are involved in sensory interpretation and execution of higher cognitive function and perception [1]. This rsfMRI study focuses on IPL due to its consistent involvement in DMN. Recently, a study on resting brain has suggested IPL to be associated with self-referential condition [2]. ITG, on the other hand, was selected due to its role in visual object recognition and perception. The involvement of IPL in DMN is related to subjects' internal representation of information while suppressing any external or internal distraction. Activation of ITG is suggested to be due to its involvement in sensory information processing while the subjects are focusing onto the visual fixation [4]. From the winning dynamic causal model, the connectivity between IPL and ITG are negatively bi-directional, from which an increase in IPL activity decreases the activity in ITG and vice versa.

This observation is based on justification that the suppressing of internal cognitive processing in resting brain is in conjunction with the sensory information processing due to subjects' attention to the visual fixation. Connectivity between IPL and ITG is externally modulated, caused by the regulation of resting brain. This observation incorporates the probability of association between resting neural inhibition and modulation of inhibition of cognitive performance [3]. A higher strength of connectivity or transfer of information between ITG and IPL comes with higher influence on the connection by external node of DMN or other network that is not under study.

**Conclusion:** LFF signal in resting brain is able to be modelled. IPL and ITG have been found to be bi-directionally connected and the connection is modulated by an external perturbation possibly by the LFF. This connectivity model determined by BMS has the best balance between accuracy (fit) and complexity.

### References:

1. Yusoff AN (2013) Psychophysiological Interaction between Right Precentral Gyrus and Superior Parietal Lobule. *Sains Malaysiana* 42(6): 765-771.
2. Davey CG, Pujol J, Harrison BJ (2016) Mapping the Self in the Brain's Default Mode Network. *NeuroImage* 132: 390-397
3. Legon W, Punzell S, Dowlati E, et al. (2016) Altered prefrontal excitation/inhibition balance and prefrontal output: markers of aging in human memory networks. *Cereb Cortex* 26(11): 4315-4326.
4. Yusoff AN, Xin Ling T, Abd Hamid AI et al. (2016) Superior Temporal Gyrus (STG) and Cerebellum Show Different Activation Profile during Simple Arithmetic Addition Task in Quiet and in Noisy Environment: An fMRI Study. *Mal. J. Health Sci.* 14(2): 119-127

Corresponding author email: nazlimtrw@ukm.edu.my

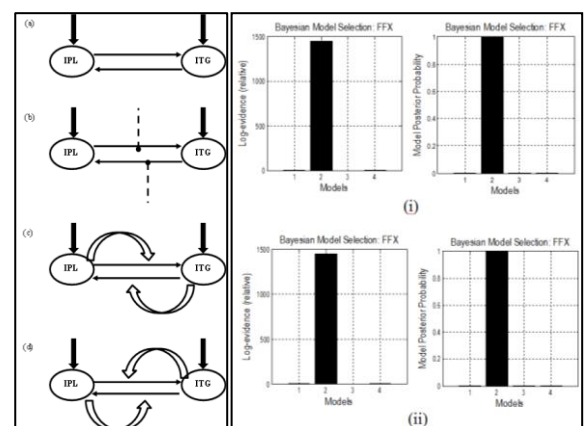


Fig. 1 Proposed dynamic causal models (left) and model comparison results (right) using BMS for respective models in (i) left and (ii) right hemisphere

## **ATTENUATED PREFRONTAL GLUTAMATERGIC METABOLISM IN ANIMAL MODEL OF POSTTRAUMATIC STRESS DISORDER BY USING PROTON MAGNETIC RESONANCE SPECTROSCOPY AT 9.4T**

Song-I Lim, Kyu-Ho Song, Chi-Hyeon Yoo, Bo-Young Choe

The Catholic University of Korea, College of Medicine, Republic of Korea

**Key words:** MRS, MRI, Posttraumatic Stress, PTSD

### **Purpose**

Single prolonged stress (SPS) is an animal model of posttraumatic stress disorder (PTSD). However, it has not been known how PTSD develops from the first exposure to traumatic events and neurochemical differences between acute/single stress and PTSD-triggering stress. Therefore, the object of this study is to determine time-dependent neurochemical changes in prefrontal cortex (PFC) of rats using proton magnetic resonance spectroscopy (1H-MRS).

### **Methods**

Male Sprague-Dawley rats (n=14; body weight=200-220g) were used. The SPS protocol was used in this study. Rats were restrained for 2h and then immediately forced to swim for 20min in water (20-24 Celsius). After a 15-min recuperation period, rats were exposed to ether (using a desiccator) until general anesthesia occurred (<5min). Acquisition of in vivo MRS spectra and MRI was performed 30min before the SPS (Base), approximately 10min after the SPS (D+0), 3 (D+3) and 7 (D+7) days after SPS to investigate time-dependent changes on metabolites levels in the PFC.

### **Results**

Statistical significance was analyzed using one-way ANOVA with post hoc Tukey HSD tests to assess the metabolite changes in the PFC. The SPS resulted in significant stress-induced differences for 7 days in glutamine (F(3,52)=6.750, P=0.001), choline-containing compounds (F(3,52)=16.442, P=0.000), glutamine/glutamate concentrations (F(3,52)=7.352, P=0.000).

### **Conclusions**

PTSD in human is associated with decreased neuronal activity in the PFC. In this study, SPS altered total choline, glutamine levels but not NAA levels in the PFC of the rats. Therefore, SPS attenuated excitatory tone and membrane turnover but did not affect neural integrity in the PFC.

## **THE ADMINISTRATION OF VARENICLINE ON REPEATED NICOTINE-INDUCED ANIMAL MODEL: IN VIVO PROTON MAGNETIC RESONANCE SPECTROSCOPY AT 9.4T**

Song-I Lim, Kyu-Ho Song, Chi-Hyeon Yoo, Bo-Young Choe

The Catholic University of Korea College of Medicine, Republic of Korea

**Key words:** MRS, MRI, Nicotine, Preclinical, hippocampus

### **Purpose**

Nicotine exerts its effects through the activation of nicotinic acetylcholine receptors (nAChRs). Varenicline, a smoking cessation aid, is a partial agonist acting at the  $\alpha 4\beta 2$  nAChRs. Although nicotine and varenicline contribute to the reward system, the influence of the substances on hippocampal neurochemical changes has not been investigated yet. We therefore studied the effects of repeated nicotine exposure and varenicline administration on hippocampus of rats by using in vivo proton magnetic resonance spectroscopy ( $^1\text{H}$  MRS) at 9.4T.

### **Methods**

Male Wistar rats ( $n = 11$ ; mean body weight,  $304.9 \pm 9.9$  g) were divided into 3 groups: control rats (control,  $n = 3$ ); nicotine-induced rats (nicotine,  $n = 4$ ); and nicotine- and varenicline-induced rats (varenicline,  $n = 4$ ). Acquisition of in vivo MRS was conducted by using 9.4 T Agilent Scanner. The LCmodel was used to quantify the metabolites in the frequency domain, using the basis metabolites.

### **Results**

In this study, the results show the tendency of increased Glu level in nicotine group than in the control and varenicline groups. Moreover, GSH and NAA levels tended to decrease in the nicotine group in comparison with those in the control and varenicline groups.

### **Conclusions**

These findings indicate that the hippocampus is integrally linked to the brain reward sensitization involved in addiction and glutamate release through mobilization of intracellular calcium stores. Further, oxidative stress and toxicity of nicotine on brain would cause the decline of GSH and NAA. In conclusion, we found that varenicline effectively inhibits the reward cycle.

## **ALTERATION OF NEUROMETABOLITES LEVEL ON PREFRONTAL CORTEX OF REPEATED MK-801 TREATMENT SCHIZOPHRENIC ANIMAL MODEL: IN VIVO PROTON MAGNETIC RESONANCE SPECTROSCOPY STUDY**

Chi-Hyeon Yoo, Kyu-Ho Song, Song-I Lim, Bo-Young Choe

The Catholic University of Korea, Republic of Korea

**Key words:** Dizocilpine (MK-801); Schizophrenia;  $^1\text{H}$  MRS

### **Purpose**

Repeated exposure to dizocilpine (MK-801) can be used as a model of schizophrenia that incorporates disease progression. Proton magnetic resonance spectroscopy ( $^1\text{H}$  MRS) has been widely used to investigate schizophrenia-related alterations in glutamate (Glu). The purpose of this study was to investigate metabolic alterations in the prefrontal cortex (PFC) in an animal model of schizophrenia by using in vivo  $^1\text{H}$  MRS.

### **Methods**

Because of the spectral overlap of Glu and glutamine (Gln), high-field  $^1\text{H}$  MRS with short echo time (TE) was used. A point-resolved spectroscopy (PRESS) sequence was used to measure the levels of Glu and Gln, and the brain metabolites in a volume of interest (22.5 l) located in the PFC region of rats ( $n = 13$ ) before and after 6 days of MK-801 (0.5 mg/kg) treatment. Analysis of the spectra showed that the cross-contamination of Glu and Gln can be considered to comparably low.

### **Results**

No metabolic parameters were altered ( $p > 0.05$ ). However, differences in the levels of Glu and N-acetylaspartate (NAA) between two times were significantly correlated ( $p < 0.01$ ). The results showed both decreased (in 6 of the 13 rats) and increased (7 of the 13 rats) levels of Glu and NAA, which suggested that these opposite metabolic alterations reflect two stage of disease progression.

### **Conclusions**

The results suggest that high-field in vivo  $^1\text{H}$  MRS with short TE can quantify Glu and Gln with reliably low level of cross-contamination and that repeated exposure to MK-801 induces the progressive development of schizophrenia.

## **ALTERATION OF METABOLITES IN A DEPRESSIVE-LIKE RAT MODEL OF CHRONIC FORCED SWIMMING STRESS: IN VIVO PROTON MAGNETIC RESONANCE SPECTROSCOPY STUDY AT 7T**

Chi-Hyeon Yoo, Song-I Lim, Kyu-Ho Song, Bo-Young Choe

The Catholic University of Korea, Republic of Korea

**Key words:** Depression; Magnetic resonance spectroscopy

### **Purpose**

A chronic forced swimming stress (CFSS) treatment was reported to inducing behavioral despair to subjected animals. Purpose of the study was to investigate the CFSS-induced effects, particularly glutamate (Glu) system, on the prefrontal cortex (PFC) of the rats by using high-field and short echo-time in vivo proton magnetic resonance spectroscopy ( $^1\text{H}$  MRS).

### **Methods**

A point-resolved spectroscopy was used to quantify target metabolites in a volume of interest (22.5 l) localized in the PFC of rats before and after the 14 days of CFSS treatment. Forced swim tests were performed before and after the treatments to investigate changes in the swimming behaviors. Spectral analysis of simulations and in vitro measurements were performed to assess cross-contamination of Glu and glutamine (Gln), because Glu and Gln overlapped in spectra.

### **Results**

The results of spectral analysis suggested that spectral overlap of Glu and Gln was not critical, in turn, in vivo  $^1\text{H}$  MRS can reliably assessed alterations in Glu metabolism. The rats showed significant decreased immobility time and increased climbing time after the CFSS treatment, suggesting that the rats were in behavioral despair. Significant alteration in the levels of Glu and Gln was not detected. Significantly increased levels of myo-inositol, total choline, N-acetyl-aspartate were consistent with the results of patients with depressive disorders, suggesting that the CFSS treatment induced metabolic alterations to the animals similar with that found in patients.

### **Conclusions**

Further investigation with enhanced in vivo  $^1\text{H}$  MRS for Glu metabolism might provide further insights into pathophysiology of depression and Glu system.

## LIPID METABOLITES IN A RAT MODEL OF HIGH-FAT-DIET-INDUCED FATTY LIVER DISEASE USING 1H MRS

Kyu-Ho Song, Chi-Hyeon Yoo, Song-I Lim, Bo-Young Choe

College of Medicine, The Catholic University of Korea

**Key words:** MRS, NAFLD

### **Purpose**

The objective of this study was to determine the metabolic changes in a rat model of high-fat-diet-induced NAFLD by using single-voxel 1H-MRS with a 3.0-T MRI scanner.

### **Methods**

The examinations were performed on a 3.0 T scanner using a 4-channel animal coil for higher resolution. This method used point-resolved spectroscopy (repetition time/echo time = 6000/35 ms; number of signal averages = 64). The HF diet pellets contained 60% fat. In order to avoid large blood vessels, a voxel ( $0.8 \times 0.8 \times 0.8$  cm<sup>3</sup>) was placed in a homogeneous area of the liver parenchyma during free breathing. To measure the lipid content, we quantified total lipids ( $(-\text{CH}_2-\text{n}) / \text{noise}$ ), total saturated fatty acids ( $3(-\text{CH}_2-)/2(-\text{CH}_3)$ ), total unsaturated fatty acids ( $3(-\text{CH}_2-\text{C}=\text{C}-\text{CH}_2-)/4(-\text{CH}_3)$ ), total unsaturated bonds index ( $3(-\text{CH}=\text{CH}-) / 2(-\text{CH}_3)$ ), and polyunsaturated bonds index ( $3(=\text{C}-\text{CH}_2-\text{C}=\text{C}) / 2(-\text{CH}_3)$ ) by separating each peak area of  $(-\text{CH}_2-\text{n})$ ,  $-\text{CH}_2-\text{C}=\text{C}-\text{CH}_2-$ ,  $=\text{C}-\text{CH}_2-\text{C}=\text{C}$ , and  $-\text{CH}=\text{CH}-$  by  $-\text{CH}_3$ . The  $-\text{CH}_3$  (0.90 ppm) peak was used as an internal chemical shift reference.

### **Results**

A significant increase in the number of polyunsaturated bonds was observed after 3 and 9 weeks. Our results show that the indices of total unsaturated fatty acids, total unsaturated bonds, and polyunsaturated bonds do not change significantly after 15 weeks of high-fat diet. Our study suggests that unsaturated fatty acids may be upregulated or downregulated in a chronic model of NAFLD.

### **Conclusions**

This study of 1H MRS at 3.0T using a four-channel animal coil shows sufficient spectral resolution and SNR for the characterization of observable total lipids and fatty acids.

## IMAGE ANALYSIS FOR DYNAMIC CONTRAST-ENHANCED MRI

Yasuhiro Sako<sup>1</sup>, Masafumi Ohki<sup>1</sup>, Anucha Chaichana<sup>2</sup>, Misa Sumi<sup>3</sup>, Takashi Nakamura<sup>3</sup>

<sup>1</sup>Department of Health Sciences, Graduate School of Medical Sciences, Kyushu University, Japan

<sup>2</sup>Department of Radiological Technology, Faculty of Medical Technology, Mahidol University

<sup>3</sup>Department of Radiology and Cancer Biology, Nagasaki University School of Dentistry

**Key words:** dynamic contrast-enhanced MRI, salivary gland tumor, image analysis

### Purpose

Temporal variation of signal intensities by contrast media can be observed in dynamic contrast-enhanced MRI (Magnetic Resonance Imaging). To quantify the variation, we made a GUI (Graphical User Interface) based application program and evaluated it on the feasibility of the differential diagnosis of salivary gland tumors.

### Methods

The application program was developed with MATLAB (MathWorks, Inc.). The program analyzed the three-dimensional MRI images from patients with benign and malignant salivary gland tumors. Three features, Tmax, ER, WR were calculated from the temporal variation of signal intensities. Tmax is a time required to reach the intensity peak, ER is an enhancement ratio of intensity by contrast media and WR represents a washout ratio of contrast media. We classified the temporal variation into five types with these features and displayed it as a pseudo-color image. We also displayed each of these features as a three-dimensional image to observe the spatial distribution of it.

### Results

The classification into five types was found to be useful for differentiating between benign and malignant tumors and between Warthin's tumors and other benign tumors. Tmax was also found to be useful for differentiating between Warthin's tumors and other benign tumors.

### Conclusions

The image analysis program for the differential diagnosis of salivary grand tumors in dynamic contrast-enhanced MRI was developed and the usefulness was evaluated by analyzing clinical images.

## AN e-LEARNING PACKAGE FOR PERSONAL DOSIMETRY TRAINING PURPOSES

M Koutalonis<sup>1</sup>, A J Porter<sup>1</sup>

<sup>1</sup>Colchester Hospital University NHS Foundation Trust, Medical Physics Department, UK

**Key words:** e-learning, education, training, personal dosimetry

**Introduction** Personal dose monitoring is a legislative requirement under the Ionising Radiations Regulations 1999 (IRR99) in the UK. Regulation 18(3) says that “An employer who has designated an area as a controlled area shall not permit a person to enter or remain in such area in accordance with the written arrangements under paragraph 2(c), unless he can demonstrate, by personal dose monitoring or other suitable measurements, that the doses are restricted in accordance with that sub-paragraph”. Members of staff who work with ionising radiation are therefore issued with personal dosimeters to monitor the doses they receive and satisfy the regulations. However, several studies have showed that awareness of personal dosimetry among staff who work with ionising radiation is low. In particular, in our hospital it was noticed that, despite given relevant written instructions, some staff members do not know how to distinguish among different types of dosimeters, where to wear each, what to do if they lose them, when to return them for replacement etc. It was therefore decided to develop an e-learning package, aiming to increase the awareness of matters relating to personal dosimetry among staff.

**Methods** The topics covered by the package include: legislation relevant to personal dosimetry; types of dosimeters and how to distinguish among each type; correct wearing of dosimeters; local investigation levels; when to return each dosimeter for replacement and what to do if it is lost; where to find dose results etc. Information was also given regarding the consequences of not complying with the regulations as well as the current dose limits and typical staff doses per department in our hospital. The e-learning package was introduced as part of the mandatory training of all new members of staff that require personal monitoring. Existing staff that are already issued with personal dosimeters were also asked to complete the training.

The e-learning package also contains a mandatory quiz that each member of staff needs to score at least 80% in order to be issued with a certificate and their personal dosimeters. The quiz consists of 10 multiple choice questions, each giving a 10% if answered correctly.

A Facility Index (FI) was calculated for each question. This is a measure of how easy or difficult is a question for the quiz-takers. It is calculated as  $FI = X_{\text{average}} / X_{\text{max}}$ , where  $X_{\text{average}}$  is the mean credit obtained by all users attempting the question and  $X_{\text{max}}$  is the maximum credit achievable for that question. In our case where most of the answers can be distributed dichotomically into correct/wrong categories,

this index coincides with the percentage of users that answered each question correctly.

A Discrimination Index (DI) was also calculated for each question. This provides a rough indication of the performance of each question to separate proficient vs. less proficient members of staff. It is calculated by first dividing learners into thirds based on the overall score in the question. Then the average score is calculated for the groups of top and bottom performers and the average score is subtracted. The DI can take values between +1 and -1. If the index goes below 0.0 it means that more of the weaker staff got the question right than the stronger ones and such questions should be considered worthless as they can reduce the accuracy of the overall score.

**Results:** Until today, 229 members of staff attempted the training and the quiz, of which nearly 16% have failed in their first attempt. 78.9% of the those that did the training, took less than 5 minutes to read through the 21 training slides and attempt the quiz (11.4% spent >10 minutes).

The lowest FI was noticed for questions related to the duration of the wearing period of each dosimeter (73%) and the regulations that are satisfied by the personal dosimetry monitoring (76%). Also, 21% of our staff do not know where they can find the local investigation levels (they are in the Local Rules for each Controlled Area) and 17% are confused as to what is the correct positioning for a whole body and a collar dosimeter (correct facing – inside/outside of personal protective equipment).

The DI for all questions was > 0.0 which shows that more of the stronger staff got the questions right than the weaker ones. The lowest DI value (0.755) was calculated for the question related to the wearing period for each type of dosimeter. This was the question that had the highest Standard Deviation (SD) too (0.42).

**Discussion:** The statistics show that some staff may not be reading the training material properly. This could be due to limited time or because they feel confident with the content of the package. The results will help us highlight areas for improvement. Questions with higher fail rate may require more explanation and attention when the package is next reviewed.

**Conclusion:** Personal dosimetry is a legislative requirement for staff who work with ionising radiation and e-learning packages can be a very useful tool towards increasing the awareness among monitored staff.

### References:

1. The Ionising Radiations Regulations 1999, <http://www.legislation.gov.uk/uksi/1999/3232/contents/made>

## **DEVELOPMENT OF A NOVEL CARBON LOK-BAR: CHALLENGE REGARDING REDUCTION OF RAY SCATTERING AND ABSORPTION IN RAPIDARC® TREATMENT PLANNING AND DOSE DELIVERY**

Hajime Monzen<sup>1</sup>, Kazuki Kubo<sup>2</sup>, Mikoto Tamura<sup>2</sup>, Kenji Matsumoto<sup>2</sup>, Yasumasa Nishimura<sup>3</sup>

<sup>1</sup> Kindai University, Japan

<sup>2</sup> Graduate School of Medical Sciences, Kindai University, Japan

<sup>3</sup> Faculty of Madeline, Kindai University, Japan

### **Purpose**

We developed a novel carbon lok-bar (HM-bar) that is used to secure the immobilizers to the treatment couch. The aim of this study was to investigate the X-ray scattering and absorption properties of the HM-bar in computer tomography (CT) simulation and radiotherapy dose delivery using the Varian Exact? lok-bar (VL-bar) as a benchmark.

### **Methods**

The attenuation rates for each lok-bar were measured using a farmer-type ionization chamber (PTW30013) and the I'mRT phantom (IBA Dosimetry GmbH). Measurement points were between gantry angles of 110 and 180 degrees. The treatment apparatus was a NovalisTx (Brainlab AG); X-ray energies were set at 6 MV and 10 MV.

### **Results**

Artifacts were seldom observed in the CT scans of the HM-bar. The attenuation rate of each lok-bar was higher when the X-ray energy was set at 6 MV than at 10 MV. The highest attenuation rate in the VL-bar was observed at a gantry angle of 112 degrees; the rates were 22.4% at 6 MV and 19.3% at 10 MV. Similarly, the highest attenuation rate for the HM-bar was also observed at a gantry angle of 112 degrees; the rates were 12.2% and 10.1% at 6 MV and 10 MV, respectively.

### **Conclusions**

The HM-bar could be used to minimize the occurrence of artifacts and provide good images in CT scans regarding radiotherapy planning and dose calculation.

### **Key words**

VMAT-SBRT, Loc-bar, patient immobilizers, artifact, X-ray scattering, absorption

## **SEQUENTIAL EVALUATION OF METAL ARTIFACT REDUCTION AND REGISTRATION USING 3D CT/MRI IMAGE**

Min-Young Lee, Kyu-Ho Song, Bo-Young Choi, Tae-Suk Suh

Catholic University, Republic of Korea

**Key words:** CT-MRI, Humanoid phantom, Metal Artifact, Implant, Heterogeneity

### **Purpose**

The purpose of this study is to quantitatively compare image acquisition between registered image of CT/MRI and of metal artifact reduced CT/MRI.

### **Methods**

The phantom comprises circle shape which shaped to simulated the anatomical structures of a human head and neck. Through applying various clinical cases, the developed phantom is closely allied to human. The phantom was filled with a solution of nickel chloride and sodium chloride. The implants and teeth were imaged by means of 3T MRI system and multi-detector CT. This study is evaluated metal artifact reduction and registration sequentially using MR image with different sequences and CT image.

### **Results**

The accuracy of dose calculations is essential to the quality of radiotherapy diagnostic. The phantom was capable of producing realistic head and neck metal artifact imaging data from which imaging devices and techniques can be evaluated. The dedicated head and neck CT/MRI phantom was performed to assess the magnitude and spatial dependence of MRI geometrical distortion and CT artifact accuracy in various sequences. The image reduced and registered CT/MRI image compared to registered and reduced CT/MRI image averagely 4% difference was observed.

### **Conclusions**

The phantom provides a unique and useful tool in head and neck dosimeter research. It can be used in the development of new imaging instrumentation, image acquisition strategies, and image processing and reconstruction methods.

## **VERIFICATION OF 6-DOF ROBOTIC BED SYSTEM FOR KHIMA PROJECT**

Yongkeun Song

Korea Institute of Radiological and Medical Sciences, Republic of Korea

**Key words:** Robotic Bed System KHIMA project Patient Positioning System

### **Purpose**

Korea Heavy Ion Medical Accelerator Project (KHIMA)'s purpose launched by Korea Institute of Radiological and Medical Sciences (KIRAMS) is to build a carbon ion treatment center in Busan, Korea. This project plans horizontal and vertical fixed beam line without rotation gantry. Therefore, we have designed and manufactured 6-DOF robotic bed system for KHIMA project with Robot Research Initiative in Chonnam National University. We also have planned to import the Computed Tomography on rail in treatment room. It has the possibility of collision with robotic bed system. So we conducted the collision simulation between the two product using simulation tool named IGRIP.

### **Methods**

In order to conduct the collision simulation, we analyzed the CT on rail and robotic bed system at first, and converted a design map to IGRIP file. While moving CT on rail in the robotic bed system direction, we look into where collision is occurred.

### **Results**

We conducted collision simulation by treatment site such as head and neck, lung, and pelvis. Collision of between robotic bed system and CT on rail mainly observed coupling part of couch top and robot base.

### **Conclusions**

In this paper, we dealt with how to verify collision between the robotic bed system and CT on rail. We assumed that current design has the potential collision. Therefore, modified design is currently considered.

## **NANO PARTICLES AS DRUG DELIVERY VEHICLES: APPLICATIONS AND HAZARDS**

Tabinda Hasan

Al Maarefa College Of Medicine, Riyadh, Ksa, Saudi Arabia

**Key words:** nano particles, drug delivery systems

### **Purpose**

The use of nanoparticles as drug delivery vehicles holds promising scope in medicine for both in vitro and in vivo diagnostics and therapeutics. This paper provides an overview of some of the current nano drug delivery systems. It also draws attention to the important issue of how to proceed with safety evaluation of engineered nanoparticles as drug delivery systems.

### **Methods**

A systematic meta-analysis approach was used to mine database on combustion derived nanoparticles (CDNP) obtained by inhalation toxicology and epidemiology studies and engineered nanoparticles repositories dating from 2010 till 2016.

### **Results**

Currently, nanoparticles are being employed in cancer therapy, to reduce side effects of routine chemo-drugs and toxicity. However, the nanoparticles have their own toxicity, the hazards of which are different from those posed by conventional delivery matrices. The potential of its interaction with tissues/cells, and thereby, its potential toxicity, depends greatly on the composition of nanoparticles formulation.

### **Conclusions**

Nanoparticles small size allows them to cross all biological barriers in the human body, including the blood brain barrier which opens novel avenues to deliver drugs effectively into the brain. Nano size allows their infiltration into inter/ intra cellular compartments and within the nucleus. A multitude of substances are currently under trial for producing nano particles including albumin, gelatin, phospholipids, polymers and metals. Despite increasing optimism about nano-particles drug-delivery vehicular applications in medicine, it cannot be expected that all aspects of nano toxicology will be detected, so probably, we need to proceed with caution and additional more specific testings.

## **THE EFFECTS OF IRIIDIUM NANOPARTICLES ON RADIATION DOSE ENHANCEMENT FOR MEGAVOLTAGE PHOTON AND ELECTRON BEAM**

Nur Amanina Md Isa, Wan Nordiana Rahman, Norhayati Dollah, Raizulnasuha Abd Rashid, Rosmazihana Mat Lazim

Universiti Sains Malaysia

**Key words:** radiotherapy, nanoparticle, radiosensitizer

### **Purpose**

Metal-based nanoparticles such as gold nanoparticles have been widely investigated for their potential to increase the therapeutic effects of radiotherapy. The purpose of this study is to investigate the effects of Iridium nanoparticles on radiation dose enhancement in Megavoltage Radiotherapy

### **Methods**

The HeLa cells were incubated with two different concentrations of Iridium nanoparticles at 0.1mM/L and 0.5 mM/L. The samples of HeLa cells were then irradiated with photon beam of 6 MV energy and electron beam of 6 MeV energy with the cumulative dose ranges from 0.5 to 10 Gy. The cells' survival after irradiation were obtained using clonogenic assay. Cells survival were analysed and fitted using linear quadratic formalism

### **Results**

DEF obtained for photon beam at 0.1 mM/L and 0.5 mM/L are 1.08 and 2.10 respectively while for electron beam the values generated at 0.1 mM/L is 1.17 and for 0.5mM/L is 1.13. The cell survival curves of HeLa cells with an inclusion of Iridium nanoparticles was steeper compared to the control cells indicated the dose enhancement effect. It is also established that the shape of the cell survival curve is affected by different radiation beams and Iridium NPs concentration.

### **Conclusions**

It can be concluded that Iridium nanoparticles are proven to be one of the potential radiosensitizers in radiotherapy. Dose enhancement effects are observed to be dependent on radiation beam types and nanoparticles concentration.

## **KINEMATIC ANALYSIS OF HUMAN GAIT FOR TYPICAL POSTURES OF WALKING, RUNNING AND CART PULLING**

Nupur Karmaker<sup>1</sup>, Hasin Anupama Azhari<sup>1</sup>, Abdul Al Mortuza<sup>2</sup>, Abhijit Chanda<sup>3</sup>, Golam Abu Zakaria<sup>4</sup>

<sup>1</sup>Dept of Medical Physics And Biomedical Engineering (MPBME) Gono Bishwabidyalay (University), Savar Dhaka, Bangladesh

<sup>2</sup>Bangladesh Atomic Energy Commission

<sup>3</sup>Jadavpur University

<sup>4</sup>Dept. of Medical Radiation Physics, Gummersbach Hospital, Academic Teaching Hospital University Of Cologne, Gummersbach, Germany.

**Key words:** Kinematic, Gait, Gait lab, Phase, force analysis, degree of rotation of joints.

### **Purpose**

The purpose of gait analysis is to determine the biomechanics of the joint, phases of gait cycle, graphical and analytical analysis of degree of rotation, analysis of the electrical activity of muscles and force exerted on the hip joint at different locomotion during walking, running and cart pulling.

### **Methods**

Cart pulling length have been divided into frames with respect to time by using video splitter software. Phases of gait cycle, degree of rotation of joints, EMG profile and force analysis during walking and running has been taken from different papers. Gait cycle and degree of rotation of joints during cart pulling has been prepared by using video camera, stop watch, video splitter software and Microsoft Excel.

### **Results**

During cart pulling, the force on hip is the vector sum of the force  $F_g = mg$ , due the body of weight of the person and  $F_a = ma$ , due to the velocity. During cart pulling shows maximum degree of rotation of hip joint, knee: running, and ankle: cart pulling. During walking, it has been observed minimum degree of rotation of hip, ankle: during running. During cart pulling, dynamic force depends on the walking velocity, body weight and load weight.

### **Conclusions**

It will be better to establish the gait laboratory to determine the gait related diseases. If the way of cart pulling is changed i.e the design of cart pulling machine, load bearing system is changed then it would possible to reduce the risk of limb loss, flat foot syndrome and varicose vein in lower limb.

## **MONTE CARLO SIMULATION OF MOLECULES AGONIST DIFFUSION IN A MODEL SYNAPSE**

Adita Sutresno, Freddy Haryanto, Sparisoma Viridi, Idam Arif

ITB, Indonesia

**Key words:** Monte Carlo Cell, Diffusion, Synapse, Agonist Molecule

### **Purpose**

Synapse is a part of the nervous system that permits a neuron to pass an electrical or chemical signal to another neuron. Chemical signal transferred with diffusion process in the synapse because there is different concentration between outside synapse and pre-synapse then synapse and cleft. In this paper focusing on diffusion between two molecule agonist those agonists, a molecule is a molecule that binds to a receptor causing activation and resultant cellular changes.

### **Methods**

This study used Monte Carlo simulation to determine a concentration of agonist ion in synapse transferred from outside synapse to pre-synapse then to synapse cleft, which one effect to a speed of diffusion process. The synapse was modeled as a sphere with receptors on a surface with several variation model receptor and receptor density.

### **Results**

The size of receptor and density receptor greatly affects the speed of molecules transfer from outside the synapse into the presynaptic and the number of molecules in the presynaptic agonist also affects the speed signal embodied in many molecules agonist releases of pre-synapse leading to the cleft. Another side, comparison amount of agonist molecules inside and outside presynaptic was investigated to an effect of diffusion.

### **Conclusions**

These simulations identify characteristics of agonist molecules base on concentration, size receptor, density receptor and irreversible process in synapse diffusion.

## **EFFECT OF SINTERING ON THERMOLUMINESCENCE INTENSITY OF $\text{CaSO}_4:\text{Tm}$ WITH ADDITION OF PTFE**

Nunung Nuraeni<sup>1</sup>, Dewi Kartikasari<sup>2</sup>, Eri Hiswara<sup>2</sup>, Ferry Iskandar<sup>3</sup>, Freddy Haryanto<sup>3</sup>, Abdul Waris<sup>3</sup>

<sup>1</sup>Institut Teknologi Bandung, Indonesia

<sup>2</sup>Ptkmr-Batan

<sup>3</sup>ITB

**Key words** :  $\text{CaSO}_4:\text{Tm}$ , PTFE, sintering, thermoluminescence

### **Purpose**

Effect of sintering treatment in thermoluminescence respons of thermoluminescent dosimeter (TLD)  $\text{CaSO}_4:\text{Tm}$  and  $\text{CaSO}_4:\text{Tm}$  with addition of PTFE (Poly Tetra Fluoro Ethylene) was investigated

### **Methods**

TLD  $\text{CaSO}_4:\text{Tm}$  was prepared by using co-precipitation method. To increase the TL response,  $\text{CaSO}_4:\text{Tm}$  were added with PTFE which has mass ratio of 2:3. The sintering treatment was done to TLD  $\text{CaSO}_4:\text{Tm}$  with PTFE addition ranging from 600, 700, 800 and 900°C for 1 hour. The thermoluminescence intensity was observed using TLD Reader Harshaw-3500 with the maximum temperature 260°C

### **Result**

From experimental result, the thermoluminescence intensity of  $\text{CaSO}_4:\text{Dy}$  with PTFE addition after sintering at 600, 700, 800 and 900°C are 596.93 nC, 1236,38 nC, 476,2 nC and 1158,11 nC, respectively.

### **Conclusion**

Generally, the thermoluminescence intensity of  $\text{CaSO}_4:\text{Tm}$  with PTFE addition increase with the increasing of temperature, but anomaly occurred at temperature 800°C.

## **THE EVALUATION OF THE PROTON BROAD BEAM USING MULTILAYER IONIZATION CHAMBER SYSTEM (*ZEBRA*)**

Yasuhiro Hasegawa<sup>1</sup>, Kunihiro Tateoka<sup>1</sup>, Yuya Azuma<sup>1</sup>

<sup>1</sup>Proton Therapy Center, Sapporo Teishinkai Hospital, Japan

**Key words:** Proton Therapy, Bragg-peak, Depth-Dose

### **Purpose**

For clinical proton beams, depth-dose is measured using three dimensional water tank dosimetry system with ionization chamber. This method needs a lot of time. In this work, the Zebra, a multilayer ionization chamber system, that can measure depth-dose for a short time, was compared with water tank dosimetry system.

### **Methods**

The Zebra can measure for broad-beam of multiple energies of spread-out Bragg peak (SOBP) using Ridge filter by SUMITOMO cyclotron delivery system. For broad-beam, the Zebra-measured depth-dose distributions were compared with those measured by the water tank system regarding range, the depth of the distal 90% dose, SOBP length, the region between the proximal 95% and distal 90% dose and distal-dose fall off (DDF): the region between the distal 80% and 20% dose.

### **Results**

The reproducibility of measured data from the Zebra was showed better than 1%. For broad-beam PDD distributions showed about 2% agreement within the SOBP, and 4% outside. Range values agreed within about 1.0mm. SOBP length values agreed within about 2 mm. DDF values agreed within 0.5mm. Moreover, the setup and measurement time for all Zebra measurements was 3 to 20 times less, respectively, compared to the water tank measurements.

### **Conclusions**

The Zebra can measure the depth-dose distributions for broad proton beams for a short time. Fathomer, SOBP length, Range values and DDF values obtained with the Zebra are within the acceptable variations compared with the water tank measurements system.

## **ICMP 2016**



## **MINI SIMPOSIA (IOMP SCHOOL)**

## **MINI SYMPOSIUM**

### **THREE-DIMENSIONAL (3D) DOSIMETRY**

Geoffrey S. Ibbott, Ph.D.,

UT MD Anderson Cancer Center.  
[gibbott@mdanderson.org](mailto:gibbott@mdanderson.org)

Three-dimensional (3D) dosimetry using volumetric dosimeters of a variety of compositions has long been suggested as a promising technique for the radiation therapy clinic. 3D dosimetry provides a unique methodology for dose measurements in the volume irradiated using complex conformal delivery techniques such as IMRT and VMAT. To date true 3D dosimetry is still not widely practiced in the community; it has been confined to centers of specialized expertise where it is employed for quality assurance or commissioning roles where other dosimetry techniques are difficult to implement. The potential for improved clinical applicability has been advanced considerably in the last decade by the development of improved 3D dosimeters (e.g., radiochromic plastics, radiochromic gel dosimeters and normoxic polymer gel systems) and by improved readout protocols using optical computed tomography or magnetic resonance imaging.

The current status of 3D dosimetry will be reviewed, several dosimeters and imaging methods for dose readout will be described, the workflow procedures required for good dosimetry will be discussed, and some limitations for applications in select settings will be analyzed. The application of 3D dosimetry to several relevant clinical situations will be presented, describing how 3D approaches can complement other dose delivery validation approaches already available in the clinic. The applications presented will be selected to inform attendees of the unique features provided by full 3D techniques.

## **MINI-SYMPOSIUM**

### ***IOMP SCHOOL:***

## **MDCT: PHYSICS, DOSIMETRY AND RADIATION PROTECTION**

ORGANIZER: John Damilakis, Professor of Medical Physics, University of Crete, Greece,

### **1st DAY : MDCT: Physics and Dosimetry**

Chair: S. Tabakov Duration: 90 minutes

- a. Physics and basic technology of CT – Kwan Hoong Ng (Malaysia)
- b. CT dosimetry - K.Matsubara (Japan)
- c. CT dose management of pregnant patients - J. Damilakis (Greece)

### **2nd DAY: Dose Tracking and Quality Assurance**

Chair: J. Damilakis, Duration: 90 minutes

- a. How tracking can help in radiation protection of patients? – M. Rehani (USA)
- b. Patient dose tracking systems: A new way of managing patient dose - N. Fitousi (Belgium)
- c. Quality Assurance in CT - V. Tsapaki (Greece)

### **Speakers:**

Kwan Hoong Ng, Prof. of Medical Physics, Malaysia

K.Matsubara, Assoc.Prof. of Health Sciences, Kanazawa University, Kanazawa, Japan,

J. Damilakis. Prof. of Medical Physics, Greece

M. Rehani, Vice President, IOMP

N. Fitousi, Ph.D, Medical Physicist, QAELUM N.V., Innovation and Incubation Center, K.U. Leuven, Belgium

V. Tsapaki, Ph.D, Konstantopouleio Nea Ionia General Hospital, Athens, Greece

### **Course Objectives:**

To understand the technical and methodological principles of computed tomography

To describe the principles of optimising protocols

To explain the concepts and tools for dose management in radiology with regard to pregnant patients

To identify informatics and tools for tracking patient radiation dose

To learn how dose tracking can help in radiation protection of patients

To understand the importance of QA in CT

## **MINI-SYMPOSIUM**

### **DOSE TRACKING AND QUALITY ASSURANCE**

Chair: J. Damilakis

Dose tracking systems collect dose data from imaging systems that can be displayed in a variety of formats for analysis and benchmarking. Reviewing practices helps identify areas for improvement. A quality assurance (QA) program in Radiology is needed to a) ensure adequate clinical performance and compliance with standards and b) maintain equipment performance with minimum radiation exposure.

The aim of this mini symposium is to a) explain how dose tracking systems can manage information related to patient doses, b) provide information on quality assurance in CT and c) explain how dose tracking systems can improve quality assurance in radiology practices and especially in CT.

The main learning objectives are to a) identify informatics and tools for tracking patient radiation dose, b) learn how dose tracking can help in radiation protection of patients, c) understand the importance of quality assurance in CT and d) outline goals for a quality assurance program to address issues associated with patient radiation doses.

This mini-symposium consists of the following presentations:

- a. How tracking can help in radiation protection of patients? M. Rehani
- b. Patient dose tracking systems: A new way of managing patient dose, N. Fitousi
- c. Quality Assurance in CT, V. Tsapaki

## MINI-SYMPOSIUM

### EUROPEAN INITIATIVES ON MEDICAL RADIATION PROTECTION

Chair: J. Damilakis Co-Chair: V. Tsapaki

The aim of this mini-symposium is to present recent EFOMP (European Federation of Organizations for Medical Physics) projects and initiatives in medical physics and medical radiation protection and also to discuss a possibility of trans-Atlantic collaboration on these issues. The ‘European DRLs for Paediatric Imaging’ project (abbreviation: PiDRL) is an EC project aimed to a) develop a methodology for establishing and using DRLs for paediatric medical imaging and b) update and extend the European DRLs to cover as many as possible procedures.

The PiDRL project has recently drafted European Guidelines on how to establish and how to use paediatric DRLs. More information about PiDRL can be found at [www.eurosafeimaging.org/pidrl](http://www.eurosafeimaging.org/pidrl). EUTEMPE-RX is a project which aims to provide training opportunities to medical physicists in diagnostic and interventional radiology to become Medical Physics Experts i.e. to reach level 8 according to the European Qualification Framework (EQF). A network of excellent teaching centers in medical physics has been set up to develop a set of modules.

The courses achieve their learning objectives combining online with face-to-face teaching. More information about EUTEMPE-RX can be found at [www.eutempe-rx.eu](http://www.eutempe-rx.eu). This mini-symposium consists of the following presentations:

- a. PiDRL: A European Commission project on Paediatric DRLs, J. Damilakis
- b. Overview of EFOMP projects on Radiation Protection, V. Tsapaki
- c. Collaboration of AAPM and EFOMP on Radiation Protection Projects, E. Lief

## **MINI-SYMPOSIUM**

### **SAFETY IN MRI**

Stephen Keevil

Guy's and St Thomas' NHS Foundation Trust and King's College London, UK

One of the main advantages of MRI as a medical imaging modality is that it is free of the hazards associated with ionising radiation. However, the modality presents a number of unique hazards of its own, some of which have in the past resulted in death or serious injury to patients or members of staff. The most serious hazards in this category relate to ferromagnetic projectiles attracted by the strong magnetic field of the scanner, burns caused by the radiofrequency field and interactions between the electromagnetic fields used in MRI and biomedical implants. It is also possible for persons to experience transient sensory and stimulation effects in the vicinity of the MR scanner which, although they are not injurious to health in the long term, can be disturbing and could affect performance and safety if experienced by staff members. In this mini-symposium, we will consider the nature of and the mechanisms behind these various hazards. We will then describe ways in which risks can be minimised through appropriate training, adoption of good working practices, screening of persons who need to enter the MRI suite, and control of access through administrative means and good design of the MRI facility.

The mini-symposium will also include an overview of international standards and guidelines relevant to MRI safety, as well as examples of legislation and guidance at national and supra-national level.

## **MINI SYMPOSIUM**

### **EXPERIENCE BASED LECTURE ON ROC OBSERVER STUDIES IN DIAGNOSTIC MEDICAL PHYSICS**

Junji Shiraishi, Ph.D., Rie Tanaka, Ph.D.

Kumamoto University, Kanazawa University, JAPAN

To understand the experimental procedure of receiver operating characteristic (ROC) observer studies, there is nothing superior to performing as both an experimenter and observer in such a study. This is a hands-on seminar prepared especially for people, who have never experienced an ROC observer study and want to know how to perform one. Please join us with writing implement and eyeglasses, if necessary.

In the first step of this lecture, a basic theory of ROC analysis is discussed and guidance on how to design and conduct an observer study is provided. In the next step, the participants will perform an ROC observer study as an observer for detecting subtle low-contrast signals on two data sets of phantom images exposed to different dose levels. Sample images are displayed on the screen. As the third step, the participant changes his/her role from an observer to an experimenter to evaluate the diagnostic accuracy of the observer for two image data sets in terms of optimization of the patient dose by hand calculation. This procedure would help the participant understand some experimental issues associated with ROC observer study. For your convenience, this lecture also provides useful information about an ROC computer software, which is publically available for all researchers.

#### **Corresponding author:**

Junji Shiraishi, PhD

Professor

Department of Medical Physics, Faculty of Life Sciences, Kumamoto University

4-24-1 Kuhonji, Chuo-ku, Kumamoto, Kumamoto, 862-0976 JAPAN

TEL/FAX: +81-96-373-5484

Email: j2s@kumamoto-u.ac.jp

## MINI SYMPOSIUM

### NOVEL RETRIEVAL TECHNOLOGIES FOR SIMILAR IMAGES AND PERSONAL IDENTIFICATION IN COMPUTER-AIDED DIAGNOSIS AND RADIATION THERAPY

H Arimura<sup>1</sup>, C Muramatsu<sup>2</sup>, H Fujita<sup>2</sup>, Y-W Chen<sup>3</sup>, K Wakasugi<sup>4</sup>, A Katsumata<sup>5</sup>, T Aoki<sup>6</sup>

<sup>1</sup>Kyushu University, <sup>2</sup>Gifu University, <sup>3</sup>Ritsumeikan University, <sup>4</sup>Panasonic Corporation, <sup>5</sup>Asahi University <sup>6</sup>Tohoku University

Muramatsu and Fujita et al have been investigating a similar image retrieval method for assisting radiologists in diagnosis and reporting of mammograms and breast ultrasound images. Based on the experts' subjective ratings, clinically relevant images are retrieved using a machine learning method.

Efficient feature extraction is a key issue for content-based medical image retrieval. Chen et al propose a multilinear sparse coding method for spatio-temporal feature extraction of multi-phase CT images and apply it to liver lesion retrieval. The multi-phase CT image is treated as a third-order tensor.

Wakasugi et al introduce the experimental result that the accuracy of diagnosis was improved with our similar case retrieval system for computed tomography (CT) images of diverse lung lesion patterns, and explore a potential of the retrieval system with convolutional neural networks.

Arimura et al will present a similar-case-based optimization framework for beam arrangements in lung stereotactic body radiation therapy for assisting treatment planners.

The usefulness of dental formula as an aid to personal identification is widely accepted within the forensic field. The panoramic radiograph is widely using in the field of dentistry. Katsumata et al studied a method to extract dental formula from panoramic radiograph.

Aoki et al report methods of victim identification used in the Great East Japan Earthquake and Tsunami on March 11, 2011, where dental identification was most effective. Aoki et al also discuss the possibility of introducing dental radiograph matching technology in future mass fatality incidents.

## **MINI SYMPOSIUM**

### **THE NEW ERA OF MEDICAL PHYSICS IN ASIA: *JOURNAL RADIOLOGICAL PHYSICS AND TECHNOLOGY***

K. Doi

University of Chicago, Chicago, USA, and Gunma Prefectural College of Health Sciences, Maebashi, Japan

Radiological Physics and Technology (RPT) is the official English-language journal of the Japanese Society of Radiological Technology (JSRT) and the Japan Society of Medical Physics (JSMP), and also the Asia-Oceania Federation of Organizations for Medical Physics (AFOMP). We believe that new ideas and new findings are the most important ingredients in scientific and technical publications. It is worthwhile to report new ideas and new findings as soon as possible, even if the supporting data might not be completely available at an early phase of research and development. Therefore, we welcome short articles clearly describing new ideas and new findings that are likely to have a significant impact on radiological physics and technology in the future. We also believe that one of the roles of the journal is to assist young researchers in nurturing their growth as a scientist, and thus our editorial policy includes trying to salvage a manuscript as much as possible by providing constructive reviews to authors, if the manuscript has at least a potentially publishable content, although the manuscript appears to be written poorly. Because the native language of many authors is not English, the RPT provides a special editing service by our Editorial Assistant, which is free to authors, for initial polishing of all manuscripts submitted, and also a final polishing only for technically accepted manuscripts.

## MINI SYMPOSIUM

### MEDICAL PHYSIC ASPECTS OF PROTON THERAPY

T Toshito

Department of Proton Therapy Physics, Nagoya Proton Therapy Center,  
Nagoya City West Medical Center  
1-1-1, Hirate-cho, Kita-ku, Nagoya, 462-8508, Japan

Proton therapy is of great dosimetric advantage against photon therapy since its characteristics to create Bragg-peak. Number of proton therapy facilities is rapidly increasing. Broad beam and scanning methods are two main approaches to deliver proton beam. The broad beam method is well established technique and has been used since its early days. On the other hand, the scanning method emerged lately to achieve higher dose concentration and becomes popular among facilities which are launched recently.

The Nagoya Proton Therapy Center (NPTC) began treatment in February 2013 as ninth proton therapy facility in Japan. The NPTC is a hospital-based facility managed by a city and designed to serve as many patients as possible efficiently. The NPTC has three treatment rooms: two rooms are equipped with isocentric gantries which rotate 360° around patient and one is equipped with a fixed horizontal beamline. One gantry treatment room has a pencil beam scanning treatment delivery nozzle. Another gantry treatment room and the fixed beam treatment room have a broad beam treatment delivery nozzle. Usage of treatment rooms are so arranged that scanning method is used to treat static tumors including head and neck, broad beam with a gantry is used to treat lung and liver which are generally accompanied by respiratory movement, and broad beam with a fixed port is used to treat prostate cancer. More than 1200 patients have been treated until the end of March 2016.

Introduction to proton therapy, treatment, equipment, and activities in medical physics including treatment planning and QA in the NPTC will be presented.

***Keywords: proton therapy, spot scanning, broad beam, gantry, quality assurance***

## MINI SYMPOSIUM

### RECENT DEVELOPMENTS IN DOSIMETRY, TREATMENT PLANNING AND QUALITY ASSURANCE FOR INTENSITY MODULATED PROTON THERAPY

N Sahoo

Department of Radiation Physics, UT MD Anderson Cancer Center, Houston, TX 77030, USA

There is a growing interest worldwide in intensity modulated proton therapy (IMPT) because of its ability to provide superior conformal dose distribution through inverse planning and optimization that can lead to higher therapeutic gain compared to passively scattered proton therapy as well as widely used radiation therapy using photons and electrons. However, there are some challenges associated with: (a) range uncertainties, (b) dose calculation in heterogeneous media, (c) dose planning in the presence of high-z materials artifacts in CT-images, (d) uncertainties in relative biological effectiveness (RBE), (e) dose planning for and delivery to moving targets and (f) dose verification, to utilize the full potential of IMPT. The dosimetry, treatment planning and quality assurance for IMPT are still evolving to overcome these challenges so as to reduce and manage the uncertainties, and improve its clinical effectiveness. This talk will review some of the recent developments in these areas. The potential use of dual energy CT, proton radiography and in vivo proton range verification methods to reduce the range uncertainties will be presented. The use of fast Monte-Carlo simulation techniques to improve the accuracy of dose calculation in heterogeneous media and better mapping of the linear energy transfer and radiobiological effectiveness will be discussed. Recent developments in treatment planning strategies for IMPT for multiple long fields with junctions like the ones used for cranio-spinal irradiation and moving targets will be reviewed. The benefits and limitations of RBE based plan optimization will be discussed. The potential benefits of intensity modulated proton arc therapy will be presented. Recent developments both in 3-D dosimetry and in methods to improve the efficiency of quality assurance procedures for IMPT will be presented. This talk will conclude with a brief discussion of the various uncertainties in IMPT and the strategies to mitigate them.

**Key words:** Intensity Modulated Proton Therapy, treatment planning, relative biological effectiveness, uncertainties

E-mail: [nsahoo@mdanderson.org](mailto:nsahoo@mdanderson.org)

## MINI SYMPOSIUM

# ROBUST OPTIMIZATION AND ROBUSTNESS QUANTIFICATION IN INTENSITY MODULATED PROTON THERAPY

W Liu

Department of Radiation Oncology, Mayo Clinic, Phoenix, AZ, USA

Intensity-Modulated Proton Therapy (IMPT) is highly sensitive to uncertainties in beam range, patient setup and organ motion. Therefore, it is essential to evaluate the robustness of the IMPT plans against these uncertainties and design robustly optimized plans to improve the plan quality. The root mean square dose volume histograms (RVH) can be used to measure the sensitivity of the dose to uncertainties and the areas under the RVH curve (AUCs) can be used to evaluate plan robustness. Results of our research have shown the following: in the worst case and nominal scenarios, robustly optimized plans have better target coverage, improved dose homogeneity, and lower or equivalent dose to organs at risk (OARs). Additionally, robust optimization provides significantly more robust dose distributions to targets and organs than conventional optimization in H&N using IMPT. Reduction of PTV and planning directly based on CTV provides better or equivalent OAR sparing. Also 4D robust optimization mitigates the influence of interplay effect than 3D robust optimization in lung cancer patients treated by IMPT. A review of the current state of art of robust optimization for IMPT treatment planning and robustness quantification will be presented.

**Key words:** Intensity modulated proton therapy, uncertainties, robust optimization

E-mail: [Liu.Wei@mayo.edu](mailto:Liu.Wei@mayo.edu)

## MINI SYMPOSIUM

### IAEA/RCA PROJECT, RAS6077, “STRENGTHENING THE EFFECTIVENESS AND EXTENT OF MEDICAL PHYSICS EDUCATION AND TRAINING”

A. Meghzifene & H. Brendan

Dosimetry & Medical Radiation Physics Section, Division of Human Health  
International Atomic Energy Agency (IAEA), Vienna, Austria

The regional project RAS6077 is an IAEA (<https://www.iaea.org/>) technical cooperation project under the auspices of the Regional Cooperative Agreement (RCA <http://www.rcaro.org/>) involving 19 countries in the Asia Pacific region. RAS6077 is a four-year project which commenced in 2014. RAS6077 follows on from a previous project RAS6038 which was influential in addressing structured clinical training of medical physicists. Under RAS6038, the IAEA published clinical training guides IAEA TCS 37, 47 and 50 covering radiation oncology, diagnostic radiology and nuclear medicine. The IAEA structured clinical training program was piloted in four countries with approximately 50 medical physicists completing the clinical training.

RAS6077 has built on the achievements of RAS6038 by extending the reach of structured clinical training programs for medical physicists. One approach to extending training to many countries is in electronic networking, so the project has developed a Moodle environment called AMPLE (Advanced Medical Physics Learning Environment) hosted by the IAEA on its CLP4NET e-learning platform (<http://clp4net.iaea.org/>). AMPLE provides a means of electronically tracking the progress of training of residents through the clinical training modules and associated competencies, allows communication between residents, supervisors and coordinators, and provides a central resource for electronic learning materials.

In a separate development under RAS6077, it is noted that structured clinical training cannot take place without accredited clinical training institutions, accredited academic institutions, and a means of certifying individuals once they have completed the clinical training. RAS6077 is seeking to develop, in cooperation with IOMP, IMPCB and AFOMP, a model for accreditation and certification that can serve as a template for participating countries.

Keywords: clinical training, residency programme, e-learning platform.

## **MINI SYMPOSIUM**

### **CURRENT STATUS AND FUTURE CHALLENGES OF MAMMOGRAPHY IN ASIA**

***THIS MINI-SYMPOSIUM IS CO-SPONSORED BY THE TMPS AND JSRT***

T Endo<sup>1</sup>, H Nishide<sup>2</sup>, P Hansakul<sup>3</sup>, A Krisanachinda<sup>4</sup>

<sup>1</sup>National Hospital Organization Higashi Nagoya National Hospital, <sup>2</sup>Gifu University of Medical Science, Japan  
<sup>3</sup>King Chulalongkorn Memorial Hospital, <sup>4</sup>Chulalongkorn University, Thailand

#### ***JSRT***

Breast cancer is the most common cancer in Japanese women, and it is similar in Asian women. We will present the current status of breast cancer diagnosis in Japan and Thailand, and introduce the quality control system for screening mammography in the Japan central organization. Objective of this Mini-Symposium is to discuss the role of mammogram in screening and diagnostic breast diseases, and the appropriate imaging modalities for early detection approach of breast cancer in Asia.

#### ***TMPS***

Breast cancer is a second leading cause of death from cancer in Thai women. Screening and early diagnosis may help to decrease the mortality from breast cancer. The aims of this course are to discuss the current guideline for screening breast cancer, the role of mammogram in screening and diagnostic breast diseases and the appropriate imaging modalities for diagnosis breast diseases in Thai population.

In this presentation the radiation dose from Digital Breast Mammography and Tomosynthesis in Thai patients will be reported for the past five years.

It is expected that this Mini-Symposium will create a cooperative relationship between the TMPS and JSRT and work in partnership for breast cancer diagnosis in future.

## **MINI SYMPOSIUM**

### **WOMEN IN MEDICAL PHYSICS: EDUCATION AND PROFESSION**

V. Tsapaki

IOMP Secretary General, Konstantopoulio General Hospital, Nea Ionia of Athens, Greece

Women have made significant contributions to science from the earliest times. It is true that the access of women to either basic education and moreover to higher education, in less resourced countries of the world, has been severely restricted in the past. However, this did not prevent women to leave their legacy in history with revolutionary discoveries.

Despite the immense steps for women so far, there are still socio-economic factors that limit the effective participation of women in higher education and professional levels. More specifically, the field of medical physics, one of the forefronts of current physics research and application, is still a male-dominated field in many regions of the world.

In the attempt to popularize the role of the women in medical physics and encourage female medical physicists to advance, the current session, proposed by the International Organization for Medical Physics Subcommittee, will present all problems, perspectives and possible solutions in education. It will also address the issue of women position in society in general and also within the professional environment. Last but not least during the session various ways to increase the participation of women in medical physics activities and action plans to improve the situation will be presented.

Keywords: Women, education, profession

## **MINI SYMPOSIUM**

### **PARTICIPATION OF WOMEN IN MEDICAL PHYSICS SCIENTIFIC EVENTS**

V. Tsapaki

IOMP Secretary General, Konstantopoulio General Hospital, Nea Ionia of Athens, Greece

According to the most recent UNESCO Science Report, women account for only 28 % of researchers across the world, with the gap deepening at the higher echelons of decision-making. Women have less access to funding, to networks, to senior positions, which puts them at a further disadvantage in high-impact science publishing.

It is also true that medical technology is improving greatly the last decades even in less resourced countries around the world. The needs in different continents such as including infrastructure development, private sector improvement of governance systems and accountability, all have a common fact which is the need for people with access to science and technology. There is no improvement in society without investing in skills, science, technology and innovation.

For all above reasons, the participation of women in scientific events and in policy-making processes is vital for The particular session, organized by the International Organization for Medical Physics Subcommittee, will address all these issues. Pilot surveys focused on participation of women in Medical Physics Congresses will be presented. Detailed experience from Spain, Brazil, Europe, as well as from Asia will be presented. Furthermore, ways to increase the participation of women in medical physics scientific events and methods to improve the situation will be discussed during this session.

Keywords: Women, scientific events

## **MINI SYMPOSIUM**

### **IOMP WORKSHOP: BUILDING PROFESSIONAL CAPACITY IN DEVELOPING COUNTRIES**

Organisers: Slavik Tabakov (President IOMP), Anchali Krisanachinda (Treasurer IOMP, Past President SEAFOMP), Yakov Pipman (Chair IOMP PRC), SD Sharma (AMPI Officer), KY Cheung (President IUPESM)

This workshop is co-sponsored by the IUPAP and IOMP. Its objective is to establish the current status and propose professional and educational activities supporting the development of medical physics in developing countries. IOMP has guided similar successful symposia on the subject and expects significant international impact from the Workshop

The Workshop will have its own Scientific and Professional Board, including Officers of the IOMP and its Regional Organisation (in particular Asian-Oceania Federation of Organizations for Medical Physics AFOMP and the South-East Asian Federation of Organisations for Medical Physics SEAFOMP). The Board will select presentation and poster from the submissions directly to the Board.

The materials from this IOMP Workshop will be published in the IOMP Professional Journal Medical Physics International (an open-source peer-review journal with approximately 4000 international readers per month).

It is expected that this IOMP Workshop will attract approximately 100 attendees from up to 20 countries and organisations (many of which from developing countries). The Workshop has its own funding through the Grant of the IUPAP.

The main speakers will include some of the organisers, representatives from developing countries, as well as from organisations as WHO and IAEA.

## MINI-SYMPOSIUM: LATEST TECHNOLOGIES OF MDCT IN JAPAN

Katsumi Tsujioka<sup>1</sup>, Katsuhiro Ichikawa<sup>2</sup>

<sup>1</sup>Fujita Health University. <sup>2</sup>Kanazawa University, Japan

The progress of the X-rays CT technique is remarkable now and the multi detector row CT (MDCT) takes the core of the field of current medical imaging. It is very important that we understand a technologies and performance evaluation of the MDCT. This symposium reports a latest CT technique of the MDCT in Japan.

### 1. The latest technologies and problems of the MDCT

The performance of the CT was greatly improved by development of the MDCT. It changed a diagnosis by the CT from the two dimensions into three dimensions and the four dimensions. The MDCT has many techniques for accomplishment of the clinical use. And it has the invention for solutions to the problem.

- (1) Helical scan and MDCT
- (2) Image display technology
- (3) Clinical application
- (4) Problems of the MDCT
- (5) Next generation CT

Three big problems occur by the expansion of the cone beam of the MDCT. The first problem is increase of the scattered radiation. The second problem is an error of the image reconfiguration. The third problem is extra radiation exposure to a patient. The technique that is high to approve these problems is necessary.

### 2. Performance evaluation of the MDCT

It is important that we evaluate performance of the MDCT. The performance evaluation of the MDCT cannot often be supported by the conventional method. Particularly, a wrong evaluation result may be given by the conventional rating system by the new iterative reconstruction. This presentation describes a new performance rating system for MDCT and iterative reconstruction.

### 3. Recommendation of the experiment using the phantom

The phantom experiment is important in a study of the CT. The phantom experiment may be effective in comparison with a clinical study and the simulation. The advantages by the phantom experiment are as follows. We can measure evaluation factor that we were not able to distinguish in the clinical study. We can evaluate the unknown effect that a guess was impossible by the simulation. We introduce the following phantoms at this symposium.

- (1) The phantom to evaluate the subtraction CT.
- (2) The phantom to evaluate the low contrast CT value.
- (3) The phantom to evaluate the cardiac movement.
- (4) The phantom to evaluate the coronary artery movement.
- (5) The phantom to evaluate the Ca-scoring.
- (6) The phantom to train the making 3D images.

By this symposium, we hope that everybody deepens understanding about the MDCT more than before.

## MINI SYMPOSIUM

### EYE LENS DOSIMETRY AND THE STUDY ON RADIATION CATARACT IN INTERVENTIONAL CARDIOLOGISTS

K.Matsubara<sup>1</sup>, S.Srimahachota<sup>2</sup>, A.Krisanachinda<sup>2</sup>

<sup>1</sup>Kanazawa University, Kanazawa, Japan, <sup>2</sup>Chulalongkorn University, Bangkok, Thailand

Cardiac catheterization has been used for decades as the gold standard for the diagnosis of different cardiovascular diseases. Cardiovascular interventional therapy is effective for cardiovascular diseases and reduces the comorbidities of coronary artery diseases, peripheral vascular disease, cardiac arrhythmia and congenital heart disease.

Cataract, or opacification of the lens, is often associated with visual impairment and may be classified into three main forms: nuclear, cortical, and posterior subcapsular (PSC), according to their anatomic location. Among the three major forms of age-related cataract, PSC is the least common but this form is most commonly associated with ionizing radiation exposure. Because of its location along the lens visual axis, relatively minor PSC can have a great impact on vision. In addition to ionizing radiation, other factors commonly associated with PSC are the use of systemic steroids and diabetes. The main symptom of a cataract is slow and progressive vision loss, i.e. a loss of the acuity of vision, varying in degree from clinically insignificant opacities to total opacification of the lens. People with cataracts are also increasingly prone to glare sensitivity as the clouded areas scatter light into the eye. Cataracts can sometimes cause double vision, and cataract patients may also see halos and starbursts around lights. Light/dark adaptation slows down, and spatial vision is reduced.

Workers involved in interventional cardiology procedures receive high eye lens dose if protection has not been used. Currently, there is no suitable method for routine measurement of eye dose. According to ICRU the operational quantity Hp (3) is the most appropriate to monitor the eye lens dose, as the lens is covered by about 3 mm of tissue. Proposals to use Hp(0.07) for eye lens dose monitoring. Correlations are being attempted with Hp(10).

The eye dose in terms of Hp (3) of the cardiologists, nurses and radiographers for interventional cardiology procedures could be measured by the optically stimulated luminescence (OSL) dosimeter for occupational exposure and the eye lens dose. The OSL badge is set at waist level and under the lead apron; the second is placed at the collar. Nano dots OSL dosimeter is taped outside and inside, on the left and the right corners of the lead eye glass to determine the eye lens dose with and without protection

Regular eye dosimetry in diagnostic imaging does not exist practically. The accurate assessment of eye lens dose is one of the most important aspects of correlating doses with observed lens opacities among workers in interventional suites and also to ascertain the compliance with regulatory limits. The eye lens dose, as organ dose, is not directly measurable. According to ICRU the operational quantity Hp (3) is the most appropriate to monitor the eye lens dose, as the lens is covered by about 3 mm of tissue. Proposals to use Hp (0.07) for eye lens dose monitoring, correlations are being attempted with Hp(10).

A total exposed were examined from interventional cardiology personnel. The mean eye lens, body and collar dose for the cardiologists, nurses and radiographers would be demonstrated. The results are compared to the current dose limit for the eye lens of radiation worker and the detection of the cataract would be reported.

## **MINI SYMPOSIUM**

### **RADIATION PROTECTION IN DENTAL RADIOLOGY**

Jenia Vassileva: IAEA program on strengthening radiation protection in dental radiology

Ruben Pauwels: Overview of CBCT – technology, patient doses, image quality, optimization

Virginia Tsapaki: EFOMP protocol for QA in CBCT

X ray imaging is extensively used in dentistry to diagnose, plan treatments and monitor both treatments and lesion development. According to the UNSCEAR, dental examinations are the most frequent type of radiological procedures, accounting for 21% of the total on a global scale. Individual doses are small but collective doses cannot be ignored due to the high volume of procedures. With the increase utilization of cone beam computed tomography (CBCT), both frequency and collective dose from dental imaging is expected to increase and this will require improved knowledge and awareness of dental practitioners on justified and optimized use of this technology. Medical physicists play important role in implementation of the quality assurance and radiation safety program, including training of health professionals. These were the motivation for the IAEA to initiate a number of activities in support to the strengthening the safe use of X ray in dentomaxillofacial radiology, including development of a free training material, informational material on benefit and risks, and other guidelines for dentists and other health professionals. This mini-symposium will focus on the role of medical physicists for ensuring optimised use of dental imaging. The objective will be to enhance the knowledge of medical physicists in approaches for achieving diagnostic image quality at lower patient dose. The IAEA program on strengthening radiation protection in dental radiology will be outlined, followed by two invited talks on proper use of CBCT.

## MINI SYMPOSIUM

### COMPREHENSIVE AUDITS IN RADIATION ONCOLOGY, NUCLEAR MEDICINE, DIAGNOSTIC AND INTERVENTIONAL RADIOLOGY

Ahmed Meghzipene<sup>1</sup>, IAEA  
Anchali Krisanachinda<sup>2</sup>

<sup>1</sup>Dosimetry & Medical Radiation Physics Section, Division of Human Health  
International Atomic Energy Agency (IAEA), Vienna, Austria

<sup>2</sup>TMPS Chulalongkorn University Bangkok Thailand

As part of a comprehensive approach to quality assurance (QA) in the diagnosis or treatment of diseases by radiation, an independent external audit (peer review) is important to ensure adequate quality of practice and delivery of safe and effective diagnosis or treatment. As part of its Human Health programme, the IAEA has developed guidelines for comprehensive audits in radiation oncology ([http://www-pub.iaea.org/MTCD/publications/PDF/Pub1297\\_web.pdf](http://www-pub.iaea.org/MTCD/publications/PDF/Pub1297_web.pdf)), nuclear medicine (<http://www-pub.iaea.org/MTCD/Publications/PDF/Pub1683Web-68161172.pdf>) and diagnostic radiology ([http://www-pub.iaea.org/MTCD/Publications/PDF/Pub1425\\_web.pdf](http://www-pub.iaea.org/MTCD/Publications/PDF/Pub1425_web.pdf)), with the aim to identify gaps in documentation and actual practice and recommend ways to improve quality of patient care. The audits are carried out only at the request of a hospital and implemented through the IAEA Technical Cooperation programme. The audits are carried out by a team of professionals composed of an experienced medical practitioner, medical physicist and radiographer or technologist, last 5 days and follow the standardized methodologies published by the IAEA. The auditing process includes a debriefing, interviews with relevant staff, observations of practice and review of documentation. In radiation oncology, independent measurements to verify the machine outputs can be done by the medical physicist, using an IAEA dosimetry kit. At the end of the audit, the team of experts brief the local staff on the findings and present the preliminary recommendations. The draft audit report is submitted to the IAEA for review and finalized, taking into account the comments, if any, by the IAEA staff and audit counterpart. The full audit report is strictly confidential. In case the auditors identify serious shortcomings in the practice, a follow-up audit mission is usually implemented.

The audits in radiation oncology and nuclear medicine have been well accepted by the medical community and missions have been carried out in about 70 Member States. These two audit methodologies have also been adopted by some countries and implemented at the national level. However, till September 2016, the level of implementation of audits in diagnostic radiology has been low. Additional efforts are needed to promote the need for quality audits in this area, especially among professionals working in radiology.

Keywords: clinical audits, comprehensive audits, QUATRO, QUANUM, QUAADRIL

## **MINI SYMPOSIUM**

### **PRACTICAL APPLICATION OF MOODLE FOR E-LEARNING COURSES IN MEDICAL PHYSICS**

**Speaker/Organiser: V Tabakova, PhD (King's College, London, UK)**

The Mini-Symposium features e-Learning as the environment most suitable for education and training in a dynamic profession such as Medical Physics. It will be delivered in two parts and will demonstrate the free e-Learning platform Moodle.

The symposium is expected to attract educators in all fields related to Medical Physics. It is not necessary to have any prior knowledge of Moodle and no advance preparation is needed.

1. Part 1 will deal with:

- Types and effectiveness of e-Learning
- Our contributions in e-Learning in Medical Physics (EMERALD, EMIT, etc.)
- e-Learning platforms, characteristics, advantages
- Introduction to the Moodle platform

2. Part 2 will look at the development of an educational e-module on Moodle – Step by Step (based on the example of the module on **Physics of Medical Imaging**).

The roles and functions on Moodle will be discussed (Manager, Teacher, Student). The symposium will deal also with Formatting and settings and an illustration of building a complete module will be given (with lectures, coursework, quizzes etc.). It will be discussed how to gather effectively information from Moodle (student participation, grade information, etc.)

Throughout the Symposium the advantages of e-Learning in general and of Moodle in particular will be highlighted and the prerequisites for successful introduction of e-Learning will be discussed.

The platform has been used continuously for the past 5 years in the MSc Medical Engineering and Physics at King's College London. It has been found very useful, easy to use and intuitive by students and lecturers alike.

## MINI SYMPOSIUM

### DOSIMETRY OF SMALL STATIC PHOTON FIELDS: CHALLENGES AND SOLUTIONS

M. Saiful Huq<sup>1</sup> and Sivalee Suriyapee<sup>2</sup>

<sup>1</sup>University of Pittsburgh Cancer Institute and UPMC CancerCenter, Pittsburgh, Pennsylvania, USA

<sup>2</sup>Chulalongkorn University, Bangkok, Thailand

Intensity modulated radiotherapy, Stereotactic radiosurgery and stereotactic body radiotherapy routinely uses radiation beams of small field sizes to treat small tumor. The increased use of small photon fields for such treatments makes it necessary to standardize the dosimetry of such fields using procedures that are consistent with those for conventional radiotherapy. To meet this need an international working group was established by the International Atomic Energy Agency (IAEA) in collaboration with the American Association of Physicists in medicine (AAPM). This group has developed a new Code of Practice (CoP) that provides recommendations for reference dosimetry using ionization chambers in machines that cannot establish a conventional 10 cm x 10 cm reference field. The formalism for reference dosimetry is based on the work of Alfonso *et al.*, Med. Phys. 35 (2008). The CoP also provides recommendations for measurements of output factors in small fields using high-resolution detectors such as diodes, diamond, and radiochromic film. Experimentally determined and/or Monte Carlo calculated correction factors for recommended ionization chambers are given for reference dosimetry in non-standard machine specific machine specific reference (msr) fields. The CoP also provides data for correction factors for high-resolution detectors such as diodes, diamond etc for measurement of output factors.

This mini-symposium will discuss the physics of small static photon fields, the recommendations given in the CoP for reference dosimetry in non-standard msr fields and the procedures for the measurement of output factors in small fields. Results of clinical implementation of the recommendations of the CoP will be presented.

## MINI SYMPOSIUM

### STEREOTACTIC BODY RADIATION THERAPY: TECHNICAL CHALLENGES AND CLINICAL ASPECTS

M. Saiful Huq<sup>1</sup>, Sornjarod Oonsiri<sup>2</sup> and Danita Kannarunimit<sup>3</sup>

<sup>1</sup>Department of Radiation Oncology, University of Pittsburgh Cancer Institute and UPMC CancerCenter, Pittsburgh, Pennsylvania, USA

<sup>2</sup>King Chulalongkorn Memorial Hospital, Bangkok, Thailand

<sup>3</sup>Chulalongkorn University Hospital, Bangkok, Thailand

Stereotactic body radiotherapy (SBRT) is a non-surgical specialized type of external beam radiation treatment in which large doses of highly accurate, precise, and conformal ionizing radiation are delivered to a well-defined target volume in a fractionated stereotactic radiosurgery scheme using image guidance. Successful clinical implementation of SBRT requires careful consideration of details of every step in the treatment process and integration of several technologies. Important considerations for SBRT treatments include, but are not limited to: i) 3D imaging and localization techniques, ii) Integration of modern imaging systems, iii) strategies for immobilization, simulation, motion assessment including 4D CT and respiratory motion management, iv) Treatment planning systems with the capability of integrating imaging information from various imaging modalities for delineating target and OAR volumes and calculating heterogeneity corrected accurate dose distributions with a sharp dose gradient using different techniques such as IMRT, VMAT etc. v) Linear accelerators and other devices designed for delivery of SBRT treatments, vi) sophisticated image guidance technologies and techniques such as 4D CBCT imaging, stereoscopic x-ray imaging, fluoroscopic verification of tumor motion, gating, tracking. In this mini-symposium, lung SBRT patient cases will be discussed to highlight real-world challenges and considerations for ensuring safe and accurate treatment planning and delivery. Discussions will focus around patient selection for lung SBRT, imaging and immobilization, motion assessment and management for moving target and OAR, target delineation for treatment planning and delivery, online treatment alignment and established prescription regimens and OAR dose limits and clinical outcomes.

## MINI SYMPOSIUM

### NEW APPROACHES TO QUALITY MANAGEMENT IN RADIATION THERAPY

M. Saiful Huq<sup>1</sup>, Puangpen Tangboonduangjit<sup>2</sup> and Taweap Sanghangthum<sup>3</sup>

<sup>1</sup>Department of Radiation Oncology, University of Pittsburgh Cancer Institute and UPMC CancerCenter, Pittsburgh, Pennsylvania, USA

<sup>2</sup>Department of Radiology, Faculty of Medicine, Ramathibodi Hospital, Mahidol University, Bangkok, Thailand

<sup>3</sup>Department of Radiology, Faculty of Medicine, Chulalongkorn University, Bangkok, Thailand

Current quality assurance (QA) guidelines provided by various professional organizations are prescriptive in nature. They focus on performance characteristics of planning and delivery devices. However, published analyses of events in radiation therapy show that these device-centric approaches to quality management (QM) in radiation therapy are not sufficient to protect patients against catastrophic or even minor events. A comprehensive quality management and safety program in radiation therapy should be based on risk assessment for clinical processes, resulting in an integrated QM approach that involves both process and traditional equipment QA. Task Group 100 (TG100) of the American Association of Physicists in Medicine has developed such an integrated approach for QM radiation therapy. The tools that TG100 recommended are: 1) process mapping, 2) failure modes and effects analysis (FMEA), and 3) Fault tree analysis (FTA). The process-mapping tool is used to design and understand a clinical process, the FMEA tool is used to prospectively identify and analyse the weak points in the process and the FTA tool is used to visualize potential locations in the process where controls can be placed so that error pathways are blocked. Information obtained from the analyses using these tools is then used to develop a risk-based QM program. Other tools such as statistical process control (SPC) is also used for monitoring and controlling processes thereby ensuring that processes operate at their full potential. SPC is a method of quality control that uses statistical methods. This mini-symposium will discuss these new approaches to quality management in radiation therapy.

## **MINI SYMPOSIUM**

### **DOSIMETRY IN RADIOPHARMACEUTICAL THERAPY TREATMENT PLANNING**

George Sgouros, Ph.D.

Johns Hopkins University, School of Medicine USA

Radiopharmaceutical Therapy is an emerging treatment modality that has the potential to improve the treatment of cancer patients. As currently implemented, this treatment modality does not take advantage of the potential to adopt a precision medicine/treatment planning approach to treating patients by using a theranostic approach to couple imaging with treatment. The presentation will highlight opportunities to taking such an approach and present examples of the advantages of doing so.

The objectives are to understand the difference between dosimetry for diagnostic imaging vs. for therapy and to describe the role of radiobiology in dosimetry and treatment planning for radiopharmaceutical therapy

## **MINI SYMPOSIUM**

### **ASEAN COLLEGE OF MEDICAL PHYSICS WORKSHOP ON DIGITAL RADIOGRAPHY**

KH Ng, N Pongnapang, N Jamal, CH Yeong

This workshop is organized by the ASEAN College of Medical Physics (ACOMP) as one of the continuing professional medical physics education programs in the region. The theme for this workshop focuses on the physical principles, image quality and quality control (QC) tests in digital radiography (DR). DR is rapidly being developed in the last decade and has been gradually replacing computer radiography (CR) in many countries. It offers the potential for improved image quality and provides opportunities for advances in medical image management, computer-aided detection and teleradiology. This workshop aims to provide comprehensive information on the physical principles and instrumentation of DR. The main optimization techniques such as the use of automatic exposure control (AEC) and exposure index (EI) will be discussed. This workshop also emphasizes the routine physical QC tests in DR where image quality and artifacts will be highlighted.

This workshop is expected to attract participants from the ASEAN and other countries. The speakers are Prof. Dr. Kwan-Hoong Ng (Director of ACOMP), Dr. Napapong Pongnapang (Thailand), Dr. Noriah Jamal (Malaysia) and Dr. Chai-Hong Yeong (Malaysia).

## **MINI SYMPOSIUM**

### **THE EVOLVING POSTURE OF MEDICAL PHYSICS AS A PROFESSION: MEDICAL PHYSICS 3.0**

Ehsan Samei, PhD, DABR, FAAPM, FSPIE

Director, Medical Physics Graduate Program  
Chief Physicist, Duke Clinical Imaging Physics Group  
Professor of Radiology, Medical Physics, Physics, Biomedical Engineering, and Electrical and Computer Engineering  
Duke University Medical Center  
2424 Erwin Road, Suite 302 (DUMC Box 2731), Durham, NC 27705

Over its existence, medical physics has made significant contribution to medicine, particularly in the design, implementation, and quality assurance of imaging and radiation therapy techniques. However, the clinical engagement has been limited. Medical Physics 3.0 is a new initiative to redefine excellence based on the crucial roles that medical physicists should play in healthcare enterprise today. It involves a set of trajectories to grow, express, and enact the value of medical physics and to position physicists to have the competence and the confidence to fulfill their unique calling as scientific agents of precision and innovation in healthcare

The objectives are :

- Understand the broad trajectory of advances in the contribution of medical physics to human health
- Understand the attributes of excellent in clinical physics
- Outline processes to position physicists to have the competence and the confidence to fulfill their unique calling as scientific agents of precision and innovation in healthcare

## **MINI SYMPOSIUM**

### **PRECISION MEDICINE THROUGH DOSE OPTIMIZATION AND MONITORING OF MEDICAL IMAGING**

Ehsan Samei, PhD, DABR, FAAPM, FSPIE

Director, Medical Physics Graduate Program  
Chief Physicist, Duke Clinical Imaging Physics Group  
Professor of Radiology, Medical Physics, Physics, Biomedical Engineering, and Electrical and Computer Engineering  
Duke University Medical Center  
2424 Erwin Road, Suite 302 (DUMC Box 2731), Durham, NC 27705

This symposium focuses on how dose optimization in terms of prospective optimized technique definitions as well as retrospective analysis of patient data pertaining imaging safety and quality can be used towards improved consistency of care.

#### Course Objective:

1. To delineate the scientific strategy to achieve optimized dose in medical imaging.
2. To delineate relevant analytical techniques to audit the prescription and the actuality of radiation dose and image quality in patient imaging.
3. To define how prospective and retrospective aspects of dose optimization can be used for holistic performance optimization and for practice of precision medicine in medical imaging.

## MINI SYMPOSIUM

### DOSIMETRY IN TERMS OF ABSORBED DOSE TO WATER IN PHOTON BRACHYTHERAPY

Golam Abu Zakaria

Department of Medical Radiation Physics, Gummersbach Hospital, Academic Teaching Hospital of the University of Cologne, Gummersbach, Germany

E-mail: GolamAbu.Zakaria@klinikum-oberberg.de

Keywords: Brachytherapy dosimetry, Absorbed dose to water, Photon radiation quality index

About 10% of all radiotherapy treatments are performed by brachytherapy (BT) mostly by photon-radiation from  $^{192}\text{Ir}$  with high BT-photon energy, HE:  $E > 50\text{keV}$ , or from  $^{125}\text{I}$  with low BT-photon energy, LE:  $E < 50\text{keV}$ . Although the absorbed dose to water  $D_W$  is best related to the radiobiological effects, BT-photon-sources are still calibrated in terms of the reference air kerma-rate. Thus, the clinical medical physicist has to determine  $D_W$  by using the AAPM-TG-43 formalism (used in most BT-treatment planning systems, expecting one BT-source in an unfinite water phantom) or more advanced model based dose calculation algorithms.

Several  $\dot{D}_{w,1}$ -primary standards have been developed in European Metrological Institutes within the Euramet-project. There is still a great need to provide more primary standards, traceably calibrated secondary and transfer standards to calibrate every BT-photon-source and BT-dosimetry-detector in terms of absorbed dose to water.

The response of BT-dosimetry-detectors is strongly energy related both the detector material to water dose-ratio and the intrinsic response. Thus, Monte Carlo (MC) simulations are used to determine the mean photon energy  $\bar{E}$  at the point of interest. A new possibility to determine the mean photon energy without new MC-calculations has just been published, utilizing the novel BT-photon radiation quality index  $Q^{\text{BT}}$ , the ratio of the primary radiation dose at 2 cm of water to that at 1 cm. This  $Q^{\text{BT}}$  can be derived easily and accurately from published primary and scatter separated (PSS) dose data.

## **MINI SYMPOSIUM**

### **DIGITAL RADIOGRAPHY DETECTORS: OVERVIEW AND ACCEPTANCE TESTING / QUALITY CONTROL UPDATE**

J.A. Seibert, PhD,

University of California Davis Health System, Sacramento, California, USA

Digital radiography detectors represent a wide variety of technologies, including computed radiography (CR), optically coupled CCD-based large area detectors, flat-panel thin-film-transistor (TFT) arrays, complementary metal-oxide (CMOS) arrays, and slot-scan arrays. Each type of detector has unique attributes in terms of x-ray latent image capture, signal conversion, and temporal acquisition capabilities, but all are characterized as having a wide exposure dynamic range and similar pre- and post-processing steps necessary to optimize the resultant images for human viewing and diagnosis. Technological advances continue, with introduction of wireless, flat panel arrays with large and small form factors, systems with variable acquisition gain, discrete photon counting devices, and energy discriminating capabilities. A brief overview of current and future x-ray detectors is discussed in the presentation.

The American Association of Physicists in Medicine is developing harmonized and holistic digital radiography acceptance test and periodic quality control procedures to encompass acquisition detectors as mentioned above in addition to the other components in the system, including the x-ray generator, x-ray tube, antiscatter grid, automatic exposure control modules, informatics components including system interfaces, HL7 - DICOM attributes, image processing/calibration issues, and image display characteristics, as examples. The efforts of the task group, now nearing completion, will be outlined and described.

## MINI SYMPOSIUM

### IMPLEMENTATION OF THE IEC 62494-1 EXPOSURE INDEX STANDARD

J.A. Seibert, PhD,

University of California Davis Health System, Sacramento, California, USA

As digital radiography detectors have a wide exposure dynamic range coupled with acquisition post-processing, appropriate image quality cannot simply be judged by its visible appearance. The generic “Exposure Index” is a method in which digital radiography manufacturers provide feedback to the radiographer regarding the estimated exposure on the detector, as an indirect indication of digital image quality and noise. Unfortunately, there are as many proprietary Exposure Index methods as there are manufacturers. The situation is even more complicated in a multi-vendor environment with a need to share data across institutions, or to a dose registry database. Fortunately, a unified Exposure Index methodology for Digital X-ray Imaging Systems, developed concurrently by the International Electrotechnical Commission (IEC) and the American Association of Physicists in Medicine in cooperation with the digital radiography system manufacturers, has been implemented as an international standard. Even though the IEC 62494-1 standard has been available since 2008, only now, in 2016, is the standard beginning to be widely adopted in the United States for digital radiography systems.

As discussed in the presentation, the standardized Exposure Index (EI) does not indicate patient dose, but is a linearly proportional estimate of the incident radiation exposure to the detector based upon the analysis of the resultant histogram distribution of digital values within the exposed region. The major value of the standard is to provide immediate feedback to the radiographer with calculation of the “Deviation Index” that indicates the amount of under- or overexposure of the incident radiation to the detector, relative to a user-determined “Target Exposure Index” ( $EI_T$ ) value. A key aspect of the implementation is the identification of the  $EI_T$  values in the imaging system protocol database, based upon the type of exam, the type of detector, and the clinical requirements in terms of image quality (noise). While an estimate of patient dose is not achieved, it is suggested that use of the standardized EI,  $EI_T$ , and DI values will lead to improved image acquisition performance in terms of reproducibility and use of optimized radiographic techniques, with the likelihood of better and safer care of the patient population needing radiographic examinations. Radiologists will benefit from standardized terminology, and institutions / clinics will be able to compare exposure index values and deviation index performance with others through a national dose index registry database.

## **MINI SYMPOSIUM**

### **RADIATION DOSE METRICS AND DOSE MONITORING FOR MEDICAL IMAGING PROCEDURES**

J.A. Seibert, PhD,

University of California Davis Health System, Sacramento, California, USA

Monitoring of radiation dose metrics is rapidly expanding in the United States to record and report radiation dose metrics, beginning with the 2012 implementation of the American College of Radiology Dose Index Registry for CT, and legislation to require reporting of dose metrics in California. Dose monitoring is now expanding to other imaging modalities that use ionizing radiation, including interventional radiology, cardiology, mammography, radiography, and nuclear medicine. Tracking and analyzing dose-metric data allows opportunities for optimizing imaging procedures and identifying outlier high-dose examinations, as well as providing a longitudinal history of patient encounters and creating a radiation dose portfolio to improve patient quality and safety. Underlying these efforts are DICOM working groups to specifically create supplements and modify existing standards to improve radiation dose data collection and extraction in structured reports, and continued development of the Integrating the Healthcare Enterprise (IHE) Radiation Exposure Monitoring (REM) profile.

This presentation will describe the implementation, training, use-cases, and future directives of the dose monitoring effort at the UC Davis Medical Center. As imaging modalities report unique radiation dose metrics that differ from patient radiation dose, medical physicist insight and informatics tools are required to objectively evaluate and optimize procedures, as well as determine reference dose benchmarks. Recent DICOM supplements (in particular the radiopharmaceutical injected dose) and radiation dose structured report content will be discussed.

## **MINI SYMPOSIUM**

### **RADIO-ADAPTIVE RESPONSE – MORE THAN TUMOR RESISTANCE**

Danupon Nantajit, Ph.D.

Department of Radiation Oncology, Chulabhorn Hospital, Bangkok 10210, Thailand

The concept of tumor adaptive resistance has long been introduced as the idea that tumor cells detoxify treatment reagents. For radiation therapy, fractionation has allowed both normal tissue as well as tumor sparing, although at a different level. The exact mechanisms of tumor acquired adaptive resistance is yet fully understood; however, other tumor adaptive response to ionizing radiation has recently been observed and introduced under different treatment conditions. In terms of tumor, stress of radiation induces cell resistance, aggressiveness as well as metastatic potentials. Phenomena such as epithelial-mesenchymal transition (EMT) are also activated as a response to radiation. Inversely, radiation-induced bystander effect, anti-tumor immune response as well as abscopal effect has also been observed under certain radiation fractionation scheme. With stereotactic body radiation therapy (SBRT), anti-angiogenesis response has been reported along with a certain degree of abscopal effect. Both the positive and negative responses of fractionated irradiation under different schemes will be discussed including responsible genes underlying such responses. Low dose radiation-induced adaptive resistance will also be mentioned to provide a clearer view of tumor biology as a system. At the moment, mechanisms underlying these radioadaptive responses are being defined; their applications should be exploited to improve efficacy of current cancer therapy

## MINI SYMPOSIUM

### TUMOR MICROENVIRONMENT: CHALLENGES AND PERSPECTIVES

Thititip Tippayamontri<sup>1,2</sup>

<sup>1</sup>Department of radiological technology and medical physics, faculty of allied health sciences, Chulalongkorn University, Bangkok Thailand. <sup>2</sup>Department of nuclear medicine and radiobiology, faculty of medicine and health sciences, University of Sherbrooke, Sherbrooke, QC, Canada.

The tumor microenvironment (TME) is being well recognized as an important factor in multiple stages of disease progression, especially for local resistance, immune-escaping, and distant metastasis. An appropriate understanding of TME is substantial important for the future development of clinical strategies in clinical oncology to overcome cancer resistance, prevent metastasis and improve therapeutic efficacy. This relate particularly to the appropriate evaluation of TME and selection of candidate agents to target TME. TME consists of a number of components including surrounding blood vessels, infiltrating immune cells, fibroblasts, bone marrow-derived inflammatory cells, lymphocytes, signalling molecules and the extracellular matrix. In addition, TME components along with cancer cells are exposed to abnormal physiologic conditions such as hypoxia and acidic extracellular pH that may induce both adaptive and constitutive changes in cancer and stromal cells. In this presentation, we will focus on the understanding of TME biology and highlights the prospect possibilities of visualization and targeting TME.

## **MINI SYMPOSIUM**

### **JOHN CAMERON MEMORIAL LECTURE (SEAFOMP): ADVANCES IN IMAGE GUIDED RADIATION THERAPY**

Geoffrey S. Ibbott, Ph.D.,

UT MD Anderson Cancer Center. [gibbott@mdanderson.org](mailto:gibbott@mdanderson.org)

The introduction of image guidance in radiation therapy has revolutionized the delivery of treatments. Modern imaging systems can supplement or even replace the historical practice of relying on external landmarks and laser alignment systems. Rather than depending on markings on the patient's skin, image-guided radiation therapy (IGRT) using techniques such as computed tomography (CT), cone-beam CT, MV on-board imaging (OBI), and kV OBI allows the patient to be positioned based on the internal anatomy. These advances in technology have enabled more accurate delivery of radiation doses to anatomically complex tumor volumes, while sparing surrounding tissues. While these imaging modalities provide excellent bony anatomy image quality, magnetic resonance imaging (MRI) surpasses them in soft tissue image contrast for better visualization and tracking of soft tissue tumors with no additional radiation dose to the patient. However, the introduction of MRI into a radiotherapy facility carries with it a number of complications including the influence of the magnetic field on the dose deposition, as well as the effects it can have on dosimetry systems. The development and introduction of these new IGRT techniques will be reviewed and the benefits and disadvantages of each will be described. Clinical examples of the capabilities of each of the systems will be discussed.

## **MINI SYMPOSIUM**

### **THE ROLE OF MEDICAL PHYSICISTS IN CLINICAL TRIALS**

Facilitator: Tomas Kron, Peter Mac Callum Cancer Centre, Melbourne Australia

Clinical trials are an essential part of clinical research and are still considered the best way to generate clinical evidence on which best practice should be based. However, medical physicists rarely engage with trials other than providing quality assurance for technical aspects. This workshop focuses on clinical trials as an opportunity for medical physicists to engage closer with clinical research bringing in not only their unique skills but also questions that are relevant to the interface between patients and technology.

Participants will learn about different phases of clinical trials, typical trial questions and the need for statistics and ethics review. The importance of data quality will be emphasised and the role of quality assurance highlighted.

The workshop will illustrate the contributions physicists can make using several radiotherapy trials as example. They range from high-tech trials for stereotactic ablative body radiotherapy (SABR) to interventions that involve the patient in her/his own treatment (eg Deep Inhalation Breath Hold, DIBH). In these trials we will illustrate the whole range of possible physics contributions from writing sections of the protocol (imaging, radiotherapy technique, quality assurance) to reviewing safety and possibly adding trial questions themselves. The latter can be secondary endpoints such as comparison of technologies to achieve the same clinical objective (eg IMRT, VMAT, tomotherapy,...) to optimisation and health economic outcomes.

Depending on the number of participants there will be an opportunity for the audience to participate in the set-up of a theoretical trial and explore what physicists can add.

## **MINI SYMPOSIUM**

### **NEW HORIZON OF MEDICAL PHYSICS AND SYNERGETIC EFFECT WITH MEDICAL ENGINEERING AND INFORMATION SCIENCE**

Kiyonari Inamura

Professor Emeritus Osaka University, Japan

To provide young researchers with topics of new horizon of cooperating medical informatics with medical engineering and of bringing synergetic effect, titles of research fields and of focusing them onto concrete method of development are raised.

Close reviews and analyses of papers from AAPM journals, IJCARS (International Journal of Computer Assisted Radiology and Surgery), IJBME, AJMI (American Journal of Medical Informatics), BIIJ, and PRT (Radiological Physics and Technology) were done. Retrospective history, present status and future prospect are sought logically.

Examples are: (1) new modalities for diagnoses and therapy such as portable CT for disaster ambulance in earthquake, (2) predictive, preventive and personalized medicine, (3). information processing in computer assisted interventions, (4). application of big data and cloud computing, (5) multiscale digital patient, (6). medical decision supports, (7). quantitative imaging biomarkers, (8) medical robotics and manipulators and deep brain stimulation and (9) Smart cyber operating theater.

Breakdown of above each item into specific detail is tried to present. Coming World Congress in 2018 and 2021 where both International Congresses of Medical Physics and IFMBE will be good opportunities for young investigators to present results of research and development. WC 2022 hopefully in Japan is the final target of harvesting fruitful results of cooperated research and development.

## **MINI SYMPOSIUM**

### **MP EDUCATION AND TRAINING IN MEFOMP COUNTRIES**

**Laila Al Balooshi**

*Head of Medical Physics Section , Dubai Hospital, Dubai - UAE*

The Education and Training of medical Physics in MEFOMP countries has evolved since the last decade to better suit the demand and fulfill the market need of physicists in our region. The programs of Medical Physics will be revised for some countries in our region.

The mission of MEFOMP Educational and Training Committee (ETC) is to promote activities related to education and training of medical physicists for the purpose of improving the quality of medical services for patients in the region through advancement in the practice of physics in medicine. ETC helps and provides support for all medical physics trainees in all member countries to have access to various levels of learning, and the types of knowledge required for higher level functions such as problem solving, creative innovations, and applied clinical applications.

Medical physics education can be much more effective and efficient when all regional chapters of IOMP share their knowledge and experience to enhance the outcome with coordination of highly qualified experts of medical physics professionals.

## **MINI SYMPOSIUM**

### **PIONEER WOMEN MEDICAL PHYSICISTS FROM MEFOMP COUNTRIES**

Huda. M. Al Naemi

Hamad Medical Corporation, Doha, Qatar, P.O.Box:3050

The establishment of Middle East Federation of Medical Physics (MEFOMP) in 2009 was part of the International Organization for Medical Physics (IOMP) efforts to organize regional medical physics societies under its umbrella and to further enhance and improve the status of medical physics across the Globe.

The main Goals of MEFOMP are: to Promote advancement of medical physics in the Middle East (ME), Educate and train local society members on new procedures and technologies, Encourage exchange of expertise and information among societies and to organize regional conferences and symposia.

The number of Female medical physicists obtained from the MEFOMP countries medical physics societies (in Lebanon, Syria, Jordan, Iraq, Palestine, King Saudi Arabia (KSA), United Arab Emirates (UAE), Kuwait, Qatar, Bahrain, Oman and Yemen) was found to be 243. Whereas the total number of medical physicists in these countries is 700 working in radiology, oncology, nuclear medicine and all other medical physics fields. This means that 35% of the medical physicists in the Middle East are women. The highest number of female medical physicists was found to be in Kingdom of Saudi Arabia – 83 (34% of the total MEFOMP female members). The highest percentage of the female medical physicists in MEFOMP countries is in the UAE as 70% of medical physicists are female.

Some of the women in MEFOMP countries are pioneers in their field, their creativity and achievements have contributed to medical physics and that is sure to inspire a new generation of young women to pursue their highest ambitions in medical physics and other fields.

## **MINI SYMPOSIUM**

### **MEDICAL PHYSICISTS CERTIFICATION PROCESS AND EXAMINATION IN THE MIDDLE EAST**

Ibrahim Duhaini<sup>1</sup>

<sup>1</sup> Rafik Hariri University Hospital, Radiation Oncology Department, Beirut, Lebanon

Certifying medical physics is becoming an essential part in recruiting medical physicists in hospitals across the Middle East region. Due to the lack of a comprehensive post graduate programs in MP in most of ME countries, hospitals find it very difficult to hire MP without the proper credentials and clinical experiences. Also, MP in the region find it very difficult to apply and travel for certification to Europe or North America due to visa and other related issues. So, if these certifying bodies are willing to cooperate with MEFOMP and/or similar organizations in the ME region, this could result in certifications being offered in the region for the region in a way to ease the process and save efforts and resources from the burdens of MP.

Certifying Medical Physicists requires an individual to obtain a university degree at the level of Master degree in Medical Physics, this is followed by at least one year of clinical residency program in the Medical Physics fields applied in a Hospital.

The existing local/national certifying organization exam models are utilized as reference to design the final exam structure which can be customized for the medical physicists who will be working in the Middle East.

Three Exam Model proposals will be discussed here, all of which aim to evaluate the competencies of the individual medical physicist knowledge and skills by following various examination approaches.

## **MINI SYMPOSIUM**

### **FETAL DOSE IN RADIOTHERAPY – MANAGING THE PHYSICS ASPECTS**

James C L Lee, SEAFOMP's President

The incidence of cancer reported is increasing worldwide. As a result, the probability of treating younger patients has also increased, including females who may be pregnant at time of radiotherapy. This presents a real challenge as the developing fetus may be irradiated with significant radiation dose. This lecture aims to give a basic overview of dose effects on developing fetus and the management of dose from the physics perspective. The reduction of fetus dose and the optimal treatment for the pregnant patient are competing demands for radiotherapy that requires optimization. Hence various strategies have been proposed and adopted for such radiotherapy treatment. Some practical aspects for fetal dose in NPC IMRT treatment will be discussed. Proton therapy will also be briefly discussed.

## **MINI SYMPOSIUM**

### **CERTIFICATION OF MEDICAL PHYSICISTS IN AFOMP COUNTRIES**

Howell Round

School of Engineering, University of Waikato, Hamilton, New Zealand

Certification of physicists by medical physics professional organizations is increasingly being recognised as important to ensure that clinical medical physics is being practiced by properly-trained, competent physicists. Increasingly, more AFOMP national member organizations (NMOs) are planning and establishing training programs that lead to certification. A survey was recently conducted to establish the current status of certification in AFOMP countries.

Two types of certification exist. One is a requirement by a government for medical physicists in its country to be registered with some sort of screening process being in place to ensure that those certified have a level of competence. For example, to practice clinical medical physics in India, individuals must be licensed/registered by India's Atomic Energy Regulatory Board. This seems to be uncommon in AFOMP countries. The other type is certification by an NMO which is generally achieved by completing a master degree in medical physics, completing a structured training program and passing written and oral examination - similar to the requirements for International Medical Physics Certification Board (IMPCB) accreditation. Over half of the AFOMP NMOs have such a certification program. The Korean Society for Medical Physics has received IMPCB accreditation while others (e.g. Australia and New Zealand) intend to apply for it in the near future.

Generally there is no government requirement for a country's medical physicists to have achieved certification by that country's NMO, although there is such a requirement in Indonesia and others are moving in that direction. Having such a requirement creates difficulties for NMOs with many senior medical physicists with a lot of experience who have never been certified. This is best overcome with some form of grandfathering, which may require some form of assessment by one's peers.

Maintenance of certification through continuing professional development, etc., is required by less than half of the NMOs offering certification, while others are planning to do so. The effort and cost required to establish and administer a continuing professional development program should not be underestimated.

There has been a lot of enthusiasm for establishing training and certification programs for medical physicists in AFOMP countries. This is challenging even for countries with high incomes, but for poorer countries with few physicists this is extremely difficult and cooperation between AFOMP NMOs is necessary if training and certification programs are to be established in all countries.

Keywords: certification, training, accreditation, continuing professional development



